



Université catholique de Louvain  
Faculté des Sciences  
Département de physique  
Unité de physique théorique  
Center for Particle Physics and Phenomenology

---

---

# New techniques in QCD

---

---

*Thèse présentée par **Claude Duhr** en vue d'obtenir le grade de  
Docteur en Sciences.*

## Composition du Jury:

Promoteur:	Pr. Fabio Maltoni	UCL
Président:	Pr. Denis Favart	UCL
Membres du jury:	Pr. Ben Craps	VUB, Bruxelles
	Pr. Vittorio Del Duca	INFN, Frascati
	Pr. Jean-Marc Gérard	UCL
	Pr. Jan Govaerts	UCL
	Pr. David A. Kosower	CEA, Saclay

---

September 2009



# Remerciements

*Je tiens tout d'abord à remercier le Professeur Fabio Maltoni de l'Université catholique de Louvain de m'avoir offert la possibilité d'effectuer ce travail grâce à l'appui du Fonds National de la Recherche Scientifique. Son support constant et nos discussions stimulantes durant ces dernières années ont constitués le fondement solide sur lequel le présent travail a été construit.*

*Un remerciement particulier va au Docteur Vittorio Del Duca des "Laboratori Nazionali di Frascati" sans lequel la majeure partie de ce travail n'aurait pas pu être réalisée. Notre collaboration m'a permis d'approfondir mes connaissances en physique tout en m'aventurant sous sa guidance dans des domaines fascinants qui me seraient restés inconnus autrement.*

*Je tiens également à remercier les autres membres de mon Jury de soutenance, les Professeurs Ben Craps, Denis Favart, Jean-Marc-Gérard, Jan Govaerts et David A. Kosower, qui ont sacrifié une partie de leur temps pour évaluer ce travail et qui avec leurs questions et commentaires m'ont permis d'améliorer le manuscrit.*

*Le travail effectué durant ces dernières années n'aurait évidemment pas été réalisable sans le soutiens de mes nombreux collaborateurs. Je remercie donc chaleureusement le Docteur U. Aglietti et les Professeurs E. W. Nigel Glover et Vladimir A. Smirnov pour nos nombreuses et longues discussions dans lesquelles ils ont partagé avec moi leurs connaissances et expériences qui sont à la base de la réalisation de ce travail. Je voudrais également remercier toutes les person-*

nes qui ont contribué au projet “FeynRules”, Priscila de Aquino, Céline De-  
grande, Neil D. Christensen, Benjamin Fuks, Michel Herquet et Steffen Schu-  
mann. Sans leurs commentaires et suggestions le projet n’aurait pas pu voir  
la lumière du jour. Dans la même lignée, je remercie aussi tous les membres  
du “MadGraph Team”, et particulièrement Johan Alwall, Rikkert Frederix, Si-  
mon de Visscher, Olivier Mattelaer et Tim Stelzer, qui ont toujours patiem-  
ment répondu à toutes mes questions. Finalement, un remerciement aussi aux  
“Laboratori Nazionali di Frascati” et au “Institute for Particle Physics Phe-  
nomenology” à Durham, où une grande partie de ce travail à été achevée et qui  
m’ont toujours chaleureusement accueilli.

Les trois dernières années n’étaient évidemment pas seulement constituées de  
travail, et je voudrais donc aussi remercier toute ma famille et mes amis qui  
ont toujours été à mes côtés, aussi bien pendant les moments agréables que  
pendant les moments difficiles. Un grand merci en particuliers à tous mes  
autres collègues du CP3 pour les bons moments qu’on a passé ensemble et qui  
me resteront toujours en mémoires.

Gilsdorf, le 10 août 2009.

# Contents

<b>Introduction</b>	<b>1</b>
<b>I Tree-level techniques in gauge theories</b>	<b>9</b>
<b>1 Tree-level scattering amplitudes in gauge theories</b>	<b>11</b>
1.1 Feynman rules in gauge theories . . . . .	11
1.2 Color decomposition . . . . .	13
1.3 Spinor-helicity formalism . . . . .	15
1.4 Berends-Giele recursive relations . . . . .	19
<b>2 Twistor techniques in gauge theories</b>	<b>23</b>
2.1 Introduction . . . . .	23
2.2 The BCFW recursive relations . . . . .	24
2.3 The MHV formalism . . . . .	26
2.4 Recursive formulation of the MHV formalism . . . . .	29

---

<b>3</b>	<b>Color-dressed recursive relations</b>	<b>37</b>
3.1	Recursive relations in gauge theories . . . . .	37
3.2	Color-dressed Berends-Giele recursive relations . . . . .	38
3.3	Color-dressed BCFW recursive relations . . . . .	43
3.4	Discussion and conclusion . . . . .	47
<b>II</b>	<b>Infrared singularities of scattering amplitudes</b>	<b>51</b>
<b>4</b>	<b>Infrared singularities in scattering amplitudes</b>	<b>53</b>
4.1	Perturbative expansion of physical observables . . . . .	53
4.2	Infrared singularities . . . . .	57
4.3	Subtraction schemes . . . . .	64
4.4	Antenna factorization . . . . .	67
<b>5</b>	<b>Antenna functions from MHV rules</b>	<b>69</b>
5.1	Power counting for antenna functions in the MHV formalism . . . . .	69
5.2	Diagrammatic evaluation of antenna functions . . . . .	78
5.3	From antenna functions to splitting amplitudes . . . . .	83
5.4	Recursive relations . . . . .	88
<b>6</b>	<b>Analytic integration of some real-virtual counterterms</b>	<b>93</b>
6.1	A general subtraction scheme at NNLO . . . . .	93
6.2	The real-virtual integrals . . . . .	96
6.3	Hypergeometric integrals from integration-by-parts identities . . . . .	99
6.4	Conclusion . . . . .	107

---

<b>III</b>	<b>The BDS ansatz and high-energy limits</b>	<b>111</b>
<b>7</b>	<b>The Bern-Dixon-Smirnov ansatz</b>	<b>113</b>
7.1	The ABDK/BDS ansatz . . . . .	113
<b>8</b>	<b>The high-energy behavior of tree-level gluon amplitudes</b>	<b>121</b>
8.1	The multi-Regge limit . . . . .	121
8.2	Quasi multi-Regge limits . . . . .	125
8.3	Multi-Regge limits and MHV rules . . . . .	129
<b>9</b>	<b>High-energy factorization beyond tree-level</b>	<b>139</b>
9.1	The high-energy prescription . . . . .	139
9.2	MSYM amplitudes in the high-energy limit . . . . .	142
9.3	Quasi multi-Regge limits beyond tree-level . . . . .	149
9.4	The analytic continuation to the physical region . . . . .	151
<b>10</b>	<b>The BDS ansatz in the high-energy limit</b>	<b>153</b>
10.1	The BDS ansatz in multi-Regge kinematics . . . . .	153
10.2	The BDS ansatz and quasi multi-Regge kinematics . . . . .	157
<b>11</b>	<b>The five-point amplitude in multi-Regge kinematics</b>	<b>163</b>
11.1	Introduction . . . . .	163
11.2	Definitions and conventions . . . . .	164
11.3	The pentagon integral from NDIM . . . . .	165
11.4	The two-loop five-point amplitude . . . . .	178
11.5	The two-loop Lipatov vertex in MSYM . . . . .	180
11.6	The physical region . . . . .	181

---

<b>Conclusion</b>	<b>187</b>
<b>IV Appendices</b>	<b>191</b>
<b>A Reconstruction functions</b>	<b>193</b>
<b>B Proof of Chapter 5</b>	<b>195</b>
B.1 Gluon insertion rule . . . . .	195
B.2 Proof of Rule 5.5 . . . . .	197
<b>C Recursive relations for soft factors</b>	<b>203</b>
<b>D Multi-Regge kinematics</b>	<b>209</b>
D.1 Multi-parton kinematics . . . . .	209
D.2 Multi-Regge kinematics . . . . .	212
<b>E Proof of the MHV rules for quasi multi-Regge limits</b>	<b>215</b>
E.1 Power counting rules for quasi multi-Regge limits . . . . .	215
E.2 Proof of the MHV rules for quasi multi - Regge limits . . . . .	219
<b>F Nested harmonic sums</b>	<b>223</b>
<b>G Multiple polylogarithms</b>	<b>225</b>
G.1 Euler's and Nielsen's polylogarithms . . . . .	225
G.2 One-dimensional harmonic polylogarithms . . . . .	226
G.3 Two-dimensional harmonic polylogarithms . . . . .	229
G.4 Goncharov's multiple polylogarithm . . . . .	231



---

<b>H</b>	<b>Hypergeometric functions</b>	<b>235</b>
H.1	The Gauss hypergeometric functions . . . . .	235
H.2	Generalized hypergeometric functions . . . . .	238
<b>I</b>	<b><math>\mathcal{M}</math> functions</b>	<b>243</b>
<b>J</b>	<b>Real-virtual integrals</b>	<b>249</b>
J.1	The soft-collinear integral $\mathcal{K}$ . . . . .	249
J.2	The collinear integrals $\mathcal{I}$ . . . . .	252
J.3	The iterated integrals . . . . .	270
<b>K</b>	<b>Scalar one-loop integrals</b>	<b>273</b>
K.1	Basic definitions and conventions . . . . .	273
K.2	The Feynman parametrization . . . . .	275
K.3	Wick rotation and analytic continuation to the Euclidean region	276
K.4	The Schwinger parametrization . . . . .	277
K.5	The Negative Dimension approach . . . . .	278
K.6	The Mellin-Barnes representation . . . . .	280
<b>L</b>	<b>Analytic continuation of the scalar massless pentagon</b>	<b>283</b>
L.1	Analytic continuation from Region II(a) to Region II(b) . . . . .	283
L.2	Symmetry properties in Region I . . . . .	285
L.3	Analytic continuation from Region II(a) to Region I . . . . .	286
<b>M</b>	<b>The pentagon integral from Mellin-Barnes integrals</b>	<b>289</b>
M.1	Evaluation of the Mellin-Barnes integral in Region I . . . . .	290
M.2	Evaluation of the Mellin-Barnes integral in Region II . . . . .	301

---

M.3	The analytic expressions of the functions $i^{(0)}$ and $i^{(1)}$ . . . . .	310
M.4	The analytic expressions of the functions $j^{(0)}$ and $j^{(1)}$ . . . . .	311
<b>N</b>	<b>Reduction of the polylogarithms in terms of <math>G</math>-functions</b>	<b>313</b>
N.1	Reduction of $\text{Li}_n$ in Region I . . . . .	313
N.2	Reduction of $\text{Li}_n$ in Region II . . . . .	318
<b>O</b>	<b>Results for tree-level Lipatov vertices</b>	<b>319</b>
O.1	NMHV-type vertices . . . . .	319
O.2	NNMHV-type vertices . . . . .	327
	<b>Bibliography</b>	<b>357</b>

# Introduction

In the last forty years high-energy physics has been dominated by the Standard Model (SM), which describes the strong and electroweak interactions of the fundamental fermions and vector bosons. These interactions are described by an  $SU(3)_C \times SU(2)_L \times U(1)_Y$  gauge theory, where the  $SU(2)_L \times U(1)_Y$  symmetry gets spontaneously broken so that the weak gauge bosons and the fermions acquire a mass.

Despite the great success of the SM, all physicists agree that, even if the last missing fundamental particle predicted by the SM, the Higgs boson, is discovered, the SM cannot be the final theory as many questions are left unanswered. Therefore one of the main challenges, both on the theory and on the experimental side, is to look for new physics beyond the SM. Due to its great experimental success and despite the fact that new physics is expected to arise at the TeV scale, physicists believe that the principles underlying the SM are correct and that gauge symmetries are among the fundamental symmetries of Nature. In particular, the theory of strong interactions, Quantum Chromodynamics (QCD), is described by an unbroken gauge symmetry based on the gauge group  $SU(3)_C$ . The study of gauge symmetries is hence among the most important tasks in theoretical physics and has a twofold interest. First, a thorough understanding of gauge theories allows to pursue our efforts towards uncovering of the underlying principles of Nature. The second interest is purely phenomenological and stems from our need to make predictions for future collider experiments. In particular, the Large Hadron collider (LHC)

starts operating this year at CERN and will search for new physics linked to the breaking of the electroweak symmetry. Since however the LHC is a proton-proton collider, the major fraction of events observed will be pure QCD events and a good understanding of this QCD background to new physics signals thus requires a thorough understanding of how to make predictions for gauge theory scattering amplitudes.

During the last decade, significant progress has been made in the computation of gauge theory scattering amplitudes, both at tree-level and beyond. At tree-level, the field has got new momentum in 2003 when Witten conjectured a duality between Yang-Mills theories and a certain type of string theory based on twistor space [1]. The main outcomes of this conjecture, the BCFW recursion and the MHV rules [2, 3, 4], have led since then not only to new explicit results for gluon scattering amplitudes for up to eight gluons, but have also provided a new insight into the internal structure of Yang-Mills tree-level scattering amplitudes by revealing their intrinsically recursive nature. The ideas inherent to these twistor approaches were soon also applied beyond tree level, where they have been combined to the pioneering work of Bern Dixon and Kosower on the unitarity based approaches of the early nineties [5, 6]. This new way of tackling one-loop amplitudes has led to a revolution in the way we think (loop) amplitudes should be computed in an efficient way and a large number of new results have recently been published that were thought impossible just a few years ago. Furthermore, two independent groups implemented this approach into a numerical code allowing for the first time an automatic evaluation of one-loop amplitudes and therefore finally bringing within reach the full automatization of next-to-leading order computations in QCD [7, 8].

Despite the impressive progress that has been made regarding one-loop scattering amplitudes in QCD, not much is known, however, about Yang-Mills amplitudes at two-loop accuracy and beyond. Progress in this direction has been made, however, in recent years in the context of planar  $\mathcal{N} = 4$  super Yang-Mills theories (MSYM). The study of this particular gauge theory has a twofold interest. First, it is known that one can always arrange the computation of QCD loop amplitudes in a way such as to make the MSYM contribution manifest, *i.e.*, MSYM amplitudes are a part of the full QCD amplitude and

so their knowledge reveals part of the full QCD result. Second, since MSYM is a supersymmetric conformal quantum field theory, it is much simpler than full QCD and therefore serves as a playground to investigate the properties of Yang-Mills theories in this simpler framework and the hope is to extend these properties to the study of QCD amplitudes. One of the most intriguing results in this context is a conjecture put forward by Bern, Dixon and Smirnov (BDS), based on the previous work of Anastasiou, Bern, Dixon and Kosower, that an MSYM gluon amplitude in a so-called *maximally helicity violating* configuration must fulfill a set of iteration relations which allow to express a generic  $\ell$ -loop amplitude for an arbitrary number of legs in terms of the one-loop amplitude [9, 10]. The BDS ansatz was shown to hold in the case of the two and three-loop four-point amplitude by direct analytical computation and in the case of the two-loop five-point amplitudes by a numerical evaluation. However, it was shown to fail independently by several groups in the finite part of the two-loop  $n$ -point case, with  $n \geq 6$  [11, 12, 13]. The question whether the ansatz is just a mirage or whether it is enough to modify the ansatz by some (yet unknown) function in order to correct it for any number of external legs is currently the aim of intense research activity.

An aim of this work is to contribute to this challenge of understanding Yang-Mills theories, both from the theoretical and from the phenomenological point of view. We concentrate in particular on the computation of gauge theory scattering amplitudes. In the first part, we investigate tree-level amplitudes and we give a review of Witten's twistor techniques in Chapter 2. Those techniques are defined at the level of the color-stripped amplitudes and need to be dressed with color when computing full QCD matrix elements. In Chapter 3 we therefore introduce a technique to dress recursive relations for color-ordered tree-level amplitudes with color and we derive the corresponding color-dressed recursive relations, showing in this way explicitly that the recursive nature of gauge theory scattering amplitudes is preserved also for the full QCD matrix elements, including color [14].

For many phenomenological applications, however, tree-level approximations to physical observables are insufficient and only orders of magnitude can be obtained. In such cases it is necessary to include higher-order corrections

coming from loop amplitudes. QCD computations beyond leading-order exhibit two different types of divergencies which have to be dealt with before any prediction for a physical quantity can be obtained. On the one hand, ultraviolet-divergencies appearing when particles with large momenta circulate inside a loop can be handled by the renormalization procedure. On the other hand, QCD loop amplitudes are also infrared divergent. The Kinoshita-Lee-Nauenberg (KLN) theorem implies that the infrared singularities coming from the real and virtual corrections arising when two or more particles become soft and / or collinear in phase space cancel out for inclusive enough quantities (cross sections, decay rates,...) at any order in perturbation theory. In the second part of this work we therefore investigate the infrared behavior of gauge theory amplitudes. In Chapter 4 we review how the infrared divergencies coming from the real and virtual corrections are handled using so-called *subtraction schemes* before performing any numerical calculation. The subtraction method relies on the fact that the infrared behavior of QCD amplitudes is universal and can be described by the so-called *splitting amplitudes* and *soft factors*. A precise knowledge of these universal quantities is thus needed to perform higher-order calculations in QCD. Besides the splitting amplitudes and soft factors, there is another set of objects that describe the infrared behavior of QCD amplitudes. These so-called antenna functions were introduced in Refs. [15, 16] and describe in a unified way the soft and collinear divergencies in QCD. In Chapter 5 we present a novel way of introducing tree-level antenna functions, based on Witten's twistor techniques [17]. We show how the MHV formalism provides a natural way of defining antenna functions as a sum over MHV diagrams, extending in this way the corresponding result by Birthwright *et al.* derived for splitting amplitudes [18, 19]. We then apply our technique to derive for the first time the a full set of tree-level gluon antenna functions up to N<sup>3</sup>LO and we present a set of recursive relations for antenna functions and splitting amplitudes, showing in this way once more that splitting amplitudes inherit all the properties of the full amplitudes: gauge invariance, symmetry relations and even a fully recursive formulation.

A general process-independent subtraction scheme at NLO was already introduced more than a decade ago [20]. Its generalization to NNLO and the

counterterms regularizing the real emissions for up to two unresolved particles, however, have only been proposed recently [21, 22, 23, 24]. In practise, it is necessary to know also the analytic expressions of these counterterms integrated over the phase space of the unresolved particles. In this work we address this problem and explicitly integrate a subset of the real virtual counterterms appearing in the generic NNLO subtraction scheme. In Chapter 6 we present our method of performing the integration, which is a generalization of techniques introduced in the last decade for the computation of (multi-) loop integrals and we extend this technique to the computation of generalized hypergeometric integrals which appear in the integrals over the phase space of the unresolved particles. We illustrate our approach on the example of the soft counterterm, which can be expressed in terms of Gauss's hypergeometric function. Details on the more general integrals are given in Appendix J.

In the third part of this work we analyze the BDS conjecture in MSYM. We review the ansatz and what is known about its breakdown in Chapter 7. Since the computation of the two-loop six-point amplitude in Ref. [12] was numerical, not much is known about the breakdown of the ansatz for  $n = 6$ . The question could be settled by the a direct analytical computation of the two-loop six-point amplitude, involving the analytic calculation of two-loop hexagon integrals, a computation which is beyond our technical capabilities for the moment. We therefore propose to perform the computation not in general kinematics, but in simplified kinematics, based on the high-energy behavior of gauge theory amplitudes, where the loop integration might become simpler. In the high-energy limit, the produced gluons are strongly ordered in rapidity and the corresponding scattering amplitudes are conjectured to factorize in terms of universal building blocks, the so-called coefficient functions and Lipatov vertices, similar to the splitting amplitudes and soft factors in the case of the infrared limits [25]. In Chapter 8 we review the high-energy factorization of tree-level gluon amplitudes and introduce our notations and conventions. We then proceed and present a novel way to compute tree-level coefficient functions and Lipatov vertices. This new approach is based on the MHV formalism and is a generalization of the methods introduced in Chapter 5 in the context of antenna functions. We explicitly use this new technique and derive for the first

time the complete set of tree-level gluon Lipatov vertices for the emission of up to four gluons. In Chapter 9 we generalize the high-energy factorization beyond tree-level (in fact we conjecture that it holds true to any number of loops in the perturbative expansion [26, 27]) and we present explicit examples of how the universal building blocks can be extracted from MSYM loop amplitudes. In Chapter 10 we then combine the results of the preceding chapters and analyze the high-energy behavior of the BDS ansatz. We show in particular that the BDS ansatz in the euclidean region where all the invariants are negative is fully consistent with high-energy factorization for any number of loops and legs. By relaxing the strong rapidity ordering of the final state gluons we can disguise the limit of simplified kinematics where a discrepancy with the BDS ansatz should arise. Since this limit involves the explicit computation of the one and two-loop hexagons (in simplified kinematics), we study in Chapter 11 for the first time the behavior of one-loop MSYM amplitudes to higher orders in the dimensional regulator  $\epsilon$ , a necessary ingredient for the BDS ansatz. In particular, we compute the one-loop scalar massless pentagon in  $D = 6 - 2\epsilon$  dimensions in the high-energy limit, which appears in the higher order contributions in  $\epsilon$  to the five-point MSYM amplitude. We show that the result can be expressed in terms of generalized hypergeometric functions, whose Laurent series needs the introduction of a new set of transcendental functions, the so-called  $\mathcal{M}$  functions [28]. The knowledge of the scalar massless pentagon allows us to derive for the first time an analytic expression for the two-loop five-point amplitude, albeit in simplified kinematics and we finally use this result to extract the two-loop Lipatov vertex in planar MSYM [29]. Further appendices including technical details omitted throughout the main text as well as details on the special functions used throughout this work are also included.

This work is based on the following papers, as well as on conference proceedings [30]:

- C. Duhr, S. Hoeche and F. Maltoni, “*Color-dressed recursive relations for multi-parton amplitudes*,” JHEP, vol. 08, p. 062, 2006, [hep-ph/0607057].
- C. Duhr and F. Maltoni, “*Antenna functions from MHV rules*,” JHEP, vol. 11, p. 002, 2008, [arXiv:0808.3319].



- U. Aglietti, V. Del Duca, C. Duhr, G. Somogyi and Z. Trocsanyi, “*Analytic integration of real-virtual counterterms in NNLO jet cross sections I,*” JHEP, vol. 09, p. 107, 2008, [arXiv:0807.0514].
- V. Del Duca, C. Duhr and E.W.N. Glover, “*Iterated amplitudes in the high-energy limit,*” JHEP, vol. 12, p. 097, 2008, [arXiv:0809.1822].
- V. Del Duca, C. Duhr, E.W.N. Glover and V.A. Smirnov, “*The one-loop pentagon to higher orders in epsilon,*” 2009, submitted to JHEP, [arXiv:0905.0097].
- V. Del Duca, C. Duhr and E.W.N. Glover, “*The five-gluon amplitude in the high-energy limit,*” 2009, submitted to JHEP, [arXiv:0905.0100].

Some of the results in Chapter 8 and Appendix E are original and have not yet been published.



## Part I

# Tree-level techniques in gauge theories



# Chapter 1

## Tree-level scattering amplitudes in gauge theories

### 1.1 Feynman rules and diagrams in gauge theories

The theory of strong interactions is a Yang-Mills gauge theory based on the gauge group  $SU(3)$ . In the following we give a short review of  $SU(N_c)$  gauge theories in general, having  $N_f$  quark flavors in the fundamental representation. The Lagrangian for an  $SU(N_c)$  gauge theory reads

$$\mathcal{L} = -\frac{1}{4} \text{Tr} (F_{\mu\nu} F^{\mu\nu}) + \bar{q}_f i \not{D} q_f - m_f \bar{q}_f q_f + \frac{1}{2\xi} (\partial^\mu G_\mu^a)^2 + \bar{c}^a \partial^\mu D_\mu c^a, \quad (1.1)$$

where  $q_f$  denotes the quark field with flavor  $f$  and mass  $m_f^*$ ,  $G_\mu^a$  is the gauge field (the gluon in the case of QCD) and  $c^a$  denote the ghost fields. The covariant derivative  $D_\mu$  and the field strength tensor  $F_{\mu\nu}$  are defined by

$$\begin{aligned} D_\mu &= \partial_\mu - ig T^a G_\mu^a \\ F_{\mu\nu} &= \frac{i}{g} [D_\mu, D_\nu] = \left( \partial_\mu G_\nu^a - \partial_\nu G_\mu^a + g \sqrt{2} f^{abc} G_\mu^b G_\nu^c \right) T^a, \end{aligned} \quad (1.2)$$

---

\*In this work we only consider massless quarks,  $m_f = 0$ .

$n$	2	3	4	5	6	...
# diagrams	4	45	510	5040	40320	...

Table 1.1: Number of Feynman diagrams contributing to  $gg \rightarrow ng$  at tree level.

where  $T^a$  denote the generators of the Lie algebra of  $SU(N_c)$ , with the normalization

$$\text{Tr}(T^a T^b) = \delta^{ab} \quad \text{and} \quad [T^a, T^b] = i\sqrt{2} f^{abc} T^c. \quad (1.3)$$

The Lagrangian in Eq. (1.1) describes all the gauge interactions between the quarks and the gluons, and all (tree-level) Feynman rules can be derived from it. The complete set of Feynman rules of an  $SU(N_c)$  gauge theory can be found in Ref. [31]. Feynman rules are at the basis of the computation of Feynman diagrams, the ‘Queen’ of all techniques to compute scattering amplitudes in quantum field theory (QFT), which has been one of the most important activities in theoretical physics over the last fifty years. Although Feynman diagrams provide a very intuitive approach to the calculation of scattering amplitudes, their use may become inefficient due the factorial growth in complexity with the number of external particles (See Table 1.1). The main reason for such an extremely fast growth stems from the fact that each individual Feynman diagram is not a gauge-invariant quantity and subsets of diagrams combine to yield a gauge-invariant result, and gauge-invariant subsets are repeated many times. On the other hand, it is known that even if the number of diagrams can be quite large, the gauge-invariant results for QCD amplitudes can very often be written in a rather simple form, and large cancellations can happen between the different non gauge invariant contributions. For this reason, new techniques have been developed over the last fifteen years that allow to take the gauge-invariant structure into account from the beginning and to avoid in this way the bad algorithmic behavior of the Feynman diagram expansion. The first chapter of this work is a short review of these alternatives to Feynman diagrams.

## 1.2 Color decomposition

In this section we review the main ingredients that allow to overcome the problem of the factorial growth in the number of Feynman diagrams. As already mentioned, the bad algorithmic behavior of the Feynman diagram-based approaches comes from organizing the computation in a way that is not compliant with the underlying gauge symmetry of the theory. The main idea is to keep all the information separated from the start, *i.e.*, to factor out the gauge structure from the kinematical dependence of the amplitude in order to preserve gauge invariance at every step in the computation. The starting point for this approach is *color decomposition*, which allows to write any scattering amplitude as a sum over the different color structures that appear in the amplitude, multiplied by a coefficient that contains the kinematical dependence of the scattering. In the following, we focus on the different color decompositions for pure gluon amplitudes at tree-level, and we briefly comment at the end of this section on generalizations to include quarks as well.

Let us consider the tree-level amplitude for the scattering of  $n$  gluons with momenta  $p_i$ , helicities  $h_i$  and color quantum numbers  $a_i$ . This amplitude can be written as [32]

$$\begin{aligned} \mathcal{A}_n(\{p_i, h_i, a_i\}) &= g^{n-2} \sum_{\sigma \in S_n / \mathbb{Z}_n} \text{Tr}(T^{a_{\sigma_1}} \dots T^{a_{\sigma_n}}) A_n(\sigma(1^{h_1}), \dots, \sigma(n^{h_n})), \end{aligned} \quad (1.4)$$

where the sum runs over all non-cyclic permutations of the gluons. The coefficients  $A_n$  of the color traces are gauge-invariant quantities called *color-ordered amplitudes*<sup>†</sup> which only depend on the gluon momenta and helicities, but not on color<sup>‡</sup>. The color-ordered amplitudes are invariant under crossing symmetry if all external momenta are taken to be outgoing, which is the convention we will follow in the rest of this work. Furthermore, they are invariant under a cyclic permutation of the gluons and they fulfill the *reflection identity*,

$$A_n(n, \dots, 1) = (-1)^n A_n(1, \dots, n). \quad (1.5)$$

<sup>†</sup>Also known as *partial amplitudes*.

<sup>‡</sup>Note that we follow the convention to label the arguments of the color-ordered amplitudes only by the gluon indices, *i.e.*,  $A_n(1, \dots, n)$  has to be understood as  $A_n(p_1, \dots, p_n)$ .

Finally, there are linear relations among the partial amplitudes, known as the *Kleiss-Kuijf relations*, which allow to reduce the number of independent partial amplitudes from  $(n-1)!$  to  $(n-3)!$  [33, 34, 35]. Several ways exist to compute the partial amplitudes, but we only mention at this point the *color-ordered Feynman rules*, extending Feynman diagram-based approaches to color-ordered amplitudes [32]. In the next chapters we will review several alternative approaches, both recursive and diagrammatic.

Since the number of partial amplitudes in Eq. (1.4) grows factorially with the number of external gluons, it is more convenient to express the amplitude in a basis where we can identify *a priori* the terms in the color sum that give a non-zero contribution. In Eq. (1.4) each gluon was labelled by an adjoint color index ranging from 1 to  $N_c^2 - 1$ . Since  $\mathbf{N}_c \otimes \overline{\mathbf{N}}_c = (\mathbf{N}_c^2 - \mathbf{1}) \oplus \mathbf{1}$ , we can alternatively label the gluons by a pair of fundamental and anti-fundamental color indices  $(i, \bar{j})$ . In Ref. [36] it was shown that in this color-basis a tree-level gluon amplitude can be written as

$$\begin{aligned} \mathcal{A}_n(\{p_i, h_i, a_i\}) &= g^{n-2} \sum_{\sigma \in S_n / \mathbb{Z}_n} \delta_{i_{\sigma_1}}^{\bar{j}_{\sigma_n}} \delta_{i_{\sigma_2}}^{\bar{j}_{\sigma_1}} \dots \delta_{i_{\sigma_n}}^{\bar{j}_{\sigma_{n-1}}} A_n(\sigma(1^{h_1}), \dots, \sigma(n^{h_n})), \end{aligned} \quad (1.6)$$

where the partial amplitudes are the same as those appearing Eq. (1.4). This color decomposition, also known as the color-flow decomposition, is well suited to be used in numerical algorithms, because the color factors in front of the partial amplitudes all evaluate to either zero or one. Hence, one can identify *a priori* the zero color flows and restrict the computation only to partial amplitude with non-zero color flow. Squaring and summing is particularly easy in the color-flow decomposition, *e.g.*,

$$\begin{aligned} &\delta_{i_{\sigma_1}}^{\bar{j}_{\sigma_n}} \delta_{i_{\sigma_2}}^{\bar{j}_{\sigma_1}} \dots \delta_{i_{\sigma_n}}^{\bar{j}_{\sigma_{n-1}}} \left( \delta_{i_{\sigma_1}}^{\bar{j}_{\sigma_n}} \delta_{i_{\sigma_2}}^{\bar{j}_{\sigma_1}} \dots \delta_{i_{\sigma_n}}^{\bar{j}_{\sigma_{n-1}}} \right)^\dagger \\ &= \delta_{i_{\sigma_1}}^{\bar{j}_{\sigma_n}} \delta_{i_{\sigma_2}}^{\bar{j}_{\sigma_1}} \dots \delta_{i_{\sigma_n}}^{\bar{j}_{\sigma_{n-1}}} \left( \delta_{j_n}^{\bar{i}_{\sigma_1}} \delta_{j_1}^{\bar{i}_{\sigma_2}} \dots \delta_{j_{\sigma_{n-1}}}^{\bar{i}_{\sigma_n}} \right) \\ &= N_c^n, \end{aligned} \quad (1.7)$$

and for the cross terms between different color flows one gets in a similar way monomials of the form  $N_c^{n-m}$ , where  $m$  is even. This is to be contrasted to the fundamental color decomposition, where products of traces of color matrices have to be computed.



The two color decompositions (1.4) and (1.6) both use the fundamental representation of  $SU(N_c)$  for the color factors. Since the gluons transform in the adjoint representation of the gauge group, we can ask for a decomposition of the amplitude that takes advantage of the adjoint nature of the gauge bosons. In Ref. [37] it was shown that a pure gluon scattering amplitude can be written as

$$\begin{aligned} \mathcal{A}_n(\{p_i, h_i, a_i\}) &= g^{n-2} \sum_{\sigma \in S_{n-2}} (F^{a_{\sigma_2}} \dots F^{a_{\sigma_{n-1}}})_{a_1 a_n} \\ &\times A_n(1^{h_1}, \sigma(2^{h_2}), \dots, \sigma((n-1)^{h_{n-1}}), n^{h_n}), \end{aligned} \quad (1.8)$$

where  $(F^b)_{ac} = if^{abc}$  denote the generators of the fundamental representation of  $SU(N_c)$ . Note that in contrast to the decompositions discussed earlier, only  $(n-2)!$  terms appear in the sum in Eq. (1.8). However, although the number of color-ordered amplitudes which need to be evaluated is much smaller than in the fundamental or the color-flow decompositions, the adjoint color basis turns out to be less efficient because it involves matrix products for the  $(N_c^2 - 1)$ -dimensional matrices  $F^a$ .

Let us conclude this section by making some comments on how color decomposition can be extended to quarks. We give the explicit example of a tree-level amplitude containing a single quark-antiquark pair and an arbitrary number of gluons. Since quarks transform in the fundamental representation of  $SU(N_c)$ , we can immediately write down the amplitude by replacing in Eq. (1.8) the generators  $F^a$  by the generators  $T^a$  of the fundamental representation [32],

$$\begin{aligned} \mathcal{A}_n(1_q^{h_1, i}, 2_{\bar{q}}^{h_2, \bar{j}}, \{p_i, h_i, a_i\}) \\ = g^{n-2} \sum_{\sigma \in S_{n-2}} (T^{a_{\sigma_3}} \dots T^{a_{\sigma_n}})_i^{\bar{j}} A_n(1_q^{h_1}, 2_{\bar{q}}^{h_2}, \sigma(3^{h_3}), \dots, \sigma(n^{h_n})). \end{aligned} \quad (1.9)$$

For amplitudes involving more than one quark pair, we can derive a similar result, the color factors being products of strings of color matrices.

## 1.3 Spinor-helicity formalism

In the previous section we showed how the problem of computing an  $n$ -point amplitude can be reduced to the computation of the corresponding  $(n-3)!$

independent partial amplitudes. In the rest of this chapter we thus concentrate on techniques for the computation of partial amplitudes<sup>§</sup>. Since color-ordered amplitudes only depend on the gluon momenta and helicities, they can be easily calculated using the spinor-helicity formalism, based on the fact that each lightlike momentum  $p$  can be decomposed into two spinors,

$$P_{a\dot{a}} = \sigma_{a\dot{a}}^\mu p_\mu = \lambda_a \tilde{\lambda}_{\dot{a}}, \quad (1.10)$$

where  $\lambda$  and  $\tilde{\lambda}$  denote two Weyl spinors with opposite chirality. We refer to  $\lambda_a$  and  $\tilde{\lambda}_{\dot{a}}$  as the holomorphic and antiholomorphic spinor components of the momentum  $p$ . It is easy to see that if  $p_\mu$  is real, then the matrix  $P_{a\dot{a}}$  must be hermitian, which implies in turn that the holomorphic and antiholomorphic components must be complex conjugated to each other (up to a sign). We define spinor products as the antisymmetric contractions of these Weyl spinors, *e.g.* if  $p_i$  and  $p_j$  denote two massless momenta, then we define

$$\langle ij \rangle = \epsilon_{ab} \lambda_i^a \lambda_j^b \quad \text{and} \quad [ij] = \epsilon_{\dot{a}\dot{b}} \tilde{\lambda}_i^{\dot{a}} \tilde{\lambda}_j^{\dot{b}}. \quad (1.11)$$

From the antisymmetry of the Levi-Civita tensor it follows immediately that spinor products are antisymmetric,

$$\langle ij \rangle = -\langle ji \rangle \quad \text{and} \quad [ij] = -[ji], \quad (1.12)$$

and for real momenta the two kinds of spinor products are complex conjugate to each other (up to a sign). Furthermore, they have a very simple physical interpretation, because the two spinor products can be identified as the complex square roots of the two-particle invariants  $s_{ij} = (p_i + p_j)^2 = 2p_i \cdot p_j$ ,

$$s_{ij} = \langle ij \rangle [ji]. \quad (1.13)$$

Spinor products enjoy many algebraic properties (See for example Ref. [32]). Let us mention here only the *Schouten identity*, a relation that will play an important role in Chapter 5,

$$\langle ij \rangle \langle kl \rangle = \langle ik \rangle \langle jl \rangle + \langle il \rangle \langle kj \rangle. \quad (1.14)$$

---

<sup>§</sup>From here on, if there is no ambiguity, we use indifferently the words ‘amplitude’ and ‘partial amplitude’.

The definitions of the previous paragraph make it possible to express every tree-level gluon amplitude as a rational function of spinor products. This result is easily obtained by making the following observation:

1. Any momentum coming from a (color-ordered) vertex and any propagator can be written in terms of spinor products using Eqs. (1.10) and (1.13).
2. We can find a representation of the polarization vectors for a gluon with momentum  $p_{a\dot{a}} = \lambda_a \tilde{\lambda}_{\dot{a}}$  in terms of spinor products [38],

$$\epsilon_{a\dot{a}}^-(p, q) = \sqrt{2} \frac{\lambda_a \tilde{\mu}_{\dot{a}}}{\langle \lambda, \mu \rangle} \quad \text{and} \quad \epsilon_{a\dot{a}}^+(p, q) = -\sqrt{2} \frac{\mu_a \tilde{\lambda}_{\dot{a}}}{[\lambda, \mu]}, \quad (1.15)$$

where  $q_{a\dot{a}} = \mu_a \tilde{\mu}_{\dot{a}}$  denotes an arbitrary lightlike momentum (but linearly independent from  $p_{a\dot{a}}$ ).

Eq. (1.15) needs some more explanation. It is easy to check that the vectors  $\epsilon_{a\dot{a}}^\pm$  defined in this way fulfill all the properties of transverse polarization vectors,

$$\begin{aligned} \epsilon^+(p, q) \cdot \epsilon^+(p, q) &= \epsilon^-(p, q) \cdot \epsilon^-(p, q) = 0 \\ \epsilon^+(p, q) \cdot \epsilon^-(p, q) &= -1, \\ p \cdot \epsilon^\pm(p, q) &= 0, \\ (\epsilon^\pm(p, q))^* &= \epsilon^\mp(p, q), \end{aligned} \quad (1.16)$$

and they also fulfill the closure relation

$$\epsilon_\mu^+(p, q) (\epsilon_\nu^+(p, q))^* + \epsilon_\mu^-(p, q) (\epsilon_\nu^-(p, q))^* = -g_{\mu\nu} + \frac{p_\mu q_\nu + p_\nu q_\mu}{p \cdot q}. \quad (1.17)$$

Finally, one can show that the choice of the arbitrary lightlike vector  $q$  is equivalent to a gauge choice, and hence it must cancel for gauge-invariant quantities. This property can be used as a cross-check in explicit computations.

For some specific helicity configurations a closed form valid for an arbitrary number of gluons can be derived:

1. At tree-level there is no way to distinguish a pure gluon amplitude in QCD from the corresponding amplitude in supersymmetric theories. Hence, the tree-level QCD amplitude must fulfill the same supersymmetric Ward

identities as in the SUSY case, which imply in turn that all tree-level amplitudes where the gluons have the same helicity or only one gluon has a different helicity must vanish [32],

$$\begin{aligned} A_n(1^\pm, 2^+, \dots, n^+) &= 0, \\ A_n(1^\mp, 2^-, \dots, n^-) &= 0. \end{aligned} \tag{1.18}$$

2. The first non-zero helicity configurations correspond to exactly two gluons of different helicity. Those *maximally helicity violating (MHV)* amplitudes were first conjectured by Parke and Taylor in Ref. [39] and later proven recursively by Berends and Giele using their recursive relations [40] (See Section 1.4). They take an extremely simple analytic form,

$$A_n(1^+, \dots, i^-, \dots, j^-, \dots, n^+) = \frac{\langle ij \rangle^4}{\langle 12 \rangle \langle 23 \rangle \dots \langle (n-1)n \rangle \langle n1 \rangle}. \tag{1.19}$$

Using parity, we can find the corresponding amplitude for exactly two positive-helicity gluons<sup>¶</sup>,

$$A_n(1^-, \dots, i^+, \dots, j^+, \dots, n^-) = (-1)^n \frac{[ij]^4}{[12][23] \dots [(n-1)n][n1]}. \tag{1.20}$$

Note that once these formulas are established for pure gluon amplitudes, we can deduce the corresponding MHV amplitudes for quarks using the effective tree-level supersymmetry of QCD.

3. Recently, a generic formula for all split-helicity amplitudes of the form  $A_n(1^-, \dots, i^-, (i+1)^+, \dots, n^+)$  has been derived [41]. Since this formula will not play any role in this work, we do not comment on this result further, but only quote it for completeness.

For  $n = 4$  and  $n = 5$  all partial amplitudes are MHV (or  $\overline{\text{MHV}}$ ) amplitudes. Starting from  $n \geq 6$ , however, no generic formula valid for arbitrary  $n$  can be given. We classify the new structures in terms of the number  $n_-$  of negative-helicity gluons in the amplitude:

1.  $n_- = 2$ : MHV amplitude.

---

<sup>¶</sup>These amplitude are sometimes referred to in the literature as  $\overline{\text{MHV}}$  amplitudes.

2.  $n_- = 3$ : Next-to-MHV (NMHV) amplitude.
3.  $n_- = 4$ : Next-to-next-to-MHV (NNMHV) amplitude.
4. *etc.*

There are several techniques to compute a generic non-MHV amplitude, and the first part of this work is in fact devoted to these techniques.

## 1.4 Berends-Giele recursive relations

In this section we discuss a recursive algorithm to compute color-ordered amplitudes for a given number of external particles. This algorithm, introduced by Berends and Giele in Ref. [40], relies on the concept of an  $n$ -point *off-shell current*  $J$ , defined as the sum over all tree-level Feynman graphs with  $n$  external on-shell legs and a single external off-shell leg. On-shell amplitudes can be obtained from off-shell currents by putting the off-shell leg on shell,

$$A_{n+1}(1, \dots, n, (n+1)^\pm) = \lim_{P_{1,n}^2 \rightarrow 0} iP_{1,n}^2 \epsilon_\mu^\pm J^\mu(1, \dots, n), \quad (1.21)$$

where  $\mu$  denotes the Lorentz index of the off-shell gluon, and where we defined  $P_{1,n} = p_1 + \dots + p_n$ . The currents can be built recursively from similar objects with fewer external legs, and the Berends-Giele (BG) recursive relations for pure gluon amplitudes read<sup>||</sup>

$$J^\mu(1, \dots, n) = \frac{-i}{P_{1,n}^2} \left[ \sum_{i=1}^{n-1} V_3^{\mu\nu\rho}(P_{1,i}, P_{i+1,n}) J_\nu(1, \dots, i) J_\rho(i+1, \dots, n) + \sum_{j=i+1}^{n-1} \sum_{i=1}^{n-2} V_4^{\mu\nu\rho\sigma} J_\nu(1, \dots, i) J_\rho(i+1, \dots, j) J_\sigma(j+1, \dots, n) \right]. \quad (1.22)$$

where by convention one defines one-point off-shell currents to correspond to the polarization vectors of the external gluons,  $J_\mu(i^\pm) = \epsilon_\mu^\pm(p_i, q_i)$ , and where

---

<sup>||</sup>In the following we review this recursive approach in the case of pure gluon amplitudes. The generalization to quarks is then straightforward.

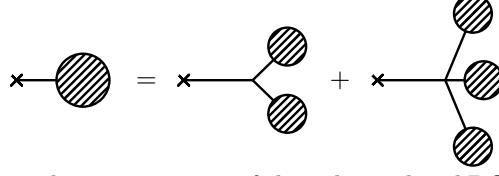


Figure 1.1: Pictorial representation of the color-ordered BG recursive relations. Blobs indicate off-shell currents, crosses off-shell lines.

$V_3$  and  $V_4$  denote the color-ordered three and four-gluon vertices

$$\begin{aligned} V_3^{\mu\nu\rho}(P, Q) &= \frac{i}{\sqrt{2}} (g^{\nu\rho}(P - Q)^\mu + 2g^{\rho\mu}Q^\nu - 2g^{\mu\nu}P^\rho), \\ V_4^{\mu\nu\rho\sigma} &= \frac{i}{2} (2g^{\mu\rho}g^{\nu\sigma} - g^{\mu\nu}g^{\rho\sigma} - g^{\mu\sigma}g^{\nu\rho}). \end{aligned} \quad (1.23)$$

A pictorial representation of the BG recursion can be found in Fig. 1.1.

For numerical purposes Eq. (1.22) is not yet in its most optimal form, because it involves both the three and the four-gluon vertices in the recursion. In order to reduce the complexity of the algorithm, we decompose the four-gluon vertex in terms of three-point building blocks. This can be achieved by introducing a fictitious tensor particle which only couples to the gluons [42]. In terms of the tensor-gluon vertex, the color-ordered four-gluon interaction can be written [14]

$$V_4^{\mu\nu\rho\sigma} = V_T^{\nu\mu\alpha\beta} iD_{\alpha\beta\gamma\delta} V_T^{\sigma\rho\gamma\delta} + V_T^{\mu\sigma\alpha\beta} iD_{\alpha\beta\gamma\delta} V_T^{\rho\nu\gamma\delta}, \quad (1.24)$$

where  $V_T^{\mu\nu\rho\sigma}$  and  $iD_{\alpha\beta\gamma\delta}$  denote the tensor-gluon vertex and the tensor propagator summarized in Table 1.2. We also introduce an  $n$ -point off-shell tensor current  $J_{\mu\nu}$  as the sum of all Feynman graphs having  $n$  external on-shell gluons and a single off-shell tensor leg. Note that this definition implies that there is no one-point tensor current. Inserting the decomposition of the four-gluon vertex into Eq. (1.22), the BG recursive relations immediately become

$$\begin{aligned} J^\mu(1, 2, \dots, n) &= \frac{-i}{P_{1,n}^2} \sum_{k=1}^{n-1} \left\{ V_3^{\mu\nu\rho}(P_{1,k}, P_{k+1,n}) J_\nu(1, \dots, k) J_\rho(k+1, \dots, n) \right. \\ &\quad + V_T^{\nu\mu\alpha\beta} J_\nu(1, \dots, k) J_{\alpha\beta}(k+1, \dots, n) \\ &\quad \left. + V_T^{\mu\sigma\alpha\beta} J_{\alpha\beta}(1, \dots, k) J_\sigma(k+1, \dots, n) \right\}, \end{aligned}$$

$$J_{\alpha\beta}(1, \dots, n) = iD_{\alpha\beta\gamma\delta} V_T^{\rho\nu\gamma\delta} \sum_{j=1}^{n-1} J_\nu(1, \dots, j) J_\rho(j+1, \dots, n). \quad (1.25)$$

The recursive relations for the gluon and tensor currents can be solved simultaneously up to the desired order in the number of external legs. Putting the external leg on-shell, we obtain an explicit representation for a given partial amplitude. The BG algorithm is known to have a very good algorithmic behavior. However, in order to build the full amplitude, we need to perform the sum over the color permutations of the external gluons. So, even if the complexity of the recursion for the partial amplitudes is very good, we end up with a factorial growth when it comes to summing over colors. This important issue will be discussed in more detail in Chapter 3 when discussing color-dressed recursive relations.

---



---


$$\mu\nu \text{ --- } \rho\sigma \quad iD_{\mu\nu\rho\sigma} = -\frac{i}{2} (g^{\mu\rho}g^{\nu\sigma} - g^{\nu\rho}g^{\mu\sigma})$$

$$\begin{array}{c} \mu \quad \nu \\ \diagdown \quad / \\ \text{---} \\ \rho\sigma \end{array} \quad V_T^{\mu\nu\rho\sigma} = -\frac{g}{2} (g^{\mu\rho}g^{\nu\sigma} - g^{\nu\rho}g^{\mu\sigma})$$


---



---

Table 1.2: The color-ordered Feynman rules for the fictitious tensor particle appearing in the decomposition of the four gluon vertex. Straight lines indicate gluons, dashed lines indicate tensors.

$$(a) \text{---} \bigcirc \text{---} = \text{---} \begin{array}{c} \bigcirc \\ / \quad \backslash \\ \bigcirc \quad \bigcirc \end{array} + \text{---} \begin{array}{c} \bigcirc \\ \backslash \quad / \\ \bigcirc \quad \bigcirc \end{array} + \text{---} \begin{array}{c} \bigcirc \\ \cdot \\ \bigcirc \quad \bigcirc \end{array}$$

$$(b) \text{---} \bigcirc \text{---} = \text{---} \begin{array}{c} \bigcirc \\ \backslash \quad / \\ \text{---} \\ \bigcirc \quad \bigcirc \end{array}$$

Figure 1.2: Berends-Giele recursive relations where the four-gluon vertex has been decomposed in terms of a fictitious tensor particle. Straight lines denote gluons, dashed lines denote tensors.



# Chapter 2

## Twistor techniques in gauge theories

### 2.1 Introduction

In the previous chapter we introduced the color-ordered Feynman rules and the BG recursion as two examples of how to compute tree-level partial amplitudes. Recently, two additional techniques have been developed, known as the MHV formalism and the BCFW recursion. They are the outcome of a conjecture by E. Witten of a duality between gauge theories and a certain type of string theory in twistor space [1]. Although originally formulated in the context of string theory, the MHV formalism and the BCFW recursion have been proven rigorously within the framework of gauge quantum field theories, and they do not need the reference to twistor space any more\*. We follow here this approach and only present the results within the framework of quantum field theory, without commenting on the original conjecture to string theory used to derive them in first place.

Before reviewing these two new approaches in more detail, let us make some general comments about their common features. The main idea is that on-shell amplitudes can be built recursively from amplitudes with fewer external legs,

---

\*The name ‘twistor techniques’ is however still used nowadays to quote those results.

where some of the external legs have to be evaluated in complex momenta. Loosely speaking, we can see an off-shell real momentum as an on-shell leg in complex kinematics. In contrast to the Berends-Giele recursive relations for example, where each current contains by definition an off-shell leg, the building blocks in this approach are full gauge-invariant amplitudes, enjoying all the properties inherent to gauge invariance. As a consequence, the analytic results obtained from the twistor techniques have a much more compact and simpler analytic structure, because some of the cancellations between non gauge-invariant pieces are built in from the start. In the next two sections we give an overview of the BCFW recursion and the MHV formalism, and how to proof them within the framework of quantum field theory.

## 2.2 The BCFW recursive relations

The BCFW recursive relations were first conjectured by Britto, Cachazo and Feng in Ref. [3] and later proven analytically by the same people together with Witten in Ref. [4]. They state that an on-shell tree-level amplitude can be built recursively from gluon amplitudes with fewer external legs, where two or more of the momenta have been shifted into the complex plane. To be more concrete, the recursion reads

$$A_n(1^+, 2, \dots, n^-) = \sum_{k=2}^{n-2} A_{k+1}(\hat{1}, 2, \dots, k, -\hat{P}_{1,k}^{-h}) \frac{1}{P_{1,k}^2} A_{n-k+1}(\hat{P}_{1,k}^h, k+1, \dots, \hat{n}), \quad (2.1)$$

where a sum over the helicities  $h$  of the intermediate gluon is implicit, and where

$$\begin{aligned} \hat{P}_{1,k} &= P_{1,k} + \frac{P_{1,k}^2}{\langle n|P_{1,k}|1 \rangle} \lambda_n \tilde{\lambda}_1, \\ \hat{p}_1 &= p_1 + \frac{P_{1,k}^2}{\langle n|P_{1,k}|1 \rangle} \lambda_n \tilde{\lambda}_1, \\ \hat{p}_n &= p_n - \frac{P_{1,k}^2}{\langle n|P_{1,k}|1 \rangle} \lambda_n \tilde{\lambda}_1, \end{aligned} \quad (2.2)$$

and  $\lambda_i$  and  $\tilde{\lambda}_i$  denote the spinor components of the momentum  $p_i$ . In Eq. (2.2) we introduced the shorthands

$$\langle i|j|k\rangle = \langle ij\rangle[jk] \quad \text{and} \quad \langle n|P_{1,k}|1\rangle = \langle n|1|1\rangle + \dots + \langle n|k|1\rangle. \quad (2.3)$$

In the following we review the proof of the recursion (2.1), which relies on standard complex analysis. Let us consider an  $n$ -point gluon amplitude  $A_n(1, \dots, n)$  and let us shift the spinor components of the momenta  $p_1$  and  $p_n$  into the complex plane,

$$\begin{aligned} p_1 &= \lambda_1 \tilde{\lambda}_1 \rightarrow \hat{p}_1(z) = \lambda_1 (\tilde{\lambda}_1 - z \tilde{\lambda}_n), \\ p_n &= \lambda_n \tilde{\lambda}_n \rightarrow \hat{p}_n(z) = (\lambda_n + z \lambda_1) \tilde{\lambda}_n. \end{aligned} \quad (2.4)$$

It is easy to check that the shifts conserve momentum and on-shellness,  $\hat{p}_1(z) + \hat{p}_n(z) = p_1 + p_n$  and  $\hat{p}_1(z)^2 = \hat{p}_n(z)^2 = 0$ ,  $\forall z \in \mathbb{C}$ . After shifting of the momenta, the amplitude is a function  $A(z)$  of the complex parameter  $z$ . BCFW showed that this function has the following properties:

1.  $A(z)$  is a meromorphic function of  $z$ .
2.  $A(z)$  has only simple poles.
3.  $A(z)$  vanishes at infinity.

The first point is trivial, it arises naturally from the fact that a color-ordered amplitude is a rational function of spinor products. The next two points are more subtle, and we suggest the interested reader should refer to Ref. [4]. To continue, let us consider the following contour integral, where the contour is taken at infinity in the  $z$ -plane. Since  $A(z)$  vanishes at infinity, Cauchy's theorem implies,

$$0 = \oint \frac{dz}{z} A(z) = A(0) + \sum_p \text{Res}_{z=z_p} \frac{A(z)}{z}, \quad (2.5)$$

where the sum runs over all the poles<sup>†</sup> of  $A(z)$ . The poles of a tree-level amplitudes stem from internal propagators going on-shell,  $P^2 = 0$ , and since at

<sup>†</sup>Note that we implicitly assumed that  $A(z)$  has no pole in  $z = 0$ . This is always true in general, because for  $z = 0$  the complex function  $A(z)$  reduces to the original amplitude.

tree-level each propagator divides a diagram into two disconnected parts, the residue of the pole is simply given by the formula

$$A(1, \dots, n) \longrightarrow \sum_h A(1, \dots, P^h) \frac{1}{P^2} A(-P^{-h}, \dots, n). \quad (2.6)$$

Inserting this relation into Eq. (2.5) we find, after some algebra, the recursion (2.1).

The main feature of Eq. (2.1) is that it is an on-shell recursion, *i.e.* the subamplitudes appearing in the recursion are full gauge-invariant on-shell amplitudes. Note however also on-shell three-point amplitudes appear that in the recursion that vanish in real kinematics. In complex kinematics, however, these quantities are non zero and have to be taken into account. Also note that, since there is nothing special about the momenta  $p_1$  and  $p_n$ , we could have made a different choice in Eq. (2.4) for the shifted momenta. Since the proof is only based on Cauchy's theorem, we could repeat the argument and derive a version of the BCFW recursion with different shifts, a property that will be used in the next section when we discuss the MHV formalism. Let us conclude by mentioning that the proof we presented here is valid for pure gluon amplitudes, but it is straightforward to extend it to more general cases, such as quarks and scalars, as well as massive vector bosons and QED processes [43, 44, 45, 46]. In Chapter 3 we will present another generalization of the BCFW recursive relations, and we will show that the recursion does not only hold for partial amplitudes, but the recursion stays true at the level of the full scattering amplitude, including color.

## 2.3 The MHV formalism

The MHV formalism is the second outcome of Witten's duality to twistor space and consists in a diagrammatic technique, similar to Feynman diagrams, but where the vertices correspond to the on-shell MHV amplitudes given in Eq. (1.19) and the propagators are just scalar propagators [2]. When using MHV amplitudes as vertices, we have to face the problem that Eq. (1.19) needs to be evaluated for off-shell momenta. Since the factorization of a momentum

into two opposite-chirality spinors only holds for lightlike momenta, we have to find a new way to evaluate the spinor products in Eq. (1.19) when off-shell momenta are involved. We can, however, note that MHV amplitudes have a quite peculiar structure, because they only depend on holomorphic spinor products, and it is hence enough to have a prescription to construct a spinor of the corresponding type. The prescription was given in Ref. [2] and reads:

**Rule 2.1.** *Each off-shell momentum  $P$  in an MHV amplitude has to be interpreted as  $P_{a\dot{a}}\eta^{\dot{a}}$ , where  $\eta^{\dot{a}}$  is an arbitrary massless spinor.*

In practise, this means that all spinor products involving an off-shell momentum  $P = P_{i,j}$  have to be interpreted as

$$\langle kP_{i,j} \rangle = \langle k|P_{i,j}|\eta \rangle = \langle ki \rangle [i\eta] + \dots + \langle kj \rangle [j\eta]. \quad (2.7)$$

Since  $\eta$  is arbitrary, this dependence is unphysical and must cancel out in the sum over all diagrams. This property can be used as a cross-check in explicit computations. An important property of the decomposition of an amplitude into MHV diagrams is that for every diagram there is a relation between the number  $n_-$  of negative-helicity gluons in the amplitude, the number  $p$  of scalar propagators and the number  $v$  of MHV vertices in the diagram,

$$p = v - 1 = n_- - 2. \quad (2.8)$$

This relation will be used extensively in Chapter 5 when deriving the infrared behavior of MHV diagrams. Note that in the trivial case of an MHV amplitude  $n_- = 2$  and Eq. (2.8) implies  $p = 0$ , in agreement with our expectation for MHV amplitudes.

Both in the BCFW recursive relations and in the MHV formalism the basic building blocks are full on-shell amplitudes connected by scalar propagators and with off-shell legs being evaluated in complex kinematics. In Ref. [47] Risager showed that there is in fact a deeper connection between the MHV formalism and the BCFW recursion. More precisely, Risager showed that the MHV formalism is a consequence of the BCFW recursive relations for a very specific choice of the complex shifts. To see this, let us shift all the momenta of the negative-helicity gluons whereas all other momenta stay real. For example,

in an NMHV amplitude containing exactly three negative-helicity gluons with momenta  $p_{m_1}$ ,  $p_{m_2}$  and  $p_{m_3}$ , the BCFW shifts considered by Risager are

$$\begin{aligned} p_{m_1} &= \lambda_{m_1} \tilde{\lambda}_{m_1} \rightarrow \hat{p}_{m_1}(z) = \lambda_{m_1} (\tilde{\lambda}_{m_1} + z \langle \lambda_{m_2} \lambda_{m_3} \rangle \eta), \\ p_{m_2} &= \lambda_{m_2} \tilde{\lambda}_{m_2} \rightarrow \hat{p}_{m_2}(z) = \lambda_{m_2} (\tilde{\lambda}_{m_2} + z \langle \lambda_{m_3} \lambda_{m_1} \rangle \eta), \\ p_{m_3} &= \lambda_{m_3} \tilde{\lambda}_{m_3} \rightarrow \hat{p}_{m_3}(z) = \lambda_{m_3} (\tilde{\lambda}_{m_3} + z \langle \lambda_{m_1} \lambda_{m_2} \rangle \eta), \end{aligned} \quad (2.9)$$

where  $\eta$  is an arbitrary antiholomorphic spinor, and all other momenta are evaluated in real kinematics. From the Schouten identity it follows that these shifts conserve momentum. Computing the contour integral (2.5) and taking residues, we find

$$\begin{aligned} A^{NMHV}(\dots, m_1^-, \dots, m_2^-, \dots, m_3^-, \dots) &= \sum_{i,j} A(i^+, \dots, \hat{m}_1^-, \dots, j, \hat{P}_{i,j}^-) \\ &\times \frac{1}{P_{i,j}} A(-\hat{P}_{i,j}^+, (k+1)^+, \dots, \hat{m}_2^-, \dots, \hat{m}_3^-, \dots, (i-1)^+) \\ &+ (m_1 \leftrightarrow m_2) + (m_1 \leftrightarrow m_3). \end{aligned} \quad (2.10)$$

The right-hand side of Eq. (2.10) expresses an NMHV as a sum of MHV amplitudes connected by scalar propagators. A straightforward computation shows that the shifts (2.9) reproduce exactly the off-shell continuation (2.7). As a consequence, every NMHV amplitude can be written as a sum of MHV diagrams. We can now repeat this procedure for a generic  $N^n$ MHV amplitude and prove recursively that the MHV decomposition holds for arbitrary  $n$ .

Many generalizations beyond pure gluon amplitudes exist for the MHV formalism, in particular for scalars and fermions [48, 49, 50]. Furthermore, it was shown that the MHV formalism is not only convenient for the computation of full scattering amplitudes, but it has been used to compute splitting amplitudes for quarks and gluons [19, 18]. In this work we will present two more applications of the MHV formalism and extend it to the computation of antenna functions, impact factors and Lipatov vertices.

## 2.4 Recursive formulation of the MHV formalism

In the previous section we presented the MHV formalism, which allows to write any tree-level gluon amplitude as a sum of MHV diagrams. Although this diagrammatic technique is very simple and intuitive, it may become inefficient for diagrams with a large number of external legs, because two different graphs may contain identical subgraphs. As a consequence, identical subgraphs are evaluated multiple times, which can slow down numerical codes. In order to improve the efficiency of numerical implementations, a recursive formulation in terms of currents, similar to the BG recursion, is desirable. In this way, each current is only computed once, avoiding in this way multiple evaluations of the same quantity. In this section we present a recursive formulation of the MHV formalism in terms of currents originally introduced in Ref. [14, 17].

Our goal is to obtain a recursion whose structure is similar to the BG recursive relations. Let us start by defining an  $n$ -point off-shell current  $J_h(1, \dots, n)$  as the sum over all MHV diagrams having  $n$  external on-shell legs and a single off-shell leg with helicity  $h^\ddagger$ . We refer to such a current as a single-line current. A specific  $(n+1)$ -point amplitude can then be obtained by putting the off-shell leg on-shell,

$$A_{n+1}(1, \dots, (n+1)^h) = \lim_{P_{1,n}^2 \rightarrow 0} P_{1,n}^2 J_{-h}(1, \dots, n). \quad (2.11)$$

Looking back to ordinary Feynman rules and the BG recursion, it is easy to write out a recursion for the single-line current,

$$\begin{aligned} & J_h(1, \dots, n) \\ &= \frac{1}{P_{1,n}^2} \left[ \sum_{i=1}^{n-1} A_3^{\text{MHV}} \left( -P_{1,n}^{-h}, P_{1,k}^{h_1}, P_{k+1,n}^{h_2} \right) J_{h_1}(1, \dots, i) J_{h_2}(i+1, \dots, n) \right] \end{aligned} \quad (2.12)$$

---

<sup>‡</sup>In the context of the MHV rules, it makes sense to talk about the helicity of an off-shell particle. Note that, as the off-shell continuation of the spinors involves an arbitrary reference spinor  $\eta^{\dot{a}}$ , these currents are not gauge-invariant objects. However, the  $\eta^{\dot{a}}$  dependence drops out in the end.

$$\begin{aligned}
& + \sum_{i=1}^{n-2} \sum_{j=i+1}^{n-1} A_4^{\text{MHV}} \left( -P_{1,n}^{-h}, P_{1,i}^{h_1}, P_{i+1,j}^{h_2}, P_{j+1,n}^{h_3} \right) J_{h_1}(1, \dots, i) \\
& \times \left. \begin{aligned} & J_{h_2}(i+1, \dots, j) J_{h_3}(j+1, \dots, n) + \dots \end{aligned} \right].
\end{aligned}$$

The dots indicate terms with higher-point MHV vertices and a sum over the helicities  $(h, h_1, h_2, \dots)$  with  $-h + h_1 + h_2 + \dots = n - 4$  is implicitly understood. Although Eq. (2.12) provides a recursion for the single-line current, it suffers from the fact that for large values of  $n$  high-multiplicity MHV vertices enter the recursion. This problem is similar to the BG recursion, where it was overcome by decomposing the four-gluon vertex in terms of a fictitious tensor particle and where we arrived in the end at a recursion that only involves three-point vertices. In the rest of this section we describe how to extend this decomposition to the MHV formalism.

Since the building blocks of MHV diagrams are MHV amplitudes, let us start by analyzing how we can decompose a generic  $n$ -point MHV amplitude in terms of effective three-point vertices. It is easy to show that an  $n$ -point MHV amplitude can be written in terms of eikonal factors

$$\begin{aligned}
& A_n(1^+, 2^+, \dots, (n-2)^+, (n-1)^-, n^-) \\
& = \frac{\langle (n-1) n \rangle^4}{\langle 1 (n-2) \rangle \langle (n-2) (n-1) \rangle \langle (n-1) n \rangle \langle n 1 \rangle} \prod_{k=3}^{n-2} D_{1,k}^{k-1}, \tag{2.13}
\end{aligned}$$

where the eikonal factors are defined by  $D_{ij}^k = \frac{\langle ij \rangle}{\langle ik \rangle \langle kj \rangle}$ . As a consequence, for an MHV-type current we can write

$$\begin{aligned}
& J_+(1^+, 2^+, \dots, (n-2)^+, (n-1)^-) \\
& = \frac{1}{P_{1,n-1}^2} \frac{\langle (n-1), P_{1,n-1} \rangle^4}{\langle 1, 2 \rangle \dots \langle (n-1), P_{1,n-1} \rangle \langle P_{1,n-1}, 1 \rangle} \\
& = \frac{1}{P_{1,n-1}^2} \frac{\langle (n-1), P_{1,n-1} \rangle^4}{\langle 1, (n-2) \rangle \langle (n-2), (n-1) \rangle \langle (n-1), P_{1,n-1} \rangle \langle P_{1,n-1}, 1 \rangle} \prod_{k=3}^{n-2} D_{1k}^{k-1} \\
& = \frac{1}{P_{1,n-1}^2} V_4(1, n-2, n-1, P_{1,n-1}) \prod_{k=3}^{n-2} D_{1k}^{k-1}, \tag{2.14}
\end{aligned}$$



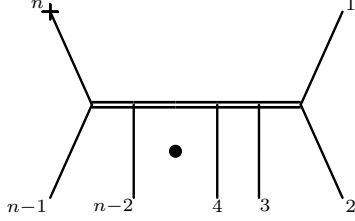


Figure 2.1: Decomposition of an MHV-amplitude where the MHV vertex has been stretched out into a double-line. The cross indicates the off-shell line.

where we define

$$V_4(a, b, c, d) = \frac{\langle cd \rangle^4}{\langle ab \rangle \langle bc \rangle \langle cd \rangle \langle da \rangle}. \quad (2.15)$$

In Fig. 2.1, we introduce a graphical representation for Eq. (2.14) in terms of an internal double-line to which the external gluons may couple. We also introduce double-line currents  $J_{uv}^m(1, \dots, n)$  defined as the double-line diagram with an external (off-shell) double-line which the gluons 1 to  $n$  are attached to. The indices  $u$  and  $v$  refer to the indices of the first particle one encounters if one follows each line of the double-line into the current, and  $m$  refers to the number of negative-helicity gluons attached to the double-line<sup>§</sup>. As a double-line is part of an MHV-amplitude with exactly two negative-helicity particles,  $J_{uv}^m(1, \dots, n) = 0$  if  $m \geq 3$ . The double-line currents contributing to the MHV single-line current  $J_+(1^+, \dots, (n-2)^+, (n-1)^-)$  can be easily constructed recursively by successively adding eikonals,

$$\begin{aligned} J_{1k}^0(1^+, \dots, k^+) \\ = D_{1k}^{k-1} J_{1(k-1)}^0(1^+, \dots, (k-1)^+), \end{aligned} \quad (2.16)$$

where we define that all one-point double-line currents are zero, and all two-point double-line currents are given by  $J_{uv}^0(1^+, 2^+) = \delta_{1u} \delta_{2v}$ . The MHV single-line current is then given by

$$\begin{aligned} J_+(1^+, \dots, (n-2)^+, (n-1)^-) \\ = V_4(1, n-2, n-1, P_{1,n}) J_{1(n-2)}^0(1^+, \dots, (n-2)^+), \end{aligned} \quad (2.17)$$

<sup>§</sup>Up to now these indices are redundant. The double-line currents contributing to an MHV single-line current of the form  $J_+(1^+, \dots, (n-2)^+, (n-1)^-)$  are all of the form  $J_{uv}^m(1^+, \dots, k^+)$  with  $u = 1$ ,  $v = k$  and  $m = 0$ . The meaning of these indices will become clear when we generalize double-line currents to the MHV formalism.

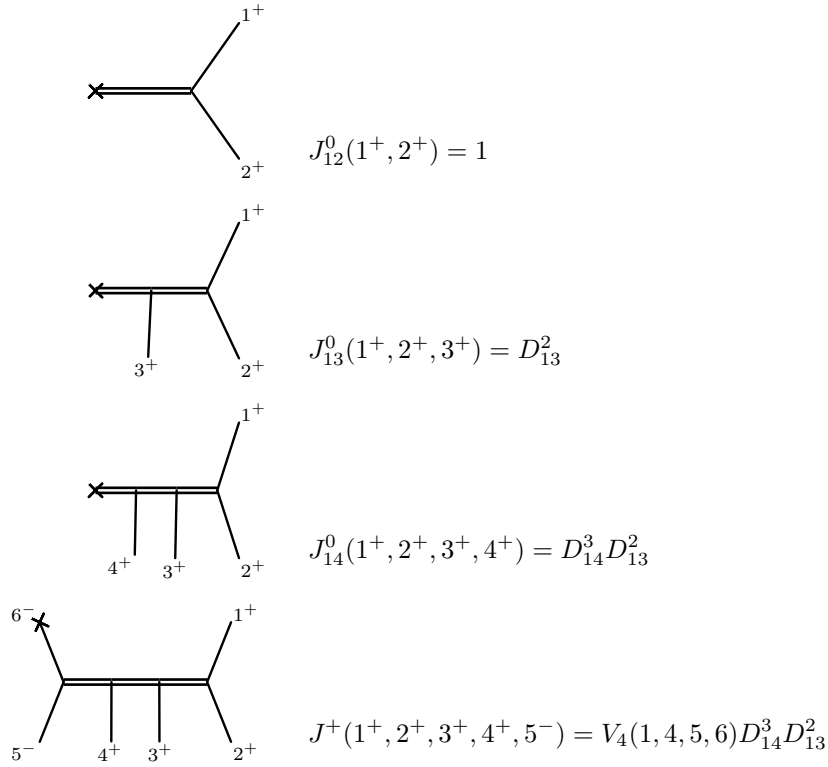


Figure 2.2: Construction of  $A_6(1^+, 2^+, 3^+, 4^+, 5^-, 6^-)$  using the recursion for the double-line current. A cross indicates an off-shell leg.

and the MHV amplitude can then be obtained by putting the off-shell leg on-shell. This procedure is illustrated in Fig. 2.2 for the six-point MHV-amplitude

Up to now we have only considered a very special class of MHV-amplitudes, namely those where the two negative-helicity gluons are adjacent in the MHV-amplitude. We now generalize this procedure to an arbitrary MHV-amplitude  $A_n(1^+, \dots, i^-, \dots, j^-, \dots, n^+)$ . The factorization (2.13) stays no longer true in this case, because an MHV-amplitude only factorizes when a soft positive-helicity gluon is radiated. A closer look at our recursive procedure reveals that

we only used this method to construct the denominator of the MHV-amplitude, whereas the numerator is completely encoded in  $V_4(1, n-2, n-1, n)$ . Thus we can generalize this procedure using the following rules:

1. Each time we add a negative-helicity particle  $j$  to a double-line current containing already  $m$  negative-helicity particles, add a  $\delta_{jm_i}$  to the double-line current, where  $i = 1$  if  $m$  passes from 0 to 1, and  $i = 2$  if  $m$  passes from 1 to 2.
2. At the last step in the recursion sum over all possible values for  $m_1$  and  $m_2$ ,

$$J_h(1, \dots, n-2, n-1) = \sum_{m_1, m_2} V_4(1, n-2, n-1, P_{1,n}; m_1, m_2) J_{1(n-2)}^m(1, \dots, n-2), \quad (2.18)$$

where we defined

$$V_4(a, b, c, d; m_1, m_2) = \frac{\langle m_1, m_2 \rangle^4}{\langle ab \rangle \langle bc \rangle \langle cd \rangle \langle da \rangle}. \quad (2.19)$$

We have now derived a way to decompose each MHV amplitude completely in terms of three-point building blocks. Since the vertices in Eq. (2.12) have the same functional form as an MHV amplitude, we can in the same way decompose all the vertices in the recursion (2.12) into three-point objects. Before turning to this task, let us introduce some notations which are useful to write down the recursion. Each line in a MHV diagram, as well internal as external, can be uniquely characterized by the momentum  $P_{i_1, i_2}$  flowing through the line, *i.e.*, each line can be labelled by a pair of integers  $I = (i_1, i_2)$ , with  $1 \leq i_1 \leq i_2 \leq n$ . We refer to such a pair  $I$  as a *multiindex*. In particular, external lines can be characterized by their momentum  $p_i$ , and we formalize this by associating the multiindex  $I = (i, i)$  to this line. In general, we have

1. To each line with momentum  $P_{i_1, i_2}$  we can associate in a unique way a multiindex  $I = (i_1, i_2)$  with  $i_1 \leq i_2$  defined by  $P_I \equiv P_{i_1, i_2}$ .
2. A line in a MHV diagram with multiindex  $I = (i_1, i_2)$  is an external line if and only if  $i_1 = i_2$ .

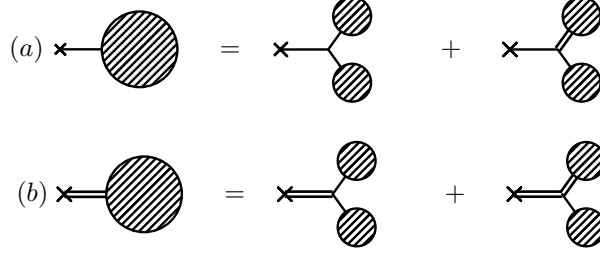


Figure 2.3: Recursion for the single-line currents (a) and the double-line currents (b). A cross indicates an off-shell line.

For later convenience, we introduce the following definitions:

- An on-shell particle with momentum  $p_i = P_{i,i}$  is labelled by the multiindex

$$\bar{i} \equiv (i, i). \quad (2.20)$$

- Kronecker-delta:

$$\delta_J^I = \delta_{j_1}^{i_1} \delta_{j_2}^{i_2}. \quad (2.21)$$

- Ordering relation:

$$I < J \Leftrightarrow i_1 \leq i_2 < j_1 \leq j_2. \quad (2.22)$$

Let us now turn to the decomposition of the higher-point vertices in the recursion (2.12). Merging the recursion relations (2.16 - 2.17) and (2.12) and replacing indices by multiindices, we obtain a system of recursive relations for the single and double-line currents,

$$J_{UV}^m(1, \dots, n) \quad (2.23)$$

$$\begin{aligned} &= \delta_{v_1-1}^{u_2} V_{TS}^{h_1 h_2 m}((1, u_2), (v_1, n), U, V) J_{h_1}(1, \dots, u_2) J_{h_2}(v_1, \dots, n) \\ &+ (1 - \delta_{v_1-1}^{u_2}) \sum_{\substack{W \\ w_2=v_1-1}} V_{TT}^{m' h m}(U, W, (v_1, n), U, V) \\ &\quad \times J_{UW}^{m'}(1, \dots, v_1 - 1) J_h(v_1, \dots, n), \end{aligned} \quad (2.24)$$

$$J_h(1, \dots, n) \tag{2.25}$$

$$= \frac{1}{P_{1,n}^2} \sum_{k=1}^{n-1} \sum_{M_1, M_2} \left[ V_{SS}^{h_1 h_2 h}((1, k), (k+1, n), (1, n); M_1, M_2) \right. \\ \left. \times J_{h_1}(1, \dots, k) J_{h_2}(k+1, \dots, n) \right] \tag{2.26}$$

$$+ \sum_{\substack{U < V \\ v_2 = k}} V_{ST}^{m h_1 h}(U, V, (k+1, n), (1, n); M_1, M_2) \\ \left. \times J_{UV}^m(1, \dots, k) J_{h_1}(k+1, \dots, n) \right], \tag{2.27}$$

where a sum over all repeated helicity indices is understood. A graphical representation of the recursion can be found in Fig. 2.3. The vertices appearing in the recursion are given in Table 2.1, and the  $\epsilon$ -functions appearing in the recursion keep track of the helicities,

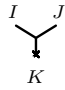

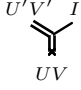
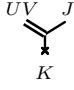
$$\begin{aligned} \epsilon_{m m'}^h(I) &= \begin{cases} \delta_I^{M_m} & , \text{if } h = -1, m = m' + 1, m \leq 2 \\ 0 & , \text{otherwise,} \end{cases} \\ \epsilon_m^{h_I h_J}(I, J) &= \begin{cases} \delta_I^{M_1} \delta_J^{M_2} & , \text{if } h_I = h_J = -1, m = 2, \\ \delta_I^{M_1} & , \text{if } h_I = -h_J = -1, m = 1, \\ \delta_J^{M_1} & , \text{if } h_I = -h_J = 1, m = 1, \\ 1 & , \text{if } h_I = h_J = 1, m = 0, \\ 0 & , \text{otherwise,} \end{cases} \tag{2.28} \\ \epsilon^{h_I h_J h_K}(I, J, K) &= \begin{cases} \delta_X^{M_1} \delta_Y^{M_2} & \text{if } h_X = h_Y = -1, h_1 + h_2 + h_3 = -1, \\ 0 & , \text{otherwise.} \end{cases} \end{aligned}$$

Note that the recursion is formally the same as the BG recursion (1.25), the two recursions differing only by the exact definition of the currents and the vertices. Let us conclude this section by noticing that the recursive relations (2.23 - 2.25) cannot only be used to compute tree-level scattering amplitudes, but, modulo some small modifications that will be discussed in Chapter 5, they are also useful to study the infrared behavior of an amplitude.

---



---

	$V_{SS}^{h_I h_J h_K}(I, J, K; M_1, M_2) = \epsilon^{h_K h_I h_J}(I, J, K) \frac{\langle M_1 M_2 \rangle^4}{\langle IJ \rangle \langle JK \rangle \langle KI \rangle}$
	$V_{TS}^{h_I h_J m}(I, J, U, V) = \epsilon_m^{h_I h_J}(U, V) \delta_U^I \delta_V^J$
	$V_{TT}^{m' h_I m}(U', V', J, U, V) = \epsilon_{mm'}^h(J) D_{UJ}^{V'} \delta_U^{U'} \delta_V^J$
	$V_{ST}^{m h_J h_K}(U, V, J, K; M_1, M_2) = \epsilon_{ 2-m }^{h_J h_K}(J, K) \frac{\langle M_1 M_2 \rangle^4}{\langle UV \rangle \langle VJ \rangle \langle JK \rangle \langle KU \rangle}$

---



---

Table 2.1: Vertices appearing in the recursion for the single and double-line currents. A cross indicates and off-shell leg.

# Chapter 3

## Color-dressed recursive relations

### 3.1 Recursive relations in gauge theories

In the previous chapters we introduced three different recursive relations to compute tree-level partial amplitudes. Since partial amplitudes are gauge-invariant quantities, their computation allows to overcome the problems of the traditional Feynman diagram expansion, where large sums of non gauge-invariant diagrams have to be performed. At the end of the day however, the partial amplitudes must be combined into the full physical amplitude using the color decomposition formulas presented in Section 1.2. Since the sum in Eq. (1.4) runs over all non-cyclic permutations of the gluons, at least  $(n - 3)!$  different partial amplitudes need to be computed in order to rebuild the full physical matrix element. The conclusion is that, whatever the algorithmic complexity of the recursion is, the last step in the computation, the sum over color permutations, scales factorially with the number of external particles and so this approach thus naturally leads to factorial algorithms.

The considerations of the previous paragraph show that the recursions presented in the previous chapters are not fully suitable for implementations into computer programs. In this chapter we present a general technique to dress

recursive relations for partial amplitudes with color. We show that it is possible to write down recursive relations valid at the level of the full colored amplitude, taking color into account from the start and avoiding in this way the problem of a factorial growth when summing over colors. Although we only illustrate this technique on the examples of the BG and BCFW, the technique itself is generic and could be extended to other cases as well. In particular, in Ref. [14] the color-dressed version of the recursive formulation of the MHV formalism was derived. Since the color dressing of these recursive relations does not add anything new to the discussion and follows exactly the same lines as the color dressing of the BG recursive relations, we do not include its derivation here but refer the reader to the literature.

## 3.2 Color-dressed Berends-Giele recursive relations

In this section we show how to dress the BG recursive relations\* with color. We start by defining a color-dressed  $n$ -point off-shell current by analogy to the color decomposition (1.6) valid at the level of the full amplitude<sup>†</sup>,

$$\mathcal{J}_{I\bar{J}}^\mu(1, 2, \dots, n) = \sum_{\sigma \in S_n} \delta_{i_{\sigma_1}}^{\bar{J}} \delta_{i_{\sigma_2}}^{\bar{J}\sigma_1} \dots \delta_I^{\bar{J}\sigma_n} J^\mu(\sigma_1, \sigma_2, \dots, \sigma_n), \quad (3.1)$$

where  $(I, \bar{J})$  is the color of the off-shell leg. Similarly, a color dressed tensor off-shell current reads

$$\mathcal{J}_{I\bar{J}}^{\mu\nu}(1, 2, \dots, n) = \sum_{\sigma \in S_n} \delta_{i_{\sigma_1}}^{\bar{J}} \delta_{i_{\sigma_2}}^{\bar{J}\sigma_1} \dots \delta_I^{\bar{J}\sigma_n} J^{\mu\nu}(\sigma_1, \sigma_2, \dots, \sigma_n). \quad (3.2)$$

After inserting the BG recursive relations (1.25) in the color-flow decomposition of the color-dressed currents, the three gluon vertex part reads

$$\begin{aligned} & \frac{-i}{P_{1,n}^2} \sum_{\sigma \in S_n} \sum_{k=1}^{n-1} \delta_{i_{\sigma_1}}^{\bar{J}} \delta_{i_{\sigma_2}}^{\bar{J}\sigma_1} \dots \delta_I^{\bar{J}\sigma_n} V_3^{\mu\nu\rho}(P_{\sigma_1, \sigma_k}, P_{\sigma_{k+1}, \sigma_n}) \\ & \times J_\nu(\sigma_1, \dots, \sigma_k) J_\rho(\sigma_{k+1}, \dots, \sigma_n), \end{aligned} \quad (3.3)$$

\*We only study here the case where the four-gluon vertex is decomposed by means of a fictitious tensor particle, Eq. (1.25).

<sup>†</sup>For clarity, we suppress in this chapter the coupling constant in Eqs. (1.6) and (1.8).



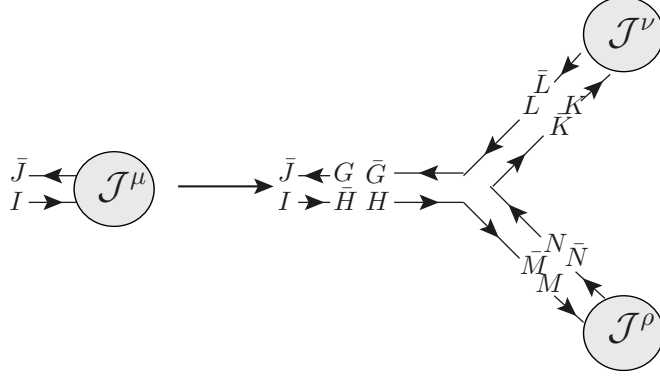


Figure 3.1: Diagrammatic representation of the decomposition (3.5) of the color factor of the three gluon vertex part.

where

$$\begin{aligned} P_{\sigma_1, \sigma_k} &= p_{\sigma_1} + p_{\sigma_2} + \dots + p_{\sigma_k}, \\ P_{\sigma_{k+1}, \sigma_n} &= p_{\sigma_{k+1}} + p_{\sigma_{k+2}} + \dots + p_{\sigma_n}. \end{aligned} \quad (3.4)$$

The color factor appearing in Eq. (3.3) can be decomposed into (See Fig. 3.1)

$$\delta_{i_{\sigma_1}}^{\bar{J}} \delta_{i_{\sigma_2}}^{\bar{J}_{\sigma_1}} \dots \delta_{i_{\sigma_n}}^{\bar{J}_{\sigma_{n-1}}} = \delta_G^{\bar{J}} \delta_I^{\bar{H}} \delta_L^{\bar{G}} \delta_N^{\bar{K}} \delta_H^{\bar{M}} \delta_{i_{\sigma_1}}^{\bar{L}} \dots \delta_{i_{\sigma_k}}^{\bar{J}_{\sigma_k}} \delta_{i_{\sigma_{k+1}}}^{\bar{N}} \dots \delta_{i_{\sigma_n}}^{\bar{J}_{\sigma_n}}. \quad (3.5)$$

In this decomposition, the color factor can be interpreted as follows:

- $\delta_G^{\bar{J}} \delta_I^{\bar{H}}$  is the color structure of the propagator appearing in the Berends-Giele recursive relations.
- $\delta_{i_{\sigma_1}}^{\bar{L}} \dots \delta_{i_{\sigma_k}}^{\bar{J}_{\sigma_k}}$  is the color structure of the subcurrent  $J_\nu(\sigma_1, \dots, \sigma_k)$ , where the off-shell leg  $\nu$  has color  $(K, \bar{L})$ .
- $\delta_{i_{\sigma_{k+1}}}^{\bar{N}} \dots \delta_{i_{\sigma_n}}^{\bar{J}_{\sigma_n}}$  is the color structure of the subcurrent  $J_\rho(\sigma_{k+1}, \dots, \sigma_n)$ , where the off-shell leg  $\rho$  has color  $(M, \bar{N})$ .
- $\delta_L^{\bar{G}} \delta_N^{\bar{K}} \delta_H^{\bar{M}}$  is part of the color structure of a three gluon vertex to which the off-shell legs  $\mu, \nu, \rho$  with colors  $(G, \bar{H}), (K, \bar{L}), (M, \bar{N})$  are attached.

At this level, we have to introduce the concept of ordered partitions of a set  $E$  into two independent parts. An ordered partition of a set  $E$  into two independent parts is a pair  $(\pi_1, \pi_2)$  of subsets of  $E$  such that  $\pi_1 \oplus \pi_2 = E$ , which means  $(\pi_1, \pi_2) \neq (\pi_2, \pi_1)$ . Furthermore, we call (unordered) partition of a set  $E$  into two independent parts a set  $\{\pi_1, \pi_2\}$  of subsets of  $E$  such that  $\pi_1 \oplus \pi_2 = E$  and  $\{\pi_1, \pi_2\} = \{\pi_2, \pi_1\}$ . These definitions can be easily extended to partitions of a set  $E$  into  $n > 2$  independent parts, for both the ordered and the unordered case. In the case encountered here,  $E = \{1, 2, \dots, n\}$ , and we denote the set of all ordered partitions of  $n$  consecutive numbers  $\{1, 2, \dots, n\}$  into  $p$  independent parts by  $OP(n, p)$ , and the set of all (unordered) partitions of  $n$  consecutive numbers  $\{1, 2, \dots, n\}$  into  $p$  independent parts by  $P(n, p)$ .

Using these definitions, the sum over permutations appearing in Eq. (3.3) can be decomposed as follows: For a given value of  $k$ ,

- Choose an ordered partition  $\pi = (\pi_1, \pi_2)$  in  $OP(n, 2)$  such that  $\#\pi_1 = k$ , where  $\#\pi_1$  is the number of elements in the set  $\pi_1$ .
- Fix the first  $k$  elements of the permutation to be in the subset  $\pi_1$ .
- Sum over all permutations of the first  $k$  elements and over all permutations of the last  $n - k$  elements.
- Sum over all possible choices for the ordered partition  $\pi = (\pi_1, \pi_2)$ .

This is equivalent to the replacement

$$\sum_{k=1}^{n-1} \sum_{\sigma \in S_n} \rightarrow \sum_{\pi \in OP(n, 2)} \sum_{\sigma \in S_k} \sum_{\sigma' \in S_{n-k}}. \quad (3.6)$$

The three gluon vertex part now reads

$$\delta_G^{\bar{J}} \delta_I^{\bar{H}} \frac{-i}{P_{1,n}^2} \sum_{\pi \in OP(n, 2)} \sum_{\sigma \in S_k} \sum_{\sigma' \in S_{n-k}} \delta_L^{\bar{G}} \delta_N^{\bar{K}} \delta_H^{\bar{M}} V_3^{\mu\nu\rho} \left( P_{\sigma_{\pi^1}, \sigma_{\pi^k}}, P_{\sigma'_{\pi^{k+1}}, \sigma'_{\pi^n}} \right) \\ \delta_{i_{\sigma_{\pi^1}}}^{\bar{L}} \dots \delta_{\bar{K}}^{\bar{J} \sigma_{\pi^k}} J_\nu(\sigma_{\pi^1}, \dots, \sigma_{\pi^k}) \delta_{i_{\sigma'_{\pi^{k+1}}}}^{\bar{N}} \dots \delta_{\bar{M}}^{\bar{J} \sigma'_{\pi^n}} J_\rho(\sigma'_{\pi^{k+1}}, \dots, \sigma'_{\pi^n}), \quad (3.7)$$

where  $\pi_1 = \{\pi^1, \pi^2, \dots, \pi^k\}$  and  $\pi_2 = \{\pi^{k+1}, \pi^{k+2}, \dots, \pi^n\}$ . Clearly,  $P_{\sigma_{\pi^1}, \sigma_{\pi^k}}$  and  $P_{\sigma'_{\pi^{k+1}}, \sigma'_{\pi^n}}$  only depend on the choice of the ordered partition  $\pi = (\pi_1, \pi_2)$ ,

but not on the order of the elements of  $\pi_1$  and  $\pi_2$ . We therefore define

$$P_{\pi_1} = p_{\pi^1} + p_{\pi^2} + \dots + p_{\pi^k}, \quad (3.8)$$

$$P_{\pi_2} = p_{\pi^{k+1}} + p_{\pi^{k+2}} + \dots + p_{\pi^n}. \quad (3.9)$$

It is now possible to identify several subcurrents in this expression, namely

$$\mathcal{J}_\nu^{K\bar{L}}(\pi_1) = \sum_{\sigma \in S_k} \delta_{i_{\sigma^1}}^{\bar{L}} \dots \delta_{K^{\sigma^k}}^{\bar{J}} J_\nu(\sigma_{\pi^1}, \dots, \sigma_{\pi^k}), \quad (3.10)$$

$$\mathcal{J}_\rho^{M\bar{N}}(\pi_2) = \sum_{\sigma' \in S_{n-k}} \delta_{i_{\sigma'^{k+1}}}^{\bar{N}} \dots \delta_{M^{\sigma'^n}}^{\bar{J}} J_\rho(\sigma'_{\pi^{k+1}}, \dots, \sigma'_{\pi^n}), \quad (3.11)$$

so that the three gluon vertex part reads

$$\delta_G^{\bar{J}} \delta_I^{\bar{H}} \frac{-i}{P_{1,n}^2} \sum_{\pi \in OP(n,2)} \delta_L^{\bar{G}} \delta_N^{\bar{K}} \delta_H^{\bar{M}} V_3^{\mu\nu\rho}(P_{\pi_1}, P_{\pi_2}) \mathcal{J}_\nu^{K\bar{L}}(\pi_1) \mathcal{J}_\rho^{M\bar{N}}(\pi_2), \quad (3.12)$$

In Ref. [36] it was shown that the (color-dressed) three gluon vertex can be expressed in the color-flow decomposition as<sup>‡</sup>

$$\mathcal{V}_3^{\mu\nu\rho}(P_{\pi_1}, P_{\pi_2}) = \delta_L^{\bar{G}} \delta_N^{\bar{K}} \delta_H^{\bar{M}} V_3^{\mu\nu\rho}(P_{\pi_1}, P_{\pi_2}) + \delta_N^{\bar{G}} \delta_L^{\bar{M}} \delta_H^{\bar{K}} V_3^{\mu\rho\nu}(P_{\pi_2}, P_{\pi_1}). \quad (3.13)$$

So, finally the three gluon vertex part can be written

$$\delta_G^{\bar{J}} \delta_I^{\bar{H}} \frac{-i}{P_{1,n}^2} \sum_{\pi \in P(n,2)} \mathcal{V}_3^{\mu\nu\rho}(P_{\pi_1}, P_{\pi_2}) \mathcal{J}_\nu^{K\bar{L}}(\pi_1) \mathcal{J}_\rho^{M\bar{N}}(\pi_2). \quad (3.14)$$

Let us now turn to the tensor-gluon part in the BG recursive relations (1.25). From Fig. 3.2 it can be seen that for the  $s$ -channel appearing in the decomposition of the four gluon vertex, each tensor-gluon vertex has the same color-flow structure as a three gluon vertex. The  $t$ -channel contribution is similar. Therefore the tensor-gluon vertex can be written in the color decomposition

$$\mathcal{V}_T^{\mu\nu\alpha\beta} = \delta_{i_1}^{\bar{J}} \delta_{i_2}^{\bar{J}_1} \delta_I^{\bar{J}_2} V_T^{\mu\nu\alpha\beta} + \delta_{i_2}^{\bar{J}} \delta_{i_1}^{\bar{J}_2} \delta_I^{\bar{J}_1} V_T^{\nu\mu\alpha\beta}, \quad (3.15)$$

where  $(I, \bar{J})$  is the color of the tensor particle. As the tensor-gluon vertex part has the same color-flow structure as the three gluon vertex, the color dressing

<sup>‡</sup>For clarity, the color indices of the vertex are not written explicitly.

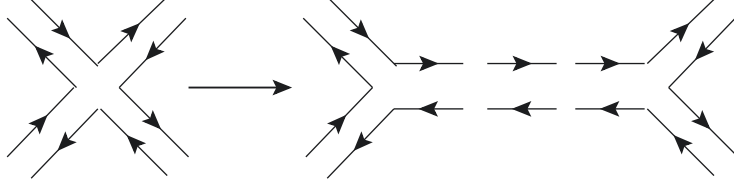


Figure 3.2: Color-flow structure of the  $s$ -channel contribution to the four-gluon vertex.

for the tensor-gluon part is exactly the same as for the pure gluon part, and the result is

$$\sum_{\pi \in OP(n,2)} \left\{ \delta_L^{\bar{G}} \delta_N^{\bar{K}} \delta_H^{\bar{M}} V_T^{\mu\nu\alpha\beta} \mathcal{J}_\nu^{K\bar{L}}(\pi_1) \mathcal{J}_{\alpha\beta}^{M\bar{N}}(\pi_2) + \delta_L^{\bar{G}} \delta_N^{\bar{K}} \delta_H^{\bar{M}} V_T^{\nu\mu\alpha\beta} \mathcal{J}_{\alpha\beta}^{K\bar{L}}(\pi_1) \mathcal{J}_\nu^{M\bar{N}}(\pi_2) \right\}. \quad (3.16)$$

As the sum runs over all elements in  $OP(n,2)$ , we can exchange in the last term  $\pi_1$  and  $\pi_2$ . The same holds true for the color indices  $(K, \bar{L})$  and  $(M, \bar{N})$ . The tensor part now becomes, using Eq. (3.15),

$$\sum_{\pi \in OP(n,2)} \mathcal{V}_T^{\mu\nu\alpha\beta} \mathcal{J}_\nu^{K\bar{L}}(\pi_1) \mathcal{J}_{\alpha\beta}^{M\bar{N}}(\pi_2). \quad (3.17)$$

Hence the color-dressed recursive relations with all four-gluon vertices replaced by tensor particles read

$$\begin{aligned} \mathcal{J}_\mu^{I\bar{J}}(1, \dots, n) &= D_{\mu\nu}(P_{1,n}) \left[ \sum_{\pi \in P(n,2)} \mathcal{V}_3^{\nu\rho\sigma}(P_{\pi_1}, P_{\pi_2}) \mathcal{J}_\rho^{K\bar{L}}(\pi_1) \mathcal{J}_\sigma^{M\bar{N}}(\pi_2) \right. \\ &\quad \left. + \sum_{\pi \in OP(n,2)} \mathcal{V}_T^{\mu\rho\alpha\beta} \mathcal{J}_\rho^{K\bar{L}}(\pi_1) \mathcal{J}_{\alpha\beta}^{M\bar{N}}(\pi_2) \right]. \end{aligned} \quad (3.18)$$

To complete the color dressing of the Berends-Giele recursive relations, we have to apply the color dressing method introduced above to the recursive relations for the off-shell tensor-current. Both the color-dressed vertex and the color-dressed off-shell tensor-current have the same form as in the pure gluon case

and the recursive relations for the tensor particle have the same structure as for the three-gluon vertex part in the previous section. Therefore, one can immediately write down the color-dressed recursive relations for the off-shell tensor-current

$$\mathcal{J}_{\mu\nu}^{I\bar{J}}(1, \dots, n) = iD_{\mu\nu\alpha\beta} \mathcal{V}_T^{\sigma\rho\alpha\beta} \sum_{\pi \in P(n,2)} \mathcal{J}_\rho^{K\bar{L}}(\pi_1) \mathcal{J}_\sigma^{M\bar{N}}(\pi_2). \quad (3.19)$$

The two recursive relations, Eqs. (3.18) and (3.19), can be solved simultaneously to construct color-dressed gluon off-shell currents for arbitrary  $n$ . The full color-dressed scattering amplitude is then recovered by putting the off-shell leg on-shell. This result is equivalent to the recursion presented in Ref. [40], as well as to the Dyson-Schwinger algorithm of Ref. [42] and the ALPHA-algorithm of Ref. [51]. Recently, the color-dressed BG recursion has been implemented into the matrix element generator COMIX [52]. It should be noticed that the color-dressed recursive relations have the same form as the color-ordered Berends-Giele recursive relations, Eq. (1.25), the only difference between the color-ordered and the color-dressed case being that in the latter we sum over unordered objects and no permutations need to be taken into account. This is a general feature which turns out to be common to all color-dressed recursive relations.

### 3.3 Color-dressed BCFW recursive relations

In this section, we apply the same method employed to construct the color-dressed BG recursive relations to the BCFW recursive relations, presented in Section 2.2. As in the BCFW recursion, Eq. (2.1), we have to choose two reference gluons, 1 and  $n$ , the color-flow decomposition and the color decomposition in the fundamental representation are not well suited to dress the BCFW recursive relations with color, because they allow us to fix only one of the two reference gluons. The most natural color decomposition which allows one to fix both reference gluons is the color decomposition in the adjoint representation,

Eq. (1.8). Inserting Eq. (2.1) into Eq. (1.8) for the color-ordered part, one finds

$$\begin{aligned} \mathcal{A}_n(1, \dots, n) &= \sum_{k=2}^{n-2} \sum_{\sigma \in S_{n-2}} (F^{a_{\sigma_2}} \dots F^{a_{\sigma_{n-1}}})_{a_1 a_n} A_{k+1}(\hat{1}, \sigma_2, \dots, \sigma_k, -\hat{P}_{1, \sigma_k}^{-h}) \\ &\times \frac{1}{P_{1, \sigma_k}^2} A_{n-k+1}(\hat{P}_{1, \sigma_k}^h, \sigma_{k+1}, \dots, \sigma_{n-1}, \hat{n}), \end{aligned} \quad (3.20)$$

where

$$P_{1, \sigma_k} = p_1 + p_{\sigma_2} + \dots + p_{\sigma_k}. \quad (3.21)$$

For a given value of  $k$ , the sum over permutations appearing in Eq. (3.20) can be decomposed in a similar way as for the three-gluon vertex part for the Berends-Giele recursive relations

- Choose an ordered partition  $\pi = (\pi_1, \pi_2)$  of  $\{2, 3, \dots, n-2, n-1\}$  such that  $\#\pi_1 = k-1$ .
- Fix the first  $k-1$  elements of the permutation to be in the subset  $\pi_1$ .
- Sum over all permutations of the first  $k-1$  elements and over all permutations of the last  $n-k-1$  elements.
- Sum over all possible choices for the ordered partition  $\pi = (\pi_1, \pi_2)$ .

This is equivalent to the replacement

$$\sum_{k=2}^{n-2} \sum_{\sigma \in S_{n-2}} \rightarrow \sum_{\pi \in OP(n-2, 2)} \sum_{\sigma \in S_{k-1}} \sum_{\sigma' \in S_{n-k-1}}, \quad (3.22)$$

where by  $OP(n-2, 2)$  we mean the set of all ordered partitions of  $\{2, 3, \dots, n-1\}$ . Furthermore, for a fixed value of  $k$ , the color factor can be written

$$(F^{a_{\sigma_2}} \dots F^{a_{\sigma_{n-1}}})_{a_1 a_n} = (F^{a_{\sigma_2}} \dots F^{a_{\sigma_k}})_{a_1 x} (F^{a_{\sigma_{k+1}}} \dots F^{a_{\sigma_{n-1}}})_{x a_n}, \quad (3.23)$$

where a sum over  $x = 1, \dots, (N_c^2 - 1)$  is understood. Finally, the propagator clearly only depends on the choice of the ordered partition  $\pi = (\pi_1, \pi_2)$  and

not on the order of the elements in  $\pi_1$  and  $\pi_2$ . If  $\pi_1 = \{\pi^2, \pi^3, \dots, \pi^k\}$ , we define

$$\begin{aligned} P_{1,\pi_1} &= p_1 + p_{\pi^2} + p_{\pi^3} + \dots + p_{\pi^k}, \\ P_{\pi_2,n} &= -P_{1,\pi_1}. \end{aligned} \quad (3.24)$$

At this point it is possible to identify subamplitudes in the expression for  $\mathcal{A}_n$ , namely

$$\begin{aligned} &\sum_{\sigma \in S_{k-1}} \left( F^{\alpha_{\sigma_{\pi^2}}} \dots F^{\alpha_{\sigma_{\pi^k}}} \right)_{a_1 x} A_{k+1} \left( \hat{1}, \sigma_{\pi^2}, \dots, \sigma_{\pi^k}, -\hat{P}_{1,\pi_1}^{-h} \right) \\ &= \mathcal{A}_{k+1} \left( \hat{1}, \pi_1, -\hat{P}_{1,\pi_1}^{-h,x} \right), \\ &\sum_{\sigma' \in S_{n-k-1}} \left( F^{\alpha_{\sigma'_{\pi^{k+1}}}} \dots F^{\alpha_{\sigma'_{\pi^{n-1}}}} \right)_{x a_n} A_{n-k+1} \left( -\hat{P}_{\pi_2,n}^{-h}, \sigma'_{\pi^{k+1}}, \dots, \sigma'_{\pi^{n-1}}, \hat{n} \right) \\ &= \mathcal{A}_{n-k+1} \left( -\hat{P}_{\pi_2,n}^{-h,x}, \pi_2, \hat{n} \right), \end{aligned} \quad (3.25)$$

where  $x$  is the color of the intermediate gluon. Collecting all the pieces, the color-dressed BCFW recursive relations read

$$\begin{aligned} &\mathcal{A}_n(1, 2, \dots, n) \\ &= \sum_{\pi \in OP(n-2,2)} \mathcal{A}_{k+1} \left( \hat{1}, \pi_1, -\hat{P}_{1,\pi_1}^{-h,x} \right) \frac{1}{P_{1,\pi_1}^2} \mathcal{A}_{n-k+1} \left( \hat{P}_{1,\pi_1}^{h,x}, \pi_2, \hat{n} \right). \end{aligned} \quad (3.26)$$

We see that using the adjoint color basis, we were able to derive new recursive relations which allow us to construct the full color-dressed scattering amplitude. Although the proof of these new recursive relations uses the adjoint color basis, the final result, Eq. (3.26), is independent of the basis choice. Furthermore, as in the case of the BG recursive relations, we see that the form of the color-dressed BCFW recursive relations is the same as in the color-ordered case, with the difference that in Eq. (3.26) the sum goes over all partitions of  $\{2, 3, \dots, n-1\}$ , *i.e.*, over unordered objects. This implies that the color-dressed BCFW recursive relations have the same properties as in the color-ordered case, namely

1. The definition of the off-shell shifts, Eq. (2.2), is independent of the color. The shifts are exactly the same in the color-ordered and in the color-dressed case.

2. As in the color-ordered BCFW recursive relations, the pole structure of the scattering amplitude is manifest in Eq. (3.26).
3. Similar to the color-ordered case, the subamplitudes in Eq. (3.26) are not independent, but they are linked via the off-shell shifts.

The result (3.26) obtained for amplitudes containing only gluons can be easily extended to include a single quark pair. The BCFW recursive relations for color-ordered amplitudes still hold when a quark pair is included, where either a quark or a gluon can be chosen as the intermediate particle [45]. If a quark is chosen for the internal line, no sum over helicities has to be carried out, because helicity is conserved all along the fermion line. The BCFW recursive relations then read

$$\begin{aligned}
A_n(1_q^h, 2, \dots, n_{\bar{q}}^{-h}) &= \sum_{k=2}^{n-2} A_{k+1}(\hat{1}_q^h, 2, \dots, k, -\hat{P}_{\bar{q},1k}^{-h}) \\
&\times \frac{1}{P_{q,1k}^2} A_{n-k+1}(\hat{P}_{q,1k}^h, k+1, \dots, n-1, \hat{n}_{\bar{q}}^{-h}),
\end{aligned} \tag{3.27}$$

where  $h$  is the helicity of the quark. Both the recursive relations and the color decomposition (1.9) have the same form as in the case of a pure gluon amplitude, with the only difference that instead of working in the adjoint representation one now has to work in the fundamental representation of  $SU(N_c)$ . So the recursive relations derived in the case of pure gluon amplitudes can be easily extended to include a single  $q\bar{q}$  pair

$$\begin{aligned}
&\mathcal{A}_n(1_q^h, 2, \dots, n_{\bar{q}}^{-h}) \\
&= \sum_{\pi \in OP(n-2,2)} \mathcal{A}_{k+1}(\hat{1}_q^h, \pi, -\hat{P}_{\bar{q},1\pi}^{-h,x}) \frac{1}{P_{q,1\pi}^2} \mathcal{A}_{n-k+1}(\hat{P}_{q,1\pi}^{h,x}, \bar{\pi}, \hat{n}_{\bar{q}}^{-h}).
\end{aligned} \tag{3.28}$$

The formula is exactly the same as in the pure gluon case, up to two small differences:

- no helicity sum has to be carried out
- $x = 1, \dots, N_c$ , because quarks carry a fundamental color index.

It is possible to extend this relation to include photons, by simply taking

$$(T^a)_i^{\bar{j}} = \delta_i^{\bar{j}}. \tag{3.29}$$



From this it follows that a QED amplitude containing a single  $q\bar{q}$  pair and  $(n-2)$  photons can be written in terms of color-ordered amplitudes as

$$\mathcal{A}_n^{QED}(1_q, 2_{\bar{q}}, 3, \dots, n) = \sum_{\sigma \in S_{n-2}} A_n(1_q, 2_{\bar{q}}, \sigma_3, \dots, \sigma_n). \quad (3.30)$$

and so the above recursive relations (3.27) still hold true for QED amplitudes. This particular result has already been pointed out in Ref. [53]. However, as shown there, for QED processes it is more efficient to take one of the fermions and one photon as reference particles. In fact, as there is no photon-photon vertex, all the terms in the recursive relations where both fermions are in the same subamplitude vanish, which may save a lot of calculation.

## 3.4 Discussion and conclusion

In the first part of this work we discussed the computation of tree-level scattering amplitudes in  $SU(N_c)$  gauge theories, appearing for example in the computation of multi-jet cross-sections at hadron colliders. We reviewed several techniques that bypass the problem of a factorial growth in the number of Feynman diagrams, a problem inherent to the non-abelian structure of an  $SU(N_c)$  gauge theory. The main idea is to keep the information coming from the gauge structure separated from the kinematical dependence. This allows to define gauge-invariant color-ordered amplitudes that have the information on the gauge symmetry built in. Several powerful techniques have recently been developed that have led to new analytic results for multi-leg scattering amplitudes that were thought inconceivable a decade ago.

We concentrated in particular on several recursive techniques for the computation of partial amplitudes. First, the almost traditional BG recursion is very intuitive from the technical point of view and at the basis of many modern implementations for the automatic generation of matrix elements. Second, we reviewed the BCFW recursive relations which have been used to derive new results that enjoy the property of a particularly simple and compact analytic structure. Finally, we introduced a new recursive approach based on the MHV formalism. We showed how to obtain an efficient recursive formulation for MHV

diagrams by introducing a fictitious particle that allows one to build higher-point MHV vertices recursively. The recursion itself is formulated in terms of currents, and has a structure which is strikingly similar to the well-known BG recursive relations.

Even though these recursive techniques are powerful tools for the computation of partial amplitudes, their use can become inefficient when partial amplitudes are combined with their relative color factors, an operation which naturally scales factorially. This step is nevertheless unavoidable to make predictions for physical quantities, and we therefore introduced a new version of the recursions that take color into account from the start. The main feature of our approach is that the form of the recursion is left unchanged, the only difference being that sums run over unordered objects in the color-dressed case. Furthermore, if the color-ordered recursion followed by color-decomposition leads naturally to a factorial growth, the new color-dressed approach in general only scales exponentially with the number of external particles. This result follows immediately from the fact that the number of building blocks entering the recursion grows with the number of (ordered) partitions, a number which is well known to scale exponentially.

In Ref. [14, 54] a (numerical) comparison of the various recursions was performed. In particular, in Ref. [14] explicit numerical implementations of the color-dressed BG, BCFW and MHV recursive relations were confronted. The result is that, for numerical purposes, the traditional BG recursion has by far the best algorithmic behavior for a large number of external particles. The reason why the twistor-inspired results perform worse has several reasons. On the one hand, the BCFW recursion suffer from its top-down structure, *i.e.*, due the off-shell shifts we have to reevaluate the subamplitudes for different off-shell continued momenta at each step in the recursion. On the other hand, the MHV-inspired recursion loses efficiency due to the larger number of different vertices that appear in the recursion compared to the BG algorithm.

In conclusion, we have shown how it is possible to dress recursive relations for partial amplitudes with color. The resulting color-dressed recursive relations can easily be derived by employing an appropriate color decomposition, and

---

retain the same very elegant form of their color-ordered counterparts. In this respect, it is suggestive to speculate that similar colored relations might be derived also for one-loop amplitudes, for which an analogous color decomposition holds.



## Part II

# Infrared singularities of scattering amplitudes



# Chapter 4

## Infrared singularities in scattering amplitudes

### 4.1 Perturbative expansion of physical observables

In the first part of this work we presented several techniques for the computation of tree-level scattering amplitudes. In quantum theories, however, approximating a physical observable by a tree-level computation is very often insufficient and only orders of magnitude can be obtained. Precise predictions for physical observables then require the inclusion of quantum corrections, *i.e.*, of higher-order terms in the perturbative expansion.

We start by analyzing the perturbative expansion for a two-particle scattering with colorless initial states (typically  $e^+e^-$  collisions), and we will comment on hadron colliders at the end of this section. Let  $\mathcal{O}_n(p_1, \dots, p_n)$  be a function of  $n$  momenta representing an observable  $\mathcal{O}$ . Then the distribution of  $\mathcal{O}$  is given by the perturbative expansion

$$\frac{d\sigma}{d\mathcal{O}} = \sum_{n=2}^{\infty} \alpha_s^n \int d\Phi_n(p_1, \dots, p_n; Q) |\bar{\mathcal{A}}_{n+2}(p_1, \dots, p_n; p_{e^-}, p_{e^+})|^2 \mathcal{O}_n, \quad (4.1)$$

with  $\mathcal{O}_n = \delta(\mathcal{O} - \mathcal{O}_n(p_1, \dots, p_n))$  and  $|\bar{\mathcal{A}}_{n+2}|^2$  denotes the squared matrix element for 2-to- $n$  scattering, summed over final state and averaged over initial state quantum numbers, and  $d\Phi_n$  is the  $n$  particle phase space measure for a total incoming momentum  $Q = p_{e^-} + p_{e^+}$ ,

$$d\Phi_n(p_1, \dots, p_n; Q) = (2\pi)^4 \delta^{(4)}\left(Q - \sum_{k=1}^n p_k\right) \prod_{k=1}^n \frac{1}{(2\pi)^3} \frac{d^3 p_k}{2E_k}. \quad (4.2)$$

Using the perturbative expansion of the amplitude in the number of loops,

$$\mathcal{A}_{n+2} = \sum_{\ell=0}^{\infty} \alpha_s^\ell \mathcal{A}_{n+2}^{(\ell)}, \quad (4.3)$$

we see that the leading-order (LO) approximation to Eq. (4.1) is just given by the tree-level result\*,

$$\frac{d\sigma^{\text{LO}}}{d\mathcal{O}} = \alpha_s^2 \int d\Phi_2(p_q, p_{\bar{q}}; Q) \left| \bar{\mathcal{A}}_4^{(0)}(p_q, p_{\bar{q}}; p_{e^-}, p_{e^+}) \right|^2 \mathcal{O}_2. \quad (4.4)$$

Expanding Eq. (4.1) to next-to-leading order (NLO) we find contributions from both the virtual one-loop corrections to the process  $e^+e^- \rightarrow q\bar{q}$  as well as the real corrections coming from the emission of an additional gluon in the final state,

$$\begin{aligned} \frac{d\sigma^{\text{NLO}}}{d\mathcal{O}} &= \alpha_s^3 \int d\Phi_3(p_q, p_{\bar{q}}, p_g; Q) \left| \bar{\mathcal{A}}_5^{(0)}(p_q, p_{\bar{q}}, p_g; p_{e^-}, p_{e^+}) \right|^2 \mathcal{O}_3 \\ &+ 2\alpha_s^3 \text{Re} \int d\Phi_2(p_q, p_{\bar{q}}; Q) \mathcal{A}_4^{(1)}(p_q, p_{\bar{q}}; p_{e^-}, p_{e^+}) \mathcal{A}_4^{(0)}(p_q, p_{\bar{q}}; p_{e^-}, p_{e^+})^* \mathcal{O}_2, \end{aligned} \quad (4.5)$$

The NLO result is thus expressed as a sum of two terms with a different number of final-state particles. As a consequence the two phase space integrals must be performed independently, but it turns out that each of these two terms is separately divergent:

1. The loop integral in  $\mathcal{A}_4^{(1)}$  in general contains infrared singularities.
2. The matrix element  $\mathcal{A}_5^{(0)}$  describing the real correction is singular if a quark emits a collinear or soft gluon. The amplitude for such an emission

---

\*In some cases the LO result is already a one-loop process, *e.g.* Higgs production via gluon fusion.



contains a propagator of the form  $1/(p_q + p_g)^2 = 1/(2E_q E_g (1 - \cos \theta))$ , where  $\theta$  denotes the angle between the quark and the gluon. It is easy to see that this quantity is divergent if either  $p_g$  is collinear to  $p_q$ ,  $\theta = 0$ , or if the gluon is soft,  $E_g \rightarrow 0$ . As a consequence the three-body phase space integral in Eq. (4.5) is divergent.

Let us have a closer look at this problem, and let us start with a very special observable, namely the total cross section, obtained by setting  $\mathcal{O}_n = 1$  in Eq. (4.1)<sup>†</sup>. Although the real and virtual corrections are separately divergent, the Kinoshita-Lee-Nauenberg (KLN) theorem implies that the total cross-section is finite order by order in perturbation theory. In particular, the NLO correction to the total cross-section must be finite,

$$\begin{aligned} \sigma^{\text{NLO}} &= 2\alpha_s^3 \text{Re} \int d\Phi_2(p_q, p_{\bar{q}}; Q) \mathcal{A}_4^{(1)}(p_q, p_{\bar{q}}; p_{e^-}, p_{e^+}) \mathcal{A}_4^{(0)*}(p_q, p_{\bar{q}}; p_{e^-}, p_{e^+}) \\ &\quad + \alpha_s^3 \int d\Phi_3(p_q, p_{\bar{q}}, p_g; Q) \left| \bar{\mathcal{A}}_5^{(0)}(p_q, p_{\bar{q}}, p_g; p_{e^-}, p_{e^+}) \right|^2 \\ &= \text{finite}. \end{aligned} \tag{4.6}$$

Let us now turn to more general observables. In this case, the KLN theorem does not imply that Eq. (4.5) is finite straightaway, because the two terms differ by the definition of the observable  $\mathcal{O}_n$ . In fact, not all physical observables are well-defined in the sense that their distributions are finite to all orders in perturbation theory. In order to get a cancellation between the singular terms in the real and virtual corrections we need a more restrictive class of observables. We define a *collinear and infrared safe observable*  $\mathcal{O}$  by the two conditions:

1. Collinear safety:

$$\lim_{p_i \parallel p_j} \mathcal{O}_{n+1}(p_1, \dots, p_i, \dots, p_j, \dots, p_{n+1}) = \mathcal{O}_n(p_1, \dots, p_i + p_j, \dots, p_{n+1}). \tag{4.7}$$

---

<sup>†</sup>We omit the flux factor in the present discussion, because it does not add anything new.

2. Infrared safety:

$$\lim_{p_i \rightarrow 0} O_{n+1}(p_1, \dots, p_i, \dots, p_{n+1}) = O_n(p_1, \dots, p_{i-1}, p_{i+1}, \dots, p_{n+1}). \quad (4.8)$$

For a collinear and infrared safe observable, the quantities  $\mathcal{O}_2$  and  $\mathcal{O}_3$  in Eq. (4.5) become equal in the singular regions, and so the cancellation of the divergences happens in exactly the same way as for the total cross-section. Note in particular that this implies that the total cross-section is a collinear and infrared safe observable.

From the previous discussion it is clear that a thorough understanding of the infrared behavior of scattering amplitudes is needed to perform higher-order corrections to physical observables. In particular, as the infrared structure of the real corrections is determined by the radiation of additional partons in the final state, the divergences cannot be dependent of the underlying hard scattering, but must be universal and independent of the LO process. In the next section we will review the description of these universal infrared divergences.

Let us conclude this section by briefly commenting on how to generalize the previous discussion to hadronic initial states. In the case of colorless initial states we only had to consider radiation coming from the final state particles. For hadron collisions, however, the initial state particles are in general themselves colored particles, so we need to take into account initial state radiation as well. Let us consider for example a collision of two protons with momenta  $P_1$  and  $P_2$  respectively. Since the proton is a non-perturbative bound state of partons (quarks and gluons), we cannot directly use the wave functions of the incoming protons in our perturbative computation. Nevertheless, we can model the collision by assuming a factorized form for the cross section, given as the convolution of a (perturbative) partonic cross section with a non-perturbative quantity describing the probability to find a certain parton inside the proton,

$$\sigma(pp \rightarrow X) = \sum_{a,b} \int_0^1 dx_1 dx_2 f_a(x_1) f_b(x_2) \hat{\sigma}(ab \rightarrow X), \quad (4.9)$$

where the sum runs over all species of partons  $a$  and  $b$ .  $\hat{\sigma}(ab \rightarrow X)$  is the partonic cross section, calculable in perturbation theory and describing the collision of two partons  $a$  and  $b$  with momenta  $p_a = x_1 P_1$  and  $p_b = x_2 P_2$

respectively.  $f_a(x_1)$  and  $f_b(x_2)$  are the so-called parton distribution functions (PDF's) and represent the probability to find a parton  $a$  ( $b$ ) inside the proton carrying a fraction  $x_1$  ( $x_2$ ) of the proton momentum. The PDF's reflect the internal structure of the proton and are non-perturbative quantities that must be taken from experiment. The partons  $a$  and  $b$  are in general colored objects, and so they can radiate additional gluons that can give rise to additional infrared singularities. It can be shown that the divergencies due to initial state radiation can be reabsorbed into the definition of the parton distribution functions (PDF's), to the price of making the PDF's scale dependent. This scale, known as the factorization scale  $\mu_F$  describes the scale at which long-distance (IR) effects are reabsorbed into the PDF's. As in this work we are only interested in final state radiation, we do not investigate this direction further, but we only quote it for completeness.

## 4.2 Infrared singularities

### 4.2.1 Infrared factorization

In this section we analyze more closely the infrared singularities associated to the emission of soft or collinear gluons. In Section 2.2 we mentioned that poles in a tree-level partial amplitude arise when an intermediate propagator goes on-shell, and the residue of the pole  $P_{1,n}^2 \rightarrow 0$  is given by,

$$A_m(1, \dots, m) \longrightarrow \sum_h A_{n+1}(1, \dots, n, -P_{n,m}^{-h}) \frac{1}{P_{1,n}^2} A_{m-n+1}(P_{1,n}^h, n+1, \dots, m). \quad (4.10)$$

In the limit where the particles  $1, \dots, n$  are unresolved (*i.e.*, soft or collinear), we can identify in the right-hand side of Eq. (4.10) the amplitude for the hard scattering of  $(m - n + 1)$  particles,  $A_{m-n+1}(P_{1,n}^h, n + 1, \dots, m)$ . The factor multiplying the hard scattering depends only on the unresolved particles and is independent of the hard scattering. Hence, close to a singularity for  $n$  unresolved particles, a partial amplitude factorizes into a product of a universal singular factor times the matrix element for the hard scattering. This important property is known as *infrared factorization*. We start by analyzing the

collinear factorization of color-ordered amplitudes arising when two or more partons become collinear, and we will analyze the soft and soft-collinear divergencies in subsequent sections. Note that we follow here the conventions of Ref. [25, 55] and study the factorization properties at the level of the color-stripped amplitudes. Alternatively, we could also study the infrared behavior of the matrix element squared  $|\bar{\mathcal{A}}|^2$  [56, 57]. In the case of collinear divergences this approach leads to the factorization of the matrix element into the matrix element for the hard scattering times the Altarelli-Parisi splitting function, which also appears as the kernel of the DGLAP equation. For soft divergences, however, no exact factorization holds at the amplitude squared level because the soft particles do not completely decouple from the hard partons, but they remain color-connected to the hard scattering. We therefore restrict ourselves to the study of the infrared factorization properties at the color-ordered level, where the amplitude factorizes exactly in all infrared limits. In the rest of this section we review how these universal factors describing the soft and collinear emissions can be extracted from tree-level amplitudes, and we briefly comment at the end on how to generalize these quantities beyond tree-level.

## 4.2.2 Collinear factorization

Collinear singularities arise when two or more adjacent particles, say  $1, \dots, n$ , in a color-ordered amplitude become collinear. In this limit, the amplitude factorizes as

$$A_m(1, \dots, m) \sim \sum_h \text{Split}_{-h}(1, \dots, n) A_{m-n+1}(P^h, n+1, \dots, m), \quad (4.11)$$

where  $P$  denotes the combined momentum  $p_1 + \dots + p_n$ , *i.e.*, the collinear direction.  $\text{Split}_{-h}(1, \dots, n)$  denotes the tree-level splitting amplitude describing the collinear splitting of a particle with momentum  $P$  and helicity  $h$  into  $n$  particles with fixed helicity. The factorization property (4.11) implies that in the region of phase space where the particles  $1, \dots, n$  are collinear, the amplitude  $A_m(1, \dots, m)$  can be approximated by the right-hand side of Eq. (4.11). Explicit results for tree-level color-ordered splitting amplitudes involving quarks and gluons have been derived in Ref. [25] up to  $n = 4$  from tree-level impact

factors and in Ref. [19, 18] using the MHV formalism up to  $n = 4$  for quarks and up to  $n = 6$  for pure gluon splitting amplitudes. Splitting amplitudes inherit many properties from the full color-ordered amplitudes. In particular they are gauge-invariant and fulfill the reflection identity

$$\text{Split}_{-h}(n, \dots, 1) = (-1)^{n+1} \text{Split}_{-h}(1, \dots, n). \quad (4.12)$$

Since splitting amplitudes are universal quantities, they can be computed once and for all, independently of the underlying hard scattering process. In the following we describe a simple algorithm to extract splitting amplitudes from the full scattering amplitude based on a simple power counting. First we restrict ourselves to the simplest of all cases,  $m - n + 1 = 4$ , *i.e.*, the factorization over the four-point amplitude,

$$A_{n+3}(1, \dots, n, a^+, b^{-h}, c^-) \sim \text{Split}_{-h}(1, \dots, n) A_4(P^h, a^+, b^{-h}, c^-). \quad (4.13)$$

Note that due to the supersymmetric Ward identities (1.18), no sum over the helicities of the intermediate particle has to be carried out. Furthermore, from Eq. (1.19) it follows that the hard four-point amplitude always has the simple analytic structure of an MHV amplitude. The splitting amplitudes can then be extracted using a simple algorithm, based on a simple power counting:

1. If  $i$  and  $j$  are particles from the collinear set, rescale the corresponding spinor products according to

$$\begin{aligned} \langle ij \rangle &\rightarrow t \langle ij \rangle, \\ [ij] &\rightarrow t [ij]. \end{aligned} \quad (4.14)$$

2. Expand the amplitude in powers of  $t$ ,

$$\begin{aligned} A_{n+3}(1, \dots, n, a^+, b^{-h}, c^-) \\ = \frac{1}{t^{n-1}} \text{Split}_{-h}(1, \dots, n) A_4(P^h, a^+, b^{-h}, c^-) + \mathcal{O}(1/t^{n-2}). \end{aligned} \quad (4.15)$$

The splitting amplitude corresponds to the leading term in the expansion, *i.e.*, if  $i$  is in the collinear set and  $a$  is not in the collinear set, then the

splitting amplitude corresponds to the coefficient of  $1/t^{n-1}$ , with

$$\begin{aligned}\langle ai \rangle &\rightarrow \sqrt{z_i} \langle aP \rangle, \\ [ai] &\rightarrow \sqrt{z_i} [aP],\end{aligned}\tag{4.16}$$

where  $z_i$  denote the longitudinal momentum fractions<sup>‡</sup>,  $p_i = z_i P$ .

Let us illustrate this procedure on the simple case of an MHV amplitude, Eq. (1.19). For  $h = +1$ , the scaling (4.14) gives

$$\begin{aligned}A_{n+3}(1^+, \dots, n^+, a^+, b^-, c^-) &= \frac{1}{t^{n-1}} \frac{\langle bc \rangle^4}{\langle 12 \rangle \dots \langle (n-1)n \rangle \sqrt{z_n} \langle Pa \rangle \langle ab \rangle \langle bc \rangle \sqrt{z_1} \langle cP \rangle} \\ &= \frac{1}{t^{n-1}} \frac{1}{\sqrt{z_1 z_n} \langle 12 \rangle \dots \langle (n-1)n \rangle} A_4(P^+, a^+, b^-, c^-).\end{aligned}\tag{4.17}$$

From this expression we immediately read off the MHV-type splitting amplitude  $\text{Split}_-(1^+, \dots, n^+)$ ,

$$\text{Split}_-(1^+, \dots, n^+) = \frac{1}{\sqrt{z_1 z_n} \langle 12 \rangle \dots \langle (n-1)n \rangle}.\tag{4.18}$$

Repeating the same argument for  $h = -1$  we find a second MHV-type splitting amplitude,

$$\text{Split}_+(1^+, \dots, i^-, \dots, n^+) = \frac{z_i^2}{\sqrt{z_1 z_n} \langle 12 \rangle \dots \langle (n-1)n \rangle}.\tag{4.19}$$

Similar relations can be derived for  $\overline{\text{MHV}}$ -type splitting amplitudes. Note however that for more general helicity assignments no generic formula for arbitrary  $n$  can be given. In Chapter 5 we will present a recursive algorithm that allows to compute splitting amplitudes for an arbitrary number of gluons for a given helicity configuration.

### 4.2.3 Soft factorization

The factorization of an amplitude in the soft limit is very different from the collinear one. Let us consider a pure gluon color-ordered amplitude at tree-level. This amplitude displays an infrared divergence as some of the gluons

<sup>‡</sup>From momentum conservation it follows immediately that  $z_1 + \dots + z_n = 1$ .

become soft, *i.e.*, some of the gluon energies vanish. Two different cases might occur, the color-connected and the color-disconnected one, that need to be considered separately [55].

Let us first consider the color-connected case where the soft gluons are all adjacent in the color-ordered amplitude, say  $s_1, \dots, s_n$ . The amplitude then factorizes as

$$\begin{aligned} A_m(1, \dots, a, s_1, \dots, s_n, b, \dots, m) \\ \sim \text{Soft}(a, s_1, \dots, s_n, b) A_{m-n}(1, \dots, a, b, \dots, m), \end{aligned} \quad (4.20)$$

where  $\text{Soft}(a, s_1, \dots, s_n, b)$  is a universal function, called soft factor, describing the emission of  $n$  unresolved soft gluons from the hard amplitude. This factorization implies that in the region of phase space where the particles  $s_1, \dots, s_n$  become soft, the amplitude  $A_m(1, \dots, a, s_1, \dots, s_n, b, \dots, m)$  can be approximated by the right-hand side of Eq. (4.20). The (color-ordered) soft factor  $\text{Soft}(a, s_1, \dots, s_n, b)$  defined in this way depends on the momenta and the helicities of the soft particles, and also on the particles  $a$  and  $b$  color-connected to the soft set. The soft factors are, however, independent of the helicities of the particles  $a$  and  $b$  [32]. Furthermore, it is quite easy to see that the soft factors again satisfy the reflection identity,

$$\text{Soft}(b, n, \dots, 1, a) = (-1)^n \text{Soft}(a, 1, \dots, n, b). \quad (4.21)$$

The color-disconnected case corresponds to the situation where the soft particles are not all adjacent, but separated by at least one hard gluon. In this case the factorization is, *e.g.* for two sets of soft particles,

$$\begin{aligned} A_m(1, \dots, a, s_1, \dots, s_n, b, \dots, c, t_1, \dots, t_l, d, \dots, m) \\ \sim \text{Soft}(a, s_1, \dots, s_n, b) \text{Soft}(c, t_1, \dots, t_l, d) A_{m-n-l}(1, \dots, a, b, \dots, c, d, \dots, m), \end{aligned} \quad (4.22)$$

*i.e.*, the color-disconnected soft factors are just products of the corresponding color-connected soft factors. In the rest of this work we will thus only deal with the color-connected case.

Similar to the case of splitting amplitudes, soft factors are universal quantities that can be calculated once and for all. We therefore again restrict the com-

putation to the simplest of all cases, namely where the hard amplitude is an MHV amplitude,

$$A_{n+4}(a^+, 1, \dots, n, b^+, c^-, d^-) \sim \text{Soft}(a, 1, \dots, m, b) A_4(a^+, b^+, c^-, d^-). \quad (4.23)$$

Note that as the soft factor is independent of the helicities of the hard particles  $a$  and  $b$ , it is unaffected by the helicity assignment in the hard part. The soft factors can be obtained by a simple power counting algorithm:

1. Rescale all spinor products according to

$$\begin{aligned} \langle ij \rangle &\rightarrow t^2 \langle ij \rangle, \\ \langle aj \rangle &\rightarrow t \langle aj \rangle, \\ [ij] &\rightarrow t^2 [ij], \\ [aj] &\rightarrow t [aj], \\ s_{ij} &\rightarrow t^4 s_{ij}, \\ s_{aj} &\rightarrow t^2 s_{aj}. \end{aligned} \quad (4.24)$$

2. Expand the amplitude in powers of  $t$ ,

$$\begin{aligned} A_{n+4}(a^+, 1, \dots, n, b^+, c^-, d^-) \\ = \frac{1}{t^{2n}} \text{Soft}(a, 1, \dots, m, b) A_4(a^+, b^+, c^-, d^-) + \mathcal{O}(1/t^{2n-1}), \end{aligned} \quad (4.25)$$

where the dots indicate terms which are less divergent than  $1/t^{2n}$ . The soft factor then corresponds to the leading term in the expansion.

Let us again illustrate this procedure on an MHV example. Using the scaling (4.24), we find

$$\begin{aligned} A_{n+4}(a^+, 1^+, \dots, n^+, b^+, c^-, d^-) \\ = \frac{1}{t^{2n}} \frac{\langle bc \rangle^4}{\langle a1 \rangle \langle 12 \rangle \dots \langle nb \rangle \langle bc \rangle \langle cd \rangle \langle da \rangle} \\ = \frac{1}{t^{2n}} \frac{\langle ab \rangle}{\langle a1 \rangle \dots \langle nb \rangle} A_4(a^+, b^+, c^-, d^-). \end{aligned} \quad (4.26)$$

Hence, the tree-level MHV-type soft factor reads,

$$\text{Soft}(a, 1^+, \dots, n^+, b) = \frac{\langle ab \rangle}{\langle a1 \rangle \dots \langle nb \rangle}. \quad (4.27)$$



Note that we could have derived the same result using a different helicity assignment for the hard particles  $a, b, c, d$ . Also note that an MHV amplitude only exhibits soft divergencies when a positive-helicity gluon becomes soft, because for a negative-helicity soft gluon the scaling (4.24) only generates subleading terms in  $1/t^{2n-4}$ . We could have anticipated this result from the fact that in this case the hard amplitude only contains a single negative-helicity gluon, and hence vanishes due to Eq. (1.18).

#### 4.2.4 Infrared factorization beyond tree-level

We conclude this section by briefly commenting on how collinear and soft factorization generalizes beyond tree-level. In Ref. [58] it was shown that collinear factorization holds to all orders in perturbation theory, and in the limit where two particles becomes collinear, an  $L$ -loop amplitude factorizes according to

$$A_n^{(L)}(1, 2, \dots, n) = \sum_{\ell=0}^L \sum_h \text{Split}_{-h}^{(\ell)}(1, 2) A_{n-1}^{(L-\ell)}(P^h, 3, \dots, n). \quad (4.28)$$

In this formula  $\text{Split}_{-h}^{(\ell)}$  denotes the  $\ell$ -loop splitting amplitude, and  $\text{Split}_{-h}^{(0)}$  corresponds to the tree-level splitting amplitudes defined in Section 4.2.2. Splitting amplitudes are known up to NNLO [6, 59, 60, 61, 62], and in particular, the NLO splitting amplitudes in dimensional regularization through  $\mathcal{O}(\epsilon^0)$  read (the result is given in the euclidean region where all invariants are taken to be negative),

$$\begin{aligned} \text{Split}_+^{(1)}(1^-, 2^-) &= (G^f + G^n) \text{Split}_+^{(0)}(1^-, 2^-), \\ \text{Split}_+^{(1)}(1^\pm, 2^\mp) &= G^n \text{Split}_+^{(0)}(1^\pm, 2^\mp), \\ \text{Split}_+^{(1)}(1^+, 2^+) &= -G^f \frac{1}{\sqrt{z_1 z_2}} \frac{[12]}{\langle 12 \rangle^2}, \end{aligned} \quad (4.29)$$

where the coefficients  $G^f$  and  $G^n$  are given by

$$\begin{aligned} G^f &= \frac{1}{48\pi^2} \left( 1 - \frac{N_f}{N_c} \right) z_1 z_2 + \mathcal{O}(\epsilon), \\ G^n &= c_\Gamma \left[ -\frac{1}{\epsilon^2} z_1^{-\epsilon} z_2^{-\epsilon} \left( \frac{\mu^2}{-s_{12}} \right)^\epsilon + 2 \ln z_1 \ln z_2 - \frac{\pi^2}{6} \right] + \mathcal{O}(\epsilon), \end{aligned} \quad (4.30)$$

with

$$c_\Gamma = \frac{\Gamma(1+\epsilon)\Gamma^2(1-\epsilon)}{(4\pi)^{2-\epsilon}\Gamma(1-2\epsilon)}, \quad (4.31)$$

and  $\Gamma(z)$  denotes the Euler  $\Gamma$  function,

$$\Gamma(z) = \int_0^\infty dt t^{z-1} e^{-t}. \quad (4.32)$$

Note the appearance of the splitting amplitude  $\text{Split}_+^{(1)}(1^+, 2^+)$  which vanishes at tree-level due to the supersymmetric Ward identities.

Unlike collinear factorization, soft factorization was only shown to hold up to one-loop accuracy in the perturbative expansion,

$$\begin{aligned} A_n^{(1)}(1, 2, \dots, n) \\ = \text{Soft}^{(1)}(1, 2, 3) A_{n-1}^{(0)}(1, 3, \dots, n) + \text{Soft}^{(0)}(1, 2, 3) A_{n-1}^{(1)}(1, 3, \dots, n), \end{aligned} \quad (4.33)$$

with

$$\text{Soft}^{(1)}(a, 1, b) = -\text{Soft}^{(0)}(a, 1, b) c_\Gamma \frac{1}{\epsilon^2} \left( \frac{\mu^2(-s_{ab})}{(-s_{a1})(-s_{1b})} \right)^\epsilon \frac{\pi\epsilon}{\sin \pi\epsilon}, \quad (4.34)$$

where  $\text{Soft}^{(1)}$  denotes the one-loop soft factor, and  $\text{Soft}^{(0)}$  is the tree-level soft factor defined in Section 4.2.3.

### 4.3 Subtraction schemes

In Section 4.1 we discussed that the infrared singularities in the real and virtual corrections contributing to the NLO correction mutually cancel for a collinear and infrared safe physical observable. Although the full NLO result is finite, we cannot use Eq. (4.5) directly in numerical computer programs because the real and virtual phase space integrals have to be performed independently. To regularize the integrals, we add and subtract an approximate cross-section to Eq. (4.5) which exactly cancels the divergencies in the real correction [63],

$$\frac{d\sigma^{\text{NLO}}}{d\mathcal{O}} = \int d\sigma_2^V \mathcal{O}_2 + \int d\sigma_3^{\text{R,app}} \mathcal{O}_3 + \int [d\sigma_3^{\text{R}} - d\sigma_3^{\text{R,app}}] \mathcal{O}_3, \quad (4.35)$$

where we defined

$$d\sigma_2^V = d\Phi_2 2 \operatorname{Re} \mathcal{A}_2^{(1)} \mathcal{A}_2^{(0)*} \quad \text{and} \quad d\sigma_3^R = d\Phi_3 \left| \bar{\mathcal{A}}_3^{(0)} \right|^2, \quad (4.36)$$

and  $d\sigma_3^{R,\text{app}}$  denotes the approximate cross-section such that  $(d\sigma_3^R - d\sigma_3^{R,\text{app}})$  is finite in every phase space point. If  $\mathcal{O}$  denotes a collinear and infrared safe observable, the KLN theorem implies that the sum of the first two terms in Eq. (4.35) is finite as well. We have seen in the previous section that the infrared behavior of tree-level amplitudes can be described by the universal splitting amplitudes and soft factors, and so the approximate cross-section can be constructed completely from these quantities,

$$d\sigma_3^{R,\text{app}} = d\Phi_3 \sum_r \left[ \sum_{i \neq r} \frac{1}{2} \mathbf{C}_{ir} + \mathbf{S}_r - \sum_{i \neq r} \mathbf{S} \mathbf{C}_{ir} \right] \left| \bar{\mathcal{A}}_2^{(0)} \right|^2. \quad (4.37)$$

The sum runs over all (pairs) of unresolved particles, and  $\mathbf{C}_{ir}$  and  $\mathbf{S}_r$  denote universal collinear and soft counterterms constructed from the splitting amplitudes and soft factors defined in the previous section<sup>§</sup>. The term  $\mathbf{S} \mathbf{C}_{ir}$  accounts for the overlapping between the soft and collinear regions of phase space and has to be added in order to avoid double counting of divergent phase space points.

Eq. (4.37), however, cannot yet serve as an approximate cross section because the factorization formulas presented in Section 4.2 are only true in the strict singular limit. To overcome this issue, we perform a change of variable in the three-body phase space integral,

$$\{p_i\} = \{p_q, p_{\bar{q}}, p_g\} \rightarrow \{\tilde{p}_i; p_r\} = \{\tilde{p}_q, \tilde{p}_{\bar{q}}; p_r\}, \quad (4.38)$$

such that all particles stay on shell and momentum is conserved,  $\tilde{p}_i^2 = p_r^2 = 0$  and  $\tilde{p}_q + \tilde{p}_{\bar{q}} = p_q + p_{\bar{q}} + p_g$ . An explicit example of such a change of variable can be found in Ref. [63]. In these new variables the approximate cross-section reads

$$d\sigma_3^{R,\text{app}} = [dp_{1;2}] \mathcal{C}(p_r) d\sigma_2^B, \quad (4.39)$$

---

<sup>§</sup>Note that in practise the counterterms have a slightly more complicated form because of color connections between the unresolved and the hard partons. Since in this work we only want to give a flavor of how to construct a subtraction scheme at NLO, we neglect all color connections in Eq. (4.37).

where  $d\sigma_2^{\text{B}} = d\Phi_2 \left| \bar{\mathcal{A}}_2^{(0)} \right|^2$  denotes the Born-level cross-section and  $\mathcal{C}$  denotes the counterterm in the new variables,

$$\mathcal{C}(\{\tilde{p}_i\}, p_r) = \sum_r \left[ \sum_{i \neq r} \frac{1}{2} \mathbf{C}_{ir} + \mathbf{S}_r - \sum_{i \neq r} \mathbf{S} \mathbf{C}_{ir} \right]_{\{\tilde{p}_i; p_r\}} \quad (4.40)$$

and

$$[dp_{1;2}] = \mathcal{J}_2(\{\tilde{p}_i\}, p_r; P) \frac{1}{(2\pi)^3} \frac{d^3 p_r}{2E_r}, \quad (4.41)$$

denotes the phase space measure of the unresolved particle and  $\mathcal{J}_2$  is the jacobian of the change of variable. Using this representation for the approximate cross-section, Eq. (4.35) becomes

$$\frac{d\sigma^{\text{NLO}}}{d\mathcal{O}} = \int \left[ d\sigma_2^{\text{V}} + d\sigma_2^{\text{B}} \int [dp_{1;2}] \mathcal{C} \right] \mathcal{O}_2 + \int \left[ d\sigma_3^{\text{R}} - d\sigma_2^{\text{B}} \int [dp_{1;2}] \mathcal{C} \right] \mathcal{O}_3, \quad (4.42)$$

The two phase space integrals in Eq. (4.42) are both finite, and they can be integrated numerically independently from each other. Note that not only the counterterm  $\mathcal{C}$  appears in Eq. (4.42), but also its integral over the phase space of the unresolved particle. Since this one-particle integral is independent of the hard matrix element, it can be done analytically once and for all. This integral is however divergent and needs to be regularized, an issue that will be addressed in Chapter 6 where we discuss the integration of some real virtual counterterms for an NNLO subtraction scheme. That the counterterms in Eq. (4.42) are independent of the underlying hard scattering. For this reason, the scheme described above is universal, and does not only apply to the specific process  $e^+e^- \rightarrow q\bar{q}$  at NLO. A generic algorithm for next-to-leading order subtraction has already been developed a decade ago in Ref. [20], where also initial state radiation was taken into account. Recently, a generic NNLO subtraction scheme has been proposed [21, 22, 24]. The construction of a subtraction scheme at higher orders is much more complicated than in the NLO case, because of several overlapping singular regions of phase space. In order to overcome this problem, a new type of factorization has been proposed, called antenna factorization, which takes into account the overlapping of the singular regions from the start.

## 4.4 Antenna factorization

In the previous section, we reviewed the basic ideas of an NLO subtraction scheme. The counterterm used to regulate the soft and collinear divergences was constructed from the universal factorization properties of gauge theory amplitudes in the soft and collinear limits, and we pointed out that beyond NLO this procedure may become cumbersome due to overlapping singular regions of phase space. In this section we present an alternative way to construct counterterms for subtractions schemes, not based on the universal soft factors and splitting amplitudes, but on a more general object, the so-called antenna function [15, 16, 64].

Let us consider an  $m$ -point pure gluon amplitude  $A_m(a, 1, \dots, n, b, \dots, m)$ . The singular limit for the particles  $1, \dots, n$  is defined as the limit where the particles  $1, \dots, n$  are either collinear to  $a$ , collinear to  $b$ , or soft. An antenna function for  $n$  unresolved particles is defined as any function  $\text{Ant}(\hat{a}^{h_{\hat{a}}}, \hat{b}^{h_{\hat{b}}} \leftarrow a, 1, \dots, n, b)$  that reproduces the correct singular limits. If splitting amplitudes and soft factors represent the residues of an amplitude, antenna function can be seen, loosely speaking, as the sum of all residues for  $n$  unresolved particles. Note that, at variance with the splitting amplitudes and the soft factors, this definition does not lead to unique functions, because two antenna function could contain all the correct poles but differ by the finite part. Nevertheless, in the singular regions of phase space the amplitude can be approximated by

$$A_m(a, 1, \dots, n, b, \dots, m) \sim \sum_{h_{\hat{a}}, h_{\hat{b}}} \text{Ant}(\hat{a}^{h_{\hat{a}}}, \hat{b}^{h_{\hat{b}}} \leftarrow a, 1, \dots, n, b) A_{m-n}(\hat{a}^{-h_{\hat{a}}}, \hat{b}^{-h_{\hat{b}}}, \dots, m), \quad (4.43)$$

where  $p_{\hat{a}}$  and  $p_{\hat{b}}$  are the so-called *reconstruction functions*,

$$\begin{aligned} p_{\hat{a}} &= f_{\hat{a}}(a, 1, \dots, n, b), \\ p_{\hat{b}} &= f_{\hat{b}}(a, 1, \dots, n, b). \end{aligned} \quad (4.44)$$

The reconstruction functions satisfy the following properties:

1. On-shellness,  $p_{\hat{a}}^2 = p_{\hat{b}}^2 = 0$ .
2. Momentum conservation,  $p_{\hat{a}} + p_{\hat{b}} = p_a + p_1 + \dots + p_n + p_b$ .

3. They reduce to the right expressions in the various singular limits, *e.g.* if  $1, \dots, n$  become collinear to  $a$ , then  $p_{\hat{a}} \rightarrow p_a + p_1 + \dots + p_n$  and  $p_{\hat{b}} \rightarrow p_b$ .
4. They leave the leading pole unchanged.

The explicit expressions for the reconstruction functions of Ref. [16] are collected in Appendix A. The reconstruction functions play the role of the change of variables introduced in the previous section. In this sense, antenna functions have the phase space mapping needed to define a subtraction scheme built in.

As already pointed out, the definition of an antenna function is not strict enough to uniquely fix its functional form and several definitions can be found in the literature. In Ref. [16], Kosower presented a way to build antenna functions based on the BG recursive relations presented in Section 1.4. In Refs. [65, 66, 67], Gehrmann *et al.* defined antenna functions as ratios between the full and the hard squared matrix elements and applied their antenna functions to the computation of the event shapes for  $e^+e^- \rightarrow 3$  jets at NNLO. In the next chapter, we present an alternative definition for antenna functions based on the MHV formalism, and we study the properties special to this approach.

# Chapter 5

## Antenna functions from MHV rules

### 5.1 Power counting for antenna functions in the MHV formalism

In Section 2.3 we presented the MHV formalism and the BCFW recursion, two powerful tools to calculate partial amplitudes. Since the twistor inspired techniques are built around the collinear factorization properties of an amplitude, one can naturally ask whether they can also be used to compute splitting amplitudes and/or soft factors. In Refs. [19, 18], Birthwright *et al.* derived a rule to compute splitting amplitudes by means of the MHV formalism and applied this technique to obtain very compact formulas for several classes of splitting amplitudes. In the following we extend this rule such that they do not only describe the collinear behavior of an amplitude, but the full infrared behavior, *i.e.*, the antenna functions.

We start by introducing the notion of *MHV pole structures* of an amplitude. We know that in the MHV formalism the building blocks are MHV amplitudes, continued off shell using Eq. (2.7) and connected by scalar propagators. Since MHV amplitudes are purely holomorphic objects, antiholomorphic spinor

products can enter the final expression for the amplitude only in a very limited way. A first source are the scalar propagators, where antiholomorphic spinor products enter through the relation  $s_{ij} = \langle ij \rangle [ji]$ . There is a second source, related to the off-shell continued spinor products inherent to the MHV formalism, Eq. (2.7). Since  $\eta$  is arbitrary and the physical result must be independent of it, all spinor products involving  $\eta$  must cancel in the end. Hence, the only source of antiholomorphic spinor products are the scalar propagators in the MHV diagrams. Furthermore, we know that the number of propagators in an amplitude is linked to the number of negative helicity gluons through Eq. (2.8). Thus, we conclude that the only place where antiholomorphic spinor products enter an amplitude for  $n_-$  negative-helicity gluons (and an arbitrary number of positive-helicity gluons) are the  $p = n_- - 2$  scalar propagators. We formalize this by saying that the MHV pole structure of an amplitude is of the form

$$A \sim \frac{1}{[\ ]^{n_-}} f(\langle \ \ \rangle). \quad (5.1)$$

Let us now extend this definition to splitting amplitudes. We know that in the collinear limit, the amplitude must factorize according to Eq. (4.11). Since the MHV pole structures of the amplitudes are known, it is a trivial exercise to match the pole structure on both sides of Eq. (4.11) and to extract the MHV pole structure of splitting amplitudes,

$$\begin{aligned} \text{Split}_- &\sim \frac{1}{[\ ]^{n_-}} f(\langle \ \ \rangle), \\ \text{Split}_+ &\sim \frac{1}{[\ ]^{n_- - 1}} f(\langle \ \ \rangle), \end{aligned} \quad (5.2)$$

where  $n_-$  is the number of negative-helicity gluons in the collinear set. This result was first derived in Ref. [19, 18] and has far reaching consequences. To see this, let us consider the simplest of all cases where we choose the hard amplitude to be a four-point amplitude, Eq. (4.13). The hard amplitude on the right-hand side is an MHV amplitude, so the MHV pole structure is trivial,

$$A_4(P^h, a^+, b^{-h}, c^-) \sim \frac{1}{[\ ]^0} f(\langle \ \ \rangle), \quad (5.3)$$

or equivalently, the splitting amplitude must have the same MHV pole structure as the amplitude on the left-hand side of Eq. (4.13). Since the splitting



amplitude captures only the leading collinear singularity, we conclude that in the collinear limit only those MHV diagrams contribute where all scalar propagators go on-shell. In other words, we can refine our algorithm to compute splitting amplitudes of Section 4.2.2 in such a way that we do not need to compute the full amplitude on the left-hand side of Eq. (4.13), but it is enough to consider only a subset of MHV diagrams, namely those where all scalar propagators go on shell.

After having identified this limited set of MHV diagrams that contribute in the collinear limit, let us see what the scaling rules (4.16) become in the collinear limit. It is easy to show that,

$$\begin{aligned}
\langle a P_{i,j} \rangle &\rightarrow \langle a P \rangle [P \eta] \sum_{\alpha=i}^j z_{\alpha}, \\
\langle k P_{i,j} \rangle &\rightarrow [P \eta] \sum_{\alpha=i}^j \sqrt{z_{\alpha}} \langle k \alpha \rangle, \\
\langle P_{i,j} P_{k,l} \rangle &\rightarrow [P \eta]^2 \sum_{\alpha=i}^j \sum_{\beta=k}^l \sqrt{z_{\alpha} z_{\beta}} \langle \alpha \beta \rangle,
\end{aligned} \tag{5.4}$$

where  $a$  is a particle which is not in the collinear set,  $k$  is in the collinear set, and  $P_{i,j}$  and  $P_{k,l}$  only contain particles from the collinear set. Introducing the following notation\*

$$\begin{aligned}
\Delta(i, j; k) &= \sum_{\alpha=i}^j \sqrt{z_{\alpha}} \langle k \alpha \rangle, \\
\Delta(i, j; k, l) &= \sum_{\alpha=i}^j \sum_{\beta=k}^l \sqrt{z_{\alpha} z_{\beta}} \langle \alpha \beta \rangle,
\end{aligned} \tag{5.5}$$

Eq. (5.4) becomes

$$\begin{aligned}
\langle k P_{i,j} \rangle &\rightarrow [P \eta] \Delta(i, j; k), \\
\langle P_{i,j} P_{k,l} \rangle &\rightarrow [P \eta]^2 \Delta(i, j; k, l).
\end{aligned} \tag{5.6}$$

As already stated in Chapter 2,  $\eta$  is an arbitrary spinor that can be thought as parametrizing the gauge-dependence of a quantity. As in the collinear limit the only  $\eta$  dependence is in  $[P \eta]$ , we can neglect these spinor products, *i.e.*,

---

\*These notations differ slightly from those used in Refs. [19, 18].

we set  $[P\eta] = 1$ . We can summarize the previous discussion in the following rule, which was first presented in Ref. [19, 18] and which gives a refinement to the algorithm to compute splitting amplitudes presented in Section 4.2.2:

**Rule 5.1** (Collinear MHV rules).

1. Consider all MHV diagrams contributing to the collinear limit of the  $(n+3)$ -point amplitude  $A_{n+3}(1, \dots, n, (n+1)^+, (n+2)^{-h}, (n+3)^-)$ . This set is obtained by including the diagrams where all the scalar propagators go on-shell in the collinear limit, or equivalently, the diagrams where  $(n+1)$ ,  $(n+2)$  and  $(n+3)$  are attached to the same MHV vertex.
2. Go to the collinear limit by applying the rules in Eq. (5.4).
3. Divide out the hard four-point amplitude  $A_4(P^h, (n+1)^+, (n+2)^{-h}, (n+3)^-)$ .

In the rest of this section we show how it is possible to extend this procedure to the extraction of antenna functions. To do so, first one has to find the MHV diagrams that contribute to a given singular limit, *i.e.*, the MHV pole structures of the antenna function, similar to Eq. (5.2), have to be identified.

Let us start with the soft limits in the MHV construction. To be concrete, let us consider an  $(n+4)$ -point gluon amplitude  $A_{n+4}(a, 1, \dots, n, b, c, d)$ , where the gluons  $1, \dots, n$  become soft. The amplitude then factorizes according to Eq. (4.23). The soft factor can be easily calculated using the following result [57],

**Rule 5.2** (Gluon insertion rule).

*In the soft limit, only Feynman diagrams where the soft gluons are radiated from the external legs of the hard amplitude contribute.*

The proof of the gluon insertion rule, based on simple power counting arguments, is presented in Appendix B.1.

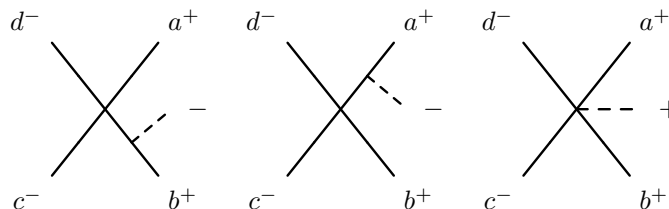


Figure 5.1: Possible MHV diagrams where a soft gluon is radiated between the external legs  $a$  and  $b$ . The dashed line corresponds to a soft gluon.

Rule 5.2 allows an easy identification of the Feynman diagrams corresponding to the emission of additional soft gluons. In order to establish the MHV pole structure of the soft emission, we need to generalize this result to MHV diagrams. Let us consider an  $(n+4)$ -point gluon amplitude  $A_{n+4}(a, 1, \dots, n, b, c, d)$ , where the gluons  $1, \dots, n$  become soft. Rule 5.2 states that in the soft limit only those Feynman diagrams contribute where the soft particles are radiated from the external legs  $a$  and  $b$ . However, it is easy to see that, given the helicity configuration, only negative-helicity gluons can be radiated from the external legs in the MHV formalism (a positive-helicity gluon would lead to a three-point MHV vertex with two positive-helicity gluons). The positive-helicity gluons must thus be radiated only from the MHV vertex which builds up the hard amplitude. Note that this is consistent with the gluon insertion rule (*cf.* the soft factorization of a pure MHV-amplitude). Similar considerations hold true for different helicity assignments of the particles  $a, b, c, d$  in the hard amplitude.

This leads us to the following new formulation of the gluon insertion rule, valid for MHV diagrams (See Fig. 5.1),

**Rule 5.3** (Gluon insertion rule in the MHV formalism).

*In the soft limit, only MHV diagrams where negative-helicity soft gluons are radiated from the external legs  $a$  and  $b$  or positive-helicity soft gluons from the MHV vertex that forms the hard amplitude contribute.*

Note that the gluon insertion rule is very restrictive on the possible diagrams (Fig. 5.1), because it forces the hard gluons  $c$  and  $d$  to be attached to the same MHV vertex. Thus only a small number of MHV diagrams contribute in the soft limit. Furthermore it is easy to see that, similar to Rule 5.1, this class of diagrams is exactly that where all scalar propagators go on-shell.

We now turn to the MHV pole structure of soft limits. Consider the situation where the set  $\{1, \dots, n\}$  contains  $n_s$  negative-helicity gluons. The set  $\{a, b, c, d\}$  contains two additional negative-helicity gluons, so that the hard amplitude  $A_4(a, b, c, d)$  is an MHV-amplitude. Using Eq. (2.8), we obtain the number of MHV propagators in the  $(n+4)$ -point amplitude,  $p = (n_s + 2) - 2 = n_s$ . As the hard four-point amplitude does not contain any MHV propagator, we come to the conclusion that a soft factor containing  $n_s$  negative-helicity gluons has the following MHV pole structure

$$\text{Soft} \sim \frac{1}{[\ ]^{n_s}} f(\langle \ \rangle). \quad (5.7)$$

Note that this result is in agreement with the MHV-type soft factors derived in Chapter 4,

$$\begin{aligned} \text{Soft}(a, 1^+, \dots, n^+, b) &= \frac{\langle ab \rangle}{\langle a1 \rangle \dots \langle nb \rangle} \sim \frac{1}{[\ ]^0} f(\langle \ \rangle), \\ \text{Soft}(a, 1^-, \dots, n^-, b) &= (-1)^n \frac{[ab]}{[a1] \dots [nb]} \sim \frac{1}{[\ ]^n} f(\langle \ \rangle). \end{aligned} \quad (5.8)$$

We can extend this result to the case of color-connected soft/collinear limits<sup>†</sup>. Let us consider to this effect the amplitude  $A_{n+3}(a, 1, \dots, k, \dots, n, b, c)$  in the limit where  $1, \dots, k$  are soft and  $k+1, \dots, n$  are collinear. In this limit the amplitude can be approximated by [55]

$$\begin{aligned} A_{n+3}(a, 1, \dots, k, \dots, n, b, c) \\ \sim \sum_h \mathcal{S}(a; 1, \dots, k; k+1, \dots, n) \text{Split}_{-h}(k+1, \dots, n) A_4(a, P^h, b, c), \end{aligned} \quad (5.9)$$

where  $\mathcal{S}$  denotes a universal soft factor. In Ref. [55] it was shown that  $\mathcal{S}$  can be obtained by taking the leading soft behavior in the splitting amplitude  $\text{Split}_{-h}(1, \dots, n)$ , *i.e.*

$$\text{Split}_{-h}(1, \dots, n) \sim \mathcal{S}(a; 1, \dots, k; k+1, \dots, n) \text{Split}_{-h}(k+1, \dots, n). \quad (5.10)$$

We now determine the MHV pole structure by applying the gluon insertion rule 5.3 to the splitting amplitude  $\text{Split}_{-h}(k+1, \dots, n)$ . From Rule 5.1 we know

---

<sup>†</sup>The color-disconnected case is trivial.

that in the limit where  $k+1, \dots, n$  are collinear, only those MHV diagrams of  $A_{n-k+3}(a, k+1, \dots, n, b, c)$  contribute where  $a, b, c$  are attached to the same MHV vertex. We apply Rule 5.3 to attach additional soft gluons to this set of diagrams. It is easy to see that, in consistency with Eq. (2.8),

- as soft negative-helicity gluons can only be emitted from the external lines, we add a new divergent propagator to the diagram each time we add a soft negative-helicity gluon.
- for the emission of soft positive-helicity gluons, the number of MHV propagators is left unchanged.

Hence, if  $n_s$  denotes the number of soft negative-helicity gluons in the set  $\{1, \dots, k\}$ , we add  $n_s$  new divergent propagators to the diagrams, and so

- if  $h = +1$ ,

$$\begin{aligned} \mathcal{S}(a; 1, \dots, k; k+1, \dots, n) \text{Split}_-(k+1, \dots, n) \\ \sim \frac{1}{[\ ]^{n_s}} \frac{1}{[\ ]^{n_-}} \sim \frac{1}{[\ ]^{n_s+n_-}}, \end{aligned} \quad (5.11)$$

- if  $h = -1$ ,

$$\begin{aligned} \mathcal{S}(a; 1, \dots, k; k+1, \dots, n) \text{Split}_+(k+1, \dots, n) \\ \sim \frac{1}{[\ ]^{n_s}} \frac{1}{[\ ]^{n_- - 1}} \sim \frac{1}{[\ ]^{(n_s+n_-) - 1}}, \end{aligned} \quad (5.12)$$

where  $n_-$  is the number of negative-helicity gluons in the collinear set  $\{k+1, \dots, n\}$ .

We can now turn to the case of antenna functions. By definition, an antenna function contains all possible infrared singularities, both soft and collinear. We analyze the MHV pole structures of the antenna functions, using the fact that they reproduce the known MHV pole structures in the various soft and collinear limits.

Let us start with  $\text{Ant}(\hat{a}^-, \hat{b}^- \leftarrow a, 1, \dots, n, b)$ , and let us consider the MHV pole structures of the different soft and collinear singularities contained in this

antenna function. Let  $n_-$  denote the number of negative helicities in the set  $\{1, \dots, n\}$  and  $N_-$  the number of negative helicities in the set  $\{a, 1, \dots, n, b\}$ . Then we have the following possibilities:

- $p_1, \dots, p_n \parallel p_a$

In this limit we have  $p_{\hat{a}} \rightarrow P \equiv p_a + p_1 + \dots + p_n$  and  $p_{\hat{b}} \rightarrow p_b$ , and

$$\begin{aligned} & \text{Ant}(\hat{a}^-, \hat{b}^- \leftarrow a, 1, \dots, n, b) \\ & \rightarrow \text{Split}_-(a, 1, \dots, n) \sim \frac{1}{[\ ]^{n_a}} \sim \frac{1}{[\ ]^{N_-}}, \end{aligned} \quad (5.13)$$

where  $n_a$  is the number of negative helicities in the set  $\{a, 1, \dots, n\}$ , and  $n_a = N_-$ . Note that if  $p_{\hat{b}} \rightarrow p_b$ , then  $h_b = -h_{\hat{b}} = +1$ .

- $p_1, \dots, p_n \parallel p_b$

In this limit we have  $p_{\hat{a}} \rightarrow p_a$  and  $p_{\hat{b}} \rightarrow P \equiv p_1 + \dots + p_n + p_b$ , and

$$\begin{aligned} & \text{Ant}(\hat{a}^-, \hat{b}^- \leftarrow a, 1, \dots, n, b) \\ & \rightarrow \text{Split}_-(1, \dots, n, b) \sim \frac{1}{[\ ]^{n_b}} \sim \frac{1}{[\ ]^{N_-}}, \end{aligned} \quad (5.14)$$

where  $n_b$  is the number of negative helicities in the set  $\{1, \dots, n, b\}$ , and  $n_b = N_-$ . Since  $p_{\hat{a}} \rightarrow p_a$ , then  $h_a = -h_{\hat{a}} = +1$ .

- $p_1, \dots, p_n \rightarrow 0$

In this limit we have  $p_{\hat{a}} \rightarrow p_a$  and  $p_{\hat{b}} \rightarrow p_b$ , and

$$\begin{aligned} & \text{Ant}(\hat{a}^-, \hat{b}^- \leftarrow a, 1, \dots, n, b) \\ & \rightarrow \text{Soft}(a, 1, \dots, n, b) \sim \frac{1}{[\ ]^{n_-}} \sim \frac{1}{[\ ]^{N_-}}, \end{aligned} \quad (5.15)$$

and  $n_- = N_-$  because if  $p_{\hat{a}} \rightarrow p_a$ , then  $h_a = -h_{\hat{a}} = +1$  and if  $p_{\hat{b}} \rightarrow p_b$ , then  $h_b = -h_{\hat{b}} = +1$ .

- $p_1, \dots, p_{i-1} \parallel p_a$  and  $p_i, \dots, p_j \rightarrow 0$  and  $p_{j+1}, \dots, p_n \parallel p_b$ .

In this limit we have  $p_{\hat{a}} \rightarrow p_a + p_1 + \dots + p_{i-1}$  and  $p_{\hat{b}} \rightarrow p_{j+1} + \dots + p_n + p_b$ , and

$$\begin{aligned} & \text{Ant}(\hat{a}^-, \hat{b}^- \leftarrow a, 1, \dots, n, b) \\ & \rightarrow \text{Split}_-(a, 1, \dots, i-1) \text{Split}_-(j+1, \dots, n, b) \\ & \times \mathcal{S}(a, 1, \dots, i-1; i, \dots, j; j+1, \dots, n, b) \\ & \sim \frac{1}{[\ ]^{n_a}} \frac{1}{[\ ]^{n_s}} \frac{1}{[\ ]^{n_b}} \sim \frac{1}{[\ ]^{N_-}}, \end{aligned} \quad (5.16)$$

where  $n_a$ ,  $n_s$  and  $n_b$  are the numbers of negative-helicity gluons in the sets  $\{a, 1, \dots, i-1\}$ ,  $\{i, \dots, j\}$  and  $\{j+1, \dots, n, b\}$  respectively, and  $n_a + n_s + n_b = N_-$ .

We are therefore able to conclude that

$$\text{Ant}(\hat{a}^-, \hat{b}^- \leftarrow a, 1, \dots, n, b) \sim \frac{1}{[\ ]^{N_-}} f(\langle \ \rangle). \quad (5.17)$$

Similar arguments for the other helicity assignments lead to

$$\begin{aligned} \text{Ant}(\hat{a}^-, \hat{b}^+ \leftarrow a, 1, \dots, n, b) &\sim \frac{1}{[\ ]^{N_- - 1}} f(\langle \ \rangle), \\ \text{Ant}(\hat{a}^+, \hat{b}^- \leftarrow a, 1, \dots, n, b) &\sim \frac{1}{[\ ]^{N_- - 1}} f(\langle \ \rangle), \\ \text{Ant}(\hat{a}^+, \hat{b}^+ \leftarrow a, 1, \dots, n, b) &\sim \frac{1}{[\ ]^{N_- - 2}} f(\langle \ \rangle). \end{aligned} \quad (5.18)$$

Eqs. (5.17 - 5.18) are the analogues for antenna functions of Eq. (5.2) for splitting amplitudes. We now show that, as it was already the case for splitting amplitudes, the MHV pole structure allows us to identify *a priori* the set of MHV diagrams that contributes to the singular limit.

Let us start with  $\text{Ant}(\hat{a}^-, \hat{b}^- \leftarrow a, 1, \dots, n, b)$ , and consider an  $(n+4)$ -point amplitude  $A_{n+4}(a, 1, \dots, n, b, c^-, d^-)$ . In the limit where the particles  $1, \dots, n$  become singular, the amplitude exhibits the factorization (4.43),

$$A_{n+4}(a, 1, \dots, n, b, c^-, d^-) \sim \text{Ant}(\hat{a}^-, \hat{b}^- \leftarrow a, 1, \dots, n, b) A_4(\hat{a}^+, \hat{b}^+, c^-, d^-). \quad (5.19)$$

If  $N_-$  denotes the number of negative-helicity gluons in the set  $\{a, 1, \dots, n, b\}$ , then the number of MHV propagators in the  $(n+4)$ -point amplitude is  $p = (N_- + 2) - 2 = N_-$ . From Eq. (5.17) we know that the MHV pole structure of this antenna function is

$$\text{Ant}(\hat{a}^-, \hat{b}^- \leftarrow a, 1, \dots, n, b) \sim \frac{1}{[\ ]^{N_-}} f(\langle \ \rangle), \quad (5.20)$$

and thus the MHV diagrams contributing to the antenna function are exactly those where all scalar propagators go on-shell. Similar conclusions can be drawn for the other helicity configurations. This brings us to the first important conclusion that Rule 5.1 can be generalized to antenna functions:

**Rule 5.4.** *The MHV diagrams that contribute to the singular limit of the  $(n + 4)$ -point amplitude  $A_{n+4}(a, 1, \dots, n, b, c^-, d^-)$  are exactly those where all scalar propagators go on-shell.*

## 5.2 Diagrammatic evaluation of antenna functions

In the previous section we showed that in the MHV formalism the MHV diagrams which contribute to the singular limit are exactly those where all scalar propagators go on-shell. This result is an extension of the corresponding Rule 5.1 for splitting amplitudes. For the antenna functions, however, it is possible to go one step further. We note that keeping only those MHV diagrams where all propagators go on-shell is equivalent to requiring that  $c$  and  $d$  must be attached to the same  $m$ -point MHV vertex with  $m \geq 4$ . We therefore formulate the following rule, which provides at the same time a possible new definition for antenna functions by means of MHV diagrams,

**Rule 5.5** (MHV rules for antenna functions).

*The antenna function  $Ant(\hat{a}^{h_a}, \hat{b}^{h_b} \leftarrow a, 1, \dots, n, b)$  can be calculated by evaluating all MHV diagrams contributing to  $A_{n+4}(a, 1, \dots, n, b, \hat{a}^{h_a}, \hat{b}^{h_b})$  and where  $\hat{a}$  and  $\hat{b}$  are attached to the same  $m$ -point MHV vertex, with  $m \geq 4$ .*

This result, which is proven analytically in Appendix B.2, allows to directly build all antenna functions using the MHV formalism and the related MHV diagrams. It is possible to identify a priori the MHV diagrams that contribute to the singular limit, and it is thus not necessary to evaluate all the MHV diagrams that contribute to the full amplitude  $A_{n+4}(a, 1, \dots, n, b, c, d)$ . This class of MHV diagrams is uniquely defined by the requirement that all the MHV propagators must go on-shell in the singular limit, which turns out to be very similar to Rule 5.1 for splitting amplitudes. The advantage of our result is, however, that the functional form of the antenna functions is exactly given by the MHV diagram, whereas in Rule 5.1 one still has to go to the collinear limit. Antenna functions can hence be represented as a special class of MHV



diagrams, the class of diagrams being the one defined by Rule 5.5. Let us make a few comments about the antenna functions obtained from Rule 5.5:

1. The antenna functions may still contain non-divergent pieces, coming from MHV diagrams that are not divergent in any limit. For example, let us consider the antenna function  $\text{Ant}(\hat{a}^-, \hat{b}^+ \leftarrow a^-, 1^-, 2^+, b^+)$ . In Ref. [16] it was shown that this antenna function is zero. Using Rule 5.5 we generate a set of four non-zero MHV diagrams. It is easy to check however that all four diagrams are finite in all the singular limits we are interested in.
2. As the antenna functions are built from MHV diagrams, it is easy to see that the antenna functions obtained from Rule 5.5 will always fulfill the reflection identity

$$\text{Ant}(\hat{a}^{h_a}, \hat{b}^{h_b} \leftarrow a, 1, \dots, n, b) = (-1)^n \text{Ant}(\hat{b}^{h_b}, \hat{a}^{h_a} \leftarrow b, n, \dots, 1, a). \quad (5.21)$$

3. The antenna functions are in general dependent of an arbitrary spinor  $\eta$ . In practise, however,  $\eta$  cannot be chosen among the momenta appearing inside the antenna functions, because this would be inconsistent with the assumption that there are no infrared poles in the amplitude coming from antiholomorphic spinor products of the form  $[\cdot\eta]$ , *e.g.* if we chose  $\eta = a$ , then  $[1\eta] = [1a]$  could lead to a pole in the limit where these two particles become collinear, which is not included in the class of diagrams defined by Rule 5.5.
4. The proof in Appendix B.2 of our result crucially relies on the fact that  $\langle a\hat{a} \rangle$  goes to zero in the singular limit. We were able to show this explicitly for the reconstruction functions given in Eq. (A.1). However, if different reconstruction functions are chosen, it should be checked that this statement still holds true for the new analytic expressions.

In Chapter 2 a recursive formulation of the MHV formalism in terms of single and double-line currents was introduced. As Rule 5.5 allows us to identify  $a$

*priori* the MHV diagrams that contribute to a given singular limit, we can use this result to write down a recursive algorithm for antenna functions in terms of the single and double-line currents. As the antenna functions contain all kinds of collinear and soft singularities, it is straightforward to derive the corresponding recursions for splitting amplitudes and soft factors. This algorithm is discussed in Section 5.4.

## 5.2.1 General formulas for NMHV antenna functions

In this section we apply Rule 5.5 to derive generic formulas for all MHV and next-to-MHV (NMHV) type antenna functions. We give explicitly the results for antenna functions of the form  $\text{Ant}(\hat{a}^-, \hat{b}^- \leftarrow a, 1, \dots, n, b)$  and  $\text{Ant}(\hat{a}^-, \hat{b}^+ \leftarrow a, 1, \dots, n, b)$ . The remaining antenna functions are related to the previous ones by parity and reflection identity (5.21).

**MHV-type antenna functions** The simplest antenna functions are those obtained from a single MHV vertex. Applying Rule 5.5 we immediately find

$$\begin{aligned} & \text{Ant}(\hat{a}^-, \hat{b}^- \leftarrow a^+, 1^+, \dots, n^+, b^+) \\ &= A_{n+4}(a^+, 1^+, \dots, n^+, b^+, \hat{a}^-, \hat{b}^-) \\ &= \frac{\langle \hat{a} \hat{b} \rangle^3}{\langle a1 \rangle \langle 12 \rangle \dots \langle nb \rangle \langle b \hat{a} \rangle \langle \hat{b} a \rangle}, \end{aligned} \tag{5.22}$$

$$\begin{aligned} & \text{Ant}(\hat{a}^-, \hat{b}^+ \leftarrow a^+, 1^+, \dots, j^-, \dots, n^+, b^+) \\ &= A_{n+4}(a^+, 1^+, \dots, j^-, \dots, n^+, b^+, \hat{a}^-, \hat{b}^+) \\ &= \frac{\langle \hat{a} j \rangle^4}{\langle a1 \rangle \langle 12 \rangle \dots \langle nb \rangle \langle b \hat{a} \rangle \langle \hat{a} \hat{b} \rangle \langle \hat{b} a \rangle}. \end{aligned} \tag{5.23}$$

**NMHV-type antenna functions** The NMHV-type antenna functions are derived from MHV diagrams containing exactly one propagator. The MHV diagrams obtained from Rule 5.5 are shown in Fig. 5.2 and Fig. 5.3. The

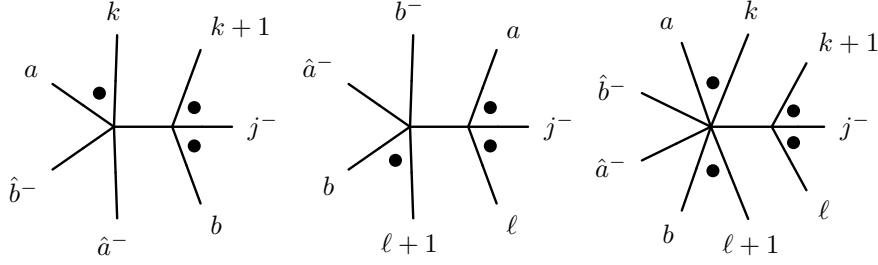


Figure 5.2: MHV diagrams contributing to NMHV-type antenna function  $\text{Ant}(\hat{a}^-, \hat{b}^- \leftarrow a^+, 1^+, \dots, j^-, \dots, n^+, b^+)$ .

generic formulas for NMHV-type antenna functions are

$$\begin{aligned}
& \text{Ant}(\hat{a}^-, \hat{b}^- \leftarrow a^+, 1^+, \dots, j^-, \dots, n^+, b^+) \\
&= \sum_{l=j}^n \frac{\langle \hat{a}\hat{b} \rangle^4 \langle jP_{a,l} \rangle^4}{s_{a,l} \langle P_{a,l}(l+1) \rangle \langle (l+1)\hat{b} \rangle \langle \hat{b}P_{a,l} \rangle \langle P_{a,l}a \rangle \langle (al) \rangle \langle lP_{a,l} \rangle} \\
&+ \sum_{k=a}^{j-1} \frac{\langle \hat{a}\hat{b} \rangle^4 \langle jP_{k+1,b} \rangle^4}{s_{k+1,b} \langle P_{k+1,b}\hat{a} \rangle \langle \hat{a}k \rangle \langle kP_{k+1,b} \rangle \langle P_{k+1,b}(k+1) \rangle \langle (k+1)b \rangle \langle bP_{k+1,b} \rangle} \\
&+ \sum_{k=a}^{j-1} \sum_{l=j}^n \frac{\langle \hat{a}\hat{b} \rangle^4 \langle jP_{k+1,l} \rangle^4}{s_{k+1,l} \langle P_{k+1,l}(l+1) \rangle \langle (l+1)k \rangle \langle kP_{k+1,l} \rangle \langle P_{k+1,l}(k+1) \rangle} \\
&\quad \times \frac{1}{\langle (k+1)l \rangle \langle lP_{k+1,l} \rangle},
\end{aligned} \tag{5.24}$$

$$\begin{aligned}
& \text{Ant}(\hat{a}^-, \hat{b}^+ \leftarrow a^+, 1^+, \dots, i^-, \dots, j^-, \dots, n^+, b^+) \\
&= \sum_{k=a}^{i-1} \frac{\langle \hat{a}P_{k+1,b} \rangle^4 \langle ij \rangle^4}{s_{k+1,b} \langle P_{k+1,b}\hat{a} \rangle \langle \hat{a}k \rangle \langle kP_{k+1,b} \rangle \langle P_{k+1,b}(k+1) \rangle \langle (k+1)b \rangle \langle bP_{k+1,b} \rangle} \\
&+ \sum_{l=j}^n \frac{\langle \hat{a}P_{a,l} \rangle^4 \langle ij \rangle^4}{s_{a,l} \langle P_{a,l}(l+1) \rangle \langle (l+1)\hat{b} \rangle \langle \hat{b}P_{a,l} \rangle \langle P_{a,l}a \rangle \langle (al) \rangle \langle lP_{a,l} \rangle} \\
&+ \sum_{k=a}^{i-1} \sum_{l=j}^n \frac{\langle \hat{a}P_{k+1,l} \rangle^4 \langle ij \rangle^4}{s_{k+1,l} \langle P_{k+1,l}(l+1) \rangle \langle (l+1)k \rangle \langle kP_{k+1,l} \rangle \langle P_{k+1,l}(k+1) \rangle} \\
&\quad \times \frac{1}{\langle (k+1)l \rangle \langle lP_{k+1,l} \rangle}
\end{aligned} \tag{5.25}$$

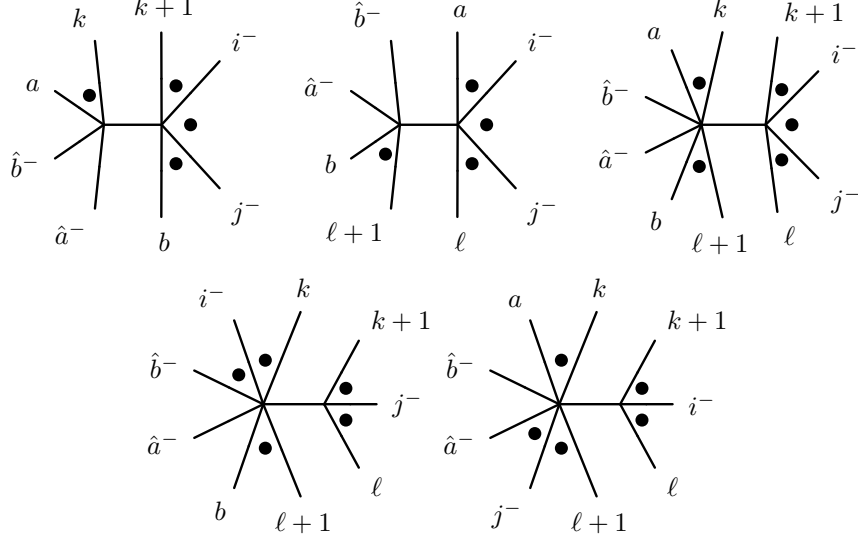


Figure 5.3: MHV diagrams contributing to the NMHV-type antenna function  $\text{Ant}(\hat{a}^-, \hat{b}^+ \leftarrow a^+, 1^+, \dots, i^-, \dots, j^-, \dots, n^+, b^+)$ .

$$\begin{aligned}
& + \sum_{k=i}^{j-1} \sum_{l=j}^b \frac{\langle \hat{a}i \rangle^4 \langle jP_{k+1,l} \rangle^4}{s_{k+1,l} \langle P_{k+1,l}(l+1) \rangle \langle (l+1)k \rangle \langle kP_{k+1,l} \rangle \langle P_{k+1,l}(k+1) \rangle} \\
& \quad \times \frac{1}{\langle (k+1)l \rangle \langle lP_{k+1,l} \rangle} \\
& + \sum_{k=\hat{a}}^{i-1} \sum_{l=i}^{j-1} \frac{\langle \hat{a}j \rangle^4 \langle iP_{k+1,l} \rangle^4}{s_{k+1,l} \langle P_{k+1,l}(l+1) \rangle \langle (l+1)k \rangle \langle kP_{k+1,l} \rangle \langle P_{k+1,l}(k+1) \rangle} \\
& \quad \times \frac{1}{\langle (k+1)l \rangle \langle lP_{k+1,l} \rangle},
\end{aligned}$$

where we introduced the notations

$$s_{i,j} = (p_i + p_{i+1} + \dots + p_j)^2 \quad \text{and} \quad \langle \langle ij \rangle \rangle = \prod_{k=i}^{j-1} \langle k(k+1) \rangle. \quad (5.26)$$

Note that the above generic formulas for NMHV-type antenna functions (together with the results for the MHV-type antenna functions) are sufficient to derive the full set of NNLO and N<sup>3</sup>LO gluon antenna functions [17]. We checked explicitly that these antenna functions reproduce the correct infrared limits and that the limits are numerically independent of  $\eta$  using the *Mathematica* pack-

age  $\mathcal{S}\mathcal{O}\mathcal{M}$  [68]. Note that our antenna functions have a slightly simpler and more compact analytic form than those presented in Ref. [16]. This fact might simplify the phase space integration of the counterterms when antenna functions are used in a subtraction method.

### 5.3 From antenna functions to splitting amplitudes

In this section we show how the antenna functions obtained from Rule 5.5 can be used to derive Rule 5.1 for splitting amplitudes presented in the previous section. Let us start with  $\text{Split}_-(a, 1, \dots, n)$ . We know that for the antenna function  $\text{Ant}(\hat{a}^-, \hat{b}^- \leftarrow a, 1, \dots, n, b)$ , we have in the limit where  $1, \dots, n$  become collinear to  $a$ ,

$$\text{Ant}(\hat{a}^-, \hat{b}^- \leftarrow a, 1, \dots, n, b) \longrightarrow \text{Split}_-(a, 1, \dots, n). \quad (5.27)$$

Furthermore, we know that the MHV pole structure of the antenna function built from Rule 5.5 is

$$\text{Ant}(\hat{a}^-, \hat{b}^- \leftarrow a, 1, \dots, n, b) \sim \frac{1}{[\ ]_{N_-}} f(\langle \ \rangle). \quad (5.28)$$

In the limit under consideration, we have  $N_- = n_a$  because in this limit  $p_b \rightarrow k_b$ , and so  $h_b = +1$ . Thus only those MHV diagrams in  $\text{Ant}(\hat{a}^-, \hat{b}^- \leftarrow a, 1, \dots, n, b)$  contribute where all  $N_- = n_a$  MHV propagators go on-shell in the collinear limit. These diagrams correspond exactly to those where  $b$  is attached to the same MHV vertex as  $\hat{a}$  and  $\hat{b}$ , which is equivalent to Rule 5.1. The derivation of the corresponding result for  $\text{Split}_+$  is similar to the  $\text{Split}_-$  case, so we do not report its derivation.

Note that unlike antenna functions, the splitting amplitudes are uniquely defined. The arbitrariness in the definition of the antenna function is lost when a specific collinear limit is taken, because the class of MHV diagrams contributing to the antenna function can be divided into two different subclasses:

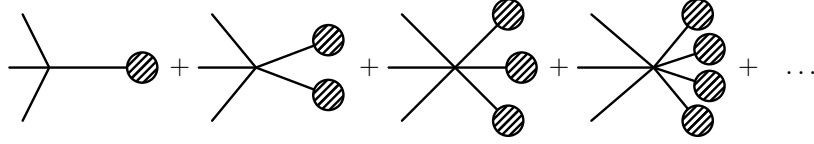


Figure 5.4: Diagrammatic expansion of the splitting amplitude. The blobs indicate MHV diagrams with a smaller number of legs.

1. The MHV diagrams where  $b$  is attached to the same MHV vertex as  $\hat{a}$  and  $\hat{b}$ : These diagrams are divergent in the collinear limit.<sup>‡</sup>
2. The MHV diagrams where  $b$  is not attached to the same MHV vertex as  $\hat{a}$  and  $\hat{b}$ : These diagrams are not divergent enough and are omitted. They contribute to the arbitrary piece from the antenna function.

### 5.3.1 Diagrammatic approach to splitting amplitudes

In the previous section we showed that in the limit where  $1, \dots, n$  become collinear to  $a$  only those MHV diagrams of the antenna contribute where  $\hat{a}$ ,  $\hat{b}$  and  $b$  are attached to the same MHV vertex. In this section we show how this result can be interpreted in terms of MHV diagrams, where the vertices are modified.

The set of diagrams defined by this condition can be easily expanded in terms of the structure of the collinear poles appearing in the diagram ( *i.e.* ,  $1/s_{a,n}$ ,  $1/s_{a,k}s_{k+1,n}$ , *etc.*). This expansion is shown in Fig. 5.4. We find

$$\text{Split}_{-h}(a, 1, \dots, n)A_4(P^h, b, c, d) \sim \sum_{\text{partitions}} \sum_j V_{\pi,j} \prod_{\pi_i} \frac{1}{s_{\pi_i}} D_{j,(\pi_i)}^{\text{MHV}}, \quad (5.29)$$

where the first sum goes over all partitions (including the set  $\{a, 1, \dots, n\}$  itself)  $\pi = (\pi_i)$  of the set  $\{a, 1, \dots, n\}$ , and the second sum runs over all diagrams corresponding to this partition.  $V_{\pi,j}$  is the MHV vertex which  $\hat{a}$ ,  $\hat{b}$  and  $b$  are attached to and  $s_{\pi_i}$  denotes the invariant formed out of the momenta which are in the subset  $\pi_i$ . Note that in this way we reproduce the pole structure of the splitting amplitude: For the partition into one subset,  $\pi = \{a, 1, \dots, n\}$ ,

<sup>‡</sup>Note that these diagrams may still contain subleading pieces.

the pole is  $1/s_{a,n}$ , for the partition into two subsets,  $\pi = \{(a, 1, \dots, k), (k + 1, \dots, n)\}$ , the pole is  $1/s_{a,k}s_{k+1,n}$ , and so on.

The diagrams  $D_{j,(\pi_i)}^{\text{MHV}}$  are MHV diagrams. They however still contain pieces that are subleading in the collinear limit. We show how it is possible to modify the definition of the MHV vertices such that the diagrams in Eq. (5.29) only contain the leading collinear pole. Let us consider a specific diagram  $D_{j,(\pi_i)}^{\text{MHV}}$ . All the vertices in  $D_{j,(\pi_i)}^{\text{MHV}}$  only depend on

- particles from the collinear set  $a, 1, 2, \dots, n$ .
- off-shell legs of the form  $P_{k,\ell}$ , where  $k$  and  $\ell$  are in the collinear set.

Let us first consider the case of a vertex which only depends on off-shell continued legs. We will give as an example the four-point vertex. The generalization is straightforward. An example of a four-point MHV-vertex with all legs continued off-shell is

$$A_4(I^-, J^-, K^+, L^+) = \frac{\langle IJ \rangle^4}{\langle IJ \rangle \langle JK \rangle \langle KL \rangle \langle LI \rangle}, \quad (5.30)$$

where we used the multiindex notation introduced in Chapter 2, *i.e.*, the amplitude  $A_4(I^-, J^-, K^+, L^+)$  has to be understood as  $A_4(P_I^-, P_J^-, P_K^+, P_L^+)$ . Applying Eq. (5.6), this vertex gives the following contribution in the collinear limit

$$A_4(I^-, J^-, K^+, L^+) \rightarrow \frac{\Delta(I, J)^4}{\Delta(I, J)\Delta(J, K)\Delta(K, L)\Delta(L, I)}, \quad (5.31)$$

The  $\Delta$ -function has been defined in Eq. (5.5), and we again use the multiindex notation,

$$\Delta(I, J) \equiv \Delta(i_1, i_2; j_1, j_2). \quad (5.32)$$

We would now like to define the object on the right-hand side of Eq. (5.31) as an effective MHV vertex in the collinear limit, which splitting amplitudes could be built up from. The idea rests on the following observations:

1. An on-shell particle with momentum  $p_i$  can be seen as labelled by the multiindex  $\bar{i} = (i, i)$ , defined in Eq. (2.20).

2. The  $\Delta$ -functions are not independent, but it is easy to see that

$$\begin{aligned}\Delta(\bar{i}, k) &= \sqrt{z_i} \langle ki \rangle, \\ \Delta(\bar{i}, J) &= \sqrt{z_i} \Delta(J, i) = -\Delta(J, \bar{i}), \\ \Delta(\bar{i}, \bar{j}) &= \sqrt{z_i} \Delta(\bar{j}, i) = \sqrt{z_i z_j} \langle ij \rangle.\end{aligned}\tag{5.33}$$

Thus we would like to extend the definition Eq. (5.31) to the case where on-shell particles are present in the vertex. For example, if the first particle (with negative helicity) in  $A_4$  is on-shell,  $I = \bar{i} = (i, i)$  and applying Eq. (5.33) we find,

$$\begin{aligned}A_4(i^-, J^-, K^+, L^+) &= A_4(\bar{i}^-, J^-, K^+, L^+) \\ &\rightarrow \frac{\Delta(\bar{i}, J)^4}{\Delta(\bar{i}, J)\Delta(J, K)\Delta(K, L)\Delta(L, \bar{i})} \\ &\rightarrow z_i \frac{-\Delta(J, i)^4}{\Delta(J, i)\Delta(J, K)\Delta(K, L)\Delta(L, i)}.\end{aligned}\tag{5.34}$$

On the other hand, a direct application of the collinear rules (5.4) leads to

$$A_4(i^-, J^-, K^+, L^+) \rightarrow \frac{-\Delta(J, i)^4}{\Delta(J, i)\Delta(J, K)\Delta(K, L)\Delta(L, i)}.\tag{5.35}$$

The difference between Eqs. (5.34) and (5.35) amounts to a factor  $z_i$ . This can be reabsorbed into the one-point current attached to the vertex, by defining the “wave function”

$$J_-(i) = \frac{1}{z_i},\tag{5.36}$$

which cancels the factor  $z_i$  in Eq. (5.34). It is easy to see that for an on-shell particle with positive helicity the wave function must then be defined as

$$J_+(i) = z_i.\tag{5.37}$$

and finally that Eq. (5.36) and (5.37) can be summarized as

$$J_h(i) = z_i^h.\tag{5.38}$$

The diagram  $D_{j,(\pi_i)}^{\text{MHV}}$  has however an additional external leg, corresponding to the incoming momentum  $P_{\pi_i}$ . We define the wave function of this external leg as

$$J_h(P_{\pi_i}) = 1.\tag{5.39}$$



We now turn to the vertex  $V_{\pi,j}$  in Eq. (5.29). Two cases are to be identified, corresponding to the value of  $h$  in Eq. (5.29).

1. If  $h = +1$ , then

$$V_{\pi,j} = \frac{\langle \hat{a}\hat{b} \rangle^3}{\langle \hat{b}P_{\pi_1} \rangle \langle \langle P_{\pi_1} P_{\pi_k} \rangle \rangle \langle P_{\pi_k} b \rangle \langle b\hat{a} \rangle}, \quad (5.40)$$

where  $k$  denotes the length of the partition. Using the properties of the reconstruction functions and the definition of the  $\Delta$ -function, we find

$$V_{\pi,j} \rightarrow \frac{1}{z_{\pi_1} z_{\pi_k}} \prod_{\ell=1}^{k-1} \frac{1}{\Delta(P_{\pi_\ell}, P_{\pi_{\ell+1}})}, \quad (5.41)$$

where we defined

$$z_{\pi_j} \equiv \sum_{\ell \in \pi_j} z_\ell. \quad (5.42)$$

2. If  $h = -1$ , then

$$V_{\pi,j} = \frac{\langle M\hat{b} \rangle^4}{\langle \hat{b}P_{\pi_1} \rangle \langle \langle P_{\pi_1} P_{\pi_k} \rangle \rangle \langle P_{\pi_k} b \rangle \langle b\hat{a} \rangle}, \quad (5.43)$$

where now  $M$  denotes the propagator with negative helicity attached to  $V_{\pi,j}$ . This yields

$$V_{\pi,j} \rightarrow \frac{z_M^4}{z_{\pi_1} z_{\pi_k}} \prod_{\ell=1}^{k-1} \frac{1}{\Delta(P_{\pi_\ell}, P_{\pi_{\ell+1}})}, \quad (5.44)$$

Putting everything together, we can write down the following diagrammatic formula for splitting amplitudes:

$$\text{Split}_{-h}(a, 1, \dots, n) = \sum_{\text{partitions}} \sum_j \mathcal{V}_{\pi,j}^{(h)} \prod_{\pi_i} \frac{1}{s_{\pi_i}} D_j^{(\pi_i)}, \quad (5.45)$$

where

$$\mathcal{V}_{\pi,j}^{(h)} = \frac{z_M^{2(1-h)}}{z_{\pi_1} z_{\pi_k}} \prod_{\ell=1}^{k-1} \frac{1}{\Delta(P_{\pi_\ell}, P_{\pi_{\ell+1}})}. \quad (5.46)$$

Let us illustrate this formula on the example of the MHV-type splitting amplitudes of Eqs. (4.18 - 4.19). For MHV-type quantities there is only one MHV diagram, so the sum over partitions is trivial. Using Eq. (5.33) we obtain,

- for  $h = +1$ ,

$$\begin{aligned}
& \text{Split}_-(1^+, \dots, n^+) \\
&= \frac{1}{z_1 z_n} \left( \prod_{\ell=1}^{n-1} \frac{1}{\sqrt{z_\ell z_{\ell+1}} \langle \ell(\ell+1) \rangle} \right) \left( \prod_{\ell=1}^n z_\ell \right) \\
&= \frac{1}{\sqrt{z_1 z_n} \langle 12 \rangle \dots \langle (n-1)n \rangle},
\end{aligned} \tag{5.47}$$

- for  $h = -1$ ,

$$\begin{aligned}
& \text{Split}_+(1^+, \dots, i^-, \dots, n^+) \\
&= \frac{z_i^4}{z_1 z_n} \left( \prod_{\ell=1}^{n-1} \frac{1}{\sqrt{z_\ell z_{\ell+1}} \langle \ell(\ell+1) \rangle} \right) \left( \prod_{\substack{\ell=1 \\ \ell \neq i}}^n z_\ell \right) \frac{1}{z_i} \\
&= \frac{z_i^2}{\sqrt{z_1 z_n} \langle 12 \rangle \dots \langle (n-1)n \rangle},
\end{aligned} \tag{5.48}$$

in agreement with the results given in Chapter 4.

## 5.4 Recursive relations

### 5.4.1 Recursive relations for antenna functions

In this section we apply the recursive formulation of the MHV formalism introduced in Section 2.4 to the calculation of antenna functions. From Rule 5.5, we build the antenna function  $\text{Ant}(\hat{a}^{h_a}, \hat{b}^{h_b} \leftarrow a, 1, \dots, n, b)$  by calculating all MHV diagrams that contribute to  $A_{n+4}(a, 1, \dots, n, b, \hat{a}^{h_a}, \hat{b}^{h_b})$  and where  $\hat{a}$  and  $\hat{b}$  are attached to the same  $n$ -point MHV vertex,  $n \geq 4$ . In the language of the recursive formulation of the MHV formalism this amplitude can be built recursively using Eq. (2.23 - 2.25), and by putting the off-shell leg on-shell.

The part of this single-line current where  $\hat{a}$  and  $\hat{b}$  are attached to the same  $n$ -point MHV vertex,  $n \geq 4$ , corresponds exactly to those diagrams where  $\hat{a}$  and  $\hat{b}$  are attached to the same double-line current (See Fig. 5.5). We can then

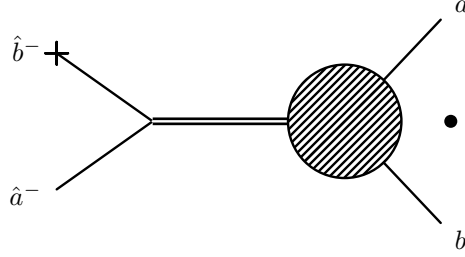


Figure 5.5: Contribution of  $J_+(a, 1, \dots, n, b, c^-)$  in the singular limit. The off-shell leg is denoted by a cross, and the double-line represents the MHV vertex to which  $\hat{a}$  and  $\hat{b}$  are attached.

write immediately

$$\text{Ant}(\hat{a}^{h_{\hat{a}}}, \hat{b}^{h_{\hat{b}}} \leftarrow a, 1, \dots, n, b) = \sum_{\substack{U < V \\ v_2 = b}} \sum_M V_4(U, V, \hat{a}, \hat{b}; M_1, M_2) \epsilon^{h_{\hat{a}} h_{\hat{b}}} J_{UV}^{(2+h_{\hat{a}}+h_{\hat{b}})/2}(a, 1, \dots, n, b) \quad (5.49)$$

where

$$\epsilon^{h_{\hat{a}} h_{\hat{b}}} = \begin{cases} \delta_{M_1}^{\hat{a}} \delta_{M_2}^{\hat{b}} & , \text{ if } h_{\hat{a}} = h_{\hat{b}} = -1, \\ \delta_{M_2}^{\hat{a}} & , \text{ if } h_{\hat{a}} = -h_{\hat{b}} = -1, \\ \delta_{M_2}^{\hat{b}} & , \text{ if } h_{\hat{a}} = -h_{\hat{b}} = +1, \\ 1 & , \text{ if } h_{\hat{a}} = h_{\hat{b}} = +1. \end{cases} \quad (5.50)$$

Note that we could have used the recursive relations in a different way to calculate the antenna function:

1. First build the full amplitude  $A_{n+4}(a, 1, \dots, n, b, c, d)$ .
2. Second extract the infrared divergent piece in the limit where  $1, \dots, n$  are unresolved, *i.e.*, the antenna function  $\text{Ant}(\hat{a}, \hat{b} \leftarrow a, 1, \dots, n, b)$ .

The calculation of the full amplitude  $A_{n+4}(a, 1, \dots, n, b, c, d)$  needs the evaluation of the  $(n+3)$ -point single-line current  $J(a, 1, \dots, n, b, c)$ , which contains

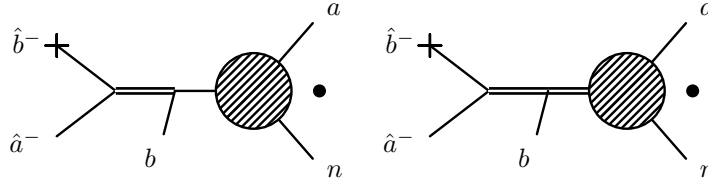


Figure 5.6: The contribution from  $\text{Ant}(\hat{a}^-, \hat{b}^- \leftarrow a, 1, \dots, n, b)$  in the limit  $k_1, \dots, k_n \parallel k_a$ . The off-shell leg is denoted by a cross, and the double-line represents the MHV vertex to which  $\hat{a}$  and  $\hat{b}$  are attached.

$(n+2)$ -point double-line currents as subcurrents. Eq. (5.49) proves that we only need to evaluate the  $(n+2)$ -point double-line current  $J_{UV}(a, 1, \dots, n, b)$ . This current contains all the information that is needed to build the antenna functions, *i.e.*, we do not need to solve the full recursion, but we stop after we have built the infrared divergent piece.

Having a recursive formula for antenna functions we can go on and derive recursive relations for splitting amplitudes, by taking the corresponding limits on Eq. (5.49). The rest of this section will be devoted to this task.

## 5.4.2 Recursive relations for splitting amplitudes

In this section we derive the recursive relations for splitting amplitudes by taking the collinear limit of the corresponding recursive relations for the antenna functions, Eq. (5.49). We already know that in the limit where  $a, 1, \dots, n$  are collinear, only those MHV diagrams contribute where  $\hat{a}$ ,  $\hat{b}$  and  $b$  are attached to the same MHV vertex. In terms of the single and double-line currents, this means that  $\hat{a}$ ,  $\hat{b}$  and  $b$  must be attached to the same double-line current (See Fig. 5.6). In addition we can recast the splitting amplitude as a sum over products of MHV diagrams, where the MHV vertices are replaced by  $\Delta$  functions and the external particles have “wave functions” corresponding to the momentum fraction  $z_i$ .

Combining these two observations with the recursive relations for the antenna functions introduced in the previous section, we are naturally led to a set of recursive relations for the splitting amplitudes themselves. We find

$$\begin{aligned} \text{Split}_{-h}(a, 1, \dots, n) \\ = J_h(a, 1, \dots, n) + \sum_{\substack{U < V, M \\ v_2 = n}} V_c^{-h}(U, V, M) J_{UV}^{(1-h)/2}(a, 1, \dots, n), \end{aligned} \quad (5.51)$$

with  $V_c^{-h}$  is similar to the quantity defined in Eq. (5.46),

$$V_c^{-h}(U, V, M) = \frac{z_M^{2(1-h)}}{z_U z_V \Delta(U, V)}. \quad (5.52)$$

Let us conclude this section with a few comments.

1. The recursive relations state that a splitting amplitude can be written as a sum of a single and a double-line current. These currents fulfill formally the same recursive relations as gluon amplitudes and antenna functions, the vertices however correspond to the MHV vertices in the collinear limit introduced in Eq. (5.31) and the one-point currents correspond to the “wave functions” introduced in Section 5.3.1,

$$J_h(i) = z_i^h. \quad (5.53)$$

2. Once again we could use the recursive relations, Eqs. (2.23 - 2.25), in a different way to calculate an  $n$ -point splitting amplitude:
  - (a) First calculate the full  $(n+3)$ -point amplitude  $A_{n+3}(1, \dots, n, a, b, c)$ .
  - (b) Then extract the splitting amplitude according to

$$A_{n+3}(1, \dots, n, a, b, c) \sim \text{Split}_{-h}(1, \dots, n) A_4(P^h, a, b, c). \quad (5.54)$$

The calculation of the full amplitude needs the calculation of an  $(n+2)$ -point single-line current  $J(1, \dots, n, a, b)$ , which contains the  $(n+1)$ -point double-line current as a subcurrent. On the other hand, Eq. (5.51) tells us that it is sufficient to evaluate  $n$ -point single and double-line currents to obtain an  $n$ -point splitting amplitude.

3. We checked the splitting amplitudes calculated using these recursive relations against the pure gluon splitting amplitudes obtained in Refs. [25, 19]. For all of them we found complete agreement.



# Chapter 6

## Analytic integration of some real-virtual counterterms

### 6.1 A general subtraction scheme at NNLO

In Chapter 4 we presented the basic ideas behind subtraction schemes at next-to-leading order. Recently a general subtraction scheme at NNLO has been presented [21, 22, 23, 24]. As we already gave a review of subtraction schemes at next-to-leading order in Section 4.3, we do not review the NNLO case in detail, but only highlight its features.

Using the notations of Chapter 4, we can write,

$$\frac{d\sigma^{\text{NNLO}}}{d\mathcal{O}} = \int d\sigma_n^{\text{VV}} \mathcal{O}_n + \int d\sigma_{n+1}^{\text{RV}} \mathcal{O}_{n+1} + \int d\sigma_{n+2}^{\text{RR}} \mathcal{O}_{n+2}, \quad (6.1)$$

where RR, RV and VV refer to the doubly real (two real emissions), the real-virtual (one-loop single emission) and the double virtual (two-loop) corrections. The three terms in this sum are separately divergent. We proceed in exactly the same way as in the NLO case and we add and subtract approximate cross-sections in order to get infrared-finite integrals. We work in dimensional regularization, and consider phase space integrals in  $D = 4 - 2\epsilon$  dimensions. After

having regularized all the integrals, we can write

$$\frac{d\sigma^{\text{NNLO}}}{d\mathcal{O}} = \int d\sigma_n^{\text{NNLO}} + \int d\sigma_{n+1}^{\text{NNLO}} + \int d\sigma_{n+2}^{\text{NNLO}}, \quad (6.2)$$

with

$$\begin{aligned} d\sigma_{n+2}^{\text{NNLO}} &= \left\{ d\sigma_{n+2}^{\text{RR}} \mathcal{O}_{n+2} \right. \\ &\quad \left. - d\sigma_{n+2}^{\text{RR,app2}} \mathcal{O}_n - \left[ d\sigma_{n+2}^{\text{RR,app1}} \mathcal{O}_{n+1} - d\sigma_{n+2}^{\text{RR,app12}} \mathcal{O}_n \right] \right\}_{\epsilon=0}, \\ d\sigma_{n+1}^{\text{NNLO}} &= \left\{ \left[ d\sigma_{n+1}^{\text{RV}} + \int d\sigma_{n+2}^{\text{RR,app1}} \right] \mathcal{O}_n \right. \\ &\quad \left. - \left[ d\sigma_{n+1}^{\text{RV,app1}} + \left( \int d\sigma_{n+2}^{\text{RR,app1}} \right)^{\text{app1}} \right] \mathcal{O}_n \right\}_{\epsilon=0}, \\ d\sigma_n^{\text{NNLO}} &= \left\{ d\sigma_n^{\text{VV}} + \int \left[ d\sigma_{n+2}^{\text{RR,app2}} - d\sigma_{n+2}^{\text{RR,app12}} \right] \right. \\ &\quad \left. + \int \left[ d\sigma_{n+1}^{\text{RV,app1}} + \left( \int d\sigma_{n+2}^{\text{RR,app1}} \right)^{\text{app1}} \right] \right\}_{\epsilon=0} \mathcal{O}_n. \end{aligned} \quad (6.3)$$

The exact form of the approximate cross-sections in terms of splitting functions and eikonal factors can be found in Ref. [21, 22]. Let us just mention here that the counterterm for the doubly real emission is constructed in a similar way as in the NLO case, *i.e.*, from the universal eikonal factors and splitting functions. In the NNLO case however, there are several new possibilities to emit two unresolved partons in the final state,

- the splitting of one parton into three partons,
- the splitting of two different partons into two partons,
- the emission of two soft partons,
- the emission of a soft parton together with a collinear splitting.

Furthermore, unlike in the NLO case where only a single unresolved gluon could be emitted, at NNLO we need to take into account the emission of unresolved  $q\bar{q}$  pairs. Also note the appearance of iterated counterterms in Eq. (6.2), *i.e.* approximate cross-sections for the approximate cross-section. These terms arise due to strongly ordered infrared limits beyond NLO, *e.g.* given when one unresolved particle is much softer than the other. In this limit, the counterterms themselves are singular, and hence we have to introduce counterterms for



the counterterms themselves. Finally, at NNLO we need to take into account the emission of soft and collinear gluons from the one-loop amplitude. The counterterms in this case are constructed from the one-loop splitting functions and soft factors discussed in Section 4.2.4.

Similar to the NLO case, the counterterms cannot be constructed directly from the universal splitting functions and soft factors, because the infrared factorization only holds in the strict soft and collinear limits. In Chapter 4 we argued that this problem can be overcome by performing a change of variables in the phase space. A main feature of the NNLO subtraction scheme of Ref. [21, 22, 23, 24] is its ‘democratic’ phase space mapping. The phase space mapping used at NLO in Ref. [20] involves only three of the original momenta  $\{p_i\}$ , corresponding to the emitter, the unresolved particle and the spectator color-connected to the emitted particle and needed to absorb the recoil. This setup requires two of the three particles - the emitter and the spectator - to be hard particles. Such a scenario is indeed always satisfied at NLO, but is no longer true for higher orders in perturbation theory. The phase space mapping of Ref. [21, 22, 23] therefore redistributes the recoil ‘democratically’ among the different colored particles in the hard process. Explicit formulas for such a phase space mapping can be found in Ref. [63].

After having defined a complete set of counterterms, we still need to compute the integrals of the approximate cross-section over the phase space of the unresolved particles. This question will be addressed in the rest of this chapter. In Section 6.2 we review the soft counterterm as a representative example of the real-virtual counterterms that appear in this scheme. In Section 6.3 we introduce our method to compute some classes of real-virtual integrals, which is a generalization of techniques used for multi-loop integrals in quantum field theory, and we illustrate this technique on the example of the integrated soft counterterm. For the more general integrals we refer to Appendix J and the literature [69].

## 6.2 The real-virtual integrals

In this section we briefly review the soft counterterm that appears in the subtraction scheme (6.2), and show that it reduces to a set of hypergeometric integrals after appropriate changes of variables have been performed. The case of the collinear counterterms is similar, up to technical complications, and we refer the reader to the literature [21, 22, 23, 24, 69].

Let us start with the phase space mapping (4.38) needed to have exact factorization of the phase space. In the case of the soft counterterm the mapping reads,

$$d\Phi_{n+1}(\{p\}_{n+1}; Q) \xrightarrow{\text{Soft}} d\Phi_n(\{\tilde{p}\}_n; Q) [dp_{1;n}], \quad (6.4)$$

and the phase space  $[dp_{1;n}]$  of the soft particle can be parametrized as [69],

$$[dp_{1;n}] = dy (1-y)^{(n-2)(1-\epsilon)-1} \frac{Q^2}{2\pi} d\Phi_2(p_r, K; Q) \theta(y) \theta(1-y), \quad (6.5)$$

where  $K$  denotes a massive timelike vector such that  $K^2 = (1-y)Q^2$ , and  $\theta$  denotes the Heaviside step function. Integrating the one-loop eikonal factor over the phase space of the unresolved particle then leads to,

$$\begin{aligned} C_A \frac{1}{\epsilon^2} \frac{\pi\epsilon}{\sin \pi\epsilon} \frac{(4\pi)^2}{S_\epsilon} (Q^2)^{(1+\kappa)\epsilon} \int [dp_{1;n}] \left( \frac{s_{ik}}{s_{ir} s_{rk}} \right)^{1+\kappa\epsilon} \\ = C_A \frac{1}{\epsilon^2} \frac{\pi\epsilon}{\sin \pi\epsilon} \frac{(4\pi)^2}{S_\epsilon} (Q^2)^{(1+\kappa)\epsilon} \frac{Q^2}{2\pi} \\ \times \int_0^1 dy (1-y)^{(n-2)(1-\epsilon)-1} \int d\Phi_2(p_r, K; Q) \left( \frac{s_{ik}}{s_{ir} s_{rk}} \right)^{1+\kappa\epsilon}. \end{aligned} \quad (6.6)$$

where  $S_\epsilon = (4\pi)^\epsilon / \Gamma(1-\epsilon)$ . Let us make some comments about this expression. Firstly, Eq. (6.6) explicitly depends on the number  $n$  of hard partons. We can get rid of this dependence by using a slightly modified version of the soft counterterm, obtained by multiplying the eikonal factor by a term that removes the dependence on  $n$  [23],

$$\left( \frac{s_{ik}}{s_{ir} s_{rk}} \right)^{1+\kappa\epsilon} \longrightarrow (1-y)^{d'_0 - (n-2)(1-\epsilon)} \left( \frac{s_{ik}}{s_{ir} s_{rk}} \right)^{1+\kappa\epsilon}, \quad (6.7)$$

with  $d'_0 = D'_0 + d'_1\epsilon$ ,  $a$  and  $b$  being integers. Note that this change in the definition of the soft counterterm is harmless, because for  $d'_{0|\epsilon=0} \geq 2$ , it does

not introduce any new divergencies in Eq. (6.6), *i.e.*, it only affects the finite part of the counterterm. Second, the integral over  $y$  in Eq. (6.6) extends over the whole range  $[0, 1]$ , *i.e.*, over the whole phase space of the soft particle. For numerical purposes, it is preferable to restrict the phase space of the unresolved particle by introducing a cut off  $y_0 \in ]0, 1]$  in the integration ( $y_0 = 1$  corresponds to subtracting over the full phase space). After these modifications, Eq. (6.6) takes the form,

$$C_A \frac{1}{\epsilon^2} \frac{\pi\epsilon}{\sin \pi\epsilon} \frac{(4\pi)^2}{S_\epsilon} (Q^2)^{(1+\kappa)\epsilon} \frac{Q^2}{2\pi} \times \int_0^{y_0} dy (1-y)^{d_0-1} \int d\Phi_2(p_r, K; Q) \left( \frac{s_{ik}}{s_{ir} s_{rk}} \right)^{1+\kappa\epsilon}. \quad (6.8)$$

To evaluate Eq. (6.8), we turn to a reference frame where

$$Q = \sqrt{s}(1, \dots), \quad \tilde{p}_i = \tilde{E}_i(1, \dots, 1), \quad \tilde{p}_k = \tilde{E}_k(1, \dots, \sin \chi, \cos \chi), \quad (6.9)$$

and

$$p_r = E_r(1, \text{“angles”}, \sin \vartheta \sin \varphi, \sin \vartheta \cos \varphi, \cos \vartheta), \quad (6.10)$$

where the dots indicate vanishing components, and “angles” denote  $(d-3)$  angular variables trivial to integrate. Introducing the quantity

$$\varepsilon_r = 2 \frac{p_r \cdot Q}{Q^2} = 2 \frac{E_r}{\sqrt{s}}, \quad (6.11)$$

the two-body phase space in Eq. (6.8) can be parametrized as,

$$d\Phi_2(p_r, K; Q) = \frac{(Q^2)^{-\epsilon}}{(4\pi)^2} S_\epsilon \frac{\Gamma(1-\epsilon)^2}{\Gamma(1-2\epsilon)} d\varepsilon_r \varepsilon_r^{1-2\epsilon} \delta(y - \varepsilon_r) \times d(\cos \vartheta) d(\cos \varphi) (\sin \vartheta)^{-2\epsilon} (\sin \varphi)^{-1-2\epsilon}. \quad (6.12)$$

In these variables the eikonal factor takes the form,

$$\frac{s_{ik}}{s_{ir} s_{rk}} = \frac{4Y_{i\bar{k},Q}}{Q^2} \frac{1 - \varepsilon_r}{\varepsilon_r^2} (1 - \cos \vartheta)^{-1} (1 - \cos \chi \cos \vartheta - \sin \chi \sin \vartheta \cos \varphi)^{-1}, \quad (6.13)$$

where we defined

$$\cos \chi = 1 - 2Y_{i\bar{k},Q} \equiv 1 - \frac{2Q^2 s_{i\bar{k}}}{s_{iQ} s_{\bar{k}Q}}. \quad (6.14)$$

Putting everything together, the integral of the soft counterterm reads [69],

$$\begin{aligned} \mathcal{J}(Y_{\bar{i}\bar{k},Q}; \epsilon, y_0, d'_0; \kappa) &= -(4Y_{\bar{i}\bar{k},Q})^{1+\kappa\epsilon} \frac{\Gamma^2(1-\epsilon)}{2\pi\Gamma(1-2\epsilon)} \Omega^{(1+\kappa\epsilon, 1+\kappa\epsilon)}(\cos\chi) \\ &\times \int_0^{y_0} dy y^{-1-2(1+\kappa)\epsilon} (1-y)^{d'_0+\kappa\epsilon}, \end{aligned} \quad (6.15)$$

where  $\Omega^{(i,k)}(\cos\chi)$  denotes the angular integral

$$\begin{aligned} \Omega^{(i,k)}(\cos\chi) &= \int_{-1}^1 d(\cos\vartheta) (\sin\vartheta)^{-2\epsilon} \int_{-1}^1 d(\cos\varphi) (\sin\varphi)^{-1-2\epsilon} \\ &\times (1-\cos\vartheta)^{-i} (1-\cos\chi\cos\vartheta - \sin\chi\sin\vartheta\cos\varphi)^{-k}. \end{aligned} \quad (6.16)$$

Our final goal is to perform the integration analytically, and to obtain the result of the integration as a Laurent series in  $\epsilon$ . The angular integral  $\Omega^{(i,k)}(\cos\chi)$  was evaluated in Ref. [70], so we can concentrate exclusively on the remaining integral over  $y$ . this integral can be identified as Gauss' hypergeometric function,

$$\int_0^1 dy y^a (1-y)^b (1-yz)^c = B(1+a, 1+b) {}_2F_1(-c, 1+a, 2+a+b; z), \quad (6.17)$$

where  $a, b, c$  and  $z$  are complex parameters and where we introduced the Euler  $B$  function,

$$B(x, y) = \frac{\Gamma(x)\Gamma(y)}{\Gamma(x+y)}. \quad (6.18)$$

Gauss' hypergeometric function  ${}_2F_1$  can be represented for  $|z| < 1$  by the power series,

$${}_2F_1(a, b, c; z) = \sum_{n=0}^{\infty} \frac{(a)_n (b)_n}{(c)_n} \frac{z^n}{n!}, \quad (6.19)$$

where the Pochhammer symbol  $(\cdot)_n$  is defined by

$$(a)_n = \frac{\Gamma(a+n)}{\Gamma(a)}. \quad (6.20)$$

In terms of Gauss' hypergeometric function, the complete soft integral (6.15) can be written as

$$\begin{aligned} \mathcal{J}(Y, \epsilon; y_0, d'_0; \kappa) &= -Y^{-(1+\kappa)\epsilon} y_0^{-2(1+\kappa)\epsilon} \frac{1}{(1+\kappa)^2 \epsilon^2} \frac{\Gamma^2(1-(1+\kappa)\epsilon)}{\Gamma(1-2(1+\kappa)\epsilon)} \\ &\times {}_2F_1(-d'_0 - \kappa\epsilon, -2(1+\kappa)\epsilon, 1-2(1+\kappa)\epsilon, y_0) \\ &\times {}_2F_1(-(1+\kappa)\epsilon, -(1+\kappa)\epsilon, 1-\epsilon, 1-Y), \end{aligned} \quad (6.21)$$

The original integral  $\mathcal{J}$  is now completely expressed in terms of Gauss' hypergeometric function, and it can therefore be expanded into a Laurent series in  $\epsilon$  using standard techniques [71, 72, 73, 74, 75, 76]. These techniques are however restricted to the special case of Gauss' hypergeometric function, and cannot be applied to more general hypergeometric integrals. Such generalized hypergeometric integrals however appear in the integrated collinear counterterms, and we therefore introduce in the next section a new method to tackle hypergeometric integrals, which is a generalization of techniques disguised for loop computations in QFT.

### 6.3 Hypergeometric integrals from integration-by-parts identities

In the previous sections we showed that after a suitable parametrization of the phase space, the soft counterterm can be expressed as a combination of a small set of basis integrals over a hypercube\*. This result is generic and applies to all the integrated counterterms. The integrands are rational functions in the integration variables as well as in some external parameters. Furthermore, some of the denominators have powers which depend on the dimensional regulator  $\epsilon$ .

In this section we introduce a general method to compute integrals of this particular type. Our approach is a generalization of techniques developed in the last twenty years to compute multi-loop Feynman diagrams [77, 78, 79, 80, 81, 82]. Similar techniques have already been used to compute the integrated antenna functions appearing the NNLO subtraction scheme of Ref. [65]. To be more precise, we introduce a method to compute integrals of the form<sup>†</sup>

$$F(\{n_i\}, \{r_i\}; \{z_i\}; \epsilon) = \int_0^1 dx_1 dx_2 \prod_j [\mathcal{R}_j(x_1, x_2; \{z_i\})]^{-n_j - r_j \epsilon}, \quad (6.22)$$

where  $n_i$  and  $r_i$  are integers, and  $z_i$  is a real parameter.  $\mathcal{R}_j$  denote rational functions in the variables  $x_i$  and  $z_i$ . Since we work in dimensional regularization,

\*In some cases the integration region is not explicitly a hypercube, but we can always rescale the integration domain such that all integrations are over the range  $[0, 1]$ .

<sup>†</sup>Note that the technique itself is *a priori* not limited to twofold integrals. In practice, however, we found that for more than two integrations the computations become so heavy that they were not feasible any more with present techniques.

our goal is to obtain a series expansion for the function  $F(\{n_i\}, \{r_i\}; \{z_i\}; \epsilon)$  in the dimensional regulator  $\epsilon$ . We can, however, not simply invert the expansion in  $\epsilon$  and the integration, because the rational functions  $\mathcal{R}_j$  might have poles in the integration region which make the integral divergent as  $\epsilon \rightarrow 0$ , *i.e.*, the poles in the integrand manifest themselves as poles in  $\epsilon$  in the Laurent expansion of  $F(\{n_i\}, \{r_i\}; \{z_i\}; \epsilon)$ .

In the following we illustrate our method on the simple example of a one-dimensional integral, namely the integral defining Gauss' hypergeometric function, Eq. (6.17). We show how our approach enables us to obtain a Laurent expansion in  $\epsilon$  for hypergeometric functions of the form  ${}_2F_1(a_1 + a_2\epsilon, b_1 + b_2\epsilon, c_1 + c_2\epsilon; z)$ ,  $a_i$ ,  $b_i$  and  $c_i$  being integers. Note that we obtain at the same time the Laurent expansion of the soft integral (6.21). Detailed results for the other real-virtual integrals including all the technical details are given in Appendix J and in Ref. [69].

From Eq. (6.17) it is easy to see that in order to obtain a Laurent expansion for  ${}_2F_1(a_1 + a_2\epsilon, b_1 + b_2\epsilon, c_1 + c_2\epsilon; z)$  we need to be able to compute a class of basic integrals of the form

$$f(x, \epsilon; n_1, n_2, n_3) = \int_0^1 d\mu(t; x, \epsilon) t^{-n_1} (1-t)^{-n_2} (1-xt)^{-n_3}, \quad (6.23)$$

where  $n_i$  are integers and the dependence on the dimensional regulator  $\epsilon$  was absorbed into the definition of the 'integration measure'

$$d\mu(t; x, \epsilon) = dt t^{-r_1\epsilon} (1-t)^{-r_2\epsilon} (1-xt)^{-r_3\epsilon}. \quad (6.24)$$

In the following we always assume that we work at fixed values for the integers  $r_i$ . Note that in the limit  $\epsilon \rightarrow 0$  the integration measure (6.24) reduces to the standard Lebesgue measure on  $[0, 1]$ .

**The case  $n_2 = 0$ .** Let us start by analyzing the particular case where  $n_2 = r_2 = 0$ . In this case the hypergeometric function reduces to an incomplete beta

function<sup>‡</sup>,

$$\begin{aligned}\beta(x, \epsilon; n_1, n_3) &= f(x, \epsilon; n_1, 0, n_3) = \int_0^1 d\mu(t; x, \epsilon) t^{-n_1} (1 - xt)^{-n_3} \\ &= x^{-1+n_1+r_1\epsilon} B_x(1 - n_1 - r_1\epsilon, 1 - n_3 - r_3\epsilon).\end{aligned}\quad (6.25)$$

The incomplete  $B$  function is defined by

$$B_\alpha(x, y) = \int_0^\alpha dt t^{x-1} (1-t)^{y-1}.\quad (6.26)$$

Our goal is to reduce the computation to the evaluation of a small set of so-called *master integrals* from which all integrals of the form (6.25) can be reconstructed. We first define the set of *independent integral* as the set of integrals for which the integrands are not related by simple algebraic relations. In the present case the independent integrals correspond exactly to the set of all integrals of the form  $\beta(x, \epsilon; n_1, n_3)$  where only one of the  $n_i$  is non zero and where  $n_3 \geq 0$ . In all other cases, the integrals are linear combinations of independent integrals, *e.g.* ,

- if  $n_1$  and  $n_3$  are simultaneously non zero, we can perform partial fractioning in the integration variable  $t$ , *e.g.* ,

$$\begin{aligned}\beta(x, \epsilon; 1, 1) &= \int_0^1 \frac{d\mu(t; x, \epsilon)}{t(1-xt)} = \int_0^1 d\mu(t; x, \epsilon) \left( \frac{1}{t} + x \frac{1}{(1-xt)} \right) \\ &= \beta(x, \epsilon; 1, 0) + x\beta(x, \epsilon; 0, 1).\end{aligned}\quad (6.27)$$

- if  $n_3 < 0$ , we can expand the integrand,

$$\begin{aligned}\beta(x, \epsilon; 0, -2) &= \int_0^1 d\mu(t; x, \epsilon) (1-xt)^2 \\ &= \beta(x, \epsilon; 0, 0) - 2x\beta(x, \epsilon; -1, 0) + x^2\beta(x, \epsilon; -2, 0).\end{aligned}\quad (6.28)$$

The set of independent integrals defined in this way is still not the most minimal one. We can derive further linear relations among the integrals using the *integration-by-parts identities (IBP's)*,

$$\begin{aligned}\int_0^1 dt \frac{\partial}{\partial t} \left( \int_0^1 d\mu(t; x, \epsilon) t^{-n_1} (1-xt)^{-n_3} \right) \\ = d\mu(t; x, \epsilon) t^{-n_1} (1-xt)^{-n_3} \Big|_{t=0}^{t=1}.\end{aligned}\quad (6.29)$$

---

<sup>‡</sup>This separation is necessary in order to avoid poles in the intermediate steps coming from  $r_2 = 0$ .

It is easy to see that in the right-hand side only the value in  $t = 1$  contributes, and carrying out the derivative under the integration sign in the left-hand side, we generate a recurrence relation for the incomplete beta function,

$$\begin{aligned} & -(n_1 + r_1\epsilon) \beta(x, \epsilon; n_1 + 1, n_3) \\ & - (n_3 + r_3\epsilon) \beta(x, \epsilon; n_1, n_3 + 1) = (1 - x)^{-n_3 - r_3\epsilon}. \end{aligned} \quad (6.30)$$

Eq. (6.30) is a recursion for the set of independent integrals  $\beta(x, \epsilon; n_1, n_3)$ . It provides an additional set of linear relations between the different integrals. We can try to solve the recursion in closed form, but in practice we only need the function  $\beta(x, \epsilon; n_1, n_3)$  for relatively small values of the integers  $n_i$ . We therefore rather generate a finite linear system from Eq. (6.30) and solve for the functions  $\beta(x, \epsilon; n_1, n_3)$  up to the desired values for  $n_1$  and  $n_3$ . In practice, it turns out that this linear system is overconstrained and that all the integrals can be expressed in terms of a single *master integral*

$$\beta^{(1)}(x, \epsilon) = \beta(x, \epsilon; 0, 0) = \int_0^1 d\mu(t; x, \epsilon). \quad (6.31)$$

All other independent integrals can be obtained recursively from the master integral by using the solutions of the IBP identities. Let us note that solving the recursion coming from the IBP identities by solving a finite-sized linear system is a variant of what is known in the context of loop computations as the *Laporta algorithm*.

At this stage we have reduced the problem of computing an integral of the form (6.25) to the computation of the corresponding master integral  $\beta^{(1)}(x, \epsilon)$ . The master integral itself can be computed as the solution of a linear differential equation. To see this, let us differentiate  $\beta^{(1)}(x, \epsilon)$  with respect to  $x$ . Carrying out the derivative on the integral representation of the master integral, we find

$$\frac{\partial}{\partial x} \beta^{(1)}(x, \epsilon) = r_3\epsilon \beta(x, \epsilon; -1, 1) = -\frac{r_3\epsilon}{x} \left( \beta^{(1)}(x, \epsilon) + \beta(x, \epsilon; 0, 1) \right), \quad (6.32)$$

where the last step follows from the reduction to independent integrals. We see that in the right-hand side of Eq. (6.32) we reproduce the master integral itself, as well as another function of the same type. We know from the recurrence relation (6.30) (or equivalently from the solution of the finite-sized linear system) how to express all the incomplete beta functions in terms of the master integral



$\beta^{(1)}$ , and so the differential equation for the master integral closes under itself.

$$\frac{\partial}{\partial x} \beta^{(1)} = \frac{r_1 \epsilon - 1}{x} \beta^{(1)} + \frac{(1-x)^{-r_3 \epsilon}}{x}, \quad (6.33)$$

The initial condition can easily be obtained by computing explicitly the master integral for  $x = 0$ ,

$$\beta^{(1)}(x = 0; \epsilon) = \int_0^1 dt t^{-r_1 \epsilon} = \frac{1}{1 - r_1 \epsilon} = \sum_{k=0}^{\infty} r_1^k \epsilon^k. \quad (6.34)$$

We have now all the ingredients to solve this differential equation. It is easy to see that the master integral is finite for  $\epsilon \rightarrow 0$ , and so we can expand it into a power series in  $\epsilon$ ,

$$\beta^{(1)}(x; \epsilon) = \sum_{n=0}^{\infty} \beta_n^{(1)}(x) \epsilon^n. \quad (6.35)$$

Inserting this expansion into the differential equation (6.33), we can solve order by order in  $\epsilon$  for the master integral. In particular, for the constant term we obtain,

$$\frac{\partial}{\partial x} \beta_0^{(1)} = -\frac{1}{x} \beta_0^{(1)} + \frac{1}{x}, \quad (6.36)$$

The general solution for  $\beta_0^{(1)}$  is easily obtained,

$$\beta_0^{(1)}(x) = \frac{C}{x} + 1, \quad (6.37)$$

where  $C$  denotes an integration constant. Matching the general solution to the initial condition at  $\epsilon = 0$ , we immediately find

$$\beta_0^{(1)}(x) = 1. \quad (6.38)$$

We can repeat this procedure order by order up to the desired order in the expansion of the master integral and obtain a Laurent series representation for the function  $\beta^{(1)}(x; \epsilon)$ .

**The case  $n_2 \neq 0$ .** Let us now turn to the generic case,  $n_2 \neq 0$ . Since the technique is exactly the same as the one employed for the computation of  $\beta(x, \epsilon; n_1, n_3)$ , we will be brief in this case. It is easy to see that the independent

integrals in the case of the function  $f(x, \epsilon; n_1, n_2, n_3)$  are defined in exactly the same way as for  $\beta(x, \epsilon; n_1, n_3)$ , *i.e.*, the set of independent integrals corresponds to the set of functions where only one of the  $n_i$ 's is non zero and  $n_2, n_3 \geq 0$ . We can now immediately write the integration-by-parts identities for the independent integrals,

$$\int_0^1 \frac{\partial}{\partial t} (d\mu(t; x, \epsilon) t^{-n_1} (1-t)^{-n_2} (1-xt)^{-n_3}) \Big|_{t=0}^{t=1} = 0. \quad (6.39)$$

Note that in this case we find zero in the right-hand side of the IBP's because both the factors  $t$  and  $(1-t)$  appear in the integrand. Carrying out the derivative under the integration sign, we find a recursion for the set of functions  $f(x, \epsilon; n_1, n_2, n_3)$ ,

$$-(n_1 + r_1\epsilon) f(x, \epsilon; n_1 + 1, n_2, n_3) + (n_2 + r_2\epsilon) f(x, \epsilon; n_1, n_2 + 1, n_3) + x(n_3 + r_3\epsilon) f(x, \epsilon; n_1, n_2, n_3 + 1) = 0. \quad (6.40)$$

We again use the recursion to generate a finite-sized linear system. Solving this system, we find that all the functions  $f(x, \epsilon; n_1, n_2, n_3)$  can be expressed as a combination of two master integrals,

$$f^{(1)}(x, \epsilon) = f(x, \epsilon; 0, 0, 0) \quad \text{and} \quad f^{(2)}(x, \epsilon) = f(x, \epsilon; 0, 0, 1). \quad (6.41)$$

These two integrals are independent and we cannot express the second one in terms of the first one. We can however still compute the master integrals as a solution of a system of differential equations. Differentiating each master integral with respect to  $x$  and carrying out the derivative under the integration sign and reducing everything to master integrals, we find,

$$\begin{aligned} \frac{\partial}{\partial x} f^{(1)} &= \frac{\epsilon r_3}{x} f^{(2)} - \frac{\epsilon r_3}{x} f^{(1)}, \\ \frac{\partial}{\partial x} f^{(2)} &= f^{(1)} \left( \frac{-\epsilon r_1 - \epsilon r_2 - \epsilon r_3 + 1}{x} + \frac{\epsilon r_1 + \epsilon r_2 + \epsilon r_3 - 1}{x-1} \right) + \\ & f^{(2)} \left( \frac{-\epsilon r_2 - \epsilon r_3}{x-1} + \frac{\epsilon r_1 + \epsilon r_2 + \epsilon r_3 - 1}{x} \right), \end{aligned} \quad (6.42)$$

with the initial condition,

$$f^{(1)}(x=0, \epsilon) = f^{(2)}(x=0, \epsilon) = B(1 - r_1\epsilon, 1 - r_2\epsilon) = 1 + \mathcal{O}(\epsilon). \quad (6.43)$$

The master integrals are finite for  $\epsilon \rightarrow 0$ , and so we expand them into a power series in  $\epsilon$ ,

$$f^{(1)}(x, \epsilon) = \sum_{n=0}^{\infty} f_n^{(1)}(x) \epsilon^n \quad \text{and} \quad f^{(2)}(x, \epsilon) = \sum_{n=0}^{\infty} f_n^{(2)}(x) \epsilon^n. \quad (6.44)$$

For the leading term, we find,

$$\begin{aligned} \frac{\partial}{\partial x} f_0^{(1)} &= 0, \\ \frac{\partial}{\partial x} f_0^{(2)} &= f^{(1)} \left( \frac{1}{x} + \frac{1}{1-x} \right) - f^{(2)} \frac{1}{x}. \end{aligned} \quad (6.45)$$

$f_0^{(1)}(x)$  is a constant with respect to  $x$ , and comparing to the initial condition (6.43) we find

$$f_0^{(1)}(x) = 1. \quad (6.46)$$

Inserting this solution into the equation for  $f_0^{(2)}(x)$ , we are left with

$$\frac{\partial}{\partial x} f_0^{(2)} = -f^{(2)} \frac{1}{x} + \frac{1}{x} + \frac{1}{1-x}. \quad (6.47)$$

The general solution to this equation is

$$f_0^{(2)}(x) = \frac{C - \ln(1-x)}{x}, \quad (6.48)$$

and matching with the initial condition (6.43), we find

$$f_0^{(2)}(x) = -\frac{\ln(1-x)}{x}. \quad (6.49)$$

We can repeat this procedure and solve for the higher orders in the power series (6.44). Since Gauss' hypergeometric function can be written in terms of the functions  $f(x, \epsilon; n_1, n_2, n_3)$ , which are themselves expressible in terms of the two master integrals  $f^{(1)}$  and  $f^{(2)}$ , we have obtained an algorithm to expand any function of the form  ${}_2F_1(a_1 + a_2\epsilon, b_1 + b_2\epsilon, c_1 + c_2\epsilon; z)$ ,  $a_i$ ,  $b_i$  and  $c_i$  being integers, into a Laurent series in  $\epsilon$ . Let us make some comments about this procedure:

1. On the one hand, the master integrals  $f^{(1)}$  and  $f^{(2)}$  are finite as  $\epsilon \rightarrow 0$  and can thus be expanded into a power series in the dimensional regulator.

On the other hand, a generic function  $f(x, \epsilon; n_1, n_2, n_3)$  can be written as a linear combination of the master integral. This combination however is not necessarily finite as  $\epsilon \rightarrow 0$ , because the solutions of the linear system used to express every integral in terms of master integrals may contain explicit poles in  $\epsilon$ .

2. We see that the solution for  $f_0^{(2)}(x)$  involves a logarithm in  $x$ . This is a generic feature, and it turns out that for higher orders in  $\epsilon$  the solution for the master integrals is written in terms of generalized polylogarithms, and in particular harmonic polylogarithms. A review of these functions is given in Appendix G.

Let us now return to the real-virtual integrals, and in particular the soft integral  $\mathcal{J}$ . In Eq. (6.21) we showed that the integral  $\mathcal{J}$  can be expressed in terms of Gauss' hypergeometric function. The considerations from the previous paragraphs provided us with an efficient technique to expand Gauss' hypergeometric function into a Laurent series in  $\epsilon$ . We can thus immediately write out a Laurent series representation for the soft integral  $\mathcal{J}$ . The results for  $\kappa = 0, 1$  and  $D'_0 = 3$  can be found in Ref. [69]. As representative examples, in Fig. 6.1 we compare the analytic and numeric results for the  $\epsilon^2$  coefficient in the expansion of  $\mathcal{J}(Y, \epsilon; y_0, 3 - 3\epsilon; \kappa)$  for  $\kappa = 0, 1$  and  $y_0 = 0.1, 1$ . The agreement between the two computations is seen to be excellent for the whole  $Y$ -range. We find a similar agreement for other (lower-order, thus simpler) expansion coefficients and/or other values of the parameters.

Let us conclude this section by making some comments about how to generalize this technique to the more general integrated counterterms. In this work, we consider a particular class of integrated counterterms, namely those that can be written as twofold integral of the form (6.22) depending on two external parameters  $z_i$ . The method employed to compute the  $\epsilon$ -expansion of the  ${}_2F_1$  functions remains applicable even in this case, with two small modifications:

1. For a twofold integral we can write out two independent IBP identities, one for each integration variable, *e.g.*, in the case where the integrand

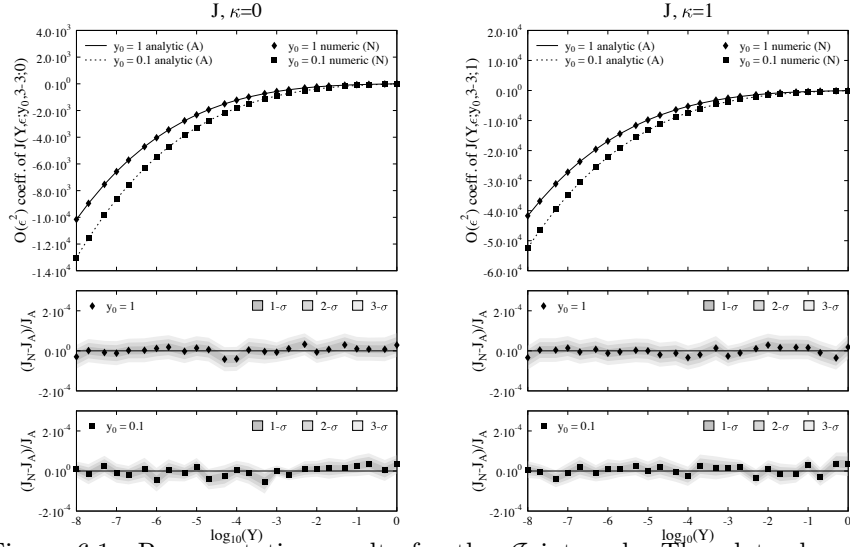


Figure 6.1: Representative results for the  $\mathcal{J}$  integral. The plots show the coefficient of the  $\mathcal{O}(\epsilon^2)$  term in  $\mathcal{J}(Y, \epsilon; y_0, 3 - 3\epsilon; \kappa)$  for  $\kappa = 0$  (left figure) and  $\kappa = 1$  (right figure) with  $y_0 = 0.1, 1$ . The plots are taken from Ref. [69].

vanishes at the border of the integration domain,

$$\begin{aligned} \int_0^1 \int_0^1 dx_1 dx_2 \frac{\partial}{\partial x_1} (\dots) &= 0, \\ \int_0^1 \int_0^1 dx_1 dx_2 \frac{\partial}{\partial x_2} (\dots) &= 0. \end{aligned} \tag{6.50}$$

2. If the integral depends on two external parameters  $z_i$ , then the master integrals fulfill a system of *partial* differential equations.

For more details on these more general integrals, we refer the reader to Appendix J as well as Ref. [69].

## 6.4 Conclusion

In the second part of this work we investigated the infrared behavior of gauge theory scattering amplitudes. We discussed how collinear and soft singularities can arise beyond leading order, and how they can be described in a uniform

way using antenna functions. Antenna functions have the property that they approximate the singular behavior of the amplitude all over the phase space, and therefore incorporate by definition the complicated phase space structure beyond next-to-leading order, facilitating in this way the construction of subtraction schemes beyond NLO. In particular, antenna subtraction is at the basis of the only exclusive NNLO description of three jet production in  $e^+e^-$  collisions.

In Chapter 5 we presented a new alternative way of defining tree-level antenna functions by means of the MHV formalism, a definition which holds at any order in perturbation theory. This method leads to very compact expressions for the antenna functions, which might simplify the analytic integration over the phase space of the unresolved particles. It also gives a very natural way of parametrizing, by means of an antiholomorphic spinor  $\eta$ , the intrinsic arbitrariness of the antenna function outside the singular regions. As an application, we have shown that it is straightforward to provide explicit expressions for MHV and NMHV antenna functions at all orders, which are sufficient to build the full set of gluon antenna functions up to N<sup>3</sup>LO. We furthermore extended this approach by combining it to the recursive formulation of the MHV formalism presented in Section 2.4, and derived recursive relations for both antenna functions and splitting amplitudes. Although the knowledge of these multi-leg antenna functions might not play a practical role at present for QCD calculations beyond leading order, their knowledge could be of interest, for instance, in testing the infrared structure of recently introduced conjectures for gluon amplitudes at all order in MSYM (See Part III of this work).

No subtraction scheme is complete without an explicit knowledge of the integrated counterterms that appear when combining the approximate cross sections with the virtual corrections. In Chapter 6 we therefore investigated new methods to perform the integrals that appear in such a scheme. The techniques we applied are a generalization of the Laporta algorithm and the master integral technique developed for (multi-) loop integrals in quantum field theory over the last decade. We extended this technique to hypergeometric Euler integrals of the form (6.22), and computed the Laurent expansion in the dimensional regularization parameter  $\epsilon$  for a class of 27 real-virtual integrals [69].

---

The technique however is much more generic, and could also be applied to the computation of the Laurent expansion of generalized hypergeometric functions that appear in loop computations (See Part III of this work), provided that an Euler integral representation is known. Unfortunately, our technique turned out to be not efficient enough in its present form to cope with all the integrated counterterms that appear in the subtraction scheme under consideration. For these classes of integrals, other techniques like for example the Mellin-Barnes approach turns out to be more efficient [83].





## Part III

# The BDS ansatz and high-energy limits



# Chapter 7

## The Bern-Dixon-Smirnov ansatz

### 7.1 The ABDK/BDS ansatz

In the last part of this work we are concerned with the computation of scattering amplitudes beyond tree-level accuracy. Although most techniques we present apply to gauge theories in general, we focus in particular on planar  $\mathcal{N} = 4$  super Yang-Mills theories (MSYM). The interest in this particular theory is manifold.

First, it is known that gluon loop amplitudes in QCD can be rearranged in a way that makes the MSYM contribution explicit, *e.g.* given at one-loop accuracy, [32],

$$A_n^{\text{QCD}} = A_n^{\mathcal{N}=4} - 4A_n^{\mathcal{N}=1} + A_n^{\text{scalar}}, \quad (7.1)$$

where  $A_n^{\mathcal{N}=4}$  denote the one-loop  $n$ -point MSYM amplitude. The knowledge of MSYM amplitudes is thus a first step to the knowledge of QCD amplitudes needed for predictions at hadron colliders.

The second reason comes from the fact that several conjectures have recently been made of what MSYM amplitudes for an arbitrary number of legs and loops should look like. In this chapter we briefly review some of these conjectures, which are at the core of this part.

In Ref. [9], Anastasiou, Bern, Dixon and Kosower (ABDK) formulated an ansatz for a two-loop MHV amplitude in MSYM for an arbitrary number of external legs. The ansatz expresses the two-loop amplitude in terms of the one-loop result,

$$M_n^{(2)}(\epsilon) = \frac{1}{2} (M_n^{(1)}(\epsilon))^2 + f^{(2)}(\epsilon) M_n^{(1)}(2\epsilon) + C^{(2)} + \mathcal{O}(\epsilon), \quad (7.2)$$

where

$$f^{(2)}(\epsilon) = \frac{\psi(1-\epsilon) + \gamma_E}{\epsilon} \quad \text{and} \quad C^{(2)} = -\frac{5}{4} \zeta_4, \quad (7.3)$$

and  $M_n^{(l)}$  denotes the  $l$ -loop coefficient, *i.e.*, the  $l$ -loop amplitude rescaled by the tree-level result,

$$A_n = A_n^{(0)} \left( 1 + \sum_{l=1}^{\infty} a^l M_n^{(l)} \right). \quad (7.4)$$

Since we work in the planar limit, we choose the 't Hooft coupling as the expansion parameter,

$$a = \frac{2g^2 N_c}{(4\pi)^{2-\epsilon}} e^{-\gamma_E \epsilon}, \quad (7.5)$$

where  $\gamma_E$  denotes the Euler-Mascheroni constant,  $\Gamma'(1) = -\gamma_E$ . Since the one-loop amplitude contains infrared poles in  $1/\epsilon^2$ , it must be known through  $\mathcal{O}(\epsilon^2)$  in Eq. (7.2). The origin of the ansatz goes back to the computation by the same people of the two-loop splitting amplitude in MSYM, which was shown to satisfy an iteration relation very similar to Eq. (7.2),

$$r_S^{(2)}(\epsilon) = \frac{1}{2} (r_S^{(1)}(\epsilon))^2 + f^{(2)}(\epsilon) r_S^{(1)}(2\epsilon), \quad (7.6)$$

where  $r_S^{(l)}$  denotes the  $l$ -loop splitting amplitude, rescaled by the tree-level result. Indeed, in the collinear limit the one and two-loop  $n$ -point MHV amplitudes must factorize according to

$$\begin{aligned} M_n^{(1)} &\rightarrow M_{n-1}^{(1)} + r_S^{(1)}, \\ M_n^{(2)} &\rightarrow M_{n-1}^{(2)} + M_{n-1}^{(1)} r_S^{(1)} + r_S^{(2)}, \end{aligned} \quad (7.7)$$

and it is easy to see that the ABDK ansatz (7.2) is the only iteration which is compatible with both the iteration of the two-loop splitting amplitude, Eq. (7.6)

and the collinear factorization (7.7). The ansatz was backed up by confronting the iteration to the analytic computation of two-loop four-point amplitude in MSYM. In Ref. [84] the ABDK ansatz was shown to hold also in the case of the five-point amplitude by numerical computation.

Bern, Dixon and Smirnov (BDS) computed the three-loop four-point MSYM amplitude [10] and showed that it satisfies an iteration similar to the ABDK ansatz for the two-loop amplitude,

$$M_4^{(3)}(\epsilon) = -\frac{1}{3} (M_4^{(1)}(\epsilon))^3 + M_4^{(1)}(\epsilon) M_4^{(2)}(\epsilon) + f^{(3)}(\epsilon) M_4^{(1)}(3\epsilon) + C^{(3)} + \mathcal{O}(\epsilon), \quad (7.8)$$

where

$$\begin{aligned} f^{(3)}(\epsilon) &= \frac{11}{2} \zeta_4 + \epsilon(6\zeta_5 + 5\zeta_2 \zeta_3) + \epsilon^3(c_1 \zeta_6 + c_2 \zeta_3^2), \\ C^{(3)} &= \left( \frac{341}{216} + \frac{2}{9} c_1 \right) \zeta_6 + \left( -\frac{17}{19} + \frac{2}{9} c_2 \right) \zeta_3^2. \end{aligned} \quad (7.9)$$

The quantities  $c_1$  and  $c_2$  are expected to be rational numbers, but they cannot be determined from the computation of the three-loop four-point amplitude, because they cancel in the final result. BDS then extended the iteration formulæ (7.2) and (7.8) and formulated an ansatz for a generic  $n$ -point MHV amplitude in MSYM. This all-order ansatz reads

$$M_n(\epsilon) = 1 + \sum_{l=1}^{\infty} a^l M_n^{(l)}(\epsilon) = \exp \sum_{l=0}^{\infty} a^l \left[ f^{(l)}(\epsilon) M_n^{(1)}(l\epsilon) + C^{(l)} + E_n^{(l)}(\epsilon) \right]. \quad (7.10)$$

The only kinematical dependence in the right-hand side of Eq. (7.10) is in the one-loop amplitude  $M_n^{(1)}(l\epsilon)$ . The quantities  $f^{(l)}(\epsilon)$  and  $C^{(l)}$  are universal and are independent of the kinematics and the number of external particles.  $f^{(l)}(\epsilon)$  is expected to be a polynomial of degree two in  $\epsilon$  and  $C^{(l)}$  to be a polynomial of uniform transcendental weight in Riemann  $\zeta$  values. The values of these functions for  $l = 2, 3$  are given in Eqs. (7.3) and (7.9). The functions  $E_n^{(l)}(\epsilon)$  are additional  $\mathcal{O}(\epsilon)$  contributions. It is easy to see that we must have  $f^{(1)}(\epsilon) = C^{(1)} = E_n^{(1)}(\epsilon) = 0$  in order to reproduce the one-loop result. Expanding the exponential in Eq. (7.10) and collecting powers of the coupling constant  $a$ , the

BDS ansatz reproduces the two and three-loop iteration formulæ (7.2) and (7.8).

The BDS ansatz was first shown to fail by Alday and Maldacena in the limit of a large number of gluons using the ADS/CFT correspondence [11]. This result was backed up by the computation of the six-edged Wilson loop and using the conjecture that the  $n$ -edged Wilson loop can be related to the MHV amplitudes in MSYM [85]. The question was settled in Ref. [12] with the explicit numerical computation of the two-loop six-point amplitude, which confirmed the Wilson loop result and demonstrated the breakdown of the BDS ansatz for  $l = 2$  and  $n = 6$  in the finite contribution of the parity-even part. Recently, also the seven and eight-edged Wilson loops have been computed [13]. Assuming that the duality between Wilson loops and MSYM scattering amplitudes holds even beyond  $n = 6$ , the conclusion is that the BDS ansatz fails for  $n = 7$  and 8 as well. The breakdown of the ansatz can be quantified by the remainder function  $R_n^{(2)}$ , defined as the difference between the left and right-hand sides of the ABDK ansatz,

$$R_n^{(2)} \equiv M_n^{(2)}(\epsilon) - \frac{1}{2} (M_n^{(1)}(\epsilon))^2 - f^{(2)}(\epsilon) M_n^{(1)}(2\epsilon) - C^{(2)}. \quad (7.11)$$

The previous results can be summarized by the statement that  $R_n^{(2)} \neq 0$  for  $n \geq 6$  and  $R_n^{(2)}$  is a constant with respect to  $\epsilon$ . Since the computation of Ref. [12] was numerical, we ignore at present the analytic expression of the remainder function  $R_6^{(2)}$ .

Even though the ABDK/BDS ansatz does not hold beyond five-points, the study of the Wilson loop duality tells us something more about the BDS ansatz. The Wilson loops in fact possess a conformal symmetry and it was shown that a particular solution to the ensuing Ward identities is given by the BDS ansatz. The general solution of the Ward identities can thus be obtained by adding to the BDS ansatz an arbitrary function which respects the conformal symmetry, *i.e.*, an arbitrary function of conformal cross-ratios. The conclusion is that, if the duality between Wilson loops and scattering amplitudes holds, then we must add to the BDS ansatz a yet unknown function of conformal ratios of Mandelstam invariants.

In the case of the four and five-point on-shell amplitudes, it was shown that there are no non-trivial such conformal ratios of invariants and hence the BDS ansatz provides the full solution for the amplitude. Starting from six points however, we can form three independent conformal ratios,

$$u_1 = \frac{s_{12} s_{45}}{s_{345} s_{456}}, \quad u_2 = \frac{s_{23} s_{56}}{s_{234} s_{456}}, \quad u_3 = \frac{s_{34} s_{61}}{s_{234} s_{345}}, \quad (7.12)$$

and so we can add an arbitrary function of these ratios to the BDS ansatz without violating the conformal Ward identities.

The conformal Ward identities hence explain why the BDS alone is insufficient to reproduce the full six-point amplitude, without however fixing the form of the remainder function. Since the computation of the six-point two-loop amplitude was purely numerical, no analytic representation for this function is known. The analytic evaluation of Eq. (7.11) would require the analytic computation of the one and two-loop hexagon integrals, which is beyond our technical capabilities for the moment.

If the analytic computation of the six-point two-loop amplitude in general kinematics is at present out of reach, one could think of performing the computation in a simpler kinematic regime where some of the invariants take particular values, or even vanish. Let us expand a little bit more on this and let us consider a generic  $n$ -point  $l$ -loop amplitude. The amplitude depends *a priori* on  $n$  four-momenta, but Lorentz invariance requires the amplitude to be a function of invariants  $s_i$  only. In a region of phase space where one of the invariants, say  $s_k$ , is much smaller than all the others,  $s_k \ll s_i, \forall i \neq k$ , we can expand the amplitude in the invariant  $s_k$ ,

$$M_n(\{s_i\}; \epsilon) = \overline{M}_n(s_k \ll s_i; \epsilon) + \text{subleading terms}, \quad (7.13)$$

where  $\overline{M}_n$  denotes the leading term in the expansion. Explicit examples of how to compute this leading term will be given in subsequent chapters. Let us only emphasize at this point that in general  $\overline{M}_n$  is easier to compute than the full amplitude, because of the kinematical constraint that might for example imply that  $\overline{M}_n$  depends on one scale less compared to the full amplitude. Instead of computing the full six-point two-loop amplitude, we could thus think of only computing its leading term in a given limit and extract the analytic expression

of the remainder function from there. However, as we will see in the following, not all kinematical limits are suitable for this task.

Let us start by analyzing the simplest kinematical limit, the double collinear limit. For example, if  $p_1$  and  $p_2$  are collinear, then their invariant mass tends to zero,  $s_{12} \simeq 0$ , and so we can repeat the previous analysis and expand the amplitude in the small parameter  $s_{12}$ . In the case of the collinear limit the leading term in the expansion is just the splitting amplitude, Eq. (4.28). We know however that the ABDK/BDS ansatz predicts correctly all the two-particle collinear limits of an amplitude, which implies that the six-point remainder function must vanish and no information on its functional can be obtained in this limit.

The two-particle collinear limit is hence too restrictive to provide some information on the analytic form of the remainder function. It is however expected that the remainder function is non zero in the triple collinear limit, because this limit appears for the first time in the six-point amplitude. This argument is backed up by the observation that in the triple collinear limit the three conformal cross-ratios stay generic and do not become subleading, *e.g.* in the limit where  $p_1$ ,  $p_2$  and  $p_3$  become collinear,

$$\begin{aligned} u_1 &\simeq \mathcal{O}\left(\frac{s_{45}}{z_3(s_{P4} + s_{P5}) + s_{45}}\right), \\ u_2 &\simeq \mathcal{O}\left(\frac{s_{56}}{z_1(s_{P5} + s_{P6}) + s_{56}}\right), \\ u_3 &\simeq \mathcal{O}\left(\frac{z_1 z_3 s_{P4} s_{P6}}{[z_1(s_{P5} + s_{P6}) + s_{56}][z_3(s_{P4} + s_{P5}) + s_{45}]}\right), \end{aligned} \quad (7.14)$$

where  $P = p_1 + p_2 + p_3$  denotes the collinear direction and  $z_i$  denote the momentum fractions. The leading term in the expansion (7.13) in the triple collinear limit corresponds to the splitting amplitude for one gluon splitting into three gluons, *e.g.*, at one and two-loop accuracy,

$$\begin{aligned} M_n^{(1)} &\rightarrow M_{n-1}^{(1)} + r_{1\rightarrow 3}^{(1)}, \\ M_n^{(2)} &\rightarrow M_{n-1}^{(2)} + M_{n-1}^{(1)} r_{1\rightarrow 3}^{(1)} + r_{1\rightarrow 3}^{(2)}, \end{aligned} \quad (7.15)$$

where  $r_{1\rightarrow 3}^{(l)}$  denotes the  $l$ -loop splitting amplitude rescaled by the tree-level result,

$$\text{Split}_{-h}^{(l)}(1, 2, 3) = \text{Split}_{-h}^{(0)}(1, 2, 3) r_{1\rightarrow 3}^{(l)}. \quad (7.16)$$



The conclusion is that it is not necessary to compute the full two-loop six-point amplitude in order to determine the functional form of  $R_6^{(2)}$ , but it would be enough to have the analytic expression of the two-loop triple collinear splitting amplitude, a computation which has however never been done so far.

In the rest of this work we extend the previous analysis from collinear limits to other classes of limits, known as the high-energy limit. In Chapter 8 and 9 we review the high-energy limit of gauge theory amplitudes, both at tree-level and beyond. Along the way, we introduce a novel way to perform computations for tree-level amplitudes in the high-energy limit, based on the MHV formalism. In Chapter 10 we analyze what the BDS ansatz becomes in the high-energy limit and we disguise several additional limits where the remainder function is expected to be non zero.



# Chapter 8

## The high-energy behavior of tree-level gluon amplitudes

### 8.1 The multi-Regge limit

Let us consider an  $n$ -point color-ordered tree-level gluon amplitude  $A_n(1, \dots, n)$  describing the 2-to- $(n-2)$  scattering  $(-p_1), (-p_2) \rightarrow p_3, \dots, p_n$ . We look at the amplitude in a very specific kinematic regime, also known as multi-Regge kinematics [86], where the final-state gluons are strongly ordered in rapidity and have comparable transverse momenta,

$$y_3 \gg y_4 \gg \dots \gg y_{n-1} \gg y_n \quad \text{and} \quad |p_{3\perp}| \simeq |p_{4\perp}| \simeq \dots \simeq |p_{n-1\perp}| \simeq |p_{n\perp}|, \quad (8.1)$$

where  $p_\perp = p^x + ip^y$  denotes the complex transverse momentum. Using light-cone coordinates\*, the two-particle invariants become, for  $3 \geq i > j \geq n$ ,

$$\begin{aligned} s_{ij} &= p_i^+ p_j^- + p_i^- p_j^+ - p_{i\perp} p_{j\perp}^* - p_{i\perp}^* p_{j\perp} \\ &= |p_{i\perp}| |p_{j\perp}| e^{y_i - y_j} + |p_{i\perp}| |p_{j\perp}| e^{y_j - y_i} - p_{i\perp} p_{j\perp}^* - p_{i\perp}^* p_{j\perp}. \end{aligned} \quad (8.2)$$

The last two terms in this relation are  $\mathcal{O}(1)$ , and the first exponential is enhanced with respect to the second one. Hence, in multi-Regge kinematics only

---

\*See Appendix D for a review.

the first exponential contributes,

$$s_{ij} \simeq |p_{i\perp}| |p_{j\perp}| e^{y_i - y_j}. \quad (8.3)$$

Similarly, one shows that,

$$\begin{aligned} s &\equiv s_{12} \simeq |p_{3\perp}| |p_{n\perp}| e^{y_3 - y_n}, \\ s_{2i} &\simeq -|p_{3\perp}| |p_{i\perp}| e^{y_3 - y_i}, \\ s_{1i} &\simeq -|p_{i\perp}| |p_{n\perp}| e^{y_i - y_n}. \end{aligned} \quad (8.4)$$

The kinematics (8.1) imply that the total scattering energy  $s$  is much larger than any other two-particle invariant, which justifies the identification of the multi-Regge limit with the high-energy limit. If we label the momenta transferred in the  $t$ -channel by

$$\begin{aligned} q_1 &= p_1 + p_n \\ q_i &= q_{i-1} + p_{n-i+1}, \quad \text{for } 2 \leq i \leq n-4 \\ q_{n-3} &= -p_2 - p_3, \end{aligned} \quad (8.5)$$

with virtualities  $t_i = q_i^2$ , then it is easy to see that in multi-Regge kinematics the  $t$ -channel momentum flow is determined by the transverse components only,  $t_i \simeq -|q_{i\perp}|^2$ . If we furthermore define  $s_i = s_{n-i, n-i+1}$ , the multi-Regge limit implies the hierarchy of scales,

$$s \gg s_1, s_2, \dots, s_{n-3} \gg -t_1, -t_2, \dots, -t_{n-3}. \quad (8.6)$$

Eq. (8.6) has the practical advantage that it is formulated in terms of two-particle invariants rather than rapidities, and it makes the high-energy behavior of the limit explicit. It does however not uniquely determine the multi-Regge limit, because we did not impose the constraint that the final state gluons should have comparable transverse momentum. Furthermore, Eq. (8.6) is a Lorentz invariant statement, whereas Eq. (8.1) is invariant only under boosts along the  $z$  axis. Let us define the transverse momentum scales

$$\kappa_i = |p_{n-i\perp}|^2, \quad \text{for } 1 \leq i \leq n-4. \quad (8.7)$$

In multi-Regge kinematics,  $\kappa_i$  is of the order of the  $t$ -type invariants and can be expressed in terms of two and three-particle invariants,

$$\kappa_i = \frac{s_i s_{i+1}}{s_{n-i-1, n-i, n-i+1}}. \quad (8.8)$$

The latter relations are known as the mass-shell conditions for the gluons. Using Eq. (8.4), we find a relation between the mass-shell conditions in the multi-Regge limit,

$$s \kappa_1 \dots \kappa_{n-4} = s_1 \dots s_{n-3}. \quad (8.9)$$

Eqs. (8.8) and (8.9) combined to the hierarchy of scales (8.6) uniquely define the multi-Regge limit in terms of multi-particle invariants, a formulation which will be used extensively in subsequent chapters when studying the high-energy behavior of gluon amplitudes beyond tree-level.

In the previous paragraph we showed how the multi-Regge limit can be defined either in terms of rapidities or in terms of particles invariants. In Chapter 1 we argued that at tree-level it is convenient to work in the spinor-helicity representation and to express an amplitude as a rational function of spinor products. Following this logic, we introduce a third equivalent way to define the multi-Regge limit based on lightcone coordinates, related to the spinor products via the relation,

$$\langle ij \rangle = p_{i\perp} \sqrt{\frac{p_j^+}{p_i^+}} - p_{j\perp} \sqrt{\frac{p_i^+}{p_j^+}}. \quad (8.10)$$

A review of multi-Regge kinematics in lightcone coordinates is given in Appendix D. It is easy to show that a strong ordering in rapidities is equivalent to a strong ordering in lightcone coordinates,

$$p_3^+ \gg p_4^+ \gg \dots \gg p_{n-1}^+ \gg p_n^+ \quad \text{and} \quad p_3^- \ll p_4^- \ll \dots \ll p_{n-1}^- \ll p_n^-, \quad (8.11)$$

where  $p^\pm = p^0 \pm p^z$ . In multi-Regge kinematics the spinor products are then written in the approximate form [25],

$$\begin{aligned} \langle ij \rangle &\simeq -p_{j\perp} \sqrt{\frac{p_i^+}{p_j^+}}, \quad \text{for } 3 \leq i < j \leq n, \\ \langle 2i \rangle &\simeq -i p_{i\perp} \sqrt{\frac{p_3^+}{p_i^+}}, \quad \text{for } 3 \leq i \leq n, \\ \langle i1 \rangle &\simeq -i \sqrt{p_i^+ p_n^-}, \quad \text{for } 3 \leq i \leq n-1, \\ \langle 12 \rangle &\simeq \sqrt{p_3^+ p_n^-}. \end{aligned} \quad (8.12)$$

Let us apply these formulas to an MHV amplitude and let us determine its form in multi-Regge kinematics. We find,

$$\begin{aligned}
A_n(1^-, 2^-, 3^+, \dots, n^+) &= \frac{\langle 12 \rangle^4}{\langle 12 \rangle \langle 23 \rangle \dots \langle (n-1)n \rangle \langle n1 \rangle} \\
&\simeq \frac{(p_3^+ p_n^-)^2}{\sqrt{p_3^+ p_n^-} (-i) p_{3\perp} (-p_{4\perp}) \sqrt{\frac{p_3^+}{p_4^+}} \dots (-p_{n\perp}) \sqrt{\frac{p_{n-1}^+}{p_n^+}} (-i) \sqrt{p_n^+ p_n^-}} \quad (8.13) \\
&\simeq p_3^+ p_n^- \frac{-1}{|p_{3\perp}|^2} \frac{p_{3\perp}^* q_{n-4\perp}}{p_{4\perp}} \frac{-1}{|q_{n-4\perp}|^2} \dots \frac{-1}{|q_{2\perp}|^2} \frac{q_{2\perp}^* p_{n\perp}}{p_{n-1\perp}} \frac{-1}{|p_{n\perp}|^2} \frac{p_{n\perp}^*}{p_{n\perp}}.
\end{aligned}$$

Using the fact that in multi-Regge kinematics  $|q_i|^2 \simeq -t_i$  and  $p_3^+ p_n^- \simeq s$ , we can recast this expression into the form,

$$A_n(1^-, 2^-, 3^+, \dots, n^+) \simeq s \frac{1}{t_{n-3}} \frac{q_{n-3\perp}^* q_{n-4\perp}}{p_{4\perp}} \frac{1}{t_{n-4}} \dots \frac{1}{t_2} \frac{q_{2\perp}^* q_{1\perp}}{p_{n-1\perp}} \frac{1}{t_1} \frac{p_{n\perp}^*}{p_{n\perp}}. \quad (8.14)$$

We see that in the multi-Regge limit the amplitude can be written as a product of terms with the same functional form,

$$\frac{q_{i+1\perp}^* q_{i\perp}}{p_{i\perp}}, \quad (8.15)$$

connected by  $t$ -channel propagators. Even though we only showed this factorization explicitly on the example of an MHV amplitude, it is conjectured that in the multi-Regge limit the leading behavior of any  $n$ -gluon color-ordered amplitude takes the factorized form [87]

$$\begin{aligned}
&A_n(1, \dots, n) \\
&= s C^{(0)}(2; 3) \frac{1}{t_n} V^{(0)}(q_{n-3}; 4; q_{n-4}) \dots \frac{1}{t_2} V^{(0)}(q_2; n-1; q_1) \frac{1}{t_1} C^{(0)}(1; n). \quad (8.16)
\end{aligned}$$

where we implicitly followed the same convention as for the color-ordered amplitudes, *i.e.* we label the external gluon momenta simply by their indices,

$$C^{(0)}(2; 3) \equiv C^{(0)}(p_2; p_3) \quad \text{and} \quad V^{(0)}(q_{n-i+1}; i; q_{n-i}) \equiv V^{(0)}(q_{n-i+1}; p_i; q_{n-i}). \quad (8.17)$$

The factorization is shown schematically in Fig. 8.1. The coefficient functions<sup>†</sup>  $C^{(0)}$  describe the  $g^* g \rightarrow g$  vertices, where  $g^*$  denotes a reggeized gluon in the

<sup>†</sup>Also known as impact factors.

$t$ -channel. They are functions of the momenta and helicities of the external gluons [87, 86],

$$\begin{aligned} C^{(0)}(2^-; 3^+) &= C^{(0)}(2^+; 3^-)^* = 1, \\ C^{(0)}(1^-; n^+) &= C^{(0)}(1^+; n^-)^* = \frac{p_{n\perp}^*}{p_{n\perp}}, \end{aligned} \quad (8.18)$$

and all other helicity configurations are subleading. The Lipatov vertex  $V^{(0)}$  describing the emission of a gluon along the  $t$ -channel ladder is given by [87, 88, 89],

$$V^{(0)}(q_{n-i+1}; i^+; q_{n-i}) = V^{(0)}(q_{n-i+1}; i^-; q_{n-i})^* = \frac{q_{n-i+1\perp}^* q_{n-i\perp}}{p_{i\perp}}. \quad (8.19)$$

Eqs. (8.18) and (8.19) are universal and do not depend on the number of external gluons. They can be used to compute any tree-level amplitude for an arbitrary number of legs in multi-Regge kinematics. Note that starting from Eq. (8.1) we can define a whole tower of new limits by successively relaxing the rapidity ordering and allowing for two or more final-state gluons with comparable rapidities. These limits, together with the corresponding factorization formulas for the amplitudes, are reviewed in the next section.

## 8.2 Quasi multi-Regge limits

When relaxing the strong rapidity ordering (8.1), we obtain kinematical configurations where two or more gluons have comparable rapidities. We can thus start from multi-Regge kinematics, and progressively approach the general kinematics, where no rapidity ordering is imposed.

Let us start with the situation where we do not impose any rapidity ordering on the gluons emitted along the ladder,

$$y_3 \gg y_4 \simeq \dots \simeq y_{n-1} \gg y_n \quad \text{and} \quad |p_{3\perp}| \simeq |p_{4\perp}| \simeq \dots \simeq |p_{n-1\perp}| \simeq |p_{n\perp}|, \quad (8.20)$$

or equivalently using lightcone coordinates,

$$p_3^+ \gg p_4^+ \simeq \dots \simeq p_{n-1}^+ \gg p_n^+. \quad (8.21)$$

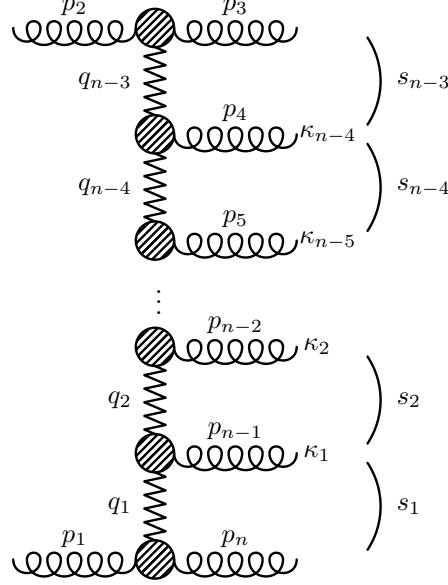


Figure 8.1: Amplitude in multi-Regge kinematics. The blobs indicate the coefficient functions (impact factors) and the Lipatov vertices describing the emission of gluons along the ladder.

Similar to the multi-Regge case, the amplitude is conjectured to factorize,

$$A_n(1, \dots, n) = s C^{(0)}(2; 3) \frac{1}{t_2} V_{n-4}^{(0)}(q_2; 4, \dots, n-1; q_1) \frac{1}{t_1} C^{(0)}(1; n), \quad (8.22)$$

where  $q_i$  and  $t_i$  denote the momenta transferred in the  $t$ -channel,

$$q_1 = p_1 + p_n, \quad \text{and} \quad q_2 = -p_2 - p_3, \quad (8.23)$$

and  $t_i = q_i^2 \simeq -|q_{i\perp}|^2$ . The coefficient functions  $C^{(0)}$  appearing in Eq. (8.22) are the same as in Eq. (8.18). The functions  $V_{n-4}^{(0)}$  are the tree-level Lipatov vertices describing the emission of  $(n-4)$  gluons with comparable rapidity along the ladder. In the special case where all the gluons have the same helicity a simple formula valid for arbitrary  $n$  can be derived from Eq. (1.19),

$$\begin{aligned} V_{n-4}^{(0)}(q_2; 4^+, \dots, (n-1)^+; q_1) &= \frac{q_{2\perp}^* q_{1\perp}}{p_{4\perp}} \sqrt{\frac{x_4}{x_{n-1}}} \frac{1}{\langle 45 \rangle \dots \langle (n-2)(n-1) \rangle}, \\ V_{n-4}^{(0)}(q_2; 4^-, \dots, (n-1)^-; q_1) &= \left[ V_{n-4}^{(0)}(q_2; 3^+, \dots, (n-1)^+; q_1) \right]^*, \end{aligned} \quad (8.24)$$



where we defined

$$x_i = \frac{p_i^+}{p_3^+ + p_4^+ + \dots + p_{n-1}^+}. \quad (8.25)$$

Note that for  $n = 5$  we recover the Lipatov vertex defined in Eq. (8.19),

$$V_1^{(0)}(q_2; 4; q_1) = V^{(0)}(q_2; 4; q_1). \quad (8.26)$$

The limit we just defined must of course encompass all other limits with a more stringent rapidity ordering, where we have two clusters of gluons separated by a large rapidity gap,

$$y_3 \gg y_4 \simeq \dots \simeq y_m \gg y_{m+1} \simeq \dots \simeq y_{n-1} \gg y_n. \quad (8.27)$$

The amplitude must factorize accordingly into a product of four building blocks, and as a consequence the Lipatov vertices themselves must factorize,

$$\begin{aligned} V_{n-4}^{(0)}(q_2; 4, \dots, n-1; q_1) \\ = V_{m-3}^{(0)}(q_2; 4, \dots, m; q_3) \frac{1}{t_3} V_{n-m-1}^{(0)}(q_3; m+1, \dots, n-1; q_1), \end{aligned} \quad (8.28)$$

where  $q_3$  denotes the momentum transferred in the  $t$ -channel,  $q_3 = q_2 - p_4 - \dots - p_m$ , and  $t_3 \simeq -|q_{3\perp}|^2$ . In particular, in the limit of strong rapidity ordering we recover the multi-Regge factorization formula (8.16). Furthermore, in the limit where a subset of the gluons, say  $i, \dots, j$ , become collinear, the amplitude must still have the correct collinear behavior, *i.e.*, the Lipatov vertex must factorize onto a splitting amplitude for the emission of collinear gluons,

$$\begin{aligned} V_{n-4}^{(0)}(q_2; 4, \dots, n-1; q_1) \\ = \sum_h V_{n+i-j-4}^{(0)}(q_2; 4, \dots, i-1, P^h, j+1, \dots, n-1; q_1) \text{Split}_{-h}(i, \dots, j), \end{aligned} \quad (8.29)$$

where  $P$  denotes the collinear direction.

The previous analysis naturally lead to the definition of generalized Lipatov vertices, describing the emission of a cluster of gluons along the  $t$ -channel ladder. We can define in exactly the same way generalized coefficient functions by not requiring a rapidity gap at the end of the gluon ladder, *e.g.*,

$$y_3 \simeq y_4 \simeq \dots \simeq y_{n-1} \gg y_n \quad \text{and} \quad |p_{3\perp}| \simeq \dots \simeq |p_{n\perp}|, \quad (8.30)$$

or equivalently in terms of lightcone coordinates,

$$p_3^+ \simeq p_4^+ \simeq \dots \simeq p_{n-1}^+ \gg p_n^+. \quad (8.31)$$

In this limit the amplitude factorizes according to

$$A_n(1, \dots, n) = s C_{n-3}^{(0)}(2; 3, \dots, n-1) \frac{1}{t} C^{(0)}(1; n), \quad (8.32)$$

where  $t \simeq -|q_\perp|^2$  with  $q = p_1 + p_n$  denotes the momentum transferred in the  $t$ -channel, and  $C^{(0)}$  was defined in Eq. (8.18). The coefficient functions  $C_{n-3}^{(0)}$  are the generalizations of the function  $C^{(0)}$  and describe the emission of  $(n-3)$  gluons with comparable rapidity at one end of the ladder. In the particular case where all the emitted gluons have the same helicity, we obtain,

$$\begin{aligned} C_{n-3}^{(0)}(2^-; 3^+, 4^+, \dots, (n-1)^+) &= -\frac{q_\perp}{p_{3\perp}} \sqrt{\frac{x_3}{x_{n-1}}} \frac{1}{\langle 34 \rangle \dots \langle (n-2)(n-1) \rangle}, \\ C_{n-3}^{(0)}(2^+; 3^-, 4^-, \dots, (n-1)^-) &= \left[ C_{n-3}^{(0)}(2^-; 3^+, 4^+, \dots, (n-1)^+) \right]^*, \end{aligned} \quad (8.33)$$

and for  $n = 4$  the generalized coefficient functions reduce to the coefficient function introduced in the previous section,

$$C_1^{(0)}(2; 3) = C^{(0)}(2; 3). \quad (8.34)$$

Similar to the case of the Lipatov vertices, the coefficient functions inherit all the factorization properties from the full amplitude. In particular, in the limit of more restrictive kinematics, say  $y_3 \simeq \dots \simeq y_m \gg y_{m+1} \simeq \dots \simeq y_{n-1}$ , the coefficient functions must factorize into a coefficient function for the emission of fewer gluons times a Lipatov vertex,

$$C_{n-3}^{(0)}(2; 3, 4, \dots, n-1) = C_{m-2}^{(0)}(2; 3, 4, \dots, m) \frac{1}{t_1} V_{n-m-1}^{(0)}(q_1; m+1, \dots, n-1; q), \quad (8.35)$$

and  $t_1 = q_1^2 \simeq -|q_{1\perp}|^2$  with  $q_1 = p_2 + p_3 + \dots + p_m$ . Note that for  $m = 3$  Eq. (8.35) reduces to Eq. (8.22). Furthermore, if a subset of particles, say  $i, \dots, j$ , becomes collinear, then the coefficient function must factorize onto a splitting amplitude,

$$\begin{aligned} &C_{n-3}^{(0)}(2; 3, 4, \dots, n-1) \\ &= \sum_h C_{n+1-j-3}^{(0)}(2; 3, 4, \dots, i-1, P^h, j+1, \dots, n-1) \text{Split}_h(i, \dots, j), \end{aligned} \quad (8.36)$$

where  $P$  denotes the collinear direction.

The generalized coefficient functions and Lipatov vertices have been computed up to  $C_4^{(0)}$  and  $V_3^{(0)}$  in Ref. [25]. The computation was performed by using the analytic expressions for color-ordered amplitudes for up to seven external gluons and taking the appropriate limit on the amplitude using the approximate form of the spinor products of Appendix D. This procedure is similar to the algorithm to extract splitting amplitudes and soft factors presented in Chapter 4. In this context, we showed that we can refine this procedure when working in the MHV formalism where we can take advantage of the fact that for MHV diagrams the pole structures are explicit. In the next section we will extend this approach and show that the MHV formalism can not only be applied to the study of the infrared behavior, but also to extract coefficient functions and Lipatov vertices.

## 8.3 Multi-Regge limits and MHV rules

### 8.3.1 Coefficient functions from MHV rules

In this section we describe how the MHV formalism can be used to extract the leading behavior of an amplitude in the multi-Regge kinematics. The MHV formalism provides an efficient way to compute the Lipatov vertices and coefficient functions by allowing one to identify *a priori* the set of diagrams that give a non-vanishing contribution in the multi-Regge limit. It is hence not necessary to compute the full set of MHV diagrams that contribute to  $A_n(1, \dots, n)$ , as it was done in Ref. [25], but we can reject *a priori* those diagrams that give only subleading contributions.

We start by analyzing the quasi multi-Regge limit describing the emission of  $(n - 3)$  gluons at one end of the ladder, Eq. (8.30). The set of MHV diagrams that contribute to this limit is defined by the following rule:

**Rule 8.1.** *In the quasi multi-Regge limit defined by the rapidity-ordering (8.30) only those MHV diagrams contribute where  $p_1$  and  $p_n$  are attached to the same  $m$ -point MHV vertex,  $m \geq 4$ .*

The proof of this rule, based on simple powercounting arguments, is given in Appendix E. Note that this rule is natural, because all diagrams defined in this way have a  $t$ -channel propagator of the form  $1/(p_1 + p_n + \dots)^2$ . The rule then defines the set of MHV diagrams that contribute in the high-energy limit, all other diagrams being subleading. Furthermore, this set also has the correct collinear behavior. Indeed we know from Rule 5.1 that in the limit where the particles  $3, 4, \dots, (n-1)$  become collinear, only those MHV diagrams contribute where  $1, 2$  and  $n$  are attached to the same MHV vertex. It is easy to see that the set of diagrams defined by Rule 8.1 encompasses this set.

Let us make some comment about the role of the arbitrary spinor  $\eta$  in this context. We know that in the full amplitude the  $\eta$  dependence always cancels out in the sum over all diagrams. In Rule 8.1, however, we only consider a subset of MHV diagrams, and so the analytic cancellation of the  $\eta$ -dependent terms is not obvious. Indeed, we know from the antenna functions studied in Chapter 5 that this cancellation is not bound to take place if only a subset of diagrams is considered. Unlike antenna functions, coefficient functions are universal gauge invariant quantities defined in a unique way, and so a dependence on the unphysical quantity  $\eta$  is inadmissible. Alternatively, we could expect the coefficient functions to be analytically dependent on  $\eta$  and only numerically independent. In the following we show that the  $\eta$  dependence always drops out analytically in the leading term in the Regge limit.

In terms of lightcone coordinates, the limit of interest in is defined by

$$p_3^+ \simeq p_4^+ \simeq \dots \simeq p_{n-1}^+ \gg p_n^+, \eta^+. \quad (8.37)$$

Since  $\eta$  is a constant and no limit is taken on it, we include  $\eta$  in the right-hand side of Eq. (8.37). We already know from Chapter 2 that the only way  $\eta$  enters a given MHV diagram is through off-shell continued spinor products of the form (2.7), *i.e.*,

$$[\ell\eta] = \eta_\perp^* \sqrt{\frac{p_\ell^+}{\eta^+}} - p_{\ell\perp}^* \sqrt{\frac{\eta^+}{p_\ell^+}}. \quad (8.38)$$

In the limit (8.37) the second term is suppressed with respect to the first one, and so we find,

$$\langle kP_{ij} \rangle \simeq \sum_{\ell=i}^j \langle k\ell \rangle \eta_{\perp}^* \sqrt{\frac{p_{\ell}^+}{\eta^+}} \simeq \frac{\eta_{\perp}^*}{\sqrt{\eta^+}} \sqrt{-p_2^+} \Delta(k, i, j), \quad (8.39)$$

where we defined

$$\Delta(k, i, j) = \sum_{\ell=i}^j \sqrt{x_{\ell}} \langle k\ell \rangle, \quad (8.40)$$

with  $x_{\ell}$  defined in Eq. (8.25). From Eq. (8.39) we see that in the high-energy limit all off-shell continued spinor products are proportional to  $\eta_{\perp}^*/\sqrt{\eta^+}$ . Furthermore, it is easy to see that an MHV diagram must contain the same number of off-shell continued spinor products in the numerator and in the denominator, and so the overall scale factor  $\eta_{\perp}^*/\sqrt{\eta^+}$  cancels out.

### 8.3.2 Lipatov vertices from MHV rules

We know from Eq. (8.35) that the coefficient function  $C_{n-3}^{(0)}$  contains the Lipatov vertex  $V_{n-4}^{(0)}$  in the limit where  $y_3$  becomes much larger than any of the  $y_i$ ,  $4 \leq i \leq (n-1)$ . Hence, the set of MHV diagrams defined by Rule 8.1 contains at the same time all the MHV diagrams that contribute to  $V_{n-4}^{(0)}$ . Our rule can thus also be used to extract the generalized Lipatov vertices by taking the appropriate limit. Furthermore, from the previous discussion it is clear that the Lipatov vertices are always analytically independent of the arbitrary spinor  $\eta$ , as they should.

In the following sections we use this approach to derive explicit expressions for the Lipatov vertices  $V_k^{(0)}$  with  $k \leq 4$  and we give explicit results for independent vertices, all other ones being related to the independent ones by parity and reflection identity,

$$\begin{aligned} V_k^{(0)}(q_1; 1^{h_1}, \dots, k^{h_k}; q_2) &= \left[ V_k^{(0)}(q_1; 1^{-h_1}, \dots, k^{-h_k}; q_2) \right]^* \\ V_k^{(0)}(q_1; 1^{h_1}, \dots, k^{h_k}; q_2) &= (-1)^k V_k^{(0)}(q_2; k^{h_k}, \dots, 1^{h_1}; q_1). \end{aligned} \quad (8.41)$$

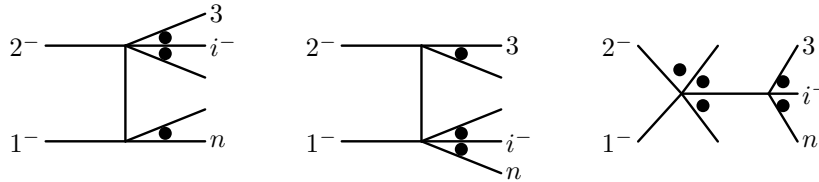


Figure 8.2: NMHV-type MHV diagrams of  $A_n(1^-, \dots, i^-, \dots, n^-)$  contributing in the high-energy limit. The dots indicate an arbitrary number of positive-helicity gluons.

Since we work with the MHV formalism, it is useful to classify the Lipatov vertices according to the number  $N$  of negative-helicity gluons in the vertex:

1.  $N = 0$ : MHV-type Lipatov vertices.  
All gluons entering the Lipatov vertex have positive helicity. All MHV-type Lipatov vertices have the same analytic structure given by Eq. (8.24).
2.  $N = 1$ : NMHV-type Lipatov vertices.  
Only one gluon has negative helicity. The MHV topologies contributing to this type of Lipatov vertex are shown in Fig. 8.2.
3.  $N = 2$ : NNMHV-type Lipatov vertices.  
Exactly two gluon have negative helicity. There are 16 MHV topologies contributing to this type of Lipatov vertex.
4. *etc.*

In the following sections we present the results for the generalized Lipatov vertices using our rule. The expressions we obtain are characterized by a much simpler form than the corresponding expressions of Ref. [25].

### 8.3.3 The $g^*g^* \rightarrow gg$ Lipatov vertices

There are two independent Lipatov vertices for  $g^*g^* \rightarrow gg$ , one of them being of MHV-type. The NMHV-type vertex is given by

$$\begin{aligned}
V_2^{(0)}(q_1; 1^+, 2^-; q_2) = & \\
& \frac{|q_{1\perp}|^2 x_1^{3/2} p_{2\perp}^3}{\sqrt{x_2} \langle 12 \rangle (x_2 |p_{1\perp}|^2 + x_1 |p_{2\perp}|^2)} p_{1\perp} (p_{1\perp} + p_{2\perp}) \\
& + \frac{q_{1\perp}^* x_1^{3/2} (q_{2\perp} + p_{2\perp})^3}{(q_{2\perp} \sqrt{x_1} - \sqrt{x_2} \langle 12 \rangle) (x_2 |p_{1\perp}|^2 + x_1 |p_{1\perp} - q_{1\perp}|^2)} p_{1\perp} \quad (8.42) \\
& + \frac{q_{1\perp} q_{2\perp} \sqrt{x_1} x_2^{3/2}}{(x_1 + x_2) \langle 12 \rangle (x_2 p_{1\perp} + x_1 (p_{1\perp} - q_{1\perp}))} \\
& - \frac{q_{1\perp}^* q_{2\perp} x_1^{3/2}}{\sqrt{x_2} (x_1 + x_2) (p_{1\perp} + p_{2\perp}) [12]}
\end{aligned}$$

We checked that our result numerically agrees with the result of Ref. [25] and that it has the correct collinear and multi-Regge limits.

### 8.3.4 The $g^*g^* \rightarrow ggg$ Lipatov vertices

There are four independent Lipatov vertices for the emission of three gluons, one of them being of MHV type, the remaining three being of NMHV type. We checked numerically that our result agrees with the result in Ref. [25] and that it has the correct collinear and multi-Regge limits. The three independent

NMHV-type vertices are given by

$$\begin{aligned}
V_3^{(0)}(q_1; 1^-, 2^+, 3^+; q_2) = & \\
& \frac{|q_{1\perp}|^2 q_{2\perp} x_2^{3/2} p_{1\perp}^3}{\langle 12 \rangle p_{2\perp} (p_{1\perp} + p_{2\perp}) (-q_{1\perp} + p_{1\perp} + p_{2\perp}) p_{3\perp} \sqrt{x_1} \left( |p_{2\perp}|^2 x_1 + |p_{1\perp}|^2 x_2 \right)} \\
& - \frac{q_{1\perp}^* q_{2\perp} \sqrt{x_2} (x_2 + x_3)^3 p_{1\perp}^3}{\langle 23 \rangle (p_{1\perp} - q_{1\perp}) \sqrt{x_3} \left( (p_{1\perp} - q_{1\perp}) x_1 + p_{1\perp} x_2 + p_{1\perp} x_3 \right)} \\
& \times \frac{1}{\sqrt{x_1 x_2} \langle 12 \rangle + p_{2\perp} x_1 + (p_{2\perp} - q_{1\perp}) x_2 + p_{2\perp} x_3} \\
& \times \frac{1}{p_{1\perp}^* \left( (p_{1\perp} - q_{1\perp}) x_1 + p_{1\perp} x_2 + p_{1\perp} x_3 \right) - q_{1\perp}^* (p_{1\perp} - q_{1\perp}) x_1} \\
& + x_2 \left( - \frac{|q_{1\perp}|^2 x_3^{3/2} p_{1\perp}^3}{(q_{2\perp} - q_{1\perp}) \langle 12 \rangle \langle 23 \rangle p_{3\perp} \sqrt{x_1}} \right. \\
& \times \frac{1}{\left( |p_{1\perp}|^2 x_2 x_3 + x_1 \left( |p_{3\perp}|^2 x_2 + |p_{2\perp}|^2 x_3 \right) \right)} \\
& \left. - \frac{q_{1\perp}^* x_3^2 p_{1\perp}^3}{\langle 12 \rangle (q_{2\perp} + p_{3\perp}) \sqrt{x_1} \left( \langle 23 \rangle \sqrt{x_3} - q_{2\perp} \sqrt{x_2} \right)} \right. \\
& \times \frac{1}{\left( |p_{1\perp}|^2 x_2 x_3 + x_1 \left( |q_{2\perp} + p_{3\perp}|^2 x_2 + |p_{2\perp}|^2 x_3 \right) \right)} \\
& + \frac{|q_{1\perp}|^2 q_{2\perp} \sqrt{x_2}}{\langle 23 \rangle (p_{1\perp} - q_{1\perp}) p_{2\perp} p_{1\perp}^* \sqrt{x_3}} - \frac{q_{1\perp}^* q_{2\perp} \langle 12 \rangle x_2^{3/2}}{s_{12} (p_{1\perp} + p_{2\perp}) \sqrt{x_1} \sqrt{x_3} \Delta(3; 1, 2)} \\
& - \frac{q_{1\perp}^* q_{2\perp} \Delta(1; 2, 3)^3}{s_{123} \langle 12 \rangle \langle 23 \rangle (p_{1\perp} + p_{2\perp} + p_{3\perp}) (x_1 + x_2 + x_3) \Delta(3; 1, 2)} \\
& + \frac{q_{1\perp} q_{2\perp} x_1^{5/2}}{\langle 12 \rangle \langle 23 \rangle \sqrt{x_3} (x_1 + x_2 + x_3) \left( (p_{1\perp} - q_{1\perp}) x_1 + p_{1\perp} x_2 + p_{1\perp} x_3 \right)}, \tag{8.43}
\end{aligned}$$



$$\begin{aligned}
V_3^{(0)}(q_1; 1^+, 2^-, 3^+; q_2) = & \\
& - \frac{|q_{1\perp}|^2 x_1^{3/2} x_3^{3/2} p_{2\perp}^4}{(q_{2\perp} - q_{1\perp}) \langle 12 \rangle \langle 23 \rangle p_{1\perp} p_{3\perp} x_2} \\
& \quad \times \frac{1}{\left( |p_{1\perp}|^2 x_2 x_3 + x_1 \left( |p_{3\perp}|^2 x_2 + |p_{2\perp}|^2 x_3 \right) \right)} \\
& + \frac{q_{1\perp}^* x_1^{3/2} x_3^2 p_{2\perp}^4}{\langle 12 \rangle p_{1\perp} (q_{2\perp} + p_{3\perp}) x_2 (q_{2\perp} \sqrt{x_2} - \langle 23 \rangle \sqrt{x_3})} \\
& \quad \times \frac{1}{\left( |p_{1\perp}|^2 x_2 x_3 + x_1 \left( |q_{2\perp} + p_{3\perp}|^2 x_2 + |p_{2\perp}|^2 x_3 \right) \right)} \\
& + \frac{|q_{1\perp}|^2 q_{2\perp} x_1^{3/2} p_{2\perp}^3}{\langle 12 \rangle p_{1\perp} (p_{1\perp} + p_{2\perp}) (-q_{1\perp} + p_{1\perp} + p_{2\perp}) p_{3\perp} \sqrt{x_2}} \\
& \quad \times \frac{1}{\left( |p_{2\perp}|^2 x_1 + |p_{1\perp}|^2 x_2 \right)} \\
& + \frac{q_{1\perp} q_{2\perp} \sqrt{x_1} x_2^2}{\langle 12 \rangle \langle 23 \rangle \sqrt{x_3} (x_1 + x_2 + x_3) ((p_{1\perp} - q_{1\perp}) x_1 + p_{1\perp} x_2 + p_{1\perp} x_3)} \\
& - \frac{q_{1\perp}^* q_{2\perp} (p_{1\perp} - q_{1\perp})^3 x_1^2 x_2^{5/2}}{\langle 23 \rangle p_{1\perp} \sqrt{x_3} (x_2 + x_3) ((p_{1\perp} - q_{1\perp}) x_1 + p_{1\perp} x_2 + p_{1\perp} x_3)} \\
& \quad \times \frac{1}{\left( \sqrt{x_1 x_2} \langle 12 \rangle + p_{2\perp} x_1 + (p_{2\perp} - q_{1\perp}) x_2 + p_{2\perp} x_3 \right)} \\
& \quad \times \frac{1}{\left( p_{1\perp}^* ((p_{1\perp} - q_{1\perp}) x_1 + p_{1\perp} x_2 + p_{1\perp} x_3) - q_{1\perp}^* (p_{1\perp} - q_{1\perp}) x_1 \right)} \\
& + \frac{q_{1\perp}^* q_{2\perp} \langle 23 \rangle \sqrt{x_1} x_3^{3/2}}{s_{23} p_{1\perp} \sqrt{x_2} (x_2 + x_3) \Delta(1; 2, 3)} \\
& - \frac{q_{1\perp}^* q_{2\perp} \langle 12 \rangle x_1^{3/2}}{s_{12} (p_{1\perp} + p_{2\perp}) \sqrt{x_2} \sqrt{x_3} \Delta(3; 1, 2)} \\
& - \frac{q_{1\perp}^* q_{2\perp} \Delta(2; 3, 1)^4}{s_{123} \langle 12 \rangle \langle 23 \rangle (p_{1\perp} + p_{2\perp} + p_{3\perp}) (x_1 + x_2 + x_3) \Delta(1; 2, 3) \Delta(3; 1, 2)}, \tag{8.44}
\end{aligned}$$

$$\begin{aligned}
V_3^{(0)}(q_1; 1^+, 2^+, 3^-; q_2) = & \\
& - \frac{q_{1\perp}^* q_{2\perp} x_1^2 \sqrt{x_2} x_3^{3/2} (p_{1\perp} - q_{1\perp})^3}{\langle 23 \rangle p_{1\perp} (x_2 + x_3) ((p_{1\perp} - q_{1\perp}) x_1 + p_{1\perp} x_2 + p_{1\perp} x_3)} \\
& \times \frac{1}{(\sqrt{x_1 x_2} \langle 12 \rangle + p_{2\perp} x_1 + (p_{2\perp} - q_{1\perp}) x_2 + p_{2\perp} x_3)} \\
& \times \frac{1}{(p_{1\perp}^* ((p_{1\perp} - q_{1\perp}) x_1 + p_{1\perp} x_2 + p_{1\perp} x_3) - q_{1\perp}^* (p_{1\perp} - q_{1\perp}) x_1)} \\
& - \frac{q_{1\perp}^* q_{2\perp} \Delta(6; 4, 5)^3}{s_{123} \langle 12 \rangle \langle 23 \rangle (p_{1\perp} + p_{2\perp} + p_{3\perp}) (x_1 + x_2 + x_3) \Delta(4; 5, 6)} + x_2 \\
& \times \left\{ \frac{q_{1\perp}^* (q_{2\perp} + p_{3\perp})^3 x_1^{3/2}}{\langle 12 \rangle p_{1\perp} (q_{2\perp} \sqrt{x_2} - \langle 23 \rangle \sqrt{x_3})} \right. \\
& \times \frac{1}{\left[ |p_{1\perp}|^2 x_2 x_3 + x_1 \left( |q_{2\perp} + p_{3\perp}|^2 x_2 + |p_{2\perp}|^2 x_3 \right) \right]} \\
& \left. - \frac{|q_{1\perp}|^2 p_{3\perp}^3 x_1^{3/2}}{(q_{2\perp} - q_{1\perp}) \langle 12 \rangle \langle 23 \rangle p_{1\perp} \sqrt{x_3}} \right\} \\
& \times \frac{1}{\left[ |p_{1\perp}|^2 x_2 x_3 + x_1 \left( |p_{3\perp}|^2 x_2 + |p_{2\perp}|^2 x_3 \right) \right]} \\
& + \frac{q_{1\perp} q_{2\perp} \sqrt{x_1} x_3^{3/2}}{\langle 12 \rangle \langle 23 \rangle (x_1 + x_2 + x_3) ((p_{1\perp} - q_{1\perp}) x_1 + p_{1\perp} x_2 + p_{1\perp} x_3)} \\
& + \frac{q_{1\perp}^* q_{2\perp} \langle 23 \rangle \sqrt{x_1} x_2^{3/2}}{s_{23} p_{1\perp} \sqrt{x_3} (x_2 + x_3) \Delta(4, 5, 6)}, \tag{8.45}
\end{aligned}$$

where  $\Delta(k, i, j)$  was defined in Eq. (8.40).

### 8.3.5 The $g^* g^* \rightarrow gggg$ Lipatov vertices

There are eight independent  $g^* g^* \rightarrow gggg$  Lipatov vertices, one of MHV type, four NMHV and three NNMHV-type vertices. As the analytic expressions are quite lengthy, they are listed explicitly in Appendix O. Note that unlike for the Lipatov vertices for the emission of two or three gluons, no analytic results for the  $g^* g^* \rightarrow gggg$  Lipatov vertices can be found in the literature. As a cross-check we checked that our results have the correct collinear and multi-Regge

factorization properties. The NMHV-type vertices can be written in the form

$$\begin{aligned}
V_4^{(0)}(q_1; 1^-, 2^+, 3^+, 4^+; q_2) &= \sum_{k=1}^{11} \frac{N^{(k)}(q_1; 1^-, 2^+, 3^+, 4^+; q_2)}{D^{(k)}(q_1; 1^-, 2^+, 3^+, 4^+; q_2)}, \\
V_4^{(0)}(q_1; 1^+, 2^-, 3^+, 4^+; q_2) &= \sum_{k=1}^{12} \frac{N^{(k)}(q_1; 1^+, 2^-, 3^+, 4^+; q_2)}{D^{(k)}(q_1; 1^+, 2^-, 3^+, 4^+; q_2)}, \\
V_4^{(0)}(q_1; 1^+, 2^+, 3^-, 4^+; q_2) &= \sum_{k=1}^{11} \frac{N^{(k)}(q_1; 1^+, 2^+, 3^-, 4^+; q_2)}{D^{(k)}(q_1; 1^+, 2^+, 3^-, 4^+; q_2)}, \\
V_4^{(0)}(q_1; 1^+, 2^+, 3^+, 4^-; q_2) &= \sum_{k=1}^8 \frac{N^{(k)}(q_1; 1^+, 2^+, 3^+, 4^-; q_2)}{D^{(k)}(q_1; 1^+, 2^+, 3^+, 4^-; q_2)},
\end{aligned} \tag{8.46}$$

where the numerator and denominator functions  $N^{(k)}$  and  $D^{(k)}$  are combinations of spinor products and lightcone components of the momenta, *e.g.* ,

$$\begin{aligned}
N^{(1)}(q_1; 1^-, 2^+, 3^+, 4^+; q_2) &= -q_{1\perp}^* q_{2\perp} p_{1\perp}^3 x_2 x_3^{3/2}, \\
D^{(1)}(q_1; 1^-, 2^+, 3^+, 4^+; q_2) &= \langle 12 \rangle \langle 23 \rangle (q_{1\perp} + p_{1\perp} + p_{2\perp}) (2q_{1\perp} + p_{1\perp} + p_{2\perp}) \\
&\quad p_{4\perp} \sqrt{x_1} \left( q_{1\perp} q_{1\perp}^* x_1 x_2 + \left( |p_{2\perp}|^2 x_1 + |p_{1\perp}|^2 x_2 \right) x_3 \right).
\end{aligned}$$

The complete set of NMHV numerator and denominator functions is listed in Appendix O.1. There are only three independent helicity configurations, all other configurations being related to the independent ones by reflection identity and parity. The NNMHV-type vertices can be written in the form,

$$\begin{aligned}
V^{4g}(q_1; 1^-, 2^-, 3^+, 4^+; q_2) &= \sum_{k=1}^{39} \frac{N^{(k)}(q_1; 1^-, 2^-, 3^+, 4^+; q_2)}{D^{(k)}(q_1; 1^-, 2^-, 3^+, 4^+; q_2)}, \\
V^{4g}(q_1; 1^-, 2^+, 3^-, 4^+; q_2) &= \sum_{k=1}^{50} \frac{N^{(k)}(q_1; 1^-, 2^+, 3^-, 4^+; q_2)}{D^{(k)}(q_1; 1^-, 2^+, 3^-, 4^+; q_2)}, \\
V^{4g}(q_1; 1^+, 2^-, 3^-, 4^+; q_2) &= \sum_{k=1}^{43} \frac{N^{(k)}(q_1; 1^+, 2^-, 3^-, 4^+; q_2)}{D^{(k)}(q_1; 1^+, 2^-, 3^-, 4^+; q_2)},
\end{aligned} \tag{8.47}$$

The complete set of NNMHV numerator and denominator functions is listed in Appendix O.2.



# Chapter 9

## High-energy factorization beyond tree-level

### 9.1 The high-energy prescription

In the previous chapter we introduced the factorization of a tree-level amplitude in the multi-Regge limit in terms of coefficient functions and Lipatov vertices. In this chapter we conjecture that high-energy factorization holds true even beyond tree-level and we introduce our notations and conventions.

The high-energy limit can be characterized by the fact that the  $s$ -type invariants are much larger than the  $t$ -type invariants, and the perturbative expansion might therefore contain large logarithms of the form  $\ln(s/t)$ . The virtual radiative corrections to Eq. (8.16) in the leading logarithmic (LL) approximation are obtained, to all orders in  $\alpha_s$ , by replacing the propagator of the  $t$ -channel gluon by its reggeized form [86]. That is, by making the replacement

$$\frac{1}{t_i} \rightarrow \frac{1}{t_i} \left( \frac{s_i}{\tau} \right)^{\alpha(t_i; \epsilon)}, \quad (9.1)$$

in Eq. (8.16), where  $\alpha(t_i; \epsilon)$  can be written in dimensional regularization in  $D = 4 - 2\epsilon$  dimensions as

$$\alpha(t_i; \epsilon) = g^2 c_\Gamma \left( \frac{\mu^2}{-t_i} \right)^\epsilon N_c \frac{2}{\epsilon}. \quad (9.2)$$

$\alpha(t_i; \epsilon)$  is the Regge trajectory and accounts for the higher order corrections due to gluon exchange in the  $t_i$  channel. In Eq. (9.1), the reggeization scale  $\tau$  is much smaller than any of the  $s$ -type invariants, and it is of the order of the  $t$ -type invariants.

In order to extend the factorization (8.16) beyond tree-level, we need a prescription that tells us how to disentangle the higher-order corrections that reggeize the gluon (9.1) from those to the Lipatov vertex and the coefficient functions, *i.e.*, we need a prescription that tells us how to distribute the radiative corrections between the different universal building blocks in a consistent way. We will give an explicit example of how this prescription works in the next section. In Ref. [26, 27] a high-energy prescription at the level of the color-ordered amplitudes was presented, which was shown to be valid up to three loops for the color-stripped four-point amplitude. We follow here this prescription, and we conjecture that in multi-Regge kinematics an  $n$ -point color-ordered gluon amplitude takes the factorized form

$$\begin{aligned} A_n(1, 2, \dots, n) &= s C(p_2, p_3; \epsilon, \tau) \frac{1}{t_{n-3}} \left( \frac{-s_{n-3}}{\tau} \right)^{\alpha(t_{n-3}; \epsilon)} \\ &\times V(q_{n-3}, p_4, q_{n-4}; \epsilon, \tau) \cdots \times \frac{1}{t_2} \left( \frac{-s_2}{\tau} \right)^{\alpha(t_2; \epsilon)} V(q_2, p_{n-1}, q_1; \epsilon, \tau) \\ &\times \frac{1}{t_1} \left( \frac{-s_1}{\tau} \right)^{\alpha(t_1; \epsilon)} C(p_1, p_n; \epsilon, \tau). \end{aligned} \quad (9.3)$$

Eq. (9.3) is explicitly given in the euclidean region where all the invariants are negative. We will comment on the analytic continuation to the physical region where all  $s$ -type invariants are positive at the end of this chapter. In the euclidean region the multi-Regge limit is defined by extending the hierarchy of scales (8.6) to the region where all invariants are negative,

$$(-s) \gg (-s_1), \dots, (-s_{n-3}) \gg (-t_1), \dots, (-t_{n-3}), \quad (9.4)$$

and the mass-shell conditions for the reggeized gluons now read

$$(-\kappa_i) = -|p_{i\perp}|^2 = \frac{(-s_i)(-s_{i+1})}{(-s_{n-i-1, n-i, n-i+1})}, \quad \text{for } 1 \leq i \leq n-4, \quad (9.5)$$

together with the constraint

$$(-s)(-\kappa_1) \dots (-\kappa_{n-4}) = (-s_1) \dots (-s_{n-3}). \quad (9.6)$$

In Eq. (9.3) the Regge trajectory  $\alpha$ , the coefficient function  $C$  and the Lipatov vertex  $V$  can be expanded into a perturbative series,

$$\begin{aligned}\alpha(t_i; \epsilon) &= \sum_{n=1}^{\infty} \bar{g}^{2n} \bar{\alpha}^{(n)}(t_i; \epsilon), \\ C(p_i, p_j; \epsilon; \tau) &= C^{(0)}(p_i; p_j) \left( 1 + \sum_{n=1}^{\infty} \bar{g}^{2n} \bar{C}^{(n)}(t_{ij}; \epsilon, \tau) \right), \\ V(q_j, p_{n-j}, q_{j+1}; \epsilon; \tau) &= V^{(0)}(q_j; p_{n-j}; q_{j+1}) \left( 1 + \sum_{n=1}^{\infty} \bar{g}^{2n} \bar{V}^{(n)}(t_{j+1}, t_j, \kappa_j; \epsilon, \tau) \right),\end{aligned}\tag{9.7}$$

with  $t_{ij} = (p_i + p_j)^2$  and

$$\bar{g}^2 = g^2 c_{\Gamma} N_c.\tag{9.8}$$

The tree-level coefficient function  $C^{(0)}$  and Lipatov vertex  $V^{(0)}$  have been defined in Chapter 8, and  $\bar{C}^{(n)}$  and  $\bar{V}^{(n)}$  denote the  $n$ -loop quantities rescaled by the tree-level quantity. For later convenience we factor out explicitly the dependence on the renormalization scale  $\mu^2$ ,

$$\begin{aligned}\bar{\alpha}^{(n)}(t_i; \epsilon) &= \left( \frac{\mu^2}{-t_i} \right)^{n\epsilon} \alpha^{(n)}(t_i; \epsilon), \\ \bar{C}^{(n)}(p_i, p_j; \epsilon, \tau) &= \left( \frac{\mu^2}{-t_k} \right)^{n\epsilon} C^{(n)}(t_{ij}; \epsilon, \tau), \\ \bar{V}^{(n)}(q_{j+1}, q_j, \kappa_j; \epsilon, \tau) &= \left( \frac{\mu^2}{-\kappa_j} \right)^{n\epsilon} V^{(n)}(t_{j+1}, t_j, \kappa_j; \epsilon, \tau).\end{aligned}\tag{9.9}$$

Inserting Eqs. (9.7) - (9.9) into Eq. (9.3), we can match the left and right-hand sides to extract the explicit expressions of the Regge trajectory, the coefficient function and the Lipatov vertex at a given order in the perturbative expansion in the rescaled coupling. We illustrate this procedure explicitly on the examples of the four and five-point MSYM amplitudes in the next section.

## 9.2 MSYM amplitudes in the high-energy limit

### 9.2.1 The four-point MSYM amplitude in the high-energy limit

In this section we analyze the multi-Regge limit of MSYM gluon amplitudes. The tree-level case was already dealt with in Chapter 8, so we only concentrate on higher-order contributions in the perturbative expansion. In Section 9.1 we defined the perturbative expansion of the building blocks in the multi-Regge limit in terms of the rescaled coupling (9.8) rather than the 't Hooft coupling,

$$A_n(1, \dots, n; \epsilon) = A_n^{(0)}(1, \dots, n) \left( 1 + \sum_{\ell=1}^{\infty} \bar{g}^{2\ell} m_n^{(\ell)}(1, \dots, n; \epsilon) \right), \quad (9.10)$$

*i.e.*, we define the quantity  $m_n^{(\ell)}$  such that

$$a^\ell M_n^{(\ell)}(1, \dots, n; \epsilon) = \bar{g}^{2\ell} m_n^{(\ell)}(1, \dots, n; \epsilon). \quad (9.11)$$

A simple calculation shows that we must have,

$$m_n^{(\ell)}(1, \dots, n; \epsilon) = 2 G(\epsilon) M_n^{(\ell)}(1, \dots, n; \epsilon), \quad (9.12)$$

with

$$G(\epsilon) = \frac{\Gamma(1-2\epsilon) e^{-\gamma_E \epsilon}}{\Gamma(1+\epsilon) \Gamma(1-\epsilon)^2} = 1 + \mathcal{O}(\epsilon^2). \quad (9.13)$$

Let us now turn to the computation of the multi-Regge building blocks, and let us start with the four-point one-loop amplitude. The high-energy prescription (9.3) reduces to

$$A_4(1, 2, 3, 4; \epsilon) = s C(p_2, p_3; \epsilon, \tau) \frac{1}{t} \left( \frac{-s}{\tau} \right)^{\alpha(t; \epsilon)} C(p_1, p_4; \epsilon, \tau). \quad (9.14)$$

Expanding Eq. (9.14) to one-loop accuracy, we find

$$m_4^{(1)}(1, \dots, n; \epsilon) = 2 \bar{C}^{(1)}(t; \epsilon, \tau) + \bar{\alpha}^{(1)}(t; \epsilon) L, \quad (9.15)$$

with  $L = \ln(-s/\tau)$ . Our aim is to extract the explicit expressions for the one-loop coefficient function and Regge trajectory from Eq. (9.15). Since these



quantities are universal, we can extract them from the four-point amplitude and reuse them in other computations. The procedure goes as follows: We can explicitly compute the one-loop four-point amplitude in the left-hand side of Eq. (9.15) in the high-energy limit, and then match the left and right-hand sides to extract the coefficient function and the Regge trajectory. The high-energy prescription introduced in the previous section instructs us how to do this matching consistently, by assigning the coefficient of the logarithm to the trajectory, and all the rest to the coefficient function. This consistent matching is required because otherwise inconsistencies arise when reusing the building blocks in other computations.

Let us now turn to the explicit computation of the one-loop four-point amplitude in the high-energy limit. The one-loop four-point amplitude can be written in terms of the scalar massless box integral,

$$m_4^{(1)}(s, t; \epsilon) = -G(\epsilon) \mu^{2\epsilon} st I_4^{4-2\epsilon}(s, t), \quad (9.16)$$

where the scalar massless box integral in  $D$  dimensions is defined by (See Appendix K),

$$I_4^D(s, t) = e^{\gamma_E \epsilon} \int \frac{d^D k}{i\pi^{D/2}} \frac{1}{D_1 D_2 D_3 D_4}, \quad (9.17)$$

with

$$D_1 = k^2 + i0, \\ D_i = \left( k + \sum_{j=1}^{i-1} p_j \right)^2 + i0, \quad i = 2, \dots, 4. \quad (9.18)$$

Although explicit expression for the massless box integral can be found in the literature, we illustrate the computation of the leading behavior in the high-energy limit by starting from the Mellin-Barnes representation of the massless box integral (See Appendix K)

$$I_4^{4-2\epsilon}(s, t) = -\frac{2 r_\Gamma e^{\gamma_E \epsilon}}{\Gamma(1+\epsilon)\Gamma(1-\epsilon)^2} (-t)^{-2-\epsilon} \\ \times \frac{1}{2\pi i} \int_{-i\infty}^{+i\infty} dz \Gamma(-z) \Gamma(2+\epsilon+z) \Gamma(1+z)^2 \Gamma(-1-\epsilon-z)^2 \left(\frac{s}{t}\right)^{z+1}, \quad (9.19)$$

with

$$r_\Gamma = \frac{\Gamma(1+\epsilon)\Gamma(1-\epsilon)^2}{\Gamma(1-2\epsilon)}. \quad (9.20)$$

Eq. (9.19) is a representation of the scalar massless box integral as a contour integral in the complex plane. We would like to close the integration contour at infinity and evaluate the integral using the residue theorem. The poles in the integrand come from the poles of the  $\Gamma$  function, which has single poles for negative integer values of the argument. The residues of the poles are given by the formula,

$$\text{Res}_{z=-n} \Gamma(z) = \frac{(-1)^n}{n!}. \quad (9.21)$$

The integral is however ill-defined, because we need a prescription of how to deal for example with the pole in  $z = 0$ , which lies on the imaginary axis. We thus need a prescription for how the contour encircles the singularity in  $z = 0$ . It can be shown that the correct prescription is that the contour should separate the poles in  $\Gamma(\dots - z)$  from those in  $\Gamma(\dots + z)$ . After having defined the contour in an unambiguous way, we can close it to the left at infinity and take residues. There are two  $\Gamma$  functions whose residues fall inside the contour,

1.  $\Gamma(1+z)$ : poles in  $z = -1 - n$ ,  $n \in \mathbb{N}$ .
2.  $\Gamma(2+\epsilon+z)$ : poles in  $z = -2 - \epsilon - n$ ,  $n \in \mathbb{N}$ .

Summing up all the residues of the  $\Gamma$  functions, we obtain a representation of the integral as a power series in  $t/s$ . Since we are not interested in the full answer for  $I_4^{4-2\epsilon}$ , but only in the leading term in the limit  $s \gg t$ , we only keep the leading term in the power series expansion, or equivalently, only the residue corresponding to the leftmost pole, *i.e.*, in  $z = -1$  [90]. We find,

$$m_4^{(1)}(s, t; \epsilon) = \left(\frac{\mu^2}{-t}\right)^\epsilon \left\{ 2 \left[ \frac{\psi(1+\epsilon) - 2\psi(-\epsilon) - \gamma_E}{\epsilon} - \frac{1}{\epsilon} \ln \frac{-t}{\tau} \right] + \frac{2}{\epsilon} L \right\}, \quad (9.22)$$

where  $\psi$  denotes the digamma function,  $\psi(z) = \frac{d}{dz} \ln \Gamma(z)$ . Comparing the expression of  $m_4^{(1)}(s, t; \epsilon)$  in Eq. (9.22) to Eq. (9.15), we can immediately read

off the expressions to all order in  $\epsilon$  for the one-loop coefficient function and the Regge trajectory [91, 92],

$$\begin{aligned} C^{(1)}(t; \epsilon, \tau) &= \frac{\psi(1+\epsilon) - 2\psi(-\epsilon) - \gamma_E}{\epsilon} - \frac{1}{\epsilon} \ln \frac{-t}{\tau} \\ \alpha^{(1)}(t; \epsilon) &= \frac{2}{\epsilon}. \end{aligned} \quad (9.23)$$

Before turning to the computation of the one-loop Lipatov vertex, let us quickly review how to iterate this procedure to extract the two-loop coefficient functions and Regge trajectory. At two loop accuracy, the high-energy prescription reads

$$\begin{aligned} m_4^{(2)} &= \frac{1}{2} \left( \bar{\alpha}^{(1)}(t; \epsilon) \right)^2 L^2 + \left( \bar{\alpha}^{(2)}(t; \epsilon) + 2\bar{C}^{(1)}(t, \tau)\bar{\alpha}^{(1)}(t; \epsilon) \right) L \\ &\quad + 2\bar{C}^{(2)}(t, \tau) + \left( \bar{C}^{(1)}(t, \tau) \right)^2 \\ &= \frac{1}{2} \left( m_4^{(1)} \right)^2 + \bar{\alpha}^{(2)}(t; \epsilon)L + 2\bar{C}^{(2)}(t, \tau) - \left( \bar{C}^{(1)}(t, \tau) \right)^2. \end{aligned} \quad (9.24)$$

Using the explicit expressions of the two-loop four-point amplitude in multi-Regge kinematics as well as the expression of the one-loop quantities (9.22) and (9.23), we can extract the two-loop Regge trajectory and the coefficient function. Explicit expressions can be found in Ref. [26].

## 9.2.2 The five-point MSYM amplitude in the high-energy limit

Let us now turn to the computation of the one-loop Lipatov vertex, which can be extracted from the five-point amplitude in the high-energy-limit. For  $n = 5$ , the high-energy prescription (9.3) reduces to,

$$\begin{aligned} A_5(1, 2, 3, 4, 5; \epsilon) &= s C(p_2, p_3; \epsilon, \tau) \frac{1}{t_2} \left( \frac{-s_2}{\tau} \right)^{\alpha(t_2; \epsilon)} \\ &\quad \times V(q_2, p_4, q_1; \epsilon, \tau) \frac{1}{t_1} \left( \frac{-s_1}{\tau} \right)^{\alpha(t_1; \epsilon)} C(p_1, p_5; \epsilon, \tau), \end{aligned} \quad (9.25)$$

and the mass-shell condition for the gluon emitted along the ladder reads

$$(-s)(-\kappa) = (-s_1)(-s_2). \quad (9.26)$$

Expanding Eq. (9.25) to one-loop accuracy, we find

$$m_5^{(1)} = \bar{\alpha}^{(1)}(t_1; \epsilon)L_1 + \bar{\alpha}^{(1)}(t_2; \epsilon)L_2 + \bar{C}^{(1)}(t_1; \epsilon, \tau) + \bar{C}^{(1)}(t_2; \epsilon, \tau) + \bar{V}^{(1)}(t_1, t_2, \kappa; \epsilon, \tau). \quad (9.27)$$

where  $L_i = \ln(-s_i/\tau)$  and  $i = 1, 2$ . The coefficient functions and Regge trajectories appearing in this expression are the same as in the four-point case. The five-point one-loop amplitude on the left-hand side can be expressed in terms of scalar one-mass boxes in  $D = 4 - 2\epsilon$  and a massless pentagon integral in  $D = 6 - 2\epsilon$  dimensions [84],

$$m_5^{(1)} = -\frac{1}{2}G(\epsilon) \sum_{\text{cyclic}} s_{12}s_{23}I_4^{1m}(1, 2, 3, 45, \epsilon) - \epsilon G(\epsilon) \epsilon_{1234}I_5^{6-2\epsilon}(\epsilon), \quad (9.28)$$

with

$$\epsilon_{1234} = \text{Tr}(p_1^\not{p}_1 p_2^\not{p}_2 p_3^\not{p}_3 p_4^\not{p}_4 \gamma^5), \quad (9.29)$$

and the cyclicity is over  $i = 1, \dots, 5$ .  $I_4^{1m}$  is the one-mass box in  $D = 4 - 2\epsilon$  dimension, with a massive leg of virtuality  $s_{45}$ , and  $I_5^{6-2\epsilon}$  denotes the massless pentagon integral in  $D = 6 - 2\epsilon$  dimensions. Note that  $I_5^{6-2\epsilon}$  is finite for  $\epsilon \rightarrow 0$ , and so it only contributes to  $\mathcal{O}(\epsilon)$  in four dimensions and can therefore be neglected. A representation to all order in  $\epsilon$  of  $I_4^{1m}$  in terms of Gauss' hypergeometric function was given in Ref. [93],

$$st I_4^{1m}(s, t, m^2; \epsilon) = \frac{2c_\Gamma}{\epsilon^2} \left\{ \left( \frac{t - m^2}{st} \right)^\epsilon {}_2F_1 \left( -\epsilon, -\epsilon, 1 - \epsilon; 1 + \frac{s}{t - m^2} \right) + \left( \frac{s - m^2}{st} \right)^\epsilon {}_2F_1 \left( -\epsilon, -\epsilon, 1 - \epsilon; 1 + \frac{t}{s - m^2} \right) - \left( \frac{(t - m^2)(s - m^2)}{-stm^2} \right)^\epsilon {}_2F_1 \left( -\epsilon, -\epsilon, 1 - \epsilon; 1 + \frac{st}{(t - m^2)(s - m^2)} \right) \right\}. \quad (9.30)$$

We want to compute the leading behavior of  $m_5^{(1)}$  in the limit defined by the hierarchy of scales (9.4). This can be achieved by expanding the hypergeometric functions in Eq. (9.30) in this limit. We give here the explicit example of  $I_4^{1m}(1, 2, 3, 45, \epsilon) = I_4^{1m}(t_2, s, s_1; \epsilon)$ . All other cases are obtained in a similar

way. Expanding the hypergeometric functions to leading order in  $t/s$ , we find

$$\begin{aligned}
& {}_2F_1\left(-\epsilon, -\epsilon, 1-\epsilon; 1 + \frac{t_2}{s-s_1}\right) \\
&= \Gamma(1+\epsilon)\Gamma(1-\epsilon) + \mathcal{O}\left(\frac{t_2}{s}\right), \\
& {}_2F_1\left(-\epsilon, -\epsilon, 1-\epsilon; 1 + \frac{s}{t_2-s_1}\right) \\
&= \epsilon\left(\frac{s}{s_1}\right)^\epsilon \left[\ln\frac{s_1}{s} + \gamma_E + \psi(-\epsilon)\right] + \mathcal{O}\left(\frac{s_1}{s}\right), \\
& {}_2F_1\left(-\epsilon, -\epsilon, 1-\epsilon; 1 + \frac{st_2}{(s-s_1)(t_2-s_1)}\right) \\
&= \Gamma(1+\epsilon)\Gamma(1-\epsilon) + \mathcal{O}\left(\frac{t_2}{s_1}\right).
\end{aligned} \tag{9.31}$$

Inserting these expressions into Eq. (9.30), it is easy to see that the first and the last term cancel, and we are left with

$$I_4^{1m}(1, 2, 3, 45, \epsilon) \simeq \epsilon(-t_2)^{-\epsilon} \left[\ln\frac{\kappa}{s_2} + \gamma_E + \psi(-\epsilon)\right], \tag{9.32}$$

where we made explicit use of Eq. (9.26). Repeating this operation for the other box integral in Eq. (9.28), we find an expression for the five-point one-loop amplitude in multi-Regge kinematics valid through  $\mathcal{O}(\epsilon^0)$ ,

$$\begin{aligned}
m_5^{(1)} = & \\
& -\frac{1}{\epsilon^2} \left(\frac{\mu^2}{\kappa}\right)^\epsilon \Gamma(1+\epsilon)\Gamma(1-\epsilon) \\
& -\frac{2}{\epsilon} \left(\frac{\mu^2}{-t_1}\right)^\epsilon (\gamma_E + \psi(-\epsilon)) \\
& +\frac{1}{\epsilon} \left(\frac{\mu^2}{-t_2}\right)^\epsilon (\psi(1+\epsilon) - 3\psi(-\epsilon) - 2\gamma_E) \\
& +\frac{1}{\epsilon^2} \left(\frac{\mu^2}{-t_1}\right)^\epsilon {}_2F_1\left(-\epsilon, 1, 1-\epsilon; \frac{t_1}{t_2}\right) \\
& -\frac{1}{\epsilon(1+\epsilon)} \left(\frac{\mu^2}{-t_2}\right)^\epsilon \frac{t_1}{t_2} {}_2F_1\left(1, 1+\epsilon, 2+\epsilon; \frac{t_1}{t_2}\right) \\
& +\frac{1}{\epsilon} \left(\frac{\mu^2}{-t_1}\right)^\epsilon \ln\frac{s_1}{\kappa} + \frac{1}{\epsilon} \left(\frac{\mu^2}{-t_2}\right)^\epsilon \ln\frac{s_2}{\kappa} \\
& +\frac{1}{\epsilon} \left(\frac{\mu^2}{-t_1}\right)^\epsilon \ln\frac{s_1}{t_2-t_1} + \frac{1}{\epsilon} \left(\frac{\mu^2}{-t_2}\right)^\epsilon \ln\frac{s_2}{t_2-t_1} + \mathcal{O}(\epsilon).
\end{aligned} \tag{9.33}$$

Eq. (9.33) is explicitly given in the euclidean region where all invariants are negative, which implies that Eq. (9.33) is manifestly real. The symmetry of the multi-Regge limit in  $t_1$  and  $t_2$  implies that  $m_5^{(1)}$  should have the same symmetry in multi-Regge kinematics. Eq. (9.33) however apparently breaks this symmetry, because only the ratio  $t_1/t_2$  appears. It can be put in a manifestly symmetric form, to the price of introducing spurious imaginary parts that cancel after combining all the terms.

We can now match this expression to the high-energy prescription (9.27). The coefficient functions and the Regge trajectories are the same as in the four-point case, so the only unknown in this relation is the one-loop Lipatov vertex through  $\mathcal{O}(\epsilon^0)$ ,

$$\begin{aligned}
\bar{V}^{(1)}(t_1, t_2, \kappa; \epsilon, \tau) = & \\
& - \frac{1}{\epsilon^2} \Gamma(1 + \epsilon) \Gamma(1 - \epsilon) \\
& + \frac{1}{\epsilon} \left( \frac{\kappa}{t_1} \right)^\epsilon \left( -\psi(1 + \epsilon) - \gamma_E + \ln \frac{-t_1}{\tau} \right) \\
& + \frac{1}{\epsilon} \left( \frac{\kappa}{t_2} \right)^\epsilon \left( -\psi(1 + \epsilon) - \gamma_E + \ln \frac{-t_2}{\tau} \right) \\
& + \frac{1}{\epsilon^2} \left( \frac{\kappa}{t_1} \right)^\epsilon {}_2F_1 \left( \epsilon, 1, 1 - \epsilon; \frac{t_1}{t_2} \right) \\
& - \frac{1}{\epsilon(1 + \epsilon)} \left( \frac{\kappa}{t_2} \right)^\epsilon \frac{t_1}{t_2} {}_2F_1 \left( 1, 1 + \epsilon, 2 + \epsilon; \frac{t_1}{t_2} \right) \\
& - \frac{1}{\epsilon} \left[ \left( \frac{\kappa}{t_1} \right)^\epsilon + \left( \frac{\kappa}{t_2} \right)^\epsilon \right] \left( \ln \frac{-\kappa}{\tau} + \ln \frac{t_1 - t_2}{\tau} \right) \\
& + \mathcal{O}(\epsilon).
\end{aligned} \tag{9.34}$$

Let us conclude this section by some comments about how this procedure extends at two loops. At two-loop accuracy, Eq. (9.25) reads

$$\begin{aligned}
m_5^{(2)} = & \frac{1}{2} \left( m_5^{(1)} \right)^2 + \bar{\alpha}^{(2)}(t_1; \epsilon) L_1 + \bar{\alpha}^{(2)}(t_2; \epsilon) L_2 \\
& + \bar{C}^{(2)}(t_1, \tau) + \bar{V}^{(2)}(t_1, t_2, \kappa, \tau) + \bar{C}^{(2)}(t_2, \tau) \\
& - \frac{1}{2} \left( \bar{C}^{(1)}(t_1, \tau) \right)^2 - \frac{1}{2} \left( \bar{V}^{(1)}(t_1, t_2, \kappa, \tau) \right)^2 - \frac{1}{2} \left( \bar{C}^{(1)}(t_2, \tau) \right)^2
\end{aligned} \tag{9.35}$$

In order to extract the two-loop Lipatov vertex from Eq. (9.35), we need to know analytically the one-loop amplitude to  $\mathcal{O}(\epsilon^2)$  and the two-loop amplitude

to  $\mathcal{O}(\epsilon^0)$  in multi-Regge kinematics. As already mentioned, the higher-order terms of the one-loop amplitude gain contributions from the scalar massless pentagon in  $D = 6 - 2\epsilon$  dimensions. We will compute these contributions explicitly in Chapter 11 to all orders in  $\epsilon$  in terms of generalized hypergeometric functions and in Appendix M as a Taylor series in  $\epsilon$  whose coefficients are combinations of generalized polylogarithms. Furthermore, we show in the next chapter that an explicit knowledge of the two-loop five-point amplitude is in fact not necessary for the extraction of the two-loop Lipatov vertex through  $\mathcal{O}(\epsilon^2)$ , but it is enough to have the one-loop vertex to higher orders in  $\epsilon$ .

### 9.3 Quasi multi-Regge limits beyond tree-level

In the previous section we introduced the multi-Regge limit for (multi-) loop amplitudes via the high-energy prescription which allows to disentangle the contributions to the different building blocks in the multi-Regge limit. In this section we briefly comment on how to define quasi multi-Regge limits beyond tree-level. Not much is known about these limits in the literature, so we will be brief and concentrate on the explicit examples of the five and six-point amplitudes.

The simplest quasi multi-Regge limit arises when two gluons with comparable rapidities are emitted at one end of the ladder,

$$y_3 \simeq y_4 \gg y_5 \quad \text{and} \quad |p_{3\perp}| \simeq |p_{4\perp}| \simeq |p_{5\perp}|, \quad (9.36)$$

In this limit we have the hierarchy of scales\*,

$$(-s) \gg (-s_1) \gg (-s_2), (-t_1), (-t_2), \quad (9.37)$$

where we used the shorthands  $t_1 = s_{51}$ ,  $t_2 = s_{23}$ ,  $s_1 = s_{45}$  and  $s_2 = s_{34}$ . Since  $y_3 \simeq y_4$ , no limit is taken on  $(-s_2)$ , and therefore this invariant can range anywhere between the  $t$ -type invariants and  $(-s_1)$ , where we recover the multi-Regge limit, Eq. (9.4). Furthermore, the high-energy prescription reads

$$A_5(1, 2, 3, 4, 5) = s C_2(p_2, p_3, p_4; \epsilon, \tau) \frac{1}{t_1} \left( \frac{-s_1}{\tau} \right)^{\alpha(t_1; \epsilon)} C(p_1, p_5; \epsilon, \tau). \quad (9.38)$$

---

\*For more details on the kinematics in this limit we refer to Ref. [27].

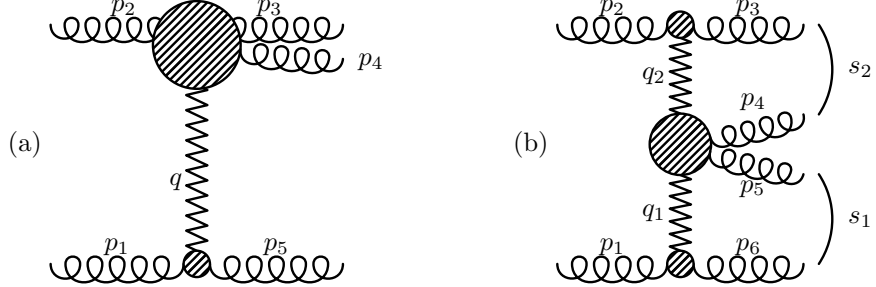


Figure 9.1: The five (a) and six (b) point amplitudes in quasi multi-Regge kinematics.

A pictorial representation of Eq. (9.38) can be found in Fig. 9.1a. In Eq. (9.38) a new building block appears, which is the generalization of the coefficient function defined in Eq. (8.32) beyond tree-level. The Regge trajectory  $\alpha$  and the coefficient function  $C$  are the same as in multi-Regge kinematics.  $C_2$  has the perturbative expansion

$$C_2(p_i, p_j, p_k; \epsilon, \tau) = C_2^{(0)}(p_i, p_j, p_k) \left( 1 + \sum_{n=1}^{\infty} \bar{g}^{2n} \bar{C}_2^{(n)}(t_{ij}, t_{ijk}, s_{ij}; \epsilon, \tau) \right), \quad (9.39)$$

with  $t_{ij} = (p_i + p_j)^2$  and  $t_{ijk} = (p_i + p_j + p_k)^2$ . Expanding Eq. (9.38) to one-loop accuracy, we find the expression of  $m_5^{(1)}$  in quasi multi-Regge kinematics,

$$m_5^{(1)}(s, s_1, s_2, t_1, t_2) = \bar{C}_2^{(1)}(t_2, t_1, s_2; \epsilon, \tau) + \bar{C}^{(1)}(t_1; \epsilon, \tau) + \bar{\alpha}^{(1)}(t_1; \epsilon) L, \quad (9.40)$$

with  $L = \ln(-s_1/\tau)$ . Although Eq. (9.40) can in principle be used to extract the generalized coefficient function  $\bar{C}_2^{(1)}$ , no expression can be found in the literature. The generalization of Eq. (9.40) to higher loops, as well as to more general coefficient functions  $\bar{C}_n^{(1)}$  is in principle straightforward.

If we go beyond five-point amplitudes, not only new types of coefficient functions appear, but we also encounter new generalized Lipatov vertices for the emission of several gluons with comparable rapidities along the ladder. Such a kinematical configuration appears for the first time in the six-point amplitude,

$$y_3 \gg y_4 \simeq y_5 \gg y_6 \quad \text{and} \quad |p_{3\perp}| \simeq |p_{4\perp}| \simeq |p_{5\perp}| \simeq |p_{6\perp}|. \quad (9.41)$$



which is equivalent to the hierarchy of scales [27],

$$(-s) \gg (-s_1), (-s_2) \gg (-t_1), (-t_2), (-s_{45}), \quad (9.42)$$

where we defined  $t_1 = s_{61}$ ,  $t_2 = s_{23}$ ,  $s_1 = s_{56}$  and  $s_2 = s_{34}$ . No limit is taken on the invariant  $s_{45}$ , so it can range from the  $t$ -type invariants to the  $s$ -type invariants, where we recover the multi-Regge limit of the six-point amplitude. In this limit, the six-point amplitude can be written in the factorized form

$$\begin{aligned} A_6(1, 2, 3, 4, 5, 6) &= s C(p_2, p_3; \epsilon, \tau) \frac{1}{t_2} \left( \frac{-s_2}{\tau} \right)^{\alpha(t_2; \epsilon)} \\ &\times V_2(q_2, p_4, p_5, q_1; \epsilon, \tau) \frac{1}{t_1} \left( \frac{-s_1}{\tau} \right)^{\alpha(t_1; \epsilon)} C(p_1, p_6; \epsilon, \tau). \end{aligned} \quad (9.43)$$

A pictorial representation of Eq. (9.43) can be found in Fig. 9.1b. The quantity  $V_2$  is the generalization of the Lipatov vertex  $V_2^{(0)}$  introduced in Chapter 8.2 beyond tree-level and describes the emission of two gluons along the ladder at two-loop accuracy. It has the perturbative expansion

$$\begin{aligned} &V_2(q_{j+1}, p_j, p_{j+1}, q_j; \epsilon, \tau) \\ &= V_2^{(0)}(q_2; p_4, p_5; q_1) \left( 1 + \sum_{n=1}^{\infty} \bar{g}^{2n} \bar{V}_2^{(n)}(t_{j+1}, t_{j,j+1}, t_j, \kappa_j, \kappa_{j+1}; \epsilon, \tau) \right). \end{aligned} \quad (9.44)$$

Explicit results for  $V_2^{(1)}$  in the case where the two emitted gluons have the same helicity can be found in Ref. [94].

## 9.4 The analytic continuation to the physical region

The high-energy prescription of Eq. (9.3), is given explicitly in the euclidean region where all invariants are negative and the amplitude is real. For physical observables, however, the  $s$ -type invariants are positive, while the  $t$ -type invariants remain negative and the amplitude develops a non-zero imaginary part. We therefore need to analytically continue the  $s$ -type invariants to the

physical region along a half circle through the complex upper half-plane such that,

$$\ln(-s - i\epsilon) = \ln|s| - i\pi\theta(s). \quad (9.45)$$

This is equivalent to the replacement,

$$(-s) \rightarrow e^{-i\pi} s, \quad (-s_i) \rightarrow e^{-i\pi} s_i, \quad (-s_{i,j,k}) \rightarrow e^{-i\pi} s_{i,j,k}. \quad (9.46)$$

The high-energy prescription (9.3), however, also depends on the transverse momentum scales  $\kappa_i$ , which become positive in the physical region. Unlike for the  $s$ -type invariants, the analytic properties of the  $\kappa_i$ 's are not determined explicitly by the usual  $i\epsilon$  prescription, because they are ratios of particle invariants. The prescription for the analytic continuation therefore needs to be inferred from Eqs. (9.5) and (9.46) and is achieved by the replacement [27],

$$(-\kappa_i) \rightarrow e^{-i\pi} \kappa_i, \quad (9.47)$$

Note that the prescription for the  $\kappa_i$ 's is similar to the one for the  $s$ -type invariants<sup>†</sup>. The analytic continuation of Eq. (9.3) to the physical region can now be derived immediately from the prescriptions (9.46) and (9.47).

Let us now analyze what the coefficient functions and the Lipatov vertices become in the physical region. Since the coefficient function and the Regge trajectory only depend on the variables  $t_i$ , they stay real in the physical region (up to overall phases in  $C^{(0)}$ ). The Lipatov vertices, however, explicitly depend on the transverse scales  $\kappa_i$ , so they must become complex,

$$\bar{V}(t_{j+1}, t_j, \kappa_j; \epsilon, \tau) = \left(\frac{\mu^2}{\kappa}\right)^{n\epsilon} V_{\text{phys}}^{(n)}(t_{j+1}, t_j, \kappa_j; \epsilon, \tau), \quad (9.48)$$

with

$$V_{\text{phys}}^{(n)}(t_{j+1}, t_j, \kappa_j; \epsilon, \tau) = e^{i\pi n\epsilon} V^{(n)}(t_{j+1}, t_j, \kappa_j; \epsilon, \tau). \quad (9.49)$$

---

<sup>†</sup>Note that if we consider the continuation to a region other than the physical region, the prescription for the analytic continuation of  $\kappa_i$  might differ from the usual prescription (9.45). E.g., in the region where  $s_i > 0$  while  $s_{ijk} < 0$ , then Eq. (9.46) combined to Eq. (9.5) implies the prescription  $(-\kappa_i) \rightarrow e^{-2i\pi} (-\kappa_i)$ .

# Chapter 10

## The BDS ansatz in the high-energy limit

### 10.1 The BDS ansatz in multi-Regge kinematics

In this chapter we study what the BDS ansatz becomes in the high-energy limit. Our goal is to disguise a limit where the remainder function for the six-point amplitude gives a non-zero contribution, similar to the triple collinear limit discussed in Chapter 7. We start by analyzing the multi-Regge limits, and we comment on quasi multi-Regge limits in the next section.

Using the approximate form of the Mandelstam invariants in multi-Regge kinematics given in Appendix D, it is trivial to show that in this limit the conformal cross-ratios appearing in  $R_6^{(2)}$  all take special values [27, 95, 96]

$$u_1 \simeq 1, \quad u_2 = \frac{t_3 \kappa_1}{t_2 s_2} \simeq \mathcal{O}\left(\frac{t}{s}\right), \quad u_3 = \frac{t_1 \kappa_2}{t_2 s_2} \simeq \mathcal{O}\left(\frac{t}{s}\right), \quad (10.1)$$

and they are in fact subleading to the desired accuracy, and so is  $R_6^{(2)}$ . This result is expected, because in multi-Regge kinematics any amplitude is determined completely by the coefficient functions, Regge trajectories and Lipatov vertices. Those quantities have been extracted in Chapter 9 from the four

and five-point amplitudes where no remainder function contributes. Hence, we do not expect the building blocks in the high-energy limit to depend on the remainder function. In the rest of this section we give a formal proof of this statement, namely we show that the coefficient function and the Lipatov vertex must fulfill iterations very similar to those fulfilled by the full amplitude and by the splitting amplitudes. As a consequence we obtain that the BDS ansatz is fully consistent with multi-Regge factorization.

Before turning to the derivation of this result, let us introduce some conventions. In Chapter 7 we presented the BDS ansatz as the resummed form of the perturbative expansion in the 't Hooft coupling. In Chapter 9, however, we defined the perturbative expansion of the building blocks in the high-energy limits in terms of the rescaled coupling  $\bar{g}^2$ , and we showed that the loop coefficients are related by a simple proportionality factor. We can therefore derive a modified version of the BDS ansatz with respect to the rescaled coupling  $\bar{g}^2$ ,

$$\begin{aligned} m_n(\epsilon) &= 1 + \sum_{l=1}^{\infty} \bar{g}^{2l} m_n^{(l)}(\epsilon) \\ &= \exp \sum_{l=0}^{\infty} \bar{g}^{2l} 2^l G^l(\epsilon) \left[ f^{(l)}(\epsilon) \frac{m_n^{(1)}(l\epsilon)}{2G(l\epsilon)} + C^{(l)} + E_n^{(l)}(\epsilon) \right]. \end{aligned} \quad (10.2)$$

In the rest of this chapter, we will always refer to Eq. (10.2) when quoting the BDS ansatz.

Let us now derive the exponentiated forms for the coefficient functions and the Lipatov vertex. Since the BDS ansatz holds true for the four-point amplitude, we can immediately insert the tree- and one-loop four-gluon amplitudes in multi-Regge kinematics, Eq. (9.15), into Eq. (10.2), such that

$$\begin{aligned} A_4 &= A_4^{(0)} \left( \frac{-s}{\tau} \right)^{\sum_{l=1}^{\infty} \bar{g}^{2l} 2^{l-1} \frac{G^l(\epsilon)}{G(l\epsilon)} f^{(l)}(\epsilon) \bar{\alpha}^{(1)}(t; l\epsilon)} \\ &\times \exp 2 \sum_{l=1}^{\infty} \bar{g}^{2l} 2^{l-1} G^l(\epsilon) \left( \frac{f^{(l)}(\epsilon)}{G(l\epsilon)} \bar{C}^{(1)}(t; l\epsilon, \tau) + C^{(l)} + E_4^{(l)}(\epsilon) \right). \end{aligned} \quad (10.3)$$

Comparing Eq. (10.3) to the general form of the high energy prescription of Eq. (9.14), we can easily identify the all-orders forms of the Regge trajectory

$$\alpha(t; \epsilon) = \sum_{l=1}^{\infty} \bar{g}^{2l} 2^{l-1} \frac{G^l(\epsilon)}{G(l\epsilon)} f^{(l)}(\epsilon) \bar{\alpha}^{(1)}(t, l\epsilon), \quad (10.4)$$

and the coefficient function,

$$\begin{aligned} & C(p_i, p_j; \epsilon, \tau) \\ &= C^{(0)}(p_i; p_j) \exp \sum_{l=1}^{\infty} \bar{g}^{2l} 2^{l-1} G^l(\epsilon) \left( \frac{f^{(l)}(\epsilon)}{G(l\epsilon)} \bar{C}^{(1)}(t; l\epsilon, \tau) + C^{(l)} + E_4^{(l)}(\epsilon) \right), \end{aligned} \quad (10.5)$$

where in the last equation  $t = (p_i + p_j)^2$ . Note that Eq. (10.4) is in agreement order by order in the expansion up to  $\mathcal{O}(\epsilon)$  with the expression of the Regge trajectory given in Ref. [26],

$$\bar{\alpha}^{(l)}(t; \epsilon) = 2^{l-1} f^{(l)}(\epsilon) \bar{\alpha}^{(1)}(t; l\epsilon). \quad (10.6)$$

The coefficient functions describing the emission of a gluon at one end of the ladder thus fulfill the same iteration as the full amplitude and the splitting functions. Expanding the exponential in Eq. (10.5) and collecting the coefficients of the coupling constant, we obtain in particular the following expression for the two-loop coefficient function in terms of the one-loop function,

$$C^{(2)}(t; \epsilon, \tau) = \frac{1}{2} \left[ C^{(1)}(t; \epsilon, \tau) \right]^2 + \frac{2G^2(\epsilon)}{G(2\epsilon)} f^{(2)}(\epsilon) C^{(1)}(t; 2\epsilon, \tau) + 2C^{(2)} + \mathcal{O}(\epsilon). \quad (10.7)$$

We can now repeat the argument for the five-point amplitude and, by reusing Eq. (10.4) and Eq. (10.5), extract the corresponding iteration for the Lipatov vertex,

$$\begin{aligned} A_5 &= C(p_2, p_3; \epsilon, \tau) C(p_1, p_5; \epsilon, \tau) \left( \frac{-s_1}{\tau} \right)^{\alpha(t_1, \epsilon)} \left( \frac{-s_2}{\tau} \right)^{\alpha(t_2, \epsilon)} \\ &\quad \times V^{(0)}(q_2; p_5; q_1) \\ &\quad \times \exp \sum_{l=1}^{\infty} \bar{g}^{2l} 2^l G^l(\epsilon) \left( \frac{f^{(l)}(\epsilon)}{2G(l\epsilon)} \bar{V}^{(1)}(t_2, t_1, \kappa_1; l\epsilon, \tau) \right. \\ &\quad \left. + E_5^{(l)}(\epsilon) - E_4^{(l)}(\epsilon) \right). \end{aligned} \quad (10.8)$$

Comparing with Eq. (9.25), we find

$$\begin{aligned} V(q_2, p, q_1; \epsilon, \tau) &= V^{(0)}(q_2; p; q_1) \\ &\quad \times \exp \sum_{l=1}^{\infty} \bar{g}^{2l} 2^l G^l(\epsilon) \left( \frac{f^{(l)}(\epsilon)}{2G(l\epsilon)} \bar{V}^{(1)}(t_2, t_1, \kappa; l\epsilon, \tau) + E_5^{(l)}(\epsilon) - E_4^{(l)}(\epsilon) \right), \end{aligned} \quad (10.9)$$

*i.e.*, also the Lipatov vertex fulfills an ABDK/BDS-type iteration. As before, expanding Eq. (10.9) in the rescaled coupling, we find an expression of the two-loop vertex in terms of the one-loop vertex,

$$\begin{aligned} V^{(2)}(t_1, t_2, \kappa; \epsilon, \tau) &= \frac{1}{2} \left[ V^{(1)}(t_1, t_2, \kappa; \epsilon, \tau) \right]^2 + \frac{2G^2(\epsilon)}{G(2\epsilon)} f^{(2)}(\epsilon) V^{(1)}(t_1, t_2, \kappa; 2\epsilon, \tau) + \mathcal{O}(\epsilon). \end{aligned} \quad (10.10)$$

We will use Eq. (10.10) explicitly in Chapter 11 where we compute the two-loop Lipatov vertex to  $\mathcal{O}(\epsilon^0)$ . Note that the iterations (10.7) and (10.10) have an important consequence. In Chapter 9 we showed that the two-loop coefficient functions and Lipatov vertices can be extracted from the four and five-point two-loop amplitudes by matching the left and right-hand sides of Eqs. (9.24 - 9.35). The iteration formulas derived in this section imply that an explicit knowledge of the two-loop amplitude is not necessary to compute the two-loop building blocks in multi-Regge kinematics, but it is enough to know the one-loop building blocks to higher-orders in  $\epsilon$ .

We now turn to the generic case. Consider an  $n$ -gluon amplitude in multi-Regge kinematics which satisfies Eq. (9.3). Inserting the exponentiated expressions for the Regge trajectory Eq. (10.4), the coefficient functions Eq. (10.5) and the Lipatov vertex Eq. (10.9), we find

$$\begin{aligned} A_n = A_n^{(0)} \exp \sum_{l=1}^{\infty} \bar{g}^{2l} 2^l G^l(\epsilon) & \left[ \frac{f^{(l)}(\epsilon)}{2G(l\epsilon)} \left( \bar{C}^{(1)}(t_1; l\epsilon, \tau) + \bar{C}^{(1)}(t_{n-3}; l\epsilon, \tau) \right. \right. \\ & + \sum_{k=1}^{n-3} \bar{\alpha}^{(1)}(t_k; l\epsilon) \ln \left( \frac{-s_k}{\tau} \right) \\ & + \sum_{k=1}^{n-4} \bar{V}^{(1)}(t_{k+1}, t_k, \kappa_k; l\epsilon, \tau) \\ & \left. \left. + C^{(l)} + E_4^{(l)}(\epsilon) + (n-4)(E_5^{(l)}(\epsilon) - E_4^{(l)}(\epsilon)) \right] \right]. \end{aligned} \quad (10.11)$$

The expression inside the brackets can now be easily identified as the one-loop amplitude in multi-Regge kinematics,

$$m_n^{(1)}(l\epsilon) = \bar{C}^{(1)}(t_1; \tau, l\epsilon) + \bar{C}^{(1)}(t_{n-3}; \tau, l\epsilon) + \sum_{k=1}^{n-3} \bar{\alpha}^{(1)}(t_k, l\epsilon) \ln\left(\frac{-s_k}{\tau}\right) + \sum_{k=1}^{n-4} \bar{V}^{(1)}(t_{k+1}, t_k, \kappa_k; \tau, l\epsilon), \quad (10.12)$$

and so we recover

$$A_n = A_n^{(0)} \exp \sum_{l=1}^{\infty} \bar{g}^{2l} 2^l G^l(\epsilon) \left( \frac{f^{(l)}(\epsilon)}{2G(l\epsilon)} m_n^{(1)}(l\epsilon) + C^{(l)} + \mathcal{O}(\epsilon) \right), \quad (10.13)$$

*i.e.*  $m_n$  satisfies the BDS ansatz up to  $\mathcal{O}(\epsilon)$ . As a corollary of Eq. (10.13) we obtain that in multi-Regge kinematics the remainder function must vanish for every  $n$ .

The previous result has two important consequences:

- Firstly, this result puts a strong constraint on all possible candidate remainder functions, because they must vanish in the multi-Regge limit.
- Secondly, since the remainder function vanishes in multi-Regge kinematics for an arbitrary number of legs, we conclude that this limit is insufficient to determine the remainder function, and more general kinematics are needed. This issue will be addressed in the next section, where we relax the constraints on the kinematics and determine a limit in which the six-point remainder function is non zero.

## 10.2 The BDS ansatz and quasi multi-Regge kinematics

In the previous section we showed that the multi-Regge limit is inappropriate to gain some information on the remainder function. We would thus like to find a limit in which the kinematics are simpler than the general kinematics, together with a non-vanishing remainder function. In Chapter 7 we argued that the triple collinear limit has this property. In the following, we argue that

some quasi multi-Regge limits have a similar property, and could thus be used to gain some information on the remainder function.

Let us start with the simplest quasi multi-Regge limit, which describes the emission of one gluon pair with comparable rapidities at one end of the ladder,

$$y_3 \simeq y_4 \gg y_5 \gg y_6 \quad \text{and} \quad |p_{3\perp}| \simeq |p_{4\perp}| \simeq |p_{5\perp}| \simeq |p_{6\perp}|. \quad (10.14)$$

This situation was analyzed in Section 9.3 in the five-point case. The generalization to the six-point amplitude is straightforward. Since the coefficient function  $C_2$  in Eq. (9.38) is completely determined by the five-point amplitude, it is easy to repeat the argument of the previous section and to show that also in this limit the remainder function must vanish for every  $n$ . Hence, even though this limit puts another strong constraint on the form of possible remainder functions, it is still too restrictive to provide some information on its functional form.

Let us now discuss the next-to-simplest Regge-type limit, the quasi multi-Regge limit for the emission of two gluon comparable helicities along the ladder,

$$y_3 \gg y_4 \simeq y_5 \gg y_6 \quad \text{and} \quad |p_{3\perp}| \simeq |p_{4\perp}| \simeq |p_{5\perp}| \simeq |p_{6\perp}|. \quad (10.15)$$

This situation was studied in Section 9.3 where we showed that a new type of Lipatov vertex appears. This limit is genuine to the six-point case, *i.e.*, this kinematic configuration arises for the first time for six external gluons. Furthermore, in this limit the conformal cross ratios all take generic values [27],

$$\begin{aligned} u_1 &\rightarrow \frac{s_{45}}{(p_4^+ + p_5^+)(p_4^- + p_5^-)} \simeq \mathcal{O}(1), \\ u_2 &\rightarrow \frac{|p_{3\perp}|^2 p_5^+ p_6^-}{(|p_{3\perp} + p_{4\perp}|^2 + p_5^+ p_4^-)(p_4^+ + p_5^+) p_6^-} \simeq \mathcal{O}(1), \\ u_3 &\rightarrow \frac{|p_{6\perp}|^2 p_3^+ p_4^-}{p_3^+ (p_4^- + p_5^-)(|p_{3\perp} + p_{4\perp}|^2 + p_5^+ p_4^-)} \simeq \mathcal{O}(1). \end{aligned} \quad (10.16)$$

Since none of the conformal ratios vanishes or approaches one, we conclude that the six-point remainder function must give a non-zero contribution. This kinematic regime could therefore provide some information on the violation of the BDS ansatz, because the remainder function is expected to be non zero. From the previous discussion it is clear that there is no simpler Regge-type limit



with this property and we conclude that this limit is the simplest Regge-type limit for which the remainder function is not subleading. We can repeat the analysis of the previous section and derive an iteration formula for the Lipatov vertex describing the emission of two gluons with comparable rapidities. We find,

$$\begin{aligned}
V_2^{(2)}(t_1, t_2, t_3, \kappa_1, \kappa_2; \epsilon, \tau) &= \frac{1}{2} \left[ V^{(1)}(t_1, t_2, t_3, \kappa_1, \kappa_2; \epsilon, \tau) \right]^2 \\
&+ \frac{2G^2(\epsilon)}{G(2\epsilon)} f^{(2)}(\epsilon) V^{(1)}(t_1, t_2, t_3, \kappa_1, \kappa_2; 2\epsilon, \tau) \\
&+ R_6^{(2)}(u_1, u_2, u_3) + \mathcal{O}(\epsilon).
\end{aligned} \tag{10.17}$$

Note that since the coefficient functions in Eq. (9.43) are completely determined by the five-point amplitude, the whole dependence on the remainder function is captured by the Lipatov vertex  $V_2$ . The conclusion is that it is enough to know the analytical form of the Lipatov vertex  $V_2$  to extract the remainder function, similar to the case of the triple collinear splitting amplitude discussed in Chapter 7. Note, however, that the triple collinear limit and the quasi-multi Regge limit are complementary, because due to the strong rapidity ordering (10.15) the momenta of the gluons 3 and 4 cannot be collinear, and hence the two limits describe completely different areas of phase space.

It is clear that every Regge-type limit defined by a rapidity ordering that encompasses Eq. (10.15) will also give rise to a non-vanishing remainder function. We could therefore relax the rapidity ordering even more, and consider the limit

$$y_3 \simeq y_4 \simeq y_5 \gg y_6 \quad \text{and} \quad |p_{3\perp}| \simeq |p_{4\perp}| \simeq |p_{5\perp}| \simeq |p_{6\perp}|, \tag{10.18}$$

*i.e.*, the production of three gluons with comparable rapidities at one end of the ladder. Also in this case the conformal cross ratios take generic values and the remainder function is expected to be non zero [27]. Indeed, the two-loop

iteration formula for the coefficient function  $\bar{C}_3^{(2)}$  reads,

$$\begin{aligned}
C_3^{(2)}(t, s_{34}, s_{45}, s_{345}; \epsilon, \tau) &= \frac{1}{2} \left[ C_3^{(1)}(t, s_{34}, s_{45}, s_{345}; \epsilon, \tau) \right]^2 \\
&+ \frac{2G^2(\epsilon)}{G(2\epsilon)} f^{(2)}(\epsilon) C_3^{(1)}(t, s_{34}, s_{45}, s_{345}; 2\epsilon, \tau) \\
&+ 2C^{(2)} + R_6^{(2)}(u_1, u_2, u_3) + \mathcal{O}(\epsilon).
\end{aligned} \tag{10.19}$$

Similar to case of the Lipatov vertex, the coefficient function  $\bar{C}_3$  must capture the whole dependence on  $R_6^{(2)}$ . Let us conclude this discussion by commenting on the relation between of the Regge-type limits and the triple collinear limit discussed in Chapter 7. In the limit where the three gluons emitted at one end of the ladder are collinear, the coefficient function must factorize into a splitting amplitude,

$$\bar{C}_3^{(2)} \rightarrow \bar{C}^{(2)} + \bar{C}^{(1)} r_{1 \rightarrow 3}^{(1)} + r_{1 \rightarrow 3}^{(2)}, \tag{10.20}$$

where  $r_{1 \rightarrow 3}^{(l)}$  denotes the  $l$ -loop triple collinear splitting amplitude defined in Chapter 7. Hence, the limit for the emission of three gluons at one end of the gluon ladder does not only encompass the production of two gluons along the ladder, but at the same time also the triple collinear limit (See Fig. 10.1).

Finally, we thus have three limits at our disposal in which the six-point remainder function is expected to be non zero:

1. the triple collinear limit, where three consecutive gluons have collinear momenta.
2. the quasi multi-Regge limit for the production of two gluon with comparable rapidities along the ladder.
3. the quasi multi-Regge limit for the production of three gluon with comparable rapidities, which encompasses the cases 1 and 2.

Although these kinematics are simpler than the general kinematics, they still require the explicit computation of the one and two-loop hexagons in the corresponding limit (unlike the multi-Regge case, which is completely determined by

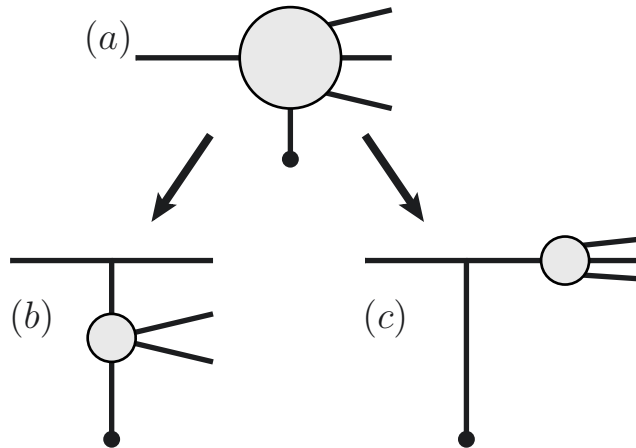


Figure 10.1: The three limits where the six-point remainder function is expected to be non zero: the impact factor for the emission of three gluons (a) encompasses the Lipatov vertex for the emission of two gluons (b) as well as the triple collinear splitting amplitude (c).

the four and five-point amplitudes). Unfortunately, not much is known in the literature about higher-point amplitudes at two-loops or at one-loop beyond  $\mathcal{O}(\epsilon^0)^*$ . As a first study of the analytic structures that appear in these kind of computations, we start from the simplest case possible, the five-point one-loop amplitude to higher orders in  $\epsilon$ , albeit in simplified kinematics, namely the multi-Regge kinematics. This computation will be performed in the next chapter.

---

\*Recall that the remainder function is essentially defined as the difference between the two-loop amplitude and the square of the one-loop amplitude.



# Chapter 11

## The five-point amplitude in multi-Regge kinematics

### 11.1 Introduction

In this chapter we present the computation of the scalar massless pentagon in  $D = 6 - 2\epsilon$  dimensions. This integral appears in the higher-order terms in the Laurent expansion of the five-point MSYM amplitude through Eq. (9.28). Since the ABDK/BDS iteration for the two-loop amplitude requires the knowledge of the one-loop amplitude through order  $\epsilon^2$ , the higher order terms in the Laurent expansion of the one-loop amplitude allows one to obtain at the same time an analytic result for the two-loop five-point amplitude.

An analytic computation of the pentagon integral in general kinematics is unfortunately beyond our technical capabilities at the moment. We therefore restrict the computation to a specific limit, namely the multi-Regge kinematics. The aim of this computation is then twofold:

- First, as we already mentioned, the computation of the pentagon integral provides us with the first analytic result for the two-loop five-point amplitude in MSYM, albeit in simplified kinematics.

- Second, we aim to study for the first time the analytic structure of higher-point one-loop amplitudes in MSYM beyond  $\mathcal{O}(\epsilon^0)$  and to get new insight into the mathematical structure of scalar one-loop integrals beyond four points. In particular, we show that in the case of the pentagon new types of generalized hypergeometric functions appear, whose Laurent expansion involves a new set of transcendental functions called  $\mathcal{M}$  functions.

The computation is performed using two different techniques\*. We first compute the pentagon integral using the negative dimension approach (NDIM), which expresses a one-loop Feynman integral as a combination of generalized hypergeometric functions in more than one variable. In Appendix M, we repeat the computation using the fourfold Mellin-Barnes representation for the scalar massless pentagon given in Ref. [84], and by transforming one Mellin-Barnes integral into an Euler integral, we arrive at a representation of the pentagon integral as a Taylor series in  $\epsilon$  whose coefficients can be expressed as combinations of Goncharov's multiple polylogarithm (See Appendix G for a review). We also include further appendices containing some technical proofs omitted throughout this chapter.

## 11.2 Definitions and conventions

The scalar pentagon integral is defined as,

$$I_5^D(\nu_1, \nu_2, \nu_3, \nu_4, \nu_5; Q_i^2) = e^{\gamma_E \epsilon} \int \frac{d^D k}{i\pi^{D/2}} \frac{1}{D_1^{\nu_1} D_2^{\nu_2} D_3^{\nu_3} D_4^{\nu_4} D_5^{\nu_5}}, \quad (11.1)$$

where the external momenta  $k_i$  are lightlike,  $k_i^2 = 0$ , and are incoming so that  $\sum_{i=1}^5 k_i^\mu = 0$ . The external momentum scales are the Mandelstam variables  $Q_i^2 = s_{12}, s_{23}, s_{34}, s_{45}, s_{15}$  and we work in the Euclidean region,  $s_{ij} < 0$ . Let us introduce the shorthands

$$\begin{aligned} s &= s_{12}, & s_1 &= s_{45}, & s_2 &= s_{34}, \\ t_1 &= s_{51}, & t_2 &= s_{23}. \end{aligned} \quad (11.2)$$

The hierarchy of scales in multi-Regge kinematics, Eq. (9.4), then implies,

$$(-s) \gg (-s_1), (-s_2) \gg (-t_1), (-t_2), \quad (11.3)$$

---

\*See Appendix K for a review of the different techniques.

together with the mass-shell condition,

$$(-\kappa)(-s) = (-s_1)(-s_2), \quad (11.4)$$

where  $(-\kappa) = -|p_{4\perp}|^2$ . Since  $\kappa$  is of the order of the  $t$ -type invariants, we must have, and the hierarchy of scales is such that

$$s_1 s_2 \sim s t_1 \sim s t_2. \quad (11.5)$$

Equivalently, we can define the limit by the scaling

$$s \rightarrow s, \quad s_1 \rightarrow \lambda s_1, \quad s_2 \rightarrow \lambda s_2, \quad t_1 \rightarrow \lambda^2 t_1, \quad t_2 \rightarrow \lambda^2 t_2, \quad (11.6)$$

and expanding in the limit  $\lambda \rightarrow 0$  and keeping only the leading term.

## 11.3 The pentagon integral from NDIM

### 11.3.1 General considerations

In this section we derive a representation for the pentagon integral from the negative dimension technique (NDIM) (See Appendix K for a review). In short, NDIM is an algorithm that allows one to transform a one-loop integral into a combination of multiple sums. In the present case, we identify 125 quadruple series contributing to the massless scalar pentagon in general kinematics. Each series has the form of a multiple generalized hypergeometric series, *e.g.* ,

$$\begin{aligned} & I^{\{n_1, n_2, n_3, n_4\}} \\ &= (-s)^{\nu_{45} - \frac{D}{2}} (-t_2)^{\nu_{51} - \frac{D}{2}} (-s_2)^{-\nu_{345} + \frac{D}{2}} (-s_1)^{\nu_{45} - \frac{D}{2}} (-t_1)^{-\nu_{512} + \frac{D}{2}} \\ &\times (-1)^{\frac{D}{2}} e^{\gamma_E \epsilon} \frac{\Gamma(\nu_1)\Gamma(\nu_2)\Gamma(\nu_3)\Gamma(\nu_4)\Gamma(\nu_5)}{\Gamma(\nu_{345} - \frac{D}{2})\Gamma(\nu_{451} - \frac{D}{2})\Gamma(\nu_{512} - \frac{D}{2})\Gamma(\frac{D}{2} - \nu_{45})\Gamma(\frac{D}{2} - \nu_{51})} \\ &\times F\left(\begin{matrix} D - \nu, & \frac{D}{2} - \nu_{45}, & \frac{D}{2} - \nu_{51} \\ 1 + \frac{D}{2} - \nu_{345}, & 1 + \frac{D}{2} - \nu_{451}, & 1 + \frac{D}{2} - \nu_{512} \end{matrix} \middle| x_1, x_2, x_3, x_4\right). \end{aligned} \quad (11.7)$$

The arguments of the hypergeometric functions are ratios of scales, *e.g.*

$$x_1 = \frac{s_2}{s}, \quad x_2 = -\frac{s_1 s_2}{s t_2}, \quad x_3 = \frac{s_1 t_1}{s t_2}, \quad x_4 = \frac{t_1}{t_2}, \quad (11.8)$$

and we introduced the definitions  $\nu_{123} = \nu_1 + \nu_2 + \nu_3$ , *etc.* For convenience we have introduced the shorthand for quadruple sums,

$$\begin{aligned}
 & F \left( \begin{array}{ccc} a, & b, & c \\ d, & e, & f \end{array} \middle| x_1, x_2, x_3, x_4 \right) \\
 &= \sum_{n_1, n_2, n_3, n_4=0}^{\infty} \frac{(a)_{n_1+n_2+n_3+n_4} (b)_{n_1+n_2+n_3} (c)_{n_2+n_3+n_4}}{(d)_{n_1+n_2} (e)_{n_2+n_3} (f)_{n_3+n_4}} \frac{x_1^{n_1}}{n_1!} \frac{x_2^{n_2}}{n_2!} \frac{x_3^{n_3}}{n_3!} \frac{x_4^{n_4}}{n_4!}.
 \end{aligned} \tag{11.9}$$

Let us make a comment about the convergence properties of these multiple series. It is well-known that for example the Gauss' hypergeometric series (6.17) is not an entire function, but it only converges inside the unit disc. It can however be analytically continued outside the unit disc by using the functional equation relating the  ${}_2F_1$  functions with arguments  $x$  and  $1/x$ , *e.g.* , for  $|\arg(-z)| < \pi$ ,

$$\begin{aligned}
 {}_2F_1(a, b, c; x) &= (-x)^{-a} \frac{\Gamma(c) \Gamma(b-a)}{\Gamma(b) \Gamma(c-a)} {}_2F_1(a, 1+a-c, 1+a-b, 1/x) \\
 &\quad + (-x)^{-b} \frac{\Gamma(c) \Gamma(a-b)}{\Gamma(a) \Gamma(c-b)} {}_2F_1(b, 1+b-c, 1+b-a, 1/x).
 \end{aligned} \tag{11.10}$$

In a similar way, the hypergeometric functions (11.9) contributing to the pentagon integral are not necessarily convergent for all values of the arguments  $x_i$ , and so we have to make sense of these divergent series. The rule is that in a given area of phase space only the convergent solutions of NDIM contribute. In other words, the phase space breaks up into several regions, in each of which the integral is represented by a different combination of hypergeometric functions of the form given in Eq. (11.7). The different regions of phase space must be related by analytic continuation, similar to Eq. (11.10). As a rule of thumb, a hypergeometric series diverges if one of its argument is greater than 1. This implies for example that the fourfold series (11.9) is divergent in the region of phase space where  $x_1 < 1$ , or equivalently in the region where  $s_2 > s$ . As a consequence, Eq. (11.7) does only contribute in the Region of phase space where  $s_2 < s$ .

Although the hypergeometric functions obtained from NDIM are a representation of the pentagon integral in arbitrary kinematics, we have to face the problem that we ignore the analytic properties of the fourfold sums. For this



reason, we restrict the computation to multi-Regge kinematics, where the hierarchy of scales (11.3) eliminates many of the 125 solutions for the pentagon integral. The procedure to reducing the number of solutions goes as follows,

1. Any solution containing a summation that contains ratios of a “large” scale divided by a “small” scale, such as

$$\left(\frac{s}{s_1}\right)^n, \quad (11.11)$$

cannot converge and is therefore discarded. This reduces the number of solutions from 125 to 22.

2. Solutions with a prefactor that are less singular than

$$\frac{1}{s_1 s_2}, \quad \frac{1}{s t_1}, \quad \frac{1}{s t_2}, \quad (11.12)$$

when  $D = 6 - 2\epsilon$  and  $\nu_i = 1$  are discarded. This reduces the number of solutions from 22 to 20.

3. Any sum that contains ratios of a “small” scale divided by a “large” scale such as

$$\left(\frac{s_1}{s}\right)^n, \quad (11.13)$$

gives its leading contribution when the summation variable  $n$  is zero. This leads to sums with fewer than four summations. In the example (11.8) this procedure would remove the dependence on  $x_1$  and  $x_3$ , which are both subleading in multi-Regge kinematics.

4. The remaining solutions contain only double sums of ratios of the three scales of Eq. (11.7), defined in Eq. (11.14).

Following the NDIM prescription that in a given region of phase space only the convergent multiple sums contribute, we can distribute the remaining double sums among three different of phase space, *i.e.*, the Euclidean region itself is divided into three distinct regions. For later convenience let us introduce the following definitions,

$$x_1 = \frac{st_1}{s_1 s_2} = \frac{t_1}{\kappa} \quad \text{and} \quad x_2 = \frac{st_2}{s_1 s_2} = \frac{t_2}{\kappa}, \quad (11.14)$$

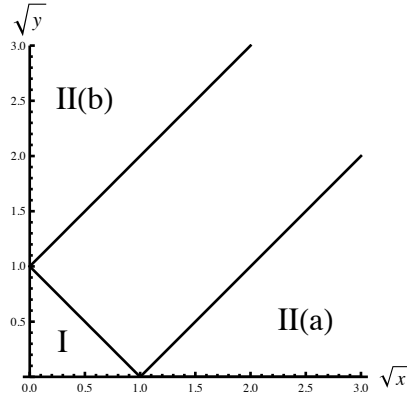


Figure 11.1: The three regions contributing to the scalar massless pentagon in Euclidean kinematics.

In terms of these quantities the Euclidean region can be divided into three regions

1. Region I, where  $\sqrt{x_1} + \sqrt{x_2} < 1$ .
2. Region II(a), where  $-\sqrt{x_1} + \sqrt{x_2} > 1$ .
3. Region II(b), where  $\sqrt{x_1} - \sqrt{x_2} > 1$ .

A graphical representation of these three regions in the  $(x_1, x_2)$  plane can be found in Fig. 11.1. Note that Region I is symmetric in  $x_1$  and  $x_2$ , whereas Regions II(a) and II(b) exchange their roles under an exchange of  $x_1$  and  $x_2$ . It is easy to see that Regions II(a) and II(b) can be furthermore characterized by

1. Region II(a):  $(-t_1) < (-t_2)$ .
2. Region II(b):  $(-t_1) > (-t_2)$ .

Note that the region where  $k_4$  is soft,  $s_1, s_2 \rightarrow 0$ , corresponds to  $x_1, x_2 \rightarrow +\infty$  in the  $(x_1, x_2)$ -plane.

### 11.3.2 The solution in Region II

As an example, we list here the solutions of the system of constraints in Region II(a),

$$I^{(IIa)}(s, s_1, s_2, t_1, t_2) = r_\Gamma e^{\gamma_E \epsilon} \frac{(-\kappa)^{-\epsilon}}{st_2} \mathcal{I}^{(IIa)}(s, s_1, s_2, t_1, t_2), \quad (11.15)$$

with

$$\mathcal{I}^{(IIa)}(s, s_1, s_2, t_1, t_2) = \sum_{i=1}^6 I_i^{(IIa)}(s, s_1, s_2, t_1, t_2), \quad (11.16)$$

and

$$\begin{aligned} I_1^{(IIa)}(s, s_1, s_2, t_1, t_2) &= -\frac{1}{\epsilon^3} y_2^{-\epsilon} \Gamma(1-2\epsilon) \Gamma(1+\epsilon)^2 \\ &\quad \times F_4\left(1-2\epsilon, 1-\epsilon, 1-\epsilon, 1-\epsilon; -y_1, y_2\right), \\ I_2^{(IIa)}(s, s_1, s_2, t_1, t_2) &= \frac{1}{\epsilon^3} \Gamma(1+\epsilon) \Gamma(1-\epsilon) F_4\left(1, 1-\epsilon, 1-\epsilon, 1+\epsilon; -y_1, y_2\right), \\ I_3^{(IIa)}(s, s_1, s_2, t_1, t_2) &= -\frac{\Gamma(1-2\epsilon) \Gamma(-\delta) \Gamma(-\epsilon-\delta+1) \Gamma(\epsilon+\delta)}{\epsilon \Gamma(1+\epsilon) \Gamma(1-\epsilon) \Gamma(1-2\epsilon-\delta)} \\ &\quad \times F_{0,2}^{2,1}\left(\begin{matrix} 1-\delta & 1-\epsilon-\delta \\ - & - \end{matrix} \middle| \begin{matrix} 1 & - & - & - \\ 1+\epsilon & 1-\epsilon-\delta & 1-\delta & - \end{matrix} \middle| -y_1, y_2\right) \\ &\quad \times (-s_1)^{-\delta} y_1^\epsilon y_2^{-\epsilon-\delta}, \\ I_4^{(IIa)}(s, s_1, s_2, t_1, t_2) &= -\frac{\Gamma(-\delta) \Gamma(1-2\epsilon) \Gamma(-\epsilon-\delta) \Gamma(\epsilon+\delta)}{\Gamma(1+\epsilon) \Gamma(1-\epsilon) \Gamma(1-2\epsilon-\delta)} \\ &\quad \times (-s_1)^{-\delta} y_1^{\epsilon+\delta} y_2^{-\epsilon-\delta} F_4\left(1, 1-\epsilon, 1+\epsilon+\delta, 1-\epsilon-\delta; -y_1, y_2\right), \\ I_5^{(IIa)}(s, s_1, s_2, t_1, t_2) &= \frac{\Gamma(\delta) \Gamma(1-2\epsilon) \Gamma(-\epsilon-\delta)}{\epsilon \Gamma(1-\epsilon) \Gamma(\delta+1) \Gamma(-2\epsilon-\delta+1)} (-s_1)^{-\delta} \\ &\quad \times y_1^\epsilon F_{0,2}^{2,1}\left(\begin{matrix} 1 & 1+\epsilon \\ - & - \end{matrix} \middle| \begin{matrix} 1 & - & - & - \\ 1+\epsilon & 1+\epsilon+\delta & 1-\delta & - \end{matrix} \middle| -y_1, y_2\right), \\ I_6^{(IIa)}(s, s_1, s_2, t_1, t_2) &= -\frac{\Gamma(-\delta) \Gamma(\delta+1) \Gamma(-\epsilon-\delta)^2 \Gamma(\epsilon+\delta+1) \Gamma(1-2\epsilon)}{\Gamma(1-\epsilon)^2 \Gamma(1+\epsilon) \Gamma(-2\epsilon-\delta+1)} \\ &\quad \times (-s_1)^{-\delta} y_1^{\epsilon+\delta} F_4\left(1+\delta, 1+\epsilon+\delta, 1+\epsilon+\delta, 1+\epsilon+\delta; -y_1, y_2\right), \end{aligned} \quad (11.17)$$

where we defined

$$y_1 = \frac{1}{x_2} = \frac{\kappa}{t_2} \quad \text{and} \quad y_2 = \frac{x_1}{x_2} = \frac{t_1}{t_2}. \quad (11.18)$$

The six solutions in Region II(a) can be entirely written in terms of generalized hypergeometric functions, and more precisely in terms of the so-called Appell  $F_4$  and Kampé de Fériet functions, defined by [97, 98],

$$\begin{aligned}
 F_4(a, b, c, d; x_1, x_2) &= \sum_{n_1=0}^{\infty} \frac{(a)_{n_1+n_2} (b)_{n_1+n_2}}{(c)_{n_1} (d)_{n_2}} \frac{x_1^{n_1}}{n_1!} \frac{x_2^{n_2}}{n_2!}, \\
 F_{p',q'}^{p,q} \left( \begin{array}{c} \alpha_i \\ \alpha'_k \end{array} \middle| \begin{array}{c} \beta_j \quad \gamma_j \\ \beta'_\ell \quad \gamma'_\ell \end{array} \middle| x_1, x_2 \right) & \quad (11.19) \\
 &= \sum_{n_1=0}^{\infty} \sum_{n_2=0}^{\infty} \frac{\prod_i (\alpha_i)_{n_1+n_2} \prod_j (\beta_j)_{n_1} (\gamma_j)_{n_2}}{\prod_k (\alpha'_k)_{n_1+n_2} \prod_\ell (\beta'_\ell)_{n_1} (\gamma'_\ell)_{n_2}} \frac{x_1^{n_1}}{n_1!} \frac{x_2^{n_2}}{n_2!}.
 \end{aligned}$$

The ‘-’ sign in the Kampé de Fériet functions in Eq. (11.17) indicates that a given index is absent in the definition of the hypergeometric series, *e.g.* ,

$$\begin{aligned}
 F_{0,2}^{2,1} \left( \begin{array}{c} a \quad b \\ - \quad - \end{array} \middle| \begin{array}{c} c \quad - \quad - \\ d \quad e \quad f \quad - \end{array} \middle| x_1, x_2 \right) & \quad (11.20) \\
 = \sum_{n_1=0}^{\infty} \sum_{n_2=0}^{\infty} \frac{(a)_{n_1+n_2} (b)_{n_1+n_2} (c)_{n_1}}{(d)_{n_1} (e)_{n_2} (f)_{n_1}} \frac{x_1^{n_1}}{n_1!} \frac{x_2^{n_2}}{n_2!}.
 \end{aligned}$$

Let us make a comment about the  $\delta$  symbol in Eq. (11.17). In Section 11.3.1 we derived a representation for the pentagon for general powers of the propagators  $\nu_i$ . Some of the coefficients of the hypergeometric functions contain, however,  $\Gamma$  functions of the form  $\Gamma(1 - \nu_i)$ , which are divergent in the limit  $\nu_i \rightarrow 1$ . We regulate this divergence by introducing a small quantity  $\delta$  such that  $\Gamma(1 - \nu_i) = \Gamma(\delta)$ . The pentagon integral must be independent of this regulator, and so the  $\delta$  dependence must cancel in the sum over all six contributions. Expanding the solutions into a Laurent series in  $\delta$ , and keeping only terms of  $\mathcal{O}(\delta^0)$ , we find,

$$\begin{aligned}
 & I_3^{(IIa)} + I_4^{(IIa)} \\
 &= -\frac{1}{\epsilon^2} y_1^\epsilon y_2^{-\epsilon} \left\{ [\ln y_1 + \psi(1 - \epsilon) - \psi(-\epsilon)] F_4(1, 1 - \epsilon, 1 + \epsilon, 1 - \epsilon; -y_1, y_2) \right. \\
 & \left. + \frac{\partial}{\partial \delta} F_{0,2}^{2,1} \left( \begin{array}{c} 1 + \delta \quad 1 + \delta - \epsilon \\ - \quad - \end{array} \middle| \begin{array}{c} 1 \quad - \quad - \\ 1 + \delta \quad 1 - \epsilon \quad 1 + \epsilon + \delta \quad - \end{array} \middle| -y_1, y_2 \right) \Big|_{\delta=0} \right\}, & (11.21)
 \end{aligned}$$

$$\begin{aligned}
& I_5^{(IIa)} + I_6^{(IIa)} \\
&= \frac{1}{\epsilon^2} y_1^\epsilon \left\{ [\ln y_1 + \psi(1 + \epsilon) - \psi(-\epsilon)] F_4(1, 1 + \epsilon, 1 + \epsilon, 1 + \epsilon; -y_1, y_2) \right. \\
& \left. + \frac{\partial}{\partial \delta} F_{0,2}^{2,1} \left( \begin{array}{ccc|ccc} 1 + \delta & 1 + \delta + \epsilon & & 1 & - & - \\ & - & & 1 + \delta & 1 + \epsilon & 1 + \epsilon + \delta \end{array} \middle| -y_1, y_2 \right) \Big|_{\delta=0} \right\},
\end{aligned}$$

and we see that these two expressions are independent of the regulator  $\delta$ . The final result for the massless scalar pentagon in multi-Regge kinematics to all orders in  $\epsilon$  in Region II(a) is then simply given by the sum

$$\begin{aligned}
& \mathcal{I}^{(IIa)}(s, s_1, s_2, t_1, t_2) \\
&= -\frac{1}{\epsilon^3} y_2^{-\epsilon} \Gamma(1 - 2\epsilon) \Gamma(1 + \epsilon)^2 F_4(1 - 2\epsilon, 1 - \epsilon, 1 - \epsilon, 1 - \epsilon; -y_1, y_2) \\
&+ \frac{1}{\epsilon^3} \Gamma(1 + \epsilon) \Gamma(1 - \epsilon) F_4(1, 1 - \epsilon, 1 - \epsilon, 1 + \epsilon; -y_1, y_2) \\
&- \frac{1}{\epsilon^2} y_1^\epsilon y_2^{-\epsilon} \left\{ [\ln y_1 + \psi(1 - \epsilon) - \psi(-\epsilon)] F_4(1, 1 - \epsilon, 1 + \epsilon, 1 - \epsilon; -y_1, y_2) \right. \\
& \left. + \frac{\partial}{\partial \delta} F_{0,2}^{2,1} \left( \begin{array}{ccc|ccc} 1 + \delta & 1 + \delta - \epsilon & & 1 & - & - \\ & - & & 1 + \delta & 1 - \epsilon & 1 + \epsilon + \delta \end{array} \middle| -y_1, y_2 \right) \Big|_{\delta=0} \right\} \\
&+ \frac{1}{\epsilon^2} y_1^\epsilon \left\{ [\ln y_1 + \psi(1 + \epsilon) - \psi(-\epsilon)] F_4(1, 1 + \epsilon, 1 + \epsilon, 1 + \epsilon; -y_1, y_2) \right. \\
& \left. + \frac{\partial}{\partial \delta} F_{0,2}^{2,1} \left( \begin{array}{ccc|ccc} 1 + \delta & 1 + \delta + \epsilon & & 1 & - & - \\ & - & & 1 + \delta & 1 + \epsilon & 1 + \epsilon + \delta \end{array} \middle| -y_1, y_2 \right) \Big|_{\delta=0} \right\}.
\end{aligned} \tag{11.22}$$

Note that the only functional dependence of  $\mathcal{I}^{(IIa)}$  is in the ratio of scales  $y_1$  and  $y_2$ , *i.e.*, in the transverse momentum scales  $t_1$ ,  $t_2$  and  $\kappa$ ,

$$\mathcal{I}^{(IIa)}(s, s_1, s_2, t_1, t_2) = \mathcal{I}^{(IIa)}(\kappa, t_1, t_2). \tag{11.23}$$

The solution in Region II(b) is related to the Region II(a) by analytic continuation according to the prescription  $t_1/t_2 \rightarrow t_2/t_1$ , or equivalently  $y_2 \rightarrow 1/y_2$ . From the symmetry of the multi-Regge limit in  $t_1$  and  $t_2$  it is easy to see that we must have

$$\mathcal{I}^{(IIb)}(\kappa, t_1, t_2) = \frac{t_2}{t_1} \mathcal{I}^{(IIa)}(\kappa, t_2, t_1). \tag{11.24}$$

In Appendix L we explicitly show that Eq. (11.22) enjoys this property.

Let us now have a closer look at the special functions in Eq. (11.22). Using the reduction formulas for the Appell function given in Appendix H, we could reexpress all the  $F_4$  in Eq. (11.22) in terms of Gauss' hypergeometric function and the Appell  $F_1$  function,

$$\begin{aligned} F_4\left(1-2\epsilon, 1-\epsilon, 1-\epsilon, 1-\epsilon, \frac{-x}{(1-x)(1-y)}, \frac{-y}{(1-x)(1-y)}\right) \\ = (1-x)^{1-\epsilon} (1-y)^{1-\epsilon} {}_2F_1(1-2\epsilon, 1-\epsilon, 1-\epsilon; xy) \\ = \frac{(1-x)^{1-\epsilon} (1-y)^{1-\epsilon}}{(1-xy)^{1-2\epsilon}}, \end{aligned} \quad (11.25)$$

$$\begin{aligned} F_4\left(1, 1-\epsilon, 1+\epsilon, 1-\epsilon, \frac{-x}{(1-x)(1-y)}, \frac{-y}{(1-x)(1-y)}\right) \\ = (1-x)(1-y) F_1(1, 2\epsilon, 1-\epsilon, 1+\epsilon; xy), \end{aligned}$$

with

$$F_1(a, b, c, d; x_1, x_2) = \sum_{n_1=0}^{\infty} \sum_{n_2=0}^{\infty} \frac{(a)_{n_1+n_2} (b)_{n_1} (c)_{n_2}}{(d)_{n_1+n_2}} \frac{x_1^{n_1}}{n_1!} \frac{x_2^{n_2}}{n_2!}. \quad (11.26)$$

The Appell  $F_1$  function appearing in this reduction can be easily expanded into a Laurent series in  $\epsilon$  using `XSummer` [76]. Note however that we do not know the corresponding reduction formulas for the Kampé de Fériet functions appearing in Eq. (11.22). For this reason, we do not apply the reduction formulas of the Appell  $F_4$  functions, but we proceed and perform the  $\epsilon$  expansion directly on the series representation of the hypergeometric functions appearing in Eq. (11.22). Since all the hypergeometric functions in Eq. (11.22) are finite for  $\epsilon = 0$ , we can safely expand the Pochhammer symbols into a power series under the summation sign,

$$\begin{aligned} (1+\epsilon)_n &= n! \left(1 + \epsilon Z_1(n) + \epsilon^2 Z_{11}(n) + \epsilon^3 Z_{111}(n) + \mathcal{O}(\epsilon^4)\right), \\ \frac{1}{(1+\epsilon)_n} &= \frac{1}{n!} \left(1 - \epsilon S_1(n) - \epsilon^2 S_{11}(n) - \epsilon^3 S_{111}(n) + \mathcal{O}(\epsilon^4)\right), \end{aligned} \quad (11.27)$$

where  $S$  and  $Z$  denote nested harmonic sums and Euler-Zagier sums, defined recursively by [99],

$$\begin{aligned} S_i(n) = Z_i(n) = H_n^{(i)} &= \sum_{k=1}^n \frac{1}{k^i}, \\ S_{i\bar{j}}(n) = \sum_{k=1}^n \frac{S_{\bar{j}}(k)}{k^i} \quad \text{and} \quad Z_{i\bar{j}}(n) &= \sum_{k=1}^n \frac{Z_{\bar{j}}(k-1)}{k^i}. \end{aligned} \quad (11.28)$$

The sum of the elements of the index vector  $\vec{i}$  is called the weight of the nested sum  $S_{\vec{i}}(n)$  or  $Z_{\vec{i}}(n)$ . The nested harmonic sums and the Euler-Zagier sums form a shuffle algebra, which allows one to express a product of sums of weight  $w_1$  and  $w_2$  respectively as a combination of sums of weight  $w_1 + w_2$ , *e.g.* ,

$$\begin{aligned} S_i(n)S_j(n) &= \sum_{k_1=1}^n \sum_{k_2=1}^n \frac{1}{k_1^i k_2^j} \\ &= \sum_{k_1=1}^n \frac{1}{k_1^i} \sum_{k_2=1}^{k_1} \frac{1}{k_2^j} + \sum_{k_2=1}^n \frac{1}{k_2^j} \sum_{k_1=1}^{k_2} \frac{1}{k_1^i} - \sum_{k=1}^n \frac{1}{k^{i+j}} \\ &= S_{ij}(n) + S_{ji}(n) - S_{i+j}(n). \end{aligned} \tag{11.29}$$

Using the algebra properties of nested sums as well as the algorithm described in Appendix F, we can express all the Euler-Zagier sums in terms of harmonic sums. Finally, using the algebra properties of the  $S$ -sums, we can reduce all the products of harmonic sums to linear combinations of the latter. Inserting Eq. (11.27) into the series representation for hypergeometric functions we obtain the desired  $\epsilon$  expansions, *e.g.* ,

$$\begin{aligned} F_4(1, 1 + \epsilon, 1 + \epsilon, 1 + \epsilon; x_1, x_2) &= \mathcal{M}(0, 0, 0; x_1, x_2) \\ &+ \epsilon \left[ \mathcal{M}(0, 0, 1; x_1, x_2) - \mathcal{M}(1, 0, 0; x_1, x_2) - \mathcal{M}(0, 1, 0; x_1, x_2) \right] \\ &+ \epsilon^2 \left[ \mathcal{M}((1, 1), 0, 0; x_1, x_2) + \mathcal{M}(0, (1, 1), 0; x_1, x_2) + \mathcal{M}(0, 0, (1, 1); x_1, x_2) \right. \\ &\quad \left. + \mathcal{M}(1, 1, 0; x_1, x_2) - \mathcal{M}(1, 0, 1; x_1, x_2) - \mathcal{M}(0, 1, 1; x_1, x_2) \right. \\ &\quad \left. - \mathcal{M}(0, 0, 2; x_1, x_2) \right] \\ &+ \mathcal{O}(\epsilon^3). \end{aligned} \tag{11.30}$$

The  $\mathcal{M}$  functions appearing in this expansion are transcendental functions defined by the double series

$$\mathcal{M}(\vec{i}, \vec{j}, \vec{k}; x_1, x_2) = \sum_{n_1=0}^{\infty} \sum_{n_2=0}^{\infty} \binom{n_1 + n_2}{n_1}^2 S_{\vec{i}}(n_1) S_{\vec{j}}(n_2) S_{\vec{k}}(n_1 + n_2) x_1^{n_1} x_2^{n_2}. \tag{11.31}$$

We define the weight of an  $\mathcal{M}$  function as the sum of the weights of the nested harmonic sums in the right-hand side of Eq. (11.31). Note that due to the

appearance of the binomial squared term in Eq. (11.31), we cannot reduce in general the double sums to known function using the standard techniques. We can however sum the series in some particular cases where we can relate the  $\mathcal{M}$ -function to the expansion of a known hypergeometric function. This issue is addressed in Appendix I.

Since Eq. (11.22) only involves Appell functions and Kampé de Fériet functions with indices  $1 + c_i\epsilon$ , it can be easily expanded in terms of  $\mathcal{M}$  functions. The first two orders read,

$$\mathcal{I}^{(IIa)}(\kappa, t_1, t_2) = i_0^{(IIa)}(y_1, y_2) + \epsilon i_1^{(IIa)}(y_1, y_2) + \mathcal{O}(\epsilon^2), \quad (11.32)$$

with

$$\begin{aligned} i_0^{(IIa)}(y_1, y_2) = & (-8 \ln y_1 - 4 \ln y_2) \mathcal{M}(0, 0, (1, 1); -y_1, y_2) \\ & - 4 \ln y_2 \mathcal{M}((1, 1), 0, 0; -y_1, y_2) + 18 \mathcal{M}(0, 0, (1, 2); -y_1, y_2) \\ & + 18 \mathcal{M}(0, 0, (2, 1); -y_1, y_2) - 24 \mathcal{M}(0, 0, (1, 1, 1); -y_1, y_2) \\ & + 8 \mathcal{M}(0, 1, (1, 1); -y_1, y_2) + 16 \mathcal{M}(1, 0, (1, 1); -y_1, y_2) \\ & - 8 \mathcal{M}((1, 1), 0, 1; -y_1, y_2) + 8 \mathcal{M}((1, 1), 1, 0; -y_1, y_2) \\ & - \mathcal{M}(0, 0, 0; -y_1, y_2) \left( \frac{\pi^2 \ln y_1}{3} + \frac{\ln^2 y_1 \ln y_2}{2} + \frac{\pi^2 \ln y_2}{2} - 2\zeta_3 \right) \\ & - \mathcal{M}(0, 0, 1; -y_1, y_2) \left( 2 \ln y_1 \ln y_2 + \ln^2 y_1 + \frac{5\pi^2}{3} \right) \\ & + (6 \ln y_1 + 3 \ln y_2) \mathcal{M}(0, 0, 2; -y_1, y_2) + 4 \ln y_1 \mathcal{M}(0, 1, 1; -y_1, y_2) \\ & + \left( 2 \ln y_1 \ln y_2 + \frac{2\pi^2}{3} \right) \mathcal{M}(1, 0, 0; -y_1, y_2) - 4 \ln y_1 \mathcal{M}(1, 1, 0; -y_1, y_2) \\ & + (4 \ln y_1 + 4 \ln y_2) \mathcal{M}(1, 0, 1; -y_1, y_2) - 2 \mathcal{M}(2, 1, 0; -y_1, y_2) \\ & + \ln y_2 \mathcal{M}(2, 0, 0; -y_1, y_2) - 12 \mathcal{M}(0, 0, 3; -y_1, y_2) - 6 \mathcal{M}(0, 1, 2; -y_1, y_2) \\ & - 12 \mathcal{M}(1, 0, 2; -y_1, y_2) - 8 \mathcal{M}(1, 1, 1; -y_1, y_2) + 2 \mathcal{M}(2, 0, 1; -y_1, y_2) \\ & + \left( \ln^2 y_1 + \pi^2 \right) \mathcal{M}(0, 1, 0; -y_1, y_2), \end{aligned} \quad (11.33)$$

The explicit expression for  $i_1^{(IIa)}$  is given in Ref. [28]. Note that  $i_0^{(IIa)}$  and  $i_1^{(IIa)}$  are of uniform transcendental weight 3 and 4, as expected.



### 11.3.3 The solution in Region I

The solutions in Region I read

$$I^{(I)}(s, s_1, s_2, t_1, t_2) = r_\Gamma e^{\gamma_E \epsilon} \frac{(-\kappa)^{-\epsilon}}{s_1 s_2} \mathcal{I}^{(I)}(s, s_1, s_2, t_1, t_2), \quad (11.34)$$

with

$$\mathcal{I}^{(I)}(s, s_1, s_2, t_1, t_2) = \sum_{i=1}^6 I_i^{(I)}(s, s_1, s_2, t_1, t_2), \quad (11.35)$$

and

$$\begin{aligned} I_1^{(I)}(s, s_1, s_2, t_1, t_2) &= -\frac{1}{\epsilon^3} x_1^{-\epsilon} x_2^{-\epsilon} \Gamma(1-2\epsilon) \Gamma(1+\epsilon)^2 \\ &\quad \times F_4(1-2\epsilon, 1-\epsilon, 1-\epsilon, 1-\epsilon; -x_1, -x_2), \\ I_2^{(I)}(s, s_1, s_2, t_1, t_2) &= \frac{1}{\epsilon^3} \Gamma(1+\epsilon) \Gamma(1-\epsilon) F_4(1, 1+\epsilon, 1+\epsilon, 1+\epsilon; -x_1, -x_2), \\ I_3^{(I)}(s, s_1, s_2, t_1, t_2) &= (-s_2)^\delta (-s_1)^{-\delta} (-t_1)^{-\delta} (-t_2)^\delta x_1^{-\epsilon} \frac{\Gamma(-\delta) \Gamma(\epsilon+\delta)}{\epsilon \Gamma(1+\epsilon)} \\ &\quad \times \sum_{n_1=0}^{\infty} \sum_{n_2=0}^{\infty} \frac{(1-\delta)_{n_2} (-\delta)_{n_1-n_2} (\delta+1)_{n_2} (1-\epsilon)_{n_2} (-\epsilon)_{n_1-n_2}}{(-\epsilon-\delta+1)_{n_1} n_1! n_2!} \\ &\quad \times \left( \frac{x_1}{x_2} \right)^{n_1} (-x_2)^{n_2}, \\ I_4^{(I)}(s, s_1, s_2, t_1, t_2) &= -(-s)^{-\delta} (-s_2)^{2\delta} (-t_1)^{-\delta} x_1^{-\epsilon} \\ &\quad \times \frac{\Gamma(1-2\delta) \Gamma(\delta) \Gamma(-\epsilon-\delta+1) \Gamma(\delta-\epsilon) \Gamma(\epsilon+\delta)}{\Gamma(1-\delta) \Gamma(\delta+1) \Gamma(1+\epsilon) \Gamma(1-\epsilon)^2} \\ &\quad \times F_{1,2}^{3,0} \left( \begin{matrix} 1 & 1-\epsilon-\delta & 1-2\delta \\ - & - & 1-\delta \end{matrix} \middle| \begin{matrix} - & - \\ 1-\epsilon-\delta & 1+\epsilon-\delta \end{matrix} \middle| -x_1, -x_2 \right), \\ I_5^{(I)}(s, s_1, s_2, t_1, t_2) &= -(-s)^\delta (-s_1)^{-2\delta} (-t_2)^\delta x_2^{-\epsilon} \\ &\quad \times \frac{\Gamma(-\delta) \Gamma(2\delta+1) \Gamma(-\epsilon-\delta) \Gamma(\epsilon-\delta) \Gamma(-\epsilon+\delta+1)}{\Gamma(1-\delta) \Gamma(\delta+1) \Gamma(1+\epsilon) \Gamma(1-\epsilon)^2} \\ &\quad \times F_{1,2}^{3,0} \left( \begin{matrix} 1 & 1-\epsilon+\delta & 1+2\delta \\ - & - & 1+\delta \end{matrix} \middle| \begin{matrix} - & - \\ 1+\epsilon+\delta & 1-\epsilon+\delta \end{matrix} \middle| -x_1, -x_2 \right), \end{aligned} \quad (11.36)$$

$$\begin{aligned}
I_6^{(I)}(s, s_1, s_2, t_1, t_2) &= -(-s_2)^\delta (-s_1)^{-\delta} x_2^{-\epsilon} \frac{\Gamma(\delta)\Gamma(-\epsilon-\delta)}{\epsilon\Gamma(1-\epsilon)} \\
&\times \sum_{n_1=0}^{\infty} \sum_{n_2=0}^{\infty} \frac{(1-\delta)_{n_2}(\delta)_{n_1-n_2}(\delta+1)_{n_2}(1-\epsilon)_{n_2}(\epsilon)_{n_1-n_2}}{(\epsilon+\delta+1)_{n_1}n_1!n_2!} \\
&\times \left(\frac{x_1}{x_2}\right)^{n_1} (-x_2)^{n_2}.
\end{aligned}$$

We again introduce a regulator  $\delta$  to prevent divergences in the  $\Gamma$  functions in the coefficients of the hypergeometric function. The cancellation of the spurious  $\delta$ -poles is not as straightforward as in Region II(a), due the appearance of a new type of hypergeometric series besides the Appell and Kampé de Fériet functions. This new series involves only Pochhammer symbols of the form  $(\cdot)_{n_1-n_2}$ ,  $(\cdot)_{n_1}$  and  $(\cdot)_{n_2}$ . In Appendix H we show that it can be reduced to Kampé de Fériet functions. We find

$$\begin{aligned}
&\sum_{n_1=0}^{\infty} \sum_{n_2=0}^{\infty} \frac{(1-\delta)_{n_2}(-\delta)_{n_1-n_2}(\delta+1)_{n_2}(1-\epsilon)_{n_2}(-\epsilon)_{n_1-n_2}}{(-\epsilon-\delta+1)_{n_1}n_1!n_2!} \left(\frac{x_1}{x_2}\right)^{n_1} (-x_2)^{n_2} \\
&= \frac{\delta\epsilon}{1-\epsilon-\delta} \frac{x_1}{x_2}
\end{aligned} \tag{11.37}$$

$$\begin{aligned}
&\times F_{2,0}^{0,3} \left( \begin{matrix} - & - \\ 2 & 2-\epsilon-\delta \end{matrix} \middle| \begin{matrix} 1+\delta & 1 & 1-\delta & 1-\delta & 1-\epsilon & 1-\epsilon \\ - & - & - & - & - & - \end{matrix} \middle| -x_1, \frac{x_1}{x_2} \right) \\
&+ F_{1,2}^{3,1} \left( \begin{matrix} 1-\delta & 1+\delta & 1-\epsilon \\ 1 & - & - \end{matrix} \middle| \begin{matrix} - & 1 & - & - \\ - & 1+\delta & 1-\delta-\epsilon & 1+\epsilon \end{matrix} \middle| -x_1, -x_2 \right),
\end{aligned}$$

$$\begin{aligned}
&\sum_{n_1=0}^{\infty} \sum_{n_2=0}^{\infty} \frac{(1-\delta)_{n_2}(\delta)_{n_1-n_2}(\delta+1)_{n_2}(1-\epsilon)_{n_2}(\epsilon)_{n_1-n_2}}{(\epsilon+\delta+1)_{n_1}n_1!n_2!} \left(\frac{x_1}{x_2}\right)^{n_1} (-x_2)^{n_2} \\
&= \frac{\delta\epsilon}{1+\epsilon+\delta} \frac{x_1}{x_2} \\
&\times F_{2,0}^{0,3} \left( \begin{matrix} - & - \\ 2 & 2+\epsilon+\delta \end{matrix} \middle| \begin{matrix} 1-\delta & 1 & 1+\delta & 1+\delta & 1-\epsilon & 1+\epsilon \\ - & - & - & - & - & - \end{matrix} \middle| -x_1, \frac{x_1}{x_2} \right) \\
&+ F_{1,2}^{3,1} \left( \begin{matrix} 1-\delta & 1+\delta & 1-\epsilon \\ 1 & - & - \end{matrix} \middle| \begin{matrix} - & 1 & - & - \\ - & 1-\delta & 1+\delta+\epsilon & 1-\epsilon \end{matrix} \middle| -x_1, -x_2 \right).
\end{aligned} \tag{11.38}$$

After inserting these expressions into Eq. (11.36), we expand the solution into a Laurent series in  $\delta$ . The poles in  $\delta$  cancel mutually between  $I_3^{(I)}$  and  $I_4^{(I)}$  and  $I_5^{(I)}$  and  $I_6^{(I)}$ . After some algebra, we find the following expression for the solution in Region I,

$$\begin{aligned}
& \mathcal{I}^{(I)}(s, s_1, s_2, t_1, t_2) \\
&= -\frac{1}{\epsilon^3} x_1^{-\epsilon} x_2^{-\epsilon} \Gamma(1-2\epsilon) \Gamma(1+\epsilon)^2 F_4(1-2\epsilon, 1-\epsilon, 1-\epsilon, 1-\epsilon; -x_1, -x_2) \\
&+ \frac{1}{\epsilon^3} \Gamma(1-\epsilon) \Gamma(1+\epsilon) F_4(1, 1+\epsilon, 1+\epsilon, 1+\epsilon; -x_1, -x_2) \\
&- \frac{1}{\epsilon^2} x_1^{-\epsilon} \left\{ \left[ \ln x_2 + \psi(1-\epsilon) - \psi(-\epsilon) \right] F_4(1, 1-\epsilon, 1-\epsilon, 1+\epsilon; -x_1, -x_2) \right. \\
&+ \left. \frac{\partial}{\partial \delta} F_{0,2}^{2,1} \left( \begin{array}{ccc|ccc} 1+\delta & 1-\epsilon+\delta & & - & - & - \\ & & & 1-\epsilon & 1+\epsilon+\delta & - \\ \hline & & & & & 1 \\ & & & & & 1+\delta \end{array} \middle| -x_1, -x_2 \right) \Big|_{\delta=0} \right\} \\
&+ \left. \frac{\epsilon}{1-\epsilon} \frac{x_1}{x_2} F_{2,0}^{0,3} \left( \begin{array}{cc|ccccc} - & - & 1 & 1 & 1 & 1-\epsilon & 1-\epsilon \\ 2 & 2-\epsilon & - & - & - & - & - \end{array} \middle| -x_1, \frac{x_1}{x_2} \right) \right\} \\
&- \frac{1}{\epsilon^2} x_2^{-\epsilon} \left\{ \left[ \ln x_2 + \psi(1-\epsilon) - \psi(\epsilon) \right] F_4(1, 1-\epsilon, 1+\epsilon, 1-\epsilon; -x_1, -x_2) \right. \\
&+ \left. \frac{\partial}{\partial \delta} F_{0,2}^{2,1} \left( \begin{array}{ccc|ccc} 1+\delta & 1-\epsilon+\delta & & - & - & - \\ & & & 1+\epsilon & 1-\epsilon+\delta & - \\ \hline & & & & & 1 \\ & & & & & 1+\delta \end{array} \middle| -x_1, -x_2 \right) \Big|_{\delta=0} \right\} \\
&- \left. \frac{\epsilon}{1+\epsilon} \frac{x_1}{x_2} F_{2,0}^{0,3} \left( \begin{array}{cc|ccccc} - & - & 1 & 1 & 1 & 1-\epsilon & 1+\epsilon \\ 2 & 2+\epsilon & - & - & - & - & - \end{array} \middle| -x_1, \frac{x_1}{x_2} \right) \right\}. \tag{11.39}
\end{aligned}$$

Note that the right-hand side of Eq. (11.39) only depends on the dimensionless quantities  $x_1$  and  $x_2$ , *i.e.*, on the transverse momentum scales  $\kappa$ ,  $t_1$  and  $t_2$ ,

$$\mathcal{I}^{(I)}(s, s_1, s_2, t_1, t_2) = \mathcal{I}^{(I)}(\kappa, t_1, t_2). \tag{11.40}$$

Furthermore, we know that the pentagon in Region I must fulfill the symmetry relation

$$\mathcal{I}^{(I)}(\kappa, t_1, t_2) = \mathcal{I}^{(I)}(\kappa, t_2, t_1). \tag{11.41}$$

The solution given in Eq. (11.39) however apparently breaks this symmetry, due to the appearance of the ratio  $x_1/x_2$ . We show in Appendix L that Eq. (11.39) indeed has the correct symmetry properties, which becomes explicit only after

a proper analytic continuation has been performed. We also show that the solution in Region I, Eq. (11.39), can be obtained from the solution in Region II(a) by performing analytic continuation according to the prescription  $y_1 \rightarrow 1/y_1$ .

## 11.4 The two-loop five-point amplitude

In this section we show how the expression for the scalar massless pentagon integral can be used to obtain an analytic expression for the two-loop five-point amplitude, albeit in simplified kinematics. The two-loop five-point MSYM amplitude is related to the corresponding one-loop amplitude through the ABDK ansatz (7.2). Since we know that the ABDK ansatz holds for  $n = 5$ , it is enough to know the one-loop amplitude to  $\mathcal{O}(\epsilon^2)$  to derive the corresponding two-loop amplitude. The decomposition of the one-loop amplitude to all orders in  $\epsilon$  in terms of scalar box and pentagon integrals was presented in Eq. (9.28). Let us decompose this relation into parity-even and odd contributions to the five-point amplitude,

$$m_5^{(1)} = m_{5e}^{(1)} + m_{5o}^{(1)}, \quad (11.42)$$

with

$$\begin{aligned} m_{5e}^{(1)} &= -\frac{1}{2} G(\epsilon) \sum_{\text{cyclic}} s_{12} s_{23} I_4^{1m}(1, 2, 3, 45, \epsilon), \\ m_{5o}^{(1)} &= -\epsilon G(\epsilon) \epsilon_{1234} I_5^{6-2\epsilon}(\epsilon). \end{aligned} \quad (11.43)$$

The even-parity contribution corresponds to the one-mass box integrals and was already given in Eq. (9.33). The pentagon contribution has been computed in the previous sections. We thus have at our disposal all the pieces needed to compute  $m_5^{(1)}$  to all orders in  $\epsilon$ .

Let us start by analyzing more closely the parity-odd contribution. The Levi-Civita tensor appearing in the parity-odd part of the five-point amplitude can be written in the form

$$\epsilon_{1234} = s_{12} s_{34} - s_{13} s_{23} + s_{14} s_{23} - 2 \langle 12 \rangle [23] \langle 34 \rangle [41]. \quad (11.44)$$

Using the approximate form of the spinor products in multi-Regge kinematics, Eq. (8.12), we obtain,

$$\epsilon_{1234} = (-s) (p_{3\perp} p_{4\perp}^* - p_{3\perp}^* p_{4\perp}). \quad (11.45)$$

Furthermore, we know that for the pentagon integral we have to distinguish several kinematic regions. Using the same notations as in the previous sections, we obtain the following representation for the parity-odd part of the five-point amplitude,

$$\begin{aligned} m_{5o}^{(1,IIa)}(s, s_1, s_1, t_1, t_2) &= -\epsilon (p_{3\perp} p_{4\perp}^* - p_{3\perp}^* p_{4\perp}) \frac{(-\kappa)^\epsilon}{t_2} \mathcal{I}^{(IIa)}(t_1, t_2, \kappa), \\ m_{5o}^{(1,I)}(s, s_1, s_1, t_1, t_2) &= -\epsilon (p_{3\perp} p_{4\perp}^* - p_{3\perp}^* p_{4\perp}) \frac{(-\kappa)^\epsilon}{\kappa} \mathcal{I}^{(I)}(t_1, t_2, \kappa), \end{aligned} \quad (11.46)$$

where  $\mathcal{I}^{(IIa)}$  and  $\mathcal{I}^{(I)}$  are defined in Eqs. (11.22) and (11.39). The expressions for  $(-t_2) < (-t_1)$  can be obtained by analytic continuation according to the prescription  $t_1/t_2 \rightarrow t_2/t_1$ . Note that since the pentagon integral is finite for  $\epsilon \rightarrow 0$ , the parity-odd contribution only starts at  $\mathcal{O}(\epsilon)$ . Combining the two terms for the parity-even and odd contributions we find immediately the expression of the one-loop five-point amplitude in multi-Regge kinematics. As a cross-check, we checked that our result has the correct behavior in the limit where  $p_4 \rightarrow 0$ .

Let us now turn to the two-loop amplitude. Using the ABDK recursion relations, it is straightforward to derive an expression of the two-loop amplitude as a function of the one-loop amplitude. Using the decomposition into parity-even and odd contributions, we obtain,

$$\begin{aligned} m_{5e}^{(2)}(\epsilon) &= \frac{1}{2} (m_{5e}^{(1)}(\epsilon))^2 + 2 f^{(2)}(\epsilon) \frac{G(\epsilon)^2}{G(2\epsilon)} m_{5e}^{(1)}(2\epsilon) + C^{(2)} + \mathcal{O}(\epsilon), \\ m_{5o}^{(2,j)}(\epsilon) &= m_{5e}^{(1)}(\epsilon) m_{5o}^{(1,j)}(\epsilon) + \mathcal{O}(\epsilon), \end{aligned} \quad (11.47)$$

with  $j = I, IIa$ . Using the explicit expressions of the parity-even and odd contributions, we see that the right-hand side of Eq. (11.47) is completely expressed in terms of known quantities. Hence, Eq. (11.47) evaluates immediately to the five-point two-loop amplitude in multi-Regge kinematics, which is the main result of this work. In previous sections, we argued that the parity-odd

contribution, which equals the contribution from the scalar massless pentagon integral, is expressed in terms of new transcendental functions not present in the parity-even contribution. This implies that the two-loop five-point amplitude is expressed in terms of this same new set of special functions, and in particular we can write out the result completely as a Laurent series in  $\epsilon$  whose coefficients are combinations of  $\mathcal{M}$  functions and Goncharov polylogarithms.

## 11.5 The two-loop Lipatov vertex in MSYM

In the previous section we computed the one-loop five-point amplitude in multi-Regge kinematics to all orders in  $\epsilon$ , and we know from Section 9.2 that the knowledge of the five-point amplitude to all orders in  $\epsilon$  enables us to extract the one-loop Lipatov vertex to same accuracy. Dividing the one-loop vertex into a parity-even and a parity-odd contribution,

$$\bar{V}^{(1)} = \bar{V}_e^{(1)} + \bar{V}_o^{(1)}, \quad (11.48)$$

we obtain the analytic expressions for the vertex by subtracting the contributions to the coefficient functions and the Regge trajectory from the five-point amplitude,

$$\begin{aligned} \bar{V}_e^{(1)}(t_1, t_2, \kappa; \epsilon, \tau) &= m_{5e}^{(1)}(s, s_1, s_2, t_1, t_2) - \bar{\alpha}^{(1)}(t_1; \epsilon) L_1 - \bar{\alpha}^{(1)}(t_2; \epsilon) L_2 - \bar{C}^{(1)}(t_1; \epsilon, \tau) \\ &\quad - \bar{C}^{(1)}(t_2; \epsilon, \tau), \\ \bar{V}_o^{(1,j)}(t_1, t_2, \kappa; \epsilon, \tau) &= m_{5o}^{(1,j)}(s, s_1, s_2, t_1, t_2) \\ &= -\epsilon (p_{3\perp} p_{4\perp}^* - p_{3\perp}^* p_{4\perp}) \frac{(-\kappa)^\epsilon}{t_2} \mathcal{I}^{(j)}(t_1, t_1, \kappa) \end{aligned} \quad (11.49)$$

with  $L_i = \ln(-s_i/\tau)$ . The explicit expression of the parity-even contribution was already derived in Eq. (9.34). Eq. (9.23) implies that there is no odd-parity contribution to the coefficient functions and the Regge trajectory, and so the parity-odd part of the vertex equals the parity-odd part of the amplitude given

in Eqs. (11.22) and (11.39). We thus have at our disposal all the pieces needed to derive the one-loop Lipatov vertex to all orders in  $\epsilon$ .

Let us now turn to the two-loop case. In Chapter 10 we showed that the BDS ansatz implies an iteration formula for the two-loop Lipatov vertex, similar to the iteration for the two-loop amplitude. Decomposing Eq. (10.10) into parity-even and odd contributions, we can write

$$\begin{aligned}
V_e^{(2)}(t_1, t_2, \kappa; \epsilon, \tau) &= \frac{1}{2} \left[ V_e^{(1)}(t_1, t_2, \kappa; \epsilon, \tau) \right]^2 + \frac{2G^2(\epsilon)}{G(2\epsilon)} f^{(2)}(\epsilon) V_e^{(1)}(t_1, t_2, \kappa; 2\epsilon, \tau) + \mathcal{O}(\epsilon), \\
V_o^{(2,j)}(t_1, t_2, \kappa; \epsilon, \tau) &= V_e^{(1)}(t_1, t_2, \kappa; \epsilon, \tau) V_o^{(1,j)}(t_1, t_2, \kappa; \epsilon, \tau) + \mathcal{O}(\epsilon).
\end{aligned} \tag{11.50}$$

As  $V_o^{(1)}$  is  $\mathcal{O}(\epsilon)$ , the parity-odd contribution only contributes starting from  $\mathcal{O}(\epsilon^{-1})$ . The right-hand side of Eq. (11.50) is known from Eq. (11.49), and hence this allows us to obtain the two-loop Lipatov vertex in MSYM. We know already that the parity-odd contribution to the one-loop vertex can be expressed in terms of  $\mathcal{M}$  functions, and hence the parity-odd contribution to the two-loop vertex can be expressed in terms of using the same set of functions.

## 11.6 The physical region

Let us conclude this section by analyzing what the two-loop Lipatov vertex becomes in the physical region where all  $s$ -type invariants are positive, obtained by performing analytic continuation on all  $s$ -type invariants according to the prescription

$$(-s) \rightarrow e^{-i\pi} s, \quad (-s_1) \rightarrow e^{-i\pi} s_1, \quad (-s_2) \rightarrow e^{-i\pi} s_2. \tag{11.51}$$

The prescription for the transverse scale  $\kappa$  is then fixed by Eq. (11.4) to be

$$(-\kappa) \rightarrow e^{-i\pi} \kappa. \tag{11.52}$$

From the previous sections, it is clear the in order to get the expression of the two-loop vertex in the physical region, it is sufficient to know the analytic

continuation of the one-loop vertex to  $\mathcal{O}(\epsilon^2)$ . In the following we give the analytic continuation of  $\bar{V}^{(1)}$  to all orders in  $\epsilon$ . The analytic continuation of the parity-even contribution (9.34) is straightforward. In the region  $(-t_2) < (-t_1)$ , we find

$$\begin{aligned}
\bar{V}_{e,\text{phys}}^{(1)}(t_1, t_2, \kappa; \epsilon, \tau) = & \\
& - \frac{1}{\epsilon^2} e^{i\pi\epsilon} \Gamma(1+\epsilon) \Gamma(1-\epsilon) \\
& + \frac{1}{\epsilon} \left( \frac{\kappa}{-t_1} \right)^\epsilon \left( -\psi(1+\epsilon) - \gamma_E + \ln \frac{-t_1}{\tau} \right) \\
& + \frac{1}{\epsilon} \left( \frac{\kappa}{-t_2} \right)^\epsilon \left( -\psi(1+\epsilon) - \gamma_E + \ln \frac{-t_2}{\tau} \right) \\
& + \frac{1}{\epsilon^2} \left( \frac{\kappa}{-t_1} \right)^\epsilon {}_2F_1 \left( \epsilon, 1, 1-\epsilon; \frac{t_1}{t_2} \right) \\
& - \frac{1}{\epsilon(1+\epsilon)} \left( \frac{\kappa}{-t_2} \right)^\epsilon \frac{t_1}{t_2} {}_2F_1 \left( 1, 1+\epsilon, 2+\epsilon; \frac{t_1}{t_2} \right) \\
& - \frac{1}{\epsilon} \left[ \left( \frac{\kappa}{-t_1} \right)^\epsilon + \left( \frac{\kappa}{-t_2} \right)^\epsilon \right] \left( \ln \frac{\kappa}{\tau} - i\pi + \ln \frac{t_1-t_2}{\tau} \right).
\end{aligned} \tag{11.53}$$

The analytic continuation of the parity-odd contribution is slightly more complicated, because it requires the analytic continuation of the pentagon integral. We address this questions for the Regions I and II(a) in the next sections.

### 11.6.1 Analytic continuation of Region II(a)

In Region II(a) the pentagon integral is expressed in terms of the dimensionless quantities  $y_1$  and  $y_2$ . The analytic continuation of  $y_1$  and  $y_2$  follows then directly from Eq. (11.18) and Eq. (11.52),

$$(-y_1) \rightarrow e^{-i\pi} y_1 \quad \text{and} \quad y_2 \rightarrow y_2. \tag{11.54}$$

In the physical region, the vertex can then be written as

$$\bar{V}_{o,\text{phys}}^{(1,IIa)}(t_1, t_2, \kappa; \epsilon, \tau) = -\epsilon (p_{3\perp} p_{4\perp}^* - p_{3\perp}^* p_{4\perp}) \frac{\kappa^\epsilon}{t_2} \mathcal{I}_{\text{phys}}^{(IIa)}(\kappa, t_1, t_2), \tag{11.55}$$

with

$$\mathcal{I}_{\text{phys}}^{(IIa)}(\kappa, t_1, t_2) = e^{i\pi\epsilon} \mathcal{I}^{(IIa)}(e^{-i\pi}(-\kappa), t_1, t_2), \tag{11.56}$$



and  $\mathcal{I}^{(IIa)}$  is given in Eq. (11.22) to all orders in  $\epsilon$  in terms of Appell and Kampé de Fériet functions. As we face the problem how of to perform the analytic continuation of these functions under the prescription (11.54), we argue in the following that the analytic continuation of the generalized hypergeometric functions that appear in  $\mathcal{I}^{(IIa)}$  is trivial, *i.e.*, the hypergeometric functions stay real in the physical region.

Indeed all the hypergeometric functions entering  $\mathcal{I}^{(IIa)}$  can be written as a nested sum, the inner sum being a one-dimensional hypergeometric function of  ${}_2F_1$  or  ${}_3F_2$  type depending on  $(-y_1)$ . For example, the first term in Eq. (11.22) can be written as

$$\begin{aligned} & -\frac{1}{\epsilon^3} y_2^{-\epsilon} \Gamma(1-2\epsilon) \Gamma(1+\epsilon)^2 F_4\left(1-2\epsilon, 1-\epsilon, 1-\epsilon, 1-\epsilon; -y_1, y_2\right) \\ & = -\frac{1}{\epsilon^3} y_2^{-\epsilon} \Gamma(1-2\epsilon) \Gamma(1+\epsilon)^2 \sum_{n=0}^{\infty} \frac{(1-2\epsilon)_n (1-\epsilon)_n}{(1-\epsilon)_n} \frac{y_2^n}{n!} \\ & \quad \times {}_2F_1\left(1-2\epsilon, 1-\epsilon, 1-\epsilon; -y_1\right). \end{aligned} \quad (11.57)$$

Since we do not perform any analytic continuation in  $y_2$ , the only way an imaginary part could arise is when we cross a branch cut during the analytic continuation in  $y_1$ . Hence the analytic properties of Eq. (11.57) are determined by the cuts in the function  ${}_2F_1\left(1-2\epsilon, 1-\epsilon, 1-\epsilon; -y_1\right)$ . We know that the  ${}_2F_1$  function has a branch cut ranging from 1 to  $+\infty$ . The convergence criterion for the  $F_4$  function requires  $|y_1| < 1$ , so we do not cross the branch cut when continuing  $y_1$  along a half circle through the upper half plane, and so we do not change the Riemann sheet during the analytic continuation. Since the Euclidean region corresponds to the Riemann sheet where the hypergeometric function is real for  $(-y_1) < 1$ , we conclude that the  ${}_2F_1$  function in Eq. (11.57) is real in the physical region, and so is the Appell function on the left-hand side of Eq. (11.57). A similar reasoning can be made for all other hypergeometric functions in Eq. (11.22), and so we can immediately write down the analytic continuation of Eq. (11.22) to the physical region where all  $s$ -type invariants

are positive,

$$\begin{aligned}
\mathcal{I}_{\text{phys}}^{(IIa)}(\kappa, t_1, t_2) = & \\
& - \frac{1}{\epsilon^3} y_2^{-\epsilon} e^{i\pi\epsilon} \Gamma(1-2\epsilon) \Gamma(1+\epsilon)^2 F_4(1-2\epsilon, 1-\epsilon, 1-\epsilon, 1-\epsilon; -y_1, y_2) \\
& + \frac{1}{\epsilon^3} e^{i\pi\epsilon} \Gamma(1+\epsilon) \Gamma(1-\epsilon) F_4(1, 1-\epsilon, 1-\epsilon, 1+\epsilon; -y_1, y_2) \\
& - \frac{1}{\epsilon^2} (-y_1)^\epsilon y_2^{-\epsilon} \left\{ \right. \\
& \times \frac{\partial}{\partial \delta} F_{0,2}^{2,1} \left( \begin{array}{cc|ccc} 1+\delta & 1+\delta-\epsilon & 1 & - & - & - \\ - & - & 1+\delta & 1-\epsilon & 1+\epsilon+\delta & - \end{array} \middle| -y_1, y_2 \right)_{|\delta=0} \\
& + [\ln(-y_1) - i\pi + \psi(1-\epsilon) - \psi(-\epsilon)] F_4(1, 1-\epsilon, 1+\epsilon, 1-\epsilon; -y_1, y_2) \left. \right\} \\
& + \frac{1}{\epsilon^2} (-y_1)^\epsilon \left\{ \right. \\
& \times \frac{\partial}{\partial \delta} F_{0,2}^{2,1} \left( \begin{array}{cc|ccc} 1+\delta & 1+\delta+\epsilon & 1 & - & - & - \\ - & - & 1+\delta & 1+\epsilon & 1+\epsilon+\delta & - \end{array} \middle| -y_1, y_2 \right)_{|\delta=0} \\
& + [\ln(-y_1) - i\pi + \psi(1+\epsilon) - \psi(-\epsilon)] F_4(1, 1+\epsilon, 1+\epsilon, 1+\epsilon; -y_1, y_2) \left. \right\}.
\end{aligned} \tag{11.58}$$

We checked explicitly that all the poles in  $\epsilon$  cancel out when expanding  $\mathcal{I}_{\text{phys}}^{(IIa)}$  into a Laurent series in  $\epsilon$ . Note that in Eq. (11.58) the same hypergeometric functions appear as in the Euclidean region, Eq. (11.22). We can therefore easily expand Eq. (11.58) in  $\epsilon$  in exactly the way as we did in the Euclidean region, and we will obtain a Laurent series whose coefficients are combinations of *real*  $\mathcal{M}$ -functions. The imaginary parts arise order by order in the Laurent series only through the explicit dependence in  $i\pi$  in Eq. (11.58). Note that if we had worked with the expression of the pentagon in terms of Goncharov's multiple polylogarithm, Eqs. (M.60) and (M.64), the complicated analytic structure of these functions would imply many spurious imaginary parts arising from individual polylogarithms, and all the spurious imaginary parts would need to cancel out in the final answer. It is therefore more natural to express the result in the physical region in terms of  $\mathcal{M}$  functions rather than the Goncharov polylogarithms.

## 11.6.2 Analytic continuation of Region I

In Region I the pentagon is expressed as a function of  $x_1$  and  $x_2$ , whose analytic continuation follows directly from Eq. (11.14) and Eq. (11.52),

$$(-x_1) \rightarrow e^{+i\pi} x_1 \quad \text{and} \quad x_2 \rightarrow e^{+i\pi} x_2, \quad (11.59)$$

and the pentagon in Region I can be expressed as

$$\bar{V}_{e,\text{phys}}^{(1,I)}(t_1, t_2, \kappa; \epsilon, \tau) = -\epsilon (p_{3\perp} p_{4\perp}^* - p_{3\perp}^* p_{4\perp}) \frac{\kappa^\epsilon}{\kappa} \mathcal{I}_{\text{phys}}^{(I)}(\kappa, t_1, t_2), \quad (11.60)$$

with

$$\mathcal{I}_{\text{phys}}^{(I)}(\kappa, t_1, t_2) = e^{i\pi\epsilon} \mathcal{I}^{(I)}(e^{-i\pi}(-\kappa), t_1, t_2), \quad (11.61)$$

and  $\mathcal{I}^{(I)}$  is given in Eq. (11.39). Using the same argument as in Region II(a), we see that the hypergeometric functions stay real even in the physical region, because the convergence of the hypergeometric functions requires  $|x_i| < 1$ ,  $i = 1, 2$ . Alternatively, we could also start from the expression of the pentagon in the physical Region II(a), Eq. (11.58), and perform the analytic continuation to Region I following the techniques described in Appendix L. We find that the two results are consistent. The final expression of the pentagon in the physical region I is then

$$\begin{aligned} \mathcal{I}_{\text{phys}}^{(I)}(\kappa, t_1, t_2) = & \\ & - \frac{1}{\epsilon^3} e^{-i\pi\epsilon} (-x_1)^{-\epsilon} (-x_2)^{-\epsilon} \Gamma(1-2\epsilon) \Gamma(1+\epsilon)^2 \\ & \times F_4(1-2\epsilon, 1-\epsilon, 1-\epsilon, 1-\epsilon; -x_1, -x_2) \\ & + \frac{1}{\epsilon^3} \Gamma(1-\epsilon) \Gamma(1+\epsilon) e^{i\pi\epsilon} F_4(1, 1+\epsilon, 1+\epsilon, 1+\epsilon; -x_1, -x_2) \\ & - \frac{1}{\epsilon^2} (-x_1)^{-\epsilon} \left\{ \right. \\ & \left. \frac{\partial}{\partial \delta} F_{0,2}^{2,1} \left( \begin{array}{c} 1+\delta \quad 1-\epsilon+\delta \\ - \quad - \end{array} \middle| \begin{array}{ccc} - & - & - \\ 1-\epsilon & 1+\epsilon+\delta & - \end{array} \begin{array}{c} 1 \\ 1+\delta \end{array} \middle| -x_1, -x_2 \right) \bigg|_{\delta=0} \right\} \end{aligned} \quad (11.62)$$

$$\begin{aligned}
& + [\ln(-x_2) + i\pi + \psi(1 - \epsilon) - \psi(-\epsilon)] F_4(1, 1 - \epsilon, 1 - \epsilon, 1 + \epsilon; -x_1, -x_2) \\
& + \frac{\epsilon}{1 - \epsilon} \frac{t_1}{t_2} F_{2,0}^{0,3} \left( \begin{array}{cc|cccc} - & - & 1 & 1 & 1 & 1 & 1 - \epsilon & 1 - \epsilon \\ 2 & 2 - \epsilon & - & - & - & - & - & - \end{array} \middle| -x_1, \frac{x_1}{x_2} \right) \Bigg\} \\
& - \frac{1}{\epsilon^2} (-x_2)^{-\epsilon} \left\{ \right. \\
& \quad \times \frac{\partial}{\partial \delta} F_{0,2}^{2,1} \left( \begin{array}{cc|ccc} 1 + \delta & 1 - \epsilon + \delta & - & - & - & 1 \\ - & - & 1 + \epsilon & 1 - \epsilon + \delta & - & 1 + \delta \end{array} \middle| -x_1, -x_2 \right) \Bigg|_{\delta=0} \\
& \quad + [\ln(-x_2) + i\pi + \psi(1 - \epsilon) - \psi(\epsilon)] F_4(1, 1 - \epsilon, 1 + \epsilon, 1 - \epsilon; -x_1, -x_2) \\
& \left. - \frac{\epsilon}{1 + \epsilon} \frac{t_1}{t_2} F_{2,0}^{0,3} \left( \begin{array}{cc|cccc} - & - & 1 & 1 & 1 & 1 & 1 - \epsilon & 1 + \epsilon \\ 2 & 2 + \epsilon & - & - & - & - & - & - \end{array} \middle| -x_1, \frac{x_1}{x_2} \right) \right\}.
\end{aligned}$$

We checked explicitly that all the poles in  $\epsilon$  cancel out when expanding  $\mathcal{I}_{\text{phys}}^{(I)}$  into a Laurent series in  $\epsilon$ .

# Conclusion

Throughout this work we investigated the structure of gauge theory scattering amplitudes, both at tree-level and beyond. A special attention was brought to the application of several cutting-edge techniques developed over the last decade to compute gauge theory scattering amplitudes in an efficient way. The main goal of this work was to apply these techniques in some concrete cases, in the double perspective of gaining a deeper understanding of the structure of gauge theory amplitudes as well as to obtain new results which could have some phenomenological interest in the future.

A first result has been to show how recursive relations for color-stripped amplitudes can be dressed with color, obtaining in this way a new version of the recursion, valid this time at the level the full amplitude, including color. The main features of this technique are that the recursive relations keep their functional form, the only difference being in the fact that in the color-dressed case the recursion runs over non-ordered objects reflecting the Bose symmetry of the full amplitude. Furthermore, the color-dressed recursions avoid the factorial growth in complexity inherent to dressing color-stripped amplitudes with color. The color-dressed recursions have by now been successfully applied in several tree-level matrix element generators [42, 52, 100]. An open question is in how far the color-dressing technique can be extended beyond tree-level where a similar color decomposition holds, especially in the context of the recently proposed automatization of one-loop computations, all operating so far only at the level of the color-stripped amplitude [7, 8].

A second result has been the application of the MHV formalism to some open issues, such as the computation of several universal quantities that describe the behavior of tree-level amplitudes in some kinematical limits. We started by studying the infrared limits of gauge theory scattering amplitudes and we showed how it is possible to extend the work by Birthwright *et al.* on splitting functions to more general kinds of infrared limits, described by the antenna functions. We showed how the MHV formalism provides a natural framework to define tree-level gluon antenna functions as a sum of MHV diagrams, a result which allowed us to derive for the first time a complete set of N<sup>3</sup>LO antenna functions, describing the soft and collinear emission of up to three gluons at tree-level. In Chapter 8 we then extended this result to the case of high-energy limits by deriving a similar rule to compute coefficient functions and Lipatov vertices in an efficient way by identifying *a priori* the MHV diagrams that give a leading contribution in the high-energy limit and we derived for the first time the complete set of tree-level Lipatov vertices describing the emission of up to four gluons. Our antenna functions and Lipatov vertices enjoy all the properties of the MHV approach and in particular, they are characterized by a much simpler analytic structure than the corresponding results in Ref. [16, 25]. Although these multi-leg antenna functions and Lipatov vertices might not have a direct phenomenological application, they might however be useful to check the infrared and multi-Regge behavior in future computations of multi-leg scattering amplitudes. In the same spirit, it could also be interesting to investigate how the techniques we introduced in this work in the context of pure gluon amplitudes can be extended to the case where one or more quark pairs are present in the amplitude.

A third result of this work was the application and development of new techniques to compute (multi-) loop amplitudes. We applied the Laporta algorithm and the differential equation technique to the computation of a class of 27 real-virtual integrated counterterms for an NNLO subtraction scheme. To our knowledge this was the first time that such techniques have been applied to hypergeometric integrals of this particular type. Although successfully applied to the computation of the twofold Euler integrals which appear in the NNLO subtraction scheme, our approach turned out to be inefficient for more compli-

cated real-virtual integrals, due to an extremely fast growth in the complexity of the algorithm. For these classes of integrals one might think of other techniques, like for example Mellin-Barnes inspired approaches, which were applied recently to the computation of the remaining real-virtual integrals [83]. The Mellin-Barnes technique, together with the negative dimension approach, was applied in this work to the computation of the scalar massless pentagon. In Chapter 11 we computed for the first time the pentagon integral to all orders in  $\epsilon$ , albeit in simplified kinematics and we found that the result can be expressed in terms of generalized hypergeometric functions, the so-called Appell and Kampé de Fériet functions, which can be expanded into a Laurent series in terms of Goncharov's multiple polylogarithms. This computation allowed us to investigate for the first time the mathematical structure of higher-point two-loop amplitudes and we studied the associated special functions and derived their main properties (See Appendices).

Recently, an expression for a general  $n$ -edged Wilson loop in QCD was presented [13]. The  $n$ -edged Wilson loop is conjectured to be related to the two-loop  $n$ -point scattering amplitude in MSYM and so it can be directly used to study the breakdown of the ABDK/BDS ansatz for more than five external legs. In Ref. [13] the Wilson loops are given as multifold Euler integrals, which remind the similarity between Feynman integrals and hypergeometric functions pointed out in Ref. [28]. Since the techniques we applied to compute the integrated counterterms and the pentagon integrals are generic and not limited to this particular class of integrals, one could think of applying these techniques also to the computation of the Euler integrals appearing in the six-edged Wilson loop, a computation which would explicitly reveal the analytical structure of the BDS remainder function. This is currently under investigation.

The techniques and functions studied in this work might hence have an impact on how we will try to understand the breakdown of the BDS ansatz in the two-loop six-point amplitude. Since the computation of this amplitude requires the knowledge of the one and two-loop hexagons, it is natural to speculate that the same kind of new mathematical structures we uncovered in the case of the five-point amplitude will also reappear in more general higher-point integrals and so the knowledge of these functions and of their properties might play an

important role in uncovering the source of the BDS ansatz violation and hence improving our knowledge of gauge theories at higher orders in the perturbative expansion.



**Part IV**

**Appendices**



# Appendix **A**

## Reconstruction functions

In this appendix we present the explicit expressions for the reconstruction functions that have been used in Chapter 4 and Chapter 5 to define antenna functions. Apart from a difference in the overall sign conventions they are the same as in Ref. [16]. They read

$$\begin{aligned}
 p_{\hat{a}} = & \\
 & \frac{1}{2(K^2 - t_{1\dots nb})} \left[ (1 + \rho)K^2 + 2R \cdot \bar{K} + \frac{1}{s_{ab}} G \left( \begin{matrix} k_a, & k_b \\ R, & P_{1,n} \end{matrix} \right) \right] k_a \\
 & + \frac{1}{2(K^2 - t_{a1\dots n})} \left[ (1 - \rho)K^2 + 2R \cdot \bar{K} + \frac{1}{s_{ab}} G \left( \begin{matrix} k_a, & k_b \\ R, & P_{1,n} \end{matrix} \right) \right] k_b \\
 & + R,
 \end{aligned} \tag{A.1}$$

$$\begin{aligned}
 p_{\hat{b}} = & \\
 & \frac{1}{2(K^2 - t_{1\dots nb})} \left[ (1 - \rho)K^2 + 2\tilde{R} \cdot \bar{K} + \frac{1}{s_{ab}} G \left( \begin{matrix} k_a, & k_b \\ \tilde{R}, & P_{1,n} \end{matrix} \right) \right] k_a \\
 & + \frac{1}{2(K^2 - t_{a1\dots n})} \left[ (1 + \rho)K^2 + 2\tilde{R} \cdot \bar{K} + \frac{1}{s_{ab}} G \left( \begin{matrix} k_a, & k_b \\ \tilde{R}, & P_{1,n} \end{matrix} \right) \right] k_b \\
 & + \tilde{R},
 \end{aligned}$$

where  $t_{1\dots nb} = (k_1 + \dots + k_n + k_b)^2$ ,  $t_{a1\dots n} = (k_a + k_1 + \dots + k_n)^2$  and,

$$K = k_a + k_1 + \dots + k_n + k_b \text{ and } \bar{K} = k_a - k_b - K. \tag{A.2}$$

Furthermore

$$R = \sum_{j=1}^n k_j r_j, \quad \tilde{R} = P_{1,n} - R = \sum_{j=1}^n k_j (1 - r_j), \quad (\text{A.3})$$

and

$$\rho = \left[ 1 + \frac{2G \begin{pmatrix} a, & R, & b \\ a, & \tilde{R}, & b \end{pmatrix}}{K^2 s_{ab}^2} + \frac{\Delta(a, R, K, b)}{(K^2)^2 s_{ab}^2} \right]^{\frac{1}{2}}. \quad (\text{A.4})$$

In these formulas,  $G$  and  $\Delta$  denote Gram determinants,

$$\begin{aligned} G \begin{pmatrix} p_1, & \dots, & p_n \\ q_1, & \dots, & q_n \end{pmatrix} &\equiv \det(2p_i \cdot q_j), \\ \Delta(p_1, \dots, p_n) &\equiv G \begin{pmatrix} p_1, & \dots, & p_n \\ p_1, & \dots, & p_n \end{pmatrix}. \end{aligned} \quad (\text{A.5})$$

A suitable choice for the coefficients  $r_j$  is [16]

$$r_j = \frac{k_j \cdot (P_{j+1,n} + k_b)}{k_j \cdot K} = \frac{t_{j\dots nb} - t_{(j+1)\dots nb}}{2k_j \cdot K}. \quad (\text{A.6})$$

# Appendix **B**

## Proof of Chapter 5

### B.1 Gluon insertion rule

In this appendix we give the explicit proof of Rules 5.3 and 5.5 which had been omitted in Chapter 5. We start with the gluon insertion rule, and comment on Rule 5.5 in the next section.

The idea behind the gluon insertion rule is to start from the Feynman diagrams of the hard amplitude and to see where a soft gluon can be radiated from in such a way that the diagram becomes divergent. There are three places in a Feynman diagram where an additional soft gluon can be emitted from:

- a three-point vertex,
- an internal line,
- an external line.

Let us examine each case separately, and let us start with the situation where a soft gluon is emitted from a three-point vertex (See Fig. B.1). It is easy to see from Fig. B.1a that if a single soft gluon is radiated from a three-point vertex, there is no propagator going on-shell, and thus there is no divergence at all in this situation. But if more than one single gluon is emitted, then there may be

a propagator going on-shell, and thus we can get a divergent diagram for more than one single soft gluon emitted from the three-point vertex (See Fig. B.1b and B.1c).

Let us first consider the situation where two soft gluons are emitted from the three-point vertex shown in Fig. B.1b. In this situation the propagator goes on-shell, and the rescaling rule, Eq. (4.24), tells us that the propagator behaves as  $t^{-2}$ . However, as a three-point vertex is proportional to the momenta of the particles, it is easy to see that the second three-point vertex behaves in the soft limit as  $t$ , and thus the diagram shown in Fig. B.1b behaves as  $t^{-2} \cdot t = t^{-1}$ , and so it is not divergent enough to contribute to the soft factor. Let us turn to the situation where three soft gluons are emitted from a three-point vertex (See Fig. B.1c). We get a divergent propagator which behaves as  $t^{-2}$ . The four-point vertex however is not divergent at all, and so the diagram shown in Fig. B.1c behaves as  $t^{-2}$ , and so it is not divergent enough to contribute to the soft limit.

Finally, we come to the conclusion that diagrams where a soft particle is radiated from a three-point vertex do not contribute in the soft limit.

Let's turn to the second case, where the soft particle is emitted from an internal line. Internal lines in a Feynman diagram correspond to off-shell propagators, *i.e.*, if  $p$  is the momentum carried by the internal line, then  $p^2 \neq 0$ . If a soft particle with momentum  $k$  is radiated from this internal line, then we get a propagator of the form  $1/(p+k)^2 = 1/(p^2 + 2p \cdot k)$ , which stays finite in the soft limit where  $k \rightarrow 0$ . So there will be no contribution from diagrams where the soft gluon is emitted from an internal line.

In the situation where a soft gluon with momentum  $k$  is emitted from an external particle with momentum  $p$ , we get a propagator  $1/(p+k)^2 = 1/(2p \cdot k)$ . In the soft limit,  $k \rightarrow 0$ , this propagator behaves as  $1/t$ , and thus has the right divergence to contribute to the soft factor.

Finally, we see that only those Feynman diagrams contribute in the soft limit where the soft gluons are radiated from the external legs of the hard amplitude, which finishes the proof.

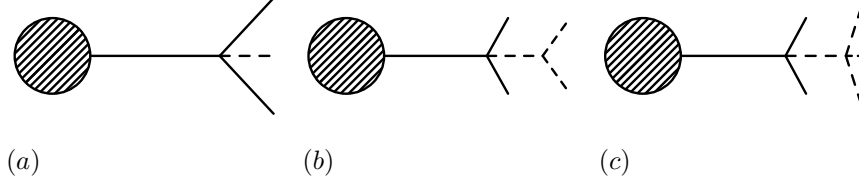


Figure B.1: The radiation of a soft gluon from a three-point vertex. Dashed lines indicate soft gluons. The blob represents any subdiagram contributing to this amplitude.

## B.2 Proof of Rule 5.5

Let us consider a generic  $(n+4)$ -point amplitude  $A_{n+4}(a, 1, \dots, n, b, c, d)$ . We want to study the limit where  $1, \dots, n$  become singular. We know from Rule 5.4 that the only MHV diagrams that contribute in the singular limit are those where all scalar propagators go on shell, which in turn implies that  $c$  and  $d$  must be attached to the same MHV vertex. Let us consider now a specific MHV diagram satisfying this condition. Then the MHV vertex with  $c$  and  $d$  attached gives a contribution

$$\frac{\langle cd \rangle^3}{\langle P_{j,b} c \rangle \langle d P_{a,i} \rangle}, \quad (\text{B.1})$$

with  $(i, j) \neq (b, a)$  because otherwise  $c$  and  $d$  would be attached to a 3-point MHV vertex, and  $i = a$  and / or  $j = b$  if  $a$  and  $b$  are attached to the same MHV vertex as  $c$  and  $d$ . Consider the following Schouten identity, Eq. (1.14),

$$\langle \hat{b} \hat{a} \rangle \langle ca \rangle = \langle \hat{b} \hat{a} \rangle \langle \hat{c} \hat{a} \rangle + \langle \hat{c} \hat{b} \rangle \langle a \hat{a} \rangle \Rightarrow \frac{\langle ca \rangle}{\langle \hat{c} \hat{a} \rangle} = \frac{\langle \hat{b} \hat{a} \rangle}{\langle \hat{b} \hat{a} \rangle} + \frac{\langle \hat{c} \hat{b} \rangle \langle a \hat{a} \rangle}{\langle \hat{c} \hat{a} \rangle \langle \hat{b} \hat{a} \rangle}, \quad (\text{B.2})$$

where  $\hat{a}$  and  $\hat{b}$  denote the reconstruction functions defined in the Appendix A. It is manifest that, if  $\langle a \hat{a} \rangle$  goes to zero in the singular limit, then Eq. (B.2) drastically simplifies. To show this, we go into the frame where  $p_a$  and  $p_b$  are aligned along the same direction. As recalled in Appendix A, the reconstruction functions can be chosen to be of the form

$$p_{\hat{a}} = A p_a + B p_b + \sum_{j=1}^n p_j r_j, \quad (\text{B.3})$$

where  $A$ ,  $B$  and  $r_j$  are functions of invariants in the particle momenta, so they are unaffected by this specific choice of reference frame. As  $p_{\hat{a}}$  is by definition lightlike, we can switch to lightcone coordinates. In the specific reference frame we chose, we get

$$\begin{aligned} p_{\hat{a}}^+ &= A p_a^+ + \sum_{j=1}^n p_j^+ r_j, \\ p_{\hat{a}}^- &= B p_b^- + \sum_{j=1}^n p_j^- r_j, \\ p_{\hat{a}\perp} &= \sum_{j=1}^n p_{j\perp} r_j. \end{aligned} \tag{B.4}$$

Furthermore it is easy to see that in this frame we can write

$$p_j \text{ singular} \Leftrightarrow p_{j\perp} \rightarrow 0, \quad \forall j = 1, \dots, n. \tag{B.5}$$

The spinor product  $\langle a\hat{a} \rangle$  can now be evaluated in this frame using the lightcone coordinates [25],

$$\langle a\hat{a} \rangle = -i \sqrt{\frac{-p_a^+}{p_{\hat{a}}^+}} p_{\hat{a}\perp} = -i \sqrt{\frac{-p_a^+}{A p_a^+ + \sum_{j=1}^n p_j^+ r_j}} \sum_{j=1}^n p_{j\perp} r_j. \tag{B.6}$$

By definition of the reconstruction functions,  $p_{\hat{a}}$  and  $p_a$  are collinear in every singular limit, and so the square root gives just a phase in the singular limit. Thus, due to Eq. (B.5),  $\langle a\hat{a} \rangle$  goes to zero in the singular limit unless there are poles in the coefficients  $r_j$  that could prevent the product  $r_j p_{j\perp}$  from going to zero as  $p_{j\perp} \rightarrow 0$ . Recalling the analytic expression for the coefficients, Eq. (A.6), we see that  $r_j$  may contain a pole if  $p_j \cdot K \rightarrow 0$ . As  $K$  always contains the momenta of the two hard particles  $a$  and  $b$ ,  $p_j \cdot K \rightarrow 0$  if and only if  $p_j \rightarrow 0$ . However, a quick look at Eq. (A.6) shows that  $r_j$  does not contain a pole in this limit, so  $r_j$  does not contain a pole in any limit. This concludes the proof that  $\langle a\hat{a} \rangle$  goes to zero in the singular limit, and allows us to conclude that in the singular limit

$$\frac{\langle ca \rangle}{\langle c\hat{a} \rangle} \rightarrow \frac{\langle \hat{b}a \rangle}{\langle \hat{b}\hat{a} \rangle}. \tag{B.7}$$

Similar conclusions can of course be drawn for  $\langle b\hat{b} \rangle$ . We can also analyze what happens to the spinor product  $\langle P_{j,b} c \rangle$  in the singular limit.



- If  $j = b$ , then  $\langle P_{j,b} c \rangle = \langle bc \rangle$ , and in the singular limit

$$\langle bc \rangle \rightarrow \langle \hat{b}c \rangle \frac{\langle \hat{a}b \rangle}{\langle \hat{a}\hat{b} \rangle}. \quad (\text{B.8})$$

- If  $j \neq b$ , then  $\langle P_{j,b} c \rangle = \langle bc \rangle [b\eta] + \sum_{k=j}^n \langle kc \rangle [k\eta]$ . The first term has already been dealt with in Eq. (B.8). The remaining terms can be rewritten using Schouten-identity

$$\langle kc \rangle = \langle \hat{b}c \rangle \frac{\langle \hat{a}k \rangle}{\langle \hat{a}\hat{b} \rangle} + \langle \hat{a}c \rangle \frac{\langle k\hat{b} \rangle}{\langle \hat{a}\hat{b} \rangle}. \quad (\text{B.9})$$

The second term on the right-hand side, proportional to  $\langle k\hat{b} \rangle$ , does not contribute in the singular limit. To see this let us first see what happens in the limit where  $p_j, \dots, p_\ell \parallel p_a$  and  $p_{\ell+1}, \dots, p_n \parallel p_b$ , with  $j < \ell \leq b$ . Then this MHV diagram would have a non-divergent scalar propagator. As we are only looking for those diagrams where all scalar propagators go on-shell, we can neglect this case. So we only need to analyze the situation where  $p_j, \dots, p_n \parallel p_b$ . Using lightcone coordinates, we find,  $\forall j \leq \ell \leq n$ ,

$$\langle \ell\hat{b} \rangle = p_{\ell\perp} \sqrt{\frac{p_{\hat{b}}^+}{p_\ell^+}} - p_{\hat{b}\perp} \sqrt{\frac{p_\ell^+}{p_{\hat{b}}^+}}. \quad (\text{B.10})$$

We know already that in the singular limit

$$p_{\hat{b}}^+ \rightarrow 0, \quad p_{\hat{b}\perp} \rightarrow 0, \quad p_{\ell\perp} \rightarrow 0, \quad \forall 1 \leq \ell \leq n, \quad (\text{B.11})$$

and  $p_{\hat{b}}$  is collinear to  $p_b$  in every singular limit. Let us have a closer look at the first term. From Eq. (B.11) it follows that in the singular limit  $p_{\ell\perp}, p_\ell^+, p_{\hat{b}}^+ \rightarrow 0$ , where we used the fact that in our specific choice of reference frame  $p_{\hat{b}}^+ = 0$ . Furthermore, all external particles must fulfill the on-shell condition  $p^+ p^- = |p_\perp|^2$ , and so

$$\frac{p_{\ell\perp}}{\sqrt{p_\ell^+}} \sim \sqrt{p_\ell^-}, \quad (\text{B.12})$$

and  $p_\ell^- \neq 0$  if  $p_j \parallel p_b$ . So the first term goes to zero as  $\sqrt{p_{\hat{b}}^+}$ . Similar arguments show that also the second term goes to zero in the singular

limit, and so we can conclude that  $\langle k\hat{b} \rangle$  vanishes. Putting everything together, we obtain

$$\langle P_{j,b}c \rangle \rightarrow \langle \hat{bc} \rangle \frac{\langle \hat{ab} \rangle}{\langle \hat{a}\hat{b} \rangle} [b\eta] + \sum_{k=j}^n \langle \hat{bc} \rangle \frac{\langle \hat{ak} \rangle}{\langle \hat{a}\hat{b} \rangle} [k\eta] = \langle \hat{bc} \rangle \frac{\langle \hat{a}P_{j,b} \rangle}{\langle \hat{a}\hat{b} \rangle}. \quad (\text{B.13})$$

Both cases can be summarized as

$$\langle P_{j,b}c \rangle \rightarrow \langle \hat{bc} \rangle \frac{\langle \hat{a}P_{j,b} \rangle}{\langle \hat{a}\hat{b} \rangle}. \quad (\text{B.14})$$

Similarly one finds

$$\langle dP_{a,i} \rangle \rightarrow \langle d\hat{a} \rangle \frac{\langle P_{a,i}\hat{b} \rangle}{\langle \hat{a}\hat{b} \rangle}. \quad (\text{B.15})$$

The contribution from Eq. (B.1) to the singular limit therefore becomes

$$\frac{\langle cd \rangle^3}{\langle P_{j,b}c \rangle \langle dP_{a,i} \rangle} \rightarrow \frac{\langle cd \rangle^3}{\langle \hat{a}\hat{b} \rangle \langle \hat{bc} \rangle \langle d\hat{a} \rangle} \frac{\langle \hat{a}\hat{b} \rangle^3}{\langle P_{j,b}\hat{a} \rangle \langle \hat{b}P_{a,i} \rangle}. \quad (\text{B.16})$$

The first factor on the right-hand side of Eq. (B.16) corresponds to the hard four-point amplitude in Eq. (5.19). The second factor has the same functional form as the left-hand side, with  $c$  and  $d$  replaced by  $\hat{a}$  and  $\hat{b}$ . This proves the following result: The antenna function  $\text{Ant}(\hat{a}^-, \hat{b}^- \leftarrow a, 1, \dots, n, b)$  can be calculated by evaluating all MHV diagrams that contribute to the  $(n+4)$ -point amplitude  $A_{n+4}(a, 1, \dots, n, b, \hat{a}^-, \hat{b}^-)$  and where  $\hat{a}$  and  $\hat{b}$  are attached to the same  $m$ -point MHV vertex, with  $m \geq 4$ .

In the rest of this section we show how this result can be generalized to the remaining antenna functions. The proof for  $\text{Ant}(\hat{a}^+, \hat{b}^+ \leftarrow a, 1, \dots, n, b)$  is similar to the previous case, and so we do not give it explicitly here.

Let us turn to  $\text{Ant}(\hat{a}^+, \hat{b}^- \leftarrow a, 1, \dots, n, b)$  and let us consider the  $(n+4)$ -point amplitude  $A_{n+4}(a, 1, \dots, n, b, c^-, d^+)$ . From Eq. (4.43) we know that in the singular limit for the particles  $1, \dots, n$ , the amplitude exhibits the factorization property

$$A_{n+4}(a, 1, \dots, n, b, c^-, d^+) \longrightarrow \sum_h \text{Ant}(\hat{a}^h, \hat{b}^{-h} \leftarrow a, 1, \dots, n, b) A_4(\hat{a}^{-h}, \hat{b}^h, c^-, d^+). \quad (\text{B.17})$$

If  $N_-$  is the number of negative-helicity gluons in the set  $\{a, 1, \dots, n, b\}$ , then the number of MHV propagators in the  $(n+4)$ -point amplitude is  $p = (N_- + 1) - 2 = N_- - 1$ . Furthermore, from the considerations in Section 5.1 we know that the MHV pole structure of this antenna function is

$$\text{Ant}(\hat{a}^+, \hat{b}^- \leftarrow a, 1, \dots, n, b) \sim \frac{1}{[\ ]_{N_- - 1}}, \quad (\text{B.18})$$

and thus the MHV diagrams contributing to the antenna function are exactly those where  $c$  and  $d$  are attached to the same  $n$ -point MHV vertex, with  $n \geq 4$ . The contribution from the MHV vertex that contains  $c$  and  $d$  is of the form

$$\frac{\langle c P_{\alpha\beta} \rangle^4}{\langle P_{j,b} c \rangle \langle cd \rangle \langle d P_{a,i} \rangle}, \quad (\text{B.19})$$

where  $P_{\alpha\beta}$  denotes the momentum of the second negative helicity leg attached to this vertex, and  $\alpha = \beta$  for an external leg. We know already that in the singular limit we have

$$\langle P_{j,b} c \rangle \rightarrow \langle \hat{b}c \rangle \frac{\langle \hat{a}P_{j,b} \rangle}{\langle \hat{a}\hat{b} \rangle}, \quad (\text{B.20})$$

$$\langle d P_{a,i} \rangle \rightarrow \langle d\hat{a} \rangle \frac{\langle P_{a,i} \hat{b} \rangle}{\langle \hat{a}\hat{b} \rangle}. \quad (\text{B.21})$$

Applying the Schouten-identity (B.2), we get for the spinor product in the numerator

$$\begin{aligned} \langle c P_{\alpha\beta} \rangle &= \sum_{k=\alpha}^{\beta} \langle cx \rangle [k\eta] \\ &= \sum_{k=\alpha}^{\beta} \left( \langle \hat{c}\hat{a} \rangle \frac{\langle k\hat{b} \rangle}{\langle \hat{a}\hat{b} \rangle} + \langle \hat{c}\hat{b} \rangle \frac{\langle k\hat{a} \rangle}{\langle \hat{b}\hat{a} \rangle} \right) [k\eta] \\ &= \langle \hat{c}\hat{a} \rangle \frac{\langle P_{\alpha\beta} \hat{b} \rangle}{\langle \hat{a}\hat{b} \rangle} + \langle \hat{c}\hat{b} \rangle \frac{\langle \hat{a} P_{\alpha\beta} \rangle}{\langle \hat{a}\hat{b} \rangle} \end{aligned} \quad (\text{B.22})$$

Inserting Eq. (B.22) into Eq. (B.19), we get five terms:

1. a term proportional to  $\langle P_{\alpha\beta} \hat{b} \rangle^4$ .
2. a term proportional to  $\langle P_{\alpha\beta} \hat{a} \rangle^4$ .

3. three “mixed” terms of the form  $\langle P_{\alpha\beta} \hat{a} \rangle^q \langle P_{\alpha\beta} \hat{b} \rangle^{4-q}$ ,  $q = 1, 2, 3$ .

We separately analyze the different limits:

- If  $k_\alpha, \dots, k_\beta \parallel k_a$ , then  $p_{\hat{a}} \rightarrow P$  and  $k_j \rightarrow z_j P$ ,  $\forall \alpha \leq j \leq \beta$  and so  $\langle P_{\alpha\beta} \hat{a} \rangle \rightarrow 0$ .
- If  $k_\alpha, \dots, k_\beta \parallel k_b$ , then  $p_{\hat{b}} \rightarrow P$  and  $k_j \rightarrow z_j P$ ,  $\forall \alpha \leq j \leq \beta$  and so  $\langle P_{\alpha\beta} \hat{b} \rangle \rightarrow 0$ .
- If  $k_\alpha, \dots, k_m \parallel k_a$  and  $k_{m'}, \dots, k_\beta \parallel k_b$ ,  $\alpha \leq m < m' \leq \beta$ , then the propagator  $1/P_{\alpha\beta}^2$  is not divergent, and thus diagrams with a propagator  $1/P_{\alpha\beta}^2$  are not divergent enough to contribute to this limit.
- If  $k_\alpha, \dots, k_\beta \rightarrow 0$ , the situation is more subtle. We show in Appendix C that in this limit only those diagrams contribute where  $\alpha = a$ , and  $P_{a\beta} \rightarrow k_a$ . Thus in this limit  $\langle P_{\alpha\beta} \hat{a} \rangle \sim \langle a\hat{a} \rangle \rightarrow 0$ .

Finally, we see that in any situation either  $\langle P_{\alpha\beta} \hat{a} \rangle$  or  $\langle P_{\alpha\beta} \hat{b} \rangle$  go to zero, and thus we can drop the “mixed” terms. So in the singular limit Eq. (B.19) becomes

$$\begin{aligned}
\frac{\langle P_{\alpha\beta} c \rangle^4}{\langle P_{j,b} c \rangle \langle cd \rangle \langle d P_{a,i} \rangle} &\rightarrow \frac{\langle c\hat{a} \rangle^4}{\langle \hat{a}\hat{b} \rangle \langle \hat{b}c \rangle \langle cd \rangle \langle d\hat{a} \rangle} \frac{\langle P_{\alpha\beta} \hat{b} \rangle^4}{\langle P_{j,b} \hat{a} \rangle \langle \hat{a}\hat{b} \rangle \langle \hat{b} P_{a,i} \rangle} \\
&+ \frac{\langle c\hat{b} \rangle^4}{\langle \hat{a}\hat{b} \rangle \langle \hat{b}c \rangle \langle cd \rangle \langle d\hat{a} \rangle} \frac{\langle P_{\alpha\beta} \hat{a} \rangle^4}{\langle P_{j,b} \hat{a} \rangle \langle \hat{a}\hat{b} \rangle \langle \hat{b} P_{a,i} \rangle}, \quad (\text{B.23}) \\
&\rightarrow A_4(\hat{a}^-, \hat{b}^+, c^-, d^+) \frac{\langle P_{\alpha\beta} \hat{b} \rangle^4}{\langle P_{j,b} \hat{a} \rangle \langle \hat{a}\hat{b} \rangle \langle \hat{b} P_{a,i} \rangle} \\
&+ A_4(\hat{a}^+, \hat{b}^-, c^-, d^+) \frac{\langle P_{\alpha\beta} \hat{a} \rangle^4}{\langle P_{j,b} \hat{a} \rangle \langle \hat{a}\hat{b} \rangle \langle \hat{b} P_{a,i} \rangle}.
\end{aligned}$$

We see that the first term contributes to  $\text{Ant}(\hat{a}^+, \hat{b}^- \leftarrow a, 1, \dots, n, b)$  and the second term contributes to  $\text{Ant}(\hat{a}^-, \hat{b}^+ \leftarrow a, 1, \dots, n, b)$ . Note that again the second factor in each term has the same functional form as the left-hand side, so we proved our claim that  $\text{Ant}(\hat{a}^{h_a}, \hat{b}^{h_b} \leftarrow a, 1, \dots, n, b)$  can be calculated by evaluating all MHV diagrams that contribute to the  $(n+4)$ -point amplitude  $A_{n+4}(a, 1, \dots, n, b, \hat{a}^{h_a}, \hat{b}^{h_b})$  and where  $\hat{a}$  and  $\hat{b}$  are attached to the same  $m$ -point MHV vertex, with  $m \geq 4$ .

# Appendix C

## Recursive relations for soft factors

In this appendix we discuss how to build recursive relations for soft factors out of the recursion for antenna functions, Eq. (5.49), in a similar way as we did for the splitting functions in Section 5.4.2.

Let us start by giving some general considerations about the off-shell continuation that appears in the MHV formalism in the soft limit. In general, a propagator involving more than two particles can be written as

$$P_{i,j}^2 = \sum_{\substack{k,l=i \\ k < l}}^j s_{kl}. \quad (\text{C.1})$$

In particular, if  $i$  is a hard particle, say  $i = a$ , and all other momenta are soft, we can write

$$P_{a,j}^2 = \sum_{l=s_1}^j s_{al} + \sum_{k=s_1}^{j-1} \sum_{l=s_2}^j s_{kl}. \quad (\text{C.2})$$

Using the power counting (4.24), it is easy to see that the second term goes to zero much faster than the first one, so we have the following behavior in the soft limit

$$P_{a,j}^2 \sim \sum_{l=s_1}^j s_{al}. \quad (\text{C.3})$$

Similar arguments hold true for spinor products involving off-shell momenta in the MHV formalism,

$$\langle k, P_{i,j} \rangle = \langle k | P_{i,j} | \eta \rangle = \sum_{l=i}^j \langle kl \rangle [l\eta]. \quad (\text{C.4})$$

Following exactly the same lines as for the propagators, we can derive the following rule for off-shell continued spinor products in the soft limit,

**Rule C.1** (Off-shell continuation in the soft limit). *In the soft limit, each spinor product of the form  $\langle k, P_{a,j} \rangle$  has to be interpreted as*

$$\langle k P_{a,j} \rangle \rightarrow \langle ka \rangle [a\eta],$$

except for  $k = a$ , because in this case we have trivially  $\langle a, P_{a,j} \rangle = \langle a, P_{1,j} \rangle$ , and equivalently for  $b$ .

In particular, this implies the following rules for off-shell continued momenta

$$\begin{aligned} \langle a, P_{j,b} \rangle &\rightarrow \langle ab \rangle [b\eta], \\ \langle P_{a,j}, b \rangle &\rightarrow \langle ab \rangle [a\eta], \\ \langle P_{i,j}, P_{k,b} \rangle &\rightarrow \langle P_{i,j}, b \rangle [b\eta], \\ \langle P_{a,i}, P_{j,k} \rangle &\rightarrow \langle a, P_{j,k} \rangle [a\eta], \\ \langle P_{a,j}, P_{k,b} \rangle &\rightarrow \langle ab \rangle [a, \eta] [b\eta]. \end{aligned} \quad (\text{C.5})$$

Let us turn now to the recursive relations. We know that in the limit where all the particles are soft, we have

$$\text{Ant}(\hat{a}^{h_a}, \hat{b}^{h_b} \leftarrow a, 1, \dots, n, b) \longrightarrow \text{Soft}(a, 1, \dots, n, b). \quad (\text{C.6})$$

As the soft factor is independent of the helicities of the reference particles  $a$  and  $b$ , some antenna functions are not divergent in this limit, but only those are divergent where  $h_{\hat{a}} = -h_a$  and  $h_{\hat{b}} = -h_b$ . Taking the soft limit of Eq. (5.49), we can derive a formula for soft factors in terms of single and double-line currents. We will show this procedure explicitly for  $\text{Ant}(\hat{a}^-, \hat{b}^- \leftarrow a^+, 1, \dots, n, b^+)$ . Applying the rules given in Chapter 4, it is easy to see that in the soft limit

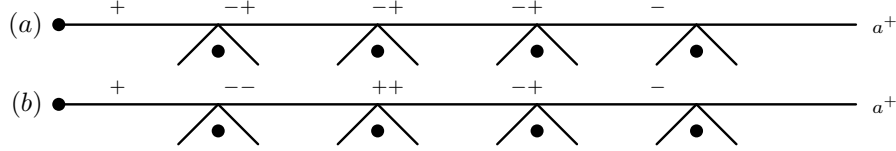


Figure C.1: Diagrams contributing to  $J_+(a^+, 1, \dots, k)$  in the soft limit.

$$\begin{aligned}
 & V_4(U, V, \hat{a}, \hat{b}; \hat{a}, \hat{b}) \\
 \rightarrow V_s(a, b, \eta) &= \begin{cases} 1 & , \text{if } U = (a, a), V = (b, b), \\ 1/[a\eta]^2 & , \text{if } U \neq (a, a), V = (b, b), \\ 1/[b\eta]^2 & , \text{if } U = (a, a), V \neq (b, b), \\ 1/([a\eta]^2[b\eta]^2) & , \text{if } U \neq (a, a), V \neq (n, n). \end{cases} \quad (\text{C.7})
 \end{aligned}$$

Finally, the contribution from an antenna function to a soft factor is

$$\sum_{\substack{U < V \\ v_2 = b}} V_s(a, b, \eta) J_{UV}^0(a^+, 1, \dots, n, b^+). \quad (\text{C.8})$$

However, Eq. (C.8) generates not only diagrams that contribute to the soft limit, but also subleading diagrams. To see this, consider the diagrams contained in  $J_+(a^+, 1, \dots, k)$  shown in Fig. C.1. Let us start with the situation where all external lines in Fig. C.1 are on-shell (except the off-shell line  $(a, k)$  indicated with a dot). Using the power counting rules (4.24), it follows that the denominators of both diagrams shown in Fig. C.1 behave as  $1/t^{2k+4k_-}$ , where  $k_-$  is the number of negative helicities in the set  $\{1, \dots, k\}$ . We then come to the following conclusion:

- For diagrams of the form shown in Fig. C.1.a, the numerator behaves as  $t^{4k_-}$ , and so these diagrams behave as  $t^{4k_-}/t^{2k+4k_-} = 1/t^{2k}$ , which is exactly the divergence we want.
- For diagrams of the form shown in Fig. C.1.b, the numerator behaves as  $t^{4k_-+8}$ , and so these diagrams behave as  $t^{4k_-+8}/t^{2k+4k_-} = 1/t^{2k-8}$ , and so these diagrams are not divergent enough to contribute to the soft factor.

Up to now we have only considered diagrams in Fig. C.1 where all external lines are on-shell. Let us turn to the situation where some of these lines may themselves be off-shell, *i.e.*, they correspond to single-line currents  $J_h(i_1, \dots, i_2)$ . First, a simple power counting argument shows that if the particles  $i_1, \dots, i_2$  are soft,

$$J_+(i_1, \dots, i_2) \sim 1/t^{2(i_2-i_1+1)-4}, \quad J_-(i_1, \dots, i_2) \sim 1/t^{2(i_2-i_1+1)}. \quad (\text{C.9})$$

Using this result, it is easy to show that

- Replacing a positive-helicity particle  $i$  by a single-line current  $J_+$  amounts to the replacement

$$\frac{1}{\langle Xi \rangle \langle iY \rangle} \rightarrow \frac{1}{\langle XI \rangle \langle IY \rangle} J_+(i_1, \dots, i_2). \quad (\text{C.10})$$

$$\sim 1/t^2 \quad \sim 1/t^4 1/t^{2(i_2-i_1+1)-4}$$

So the divergence in  $1/t^2$  of the soft particle  $i$  gets replaced by the divergence in  $1/t^{2(i_2-i_1+1)}$  of the soft particles  $i_1, \dots, i_2$ .

- Replacing a negative-helicity particle  $i$  by a single-line current  $J_-$  amounts to the replacement

$$\frac{\langle Zi \rangle^4}{\langle Xi \rangle \langle iY \rangle} \rightarrow \frac{\langle ZI \rangle^4}{\langle XI \rangle \langle IY \rangle} J_-(i_1, \dots, i_2). \quad (\text{C.11})$$

$$\sim t^2 \quad \sim t^4/t^{2(i_2-i_1+1)}$$

Furthermore, there must be somewhere in the diagram a  $1/t^4$  factor knocking the  $t^2$  on the left-hand side down to a divergence in  $1/t^2$  for the soft particle  $i$ . On the right-hand side, this same term now kills the  $t^4$  in the numerator, giving the divergence in  $1/t^{2(j_2-j_1+1)}$  for the soft particles  $i_1, \dots, i_2$ .

So we come to the conclusion that only the diagrams in  $J_+(a^+, 1, \dots, k)$  of the form shown in Fig. C.1.a contribute in the soft limit. These diagrams are exactly those which do not contain any subcurrent of the form  $J_-(a^+, 1, \dots, l)$ . A similar result holds of course for  $b$ , *i.e.*, only those diagrams contribute to the soft limit which do not contain a subcurrent of the form  $J_-(l, \dots, n, b^+)$ .



Finally we can write

$$\text{Soft}(a, 1, \dots, n, b) = \sum_{\substack{U < V \\ v_2 = b}} V_s(a, b, \eta) \bar{J}_{UV}^0(a^+, 1, \dots, n, b^+), \quad (\text{C.12})$$

where  $\bar{J}_{UV}^0(a^+, 1, \dots, n, b^+)$  denotes a double-line current which does not contain any subcurrent of the form  $J_-(a^+, 1, \dots, l)$  or  $J_-(l, \dots, n, b^+)$ .

Of course we could have used a different antenna function to extract the soft factors. In general, we get the result

$$\text{Soft}(a, 1, \dots, n, b) = \sum_{\substack{U < V \\ v_2 = b}} V_s(a, b, \eta) \epsilon^{h_a h_b} \bar{J}_{UV}^{(2-h_a-h_b)/2}(a^{h_a}, 1, \dots, n, b^{h_b}), \quad (\text{C.13})$$

where  $\bar{J}_{UV}^0(a^{h_a}, 1, \dots, n, b^{h_b})$  is the double-line current which does not contain any subcurrents of the form  $J_{-h_a}(a^{h_a}, 1, \dots, l)$  or  $J_{-h_b}(l, \dots, n, b^{h_b})$ , and

$$\begin{aligned} \epsilon^{++} &= 1, & \epsilon^{+-} &= \frac{\langle aM \rangle^4}{\langle ab \rangle^4}, \\ \epsilon^{+-} &= \frac{\langle Mb \rangle^4}{\langle ab \rangle^4}, & \epsilon^{--} &= \frac{\langle M_1 M_2 \rangle^4}{\langle ab \rangle^4}. \end{aligned} \quad (\text{C.14})$$

We calculated numerically the soft factors for one, two or three soft particles, and we checked numerically that these quantities are independent of the arbitrary spinor  $\eta$  as well as of the helicities of the spectator particles  $a$  and  $b$ .



# Appendix **D**

## Multi-Regge kinematics

### D.1 Multi-parton kinematics

We consider the production of  $n - 2$  gluons of momentum  $p_i$ , with  $i = 3, \dots, n$  in the scattering between two partons of momenta  $p_1$  and  $p_2^*$ .

Using lightcone coordinates  $p^\pm = p_0 \pm p_z$ , and complex transverse coordinates  $p_\perp = p^x + ip^y$ , with scalar product  $2p \cdot q = p^+ q^- + p^- q^+ - p_\perp q_\perp^* - p_\perp^* q_\perp$ , the 4-momenta are,

$$\begin{aligned}
 p_2 &= (p_2^+/2, 0, 0, p_2^+/2) = (p_2^+, 0; 0, 0) , \\
 p_1 &= (p_1^-/2, 0, 0, -p_1^-/2) = (0, p_1^-; 0, 0) , \\
 p_i &= ((p_i^+ + p_i^-)/2, \text{Re}[p_{i\perp}], \text{Im}[p_{i\perp}], (p_i^+ - p_i^-)/2) \\
 &= (|p_{i\perp}|e^{y_i}, |p_{i\perp}|e^{-y_i}; |p_{i\perp}| \cos \phi_i, |p_{i\perp}| \sin \phi_i) ,
 \end{aligned} \tag{D.1}$$

where  $y$  is the rapidity. The first notation above is the standard representation  $p^\mu = (p^0, p^x, p^y, p^z)$ , while in the second we have the  $+$  and  $-$  components on the left of the semicolon, and on the right the transverse components. In the following, if not differently stated,  $p_i$  and  $p_j$  are always understood to lie in

---

\*By convention we consider the scattering in the unphysical region where all momenta are taken as outgoing, and then we analytically continue to the physical region where  $p_1^0 < 0$  and  $p_2^0 < 0$ .

the range  $3 \leq i, j \leq n$ . The mass-shell condition is  $|p_{i\perp}|^2 = p_i^+ p_i^-$ . From the momentum conservation,

$$\begin{aligned} 0 &= \sum_{i=3}^n p_{i\perp}, \\ p_2^+ &= -\sum_{i=3}^n p_i^+, \\ p_1^- &= -\sum_{i=3}^n p_i^-, \end{aligned} \tag{D.2}$$

the Mandelstam invariants may be written as,

$$s_{ij} = 2p_i \cdot p_j = p_i^+ p_j^- + p_i^- p_j^+ - p_{i\perp} p_{j\perp}^* - p_{i\perp}^* p_{j\perp}, \tag{D.3}$$

so that

$$\begin{aligned} s &= 2p_1 \cdot p_2 = \sum_{i,j=3}^n p_i^+ p_j^-, \\ s_{2i} &= 2p_2 \cdot p_i = -\sum_{j=3}^n p_i^- p_j^+, \\ s_{1i} &= 2p_1 \cdot p_i = -\sum_{j=3}^n p_i^+ p_j^-. \end{aligned} \tag{D.4}$$

Using the spinor representation of Ref. [25],

$$\begin{aligned}
\psi_+(p_i) &= \begin{pmatrix} \sqrt{p_i^+} \\ \sqrt{p_i^-} e^{i\phi_i} \\ 0 \\ 0 \end{pmatrix}, & \psi_-(p_i) &= \begin{pmatrix} 0 \\ 0 \\ \sqrt{p_i^-} e^{-i\phi_i} \\ -\sqrt{p_i^+} \end{pmatrix}, \\
\psi_+(p_2) &= i \begin{pmatrix} \sqrt{-p_2^+} \\ 0 \\ 0 \\ 0 \end{pmatrix}, & \psi_-(p_2) &= i \begin{pmatrix} 0 \\ 0 \\ 0 \\ -\sqrt{-p_2^+} \end{pmatrix}, \\
\psi_+(p_1) &= -i \begin{pmatrix} 0 \\ \sqrt{-p_1^-} \\ 0 \\ 0 \end{pmatrix}, & \psi_-(p_1) &= -i \begin{pmatrix} 0 \\ 0 \\ \sqrt{-p_1^-} \\ 0 \end{pmatrix}.
\end{aligned} \tag{D.5}$$

for the momenta (D.1)<sup>†</sup>, the spinor products are

$$\begin{aligned}
\langle 21 \rangle &= -\sqrt{s}, \\
\langle 2i \rangle &= -i \sqrt{\frac{-p_2^+}{p_i^+}} p_{i\perp}, \\
\langle i1 \rangle &= i \sqrt{-p_1^- p_i^+}, \\
\langle ij \rangle &= p_{i\perp} \sqrt{\frac{p_j^+}{p_i^+}} - p_{j\perp} \sqrt{\frac{p_i^+}{p_j^+}},
\end{aligned} \tag{D.6}$$

<sup>†</sup>The spinors of the incoming partons must be continued to negative energy after the complex conjugation, *e.g.*  $\overline{\psi_+(p_2)} = i \left( \sqrt{-p_2^+}, 0, 0, 0 \right)$ .

where we have used the mass-shell condition  $|p_{i\perp}|^2 = p_i^+ p_i^-$ . The spinor products fulfill the usual identities,

$$\begin{aligned}
\langle ij \rangle &= -\langle ji \rangle \\
[ij] &= -[ji] \\
\langle ij \rangle^* &= \text{sign}(p_i^0 p_j^0) [ji] \\
(\langle i + |\gamma^\mu| j + \rangle)^* &= \text{sign}(p_i^0 p_j^0) \langle j + |\gamma^\mu| i + \rangle \\
\langle ij \rangle [ji] &= 2p_i \cdot p_j = \hat{s}_{ij} \\
\langle i + |k| j + \rangle &= [ik] \langle kj \rangle \\
\langle i - |k| j - \rangle &= \langle ik \rangle [kj] \\
\langle ij \rangle \langle kl \rangle &= \langle ik \rangle \langle jl \rangle + \langle il \rangle \langle kj \rangle
\end{aligned} \tag{D.7}$$

and if  $\sum_{i=1}^n p_i = 0$  then

$$\sum_{i=1}^n [ji] \langle ik \rangle = 0. \tag{D.8}$$

## D.2 Multi-Regge kinematics

In the multi-Regge kinematics, we require that the gluons are strongly ordered in rapidity and have comparable transverse momentum (8.1). This is equivalent to require a strong ordering of the lightcone coordinates,

$$p_3^+ \gg p_4^+ \cdots \gg p_n^+; \quad p_3^- \ll p_4^- \cdots \ll p_n^-. \tag{D.9}$$

In the high-energy limit, momentum conservation (D.2) then becomes

$$\begin{aligned}
0 &= \sum_{i=3}^n p_{i\perp}, \\
p_2^+ &= -p_3^+, \\
p_1^- &= -p_n^-,
\end{aligned} \tag{D.10}$$

where the = sign is understood to mean “equals up to corrections of next-to-leading accuracy”. The Mandelstam invariants (D.4) are reduced to,

$$\begin{aligned}
s &= 2p_1 \cdot p_2 = p_3^+ p_n^-, \\
s_{2i} &= 2p_2 \cdot p_i = -p_3^+ p_i^-, \\
s_{1i} &= 2p_1 \cdot p_i = -p_i^+ p_n^-, \\
s_{ij} &= 2p_i \cdot p_j = p_i^+ p_j^- \quad i < j.
\end{aligned} \tag{D.11}$$

The product of two successive invariants of type  $s_{ij}$  fixes the mass shell. For example,

$$\begin{aligned}
s_{k-1,k} s_{k,k+1} &= p_{k-1}^+ p_k^- p_k^+ p_{k+1}^- = |p_{k\perp}|^2 p_{k-1}^+ p_{k+1}^- \\
&= |p_{k\perp}|^2 s_{k-1,k+1} = |p_{k\perp}|^2 s_{k-1,k,k+1}.
\end{aligned} \tag{D.12}$$

Thus,

$$|p_{k\perp}|^2 = \frac{s_{k-1,k} s_{k,k+1}}{s_{k-1,k,k+1}}. \tag{D.13}$$

The spinor products (D.6) are,

$$\begin{aligned}
\langle 21 \rangle &= -\sqrt{p_3^+ p_n^-}, \\
\langle 2i \rangle &= -i \sqrt{\frac{p_3^+}{p_i^+}} p_{i\perp}, \\
\langle i1 \rangle &= i \sqrt{p_i^+ p_n^-}, \\
\langle ij \rangle &= -\sqrt{\frac{p_i^+}{p_j^+}} p_{j\perp} \quad \text{for } y_i > y_j.
\end{aligned} \tag{D.14}$$





# Appendix E

## Proof of the MHV rules for quasi multi-Regge limits

### E.1 Power counting rules for quasi multi-Regge limits

In this appendix we give the proof of the MHV rules for quasi multi-Regge limits which state that in the quasi multi-Regge limit defined by

$$y_3 \simeq y_4 \simeq \dots \simeq y_{n-1} \gg y_n \quad \text{and} \quad |p_{3\perp}| \simeq |p_{4\perp}| \simeq \dots \simeq |p_{n-1\perp}| \simeq |p_{n\perp}|, \quad (\text{E.1})$$

only those MHV diagrams contribute where  $p_1$  and  $p_n$  are attached to an  $m$ -point MHV vertex,  $m \geq 4$ . Since strong ordering in rapidity is equivalent to a strong ordering in lightcone coordinates, we can define the limit by following rescaling\*,

$$\begin{aligned} p_i^+ &\rightarrow \frac{1}{\lambda} p_i^+, \quad i \in \{3, 4, \dots, n-1\}, \\ p_n^+ &\rightarrow p_n^+, \\ p_{i\perp} &\rightarrow p_{i\perp}, \quad \forall i. \end{aligned} \quad (\text{E.2})$$

---

\*Note that we do not include the lightcone components  $p^-$  into this power counting, because they can always be reexpressed in terms of  $p^+$  and  $p_\perp$  using the on-shell condition  $p^- p^+ = |p_\perp|^2$ .

where  $\lambda \rightarrow 0$ . Since in quasi multi-Regge kinematics we have  $p_2^+ \simeq -p_3^+ - p_4^+ - \dots - p_{n-1}^+$  and  $p_1^- \simeq -p_n^-$ , we obtain the scaling of the incoming momenta,

$$p_2^+ \rightarrow \frac{1}{\lambda} p_2^+ \quad \text{and} \quad p_1^+ \rightarrow p_1^+. \quad (\text{E.3})$$

Using the lightcone representation of the spinor products, we can derive the scaling of the spinor product, *e.g.* if  $k \in \{3, 4, \dots, (n-1)\}$ ,

$$\begin{aligned} \langle jk \rangle &= p_{j\perp} \sqrt{\frac{p_k^+}{p_j^+}} - p_{k\perp} \sqrt{\frac{p_j^+}{p_k^+}} \sim 1, \\ \langle 1k \rangle &= -i \sqrt{-p_1^- p_k^+} \simeq -i \frac{|p_{n\perp}|}{\sqrt{p_n^+}} \sqrt{p_k^+} \sim \frac{1}{\sqrt{\lambda}}, \\ \langle 1n \rangle &= -i \sqrt{-p_1^- p_1^+} \simeq -i |p_{n\perp}| \sim 1, \\ \langle kn \rangle &= p_{k\perp} \sqrt{\frac{p_n^+}{p_k^+}} - p_{n\perp} \sqrt{\frac{p_k^+}{p_n^+}} \sim \frac{1}{\sqrt{\lambda}}. \end{aligned} \quad (\text{E.4})$$

Applying these rules to the MHV amplitude  $A_n(1^-, 2^-, 3^+ \dots, (n-1)^+, n^+)$ , we obtain the leading behavior in quasi multi-Regge kinematics,

$$A_n(1^-, 2^-, 3^+ \dots, (n-1)^+, n^+) \sim 1/\lambda. \quad (\text{E.5})$$

This result is generic and extends to non-MHV amplitudes. We therefore get the following simple algorithm to compute the leading behavior of a tree-level gluon amplitude in quasi multi-Regge kinematics,

**Rule E.1.**

1. Apply the power counting rule defined by Eq. (E.2) to  $A_n(1, \dots, n)$ .
2. The coefficient function  $C_{n-3}^{(0)}$  is obtained by taking the leading behavior in  $\lambda$ ,

$$A_n(1, \dots, n) \simeq \frac{1}{\lambda} C^{(0)}(2; 3, \dots, n-1) \frac{s}{t} C^{(0)}(1; n) + \mathcal{O}(1/\sqrt{\lambda}).$$

In the following we extend this algorithm to the MHV formalism, where the amplitude is completely determined by MHV vertices connected by scalar propagators. To this effect, we need to extend the power counting rules introduced at the beginning of this section to the off-shell continued spinor products (2.7).

Let us start by analyzing more closely the scalar propagators in a MHV diagram. Since at tree-level every propagator divides a diagram into two distinct parts, the scalar propagators in every MHV diagram can be divided into two types,

- $p_1$  and  $p_n$  lie on the same side with respect to the propagator (Type A).
- $p_1$  and  $p_n$  lie on different sides (Type B).

Let us start with the propagators of type A. Such a propagator can always be written as

$$P_{i,j}^2 = s_{1n} + \sum_{\substack{\alpha=i \\ \alpha \neq n}}^j s_{1\alpha} + \sum_{\substack{\alpha=i \\ \alpha \neq 1}}^j s_{n\alpha} + \sum_{\substack{\alpha=i \\ \alpha \neq 1, n}}^j \sum_{\substack{\beta=j \\ \beta \neq 1, n}}^j s_{\alpha\beta}. \quad (\text{E.6})$$

Using the power counting (E.2), it is easy to see that the first and the last term in this equation scale as  $\mathcal{O}(\lambda^0)$ . The two remaining terms scale at first sight as  $\mathcal{O}(\lambda^{-1/2})$ . However, using the lightcone representation of the momenta, we see that the singularities cancel between the two terms,

$$\begin{aligned} s_{1\alpha} + s_{n\alpha} &= p_1^- p_\alpha^+ + p_n^- p_\alpha^+ + p_n^+ p_\alpha^- + p_{n\perp} p_{\alpha\perp}^* + p_{n\perp}^* p_{\alpha\perp} \\ &= - \sum_{\beta=3}^n p_\beta^- p_\alpha^+ + p_n^- p_\alpha^+ + p_n^+ p_\alpha^- + p_{n\perp} p_{\alpha\perp}^* + p_{n\perp}^* p_{\alpha\perp} \\ &= - \sum_{\beta=3}^{n-1} p_\beta^- p_\alpha^+ + p_n^+ p_\alpha^- + p_{n\perp} p_{\alpha\perp}^* + p_{n\perp}^* p_{\alpha\perp}, \end{aligned} \quad (\text{E.7})$$

and all terms in this sum are  $\mathcal{O}(\lambda^0)$ . Furthermore, using the power counting (E.2), it is easy to check that for  $i, j, k \in \{3, 4, \dots, n-1\}$  the off-shell continued spinors products behave as

$$\begin{aligned} \langle k P_{i,j} \rangle &= \sum_{\alpha=i}^j \langle k\alpha \rangle [\alpha\eta] \sim 1/\sqrt{\lambda}, \\ \langle 1 P_{i,j} \rangle &= \sum_{\alpha=i}^j \langle 1\alpha \rangle [\alpha\eta] \sim 1/\lambda, \\ \langle n P_{i,j} \rangle &= \sum_{\alpha=i}^j \langle n\alpha \rangle [\alpha\eta] \sim 1/\lambda. \end{aligned} \quad (\text{E.8})$$

Let us now turn to propagators of type B. Without loss of generality, we can assume that such a propagator has the form  $P_{1,j}^2$ , with  $j \in \{2, 3, \dots, n-2\}$ , and it can be written

$$P_{1,j}^2 = \sum_{\alpha=2}^j s_{1\alpha} + 2 \sum_{\alpha=2}^{j-1} \sum_{\beta=\alpha+1}^j s_{\alpha\beta}. \quad (\text{E.9})$$

The second term is obviously finite whereas the first term scales as  $\mathcal{O}(1/\lambda)$ ,

$$s_{1\alpha} = p_1^- p_\alpha^+ \sim 1/\lambda. \quad (\text{E.10})$$

Finally, for off-shell continued spinor products involving type B propagators we find,

$$\begin{aligned} \langle iP_{1,j} \rangle &= \sum_{\alpha=1}^j \langle i\alpha \rangle [\alpha\eta] \sim 1/\sqrt{\lambda}, \\ \langle P_{i,j} P_{1,k} \rangle &= \sum_{\alpha=i}^j \sum_{\beta=1}^k \langle \alpha\beta \rangle [\beta\eta] [\alpha\eta] \sim 1/\lambda, \\ \langle 1P_{1,j} \rangle &= \langle 1P_{2,j} \rangle \sim 1/\lambda, \\ \langle nP_{1,j} \rangle &= \langle n1 \rangle [1\eta] + \langle nP_{2,j} \rangle \sim 1/\lambda. \end{aligned} \quad (\text{E.11})$$

Eqs. (E.8) and (E.11) show how the power counting (E.2) can be extended to off-shell continued spinor products. Looking at the scaling (E.2), (E.8), (E.11), we see that only those spinor products involving  $p_1$ ,  $p_n$  or  $P_{i,j}$  are divergent in the limit  $\lambda \rightarrow 0$  (except for  $\langle 1n \rangle$ ). We can therefore formulate the power counting in the MHV formalism directly in terms of the holomorphic spinor components,

**Rule E.2** (Power counting rules in the MHV formalism).

1. Rescale the spinors  $|1\rangle$ ,  $|n\rangle$  and  $|P_{i,j}\rangle$  by  $1/\sqrt{\lambda}$  (except for  $\langle 1n \rangle$ ).
2. Rescale all propagators type B by  $\lambda$ .
3. The coefficient function  $C_{n-3}^{(0)}$  is obtained by taking the leading behavior in  $\lambda$ ,

$$A_n(1, \dots, n) \simeq \frac{1}{\lambda} C^{(0)}(2; 3, \dots, n-1) \frac{s}{t} C^{(0)}(1; n) + \mathcal{O}(1/\sqrt{\lambda}).$$

## E.2 Proof of the MHV rules for quasi multi - Regge limits

In this section we use the power counting defined in Rule E.2 to proof the MHV rules for quasi multi-Regge limits. We first need to proof the following lemma,

**Rule E.3.** *In the quasi multi-Regge limit, the off-shell MHV currents of Chapter 2 scale as*

$$J_h(i, \dots, j) \sim \lambda^{-h}, \quad \text{if } i, j \in \{2, \dots, n-1\}, \quad (\text{E.12})$$

$$J_h(i, \dots, n) \sim \lambda^{2-h}, \quad \text{if } i \in \{4, \dots, n-1\}. \quad (\text{E.13})$$

Let us start with Eq. (E.12), and let us apply the power counting of the previous section to the diagram shown in Fig. E.1, *i.e.*, a MHV diagram having an off-shell leg, and all other legs in Fig. E.1 are external on-shell legs (In the following we refer to a diagram of this type as a *chain*). We know from Rule E.2 that the only scaling can arise from propagators of type B or from the spinors  $|1\rangle$ ,  $|n\rangle$  and  $|P_{k,l}\rangle$ . Since  $i, j \in \{2, 3, 4, \dots, n-1\}$ , it is easy to see that all the propagators in the chain are of type A, and the chain does not contain the spinors  $|1\rangle$ ,  $|n\rangle$ . Hence factors of  $\lambda$  can only arise from off-shell continued spinors  $|P_{k,l}\rangle$ . Except for  $P_{i,j}$ , all the off-shell continued momenta are connected to exactly two different MHV vertices, *i.e.*, they only appear in combinations of the form

$$\frac{\langle XP_{k,l}\rangle^4}{\langle YP_{k,l}\rangle\langle P_{k,l}Z\rangle} \frac{1}{P_{k,l}^2} \frac{1}{\langle Y'P_{k,l}\rangle\langle P_{k,l}Z'\rangle} \sim 1. \quad (\text{E.14})$$

So the only off-shell continued spinor which can give a contribution is  $P_{i,j}$ , who appears in the combination,

- If  $h = -1$ ,

$$\frac{1}{P_{i,j}^2} \frac{1}{\langle YP_{i,j}\rangle\langle P_{i,j}Z\rangle} \sim \sqrt{\lambda}^2 \sim \lambda. \quad (\text{E.15})$$

- If  $h = +1$ ,

$$\frac{1}{P_{i,j}^2} \frac{\langle XP_{i,j}\rangle^4}{\langle YP_{i,j}\rangle\langle P_{i,j}Z\rangle} \sim \sqrt{\lambda}^2 \sqrt{\lambda}^{-4} \sim \lambda^{-1}. \quad (\text{E.16})$$

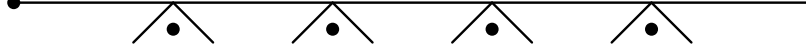


Figure E.1: Definition of a chain. The dotted line is off-shell, all other external lines are on-shell.

This proves that every chain respects the scaling given in Eq. (E.12). Since every MHV current can obviously be obtained by replacing external lines in a chain by other chains, we can now prove recursively the same results for MHV currents. Let us start by analyzing what happens if we replace one external line, say  $k$ , in a chain by a chain itself. This amounts to the replacement

- If  $h_k = -1$ ,

$$\frac{\langle Xk \rangle^4}{\langle Yk \rangle \langle kZ \rangle} \rightarrow \frac{\langle XP_{k_1, k_2} \rangle^4}{\langle YP_{k_1, k_2} \rangle \langle P_{k_1, k_2} Z \rangle} J_-(k_1, \dots, k_2) \sim \sqrt{\lambda}^{-4} \sqrt{\lambda}^2 \lambda \sim 1. \quad (\text{E.17})$$

- If  $h_k = +1$ ,

$$\frac{1}{\langle Yk \rangle \langle kZ \rangle} \rightarrow \frac{1}{\langle YP_{k_1, k_2} \rangle \langle P_{k_1, k_2} Z \rangle} J_+(k_1, \dots, k_2) \sim \sqrt{\lambda}^2 \lambda^{-1} \sim 1. \quad (\text{E.18})$$

We see that replacing an external line by a chain does not alter the scaling behavior, and the result thus follows by induction.

The proof of Eq. (E.13) follows exactly the same lines as for Eq. (E.12), so we do not repeat it here.

We now turn to the proof of the MHV rules for quasi multi-Regge limits. We analyze the different MHV diagrams that can contribute to the amplitude  $A_n(1^-, 2^-, 4, \dots, n-1, n^+)$  in quasi multi-Regge kinematics. We know that in this limit a generic amplitude scales as  $1/\lambda$ . Hence, we need to identify those MHV diagrams that exhibit this scaling behavior. Let us start by considering those MHV diagrams where  $p_1$  and  $p_n$  are attached to the same MHV vertex. Again, replacing a current by an external line does not alter the scaling, and hence we obtain the scaling of a pure MHV amplitude,  $1/\lambda$ , and so all the

diagrams in this class contribute in the quasi multi-Regge limit. However, some care is needed for the three-point MHV vertex involving  $p_1$  and  $p_n$ . In that case we obtain,

$$\frac{\langle P_{n,1}1 \rangle^4}{\langle P_{n,1}n \rangle \langle n1 \rangle \langle nP_{n,1} \rangle} J_-(2, \dots, n-1) \sim \lambda, \quad (\text{E.19})$$

*i.e.* , those diagrams are always subleading in the quasi multi-Regge limit.

Let us now turn to the set of MHV diagrams where  $p_1$  and  $p_n$  are not attached to the same MHV vertex. Let us focus on the diagrams where  $p_1$  and  $p_2$  are attached to the same vertex. The helicity configuration we chose implies that all other legs attached to this vertex must have positive helicity, and so

$$\frac{\langle 12 \rangle^3}{\langle P_{k+1,n}1 \rangle \langle 2X \rangle} J_+(k+1, \dots, n) \sim \sqrt{\lambda}. \quad (\text{E.20})$$

All other topologies in this class can be treated in a similar way, and it is easy to show that all those diagrams are subleading, which finishes the proof.





# Appendix F

## Nested harmonic sums

In this appendix we review the most important properties of the nested harmonic sums defined in Eq. (11.28). The  $S$  and  $Z$  sums fulfill an algebra. Let us illustrate this with a simple example:

$$\begin{aligned}
 S_i(n)S_j(n) &= \sum_{k_1=1}^n \sum_{k_2=1}^n \frac{1}{k_1^i k_2^j} \\
 &= \sum_{k_1=1}^n \frac{1}{k_1^i} \sum_{k_2=1}^{k_1} \frac{1}{k_2^j} + \sum_{k_2=1}^n \frac{1}{k_2^j} \sum_{k_1=1}^{k_2} \frac{1}{k_1^i} - \sum_{k=1}^n \frac{1}{k^{i+j}} \\
 &= S_{ij}(n) + S_{ji}(n) - S_{i+j}(n).
 \end{aligned} \tag{F.1}$$

A similar result can be obtained for the  $Z$ -sums\*,

$$Z_i(n)Z_j(n) = Z_{ij}(n) + Z_{ji}(n) + Z_{i+j}(n). \tag{F.2}$$

For sums of higher weight, a recursive application of the above procedure leads then to the reduction of any product of  $S$  or  $Z$  sums to a linear combination of those sums. Furthermore,  $S$  and  $Z$  sums can be interchanged, *e.g.*

$$\begin{aligned}
 Z_{11}(n) &= \sum_{k=1}^n \frac{Z_1(k-1)}{k} = \sum_{k=1}^n \frac{1}{k} \sum_{\ell=1}^{k-1} \frac{1}{\ell} = \sum_{k=1}^n \frac{1}{k} \left( -\frac{1}{k} + \sum_{\ell=1}^k \frac{1}{\ell} \right) \\
 &= -\sum_{k=1}^n \frac{1}{k^2} + \sum_{k=1}^n \frac{1}{k} S_1(k) = -S_2(n) + S_{11}(n).
 \end{aligned} \tag{F.3}$$

---

\*Note the sign difference with respect to Eq. (F.1).

For  $n \rightarrow \infty$ , the Euler-Zagier sums converge to multiple zeta values,

$$\lim_{n \rightarrow \infty} Z_{m_1 \dots m_k}(n) = \zeta(m_k, \dots, m_1). \quad (\text{F.4})$$

In Ref. [75] Moch *et al.* introduced generalizations of the  $S$  and  $Z$ -sums to make them dependent on some variables,

$$\begin{aligned} S_i(n; x) &= Z_i(n; x) = \sum_{k=1}^n \frac{x^k}{k^i}, \\ S_{i\bar{j}}(n; x_1, \dots, x_\ell) &= \sum_{k=1}^n \frac{x_1^k}{k^i} S_{\bar{j}}(k; x_2, \dots, x_n), \\ Z_{i\bar{j}}(n; x_1, \dots, x_\ell) &= \sum_{k=1}^n \frac{x_1^k}{k^i} Z_{\bar{j}}(k-1; x_2, \dots, x_n). \end{aligned} \quad (\text{F.5})$$

Those sums share of course all the properties of the corresponding number sums introduced in the previous paragraph. In particular, for  $n \rightarrow \infty$ , the  $Z$  sums converge to Goncharov's multiple polylogarithm,

$$\lim_{n \rightarrow \infty} Z_{m_1 \dots m_k}(n; x_1, \dots, x_k) = \text{Li}_{m_k, \dots, m_1}(x_1, \dots, x_k). \quad (\text{F.6})$$

These multiple polylogarithms will be reviewed in the Appendix G.

# Appendix **G**

## Multiple polylogarithms

### G.1 Euler's and Nielsen's polylogarithms

Euler's polylogarithm is defined recursively by

$$\text{Li}_n(x) = \int_0^x \frac{dt}{t} \text{Li}_{n-1}(t), \quad (\text{G.1})$$

where one puts by convention  $\text{Li}_1(x) = -\ln(1-x)$ . Euler's polylogarithm has a branch cut over the range  $[1, +\infty[$ ,

$$\text{Disc Li}_n(x) = 2\pi i \text{Li}_{n-1}(x), \quad (\text{G.2})$$

and for  $|x| \leq 1$  it can be expanded into a power series

$$\text{Li}_n(x) = \sum_{k=1}^{\infty} \frac{x^k}{k^n}. \quad (\text{G.3})$$

This identity implies that for  $x = 1$  Euler's polylogarithm takes the special value  $\text{Li}_n(1) = \zeta_n$ .

Several generalizations of Euler's polylogarithm can be found in the literature. In particular, in Ref. [101] Nielsen generalized the integral (G.1) and defined

$$S_{n,p}(x) = \frac{(-1)^{n+p-1}}{(n-1)!p!} \int_0^1 \frac{dt}{t} \ln^{n-1} t \ln^p(1-xt), \quad (\text{G.4})$$

which for  $p = 1$  reduces to Euler's polylogarithm,  $S_{n,p}(x) = -\text{Li}_{n+1}(x)$ . In the following section we review several other generalizations of Euler's polylogarithm, both in the perspective of generalizing integrals of the form (G.1) and of introducing polylogarithms of more than one variable.

## G.2 One-dimensional harmonic polylogarithms

Harmonic polylogarithms (*HPL's*) have been introduced by Remiddi and Vermaseren in Ref. [102]. The *HPL's* of weight one, *i.e.* depending on one index  $w = -1, 0, 1$ , are defined as:

$$H(-1; x) \equiv \ln(1+x); \quad H(0; x) \equiv \ln x; \quad H(1; x) \equiv -\ln(1-x). \quad (\text{G.5})$$

These functions are then just logarithms of linear functions of  $x$ . The *HPL's* of higher weight are defined recursively by the relation

$$H(a, \vec{w}; x) \equiv \int_0^x dx' f(a; x') H(\vec{w}; x') \quad \text{for } a \neq 0 \text{ and } \vec{w} \neq \vec{0}_n, \quad (\text{G.6})$$

*i.e.* in the case in which not all the indices are zero. The left-most index takes the values  $a = -1, 0, 1$  and  $\vec{w}$  is an  $n$ -dimensional vector with components  $w_i = -1, 0, 1$ . We call  $n$  the weight of the *HPL's*, so the above relation allows one to increase the weight  $w$  by one unit. The basis functions  $f(a; x)$  are given by

$$f(-1; x) \equiv \frac{1}{1+x}; \quad f(0; x) \equiv \frac{1}{x}; \quad f(1; x) \equiv \frac{1}{1-x}. \quad (\text{G.7})$$

In the case in which all indices are zero, one defines instead,

$$H(\vec{0}_n; x) \equiv \frac{1}{n!} \ln^n x. \quad (\text{G.8})$$

The *HPL's* introduced above fulfill many interesting relations, one of the most important ones being that of generating a *shuffle algebra*,

$$H(\vec{w}_1; x) H(\vec{w}_2; x) = \sum_{\vec{w}=\vec{w}_1 \uplus \vec{w}_2} H(\vec{w}; x), \quad (\text{G.9})$$

where  $\vec{w}_1 \uplus \vec{w}_2$  denotes the merging of the two weight vectors  $\vec{w}_1$  and  $\vec{w}_2$ , *i.e.* all possible concatenations of  $\vec{w}_1$  and  $\vec{w}_2$  in which relative orderings of  $\vec{w}_1$  and  $\vec{w}_2$  are preserved.

All *HPL*'s up to weight 3 can be expressed in terms of Euler's and Nielsen's polylogarithms. From weight 4 on, the *HPL*'s in general define new transcendental functions. However, there are some special cases in which we can reduce the *HPL*'s to known polylogarithms,

$$H(\vec{0}_n, 1; x) = \text{Li}_{n+1}(x) \quad \text{and} \quad H(\vec{0}_n, \vec{1}_p; x) = S_{n,p}(x). \quad (\text{G.10})$$

The *HPL*'s can be evaluated numerically in a fast and accurate way; there are various packages available for this purpose [103, 104, 105].

The basis of *HPL*'s can be extended by adding some new basis functions  $f(a; x)$  for some  $a \in \mathbb{R}$  to the set in Eq. (G.7). It is easy to convince oneself that this extended set of transcendental functions still forms a shuffle algebra (G.9).

Some special values include

$$\begin{aligned} H(\vec{a}_n; x) &= \frac{1}{n!} \ln^n \left( 1 - \frac{x}{a} \right), \\ H(\vec{0}_n, a; x) &= \text{Li}_n \left( \frac{x}{a} \right), \\ H(\vec{0}_n, \vec{a}_p; x) &= (-1)^p S_{n,p} \left( \frac{x}{a} \right). \end{aligned} \quad (\text{G.11})$$

### G.2.1 Reduction algorithms

The shuffle algebra (G.9) can be used to derive several reduction algorithms for *HPL*'s with related arguments. The relations obtained in this way in general contain several formulas given in the literature and involving Euler's and Nielsen's polylogarithms. In the following we present two algorithms to reduce *HPL*'s evaluated in  $1-x$  and  $1/x$  to *HPL*'s in  $x$ .

Let us start with the transformation  $x \rightarrow 1/x$ . If  $a < 0$  and  $0 < x < 1$ , then for *HPL*'s of weight one we find immediately

$$\begin{aligned} H(a; 1/x) &= \ln \left( 1 - \frac{1}{xa} \right) = -\ln(-a) - \ln x + \ln(1-ax) \\ &= -\ln(-a) - \ln a + H(1/a; x). \end{aligned} \quad (\text{G.12})$$

For *HPL*'s of arbitrary weight, if the rightmost index is non zero\* we can use the integral representation (G.6). Performing the change of variable  $t \rightarrow 1/t$ ,

\*If the rightmost index is zero, we use the shuffle algebra and go to an *irreducible basis*, where  $H(a, \vec{w}; x)$  is expressed as a combination of *HPL*'s with non zero rightmost index and *HPL*'s of the form (G.8).

we find,

$$\begin{aligned} H(a, \vec{w}; 1/x) &= \int_0^{1/x} dt \frac{H(\vec{w}; t)}{t-a} = H(a, \vec{w}; 1) - \int_1^x dt \frac{H(\vec{w}; 1/t)}{t(1-at)} \\ &= H(a, \vec{w}; 1) + \int_1^x dt [f(0; t) - f(1/a; t)] H(\vec{w}; 1/t). \end{aligned} \quad (\text{G.13})$$

The first term is just a transcendental number (independent of  $x$ ). The *HPL* in the remaining integral is of lower weight, and hence known recursively. Since the upper integration limit is  $x$ , the integration will yield *HPL*'s in  $x$ . Note that the transformation  $x \rightarrow 1/x$  has a fixed point in  $x = 1$ . We can hence use this algorithm to extract the special values of the *HPL*'s in  $x = 1$ .

Let us now turn to the transformation  $x \rightarrow 1 - x$ . If  $a > 1$  and  $0 < x < 1$ , for *HPL*'s of weight one we immediately get

$$\begin{aligned} H(a; 1-x) &= \ln \left( 1 - \frac{1-x}{a} \right) = \ln(a-1) - \ln a + \ln \left( 1 - \frac{x}{1-a} \right) \\ &= \ln(a-1) - \ln a + H(1-a; x). \end{aligned} \quad (\text{G.14})$$

For *HPL*'s of arbitrary weight, if the rightmost index is non zero<sup>†</sup> we can use the integral representation (G.6). Performing the change of variable  $t \rightarrow 1-t$ , we find,

$$\begin{aligned} H(a, \vec{w}; 1-x) &= \int_0^{1-x} dt \frac{H(\vec{w}; t)}{t-a} = \int_1^x dt \frac{H(\vec{w}; 1-t)}{t+a-1} \\ &= -H(1-a, \vec{w}; 1) + \int_1^x dt f(1-a; t) H(\vec{w}; 1-t). \end{aligned} \quad (\text{G.15})$$

The first term is a transcendental number, and in the second integral the *HPL* in  $1-t$  is known recursively, and hence we can completely reduce the *HPL*'s in  $1-x$ . Note that the transformation  $x \rightarrow 1-x$  has a fixed point in  $x = 1/2$ . We can hence use this algorithm to extract the special values of the *HPL*'s in  $x = 1/2$ .

---

<sup>†</sup>If the rightmost index is zero, we use the shuffle algebra and go to an *irreducible basis*, where  $H(a, \vec{w}; x)$  is expressed as a combination of *HPL*'s with non zero rightmost index and *HPL*'s of the form (G.8).

## G.3 Two-dimensional harmonic polylogarithms

For integrals depending on two arguments, an extension of the *HPL*'s to functions of two variables proves to be convenient [106]. Since a harmonic polylogarithm is basically a repeated integration on *one* variable, a second independent variable is introduced as a parameter entering the basis functions:  $f(i; x) \rightarrow f(i, \alpha; x)$ . We may say that in addition to the discrete index  $i$ , we have now a continuous index  $\alpha$ . In Ref. [106] the following basis functions were originally introduced:

$$f(b_i(\alpha); x) = \frac{1}{x - b_i(\alpha)}, \quad (\text{G.16})$$

where

$$b_1(\alpha) = 1 - \alpha \quad \text{or} \quad b_2(\alpha) = -\alpha. \quad (\text{G.17})$$

Let us remark that the above extension keeps most of the properties of the one-dimensional *HPL*'s. In Ref. [69] a new set of basis functions was introduced that is slightly more complicated than the one above,

$$f(c_1(\alpha); x) = \frac{1}{x - c_1(\alpha)} \quad f(c_2(\alpha); x) = \frac{1}{x - c_2(\alpha)}, \quad (\text{G.18})$$

with

$$c_1(\alpha) = \frac{\alpha}{\alpha - 1}, \quad c_2(\alpha) = \frac{2\alpha}{\alpha - 1}. \quad (\text{G.19})$$

The definition of the two-dimensional harmonic polylogarithms (*2dHPL*'s) reads:

$$H(c_i(\alpha), \bar{w}(\alpha); x) \equiv \int_0^x f(c_i(\alpha); x') H(\bar{w}(\alpha); x') dx'. \quad (\text{G.20})$$

In general, the *2dHPL*'s have complicated analyticity properties, with imaginary parts coming from integrating over the zeroes of the basis functions. However, for  $0 \leq x, \alpha \leq 1$ , the denominators are never singular and thus the *2dHPL*'s are real. The numerical evaluation of our *2dHPL*'s can be achieved by extending the algorithm described and implemented in Ref. [107].

### G.3.1 Special values

For some special values of the arguments, the  $2dHPL$ 's reduce to ordinary one-dimensional  $HPL$ 's. It is easy to see that for  $\alpha = 0$  and  $\alpha = 1$  we have

$$f(c_k(\alpha = 0); x) = f(0; x), \quad \lim_{\alpha \rightarrow 1} f(c_k(\alpha); x) = 0. \quad (\text{G.21})$$

From this it follows that

$$\begin{aligned} H(\dots, c_i(\alpha = 0), \dots; x) &= H(\dots, 0, \dots; x), \\ \lim_{\alpha \rightarrow 1} H(\dots, c_i(\alpha), \dots; x) &= 0. \end{aligned} \quad (\text{G.22})$$

Similarly, for  $x = 1$ , the  $2dHPL$ 's reduce to combinations of one-dimensional  $HPL$ 's in  $\alpha$ . This reduction can be performed using an extension of the algorithm presented in [106]. We first write the  $2dHPL$ 's in  $x = 1$  as the integral of the derivative with respect to  $\alpha$ ,

$$H(\vec{w}(\alpha); 1) = H(\vec{w}(\alpha = 1); 1) + \int_1^\alpha d\alpha' \frac{\partial}{\partial \alpha'} H(\vec{w}(\alpha'); 1). \quad (\text{G.23})$$

In the case where  $\vec{w}$  only contains objects of the type  $c_i$ , we have  $H(\vec{w}(\alpha = 1); x) = 0$ . Thus,

$$H(\vec{w}(\alpha); 1) = \int_1^\alpha d\alpha' \frac{\partial}{\partial \alpha'} H(\vec{w}(\alpha'); 1). \quad (\text{G.24})$$

The derivative is then carried out on the integral representation of  $H(\vec{w}(\alpha'); 1)$ , and integrating back gives the desired reduction of  $H(\vec{w}(\alpha); 1)$  to ordinary  $HPL$ 's in  $\alpha$ , *e.g.*

$$\begin{aligned} H(c_1(\alpha); 1) &= -H(0; \alpha), \\ H(c_2(\alpha); 1) &= H(-1; \alpha) - H(0; \alpha) - \ln 2. \end{aligned} \quad (\text{G.25})$$

### G.3.2 Interchange of arguments

The basis of  $2dHPL$ 's introduced above selects  $x$  as the explicit (integration) variable and  $\alpha$  as a parameter, but an alternative representation involving a repeated integration over  $\alpha$  of (different) basis functions depending on  $x$  as an external parameter is also possible.



In Ref. [69, 103], an algorithm was presented which allows to express  $2dHPL$ 's of the form  $H(\vec{w}(a); z)$  in  $z = 1$  in terms of ordinary  $HPL$ 's in  $a$ . First write  $H(\vec{w}(a); 1)$  as the integral of the derivative,

$$H(\vec{w}(a); 1) = H(\vec{w}(a_0); 1) + \int_{a_0}^a da' \frac{\partial}{\partial a'} H(\vec{w}(a'); 1), \quad (\text{G.26})$$

where  $a_0$  is arbitrary, provided that  $H(\vec{w}(a_0); 1)$  exists. The derivative is now carried out on the integral representation of  $H$ , and then we integrate back. Since differentiation lowers the weight by one unit and since we know recursively how to reduce all  $H(\vec{w}'(a); 1)$  with  $w' < w$ , we obtain now the function  $H(\vec{w}(a); 1)$  with  $a$  being the limit of the last integration.

If we apply this algorithm to the  $2dHPL$ 's defined in Eq. (G.20), then we can express all the  $2dHPL$ 's in terms of an enlarged set of basis functions,

$$f(d_k(x); \alpha) = \frac{1}{\alpha + d_k(x)}, \quad (\text{G.27})$$

where

$$d_k(x) = \frac{x}{x - k}. \quad (\text{G.28})$$

All the properties defined at the beginning of this section can be easily extended to this new class of denominators. One finds for example:

$$\begin{aligned} H(c_1(\alpha); x) &= H(0; x) - H(0; \alpha) + H(d_1(x); \alpha), \\ H(c_2(\alpha); x) &= H(0; x) - H(0; \alpha) - \ln 2 + H(d_2(x); \alpha). \end{aligned} \quad (\text{G.29})$$

## G.4 Goncharov's multiple polylogarithm

In the previous section we reviewed the harmonic polylogarithms and their two-dimensional generalization, which arise from iterated integrations in one or two variables. In this section we will extend this procedure to arbitrary iterated integration, which leads naturally to the definition of Goncharov's multiple polylogarithm. Let us define [108, 109]

$$\Omega(a) = \frac{dt}{t - a}, \quad (\text{G.30})$$

and iterated integrations by

$$\int_0^z \Omega(a_1) \circ \dots \circ \Omega(a_n) = \int_0^z \frac{dt}{t - a_1} \int_0^t \Omega(a_2) \circ \dots \circ \Omega(a_n). \quad (\text{G.31})$$

We can then define the  $G$  and  $M$ -functions as

$$\begin{aligned} G(a_1, \dots, a_n; z) &= \int_0^z \Omega(a_1) \circ \dots \circ \Omega(a_n), \\ M(a_1, \dots, a_n) &= G(a_1, \dots, a_n; 1) = \int_0^1 \Omega(a_1) \circ \dots \circ \Omega(a_n). \end{aligned} \quad (\text{G.32})$$

The  $M$ -functions are nothing but Goncharov's multiple polylogarithm, up to a sign<sup>‡</sup>,

$$M(a_1, \dots, a_n) = (-1)^k \text{Li}_{m_k, \dots, m_1}(z_k, \dots, z_1), \quad (\text{G.33})$$

where  $k$  is the number of nonzero elements in  $(a_1, \dots, a_n)$ .

Iterated integrals form a shuffle algebra, and hence we can immediately write

$$\begin{aligned} G(\vec{w}_1; z) G(\vec{w}_2; z) &= \sum_{\vec{w} = \vec{w}_1 \uplus \vec{w}_2} G(\vec{w}; z), \\ M(\vec{w}_1) M(\vec{w}_2) &= \sum_{\vec{w} = \vec{w}_1 \uplus \vec{w}_2} M(\vec{w}). \end{aligned} \quad (\text{G.34})$$

It is easy to see that in general<sup>§</sup>

$$\lim_{a_1 \rightarrow 1} M(a_1, \dots, a_n) = \infty, \quad (\text{G.35})$$

or equivalently

$$\lim_{z \rightarrow 1} G(1, a_2, \dots, a_n; z) = \infty, \quad (\text{G.36})$$

We can however extract the divergence by choosing an irreducible basis for the  $G$ -functions where the leftmost index is different from 1, except for functions of the form  $G(\vec{1}_n; z)$ , *e.g.*

$$G(1, 0; z) = G(1; z) G(0; z) - G(0, 1; z). \quad (\text{G.37})$$

In this basis the singularity structure in  $z = 1$  is explicit.

<sup>‡</sup>For the meaning of the indices  $m_i$  and  $z_i$ , the reader should refer to Ref. [75]. They are equivalent to the corresponding notation for *HPL*'s, *e.g.*  $H(0, 1; z) = H_2(z)$ .

<sup>§</sup>In some cases the divergence is tamed, *e.g.*  $\lim_{z \rightarrow 1} \ln z \ln(1 - z) = 0$ .

Since  $M$ -functions are nothing but the values in  $z = 1$  of the  $G$  functions, and since  $G$ -functions are straightforward generalizations of the  $HPL$ 's, the algorithm for interchanging the arguments presented in Section G.3.2 immediately generalizes to the  $M$ -functions, and allows in principle to reduce functions of the form  $M(\dots, \lambda_1, \dots)$  to  $HPL$ 's of the form  $H(\dots; \lambda_1)$ , the algorithm being a straightforward generalization of Eq. (G.26)

$$M(\vec{w}(a)) = M(\vec{w}(a_0)) + \int_{a_0}^a da' \frac{\partial}{\partial a'} M(\vec{w}(a')), \quad (\text{G.38})$$

where  $a_0$  is arbitrary, provided that  $M(\vec{w}(a_0))$  exists.



# Appendix H

## Hypergeometric functions

### H.1 The Gauss hypergeometric functions

In this appendix we briefly review the different representations of hypergeometric functions which appear throughout this work. We start with Gauss' hypergeometric function,

$${}_2F_1(a, b, c; x) = \sum_{n=0}^{\infty} \frac{(a)_n (b)_n}{(c)_n} \frac{x^n}{n!}, \quad (\text{H.1})$$

and we comment on hypergeometric functions in two variables in subsequent sections. We also refer the interested reader to the literature [98, 110, 97]. Eq. (H.1) defines the series representation of the hypergeometric function. The series is absolutely convergent inside the unit disc  $|x| < 1$ . The hypergeometric *function* however is defined over the complex plane, so we need to analytically continue the series (H.1) outside the unit disc according to the prescription  $x \rightarrow 1/x$ . Furthermore, in physical applications, one often encounters special cases where the indices  $a, b$  and  $c$  are of the form  $\alpha + \beta\epsilon$ ,  $\alpha, \beta$  being integers\*, and it is desired to have the hypergeometric function in the form of a Laurent expansion up to a given order in  $\epsilon$ . We review in the following several other

---

\*In some applications, also half-integer values can be found. In the following we restrict the discussion to integer values.

representations of the hypergeometric function, sometimes more suitable for specific problems.

Let us first turn to the *Euler integral representation*,

$${}_2F_1(a, b, c; x) = \frac{\Gamma(c)}{\Gamma(b)\Gamma(c-b)} \int_0^1 dt t^{b-1} (1-t)^{c-b-1} (1-xt)^{-a}. \quad (\text{H.2})$$

This identity follows immediately from the fact that for  $|x| < 1$ , we can insert the series expansion of  $(1-xt)^{-a}$  in the integrand,

$$\begin{aligned} & \frac{\Gamma(c)}{\Gamma(b)\Gamma(c-b)} \int_0^1 dt t^{b-1} (1-t)^{c-b-1} (1-xt)^{-a} \\ &= \sum_{n=0}^{\infty} \frac{(a)_n}{n!} x^n \frac{\Gamma(c)}{\Gamma(b)\Gamma(c-b)} \int_0^1 dt t^{b+n-1} (1-t)^{c-b-1} \\ &= \sum_{n=0}^{\infty} \frac{(a)_n}{n!} x^n \frac{\Gamma(c)}{\Gamma(b)\Gamma(c-b)} \frac{\Gamma(b+n)\Gamma(c-b)}{\Gamma(c+n)} \\ &= {}_2F_1(a, b, c; x), \end{aligned} \quad (\text{H.3})$$

and the identity follows by analytic continuation for  $|x| > 1$ . Note however that the Euler integral representation is meaningless if  $x$  is real and greater than 1 and  $a$  is a positive integer, since in that case the integral (H.2) is divergent. The Euler integral has the nice property that in the situation where all indices are of the form  $\alpha + \beta\epsilon$ , the expansion in  $\epsilon$  can be easily performed using integration-by-parts identities and the Laporta algorithm [69] (See Chapter 6). Indeed, since  $t$  and  $(1-t)$  vanish at the integration limits, we can write,

$$\int_0^1 dt \frac{\partial}{\partial t} \left( t^{b-1} (1-t)^{c-b-1} (1-xt)^{-a} \right) = 0, \quad (\text{H.4})$$

and carrying out the derivative on the integrand generates a set of recursive relations for the hypergeometric function. Using the Laporta algorithm we can solve the recursion and express every integral of Euler type in terms of a small set of master integrals. We can write down a set of differential equations for the master integrals that can be solved order by order in  $\epsilon$  in terms of harmonic polylogarithms (See Appendix G.4 for a review of generalized polylogarithms). Note that in the case of Gauss' hypergeometric function this procedure might look like an overkill, since we could as well expand the Pochhammer symbols in the series (H.1) and sum the resulting series in terms of nested sums. However,

for more general hypergeometric functions, this naive approach might lead to series for which the sum is not necessarily known.

A third way of representing a hypergeometric function is in terms of a Mellin-Barnes integral,

$${}_2F_1(a, b, c; x) = \frac{\Gamma(c)}{\Gamma(a)\Gamma(b)} \int_{-i\infty}^{+i\infty} dz \Gamma(-z) \frac{\Gamma(a+z)\Gamma(b+z)}{\Gamma(c+z)} (-x)^z, \quad (\text{H.5})$$

where the contour is chosen according to the usual prescription, *i.e.* the contour should separate the poles in  $\Gamma(-z)$  from the poles in  $\Gamma(\dots + z)$ . The identity (H.5) follows simply from the fact that for  $|x| < 1$  we can close the integration contour to the left and sum up the residues of  $\Gamma(-z)$ , which immediately results in the series (H.1). The Mellin-Barnes representation is however much more general, because the integral (H.5) is convergent even for  $|x| > 1$ , in which case it suffices to close the contour to the right. In this sense, the integral (H.5) really represents the hypergeometric *function*, because it is valid in all the regions<sup>†</sup>. This property gives us at the same time an effective way to perform the analytic continuation of the hypergeometric function outside the unit disc. Closing the integration contour to the right and taking residues in  $z = -a - n$  and  $z = -b - n$ ,  $n \in \mathbb{N}$ , we find

$$\begin{aligned} {}_2F_1(a, b, c; x) &= \frac{\Gamma(c)\Gamma(b-a)}{\Gamma(b)\Gamma(c-a)} (-z)^{-a} {}_2F_1(a, 1+a-c, 1+a-b; 1/z) \\ &\quad + \frac{\Gamma(c)\Gamma(a-b)}{\Gamma(a)\Gamma(c-b)} (-z)^{-b} {}_2F_1(b, 1+b-c, 1+b-a; 1/z), \end{aligned} \quad (\text{H.6})$$

where we used the formula

$$\Gamma(a-n) = (-1)^n \frac{\Gamma(a)}{(1-a)_n}. \quad (\text{H.7})$$

Finally, let us also mention the *Laplace integral representation*,

$${}_2F_1(a, b, c; x) = \frac{\Gamma(c)}{\Gamma(b)} \int_0^\infty dt_1 dt_2 e^{-t_1-t_2} t_1^{b-1} t_2^{c-1} (1-t_1 t_2 z)^{-a}, \quad (\text{H.8})$$

which follows directly from the integral representation of the  $\Gamma$  function,

$$\Gamma(z) = \int_0^\infty dt e^{-t} t^{z-1}. \quad (\text{H.9})$$

---

<sup>†</sup>In Ref. [111], Appell and Kampé de Fériet propose for this reason to *define* the hypergeometric function through the Mellin-Barnes integral (H.5).

We do not use this representation explicitly in this work, but we only quote it for completeness.

## H.2 Generalized hypergeometric functions

### H.2.1 Appell functions

The Appell functions are defined by the double series,

$$\begin{aligned}
 F_1(a, b, c, d; x, y) &= \sum_{m=0}^{\infty} \sum_{n=0}^{\infty} \frac{(a)_{m+n} (b)_m (c)_n}{(d)_{m+n}} \frac{x^m}{m!} \frac{y^n}{n!}, \\
 F_2(a, b, c, d, e; x, y) &= \sum_{m=0}^{\infty} \sum_{n=0}^{\infty} \frac{(a)_{m+n} (b)_m (c)_n}{(d)_m (e)_n} \frac{x^m}{m!} \frac{y^n}{n!}, \\
 F_3(a, b, c, d, e; x, y) &= \sum_{m=0}^{\infty} \sum_{n=0}^{\infty} \frac{(a)_m (b)_n (c)_m (d)_n}{(e)_{m+n}} \frac{x^m}{m!} \frac{y^n}{n!}, \\
 F_4(a, b, c, d; x, y) &= \sum_{m=0}^{\infty} \sum_{n=0}^{\infty} \frac{(a)_{m+n} (b)_{m+n}}{(c)_m (d)_n} \frac{x^m}{m!} \frac{y^n}{n!}.
 \end{aligned} \tag{H.10}$$

From the series representation the Mellin-Barnes representation is trivially obtained. For some special values of the indices, the Appell functions reduce to simpler hypergeometric functions, *e.g.* ,

$$\begin{aligned}
 F_4\left(\alpha, \beta, \alpha, \beta; \frac{-x}{(1-x)(1-y)}, \frac{-y}{(1-x)(1-y)}\right) &= \frac{(1-x)^\beta (1-y)^\alpha}{1-xy}, \\
 F_4\left(\alpha, \beta, \beta, \beta; \frac{-x}{(1-x)(1-y)}, \frac{-y}{(1-x)(1-y)}\right) & \\
 &= (1-x)^\alpha (1-y)^\alpha {}_2F_1(\alpha, 1+\alpha-\beta, \beta; xy), \\
 F_4\left(\alpha, \beta, 1+\alpha-\beta, \beta; \frac{-x}{(1-x)(1-y)}, \frac{-y}{(1-x)(1-y)}\right) & \\
 &= (1-y)^\alpha {}_2F_1\left(\alpha, \beta, 1+\alpha-\beta; -\frac{x(1-y)}{1-x}\right), \\
 F_4\left(\alpha, \beta, \gamma, \beta; \frac{-x}{(1-x)(1-y)}, \frac{-y}{(1-x)(1-y)}\right) & \\
 &= (1-x)^\alpha (1-y)^\alpha F_1(\alpha, \gamma-\beta, 1+\alpha-\gamma, \gamma; x, xy).
 \end{aligned} \tag{H.11}$$



The analytic continuation of the Appell  $F_4$  function reads

$$\begin{aligned}
 F_4(a, b, c, d; x, y) &= \frac{\Gamma(d)\Gamma(b-a)}{\Gamma(b)\Gamma(d-a)} (-y)^{-a} F_4\left(a, 1+a-d, c, 1+a-b; \frac{x}{y}, \frac{1}{y}\right) \\
 &\quad + \frac{\Gamma(d)\Gamma(a-b)}{\Gamma(a)\Gamma(d-b)} (-y)^{-b} F_4\left(1+b-d, b, c, 1+b-a; \frac{x}{y}, \frac{1}{y}\right).
 \end{aligned}
 \tag{H.12}$$

## H.2.2 Kampé de Fériet functions

The Kampé de Fériet functions are defined by the series

$$\begin{aligned}
 F_{p',q'}^{p,q} \left( \begin{array}{c} \alpha_i \\ \alpha'_k \end{array} \middle| \begin{array}{c} \beta_j \\ \beta'_\ell \end{array} \begin{array}{c} \gamma_j \\ \gamma'_\ell \end{array} \middle| x, y \right) \\
 = \sum_{m=0}^{\infty} \sum_{n=0}^{\infty} \frac{\prod_i (\alpha_i)_{m+n} \prod_j (\beta_j)_m (\gamma_j)_n}{\prod_k (\alpha'_k)_{m+n} \prod_\ell (\beta'_\ell)_m (\gamma'_\ell)_n} \frac{x^m}{m!} \frac{y^n}{n!},
 \end{aligned}
 \tag{H.13}$$

with  $1 \leq i \leq p$ ,  $1 \leq j \leq q$ ,  $1 \leq k \leq p'$  and  $1 \leq \ell \leq q'$ , and convergence requires  $p+q \leq p'+q'+1$  [111]. The order of a Kampé de Fériet function is defined by  $\omega = p'+q'$ . If  $p+q = \omega + 1$ , the function is called *complete*, and all other cases are obtained as a confluent limiting case of a complete function. From its definition it is clear that the Kampé de Fériet function enjoys the following symmetry property,

$$F_{p',q'}^{p,q} \left( \begin{array}{c} \alpha_i \\ \alpha'_k \end{array} \middle| \begin{array}{c} \beta_j \\ \beta'_\ell \end{array} \begin{array}{c} \gamma_j \\ \gamma'_\ell \end{array} \middle| x, y \right) = F_{p',q'}^{p,q} \left( \begin{array}{c} \alpha_i \\ \alpha'_k \end{array} \middle| \begin{array}{c} \gamma_j \\ \gamma'_\ell \end{array} \begin{array}{c} \beta_j \\ \beta'_\ell \end{array} \middle| y, x \right).
 \tag{H.14}$$

The Kampé de Fériet functions encompass the Appell functions for particular values of the parameters,

$$\begin{aligned}
 F_{1,0}^{1,1} \left( \begin{array}{c} a \\ d \end{array} \middle| \begin{array}{c} b \\ - \end{array} \begin{array}{c} c \\ - \end{array} \middle| x, y \right) &= F_1(a, b, c, d; x, y), \\
 F_{0,1}^{1,1} \left( \begin{array}{c} a \\ - \end{array} \middle| \begin{array}{c} b \\ d \end{array} \begin{array}{c} c \\ e \end{array} \middle| x, y \right) &= F_2(a, b, c, d, e; x, y), \\
 F_{1,0}^{0,2} \left( \begin{array}{c} - \\ e \end{array} \middle| \begin{array}{c} a \\ - \end{array} \begin{array}{c} b \\ - \end{array} \begin{array}{c} c \\ - \end{array} \begin{array}{c} d \\ - \end{array} \middle| x, y \right) &= F_3(a, b, c, d, e; x, y), \\
 F_{0,1}^{2,0} \left( \begin{array}{c} a \\ - \end{array} \begin{array}{c} b \\ - \end{array} \middle| \begin{array}{c} - \\ c \end{array} \begin{array}{c} - \\ d \end{array} \middle| x, y \right) &= F_4(a, b, c, d; x, y).
 \end{aligned}
 \tag{H.15}$$

The Kampé de Fériet function involves only Pochhammer symbols of the form  $(\cdot)_{n_1+n_2}$ ,  $(\cdot)_{n_1}$ ,  $(\cdot)_{n_2}$ . We could alternatively define a series involving Pochhammer symbols of the form  $(\cdot)_{n_1-n_2}$ . Let us consider the double series

$$\begin{aligned} \tilde{F}_{p',q',r'}^{p,q,r} \left( \begin{array}{c} a_i \\ a'_k \end{array} \middle| \begin{array}{c} b_j \\ b'_l \\ c'_m \end{array} \middle| x, y \right) \\ = \sum_{n_1=0}^{\infty} \sum_{n_2=0}^{\infty} \frac{\prod_i (a_i)_{n_1-n_2} \prod_j (b_j)_{n_1} \prod_h (c_h)_{n_2}}{\prod_k (a'_k)_{n_1-n_2} \prod_l (b'_l)_{n_1} \prod_m (c'_m)_{n_2}} \frac{x^{n_1}}{n_1!} \frac{y^{n_2}}{n_2!}. \end{aligned} \quad (\text{H.16})$$

Note that this function can appear in the analytic continuation of the Kampé de Fériet function. In the following we prove that the generalized hypergeometric series  $\tilde{F}$  can always be reduced to hypergeometric series involving only Pochhammer symbols of the form  $(\cdot)_{n_1+n_2}$ ,  $(\cdot)_{n_1}$ ,  $(\cdot)_{n_2}$ . We rewrite the double sum according to

$$\begin{aligned} \sum_{n_1=0}^{\infty} \sum_{n_2=0}^{\infty} &= \sum_{n_1=0}^{\infty} \sum_{n_2=0}^{n_1} + \sum_{n_1=0}^{\infty} \sum_{n_2=n_1}^{\infty} - \sum_{n_1=n_2=0}^{\infty} \\ &= \sum_{n_1=0}^{\infty} \sum_{n_2=0}^{n_1} + \sum_{n_2=0}^{\infty} \sum_{n_1=0}^{n_2} - \sum_{n_1=n_2=0}^{\infty}. \end{aligned} \quad (\text{H.17})$$

The double sums are now reshuffled into double sums up to infinity, *e.g.*

$$\sum_{n_1=0}^{\infty} \sum_{n_2=0}^{n_1} \rightarrow \sum_{N=0}^{\infty} \sum_{n_2=0}^N, \quad \text{with } n_1 = N + n_2, \quad (\text{H.18})$$

and equivalently for  $\sum_{n_2=0}^{\infty} \sum_{n_1=0}^{n_2}$ . In the second sum we then rewrite all Pochhammer symbols with negative index according to

$$(a)_{-n} = \frac{(-1)^n}{(1-a)_n}. \quad (\text{H.19})$$

We then arrive at

$$\begin{aligned} \tilde{F}_{p',q',r'}^{p,q,r} \left( \begin{array}{c} a_i \\ a'_k \end{array} \middle| \begin{array}{c} b_j \\ b'_l \\ c'_m \end{array} \middle| x, y \right) \\ = \sum_{n_1=0}^{\infty} \sum_{n_2=0}^{\infty} \frac{\prod_i (a_i)_{n_1} \prod_j (b_j)_{n_1+n_2} \prod_h (c_h)_{n_2}}{\prod_k (a'_k)_{n_1} \prod_l (b'_l)_{n_1+n_2} \prod_m (c'_m)_{n_2}} \frac{(1)_{n_1}}{(1)_{n_1+n_2}} \frac{x^{n_1}}{n_1!} \frac{(xy)^{n_2}}{n_2!} \\ + \sum_{n_1=0}^{\infty} \sum_{n_2=0}^{\infty} (-1)^{(p+p')n_2} \frac{\prod_k (1-a'_k)_{n_2} \prod_j (b_j)_{n_1} \prod_h (c_h)_{n_1+n_2}}{\prod_i (1-a_i)_{n_2} \prod_l (b'_l)_{n_1} \prod_m (c'_m)_{n_1+n_2}} \\ \times \frac{(xy)^{n_1}}{n_1!} \frac{y^{n_2}}{(n_1+n_2)!} \end{aligned} \quad (\text{H.20})$$

$$- \sum_{n=0}^{\infty} \frac{\prod_j (b_j)_n \prod_h (c_h)_n}{(1)_n \prod_l (b'_l)_n \prod_m (c'_m)_n} \frac{(xy)^n}{n!}. \tag{H.21}$$

We see that in Eq. (H.20) only Pochhammer symbols of the form  $(\cdot)_{n_1+n_2}$ ,  $(\cdot)_{n_1}$  and  $(\cdot)_{n_2}$  appear. Note however that this class of functions encompasses a larger class of functions than the one defined by the Kampé de Fériet function.

The analytic continuation of the Kampé de Fériet function is easily carried out using its Mellin-Barnes representation. In particular, we use here the following results, derived from Mellin-Barnes integrals,

$$\begin{aligned} & F_{0,2}^{2,1} \left( \begin{matrix} a & b & & & \\ - & - & & & \end{matrix} \middle| \begin{matrix} c & - & - & - \\ d & e & f & - \end{matrix} \middle| x, y \right) \\ &= \frac{\Gamma(e)\Gamma(b-a)}{\Gamma(b)\Gamma(e-a)} (-y)^{-a} F_{0,2}^{2,1} \left( \begin{matrix} a & 1+a-e & & & \\ - & - & & & \end{matrix} \middle| \begin{matrix} c & - & - & - \\ d & 1+a-b & f & - \end{matrix} \middle| x, y \right) \\ &= \frac{\Gamma(e)\Gamma(a-b)}{\Gamma(a)\Gamma(e-b)} (-y)^{-b} F_{0,2}^{2,1} \left( \begin{matrix} 1+b-e & b & & & \\ - & - & & & \end{matrix} \middle| \begin{matrix} c & - & - & - \\ d & 1+b-a & f & - \end{matrix} \middle| \frac{x}{y}, \frac{1}{y} \right). \end{aligned} \tag{H.22}$$

$$\begin{aligned} & F_{0,2}^{2,1} \left( \begin{matrix} a & b & & & \\ - & - & & & \end{matrix} \middle| \begin{matrix} c & - & - & - \\ d & e & f & - \end{matrix} \middle| x, y \right) \\ &= \frac{\Gamma(d)\Gamma(f)\Gamma(b-a)\Gamma(c-a)}{\Gamma(b)\Gamma(c)\Gamma(d-a)\Gamma(f-a)} (-x)^{-a} \\ &\quad \times F_{1,1}^{3,0} \left( \begin{matrix} a & 1+a-d & 1+a-f & & \\ - & - & 1+a-c & & \end{matrix} \middle| \begin{matrix} - & - \\ 1+a-b & e \end{matrix} \middle| \frac{1}{x}, \frac{y}{x} \right) \\ &+ \frac{\Gamma(d)\Gamma(f)\Gamma(a-b)\Gamma(c-b)}{\Gamma(a)\Gamma(c)\Gamma(d-b)\Gamma(f-b)} (-x)^{-b} \\ &\quad \times F_{1,1}^{3,0} \left( \begin{matrix} b & 1+b-d & 1+b-f & & \\ - & - & 1+b-c & & \end{matrix} \middle| \begin{matrix} - & - \\ 1+b-a & e \end{matrix} \middle| \frac{1}{x}, \frac{y}{x} \right) \\ &+ \frac{\Gamma(d)\Gamma(f)\Gamma(a-c)\Gamma(b-c)}{\Gamma(a)\Gamma(b)\Gamma(d-c)\Gamma(f-c)} (-x)^{-c} \\ &\quad \times \tilde{F}_{0,0,1}^{2,3,0} \left( \begin{matrix} a-c & b-c & & & \\ - & - & & & \end{matrix} \middle| \begin{matrix} c & 1+c-d & 1+c-f \\ - & - & e \end{matrix} \middle| y, \frac{1}{x} \right), \end{aligned} \tag{H.23}$$

and the  $\tilde{F}$  function can reshuffled into Kampé de Fériet-type series using the algorithm described in the previous paragraph.



## $\mathcal{M}$ functions

In this section we apply the techniques combining the Mellin-Barnes and series representations to study the analytic properties of the  $\mathcal{M}$  functions that appear in the  $\epsilon$ -expansion of the  $F_4$  function, Eq. (11.31). We start by analyzing some general properties of these new transcendental functions, and study more specific properties like analytic continuation and reduction to known functions in subsequent sections. First, it is easy to see that  $\mathcal{M}$  functions are symmetric,

$$\mathcal{M}(\vec{i}, \vec{j}, \vec{k}; x, y) = \mathcal{M}(\vec{j}, \vec{i}, \vec{k}; y, x). \quad (\text{I.1})$$

Second, when one of the arguments is zero, then this function reduces either to 0 or to an  $S$ -sum at infinity. Indeed, if say  $y$  is equal to zero, then only the term  $n = 0$  in the sum contributes, and since  $S_{\vec{i}}(0) = 0$ , we get

- If  $\vec{j} \neq 0$ , then

$$\mathcal{M}(\vec{i}, \vec{j}, \vec{k}; x, 0) = \sum_{m=0}^{\infty} \binom{m}{0}^2 x^m S_{\vec{i}}(m) S_{\vec{j}}(0) S_{\vec{k}}(m) = 0. \quad (\text{I.2})$$

- If  $\vec{j} = 0$ , then

$$\mathcal{M}(\vec{i}, 0, \vec{k}; x, 0) = \sum_{m=0}^{\infty} \binom{m}{0}^2 x^m S_{\vec{i}}(m) S_{\vec{k}}(m) = \sum_{m=0}^{\infty} x^m S_{\vec{i}}(m) S_{\vec{k}}(m). \quad (\text{I.3})$$

The product of nested harmonic sums can now be reduced using their algebra, and so we get

$$\mathcal{M}(\vec{i}, 0, \vec{k}; x, 0) = \sum_{\ell} S(\infty; 0, \vec{i}_{\ell}; x, 1, \dots, 1). \quad (\text{I.4})$$

where the  $S$ -sums are defined recursively in a similar way as the nested harmonic numbers, [75]

$$S(N; \vec{i}; \vec{x}) = \sum_{k=1}^N \frac{x_1^k}{k^{i_1}} S(k; \vec{i}'; \vec{x}'), \quad (\text{I.5})$$

and the values of the  $S$ -sums for  $N = \infty$  are related to Goncharov's multiple polylogarithm.

We now analyze the analytic continuation of some of these functions under the transformation  $y \rightarrow 1/y$ . Due to the symmetry property (I.1) the analytic continuation in  $x$  follows the same lines. For  $k \geq 1$  we have,

$$\begin{aligned} \psi(1+n) &= -\gamma_E + S_1(n), \\ \psi^{(k)}(1+n) &= (-1)^{k+1} k! (\zeta_{k+1} - S_{k+1}(n)), \end{aligned} \quad (\text{I.6})$$

where  $\psi^{(k)}$  denote the polygamma functions

$$\psi^{(k)}(z) = \left( \frac{d}{dz} \right)^{k+1} \ln \Gamma(z). \quad (\text{I.7})$$

We can easily relate the function  $\mathcal{M}$  to Mellin-Barnes integrals of the form

$$\begin{aligned} \frac{1}{(2\pi i)^2} \int_{-i\infty}^{+i\infty} dz_1 dz_2 \Gamma(-z_1) \Gamma(-z_2) \frac{\Gamma(1+z_1+z_2)^2}{\Gamma(1+z_1)\Gamma(1+z_2)} \\ \times (-x)^{z_1} (-y)^{z_2} \Psi(z_1, z_2), \end{aligned} \quad (\text{I.8})$$

where  $\Psi(z_1, z_2)$  denotes any product of polygamma functions with arguments  $1+z_1$ ,  $1+z_2$  or  $1+z_1+z_2$ . For example we can write

$$\begin{aligned} \frac{1}{(2\pi i)^2} \int_{-i\infty}^{+i\infty} dz_1 dz_2 \Gamma(-z_1) \Gamma(-z_2) \frac{\Gamma(1+z_1+z_2)^2}{\Gamma(1+z_1)\Gamma(1+z_2)} \psi(1+z_1) \\ \times (-x)^{z_1} (-y)^{z_2} \\ = \mathcal{M}(1, 0, 0; x, y) - \gamma_E \mathcal{M}(0, 0, 0; x, y). \end{aligned} \quad (\text{I.9})$$

It follows then that studying the analytic continuation properties of certain classes of  $\mathcal{M}$ -functions is equivalent to study the properties of the Mellin-Barnes

integral (I.8). If both  $x$  and  $y$  are smaller than 1, then we close both contours to the right, and we take residues, and we find the series definition of the  $\mathcal{M}$ -functions.

$$\begin{aligned}
 \mathcal{M}(0, 0, 0; x, y) &= -\frac{1}{y} \mathcal{M}\left(0, 0, 0; \frac{x}{y}, \frac{1}{y}\right), \\
 \mathcal{M}(1, 0, 0; x, y) &= -\frac{1}{y} \mathcal{M}\left(1, 0, 0; \frac{x}{y}, \frac{1}{y}\right), \\
 \mathcal{M}(0, 1, 0; x, y) &= \frac{2}{y} \mathcal{M}\left(0, 1, 0; \frac{x}{y}, \frac{1}{y}\right) - \frac{3}{y} \mathcal{M}\left(0, 0, 1; \frac{x}{y}, \frac{1}{y}\right) \\
 &\quad + \frac{\ln(-y)}{y} \mathcal{M}\left(0, 0, 0; \frac{x}{y}, \frac{1}{y}\right), \\
 \mathcal{M}(0, 0, 1; x, y) &= \frac{1}{y} \mathcal{M}\left(0, 1, 0; \frac{x}{y}, \frac{1}{y}\right) - \frac{2}{y} \mathcal{M}\left(0, 0, 1; \frac{x}{y}, \frac{1}{y}\right) \\
 &\quad + \frac{\ln(-y)}{y} \mathcal{M}\left(0, 0, 0; \frac{x}{y}, \frac{1}{y}\right).
 \end{aligned} \tag{I.10}$$

Note the appearance of  $\ln(-y)$ , which produces an imaginary part for  $y > 0$ .

In some cases it is possible to express the  $\mathcal{M}$ -functions in terms of known functions. This becomes possible by relating those functions back to simple cases of the expansion of the Appell  $F_4$  function, in which cases we can apply the reduction formulae (H.11) given in Appendix H. As an example, let us consider the reduction formulas

$$F_4\left(\alpha, \beta, \alpha, \beta; \frac{-\tilde{x}}{(1-\tilde{x})(1-\tilde{y})}, \frac{-\tilde{y}}{(1-\tilde{x})(1-\tilde{y})}\right) = \frac{(1-\tilde{x})^\alpha(1-\tilde{y})^\beta}{1-\tilde{x}\tilde{y}}, \tag{I.11}$$

where  $\tilde{x}$  and  $\tilde{y}$  are solutions of

$$x = \frac{-\tilde{x}}{(1-\tilde{x})(1-\tilde{y})}, \quad y = \frac{-\tilde{y}}{(1-\tilde{x})(1-\tilde{y})}. \tag{I.12}$$

Solving this system we arrive at

$$\tilde{x} = \frac{1}{2y} \left(x + y - 1 + \sqrt{\lambda(1, x, y)}\right), \quad \tilde{y} = \frac{1}{2x} \left(x + y - 1 + \sqrt{\lambda(1, x, y)}\right). \tag{I.13}$$

From this we can immediately read of the  $\mathcal{M}$ -function of weight 0,

$$\mathcal{M}(0, 0, 0; x, y) = F_4(1, 1, 1, 1; x, y) = \frac{(1-\tilde{x})(1-\tilde{y})}{1-\tilde{x}\tilde{y}}. \tag{I.14}$$

Using Eq. (11.27), we can easily obtain all the  $\mathcal{M}$ -functions of weight 1, *e.g.*

$$\begin{aligned}\mathcal{M}(1, 0, 0; x, y) &= \frac{\partial}{\partial \epsilon} F_4(1 + \epsilon, 1, 1, 1; x, y)|_{\epsilon=0} \\ &= \frac{\partial}{\partial \epsilon} [(1 - \tilde{x})^{1+\epsilon}(1 - \tilde{y})^{1+\epsilon} {}_2F_1(1 + \epsilon, 1 + \epsilon, 1; \tilde{x}\tilde{y})]|_{\epsilon=0} \quad (\text{I.15}) \\ &= \frac{(1 - \tilde{x})(1 - \tilde{y})}{1 - \tilde{x}\tilde{y}} (\ln(1 - \tilde{x}) + \ln(1 - \tilde{y}) - 2\ln(1 - \tilde{x}\tilde{y})).\end{aligned}$$

Similarly one can obtain

$$\begin{aligned}\mathcal{M}(0, 1, 0; x, y) &= \frac{(1 - \tilde{x})(1 - \tilde{y})}{1 - \tilde{x}\tilde{y}} (\ln(1 - \tilde{x}) - 2\ln(1 - \tilde{x}\tilde{y})), \\ \mathcal{M}(0, 0, 1; x, y) &= \frac{(1 - \tilde{x})(1 - \tilde{y})}{1 - \tilde{x}\tilde{y}} (\ln(1 - \tilde{y}) - 2\ln(1 - \tilde{x}\tilde{y})).\end{aligned} \quad (\text{I.16})$$

Note however that starting from weight 2 we cannot obtain a reduction in this way in all cases, since from Eq. (11.27) we see that by expanding Pochhammer symbols in the denominator we only produce  $S_{11}(n)$ , so we cannot obtain  $S_2(n) = S_{11}(n) - Z_{11}(n)$ , which needs the contribution from a Pochhammer symbol in the numerator. This however cannot be achieved by the Appell  $F_4$  function, and we have to consider more general functions, like the Kampé de Fériet functions. In the particular situation however where the  $\mathcal{M}$  function can be related to an Appell  $F_4$  function, we can sum up the series. For functions of weight 2 we can sum up all the series except for  $\mathcal{M}(2, 0, 0; x, y)$  (and the related function  $\mathcal{M}(0, 2, 0; x, y) = \mathcal{M}(2, 0, 0; y, x)$ ).

$$\begin{aligned}\mathcal{M}((1, 1), 0, 0; x, y) &= \frac{(1 - \tilde{x})(1 - \tilde{y})}{1 - \tilde{x}\tilde{y}} \left( \frac{(\tilde{x} - 2)\text{Li}(\tilde{x}\tilde{y})}{2(\tilde{x} - 1)} + \frac{\tilde{x} \log^2(1 - \tilde{y})}{4 - 4\tilde{x}} \right. \\ &\quad \left. - \log(1 - \tilde{x}) \log(1 - \tilde{y}) + \log(1 - \tilde{x}) \log(1 - \tilde{x}\tilde{y}) + \frac{\tilde{x} \log(1 - \tilde{y}) \log(1 - \tilde{x}\tilde{y})}{\tilde{x} - 1} \right. \\ &\quad \left. + \frac{\log^2(1 - \tilde{x}\tilde{y})}{1 - \tilde{x}} - \frac{3}{4} \log^2(1 - \tilde{x}) \right), \\ \mathcal{M}(0, (1, 1), 0; x, y) &= \mathcal{M}((1, 1), 0, 0; y, x),\end{aligned} \quad (\text{I.17})$$



$$\begin{aligned}
\mathcal{M}(0, 0, (1, 1); x, y) &= \frac{(1 - \tilde{x})(1 - \tilde{y})}{1 - \tilde{x}\tilde{y}} \left( -\frac{(\tilde{x} + \tilde{y} - 2)\text{Li}(\tilde{x}\tilde{y})}{2(\tilde{x} - 1)(\tilde{y} - 1)} \right. \\
&\quad + \frac{(3 - 4\tilde{x})\log^2(1 - \tilde{y})}{4(\tilde{x} - 1)} + \frac{(1 - \tilde{x}\tilde{y})\log^2(1 - \tilde{x}\tilde{y})}{(\tilde{x} - 1)(\tilde{y} - 1)} - \frac{3}{2}\log(1 - \tilde{x})\log(1 - \tilde{y}) \\
&\quad + \frac{(2\tilde{y} - 1)\log(1 - \tilde{x})\log(1 - \tilde{x}\tilde{y})}{\tilde{y} - 1} + \frac{(2\tilde{x} - 1)\log(1 - \tilde{y})\log(1 - \tilde{x}\tilde{y})}{\tilde{x} - 1} \\
&\quad \left. + \frac{(3 - 4\tilde{y})\log^2(1 - \tilde{x})}{4(\tilde{y} - 1)} \right), \\
\mathcal{M}(1, 1, 0; x, y) &= \frac{(1 - \tilde{x})(1 - \tilde{y})}{1 - \tilde{x}\tilde{y}} \left( 2\log^2(1 - \tilde{x}\tilde{y}) - \log(1 - \tilde{x})\log(1 - \tilde{x}\tilde{y}) \right. \\
&\quad \left. + \frac{3\text{Li}(\tilde{x}\tilde{y})}{2} + \log(1 - \tilde{y})\log(1 - \tilde{x}\tilde{y}) + \frac{1}{2}\log(1 - \tilde{x})\log(1 - \tilde{y}) \right), \\
\mathcal{M}(1, 0, 1; x, y) &= \frac{(1 - \tilde{x})(1 - \tilde{y})}{1 - \tilde{x}\tilde{y}} \left( \frac{(2\tilde{x} - 3)\text{Li}(\tilde{x}\tilde{y})}{2(\tilde{x} - 1)} + \frac{\tilde{x}\log^2(1 - \tilde{y})}{4 - 4\tilde{x}} \right. \\
&\quad - \frac{1}{2}\log(1 - \tilde{x})\log(1 - \tilde{y}) + \frac{\log(1 - \tilde{y})\log(1 - \tilde{x}\tilde{y})}{\tilde{x} - 1} - \frac{1}{2}\log^2(1 - \tilde{x}) \\
&\quad \left. + \frac{(\tilde{x} - 2)\log^2(1 - \tilde{x}\tilde{y})}{\tilde{x} - 1} \right), \\
\mathcal{M}(0, 1, 1; x, y) &= \mathcal{M}(1, 0, 1; y, x), \\
\mathcal{M}(0, 0, 2; x, y) &= \frac{(1 - \tilde{x})(1 - \tilde{y})}{1 - \tilde{x}\tilde{y}} \left( -\frac{(\tilde{x}\tilde{y} - 1)\text{Li}(\tilde{x}\tilde{y})}{2(\tilde{x} - 1)(\tilde{y} - 1)} + \frac{(4 - 5\tilde{y})\log^2(1 - \tilde{x})}{4(\tilde{y} - 1)} \right. \\
&\quad + \frac{(4 - 5\tilde{x})\log^2(1 - \tilde{y})}{4(\tilde{x} - 1)} + \frac{(-2\tilde{x}\tilde{y} + \tilde{x} + \tilde{y})\log^2(1 - \tilde{x}\tilde{y})}{(\tilde{x} - 1)(\tilde{y} - 1)} \\
&\quad + \frac{(3\tilde{y} - 2)\log(1 - \tilde{x})\log(1 - \tilde{x}\tilde{y})}{\tilde{y} - 1} + \frac{(3\tilde{x} - 2)\log(1 - \tilde{y})\log(1 - \tilde{x}\tilde{y})}{\tilde{x} - 1} \\
&\quad \left. - 2\log(1 - \tilde{x})\log(1 - \tilde{y}) \right).
\end{aligned}$$

(I.18)



# Appendix J

## Real-virtual integrals

In this appendix we give the details on the computation of 26 real virtual integrals for the NNLO subtraction scheme presented in Chapter 6. We start with the soft collinear integral,

$$\begin{aligned} \mathcal{K}(\epsilon; y_0, d'_0; \kappa) &= 2 \int_0^{y_0} dy \int_0^1 d\xi y^{-1-2(1+\kappa)\epsilon} (1-y)^{d'_0-1} \xi^{-\epsilon} \\ &\times (1-\xi)^{-1-(1+\kappa)\epsilon} (1-y\xi)^{1+\kappa\epsilon}, \end{aligned} \quad (\text{J.1})$$

and then we turn to the collinear integrals, which have the form

$$\begin{aligned} \mathcal{I}(x; \epsilon, \alpha_0, d_0; \kappa, k, \delta, g_I^{(\pm)}) &= x \int_0^{\alpha_0} d\alpha \alpha^{-1-(1+\kappa)\epsilon} (1-\alpha)^{2d_0-1} [\alpha + (1-\alpha)x]^{-1-(1+\kappa)\epsilon} \\ &\times \int_0^1 dv [v(1-v)]^{-\epsilon} \left( \frac{\alpha + (1-\alpha)xv}{2\alpha + (1-\alpha)x} \right)^{k+\delta\epsilon} g_I^{(\pm)} \left( \frac{\alpha + (1-\alpha)xv}{2\alpha + (1-\alpha)x} \right), \end{aligned} \quad (\text{J.2})$$

with  $\kappa = 0, 1$ ,  $k = -1, 0, 1, 2$  and  $\delta$  defined in Table J.1. We will explicitly evaluate this integral for  $I = A$  and  $I = B$  in Section J.2.

### J.1 The soft-collinear integral $\mathcal{K}$

In this section we calculate analytically the soft-collinear integral defined in Eq. (J.1) for  $\kappa = 0, 1$  and  $d'_0 = D'_0 + d'_1\epsilon$ ,  $D'_0$  being an integer.

$\delta$	Function	$g_I^{(\pm)}(z; \epsilon)$
0	$g_A$	1
$\mp 1$	$g_B^{(\pm)}$	$(1-z)^{\pm\epsilon}$
0	$g_C^{(\pm)}$	$(1-z)^{\pm\epsilon} {}_2F_1(\pm\epsilon, \pm\epsilon, 1 \pm \epsilon, z)$
$\pm 1$	$g_D^{(\pm)}$	${}_2F_1(\pm\epsilon, \pm\epsilon, 1 \pm \epsilon, 1-z)$

Table J.1: The values of  $\delta$  and  $g_I^{(\pm)}(z_r)$  at which Eq. (J.2) needs to be evaluated.

### J.1.1 Analytic result for $\kappa = 0$

For  $\kappa = 0$ , the integral decouples into a product of two one-dimensional integrals and we get

$$\mathcal{K}(\epsilon; y_0, d'_0; 0) = 2 B_{y_0}(-2\epsilon, d'_0) B(1-\epsilon, -\epsilon) - 2 B_{y_0}(1-2\epsilon, d'_0) B(2-\epsilon, -\epsilon), \quad (\text{J.3})$$

Using the expansion of the incomplete  $B$ -function, carried out in Section 6.3, we can immediately write down the expansion of  $\mathcal{K}$  for  $\kappa = 0$ . The result for  $D'_0 = 3$  can be found in Ref. [69].

### J.1.2 Analytic result for $\kappa = 1$

The integral (J.1) for  $\kappa = 1$  reads

$$\mathcal{K}(\epsilon; y_0, d'_0; 1) = 2 \int_0^{y_0} dy \int_0^1 d\xi y^{-1-4\epsilon} (1-y)^{d'_0-1} \xi^{-\epsilon} (1-\xi)^{-1-2\epsilon} (1-y\xi)^{1+\epsilon}. \quad (\text{J.4})$$

The analytic solution for this integral cannot be obtained in a straightforward way, due to the presence of the factor  $(1-y\xi)^\epsilon$  that couples the two integrals. Therefore, we rewrite the integral in the form

$$\mathcal{K}(\epsilon; y_0, d'_0; 1) = 2 y_0^{-4\epsilon} K(\epsilon; y_0, d'_1; 1, 1 - D'_0, 0, 1, -1), \quad (\text{J.5})$$

where

$$\begin{aligned} & K(\epsilon; y_0, d'_1; n_1, n_2, n_3, n_4, n_5) \\ &= \int_0^1 dy \int_0^1 d\xi y^{-n_1-4\epsilon} (1-y_0y)^{-n_2-d'_1\epsilon} \xi^{-n_3-\epsilon} (1-\xi)^{-n_4-2\epsilon} \\ & \quad \times (1-y_0y\xi)^{-n_5+\epsilon}. \end{aligned} \quad (\text{J.6})$$

We now calculate the integral  $K$  using the Laporta algorithm. The independent integrals can be obtained by partial fractioning in  $y$  and  $\xi$ , using the prescription that denominators depending on both integration variables are only partial fractioned in  $\xi$ , *e.g.*

$$\begin{aligned} \frac{1}{\xi(1-y_0y\xi)} &\rightarrow \frac{1}{\xi} + \frac{y_0y}{1-y_0y\xi}, \\ \frac{1}{y(1-y_0y\xi)} &\rightarrow \frac{1}{y(1-y_0y\xi)}. \end{aligned} \quad (\text{J.7})$$

When writing down the integration-by-parts identities for the independent integrals, we have to take into account a surface term coming from the fact that the denominator in  $(1-y_0y)$  does not vanish in  $y=1$ ,

$$\begin{aligned} & \int_0^1 dy \int_0^1 d\xi \frac{\partial}{\partial \xi} \left( y^{-n_1-4\epsilon} (1-y_0y)^{-n_2-d'_1\epsilon} \xi^{-n_3-\epsilon} (1-\xi)^{-n_4-2\epsilon} \right. \\ & \quad \left. \times (1-y_0y\xi)^{-n_5+\epsilon} \right) = 0 \\ & \int_0^1 dy \int_0^1 d\xi \frac{\partial}{\partial y} \left( y^{-n_1-4\epsilon} (1-y_0y)^{-n_2-d'_1\epsilon} \xi^{-n_3-\epsilon} (1-\xi)^{-n_4-2\epsilon} \right. \\ & \quad \left. \times (1-y_0y\xi)^{-n_5+\epsilon} \right) = (1-y_0)^{-n_3-d'_1\epsilon} K_S(\epsilon; y_0, d'_1; n_3, n_4, n_5), \end{aligned} \quad (\text{J.8})$$

with

$$K_S(\epsilon; y_0, d'_1; n_3, n_4, n_5) = \int_0^1 d\xi \xi^{-n_3-\epsilon} (1-\xi)^{-n_4-2\epsilon} (1-y_0\xi)^{-n_5+\epsilon}. \quad (\text{J.9})$$

$K_S$  is just a hypergeometric function,

$$\begin{aligned} & K_S(\epsilon; y_0, d'_1; n_3, n_4, n_5) \\ &= B(1-n_3-\epsilon, 1-n_4-\epsilon) {}_2F_1(1-n_3-\epsilon, n_5-2\epsilon, 2-n_2-n_4-3\epsilon; y_0), \end{aligned} \quad (\text{J.10})$$

and can thus be calculated using the technique presented in Section 6.3.

Knowing the series expansion for the surface term  $K_S$ , we can solve the IBP identities for the  $K$  integrals, Eq. (J.8). We find the following two master integrals,

$$\begin{aligned} K^{(1)}(\epsilon; y_0, d'_1) &= K(\epsilon; y_0, d'_1; 0, 0, 0, 0, 0), \\ K^{(2)}(\epsilon; y_0, d'_1) &= K(\epsilon; y_0, d'_1; -1, 0, 0, 0, 0), \end{aligned} \quad (\text{J.11})$$

fulfilling the following differential equations,

$$\begin{aligned} \frac{\partial}{\partial y_0} K^{(1)} &= \frac{4\epsilon - 1}{y_0} K^{(1)} + \frac{(1 - y_0)^{d'_1 \epsilon}}{y_0} f^{(1)}, \\ \frac{\partial}{\partial y_0} K^{(2)} &= 2 \frac{2\epsilon - 1}{y_0} K^{(2)} + \frac{(1 - y_0)^{d'_1 \epsilon}}{y_0} f^{(1)}, \end{aligned} \quad (\text{J.12})$$

where  $f^{(1)}$  denotes the master integral of the hypergeometric function calculated in Section 6.3 and where the initial conditions are given by

$$\begin{aligned} K^{(1)}(\epsilon; y_0 = 0, d'_1) &= B(1 - 4\epsilon, 1) B(1 - \epsilon, 1 - 2\epsilon), \\ K^{(2)}(\epsilon; y_0 = 0, d'_1) &= B(2 - 4\epsilon, 1) B(1 - \epsilon, 1 - 2\epsilon). \end{aligned} \quad (\text{J.13})$$

Plugging in the series expansion of  $f^{(1)}$  and expanding  $(1 - y_0)^{d'_1 \epsilon}$  into a power series in  $\epsilon$ , we can solve for the  $K^{(1)}$  and  $K^{(2)}$  as a power series in  $\epsilon$  whose coefficients are written in terms of *HPL*'s in  $y_0$ .

Knowing the series expansions of  $K^{(1)}$  and  $K^{(2)}$ , we can obtain the integral  $\mathcal{K}(\epsilon; y_0, d'_0; 1)$  for any fixed integer  $D'_0$ . The result for  $D'_0 = 3$  can be found in Ref. [69].

## J.2 The collinear integrals $\mathcal{I}$

In this section, we calculate the collinear integrals defined in Eq. (J.2) for  $g_I = g_A$  and  $g_I = g_B$  analytically.

### J.2.1 The $\mathcal{A}$ -type collinear integrals for $k \geq 0$

The collinear integral for  $g_I = g_A$  requires the evaluation of an integral of the form

$$\begin{aligned} \mathcal{A}(x, \epsilon; \alpha_0, d_0; \kappa, k) &= \frac{1}{x} \mathcal{I}(x, \epsilon; \alpha_0, d_0; \kappa, k, 0, g_A) \\ &= \int_0^{\alpha_0} d\alpha \int_0^1 dv \alpha^{-1-(1+\kappa)\epsilon} (1-\alpha)^{2d_0-1} [\alpha + (1-\alpha)x]^{-1-(1+\kappa)\epsilon} \\ &\quad \times v^{-\epsilon} (1-v)^{-\epsilon} \left( \frac{\alpha + (1-\alpha)xv}{2\alpha + (1-\alpha)x} \right)^k, \end{aligned} \tag{J.14}$$

where  $k = -1, 0, 1, 2$ ,  $\kappa = 0, 1$  and  $d_0 = D_0 + d_1\epsilon$  with  $D_0$  an integer. For  $k \geq 0$  this two-dimensional integral decouples into the product of two one-dimensional integrals, out of which one is straightforward,

$$\mathcal{A}(x, \epsilon; \alpha_0, d_0; \kappa, k) = \sum_{j=0}^k \binom{k}{j} x^j B(1+j-\epsilon, 1-\epsilon) \tag{J.15}$$

$$\begin{aligned} &\times \int_0^{\alpha_0} d\alpha \alpha^{k-j-1-(1+\kappa)\epsilon} (1-\alpha)^{j+2d_0-1} [\alpha + (1-\alpha)x]^{-1-(1+\kappa)\epsilon} \\ &\times [2\alpha + (1-\alpha)x]^{-k}. \end{aligned} \tag{J.16}$$

We will therefore treat separately the cases  $k \geq 0$  and  $k < 0$ .

For  $k \geq 0$  the calculation of the  $\mathcal{A}$  integrals reduces to the calculation of a one-dimensional integral of the form

$$\begin{aligned} A_+(x, \epsilon; \alpha_0, d_1; \kappa; n_1, n_2, n_3, n_4) &= \int_0^{\alpha_0} d\alpha \alpha^{-n_1-(1+\kappa)\epsilon} (1-\alpha)^{-n_2+2d_1\epsilon} [\alpha + (1-\alpha)x]^{-n_3-(1+\kappa)\epsilon} \\ &\times [2\alpha + (1-\alpha)x]^{-n_4}, \end{aligned} \tag{J.17}$$

$n_i$  being integers. The integration-by-parts identities, including a surface term for the independent integrals, are

$$\begin{aligned} &\int_0^{\alpha_0} d\alpha \frac{\partial}{\partial \alpha} \left( \alpha^{-n_1-(1+\kappa)\epsilon} (1-\alpha)^{-n_2+2d_1\epsilon} [\alpha + (1-\alpha)x]^{-n_3-(1+\kappa)\epsilon} \right. \\ &\quad \left. \times [2\alpha + (1-\alpha)x]^{-n_4} \right) \\ &= \alpha_0^{-n_1-(1+\kappa)\epsilon} (1-\alpha_0)^{-n_2+2d_1\epsilon} [\alpha_0 + (1-\alpha_0)x]^{-n_3-(1+\kappa)\epsilon} \\ &\quad \times [2\alpha_0 + (1-\alpha_0)x]^{-n_4}. \end{aligned} \tag{J.18}$$

Using the Laporta algorithm we find three master integrals for  $A_+$ ,

$$\begin{aligned} A_+^{(1)}(x, \epsilon; \alpha_0, d_1; \kappa) &= A_+(x, \epsilon; \alpha_0, d_1; \kappa; 0, 0, 0, 0) = \int_0^{\alpha_0} d\mu_\epsilon(\alpha; x), \\ A_+^{(2)}(x, \epsilon; \alpha_0, d_1; \kappa) &= A_+(x, \epsilon; \alpha_0, d_1; \kappa; -1, 0, 0, 0) = \int_0^{\alpha_0} d\mu_\epsilon(\alpha; x) \alpha, \\ A_+^{(3)}(x, \epsilon; \alpha_0, d_1; \kappa) &= A_+(x, \epsilon; \alpha_0, d_1; \kappa; 0, 0, 0, 1) = \int_0^{\alpha_0} \frac{d\mu_\epsilon(\alpha; x)}{2\alpha + (1-\alpha)x}. \end{aligned} \quad (\text{J.19})$$

where

$$\begin{aligned} d\mu_\epsilon(\alpha, x) &= d\alpha \alpha^{-(1+\kappa)\epsilon} (1-\alpha)^{2d_1\epsilon} (\alpha + (1-\alpha)x)^{-(1+\kappa)\epsilon}, \\ &= d\alpha + \epsilon d\alpha (2d_1 \ln(1-\alpha) - (1+\kappa) \ln \alpha - (1+\kappa) \ln(\alpha + x - \alpha x)) \\ &\quad + \mathcal{O}(\epsilon^2), \\ &= d\alpha + \epsilon d\alpha (-(1+\kappa)H(0; \alpha) - (1+\kappa)H(0; x) - 2d_1H(1; \alpha) \\ &\quad - (\kappa+1)H(d_1(x); \alpha)) + \mathcal{O}(\epsilon^2). \end{aligned} \quad (\text{J.20})$$

where we used the  $d$ -representation of the two-dimensional  $HPL$ 's defined in Section G.3,

$$\begin{aligned} H(d_1(x); \alpha) &= \ln \left( 1 + \frac{1-x}{x} \alpha \right), \\ H(d_1(x), d_1(x); \alpha) &= \frac{1}{2} \ln^2 \left( 1 + \frac{1-x}{x} \alpha \right), \\ &\text{etc.} \end{aligned} \quad (\text{J.21})$$

Notice that all three master integrals are finite for  $\epsilon = 0$ . This allows us to expand the integrand into a power series in  $\epsilon$  and integrate order by order in  $\epsilon$ , using the defining property of the  $HPL$ 's, Eq. (G.6). We obtain in this way the series expansion of the master integrals as a power series in  $\epsilon$  whose coefficients are written in terms of the  $d$ -representation of the two-dimensional  $HPL$ 's. We can then switch back to the  $c$ -representation using the algorithm described in Section G.3.

Having a representation of the master integrals, we can immediately write down the solutions for  $\mathcal{A}(x, \epsilon; \alpha_0, d_0; \kappa, k)$  for  $k \geq 0$  and fixed  $D_0$  using Eq. (J.15). The results for  $D_0 = 3$  can be found in Ref. [69].



### J.2.2 The $\mathcal{A}$ -type collinear integrals for $k = -1$

For  $k = -1$ , the integral (J.14) does not decouple, so we have to use the Laporta algorithm to calculate the full two-dimensional integral. However, for  $k = -1$ , we can get rid of the denominator in  $(2\alpha + (1 - \alpha)x)$  in the integrand. So we only have to deal with an integral of the form

$$\begin{aligned}
 A_-(x, \epsilon; \alpha_0, d_1; \kappa; n_1, n_2, n_3, n_4, n_5, n_6) &= \\
 &= \int_0^{\alpha_0} d\alpha \int_0^1 dv \alpha^{-n_1-(1+\kappa)\epsilon} (1-\alpha)^{-n_2+2d_1\epsilon} [\alpha + (1-\alpha)x]^{-n_3-(1+\kappa)\epsilon} \\
 &\quad \times v^{-n_4-\epsilon} (1-v)^{-n_5-\epsilon} [\alpha + (1-\alpha)xv]^{-n_6},
 \end{aligned}
 \tag{J.22}$$

$n_i$  being integers.

We write down the integration-by-parts identities for  $A_-$  including a surface term for  $\alpha$ ,

$$\begin{aligned}
 &\int_0^{\alpha_0} d\alpha \int_0^1 dv \frac{\partial}{\partial v} \left( \alpha^{-n_1-(1+\kappa)\epsilon} (1-\alpha)^{-n_2+2d_1\epsilon} [\alpha + (1-\alpha)x]^{-n_3-(1+\kappa)\epsilon} \right. \\
 &\quad \left. \times v^{-n_4-\epsilon} (1-v)^{-n_5-\epsilon} [\alpha + (1-\alpha)xv]^{-n_6} \right) = 0, \\
 &\int_0^{\alpha_0} d\alpha \int_0^1 dv \frac{\partial}{\partial \alpha} \left( \alpha^{-n_1-(1+\kappa)\epsilon} (1-\alpha)^{-n_2+2d_1\epsilon} [\alpha + (1-\alpha)x]^{-n_3-(1+\kappa)\epsilon} \right. \\
 &\quad \left. \times v^{-n_4-\epsilon} (1-v)^{-n_5-\epsilon} [\alpha + (1-\alpha)xv]^{-n_6} \right) \\
 &= \alpha_0^{-n_1-(1+\kappa)\epsilon} (1-\alpha_0)^{-n_2+2d_1\epsilon} [\alpha_0 + (1-\alpha_0)x]^{-n_3-(1+\kappa)\epsilon} \\
 &\quad \times A_{-,S}(x, \epsilon; \alpha_0, d_1; n_4, n_5, n_6),
 \end{aligned}
 \tag{J.23}$$

with

$$\begin{aligned}
 A_{-,S}(x, \epsilon; \alpha_0, d_1; n_4, n_5, n_6) &= \int_0^1 dv v^{-n_4-\epsilon} (1-v)^{-n_5-\epsilon} [\alpha_0 + (1-\alpha_0)xv]^{-n_6} \\
 &= \alpha_0^{-n_6} B(1-n_4-\epsilon, 1-n_5-\epsilon) \\
 &\quad \times {}_2F_1 \left( 1-n_4-\epsilon, n_6, 2-n_4-n_5-2\epsilon; \frac{\alpha_0-1}{\alpha_0} x \right).
 \end{aligned}
 \tag{J.24}$$

As in the case of  $\mathcal{K}$  we are going to evaluate this surface term using the Laporta algorithm, especially to get rid of the strange argument the hypergeometric function depends on and to get an expression for  $A_{-,S}$  in terms of two-dimensional *HPL*'s in  $\alpha_0$  and  $x$ .

**Evaluation of the surface term  $A_{-,S}$ .** Because the  $v$  integration is over the whole range  $[0, 1]$ , we do not have to take into account a surface term in the integration-by-parts identities for  $A_{-,S}$ ,

$$\int_0^1 dv \frac{\partial}{\partial v} (v^{-n_4-\epsilon}(1-v)^{-n_5-\epsilon}[\alpha_0 + (1-\alpha_0)xv]^{-n_6}) = 0. \quad (\text{J.25})$$

Using the Laporta algorithm we see that  $A_{-,S}$  has two master integrals,

$$\begin{aligned} A_{-,S}^{(1)}(x, \epsilon; \alpha_0, d_1) &= A_{-,S}(x, \epsilon; \alpha_0, d_1; 0, 0, 0), \\ A_{-,S}^{(2)}(x, \epsilon; \alpha_0, d_1) &= A_{-,S}(x, \epsilon; \alpha_0, d_1; 0, 0, 1). \end{aligned} \quad (\text{J.26})$$

$A_{-,S}^{(i)}(x, \epsilon; \alpha_0, d_1)$ ,  $i = 1, 2$ , are functions of the two variables  $x$  and  $\alpha_0$  defined on the square  $[0, 1] \times [0, 1]$ , so in principle we should write down a set of partial differential equations for the evolution of both  $\alpha_0$  and  $x$ . However, it is easy to see that in  $x = 0$  we have

$$\begin{aligned} A_{-,S}^{(1)}(x = 0, \epsilon; \alpha_0, d_1) &= B(1 - \epsilon, 1 - \epsilon), \\ A_{-,S}^{(2)}(x = 0, \epsilon; \alpha_0, d_1) &= \frac{1}{\alpha_0} B(1 - \epsilon, 1 - \epsilon), \end{aligned} \quad (\text{J.27})$$

for arbitrary  $\alpha_0$ . So we are in the special situation where we know the solutions on the line  $\{x = 0\} \times [0, 1]$  and so we only need to consider the evolution for the  $x$  variable. In other words, we consider  $A_{-,S}^{(i)}$  as a function of  $x$  only, keeping  $\alpha_0$  as a parameter.

The differential equations for the evolution in the  $x$  variable read

$$\begin{aligned} \frac{\partial}{\partial x} A_{-,S}^{(1)} &= 0, \\ \frac{\partial}{\partial x} A_{-,S}^{(2)} &= A_{-,S}^{(1)} \left( \frac{1-2\epsilon}{\alpha_0 x} + \frac{(\alpha_0-1)(2\epsilon-1)}{\alpha_0(\alpha_0 x - x - \alpha_0)} \right) \\ &\quad + A_{-,S}^{(2)} \left( \frac{2\epsilon-1}{x} - \frac{(\alpha_0-1)\epsilon}{\alpha_0 x - x - \alpha_0} \right), \end{aligned} \quad (\text{J.28})$$

and the initial condition for this system is given by Eq. (J.27). As the system is already triangular, we can immediately solve for  $A_{-,S}^{(1)}$  and  $A_{-,S}^{(2)}$ . Notice

in particular that the denominator in  $(\alpha_0 + x - x\alpha_0)$  will give rise to two-dimensional *HPL*'s of the form  $H(c_1(\alpha_0); x)$ , *etc.*

**Evaluation of  $A_-$ .** Having an expression for the  $\epsilon$ -expansion of the surface term, we can solve the integration-by-parts identities for  $A_-$ , Eq. (J.23). We find four master integrals,

$$\begin{aligned} A_-^{(1)}(x, \epsilon; \alpha_0, d_1; \kappa) &= A_-(x, \epsilon; \alpha_0, d_1; \kappa; 0, 0, 0, 0, 0, 0), \\ A_-^{(2)}(x, \epsilon; \alpha_0, d_1; \kappa) &= A_-(x, \epsilon; \alpha_0, d_1; \kappa; -1, 0, 0, 0, 0, 0), \\ A_-^{(3)}(x, \epsilon; \alpha_0, d_1; \kappa) &= A_-(x, \epsilon; \alpha_0, d_1; \kappa; -1, 0, 0, 0, 0, 1), \\ A_-^{(4)}(x, \epsilon; \alpha_0, d_1; \kappa) &= A_-(x, \epsilon; \alpha_0, d_1; \kappa; -2, 0, 0, 0, 0, 1). \end{aligned} \tag{J.29}$$

It is easy to see that all of the master integrals are finite for  $\epsilon = 0$ .

As in the case of the surface terms, we are only interested in the  $x$  evolution, because the master integrals are known for  $x = 0$  for any value of  $\alpha_0$ ,

$$\begin{aligned} A_-^{(1)}(x = 0, \epsilon; \alpha_0, d_1; \kappa) &= B_{\alpha_0}(1 - 2(1 + \kappa)\epsilon, 1 + 2d_1\epsilon) B(1 - \epsilon, 1 - \epsilon), \\ A_-^{(2)}(x = 0, \epsilon; \alpha_0, d_1; \kappa) &= B_{\alpha_0}(2 - 2(1 + \kappa)\epsilon, 1 + 2d_1\epsilon) B(1 - \epsilon, 1 - \epsilon), \end{aligned} \tag{J.30}$$

and

$$\begin{aligned} A_-^{(3)}(x = 0, \epsilon; \alpha_0, d_1; \kappa) &= A_-^{(1)}(x = 0, \epsilon; \alpha_0, d_1; \kappa), \\ A_-^{(4)}(x = 0, \epsilon; \alpha_0, d_1; \kappa) &= A_-^{(2)}(x = 0, \epsilon; \alpha_0, d_1; \kappa). \end{aligned} \tag{J.31}$$

The master integrals  $A_-^{(1)}$  and  $A_-^{(2)}$  form a subtopology, *i.e.* the differential equations for these two master integrals close under themselves:

$$\begin{aligned} \frac{\partial}{\partial x} A_-^{(1)} &= \frac{1 - 2(1 + \kappa)\epsilon}{x} A_-^{(1)} - \frac{2(d_1\epsilon - (1 + \kappa)\epsilon + 1)}{x} A_-^{(2)} \\ &\quad - \frac{(1 - \alpha_0)^{1+2d_1\epsilon} (-x\alpha_0 + \alpha_0 + x)^{-(1+\kappa)\epsilon} \alpha_0^{1-(1+\kappa)\epsilon}}{x} A_{-,S}^{(1)}, \\ \frac{\partial}{\partial x} A_-^{(2)} &= \frac{1 - (1 + \kappa)\epsilon}{x - 1} A_-^{(1)} + \frac{-2d_1\epsilon + (1 + \kappa)\epsilon - 2}{x - 1} A_-^{(2)} \\ &\quad - \frac{(1 - \alpha_0)^{1+2d_1\epsilon} (-x\alpha_0 + \alpha_0 + x)^{-(1+\kappa)\epsilon} \alpha_0^{1-(1+\kappa)\epsilon}}{x - 1} A_{-,S}^{(1)}. \end{aligned} \tag{J.32}$$

The two equations can be triangularized by the change of variable

$$\begin{aligned} \tilde{A}_-^{(1)} &= A_-^{(1)} - 2A_-^{(2)}, \\ \tilde{A}_-^{(2)} &= A_-^{(2)}. \end{aligned} \tag{J.33}$$

The equations for the subtopology now take the triangularized form

$$\begin{aligned}
\frac{\partial}{\partial x} \tilde{A}_-^{(1)} &= \left( \frac{2\epsilon - 2}{x - 1} + \frac{1 - 2\epsilon}{x} \right) \tilde{A}_-^{(1)} + \left( \frac{4d_1 + 2}{x - 1} - \frac{2d_1 + 2}{x} \right) \epsilon \tilde{A}_-^{(2)} \\
&\quad + (1 - \alpha_0)^{2d_1\epsilon} (-x\alpha_0 + \alpha_0 + x)^{-\epsilon} \alpha_0^{1-\epsilon} \left( \frac{2 - 2\alpha_0}{x - 1} + \frac{\alpha_0 - 1}{x} \right) A_{-,S}^{(1)}, \\
\frac{\partial}{\partial x} \tilde{A}_-^{(2)} &= \frac{1 - \epsilon}{x - 1} \tilde{A}_-^{(1)} - \frac{2d_1 + 1}{x - 1} \epsilon \tilde{A}_-^{(2)} \\
&\quad + (1 - \alpha_0)^{2d_1\epsilon} \alpha_0^{1-\epsilon} (-x\alpha_0 + \alpha_0 + x)^{-\epsilon} \frac{\alpha - 1}{x - 1} A_{-,S}^{(1)}.
\end{aligned} \tag{J.34}$$

The initial condition for  $\tilde{A}_-^{(2)}$  can be obtained from Eq. (J.30). For  $\tilde{A}_-^{(1)}$  however, Eq. (J.30) gives only trivial information. Furthermore, the solution of the differential equation has in general a pole in  $x = 1$ , but it is easy to convince oneself that  $\tilde{A}_-^{(1)}$  is finite in  $x = 1$ , which serves as the initial condition.

We can now solve for the remaining two master integrals. The differential equations for  $A_-^{(3)}$  and  $A_-^{(4)}$  read

$$\begin{aligned}
\frac{\partial}{\partial x} A_-^{(3)} &= \frac{1 - 2(1 + \kappa)\epsilon}{x} A_-^{(3)} - \frac{2(d_1\epsilon - (1 + \kappa)\epsilon + 1)}{x} A_-^{(4)} \\
&\quad - \frac{(1 - \alpha_0)^{2d_1\epsilon} (-x\alpha_0 + \alpha_0 + x)^{-(1+\kappa)\epsilon} \alpha_0^{2-(1+\kappa)\epsilon}}{x} A_{-,S}^{(2)}, \\
\frac{\partial}{\partial x} A_-^{(4)} &= \left( \frac{1 - 2\epsilon}{x} + \frac{2\epsilon - 1}{x - 1} \right) A_-^{(2)} - \frac{(2 + \kappa)\epsilon - 2}{x - 1} A_-^{(3)} \\
&\quad + \left( \frac{2\epsilon - 1}{x} - \frac{(2d_1 + \kappa)\epsilon}{x - 1} \right) A_-^{(4)} \\
&\quad - \frac{(1 - \alpha_0)^{1+2d_1\epsilon} (-x\alpha_0 + \alpha_0 + x)^{-(1+\kappa)\epsilon} \alpha_0^{2-(1+\kappa)\epsilon}}{x - 1} A_{-,S}^{(2)}.
\end{aligned} \tag{J.35}$$

These equations can be brought into a triangularized form via the change of variable

$$\begin{aligned}
\tilde{A}_-^{(3)} &= A_-^{(3)} - A_-^{(4)}, \\
\tilde{A}_-^{(4)} &= A_-^{(4)},
\end{aligned} \tag{J.36}$$

and Eq. (J.35) now reads

$$\begin{aligned}
\frac{\partial}{\partial x} \tilde{A}_-^{(3)} &= \left( \frac{1-2\epsilon}{x} + \frac{2(\epsilon-1)}{x-1} \right) \tilde{A}_-^{(3)} + \left( \frac{2(d_1+1)\epsilon}{x-1} - \frac{2(d_1+1)\epsilon}{x} \right) \tilde{A}_-^{(4)} \\
&\quad - (1-\alpha_0)^{1+2d_1\epsilon} \alpha_0^{2-\epsilon} (-x\alpha_0 + \alpha_0 + x)^{-\epsilon} \left( \frac{1}{x} - \frac{1}{x-1} \right) A_{-,S}^{(2)} \\
&\quad + \left( \frac{1-2\epsilon}{x-1} + \frac{2\epsilon-1}{x} \right) A_-^{(2)}, \\
\frac{\partial}{\partial x} \tilde{A}_-^{(4)} &= \frac{2-2\epsilon}{x-1} \tilde{A}_-^{(3)} + \left( \frac{2\epsilon-1}{x} - \frac{2(d_1\epsilon+\epsilon)}{x-1} \right) \tilde{A}_-^{(4)} \\
&\quad + \left( \frac{1-2\epsilon}{x} + \frac{2\epsilon-1}{x-1} \right) A_-^{(2)} \\
&\quad - \frac{(1-\alpha_0)^{1+2d_1\epsilon} (-x\alpha_0 + \alpha_0 + x)^{-\epsilon} \alpha_0^{2-\epsilon}}{x-1} A_{-,S}^{(2)}.
\end{aligned} \tag{J.37}$$

The initial condition for  $A_-^{(3)}$  and  $A_-^{(4)}$  can again be obtained from Eq. (J.30) and requiring  $A_-^{(3)}$  to be finite in  $x = 1$ .

Having the analytic expressions for the master integrals, we can now easily obtain the solutions for  $\mathcal{A}$  for  $k = -1$  for a fixed value of  $D_0$ . The results for  $D_0 = 3$  can be found in Ref. [69].

In Fig. J.1 we compare the analytic and numeric results for the  $\epsilon^2$  coefficient in the expansion of  $\mathcal{I}(x, \epsilon; \alpha_0, 3-3\epsilon; 1, k, 0, g_A)$  for  $k = -1, 2$  and  $\alpha_0 = 0.1, 1$  as representative examples. The dependence on  $\alpha_0$  is not visible on the plots. The agreement between the two computations is excellent for the whole  $x$ -range. We find a similar agreement for other (lower-order, thus simpler) expansion coefficients and/or other values of the parameters.

### J.2.3 The $\mathcal{B}$ -type collinear integrals

The  $\mathcal{B}$ -type collinear integrals require the evaluation of an integral of the form

$$\begin{aligned}
\mathcal{B}(x, \epsilon; \alpha_0, d_0; \delta, k) &= \frac{1}{x} \mathcal{I}(x, \epsilon; \alpha_0, d_0; 1, k, \delta, g_B) \\
&= \int_0^{\alpha_0} d\alpha \int_0^1 dv \alpha^{-1-2\epsilon} (1-\alpha)^{2d_0-1} v^{-\epsilon} (1-v)^{-\epsilon} [\alpha + (1-\alpha)x]^{-1-2\epsilon} \\
&\quad \times [2\alpha + (1-\alpha)x]^{-k} [\alpha + (1-\alpha)xv]^{k+\delta\epsilon} [\alpha + (1-\alpha)(1-v)x]^{-\delta\epsilon},
\end{aligned}$$

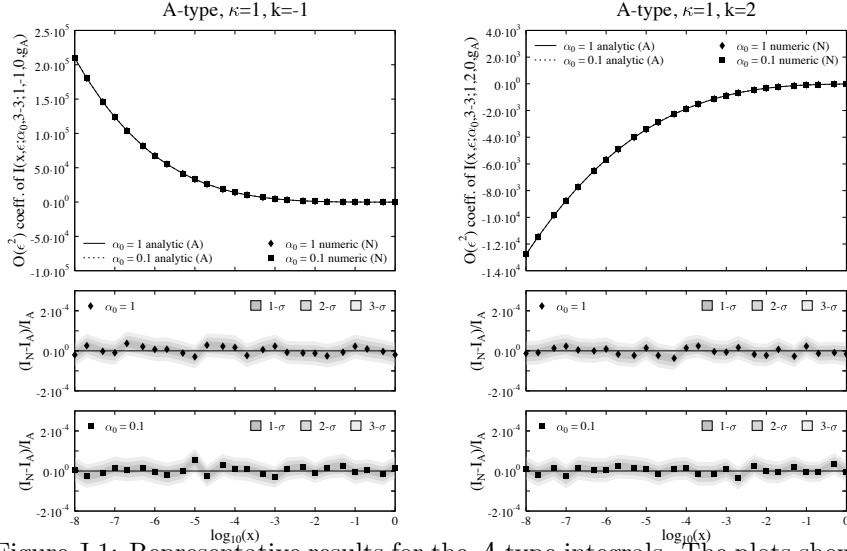


Figure J.1: Representative results for the  $\mathcal{A}$ -type integrals. The plots show the coefficient of the  $\mathcal{O}(\epsilon^2)$  term in  $\mathcal{I}(x, \epsilon; \alpha_0, 3 - 3\epsilon; 1, k, 0, g_A)$  for  $k = -1$  (left figure) and  $k = 2$  (right figure) with  $\alpha_0 = 0.1, 1$ . The plots are taken from Ref. [69].

(J.38)

where  $k = -1, 0, 1, 2$ ,  $\delta = \pm 1$  and  $d_0 = D_0 + d_1\epsilon$  (as before  $D_0$  is an integer). Unlike the  $\mathcal{A}$ -type integrals, the  $\mathcal{B}$ -type integrals do not decouple for  $k \geq 0$ , due to the appearance of the  $\epsilon$  pieces in the exponents, so we have to consider the denominators altogether and have to deal with an integral of the form

$$\begin{aligned}
 B(x, \epsilon; \alpha_0, d_1; \delta; n_1, n_2, n_3, n_4, n_5, n_6, n_7, n_8) &= \\
 &= \int_0^{\alpha_0} d\alpha \int_0^1 dv \alpha^{-n_1-2\epsilon} (1-\alpha)^{-n_2+2d_1} v^{-n_5-\epsilon} (1-v)^{-n_6-\epsilon} \\
 &\times [\alpha + (1-\alpha)x]^{-n_3-2\epsilon} [2\alpha + (1-\alpha)x]^{-n_4} \\
 &\times [\alpha + (1-\alpha)xv]^{-n_7+\delta\epsilon} [\alpha + (1-\alpha)(1-v)x]^{-n_8-\delta\epsilon}.
 \end{aligned}
 \tag{J.39}$$

We use again the Laporta algorithm and write down the integration-by-parts identities for  $B$ ,

$$\begin{aligned}
 & \int_0^{\alpha_0} d\alpha \int_0^1 dv \frac{\partial}{\partial v} (\alpha^{-n_1-2\epsilon}(1-\alpha)^{-n_2+2d_1} v^{-n_5-\epsilon}(1-v)^{-n_6-\epsilon} \\
 & \quad \times [\alpha + (1-\alpha)x]^{-n_3-2\epsilon} [2\alpha + (1-\alpha)x]^{-n_4} \\
 & \quad \times [\alpha + (1-\alpha)xv]^{-n_7+\delta\epsilon} [\alpha + (1-\alpha)(1-v)x]^{-n_8-\delta\epsilon}) \\
 & = 0, \\
 & \int_0^{\alpha_0} d\alpha \int_0^1 dv \frac{\partial}{\partial \alpha} (\alpha^{-n_1-2\epsilon}(1-\alpha)^{-n_2+2d_1} v^{-n_5-\epsilon}(1-v)^{-n_6-\epsilon} \\
 & \quad \times [\alpha + (1-\alpha)x]^{-n_3-2\epsilon} [2\alpha + (1-\alpha)x]^{-n_4} \\
 & \quad \times [\alpha + (1-\alpha)xv]^{-n_7+\delta\epsilon} [\alpha + (1-\alpha)(1-v)x]^{-n_8-\delta\epsilon}) \\
 & = \alpha_0^{-n_1-2\epsilon}(1-\alpha_0)^{-n_2+2d_1} [\alpha_0 + (1-\alpha_0)x]^{-n_3-2\epsilon} [2\alpha_0 + (1-\alpha_0)x]^{-n_4} \\
 & \quad \times B_S(x, \epsilon; \alpha_0, d_1; \delta, k; n_5, n_6, n_7, n_8),
 \end{aligned} \tag{J.40}$$

where the surface term is given by

$$\begin{aligned}
 B_S(x, \epsilon; \alpha_0, d_1; \delta; n_5, n_6, n_7, n_8) & = \\
 & = \int_0^1 dv v^{-n_5-\epsilon}(1-v)^{-n_6-\epsilon} [\alpha_0 + (1-\alpha_0)xv]^{-n_7+\delta\epsilon} \\
 & \quad \times [\alpha_0 + (1-\alpha_0)(1-v)x]^{-n_8-\delta\epsilon}.
 \end{aligned} \tag{J.41}$$

**Evaluation of the surface term  $B_S$ .** The surface term  $B_S$  is no longer a hypergeometric function as it was the case for the  $\mathcal{K}$  and  $\mathcal{A}$ -type integrals. It can nevertheless be easily calculated using the Laporta algorithm. The integration-by-parts identities for  $B_S$  read

$$\begin{aligned}
 & \int_0^1 dv \frac{\partial}{\partial v} (v^{-n_5-\epsilon}(1-v)^{-n_6-\epsilon} [\alpha_0 + (1-\alpha_0)xv]^{-n_7+\delta\epsilon} \\
 & \quad \times [\alpha_0 + (1-\alpha_0)(1-v)x]^{-n_8-\delta\epsilon}) = 0.
 \end{aligned} \tag{J.42}$$

We find three master integrals for  $B_S$ ,

$$\begin{aligned}
 B_S^{(1)}(x, \epsilon; \alpha_0, d_1; \delta) & = B_S(x, \epsilon; \alpha_0, d_1; \delta; 0, 0, 0, 0), \\
 B_S^{(2)}(x, \epsilon; \alpha_0, d_1; \delta) & = B_S(x, \epsilon; \alpha_0, d_1; \delta; -1, 0, 0, 0), \\
 B_S^{(3)}(x, \epsilon; \alpha_0, d_1; \delta) & = B_S(x, \epsilon; \alpha_0, d_1; \delta; 0, 0, 1, 0),
 \end{aligned} \tag{J.43}$$

fulfilling the differential equations

$$\begin{aligned}
\frac{\partial}{\partial x} B_S^{(1)} &= B_S^{(1)} \left( \frac{-2\alpha_0\epsilon^2 + 2\epsilon^2 + 3\alpha_0\delta\epsilon - 3\delta\epsilon - \alpha_0 + 1}{\alpha_0((\alpha_0 - 1)x - \alpha_0)(\epsilon\delta - 1)} \right. \\
&\quad + \frac{2(\epsilon\alpha_0 - \alpha_0 - \epsilon + 1)}{\alpha_0((\alpha_0 - 1)x - 2\alpha_0)} + \frac{-2\delta\epsilon^2 + 2\epsilon^2 - \delta\epsilon + 2\epsilon - 1}{\alpha_0x(\epsilon\delta - 1)} \Big) \\
&\quad + B_S^{(2)} \left( \frac{4(\alpha_0 - 1)(\epsilon - 1)}{\alpha_0((\alpha_0 - 1)x - \alpha_0)} - \frac{4(\alpha_0 - 1)(\epsilon - 1)}{\alpha_0((\alpha_0 - 1)x - 2\alpha_0)} \right) \\
&\quad + B_S^{(3)} \left( \frac{(\alpha_0 - 1)(\delta\epsilon^2 - \epsilon^2 - \epsilon + 1)}{(x\alpha_0 - \alpha_0 - x)(\epsilon\delta - 1)} \right. \\
&\quad + \frac{2\delta\epsilon^2 - 2\epsilon^2 + \delta\epsilon - 2\epsilon + 1}{x(\epsilon\delta - 1)} \\
&\quad \left. - \frac{(\alpha_0 - 1)(2\delta\epsilon^2 - 2\epsilon^2 + \delta\epsilon - 2\epsilon + 1)}{((\alpha_0 - 1)x - \alpha_0)(\epsilon\delta - 1)} \right), \\
\frac{\partial}{\partial x} B_S^{(2)} &= -B_S^{(1)} \frac{(-\delta\epsilon + \epsilon - 1)}{x} + B_S^{(2)} \frac{2(\epsilon - 1)}{x} - B_S^{(3)} \frac{\alpha_0\epsilon\delta}{x}, \\
\frac{\partial}{\partial x} B_S^{(3)} &= B_S^{(1)} \left( \frac{2\delta\epsilon^2 - 2\epsilon^2 + \delta\epsilon - 2\epsilon + 1}{\alpha_0x(1 - \epsilon\delta)} \right. \\
&\quad - \frac{\delta(2\alpha_0\epsilon^2 - 2\epsilon^2 - 2\alpha_0\epsilon - 2\alpha_0\delta\epsilon + 2\delta\epsilon + 2\epsilon + 2\alpha_0\delta - 2\delta)}{\alpha_0((\alpha_0 - 1)x - 2\alpha_0)(1 - \epsilon\delta)} \\
&\quad \left. - \frac{\delta(-2\alpha_0\delta\epsilon^2 + 2\delta\epsilon^2 + 3\alpha_0\epsilon - 3\epsilon - \alpha_0\delta + \delta)}{\alpha_0((\alpha_0 - 1)x - \alpha_0)(1 - \epsilon\delta)} \right) \\
&\quad + B_S^{(2)} \left( \frac{2(\alpha_0 - 1)(\epsilon - 1)(2\epsilon - 2\delta)\delta}{\alpha_0((\alpha_0 - 1)x - 2\alpha_0)(1 - \epsilon\delta)} \right. \\
&\quad \left. - \frac{2(\alpha_0 - 1)(\epsilon - 1)(2\epsilon - 2\delta)\delta}{\alpha_0((\alpha_0 - 1)x - \alpha_0)(1 - \epsilon\delta)} \right) \\
&\quad + B_S^{(3)} \left( \frac{-2\delta\epsilon^2 + 2\epsilon^2 - \delta\epsilon + 2\epsilon - 1}{x(1 - \epsilon\delta)} \right. \\
&\quad - \frac{(\alpha_0 - 1)(-2\delta\epsilon^2 + 2\epsilon^2 - \delta\epsilon + 2\epsilon - 1)}{((\alpha_0 - 1)x - \alpha_0)(1 - \epsilon\delta)} \\
&\quad \left. + \frac{(\alpha_0 - 1)(-\delta\epsilon^2 + \epsilon^2 + \epsilon - 1)}{(x\alpha_0 - \alpha_0 - x)(1 - \epsilon\delta)} \right). \tag{J.44}
\end{aligned}$$



The initial conditions for the differential equations are

$$\begin{aligned} B_S^{(1)}(x=0, \epsilon; \alpha_0, d_1; \delta) &= B(1-\epsilon, 1-\epsilon), \\ B_S^{(2)}(x=0, \epsilon; \alpha_0, d_1; \delta) &= B(2-\epsilon, 1-\epsilon), \\ B_S^{(3)}(x=0, \epsilon; \alpha_0, d_1; \delta) &= \frac{1}{\alpha_0} B(1-\epsilon, 1-\epsilon), \end{aligned} \tag{J.45}$$

The system can be triangularized by the change of variable

$$\tilde{B}_S^{(1)} = B_S^{(1)} - 2B_S^{(2)}, \quad \tilde{B}_S^{(2)} = B_S^{(2)}, \quad \tilde{B}_S^{(3)} = B_S^{(3)}, \tag{J.46}$$

and then solved in the usual way.

**Evaluation of the  $B$  integral.** Solving the integration-by-parts identities for the  $B$  integrals, we find nine master integrals

$$\begin{aligned} B^{(1)}(x, \epsilon; \alpha_0, d_1; \delta) &= B(x, \epsilon; \alpha_0, d_1; \delta; 0, 0, 0, 0, 0, 0, 0, 0), \\ B^{(2)}(x, \epsilon; \alpha_0, d_1; \delta) &= B(x, \epsilon; \alpha_0, d_1; \delta; 0, 0, 0, 0, 0, 0, 0, 1), \\ B^{(3)}(x, \epsilon; \alpha_0, d_1; \delta) &= B(x, \epsilon; \alpha_0, d_1; \delta; 0, 0, 0, 0, 0, 0, 1, 0), \\ B^{(4)}(x, \epsilon; \alpha_0, d_1; \delta) &= B(x, \epsilon; \alpha_0, d_1; \delta; 0, 0, 0, 1, 0, 0, 0, 0), \\ B^{(5)}(x, \epsilon; \alpha_0, d_1; \delta) &= B(x, \epsilon; \alpha_0, d_1; \delta; 0, 0, 1, 0, 0, 0, 0, 0), \\ B^{(6)}(x, \epsilon; \alpha_0, d_1; \delta) &= B(x, \epsilon; \alpha_0, d_1; \delta; -1, 0, 0, 0, 0, 0, 1, 0), \\ B^{(7)}(x, \epsilon; \alpha_0, d_1; \delta) &= B(x, \epsilon; \alpha_0, d_1; \delta; 0, 0, 0, 1, 0, 0, 1, 0), \\ B^{(8)}(x, \epsilon; \alpha_0, d_1; \delta) &= B(x, \epsilon; \alpha_0, d_1; \delta; 0, 0, 1, 0, 0, 0, 1, 0), \\ B^{(9)}(x, \epsilon; \alpha_0, d_1; \delta) &= B(x, \epsilon; \alpha_0, d_1; \delta; 0, 0, 1, 0, 0, 0, 0, 1), \end{aligned} \tag{J.47}$$

The master integrals  $B^{(i)}$ ,  $i \neq 4, 7$ , form a subtopology, *i.e.* the differential equations for these master integrals close under themselves. Furthermore the differential equations for  $B^{(1)}, B^{(3)}, B^{(5)}$  and  $B^{(6)}$  have a triangular structure in  $\epsilon$ , *i.e.* all other master integrals are suppressed by a power of  $\epsilon$ . For  $\delta = +1$ ,

the corresponding differential equations are given by

$$\begin{aligned}
\frac{\partial}{\partial x} B^{(1)} &= \frac{2(\varepsilon - 1)B_S^{(2)}(\alpha_0 - 1)^2}{(2d_1\varepsilon - 4\varepsilon + 1)(x\alpha_0 - \alpha_0 - x)} - \frac{2\varepsilon B^{(1)}}{x - 1} \\
&+ \left( \frac{4\varepsilon^2}{(2d_1\varepsilon - 4\varepsilon + 1)(x - 1)} - \frac{\varepsilon(8\varepsilon - 1)}{(2d_1\varepsilon - 4\varepsilon + 1)x} \right) B^{(2)} \\
&+ \left( \frac{2\varepsilon^2}{(2d_1\varepsilon - 4\varepsilon + 1)(x - 1)} - \frac{\varepsilon(4\varepsilon - 1)}{(2d_1\varepsilon - 4\varepsilon + 1)x} \right) B^{(3)} + \\
&\left( \frac{2\varepsilon}{x - 1} + \frac{2(2\varepsilon - 1)\varepsilon}{(2d_1\varepsilon - 4\varepsilon + 1)x} \right) B^{(5)} - \frac{2\varepsilon B^{(6)}}{x} \\
&- \frac{2\varepsilon^2 B^{(8)}}{(2d_1\varepsilon - 4\varepsilon + 1)(x - 1)} - \frac{4\varepsilon^2 B^{(9)}}{(2d_1\varepsilon - 4\varepsilon + 1)(x - 1)} \\
&+ \left( -\frac{2\varepsilon(\alpha_0 - 1)^2}{(2d_1\varepsilon - 4\varepsilon + 1)((\alpha_0 - 1)x - \alpha_0)} + \right. \\
&\left. \frac{(\alpha_0 - 1)^2}{(2d_1\varepsilon - 4\varepsilon + 1)(x\alpha_0 - \alpha_0 - x)} + \frac{2\varepsilon(\alpha_0 - 1)}{(2d_1\varepsilon - 4\varepsilon + 1)x} \right) B_S^{(1)}, \\
\frac{\partial}{\partial x} B^{(3)} &= -\frac{4\varepsilon B^{(3)}}{x} + \frac{(-2d_1\varepsilon + 4\varepsilon - 1) B^{(6)}}{x} + \frac{(\alpha_0 - 1)\alpha_0 B_S^{(3)}}{x}, \\
\frac{\partial}{\partial x} B^{(5)} &= \left( \frac{-2d_1\varepsilon + 4\varepsilon - 1}{x} + \frac{2d_1\varepsilon - 4\varepsilon + 1}{x - 1} \right) B^{(1)} \\
&+ \left( \frac{-2d_1\varepsilon + 4\varepsilon - 1}{x - 1} - \frac{4\varepsilon}{x} \right) B^{(5)} + \left( \frac{\alpha_0 - 1}{x} - \frac{(\alpha_0 - 1)^2}{(\alpha_0 - 1)x - \alpha_0} \right) B_S^{(1)}, \\
\frac{\partial}{\partial x} B^{(6)} &= \left( \frac{1 - 2\varepsilon}{x} + \frac{2\varepsilon - 1}{x - 1} \right) B^{(1)} + \left( \frac{8\varepsilon^2}{(2d_1\varepsilon - 4\varepsilon + 1)(x - 1)} \right. \\
&- \left. \frac{\varepsilon}{(2d_1\varepsilon - 4\varepsilon + 1)(x - 2)} - \frac{(8\varepsilon - 1)\varepsilon}{(2d_1\varepsilon - 4\varepsilon + 1)x} \right) B^{(2)} \\
&+ \left( -\frac{2\varepsilon}{(x - 1)^2} + \frac{2d_1\varepsilon - 5\varepsilon + 1}{(2d_1\varepsilon - 4\varepsilon + 1)(x - 2)} - \right. \\
&\left. \frac{2(2d_1\varepsilon^2 - 6\varepsilon^2 + \varepsilon)}{(2d_1\varepsilon - 4\varepsilon + 1)(x - 1)} + \frac{\varepsilon - 4\varepsilon^2}{(2d_1\varepsilon - 4\varepsilon + 1)x} \right) B^{(3)} \\
&+ \left( \frac{1 - 2\varepsilon}{x - 1} + \frac{4d_1\varepsilon^2 - 12\varepsilon^2 - 2d_1\varepsilon + 8\varepsilon - 1}{(2d_1\varepsilon - 4\varepsilon + 1)(x - 2)} + \frac{2\varepsilon(2\varepsilon - 1)}{(2d_1\varepsilon - 4\varepsilon + 1)x} \right) B^{(5)} \\
&+ \left( -\frac{2\varepsilon}{x - 1} + \frac{-2d_1\varepsilon + 4\varepsilon - 1}{x - 2} - \frac{1}{x} \right) B^{(6)}
\end{aligned}$$

$$\begin{aligned}
 & + \left( \frac{2\epsilon}{(x-1)^2} - \frac{4(2d_1\epsilon^2 - 5\epsilon^2 + \epsilon)}{(2d_1\epsilon - 4\epsilon + 1)(x-2)} + \frac{4(2d_1\epsilon^2 - 5\epsilon^2 + \epsilon)}{(2d_1\epsilon - 4\epsilon + 1)(x-1)} \right) B^{(8)} \\
 & + \left( \frac{8\epsilon^2}{(2d_1\epsilon - 4\epsilon + 1)(x-2)} - \frac{8\epsilon^2}{(2d_1\epsilon - 4\epsilon + 1)(x-1)} \right) B^{(9)} \\
 & + \left( \frac{4(\alpha_0 - 1)^3(\epsilon - 1)}{(\alpha_0 - 2)(2d_1\epsilon - 4\epsilon + 1)((\alpha_0 - 1)x - \alpha_0)} - \right. \\
 & \left. \frac{4(\alpha_0 - 1)^2(\epsilon - 1)}{(\alpha_0 - 2)(2d_1\epsilon - 4\epsilon + 1)(x-2)} \right) B_S^{(2)} + \\
 & \left( - \frac{2(2\epsilon - 1)(\alpha_0 - 1)^3}{(\alpha_0 - 2)(2d_1\epsilon - 4\epsilon + 1)((\alpha_0 - 1)x - \alpha_0)} + \frac{2\epsilon(\alpha_0 - 1)}{(2d_1\epsilon - 4\epsilon + 1)x} + \right. \\
 & \left. \frac{2(\epsilon\alpha_0^2 - \alpha_0^2 - \epsilon\alpha_0 + 2\alpha_0 - 1)}{(\alpha_0 - 2)(2d_1\epsilon - 4\epsilon + 1)(x-2)} \right) B_S^{(1)} + \frac{(\alpha_0 - 1)\alpha_0 B_S^{(3)}}{x-2},
 \end{aligned} \tag{J.48}$$

whereas for  $\delta = -1$ , the differential equations are

$$\begin{aligned}
 \frac{\partial}{\partial x} B^{(1)} & = \frac{2(\epsilon - 1)B_S^{(2)}(\alpha_0 - 1)^2}{(2d_1\epsilon - 4\epsilon + 1)(x\alpha_0 - \alpha_0 - x)} - \frac{2\epsilon B^{(1)}}{x-1} \\
 & + \left( \frac{\epsilon(4\epsilon - 1)}{(2d_1\epsilon - 4\epsilon + 1)x} - \frac{2\epsilon^2}{(2d_1\epsilon - 4\epsilon + 1)(x-1)} \right) B^{(2)} \\
 & + \left( \frac{\epsilon(8\epsilon - 1)}{(2d_1\epsilon - 4\epsilon + 1)x} - \frac{4\epsilon^2}{(2d_1\epsilon - 4\epsilon + 1)(x-1)} \right) B^{(3)} \\
 & + \left( \frac{2\epsilon}{x-1} - \frac{2\epsilon(2\epsilon - 1)}{(2d_1\epsilon - 4\epsilon + 1)x} \right) B^{(5)} + \frac{2\epsilon B^{(6)}}{x} \\
 & + \frac{4\epsilon^2 B^{(8)}}{(2d_1\epsilon - 4\epsilon + 1)(x-1)} + \frac{2\epsilon^2 B^{(9)}}{(2d_1\epsilon - 4\epsilon + 1)(x-1)} \\
 & + \left( \frac{2\epsilon(\alpha_0 - 1)^2}{(2d_1\epsilon - 4\epsilon + 1)((\alpha_0 - 1)x - \alpha_0)} - \right. \\
 & \left. \frac{(2\epsilon - 1)(\alpha_0 - 1)^2}{(2d_1\epsilon - 4\epsilon + 1)(x\alpha_0 - \alpha_0 - x)} - \frac{2\epsilon(\alpha_0 - 1)}{(2d_1\epsilon - 4\epsilon + 1)x} \right) B_S^{(1)},
 \end{aligned} \tag{J.49}$$

$$\begin{aligned}
\frac{\partial}{\partial x} B^{(3)} &= -\frac{4\epsilon B^{(3)}}{x} + \frac{(-2d_1\epsilon + 4\epsilon - 1) B^{(6)}}{x} + \frac{(\alpha_0 - 1)\alpha_0 B_S^{(3)}}{x}, \\
\frac{\partial}{\partial x} B^{(5)} &= \left( \frac{-2d_1\epsilon + 4\epsilon - 1}{x} + \frac{2d_1\epsilon - 4\epsilon + 1}{x-1} \right) B^{(1)} \\
&\quad + \left( \frac{-2d_1\epsilon + 4\epsilon - 1}{x-1} - \frac{4\epsilon}{x} \right) B^{(5)} \\
&\quad + \left( \frac{\alpha_0 - 1}{x} - \frac{(\alpha_0 - 1)^2}{(\alpha_0 - 1)x - \alpha_0} \right) B_S^{(1)}, \\
\frac{\partial}{\partial x} B^{(6)} &= \left( \frac{1-2\epsilon}{x} + \frac{2\epsilon-1}{x-1} \right) B^{(1)} \\
&\quad + \left( -\frac{4\epsilon^2}{(2d_1\epsilon - 4\epsilon + 1)(x-1)} + \frac{\epsilon}{(2d_1\epsilon - 4\epsilon + 1)(x-2)} \right. \\
&\quad \left. + \frac{(4\epsilon-1)\epsilon}{(2d_1\epsilon - 4\epsilon + 1)x} \right) B^{(2)} \\
&\quad + \left( -\frac{4\epsilon}{(x-1)^2} + \frac{2d_1\epsilon - 3\epsilon + 1}{(2d_1\epsilon - 4\epsilon + 1)(x-2)} \right. \\
&\quad \left. - \frac{4(2d_1\epsilon^2 - 2\epsilon^2 + \epsilon)}{(2d_1\epsilon - 4\epsilon + 1)(x-1)} + \frac{8\epsilon^2 - \epsilon}{(2d_1\epsilon - 4\epsilon + 1)x} \right) B^{(3)} \\
&\quad + \left( \frac{1-2\epsilon}{x-1} + \frac{4d_1\epsilon^2 - 4\epsilon^2 - 2d_1\epsilon + 4\epsilon - 1}{(2d_1\epsilon - 4\epsilon + 1)(x-2)} - \frac{2\epsilon(2\epsilon-1)}{(2d_1\epsilon - 4\epsilon + 1)x} \right) B^{(5)} \\
&\quad + \left( -\frac{4\epsilon}{x-1} + \frac{-2d_1\epsilon + 4\epsilon - 1}{x-2} + \frac{4\epsilon-1}{x} \right) B^{(6)} \\
&\quad + \left( \frac{4\epsilon}{(x-1)^2} - \frac{8(2d_1\epsilon^2 - 3\epsilon^2 + \epsilon)}{(2d_1\epsilon - 4\epsilon + 1)(x-2)} \right. \\
&\quad \left. + \frac{8(2d_1\epsilon^2 - 3\epsilon^2 + \epsilon)}{(2d_1\epsilon - 4\epsilon + 1)(x-1)} \right) B^{(8)} \\
&\quad + \left( \frac{4\epsilon^2}{(2d_1\epsilon - 4\epsilon + 1)(x-1)} - \frac{4\epsilon^2}{(2d_1\epsilon - 4\epsilon + 1)(x-2)} \right) B^{(9)}
\end{aligned} \tag{J.50}$$

$$\begin{aligned}
 & + \left( \frac{4(\alpha_0 - 1)^3(\epsilon - 1)}{(\alpha_0 - 2)(2d_1\epsilon - 4\epsilon + 1)((\alpha_0 - 1)x - \alpha_0)} - \right. \\
 & \left. \frac{4(\alpha_0 - 1)^2(\epsilon - 1)}{(\alpha_0 - 2)(2d_1\epsilon - 4\epsilon + 1)(x - 2)} \right) B_S^{(2)} + \\
 & \left( \frac{2(\alpha_0 - 1)^3}{(\alpha_0 - 2)(2d_1\epsilon - 4\epsilon + 1)((\alpha_0 - 1)x - \alpha_0)} - \frac{2\epsilon(\alpha_0 - 1)}{(2d_1\epsilon - 4\epsilon + 1)x} + \right. \\
 & \left. \frac{2(\epsilon\alpha_0^2 - \alpha_0^2 - 3\epsilon\alpha_0 + 2\alpha_0 + 2\epsilon - 1)}{(\alpha_0 - 2)(2d_1\epsilon - 4\epsilon + 1)(x - 2)} \right) B_S^{(1)} + \frac{(\alpha_0 - 1)\alpha_0 B_S^{(3)}}{x - 2}.
 \end{aligned}$$

The differential equations for  $B^{(2)}$ ,  $B^{(8)}$  and  $B^{(9)}$  read, for  $\delta = +1$ ,

$$\begin{aligned}
 \frac{\partial}{\partial x} B^{(2)} &= \left( \frac{4\epsilon - 1}{x} - \frac{4\epsilon}{x - 1} \right) B^{(2)} + \left( \frac{4\epsilon - 1}{x} - \frac{2\epsilon}{x - 1} \right) B^{(3)} - \frac{2(2\epsilon - 1)B^{(5)}}{x} \\
 &+ \frac{(2d_1\epsilon - 4\epsilon + 1) B^{(6)}}{x} + \frac{2\epsilon B^{(8)}}{x - 1} + \frac{4\epsilon B^{(9)}}{x - 1} - \frac{(\alpha_0 - 1)\alpha_0 B_S^{(3)}}{x}, \\
 \frac{\partial}{\partial x} B^{(8)} &= \left( \frac{2(d_1 - 2)\epsilon}{x - 1} - \frac{2(d_1 - 2)\epsilon}{x} \right) B^{(3)} + \left( \frac{-4\epsilon - 1}{x} - \frac{2(d_1\epsilon - 2\epsilon)}{x - 1} \right) B^{(8)} \\
 &+ \left( \frac{\alpha_0 - 1}{x} - \frac{(\alpha_0 - 1)^2}{(\alpha_0 - 1)x - \alpha_0} \right) B_S^{(3)}, \\
 \frac{\partial}{\partial x} B^{(9)} &= -\frac{2(\epsilon - 1)B_S^{(2)}(\alpha_0 - 1)^2}{\epsilon(x\alpha_0 - \alpha_0 - x)^2} + \left( \frac{2(d_1 - 2)\epsilon}{x - 1} - \frac{2(d_1 - 2)\epsilon}{x} \right) B^{(2)} \\
 &+ \left( \frac{-4\epsilon - 1}{x} - \frac{2(d_1\epsilon - 2\epsilon)}{x - 1} \right) B^{(9)} + \left( -\frac{2(\alpha_0 - 1)^2}{\alpha_0(x\alpha_0 - \alpha_0 - x)} \right. \\
 &+ \left. \frac{2(\alpha_0 - 1)}{\alpha_0 x} + \frac{2\epsilon\alpha_0^2 - \alpha_0^2 - 4\epsilon\alpha_0 + 2\alpha_0 + 2\epsilon - 1}{\epsilon(x\alpha_0 - \alpha_0 - x)^2} \right) B_S^{(1)} \\
 &+ \left( \frac{(\alpha_0 - 1)^2}{(\alpha_0 - 1)x - \alpha_0} + \frac{1 - \alpha_0}{x} \right) B_S^{(3)},
 \end{aligned}$$

(J.51)

and for  $\delta = -1$

$$\begin{aligned}
\frac{\partial}{\partial x} B^{(2)} &= \left( -\frac{2\epsilon}{x-1} - \frac{1}{x} \right) B^{(2)} + \left( \frac{8\epsilon-1}{x} - \frac{4\epsilon}{x-1} \right) B^{(3)} - \frac{2(2\epsilon-1) B^{(5)}}{x} \\
&\quad + \frac{(2d_1\epsilon-4\epsilon+1)B^{(6)}}{x} + \frac{4\epsilon B^{(8)}}{x-1} + \frac{2\epsilon B^{(9)}}{x-1} - \frac{(\alpha_0-1)\alpha_0 B_S^{(3)}}{x}, \\
\frac{\partial}{\partial x} B^{(8)} &= \left( \frac{2(d_1-2)\epsilon}{x-1} - \frac{2(d_1-2)\epsilon}{x} \right) B^{(3)} + \left( \frac{-4\epsilon-1}{x} - \frac{2(d_1\epsilon-2\epsilon)}{x-1} \right) B^{(8)} \\
&\quad + \left( \frac{\alpha_0-1}{x} - \frac{(\alpha_0-1)^2}{(\alpha_0-1)x-\alpha_0} \right) B_S^{(3)}, \\
\frac{\partial}{\partial x} B^{(9)} &= \frac{2(\epsilon-1)B_S^{(2)}(\alpha_0-1)^2}{\epsilon(x\alpha_0-\alpha_0-x)^2} + \left( \frac{2(d_1-2)\epsilon}{x-1} - \frac{2(d_1-2)\epsilon}{x} \right) B^{(2)} + \\
&\quad \left( \frac{-4\epsilon-1}{x} - \frac{2(d_1\epsilon-2\epsilon)}{x-1} \right) B^{(9)} + \left( -\frac{2(\alpha_0-1)^2}{\alpha_0(x\alpha_0-\alpha_0-x)} \right. \\
&\quad \left. + \frac{(\alpha_0-1)^2}{\epsilon(x\alpha_0-\alpha_0-x)^2} + \frac{2(\alpha_0-1)}{\alpha_0 x} \right) B_S^{(1)} \\
&\quad + \left( \frac{(\alpha_0-1)^2}{(\alpha_0-1)x-\alpha_0} + \frac{1-\alpha_0}{x} \right) B_S^{(3)}.
\end{aligned} \tag{J.52}$$

Knowing the solutions for the subtopology, we can solve for the remaining two master integrals  $B^{(4)}$  and  $B^{(7)}$ . They fulfill the following differential equations, for  $\delta = +1$ ,

$$\begin{aligned}
\frac{\partial}{\partial x} B^{(4)} &= \left( \frac{-2d_1\epsilon+4\epsilon-1}{2x} + \frac{2d_1\epsilon-4\epsilon+1}{2(x-2)} \right) B^{(1)} \\
&\quad + \left( \frac{-2d_1\epsilon+4\epsilon-1}{x-2} - \frac{4\epsilon}{x} \right) B^{(4)} \\
&\quad + \left( \frac{\alpha_0-1}{2x} - \frac{(\alpha_0-1)^2}{2((\alpha_0-1)x-2\alpha_0)} \right) B_S^{(1)}, \\
\frac{\partial}{\partial x} B^{(7)} &= \left( \frac{(d_1-2)\epsilon}{x-2} - \frac{(d_1-2)\epsilon}{x} \right) B^{(3)} + \left( \frac{-4\epsilon-1}{x} - \frac{2(d_1\epsilon-2\epsilon)}{x-2} \right) B^{(7)} \\
&\quad + \left( \frac{\alpha_0-1}{2x} - \frac{(\alpha_0-1)^2}{2((\alpha_0-1)x-2\alpha_0)} \right) B_S^{(3)},
\end{aligned} \tag{J.53}$$

whereas for  $\delta = -1$  the differential equations read

$$\begin{aligned} \frac{\partial}{\partial x} B^{(4)} &= \left( \frac{-2d_1\epsilon + 4\epsilon - 1}{2x} + \frac{2d_1\epsilon - 4\epsilon + 1}{2(x-2)} \right) B^{(1)} \\ &+ \left( \frac{-2d_1\epsilon + 4\epsilon - 1}{x-2} - \frac{4\epsilon}{x} \right) B^{(4)} \\ &+ \left( \frac{\alpha_0 - 1}{2x} - \frac{(\alpha_0 - 1)^2}{2((\alpha_0 - 1)x - 2\alpha_0)} \right) B_S^{(1)}, \\ \frac{\partial}{\partial x} B^{(7)} &= \left( \frac{(d_1 - 2)\epsilon}{x-2} - \frac{(d_1 - 2)\epsilon}{x} \right) B^{(3)} + \left( \frac{-4\epsilon - 1}{x} - \frac{2(d_1\epsilon - 2\epsilon)}{x-2} \right) B^{(7)} \\ &+ \left( \frac{\alpha_0 - 1}{2x} - \frac{(\alpha_0 - 1)^2}{2((\alpha_0 - 1)x - 2\alpha_0)} \right) B_S^{(3)}. \end{aligned} \tag{J.54}$$

The initial conditions are the following. At  $x = 0$ , we have

$$\begin{aligned} B^{(1)}(x = 0, \epsilon; \alpha_0, d_1; \delta) \\ = B^{(6)}(x = 0, \epsilon; \alpha_0, d_1; \delta) = B_{\alpha_0}(1 - 4\epsilon, 1 + 2d_1\epsilon) B(1 - \epsilon, 1 - \epsilon). \end{aligned} \tag{J.55}$$

At  $x = 1$ , we have

$$\begin{aligned} B^{(5)}(x = 1, \epsilon; \alpha_0, d_1; \delta) &= B^{(1)}(x = 1, \epsilon; \alpha_0, d_1; \delta), \\ B^{(8)}(x = 1, \epsilon; \alpha_0, d_1; \delta) &= B^{(2)}(x = 1, \epsilon; \alpha_0, d_1; \delta), \\ B^{(9)}(x = 1, \epsilon; \alpha_0, d_1; \delta) &= B^{(3)}(x = 1, \epsilon; \alpha_0, d_1; \delta). \end{aligned} \tag{J.56}$$

At  $x = 2$ , we have

$$\begin{aligned} B^{(4)}(x = 2, \epsilon; \alpha_0, d_1; \delta) &= \frac{1}{2} B^{(1)}(x = 2, \epsilon; \alpha_0, d_1; \delta), \\ B^{(7)}(x = 2, \epsilon; \alpha_0, d_1; \delta) &= \frac{1}{2} B^{(3)}(x = 2, \epsilon; \alpha_0, d_1; \delta). \end{aligned} \tag{J.57}$$

It is easy to check that  $B^{(1)}$  is finite at  $x = 0$  and  $x = 2$ . The integration constants of  $B^{(2)}$  and  $B^{(3)}$  can then be fixed in an implicit way by requiring the residues of the general solution for  $B^{(1)}$  to vanish at  $x = 0$  and  $x = 2$ .

Having the analytic expression for the master integrals, we can calculate the  $\mathcal{B}$ -type integrals for a fixed integer value of  $D_0$ . The results for  $D_0 = 3$  can be found in Ref. [69].

In Fig. J.2 we show some representative results of comparing the analytic and numeric computations for the  $\epsilon^2$  coefficient in the expansion of  $\mathcal{I}(x, \epsilon; \alpha_0, 3 -$

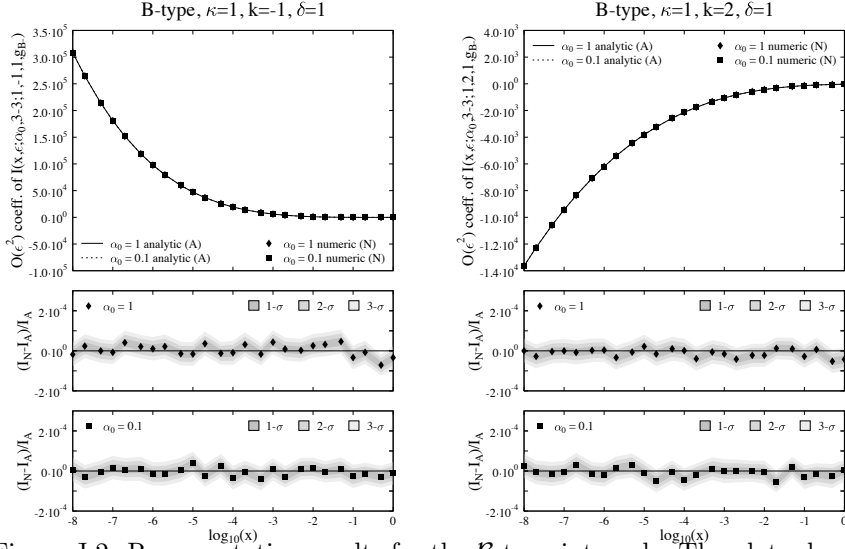


Figure J.2: Representative results for the  $\mathcal{B}$ -type integrals. The plots show the coefficient of the  $\mathcal{O}(\epsilon^2)$  term in  $\mathcal{I}(x, \epsilon; \alpha_0, 3 - 3\epsilon; 1, k, 1, g_{B-})$  for  $k = -1$  (left figure) and  $k = 2$  (right figure) with  $\alpha_0 = 0.1, 1$ . The plots are taken from Ref. [69].

$3\epsilon; 1, k, 1, g_{B-})$  for  $k = -1, 2$  and  $\alpha_0 = 0.1, 1$ . The dependence on  $\alpha_0$  is not visible on the plots. The two sets of results are in excellent agreement for the whole  $x$ -range. For other (lower-order, thus simpler) expansion coefficients and/or other values of the parameters, we find similar agreement.

## J.3 The iterated integrals

### J.3.1 The soft $\mathcal{J}*\mathcal{I}$ integrals

In this section we calculate some of the iterated integrals that appear in the doubly-approximate cross-section. The iterated soft integrals arise from a convolution of a soft and a collinear integral. they have the form [69],

$$\begin{aligned} \mathcal{J}*\mathcal{I}(Y, \epsilon; y_0, d'_0, \alpha_0, d_0; k) &= -Y B(-\epsilon, -\epsilon) {}_2F_1(1, 1, 1 - \epsilon; 1 - Y) \\ &\times \int_0^{y_0} dy y^{-1-2\epsilon} (1-y)^{d'_0} \mathcal{I}(y; \epsilon, \alpha_0, d_0; 0, k, 0, g_A). \end{aligned} \quad (\text{J.58})$$



The hypergeometric function can be easily evaluated using the technique described in Section 6.3. The evaluation of the  $y$  integral order by order in  $\epsilon$  is a little bit more cumbersome because the integrand has two kinds of singularities,

1. The pole in  $y = 0$ .
2. The integral  $\mathcal{I}$  is order by order logarithmically divergent for  $y \sim 0$ .

The pole in  $y = 0$  can easily be factorized by performing the integration by parts in  $y$ . The logarithmic singularities in  $\mathcal{I}$  however are more subtle. We have to resum all these singularities before expanding the integral. We find that we can write

$$\mathcal{I}(y; \epsilon, \alpha_0, d_0; 0, k, 0, g_A) = y^{-2\epsilon} I(y; \epsilon, \alpha_0, d_0; 0, k, 0, g_A), \tag{J.59}$$

where  $I$  is a function that is order by order finite in  $y = 0$ . Eq. (J.58) can now be written as

$$\begin{aligned} \mathcal{J}*\mathcal{I}(Y, \epsilon; y_0, d'_0, \alpha_0, d_0; k) &= -Y B(-\epsilon, -\epsilon) {}_2F_1(1, 1, 1 - \epsilon; 1 - Y) \\ &\times \left\{ -\frac{1}{4\epsilon} y_0^{-4\epsilon} (1 - y_0)^{d'_0} I(y_0; \epsilon, \alpha_0, d_0; 0, k, 0, g_A) \right. \\ &\left. + \frac{1}{4\epsilon} \int_0^{y_0} dy y^{-4\epsilon} \frac{\partial}{\partial y} \left[ (1 - y)^{d'_0} I(y; \epsilon, \alpha_0, d_0; 0, k, 0, g_A) \right] \right\}. \end{aligned} \tag{J.60}$$

As  $I$  does not have logarithmic divergences, the derivative does not produce any poles and so the integral is uniformly convergent. We can thus just expand the integrand into a power series in  $\epsilon$  and integrate order by order, using the definition of the *HPL's* \*, Eq. (G.6). As representative examples, in Fig. J.3 we compare the analytic and numeric results for the  $\epsilon^0$  coefficient in the expansion of  $\mathcal{J}*\mathcal{I}(Y, \epsilon; y_0, 3 - 3\epsilon, \alpha_0, 3 - 3\epsilon; k)$  for  $k = -1, 2$  and  $y_0 = \alpha_0 = 0.1, 1$ . The two computations agree very well over the whole  $Y$ -range. Other (lower-order, thus simpler) expansion coefficients and/or other values of the parameters show similar agreement. The results for  $D_0 = D'_0 = 3$  can be found in Ref. [69].

---

\*Notice that the rational part of  $I$  gives a non-vanishing contribution to the lower integration limit that has to be subtracted.

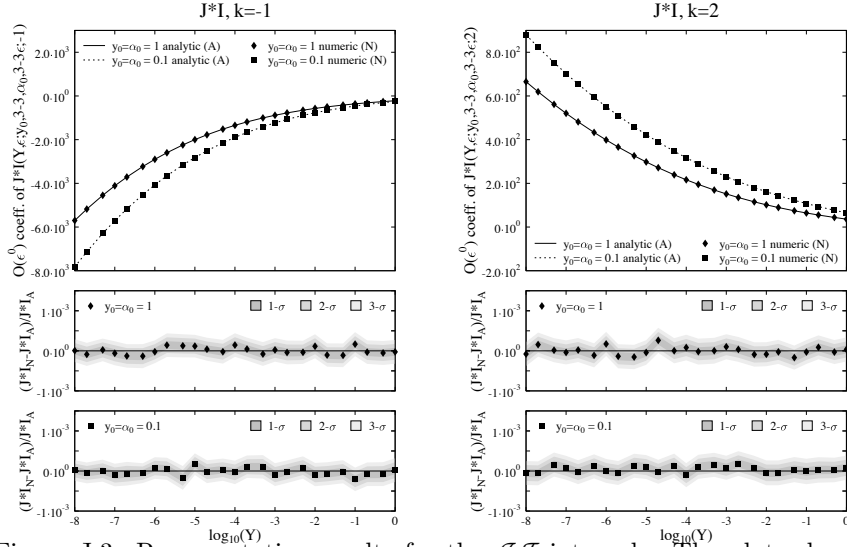


Figure J.3: Representative results for the  $\mathcal{J}^*\mathcal{I}$  integrals. The plots show the coefficient of the  $\mathcal{O}(\epsilon^0)$  term in  $\mathcal{J}^*\mathcal{I}(Y, \epsilon; y_0, 3 - 3\epsilon, \alpha_0, 3 - 3\epsilon; k)$  for  $k = -1$  (left figure) and  $k = 2$  (right figure) with  $y_0 = \alpha_0 = 0.1, 1$ . The plots are taken from Ref. [69].

### J.3.2 The soft-collinear $\mathcal{K}^*\mathcal{I}$ integrals

The iterated soft-collinear integrals arise from a convolution of a soft-collinear and a collinear integral. they have the form [69],

$$\begin{aligned}
 \mathcal{K}^*\mathcal{I}(\epsilon; y_0, d'_0, \alpha_0, d_0; k) = & \\
 & 2B(1 - \epsilon, -\epsilon) \int_0^{y_0} dy y^{-1-4\epsilon} (1 - y)^{d'_0} I(y; \epsilon, \alpha_0, d_0; 0, k, 0, g_A) \\
 & + 2B(1 - \epsilon, 1 - \epsilon) \int_0^{y_0} dy y^{-4\epsilon} (1 - y)^{d'_0-1} I(y; \epsilon, \alpha_0, d_0; 0, k, 0, g_A),
 \end{aligned} \tag{J.61}$$

where  $I$  was defined in Eq. (J.59). The first integral is exactly the same as in Section J.3.1. The second integral is uniformly convergent, so we can just expand under the integration sign and integrate order by order. The results for  $D_0 = D'_0 = 3$  can be found in Ref. [69].

# Appendix **K**

## Scalar one-loop integrals

### K.1 Basic definitions and conventions

In this appendix we give a review of scalar one-loop Feynman integral, and the basic notations and conventions we used throughout this work. A scalar on-loop integral in  $D$  dimensions is defined by

$$I_n^D(\{\nu_i\}; \{Q_i^2\}; \{M_i\}) = e^{\gamma_E \epsilon} \int \frac{d^D k}{i\pi^{D/2}} \prod_{i=1}^n \frac{1}{D_i^{\nu_i}}, \quad (\text{K.1})$$

where the external momenta  $k_i$  are incoming such that  $\sum_{i=1}^n k_i = 0$  and the propagators have the form

$$D_1 = k^2 - M_1^2 + i0, \\ D_i = \left( k + \sum_{j=1}^{i-1} k_j \right)^2 - M_i^2 + i0, \quad i = 2, \dots, n. \quad (\text{K.2})$$

Note that, although everything we say in this chapter is true in general, we are particularly interested in this work in the case where all internal masses are zero,  $M_i^2 = 0$ . The integral (K.1) is in general divergent if  $D$  is a positive integer, and we therefore need to regularize the integral. We work in dimensional regularization, *i.e.*, we evaluate Eq. (K.1) for non-integer values of  $D = D_0 - 2\epsilon$ , where  $D_0$  is an integer. We now have to face the problem

of how to define the integration in a non-integer dimensional space. Such an integration can be defined consistently by considering an infinite dimensional vector space  $V$  endowed with a non-degenerate bilinear form (*e.g.* Minkowski or euclidean metric) [112]. Let us consider now the space of covariant functions over  $V$ , *i.e.*, the space of functions of the form  $f(k^2, k \cdot p_1, \dots, k \cdot p_n) \equiv f(k)$ , where  $k, q_i \in V$ . For any complex  $D$ , the integration (K.1) can now be introduced as a linear functional on this space of covariant functions,

$$f \rightarrow \int d^D k f(k^2, k \cdot p_1, \dots, k \cdot p_n) \equiv \int d^D k f(k). \quad (\text{K.3})$$

fulfilling the following four axioms:

**1. Linearity:**

$$\int d^D k (a f(k) + b g(k)) = a \int d^D k f(k) + b \int d^D k g(k). \quad (\text{K.4})$$

**2. Translational invariance:**

$$\int d^D k f(k + p) = \int d^D k f(k). \quad (\text{K.5})$$

**3. Scaling:**

$$\int d^D k f(a \cdot k) = a^{-D} \int d^D k f(k). \quad (\text{K.6})$$

**4. Normalization\*:**

$$\int d^D k e^{-k^2} = \pi^{D/2}. \quad (\text{K.7})$$

These four axioms uniquely fix the integral of the function  $f(k) = e^{-a k^2 + k \cdot p}$ ,

$$\begin{aligned} \int d^D k e^{-a k^2 + k \cdot p} &= e^{p^2/4a} \int d^D k e^{-a(k-p/2a)^2} \\ &= a^{-D/2} e^{p^2/4a} \int d^D k e^{-k^2} = \left(\frac{\pi}{a}\right)^{D/2} e^{p^2/4a}. \end{aligned} \quad (\text{K.8})$$

The integral of a generic function  $f(k)$  can then be computed by taking linear combinations of derivatives of the generating function  $e^{-a k^2 + b k \cdot p}$ , *e.g.*,

$$k^2 + \lambda(k \cdot p) = \left( -\frac{\partial}{\partial a} + \lambda \frac{\partial}{\partial b} \right) e^{-a k^2 + b k \cdot p} \Big|_{a=b=0}. \quad (\text{K.9})$$

---

\*We choose the normalization such that it agrees with the usual Gaussian integral in  $\mathbb{R}^D$ , where  $D$  is a positive integer.

The axiomatic approach we just presented uniquely defines the scalar Feynman integrals (K.1). They can often be expressed in terms of (generalized) hypergeometric functions. In Appendix H we showed that different representations of hypergeometric functions are useful to derive different properties. In the following we argue that the different parametrizations used to evaluate Feynman integrals, Schwinger and Feynman parameters, series and Mellin-Barnes representations, are the equivalents to the four representations of the representations of the hypergeometric function, and switching from one parametrization to another might allow one to obtain valuable information about the Feynman integral. I

## K.2 The Feynman parametrization

The Feynman parametrization is based on the identity

$$\prod_{i=1}^n \frac{1}{D_i^{\nu_i}} = \frac{\Gamma(\nu)}{\Gamma(\nu_1) \dots \Gamma(\nu_n)} \prod_{i=1}^n \int_0^1 dx_i x_i^{\nu_i-1} \frac{\delta(1-x_1 \dots - x_n)}{(x_1 D_1 + \dots + x_n D_n)^\nu}, \quad (\text{K.10})$$

with  $\nu = \sum_{i=1}^n \nu_i$ . Inserting this relation into Eq. (K.1), we obtain the following representation for the Feynman integral,

$$I_n^D(\{\nu_i\}; \{Q_i^2\}; \{M_i\}) = \Gamma(\nu) \int \mathcal{D}x \int \frac{d^D k}{i\pi^{D/2}} \frac{1}{(k^2 - 2\mathcal{Q} \cdot k + \mathcal{J})^\nu}, \quad (\text{K.11})$$

where we introduced the shorthand

$$\int \mathcal{D}x = e^{\gamma_E \epsilon} \prod_{i=1}^n \int_0^1 dx_i \frac{x_i^{\nu_i-1}}{\Gamma(\nu_i)} \delta\left(1 - \sum_{i=1}^n x_i\right). \quad (\text{K.12})$$

The coefficients  $\mathcal{Q}$  and  $\mathcal{J}$  are given by

$$\begin{aligned} \mathcal{Q} &= - \sum_{i=2}^n x_i \sum_{j=1}^{i-1} k_j, \\ \mathcal{J} &= \sum_{i=1}^n x_i \left( \sum_{j=1}^{i-1} k_j \right)^2 - \sum_{i=1}^n x_i M_i^2. \end{aligned} \quad (\text{K.13})$$

Performing the loop integration, we can reduce the Feynman integral to

$$I_n^D(\{\nu_i\}; \{Q_i^2\}; \{M_i\}) = (-1)^\nu \Gamma(\nu - D/2) \int \mathcal{D}x \frac{1}{F^{\nu-D/2}}, \quad (\text{K.14})$$

where the  $F$ -polynomial is defined by

$$F = \mathcal{Q}^2 - \mathcal{J}. \quad (\text{K.15})$$

We have reduced the Feynman integral to an integral of a rational function over the unit cube in  $n$  dimensions. Note the formal equivalence of Eq. (K.14) with the Euler integral representation of the hypergeometric function, Eq. (H.2).

### K.3 Wick rotation and analytic continuation to the Euclidean region

The integral (K.1) is explicitly defined in Minkowski space, and from Eq. (K.11) is clear that a Feynman integral can always be written in the form

$$I_n^D(\{\nu_i\}; \{Q_i^2\}; \{M_i\}) = \int d^D k f(k^2). \quad (\text{K.16})$$

Separating the integration of the time component from the spatial components, we can write, with  $d^D k = dk_0 d^{D-1} \vec{k}$ ,

$$I_n^D(\{\nu_i\}; \{Q_i^2\}; \{M_i\}) = \int_{-\infty}^{+\infty} dk_0 \int d^{D-1} k f(k_0^2 - \vec{k}^2). \quad (\text{K.17})$$

We now consider the contour shown in Fig. K.1 in the complex  $k^0$ -plane. If we send the contour to infinity, we find the relation

$$\int_{-\infty}^{+\infty} dk_0 f(k_0^2 - \vec{k}^2) = \int_{+i\infty}^{-i\infty} dk_0 f(k_0^2 - \vec{k}^2) = i \int_{-\infty}^{+\infty} dk_{E0} f(-k_E^2), \quad (\text{K.18})$$

where we defined  $k_E = (ik_0, \vec{k})$ . This operation, known as the Wick rotation, transforms the integral into

$$I_n^D(\{\nu_i\}; \{Q_i^2\}; \{M_i\}) = i \int d^D k_E f(-k_E^2). \quad (\text{K.19})$$

Eq. (K.19) can now be interpreted as an integral in the Euclidean vector space spanned by  $k_E$ .

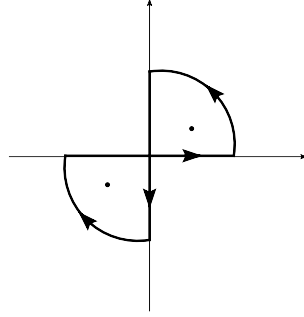


Figure K.1: The integration contour in the  $k_0$ -plane used in the Wick rotation.

## K.4 The Schwinger parametrization

The Schwinger parametrization<sup>†</sup> is based on the identity

$$\frac{1}{D_i^{\nu_i}} = \frac{(-1)^{\nu_i}}{\Gamma(\nu_i)} \int_0^\infty d\alpha_i \alpha_i^{\nu_i-1} e^{\alpha_i D_i}, \quad (\text{K.20})$$

Note that we explicitly derived Eq. (K.20) in Euclidean space, where we used the fact that in the Euclidean region  $D_i < 0$  in order to get a convergent integral. The corresponding relation in Minkowski space is similar, up to some factors of  $i$  in the exponent. Inserting Eq. (K.20) into the loop integral (K.1), we obtain,

$$I_n^D(\{\nu_i\}; \{Q_i^2\}; \{M_i\}) = \int \mathcal{D}\alpha \int \frac{d^D k}{i\pi^{D/2}} \exp\left(\sum_{i=1}^n \alpha_i D_i\right), \quad (\text{K.21})$$

where we introduced the shorthand

$$\int \mathcal{D}\alpha = e^{\gamma_E \epsilon} \prod_{i=1}^n \frac{(-1)^{\nu_i}}{\Gamma(\nu_i)} \int_0^\infty d\alpha_i \alpha_i^{\nu_i-1}, \quad (\text{K.22})$$

and performing the Gaussian integral in Eq. (K.21) leads to

$$I_n^D(\{\nu_i\}; \{Q_i^2\}; \{M_i\}) = \int \mathcal{D}\alpha \frac{1}{\mathcal{P}^{D/2}} \exp(\mathcal{Q}/\mathcal{P}) \exp(-\mathcal{M}). \quad (\text{K.23})$$

<sup>†</sup>Also known as  $\alpha$  parametrization.

The quantities  $\mathcal{P}$ ,  $\mathcal{Q}$  and  $\mathcal{M}$  are polynomials in the Schwinger parameters  $\alpha_i$ , the internal masses  $M_i^2$  and the momentum scales  $Q_i^2$ ,

$$\begin{aligned}\mathcal{P} &= \sum_{i=1}^n \alpha_i, \\ \mathcal{Q} &= \sum_{i=1}^{n-1} \sum_{j=i+1}^n \alpha_i \alpha_j \left( \sum_{l=i}^{j-1} k_l \right)^2, \\ \mathcal{M} &= \sum_{i=1}^n \alpha_i M_i^2.\end{aligned}\tag{K.24}$$

Note that the polynomials can directly be read off from the Feynman diagram in terms of trees and two-trees [90, 113, 114, 115].

The Schwinger parametrization is the starting point of the NDIM method, which we describe in the next section. Note however at this point the formal similarity between the Schwinger parametrization (K.24) and the Laplace integral representation of the hypergeometric function, Eq. (H.8).

## K.5 The Negative Dimension approach

The crucial point in the NDIM approach is that the Gaussian integral (K.21) is an analytic function of the space-time dimension. Hence it is possible to consider  $D < 0$  and to make the definition [116, 117]

$$\int \frac{d^D k}{i\pi^{D/2}} (k^2)^n = n! \delta_{n+\frac{D}{2}, 0}\tag{K.25}$$

for positive values of  $n$ .

For the one-loop integrals we are interested in here, we view Eqs. (K.21) and (K.23) as existing in negative dimensions. Making the same series expansion of the exponential as above, Eq. (K.21) becomes

$$\begin{aligned}I_n^D(\{\nu_i\}; \{Q_i^2\}; \{M_i\}) &= \int \mathcal{D}\alpha \sum_{n_1, \dots, n_n=0}^{\infty} \int \frac{d^D k}{i\pi^{D/2}} \prod_{i=1}^n \frac{(x_i D_i)^{n_i}}{n_i!} \\ &= \int \mathcal{D}\alpha \sum_{n_1, \dots, n_n=0}^{\infty} I_n^D(-n_1, \dots, -n_n; \{Q_i^2\}, \{M_i^2\}) \prod_{i=1}^n \frac{x_i^{n_i}}{n_i!},\end{aligned}\tag{K.26}$$



where the  $n_i$  are positive integers. The target loop integral is an infinite sum of (integrals over the Schwinger parameters of) loop integrals with negative powers of the propagators.

Likewise, we expand the exponentials in Eq. (K.23)

$$I_n^D(\{\nu_i\}; \{Q_i^2\}; \{M_i\}) = \int \mathcal{D}\alpha \sum_{n=0}^{\infty} \frac{\mathcal{Q}^n \mathcal{P}^{-n-\frac{D}{2}}}{n!} \sum_{m=0}^{\infty} \frac{(-\mathcal{M})^m}{m!}, \quad (\text{K.27})$$

and introduce the integers  $q_1, \dots, q_q, p_1, \dots, p_n$  and  $m_1, \dots, m_n$  to make multinomial expansions of  $\mathcal{Q}$ ,  $\mathcal{P}$  and  $\mathcal{M}$  respectively

$$\begin{aligned} \mathcal{Q}^n &= \sum_{q_1, \dots, q_q=0}^{\infty} \frac{\mathcal{Q}_1^{q_1}}{q_1!} \dots \frac{\mathcal{Q}_q^{q_q}}{q_q!} (q_1 + \dots + q_q)!, \\ \mathcal{P}^{-n-\frac{D}{2}} &= \sum_{p_1, \dots, p_n=0}^{\infty} \frac{\alpha_1^{p_1}}{p_1!} \dots \frac{\alpha_n^{p_n}}{p_n!} (p_1 + \dots + p_n)!, \\ (-\mathcal{M})^m &= \sum_{m_1, \dots, m_n=0}^{\infty} \frac{(-\alpha_1 M_1^2)^{m_1}}{m_1!} \dots \frac{(-\alpha_n M_n^2)^{m_n}}{m_n!} (m_1 + \dots + m_n)!, \end{aligned} \quad (\text{K.28})$$

subject to the constraints

$$\begin{aligned} \sum_{i=1}^q q_i &= n, \\ \sum_{i=1}^n p_i &= -n - \frac{D}{2}, \\ \sum_{i=1}^n m_i &= m, \\ p_1 + \dots + p_n + q_1 + \dots + q_q &= -\frac{D}{2}. \end{aligned} \quad (\text{K.29})$$

Altogether, Eqs. (K.27) and (K.28) give

$$\begin{aligned} I_n^D(\{\nu_i\}; \{Q_i^2\}; \{M_i\}) &= \int \mathcal{D}\alpha \sum_{\substack{p_1, \dots, p_n=0 \\ q_1, \dots, q_q=0 \\ m_1, \dots, m_n=0}}^{\infty} \frac{\mathcal{Q}_1^{q_1} \dots \mathcal{Q}_q^{q_q}}{q_1! \dots q_q!} \\ &\times \frac{\alpha_1^{p_1} \dots \alpha_n^{p_n}}{p_1! \dots p_n!} \frac{(-\alpha_1 M_1^2)^{m_1}}{m_1!} \dots \frac{(-\alpha_n M_n^2)^{m_n}}{m_n!} (p_1 + \dots + p_n)!, \end{aligned} \quad (\text{K.30})$$

with the constraints expressed by Eq. (K.29).

We recall that each of the  $\mathcal{Q}_i$  is a bilinear in the Schwinger parameters, so that the target loop integral is now an infinite sum of powers of the scales of the process (with each of the  $M_i^2$  and the  $Q_i^2$  raised to a different summation variable) integrated over the Schwinger parameters.

Equations (K.26) and (K.30) are two different expressions for the same quantity:  $I_n^D$ . Matching up powers of the Schwinger parameters, we obtain an expression for the loop integral with negative powers of the propagators in negative dimensions

$$\begin{aligned}
I_n^D(\{\nu_i\}; \{Q_i^2\}; \{M_i\}) & \\
&\equiv e^{\gamma_E \epsilon} \sum_{\substack{p_1, \dots, p_n=0 \\ q_1, \dots, q_q=0 \\ m_1, \dots, m_n=0}}^{\infty} (Q_1^2)^{q_1} \dots (Q_q^2)^{q_q} (-M_1^2)^{m_1} \dots (-M_n^2)^{m_n} \\
&\times \left( \prod_{i=1}^n \frac{\Gamma(1 - \nu_i)}{\Gamma(1 + m_i) \Gamma(1 + p_i)} \right) \left( \prod_{i=1}^q \frac{1}{\Gamma(1 + q_i)} \right) \Gamma \left( 1 + \sum_{k=1}^n p_k \right), \tag{K.31}
\end{aligned}$$

subject to the constraints Eq. (K.29). This is the main result of the negative dimension approach. The loop integral is written directly as an infinite sum. Given that  $\mathcal{Q}$  can be read off directly from the Feynman graph, so can the precise form of Eq. (K.31) as well as the system of constraints. Of course, strictly speaking we have assumed that both  $\nu_i$  and  $D/2$  are negative integers and we must be careful in interpreting this result in the physically interesting domain where the  $\nu_i$  and  $D$  are all positive. Furthermore, of the many possible solutions, only those that converge in the appropriate kinematic region should be retained.

## K.6 The Mellin-Barnes representation

The Mellin-Barnes techniques rely on the following identity,

$$\frac{1}{(A+B)^\lambda} = \frac{1}{\Gamma(\lambda)} \frac{1}{2\pi i} \int_{-i\infty}^{+i\infty} dz \Gamma(-z) \Gamma(\lambda+z) \frac{B^z}{A^{\lambda+z}}. \tag{K.32}$$

The contour in Eq. (K.32) is chosen in the standard way, *i.e.* it should separate the poles in  $\Gamma(-z)$  from the poles in  $\Gamma(\lambda+z)$ . We can apply Eq. (K.32) to the  $F$ -polynomial in Eq. (K.14), and break it up into monomials in the Feynman

parameters  $x_i$ . The integration over the Feynman parameters can now be easily performed in terms of  $\Gamma$  functions,

$$\int_0^1 \prod_{i=1}^n dx_i x_i^{a_i-1} \delta(1 - x_1 - \dots - x_n) = \frac{\Gamma(a_1) \dots \Gamma(a_n)}{\Gamma(a_1 + \dots + a_n)}. \quad (\text{K.33})$$

In this way we have eliminated all the Feynman parameter integrals in terms of Mellin-Barnes integrals, and we obtain a representation equivalent to the Mellin-Barnes representation of the hypergeometric function, Eq. (H.5).



# Analytic continuation of the scalar massless pentagon

## L.1 Analytic continuation from Region II(a) to Region II(b)

In this section we explicitly perform the analytic continuation in  $t_1/t_2 \rightarrow t_2/t_1$  (or equivalently  $y_2 \rightarrow 1/y_2$ ) of the solution (11.22) valid in Region II(a) to Region II(b), and we prove in this way explicitly the relation (11.24). Let us start with the first term in Eq. (11.22). Using Eq. (H.12), we find

$$\begin{aligned} & I_1^{(IIb)}(s, s_1, s_2, t_1, t_2) \\ &= \frac{1}{\epsilon^3} (-1)^{2\epsilon} \Gamma(1-2\epsilon) \Gamma(1+\epsilon)^2 y_2^{\epsilon-1} F_4\left(1-2\epsilon, 1-\epsilon, 1-\epsilon, 1-\epsilon; -\frac{y_1}{y_2}, \frac{1}{y_2}\right). \end{aligned} \quad (\text{L.1})$$

Similarly, the second term becomes,

$$\begin{aligned} & I_2^{(IIb)}(s, s_1, s_2, t_1, t_2) \\ &= -\frac{2}{\epsilon^3} (-1)^\epsilon \Gamma(1-2\epsilon) \Gamma(1+\epsilon)^2 \cos(\pi\epsilon) y_2^{\epsilon-1} \\ &\quad \times F_4\left(1-2\epsilon, 1-\epsilon, 1-\epsilon, 1-\epsilon; -\frac{y_1}{y_2}, \frac{1}{y_2}\right) \\ &\quad + \frac{1}{\epsilon^3} \Gamma(1+\epsilon) \Gamma(1-\epsilon) y_2^{-1} F_4\left(1, 1-\epsilon, 1-\epsilon, 1+\epsilon; -\frac{y_1}{y_2}, \frac{1}{y_2}\right). \end{aligned} \quad (\text{L.2})$$

Combining the two results, and using the identity

$$(-1)^{2\epsilon} - 2(-1)^\epsilon \cos(\pi\epsilon) = -1 \quad (\text{L.3})$$

yields

$$\begin{aligned} & I_1^{(IIb)}(s, s_1, s_2, t_1, t_2) + I_2^{(IIb)}(s, s_1, s_2, t_1, t_2) \\ &= \frac{t_2}{t_1} \left( I_1^{(IIa)}(s, s_2, s_1, t_2, t_1) + I_2^{(IIa)}(s, s_2, s_1, t_2, t_1) \right). \end{aligned} \quad (\text{L.4})$$

The third term becomes

$$\begin{aligned} & I_3^{(IIb)}(s, s_1, s_2, t_1, t_2) + I_4^{(IIb)}(s, s_1, s_2, t_1, t_2) \\ &= \frac{t_2}{t_1} \left\{ \frac{1}{\epsilon^2} y_1^\epsilon y_2^{-\epsilon} [\ln y_1 - \ln y_2 - i\pi] F_4 \left( 1, 1 + \epsilon, 1 + \epsilon, 1 + \epsilon; -\frac{y_1}{y_2}, \frac{1}{y_2} \right) \right. \\ &\quad - \frac{1}{\epsilon^3} y_1^\epsilon (-1)^\epsilon \Gamma(1 + \epsilon) \Gamma(1 - \epsilon) F_4 \left( 1, 1 - \epsilon, 1 + \epsilon, 1 - \epsilon; -\frac{y_1}{y_2}, \frac{1}{y_2} \right) \\ &\quad + \frac{1}{\epsilon^2} y_1^\epsilon y_2^{-\epsilon} \\ &\quad \left. \times \frac{\partial}{\partial \delta} F \left( \begin{matrix} 1 + \delta & 1 + \delta + \epsilon \\ - & - \end{matrix} \middle| \begin{matrix} 1 & - & - & - \\ 1 + \delta & 1 + \epsilon & 1 + \delta + \epsilon & - \end{matrix} \middle| -\frac{y_1}{y_2}, \frac{1}{y_2} \right) \Big|_{\delta=0} \right\}. \end{aligned} \quad (\text{L.5})$$

Similarly,

$$\begin{aligned} & I_5^{(IIb)}(s, s_1, s_2, t_1, t_2) + I_6^{(IIb)}(s, s_1, s_2, t_1, t_2) \\ &= \frac{t_2}{t_1} \left\{ \frac{1}{\epsilon^2} y_1^\epsilon \left[ \ln \frac{y_2}{y_1} + \psi(-\epsilon) - \psi(\epsilon) + i\pi \right] F_4 \left( 1, 1 - \epsilon, 1 + \epsilon, 1 - \epsilon; -\frac{y_1}{y_2}, \frac{1}{y_2} \right) \right. \\ &\quad - \frac{1}{\epsilon^3} y_1^\epsilon (-1)^{-\epsilon} y_2^{-\epsilon} \Gamma(1 + \epsilon) \Gamma(1 - \epsilon) F_4 \left( 1, 1 + \epsilon, 1 + \epsilon, 1 + \epsilon; -\frac{y_1}{y_2}, \frac{1}{y_2} \right) \\ &\quad - \frac{1}{\epsilon^2} y_1^\epsilon \\ &\quad \left. \times \frac{\partial}{\partial \delta} F \left( \begin{matrix} 1 + \delta & 1 + \delta - \epsilon \\ - & - \end{matrix} \middle| \begin{matrix} 1 & - & - & - \\ 1 + \delta & 1 - \epsilon & 1 + \delta + \epsilon & - \end{matrix} \middle| -\frac{y_1}{y_2}, \frac{1}{y_2} \right) \Big|_{\delta=0} \right\}. \end{aligned} \quad (\text{L.6})$$

The Kampé de Fériet function have already the correct form. Combining the remaining Appell functions, and using the fact that  $\ln y_2 - \ln y_1 = -\ln \frac{s_1 s_2}{s t_1}$  and

$$-i\pi + \frac{1}{\epsilon} (-1)^\epsilon \Gamma(1 - \epsilon) \Gamma(1 + \epsilon) = \psi(1 - \epsilon) - \psi(\epsilon), \quad (\text{L.7})$$

we find the desired result

$$\mathcal{I}_{\text{ND}}^{(IIb)}(\kappa, t_1, t_2) = \frac{t_2}{t_1} \mathcal{I}_{\text{ND}}^{(IIa)}(\kappa, t_2, t_1). \tag{L.8}$$

## L.2 Symmetry properties in Region I

In this section we proof that the solution  $\mathcal{I}_{\text{ND}}^{(I)}$  has the correct symmetry properties under the exchange of the dimensionless quantities  $x_1$  and  $x_2$ ,

$$\mathcal{I}_{\text{ND}}^{(I)}(\kappa, t_1, t_2) = \mathcal{I}_{\text{ND}}^{(I)}(\kappa, t_1, t_2). \tag{L.9}$$

The expression (11.36) apparently violates this relation, due to the explicit appearance of the argument  $x_1/x_2$  in the hypergeometric functions. In the following we show that if we perform the analytic continuation of one of the hypergeometric functions according to the prescription  $x_1/x_2 \rightarrow x_2/x_1$ , then the resulting expression is manifestly symmetric.

Since  $I_1^{(I)}$  and  $I_2^{(I)}$  are obviously symmetric, we focus here only on the remaining terms. Using the Mellin-Barnes representation of the Kampé de Fériet function, we find that

$$\begin{aligned} & \frac{\epsilon}{1-\epsilon} F_{2,0}^{0,3} \left( \begin{matrix} - & - \\ 2 & 2-\epsilon \end{matrix} \middle| \begin{matrix} 1 & 1 & 1 & 1 & 1-\epsilon & 1-\epsilon \\ - & - & - & - & - & - \end{matrix} \middle| -x_1, \frac{x_1}{x_2} \right) \\ &= (-1)^\epsilon \epsilon \Gamma(\epsilon) \Gamma(-\epsilon) t_2^{-\epsilon+1} t_1^{\epsilon-1} F_4(1, 1-\epsilon, 1+\epsilon, 1-\epsilon; -x_1, -x_2) \\ & - \frac{\epsilon}{1+\epsilon} \frac{t_2^2}{t_1^2} F_{2,0}^{0,3} \left( \begin{matrix} - & - \\ 2 & 2+\epsilon \end{matrix} \middle| \begin{matrix} 1 & 1 & 1 & 1 & 1-\epsilon & 1+\epsilon \\ - & - & - & - & - & - \end{matrix} \middle| -x_2, \frac{x_2}{x_1} \right) \\ & + \frac{t_1}{t_1} \left[ \ln \frac{t_1}{t_2} - i\pi - \psi(1-\epsilon) - \psi(-\epsilon) \right] F_4(1, 1-\epsilon, 1-\epsilon, 1+\epsilon; -x_1, x_2) + \\ & \frac{\partial}{\partial \delta} F_{0,2}^{2,1} \left( \begin{matrix} 1 & 1-\epsilon \\ - & - \end{matrix} \middle| \begin{matrix} 1 & 1 & - & - \\ 1+\delta & 1-\delta & 1-\epsilon+\delta & 1+\epsilon-\delta \end{matrix} \middle| -x_1, -x_2 \right) \Big|_{\delta=0}. \end{aligned} \tag{L.10}$$

We already see in this expression that the terms involving  $F_{2,0}^{0,3}$  exchange their roles under the transformation  $t_1 \rightarrow t_2$ . Let us now show that the same hold true for the remaining terms, and let us concentrate on the terms in

Eq. (11.39) having a coefficient involving  $(-t_1)^{-\epsilon}$ . The terms involving derivatives of Kampé de Fériet functions become

$$\begin{aligned} & \frac{\partial}{\partial \delta} F_{0,2}^{2,1} \left( \begin{matrix} 1 & 1-\epsilon \\ - & - \end{matrix} \middle| \begin{matrix} 1 & 1 & - & - \\ 1+\delta & 1-\delta & 1-\epsilon+\delta & 1+\epsilon-\delta \end{matrix} \middle| -x_1, -x_2 \right)_{|\delta=0} \\ & + \frac{\partial}{\partial \delta} F_{0,2}^{2,1} \left( \begin{matrix} 1+\delta & 1+\delta-\epsilon \\ - & - \end{matrix} \middle| \begin{matrix} - & 1 & - & - \\ - & 1+\delta & 1-\epsilon & 1+\epsilon+\delta \end{matrix} \middle| -x_1, -x_2 \right)_{|\delta=0} \\ & = \frac{\partial}{\partial \delta} F_{0,2}^{2,1} \left( \begin{matrix} 1+\delta & 1+\delta-\epsilon \\ - & - \end{matrix} \middle| \begin{matrix} 1 & - & - & - \\ 1+\delta & - & 1-\epsilon+\delta & 1+\epsilon \end{matrix} \middle| -x_1, -x_2 \right)_{|\delta=0}, \end{aligned} \quad (\text{L.11})$$

where we used the fact that for any function  $f$

$$\frac{\partial}{\partial \delta} \left( f(\delta) + f(-\delta) \right)_{|\delta=0} = 0. \quad (\text{L.12})$$

The resulting function is now symmetric to the corresponding one with coefficient  $(-t_2)^{-\epsilon}$ . Finally for the terms involving an Appell  $F_4$  function we find

$$\begin{aligned} & \left[ \ln x_1 - i\pi \right] F_4(1, 1-\epsilon, 1-\epsilon, 1+\epsilon; -x_1, -x_2) \\ & = \left[ \ln x_1 - \frac{1}{\epsilon} + \psi(-\epsilon) - \psi(\epsilon) + (-1)^\epsilon \epsilon \Gamma(-\epsilon) \Gamma(\epsilon) \right] \\ & \quad \times F_4(1, 1-\epsilon, 1-\epsilon, 1+\epsilon; -x_1, -x_2), \end{aligned} \quad (\text{L.13})$$

where the last step follows from Eq. (L.7). This term is symmetric to the corresponding one with coefficient  $(-t_2)^{-\epsilon}$  after the latter has been combined with the first term in Eq. (L.10), and this finishes the proof that Eq. (11.39) is indeed symmetric under the transformation  $(t_1 \leftrightarrow t_2, s_1 \leftrightarrow s_2)$ .

### L.3 Analytic continuation from Region II(a) to Region I

In this section we show how the solution in Region I, Eq. (11.36) can be obtained by performing analytic continuation from Region II(a), Eq. (11.22), according to the prescription  $y_1 \rightarrow 1/y_1$ .



Let us start with  $I_1^{(IIa)}$  and  $I_2^{(IIa)}$ . Using the analytic continuation formulas for the Appell  $F_4$  function, Eq. (H.12), we find

$$\begin{aligned}
I_1^{(IIa)}(s, s_1, s_2, t_1, t_2) &= -\frac{1}{\epsilon^3} x_1^{-\epsilon} x_2^{1-\epsilon} \Gamma(1-2\epsilon) \Gamma(1+\epsilon)^2 F_4(1-2\epsilon, 1-\epsilon, 1-\epsilon, 1-\epsilon; -x_1, -x_2) \\
&= I_1^{(I)}(s, s_1, s_2, t_1, t_2) \Big|_{y_1 \rightarrow 1/y_1}, \\
I_2^{(IIa)}(s, s_1, s_2, t_1, t_2) &= \frac{1}{\epsilon^3} x_2 \Gamma(1+\epsilon) \Gamma(1-\epsilon) F_4(1, 1+\epsilon, 1+\epsilon, 1+\epsilon; -x_1, -x_2) \\
&= I_2^{(I)}(s, s_1, s_2, t_1, t_2) \Big|_{y_1 \rightarrow 1/y_1}.
\end{aligned} \tag{L.14}$$

Performing the analytic continuation for  $I_3^{(IIa)} + I_4^{(IIa)}$  and collecting all the terms we find,

$$\begin{aligned}
& -\frac{1}{\epsilon(1-\epsilon)} x_1^{-\epsilon} x_2 \frac{t_1}{t_2} \\
& \times F_{2,0}^{0,3} \left( \begin{matrix} - & - \\ 2 & 2-\epsilon \end{matrix} \middle| \begin{matrix} 1 & 1 & 1 & 1 & 1-\epsilon & 1-\epsilon \\ - & - & - & - & - & - \end{matrix} \middle| -x_1, \frac{x_1}{x_2} \right) \\
& -\frac{1}{\epsilon^2} x_1^{-\epsilon} x_2 \left[ \ln x_2 + \psi(1-\epsilon) - \psi(-\epsilon) \right] F_4(1, 1-\epsilon, 1-\epsilon, 1+\epsilon; -x_1, -x_2) \\
& -\frac{1}{\epsilon^2} x_1^{-\epsilon} x_2 \\
& \times \frac{\partial}{\partial \delta} F_{0,2}^{2,1} \left( \begin{matrix} 1+\delta & 1-\epsilon+\delta \\ - & - \end{matrix} \middle| \begin{matrix} - & 1 & - & - \\ - & 1+\delta & 1-\epsilon & 1+\epsilon+\delta \end{matrix} \middle| -x_1, -x_2 \right) \Big|_{\delta=0}.
\end{aligned} \tag{L.15}$$

Comparing with Eq. (11.39), we see that we find the correct terms. The analytic continuation of  $I_5^{(IIa)} + I_6^{(IIa)}$  follows similar lines. We immediately find the remaining terms in Eq. (11.39).



# Appendix **M**

## The pentagon integral from Mellin-Barnes integrals

In this appendix we compute the scalar massless pentagon as a Laurent series in  $\epsilon$  using Mellin-Barnes integral techniques. In Ref. [118] a Mellin-Barnes representation for the pentagon was given,

$$\begin{aligned}
 I_5^D(\nu_1, \nu_2, \nu_3, \nu_4, \nu_5; Q_i^2) &= \frac{(-1)^{N_\nu} e^{\gamma_E \epsilon}}{\Gamma(D - N_\nu)} \\
 &\times \frac{1}{(2\pi i)^4} \int_{-i\infty}^{+i\infty} \prod_{i=1}^4 dz_i \Gamma(-z_i) \\
 &\times (-s)^{\frac{D}{2} - N_\nu} \left(\frac{s_1}{s}\right)^{z_4} \left(\frac{s_2}{s}\right)^{z_1} \left(\frac{t_1}{s}\right)^{z_2} \left(\frac{t_2}{s}\right)^{z_3} \\
 &\times \Gamma(\nu_5 + z_1 + z_2) \Gamma\left(\frac{D}{2} - N_\nu + \nu_1 - z_1 - z_2 - z_3\right) \Gamma(\nu_2 + z_2 + z_3) \\
 &\times \Gamma\left(\frac{D}{2} - N_\nu + \nu_3 - z_2 - z_3 - z_4\right) \Gamma(\nu_4 + z_3 + z_4) \\
 &\times \Gamma\left(-\frac{D}{2} + N_\nu + z_1 + z_2 + z_3 + z_4\right),
 \end{aligned} \tag{M.1}$$

where  $N_\nu = \sum \nu_i$ . In particular, if we put  $\nu_i = 1$  and  $D = 6 - 2\epsilon$ , then we get

$$\begin{aligned}
I_5^D(1,1,1,1,1; Q_i^2) &= \frac{-e^{\gamma_E \epsilon} (-s)^{-2-\epsilon}}{\Gamma(1-2\epsilon)} \\
&\times \frac{1}{(2\pi i)^4} \int_{-i\infty}^{+i\infty} \prod_{i=1}^4 dz_i \Gamma(-z_i) \left(\frac{s_1}{s}\right)^{z_4} \left(\frac{s_2}{s}\right)^{z_1} \left(\frac{t_1}{s}\right)^{z_2} \left(\frac{t_2}{s}\right)^{z_3} \\
&\times \Gamma(z_1 + z_2 + 1) \Gamma(-\epsilon - z_1 - z_2 - z_3 - 1) \Gamma(z_2 + z_3 + 1) \\
&\times \Gamma(-\epsilon - z_2 - z_3 - z_4 - 1) \Gamma(z_3 + z_4 + 1) \Gamma(\epsilon + z_1 + z_2 + z_3 + z_4 + 2).
\end{aligned} \tag{M.2}$$

In the following we extract the leading behavior of this integral in the limit defined by the scaling (11.6), and we show that this leading behavior is described in all the regions by a twofold Mellin-Barnes integral, which can be evaluated in terms of multiple polylogarithms.

## M.1 Evaluation of the Mellin-Barnes integral in Region I

Performing this rescaling (11.6) in the Mellin-Barnes representation (M.2) and after the change of variable  $z_4 = z - z_1 - z_2 - z_3$ , we find

$$\begin{aligned}
I_5^D(1,1,1,1,1; Q_i^2) &= \frac{-e^{\gamma_E \epsilon} (-s)^{-\epsilon-2}}{\Gamma(1-2\epsilon)} \frac{1}{(2\pi i)^4} \int_{-i\infty}^{+i\infty} dz dz_1 dz_2 dz_3 \\
&\times \left(\frac{s_1}{s}\right)^{z-z_1-z_2-z_3} \left(\frac{s_2}{s}\right)^{z_1-z_2-z_3} \left(\frac{t_1}{s}\right)^{z_2} \left(\frac{t_2}{s}\right)^{z_3} \lambda^z \\
&\times \Gamma(-\epsilon - z_1 - 1) \Gamma(-\epsilon - z + z_1 - 1) \Gamma(z - z_1 - z_2 + 1) \Gamma(-z_2) \\
&\times \Gamma(\epsilon + z - z_2 - z_3 + 2) \Gamma(-z_3) \Gamma(z_2 + z_3 + 1) \\
&\times \Gamma(-z_1 + z_2 + z_3) \Gamma(-z + z_1 + z_2 + z_3) \Gamma(z_1 - z_3 + 1).
\end{aligned} \tag{M.3}$$

To obtain the leading behavior in our limit  $\lambda \rightarrow 0$  let us follow the strategy formulated, e.g., in Chap. 4 of [113, 90]. We close the contours to the right, and we think of the integration over  $z$  as the last one, and we analyze how poles in  $\Gamma(\dots - z)$  with leading behavior  $\lambda^{-2}$  might arise. There is only one possibility, coming from the product  $\Gamma(-\epsilon - z + z_1 - 1) \Gamma(-\epsilon - z_1 - 1)$ . Taking the residues at  $z_1 = -1 - \epsilon + n_1$ ,  $n_1 \in \mathbb{N}$ , we find

$$\lambda^z \Gamma(-\epsilon - z + z_1 - 1) \rightarrow \lambda^z \Gamma(-2\epsilon - 2 - z + n_1). \tag{M.4}$$

If we now take the residues at  $z = -2 - 2\epsilon + n_1 + n_2$ ,  $n_2 \in \mathbb{N}$ , we find

$$\lambda^z \Gamma(-2\epsilon - 2 - z + n_1) \rightarrow \lambda^{-2-2\epsilon+n_1+n_2}. \quad (\text{M.5})$$

Since we are only interested in the leading behavior in  $\lambda^{-2}$ , we only keep the terms in  $n_1 = n_2 = 0$ . Hence, we find a twofold Mellin-Barnes representation for the pentagon in multi-Regge kinematics,

$$I_5^D(1,1,1,1,1; Q_i^2) = r_\Gamma e^{\gamma_E \epsilon} \frac{(-\kappa)^{-\epsilon}}{s_1 s_2} \mathcal{I}^{(I)}(\kappa, t_1, t_2) \quad (\text{M.6})$$

with

$$\begin{aligned} \mathcal{I}^{(I)}(\kappa, t_1, t_2) &= \frac{-1}{\Gamma(1+\epsilon)\Gamma(1-\epsilon)^2} \frac{1}{(2\pi i)^2} \int_{-i\infty}^{+i\infty} dz_1 dz_2 x_1^{z_1} x_2^{z_2} \\ &\quad \times \Gamma(-\epsilon - z_1) \Gamma(-z_1) \\ &\quad \Gamma(-\epsilon - z_2) \\ &\quad \times \Gamma(-\epsilon - z_1 - z_2) \Gamma(-z_2) \Gamma(z_1 + z_2 + 1) \Gamma(\epsilon + z_1 + z_2 + 1)^2, \end{aligned} \quad (\text{M.7})$$

where  $x_1$  and  $x_2$  are defined in Eq. (11.14). The contours are taken following the usual Mellin-Barnes prescription, *i.e.*, the contour should separate the poles in  $\Gamma(\dots + z_i)$  from the poles in  $\Gamma(\dots - z_i)$ . Note that this expression is symmetric in  $x_1$  and  $x_2$ , as expected in Region I. We checked that if we close the integration contours to the right, and take residues, we reproduce exactly the expression of the pentagon obtained from NDIM, Eq. (11.39).

We evaluate the Mellin-Barnes representation (M.6) and we derive an Euler integral representation for the pentagon in multi-Regge kinematics. Let us concentrate only on the Mellin-Barnes integral. We start with the change of variable  $z_2 = z - z_1$  and we find

$$\begin{aligned} \mathcal{I}^{(I)}(\kappa, t_1, t_2) &= \frac{-1}{\Gamma(1+\epsilon)\Gamma(1-\epsilon)^2} \frac{1}{(2\pi i)^2} \int_{-i\infty}^{+i\infty} dz_1 dz x_1^{z_1} x_2^{z-z_1} \\ &\quad \times \Gamma(\epsilon + z + 1)^2 \Gamma(-\epsilon - z_1) \Gamma(-z_1) \Gamma(z_1 - z) \Gamma(-\epsilon - z + z_1) \\ &\quad \times \Gamma(-\epsilon - z) \Gamma(z + 1) \end{aligned} \quad (\text{M.8})$$

We now replace the Mellin-Barnes integral over  $z_1$  by an Euler integral by using the transformation formula,

$$\begin{aligned} & \frac{1}{2\pi i} \int_{-i\infty}^{+i\infty} dz_1 \Gamma(-z_1) \Gamma(c - z_1) \Gamma(b + z_1) \Gamma(a + z_1) X^{z_1} \\ &= \Gamma(a) \Gamma(b + c) \int_0^1 dv v^{b-1} (1-v)^{a+c-1} (1 - (1-X)v)^{-a}, \end{aligned} \quad (\text{M.9})$$

and we find

$$\begin{aligned} \mathcal{I}^{(I)}(\kappa, t_1, t_2) &= \frac{-1}{\Gamma(1+\epsilon)\Gamma(1-\epsilon)^2} \frac{1}{2\pi i} \int_{-i\infty}^{+i\infty} dz \int_0^1 dv x_2^z (1-v)^{-2\epsilon-z-1} \\ &\times v^{-z-1} \left(1 - v \left(1 - \frac{x_1}{x_2}\right)\right)^{\epsilon+z} \Gamma(-\epsilon-z)^3 \Gamma(z+1) \Gamma(\epsilon+z+1)^2. \end{aligned} \quad (\text{M.10})$$

To continue, we exchange the Euler and the Mellin-Barnes integration. Note that we must be careful when doing this, because some of the poles in  $z$  could be generated by the Euler integration. We checked numerically that in the present case the exchange of the two integrations is allowed and produces the same answer. We now close the  $z$ -contour to the right and take residues at  $z = n - \epsilon, n \in \mathbb{N}$ .

$$\begin{aligned} \mathcal{I}^{(I)}(\kappa, t_1, t_2) &= -\frac{x_2^{-\epsilon}}{2\Gamma(1+\epsilon)\Gamma(1-\epsilon)} \int_0^1 dv \sum_{n=0}^{\infty} \frac{(1-\epsilon)_n}{n!} (-x_2)^n \\ &\times v^{\epsilon-1-n} (1-v)^{-\epsilon-1-n} \left(1 - v \left(1 - \frac{x_1}{x_2}\right)\right)^n \\ &\times \left\{ \ln^2(1-v) + \ln^2 v + \ln^2 \left(1 - v \left(1 - \frac{x_1}{x_2}\right)\right) + \ln^2 x_2 + \psi(n+1)^2 \right. \\ &\quad + \pi^2 + 2 \ln(1-v) \ln v - 2 \ln(1-v) \ln \left(1 - v \left(1 - \frac{x_1}{x_2}\right)\right) \\ &\quad - 2 \ln v \ln \left(1 - v \left(1 - \frac{x_1}{x_2}\right)\right) - 2 \ln(1-v) \ln x_2 - 2 \ln v \ln x_2 \\ &\quad + 2 \ln \left(1 - v \left(1 - \frac{x_1}{x_2}\right)\right) \ln x_2 + 2 \ln(1-v) \psi(n+1) \\ &\quad \left. - 2 \ln \left(1 - v \left(1 - \frac{x_1}{x_2}\right)\right) \psi(n+1) - 2 \ln x_2 \psi(n+1) \right\} \end{aligned} \quad (\text{M.11})$$

$$\begin{aligned}
 & + \psi(-\epsilon + n + 1)^2 + 2 \ln v \psi(n + 1) - 2 \ln(1 - v) \psi(-\epsilon + n + 1) \\
 & - 2 \ln v \psi(-\epsilon + n + 1) + 2 \ln \left( 1 - v \left( 1 - \frac{x_1}{x_2} \right) \right) \psi(-\epsilon + n + 1) \\
 & + 2 \ln x_2 \psi(-\epsilon + n + 1) - 2 \psi(n + 1) \psi(-\epsilon + n + 1) - \psi^{(1)}(n + 1) \\
 & + \psi^{(1)}(-\epsilon + n + 1) \Big\}.
 \end{aligned}$$

To continue, we perform the  $\epsilon$ -expansion under the integration sign\*

$$\mathcal{I}^{(I)}(\kappa, t_1, t_2) = \mathcal{I}_0^{(I)}(x_1, x_2) + \epsilon \mathcal{I}_1^{(I)}(x_1, x_2) + \mathcal{O}(\epsilon^2). \tag{M.12}$$

We find

$$\mathcal{I}_0^{(I)}(x_1, x_2) = \int_0^1 dv \frac{i^{(0)}(x_1, x_2, v)}{v^2 - x_1 v + x_2 v - v - x_2}, \tag{M.13}$$

and

$$\mathcal{I}_1^{(I)}(x_1, x_2) = \int_0^1 dv \frac{i^{(1)}(x_1, x_2, v)}{v^2 + (-x_1 + x_2 - 1)v - x_2}. \tag{M.14}$$

where  $i^{(0)}$  and  $i^{(1)}$  are functions depending on (poly)logarithms of weight 2 and 3 respectively in  $x_1$ ,  $x_2$  and  $v$  (Since the expressions are quite long and do not add anything new to the discussion, we prefer to show them in Section M.3). Note that this implies that  $\mathcal{I}_0^{(I)}(x_1, x_2)$  and  $\mathcal{I}_1^{(I)}(x_1, x_2)$  will have uniform weight 3 and 4 respectively, as expected. Furthermore note that the poles in  $v = 0$  and  $v = 1$  have cancelled out. However, we still need to be careful with the quadratic polynomial in the denominator of the integrand, since it might vanish in the integration region. We analyze this situation in the rest of this section.

We know already that the phase space boundaries in Region I require

$$\sqrt{x_1} + \sqrt{x_2} < 1. \tag{M.15}$$

This subspace of the square  $[0, 1] \times [0, 1]$  is at the same time the domain of the integral  $\mathcal{I}(x_1, x_2; \epsilon)$ . We can divide this domain further into

---

\*Note that we must be careful when we do this, since the integrals might contain poles coming from the terms  $1/v(1 - v)$ . As we will see in the following however these poles are spurious and cancel out.

1. Region I(a):  $x_1 < x_2$ .
2. Region I(b):  $x_2 < x_1$ .

We now turn to the quadratic denominator in Eqs. (M.13) and (M.14). The roots of this quadratic polynomial are

$$\begin{aligned}\lambda_1 &\equiv \lambda_1(x_1, x_2) = \frac{1}{2} \left( 1 + x_1 - x_2 - \sqrt{\lambda_K} \right), \\ \lambda_2 &\equiv \lambda_1(x_1, x_2) = \frac{1}{2} \left( 1 + x_1 - x_2 + \sqrt{\lambda_K} \right),\end{aligned}\tag{M.16}$$

where  $\lambda_K$  denotes the Källén function

$$\lambda_K \equiv \lambda_K(x_1, x_2) = \lambda(x_1, x_2, -1) = 1 + x_1^2 + x_2^2 + 2x_1 + 2x_2 - 2x_1x_2.\tag{M.17}$$

First, let us note that  $\lambda_K(x_1, x_2) > 0$ ,  $\forall (x_1, x_2) \in [0, 1] \times [0, 1]$ , and hence the square root in Eq. (M.16) is well defined in the Region I. Second, it is easy to show that on the square  $[0, 1] \times [0, 1]$  we have,

$$-1 < \lambda_1(x_1, x_2) < 0 \quad \text{and} \quad 1 < \lambda_2(x_1, x_2) < 2.\tag{M.18}$$

For later convenience, let us note at this point the following useful identities

$$\begin{aligned}\lambda_1 \lambda_2 &= -x_2, \\ \lambda_1 + \lambda_2 &= 1 + x_1 - x_2, \\ \lambda_1 - \lambda_2 &= -\sqrt{\lambda_K}, \\ \left(1 - \frac{1}{\lambda_1}\right) \left(1 - \frac{1}{\lambda_2}\right) &= \frac{x_1}{x_2}.\end{aligned}\tag{M.19}$$

From Eq. (M.18) it follows now immediately that the quadratic denominators in Eqs. (M.13) and (M.14) do not vanish in the whole integration range  $[0, 1]$ , and hence all the integrals in Eqs. (M.13) and (M.14) are convergent. Using partial fractioning and the relations (M.19) we can write

$$\begin{aligned}\mathcal{I}_0^{(I)}(x_1, x_2) &= \frac{1}{\sqrt{\lambda_K}} \int_0^1 dv \frac{i^{(0)}(x_1, x_2, v)}{v - \lambda_2} - \frac{1}{\sqrt{\lambda_K}} \int_0^1 dv \frac{i^{(0)}(x_1, x_2, v)}{v - \lambda_1},\end{aligned}\tag{M.20}$$

and

$$\begin{aligned}\mathcal{I}_1^{(I)}(x_1, x_2) &= \frac{1}{\sqrt{\lambda_K}} \int_0^1 dv \frac{i^{(1)}(x_1, x_2, v)}{v - \lambda_2} - \frac{1}{\sqrt{\lambda_K}} \int_0^1 dv \frac{i^{(1)}(x_1, x_2, v)}{v - \lambda_1}.\end{aligned}\tag{M.21}$$



Let us introduce at this point the function

$$\lambda_3 \equiv \lambda_3(x_1, x_2) = \frac{x_2}{x_2 - x_1} = \frac{\lambda_1 \lambda_2}{\lambda_1 + \lambda_2 - 1}. \tag{M.22}$$

This function appears in  $i^{(0)}$  and  $i^{(1)}$  through the logarithm

$$\ln \left( 1 - v \left( 1 - \frac{x_1}{x_2} \right) \right) = \ln \left( 1 - \frac{v}{\lambda_3} \right) = \int_0^v \frac{dt}{t - \lambda_3}. \tag{M.23}$$

It is easy to see that this logarithm is well defined in Region I, since

1. In Region I(a),  $x_1 < x_2$ , and hence  $\lambda_3 > 1$ .
2. In Region I(b),  $x_2 < x_1$ , and hence  $\lambda_3 < 0$ .

Note however that  $\lambda_3$  diverges on the diagonal  $x_1 = x_2$ . This is not a contradiction since

$$\lim_{x_2 \rightarrow x_1} \int_0^v \frac{dt}{t - \lambda_3(x_1, x_2)} = \lim_{\lambda_3 \rightarrow \infty} \int_0^v \frac{dt}{t - \lambda_3} = 0, \tag{M.24}$$

in agreement with

$$\lim_{x_2 \rightarrow x_1} \ln \left( 1 - v \left( 1 - \frac{x_1}{x_2} \right) \right) = 0. \tag{M.25}$$

We now evaluate the integrals  $\mathcal{I}_0^{(I)}$  and  $\mathcal{I}_1^{(I)}$  explicitly. To this effect, let us introduce some generalized multiple polylogarithms defined by

$$G(a, \vec{w}; z) = \int_0^z dt f(a, t) G(\vec{w}; t), \tag{M.26}$$

where

$$f(a, t) = \frac{1}{t - a}. \tag{M.27}$$

If all indices are zero we define

$$G(\vec{0}_n; z) = \int_1^z \frac{dt}{t} G(\vec{0}_{n-1}; t) = \frac{1}{n!} \ln^n z. \tag{M.28}$$

In particular cases the  $G$ -functions reduce to ordinary logarithms and polylogarithms,

$$G(\vec{a}_n; z) = \frac{1}{n!} \ln^n \left( 1 - \frac{z}{a} \right), \quad G(\vec{0}_{n-1}, a; z) = -\text{Li}_n \left( \frac{z}{a} \right). \tag{M.29}$$

Note that these definitions are straightforward generalizations of the harmonic polylogarithms, and hence these functions inherit all the properties of the *HPL*'s. In particular they fulfill a shuffle algebra

$$G(\vec{w}_1; z) G(\vec{w}_2; z) = \sum_{\vec{w}=\vec{w}_1 \uplus \vec{w}_2} G(\vec{w}; z). \quad (\text{M.30})$$

If the weight vector  $\vec{w}$  has a parametric dependence on a second variable, then we obtain multidimensional harmonic polylogarithms. Finally, let us introduce the following other set of functions, which will be useful to write down the answer for the pentagon

$$M(\vec{w}) \equiv G(\vec{w}; 1). \quad (\text{M.31})$$

The  $M$ -functions defined in this way are in fact Goncharov's multiple polylogarithm (up to a sign) [108, 109]. For a more detailed discussions of these functions, and their relations to Goncharov's multiple polylogarithm, see Appendix G.4. It is clear from the definition that these functions form a shuffle algebra

$$M(\vec{w}_1) M(\vec{w}_2) = \sum_{\vec{w}=\vec{w}_1 \uplus \vec{w}_2} M(\vec{w}). \quad (\text{M.32})$$

Using these functions we can easily integrate  $\mathcal{I}_0^{(I)}$  and  $\mathcal{I}_1^{(I)}$ . We illustrate this procedure explicitly for the integral

$$\int_0^1 \frac{dv}{v - \lambda_1} \ln \left( v \left( \frac{x_1}{x_2} - 1 \right) + 1 \right) \ln(1 - v). \quad (\text{M.33})$$

First we can express all logarithms in terms of the  $G$ -functions we defined:

$$\begin{aligned} \ln \left( v \left( \frac{x_1}{x_2} - 1 \right) + 1 \right) \ln(1 - v) &= \ln \left( 1 - \frac{v}{\lambda_3} \right) \ln(1 - v) \\ &= G(\lambda_3; v) G(1; v) \\ &= G(\lambda_3, 1; v) + G(1, \lambda_3; v). \end{aligned} \quad (\text{M.34})$$

Then we get

$$\begin{aligned} &\int_0^1 \frac{dv}{v - \lambda_1} \ln \left( v \left( \frac{x_1}{x_2} - 1 \right) + 1 \right) \ln(1 - v) \\ &= \int_0^1 dv \frac{G(\lambda_3, 1; v)}{v - \lambda_1} + \int_0^1 dv \frac{G(1, \lambda_3; v)}{v - \lambda_1} \\ &= G(\lambda_1, \lambda_3, 1; 1) + G(\lambda_1, 1, \lambda_3; 1) \\ &= M(\lambda_1, \lambda_3, 1) + M(\lambda_1, 1, \lambda_3). \end{aligned} \quad (\text{M.35})$$

All other integrals can be performed in exactly the same way, and we can hence express  $\mathcal{I}_0^{(I)}$  as a combination of  $M$ -functions. We find

$$\begin{aligned} \mathcal{I}_0^{(I)}(x_1, x_2) = & \\ & \frac{1}{\sqrt{\lambda_K}} \left\{ \left( \frac{1}{2} \ln^2 x_2 + \frac{\pi^2}{2} \right) M(\lambda_1) + \left( -\frac{1}{2} \ln^2 x_2 - \frac{\pi^2}{2} \right) M(\lambda_2) - \ln x_2 M(\lambda_1, 0) - \right. \\ & \ln x_2 M(\lambda_1, 1) + \ln x_2 M(\lambda_1, \lambda_3) + \ln x_2 M(\lambda_2, 0) + \ln x_2 M(\lambda_2, 1) - \\ & \ln x_2 M(\lambda_2, \lambda_3) + M(\lambda_1, 0, 0) + M(\lambda_1, 0, 1) - M(\lambda_1, 0, \lambda_3) + M(\lambda_1, 1, 0) + \\ & M(\lambda_1, 1, 1) - M(\lambda_1, 1, \lambda_3) - M(\lambda_1, \lambda_3, 0) - M(\lambda_1, \lambda_3, 1) + M(\lambda_1, \lambda_3, \lambda_3) - \\ & M(\lambda_2, 0, 0) - M(\lambda_2, 0, 1) + M(\lambda_2, 0, \lambda_3) - M(\lambda_2, 1, 0) - M(\lambda_2, 1, 1) + \\ & \left. M(\lambda_2, 1, \lambda_3) + M(\lambda_2, \lambda_3, 0) + M(\lambda_2, \lambda_3, 1) - M(\lambda_2, \lambda_3, \lambda_3) \right\}. \end{aligned} \tag{M.36}$$

Note that this expression is of uniform weight 3, as expected.

The integration of  $\mathcal{I}_1^{(I)}$  can be done in a similar way as for  $\mathcal{I}_0^{(I)}$ . However, there is a slight complication. The function  $i^{(1)}$  contains polylogarithms of the form

$$\text{Li}_n \left( \frac{v(x_1 - x_2) + x_2}{v(v - 1)} \right). \tag{M.37}$$

In order to perform the integration in terms of  $G$ -functions, we have to express these functions in terms of objects of the form  $G(\dots; v)$ . In Appendix N.1 we show that the following identities hold:

$$\begin{aligned} \text{Li}_2 \left( \frac{v(x_1 - x_2) + x_2}{v(v - 1)} \right) = & \\ & -\frac{1}{2} \ln^2 x_1 + \ln x_2 \ln x_1 - \ln^2 x_2 - G(0, 0; v) - G(0, 1; v) + G(0, \lambda_1; v) + \\ & G(0, \lambda_2; v) - G(1, 0; v) - G(1, 1; v) + G(1, \lambda_1; v) + G(1, \lambda_2; v) + G(\lambda_3, 0; v) + \\ & G(\lambda_3, 1; v) - G(\lambda_3, \lambda_1; v) - G(\lambda_3, \lambda_2; v) + G(0; v) \ln x_2 + G(1; v) \ln x_2 - \\ & G(\lambda_3; v) \ln x_2 - M(0, \lambda_1) - M(0, \lambda_2) + M(\lambda_1, 1) + M(\lambda_2, 1) - M(\lambda_3, 0) - \\ & M(\lambda_3, 1) + M(\lambda_3, \lambda_1) + M(\lambda_3, \lambda_2) - \frac{\pi^2}{6}. \end{aligned} \tag{M.38}$$

$$\begin{aligned}
& \operatorname{Li}_3\left(\frac{v(x_1-x_2)+x_2}{v(v-1)}\right) = \\
& \left( \frac{1}{6} \ln^3 x_1 - \frac{1}{2} G(0; v) \ln^2 x_1 - \frac{1}{2} G(1; v) \ln^2 x_1 + \frac{1}{2} G(\lambda_3; v) \ln^2 x_1 - \right. \\
& \frac{1}{2} M(\lambda_3) \ln^2 x_1 + G(0; v) \ln x_2 \ln x_1 + G(1; v) \ln x_2 \ln x_1 - G(\lambda_3; v) \ln x_2 \ln x_1 + \\
& \ln x_2 M(\lambda_3) \ln x_1 + \frac{1}{6} \pi^2 \ln x_1 - G(0; v) \ln^2 x_2 - G(1; v) \ln^2 x_2 + \\
& G(\lambda_3; v) \ln^2 x_2 - \frac{1}{6} \pi^2 G(0; v) - \frac{1}{6} \pi^2 G(1; v) + \frac{1}{6} \pi^2 G(\lambda_3; v) - G(0, 0, 0; v) - \\
& G(0, 0, 1; v) + G(0, 0, \lambda_1; v) + G(0, 0, \lambda_2; v) - G(0, 1, 0; v) - G(0, 1, 1; v) + \\
& G(0, 1, \lambda_1; v) + G(0, 1, \lambda_2; v) + G(0, \lambda_3, 0; v) + G(0, \lambda_3, 1; v) - G(0, \lambda_3, \lambda_1; v) - \\
& G(0, \lambda_3, \lambda_2; v) - G(1, 0, 0; v) - G(1, 0, 1; v) + G(1, 0, \lambda_1; v) + G(1, 0, \lambda_2; v) - \\
& G(1, 1, 0; v) - G(1, 1, 1; v) + G(1, 1, \lambda_1; v) + G(1, 1, \lambda_2; v) + G(1, \lambda_3, 0; v) + \\
& G(1, \lambda_3, 1; v) - G(1, \lambda_3, \lambda_1; v) - G(1, \lambda_3, \lambda_2; v) + G(\lambda_3, 0, 0; v) + G(\lambda_3, 0, 1; v) - \\
& G(\lambda_3, 0, \lambda_1; v) - G(\lambda_3, 0, \lambda_2; v) + G(\lambda_3, 1, 0; v) + G(\lambda_3, 1, 1; v) - G(\lambda_3, 1, \lambda_1; v) - \\
& G(\lambda_3, 1, \lambda_2; v) - G(\lambda_3, \lambda_3, 0; v) - G(\lambda_3, \lambda_3, 1; v) + G(\lambda_3, \lambda_3, \lambda_1; v) + \\
& G(\lambda_3, \lambda_3, \lambda_2; v) + G(0, 0; v) \ln x_2 + G(0, 1; v) \ln x_2 - G(0, \lambda_3; v) \ln x_2 + \\
& G(1, 0; v) \ln x_2 + G(1, 1; v) \ln x_2 - G(1, \lambda_3; v) \ln x_2 - G(\lambda_3, 0; v) \ln x_2 - \\
& G(\lambda_3, 1; v) \ln x_2 + G(\lambda_3, \lambda_3; v) \ln x_2 - \ln^2 x_2 M(\lambda_3) - \frac{1}{6} \pi^2 M(\lambda_3) - \\
& G(0; v) M(0, \lambda_1) - G(1; v) M(0, \lambda_1) + G(\lambda_3; v) M(0, \lambda_1) - M(\lambda_3) M(0, \lambda_1) - \\
& G(0; v) M(0, \lambda_2) - G(1; v) M(0, \lambda_2) + G(\lambda_3; v) M(0, \lambda_2) - M(\lambda_3) M(0, \lambda_2) + \\
& \ln x_2 M(0, \lambda_3) + G(0; v) M(\lambda_1, 1) + G(1; v) M(\lambda_1, 1) - G(\lambda_3; v) M(\lambda_1, 1) + \\
& M(\lambda_3) M(\lambda_1, 1) + G(0; v) M(\lambda_2, 1) + G(1; v) M(\lambda_2, 1) - G(\lambda_3; v) M(\lambda_2, 1) + \\
& M(\lambda_3) M(\lambda_2, 1) - G(0; v) M(\lambda_3, 0) - G(1; v) M(\lambda_3, 0) + G(\lambda_3; v) M(\lambda_3, 0) + \\
& \ln x_2 M(\lambda_3, 0) - M(\lambda_3) M(\lambda_3, 0) - G(0; v) M(\lambda_3, 1) - G(1; v) M(\lambda_3, 1) + \\
& G(\lambda_3; v) M(\lambda_3, 1) - M(\lambda_3) M(\lambda_3, 1) + G(0; v) M(\lambda_3, \lambda_1) + G(1; v) M(\lambda_3, \lambda_1) - \\
& G(\lambda_3; v) M(\lambda_3, \lambda_1) + M(\lambda_3) M(\lambda_3, \lambda_1) + G(0; v) M(\lambda_3, \lambda_2) + \\
& G(1; v) M(\lambda_3, \lambda_2) - G(\lambda_3; v) M(\lambda_3, \lambda_2) + M(\lambda_3) M(\lambda_3, \lambda_2) - \ln x_2 M(\lambda_3, \lambda_3) - \\
& M(0, 0, \lambda_1) - M(0, 0, \lambda_2) + M(0, \lambda_1, 1) + M(0, \lambda_2, 1) - M(0, \lambda_3, 0) - \\
& M(0, \lambda_3, 1) + M(0, \lambda_3, \lambda_1) + M(0, \lambda_3, \lambda_2) - M(\lambda_1, 1, 1) - M(\lambda_2, 1, 1) - \\
& M(\lambda_3, 0, 0) + M(\lambda_3, 0, \lambda_1) + M(\lambda_3, 0, \lambda_2) + M(\lambda_3, 1, 1) - M(\lambda_3, \lambda_1, 1) - \\
& \left. M(\lambda_3, \lambda_2, 1) + M(\lambda_3, \lambda_3, 0) + M(\lambda_3, \lambda_3, 1) - M(\lambda_3, \lambda_3, \lambda_1) - M(\lambda_3, \lambda_3, \lambda_2) \right).
\end{aligned}
\tag{M.39}$$

Using these identities we can express  $i^{(1)}$  completely in terms of  $G$  and  $M$ -functions, and perform the integration in exactly the same way as for  $\mathcal{I}_0^{(I)}$ . The result is

$$\begin{aligned}
 \mathcal{I}_1^{(I)}(x_1, x_2) = & \hspace{20em} \text{(M.40)} \\
 & \frac{1}{\sqrt{\lambda_K}} \left\{ \left( \ln^2 x_2 + \frac{\pi^2}{6} \right) M(\lambda_1, 0) - \frac{5}{6} \pi^2 M(\lambda_1, 1) + \left( \frac{1}{2} \ln^2 x_2 + \frac{\pi^2}{2} \right) M(\lambda_1, \lambda_1) + \right. \\
 & \left( \frac{1}{2} \ln^2 x_2 + \frac{\pi^2}{2} \right) M(\lambda_1, \lambda_2) + \left( -\frac{1}{2} \ln^2 x_1 + \ln x_2 \ln x_1 - 2 \ln^2 x_2 - \frac{\pi^2}{3} \right) M(\lambda_1, \lambda_3) + \\
 & \left( -\ln^2 x_2 - \frac{\pi^2}{6} \right) M(\lambda_2, 0) + \frac{5}{6} \pi^2 M(\lambda_2, 1) + \left( -\frac{1}{2} \ln^2 x_2 - \frac{\pi^2}{2} \right) M(\lambda_2, \lambda_1) + \\
 & \left( -\frac{1}{2} \ln^2 x_2 - \frac{\pi^2}{2} \right) M(\lambda_2, \lambda_2) + \left( \frac{1}{2} \ln^2 x_1 - \ln x_2 \ln x_1 + 2 \ln^2 x_2 + \frac{\pi^2}{3} \right) M(\lambda_2, \lambda_3) + \\
 & \left( -\frac{1}{2} \ln^2 x_1 + \ln x_2 \ln x_1 - \ln^2 x_2 - \frac{\pi^2}{6} \right) M(\lambda_3, \lambda_1) + \\
 & \left( \frac{1}{2} \ln^2 x_1 - \ln x_2 \ln x_1 + \ln^2 x_2 + \frac{\pi^2}{6} \right) M(\lambda_3, \lambda_2) - 2 \ln x_2 M(0, \lambda_1, \lambda_1) + \\
 & \ln x_2 M(0, \lambda_1, \lambda_3) + 2 \ln x_2 M(0, \lambda_2, \lambda_2) - \ln x_2 M(0, \lambda_2, \lambda_3) + \\
 & \ln x_2 M(0, \lambda_3, \lambda_1) - \ln x_2 M(0, \lambda_3, \lambda_2) - 2 \ln x_2 M(\lambda_1, 0, 0) - \ln x_2 M(\lambda_1, 0, \lambda_1) - \\
 & \ln x_2 M(\lambda_1, 0, \lambda_2) + 2 \ln x_2 M(\lambda_1, 0, \lambda_3) + 2 \ln x_2 M(\lambda_1, 1, 1) + \\
 & \ln x_2 M(\lambda_1, 1, \lambda_1) - \ln x_2 M(\lambda_1, 1, \lambda_2) - \ln x_2 M(\lambda_1, 1, \lambda_3) - \ln x_2 M(\lambda_1, \lambda_1, 0) + \\
 & \ln x_2 M(\lambda_1, \lambda_1, 1) + \ln x_2 M(\lambda_1, \lambda_1, \lambda_3) - \ln x_2 M(\lambda_1, \lambda_2, 0) - \ln x_2 M(\lambda_1, \lambda_2, 1) + \\
 & \ln x_2 M(\lambda_1, \lambda_2, \lambda_3) + 2 \ln x_2 M(\lambda_1, \lambda_3, 0) - \ln x_2 M(\lambda_1, \lambda_3, 1) + \\
 & \ln x_2 M(\lambda_1, \lambda_3, \lambda_1) + \ln x_2 M(\lambda_1, \lambda_3, \lambda_2) - 2 \ln x_2 M(\lambda_1, \lambda_3, \lambda_3) + \\
 & 2 \ln x_2 M(\lambda_2, 0, 0) + \ln x_2 M(\lambda_2, 0, \lambda_1) + \ln x_2 M(\lambda_2, 0, \lambda_2) - 2 \ln x_2 M(\lambda_2, 0, \lambda_3) - \\
 & 2 \ln x_2 M(\lambda_2, 1, 1) + \ln x_2 M(\lambda_2, 1, \lambda_1) - \ln x_2 M(\lambda_2, 1, \lambda_2) + \ln x_2 M(\lambda_2, 1, \lambda_3) + \\
 & \ln x_2 M(\lambda_2, \lambda_1, 0) + \ln x_2 M(\lambda_2, \lambda_1, 1) - \ln x_2 M(\lambda_2, \lambda_1, \lambda_3) + \ln x_2 M(\lambda_2, \lambda_2, 0) - \\
 & \ln x_2 M(\lambda_2, \lambda_2, 1) - \ln x_2 M(\lambda_2, \lambda_2, \lambda_3) - 2 \ln x_2 M(\lambda_2, \lambda_3, 0) + \\
 & \ln x_2 M(\lambda_2, \lambda_3, 1) - \ln x_2 M(\lambda_2, \lambda_3, \lambda_1) - \ln x_2 M(\lambda_2, \lambda_3, \lambda_2) + \\
 & 2 \ln x_2 M(\lambda_2, \lambda_3, \lambda_3) - \ln x_2 M(\lambda_3, 1, \lambda_1) + \ln x_2 M(\lambda_3, 1, \lambda_2) - \\
 & \ln x_2 M(\lambda_3, \lambda_1, 1) + 2 \ln x_2 M(\lambda_3, \lambda_1, \lambda_1) - \ln x_2 M(\lambda_3, \lambda_1, \lambda_3) + \\
 & \ln x_2 M(\lambda_3, \lambda_2, 1) - 2 \ln x_2 M(\lambda_3, \lambda_2, \lambda_2) + \ln x_2 M(\lambda_3, \lambda_2, \lambda_3) - \\
 & \ln x_2 M(\lambda_3, \lambda_3, \lambda_1) + \ln x_2 M(\lambda_3, \lambda_3, \lambda_2) - 2M(0, 0, \lambda_1, \lambda_1) + 2M(0, 0, \lambda_2, \lambda_2) - \\
 & M(0, \lambda_1, 0, \lambda_1) - M(0, \lambda_1, 0, \lambda_2) + M(0, \lambda_1, 1, \lambda_1) - M(0, \lambda_1, 1, \lambda_2) + \\
 & 2M(0, \lambda_1, \lambda_1, 1) - 2M(0, \lambda_1, \lambda_1, \lambda_3) - M(0, \lambda_1, \lambda_3, 0) - M(0, \lambda_1, \lambda_3, 1) - \\
 & M(0, \lambda_1, \lambda_3, \lambda_1) + M(0, \lambda_1, \lambda_3, \lambda_2) + M(0, \lambda_2, 0, \lambda_1) + M(0, \lambda_2, 0, \lambda_2) +
 \end{aligned}$$

$$\begin{aligned}
& M(0, \lambda_2, 1, \lambda_1) - M(0, \lambda_2, 1, \lambda_2) - 2M(0, \lambda_2, \lambda_2, 1) + 2M(0, \lambda_2, \lambda_2, \lambda_3) + \\
& M(0, \lambda_2, \lambda_3, 0) + M(0, \lambda_2, \lambda_3, 1) - M(0, \lambda_2, \lambda_3, \lambda_1) + M(0, \lambda_2, \lambda_3, \lambda_2) - \\
& M(0, \lambda_3, 0, \lambda_1) + M(0, \lambda_3, 0, \lambda_2) - M(0, \lambda_3, 1, \lambda_1) + M(0, \lambda_3, 1, \lambda_2) - \\
& M(0, \lambda_3, \lambda_1, 0) - M(0, \lambda_3, \lambda_1, 1) + M(0, \lambda_3, \lambda_2, 0) + M(0, \lambda_3, \lambda_2, 1) + \\
& 2M(\lambda_1, 0, 0, 0) - M(\lambda_1, 0, 0, \lambda_1) - M(\lambda_1, 0, 0, \lambda_2) - M(\lambda_1, 0, 0, \lambda_3) - \\
& 2M(\lambda_1, 0, 1, 1) + M(\lambda_1, 0, 1, \lambda_3) + M(\lambda_1, 0, \lambda_1, 1) - M(\lambda_1, 0, \lambda_1, \lambda_3) + \\
& M(\lambda_1, 0, \lambda_2, 1) - M(\lambda_1, 0, \lambda_2, \lambda_3) - 2M(\lambda_1, 0, \lambda_3, 0) - 2M(\lambda_1, 1, 0, 1) + \\
& M(\lambda_1, 1, 0, \lambda_3) - 2M(\lambda_1, 1, 1, 0) - 4M(\lambda_1, 1, 1, 1) - M(\lambda_1, 1, 1, \lambda_1) + \\
& M(\lambda_1, 1, 1, \lambda_2) + 3M(\lambda_1, 1, 1, \lambda_3) - M(\lambda_1, 1, \lambda_1, 1) + M(\lambda_1, 1, \lambda_1, \lambda_3) + \\
& M(\lambda_1, 1, \lambda_2, 1) - M(\lambda_1, 1, \lambda_2, \lambda_3) + M(\lambda_1, 1, \lambda_3, 0) + 3M(\lambda_1, 1, \lambda_3, 1) + \\
& M(\lambda_1, 1, \lambda_3, \lambda_1) - M(\lambda_1, 1, \lambda_3, \lambda_2) - 2M(\lambda_1, 1, \lambda_3, \lambda_3) + M(\lambda_1, \lambda_1, 0, 0) + \\
& M(\lambda_1, \lambda_1, 0, 1) - M(\lambda_1, \lambda_1, 0, \lambda_3) + M(\lambda_1, \lambda_1, 1, 0) - M(\lambda_1, \lambda_1, 1, 1) + \\
& M(\lambda_1, \lambda_1, 1, \lambda_3) - M(\lambda_1, \lambda_1, \lambda_3, 0) + M(\lambda_1, \lambda_1, \lambda_3, 1) + M(\lambda_1, \lambda_1, \lambda_3, \lambda_3) + \\
& M(\lambda_1, \lambda_2, 0, 0) + M(\lambda_1, \lambda_2, 0, 1) - M(\lambda_1, \lambda_2, 0, \lambda_3) + M(\lambda_1, \lambda_2, 1, 0) + \\
& M(\lambda_1, \lambda_2, 1, 1) - M(\lambda_1, \lambda_2, 1, \lambda_3) - M(\lambda_1, \lambda_2, \lambda_3, 0) - M(\lambda_1, \lambda_2, \lambda_3, 1) + \\
& M(\lambda_1, \lambda_2, \lambda_3, \lambda_3) - 3M(\lambda_1, \lambda_3, 0, 0) + 3M(\lambda_1, \lambda_3, 1, 1) + M(\lambda_1, \lambda_3, 1, \lambda_1) - \\
& M(\lambda_1, \lambda_3, 1, \lambda_2) - 2M(\lambda_1, \lambda_3, 1, \lambda_3) + M(\lambda_1, \lambda_3, \lambda_1, 1) + M(\lambda_1, \lambda_3, \lambda_1, \lambda_3) - \\
& M(\lambda_1, \lambda_3, \lambda_2, 1) + M(\lambda_1, \lambda_3, \lambda_2, \lambda_3) - 2M(\lambda_1, \lambda_3, \lambda_3, 1) + M(\lambda_1, \lambda_3, \lambda_3, \lambda_1) + \\
& M(\lambda_1, \lambda_3, \lambda_3, \lambda_2) - 2M(\lambda_2, 0, 0, 0) + M(\lambda_2, 0, 0, \lambda_1) + M(\lambda_2, 0, 0, \lambda_2) + \\
& M(\lambda_2, 0, 0, \lambda_3) + 2M(\lambda_2, 0, 1, 1) - M(\lambda_2, 0, 1, \lambda_3) - M(\lambda_2, 0, \lambda_1, 1) + \\
& M(\lambda_2, 0, \lambda_1, \lambda_3) - M(\lambda_2, 0, \lambda_2, 1) + M(\lambda_2, 0, \lambda_2, \lambda_3) + 2M(\lambda_2, 0, \lambda_3, 0) + \\
& 2M(\lambda_2, 1, 0, 1) - M(\lambda_2, 1, 0, \lambda_3) + 2M(\lambda_2, 1, 1, 0) + 4M(\lambda_2, 1, 1, 1) - \\
& M(\lambda_2, 1, 1, \lambda_1) + M(\lambda_2, 1, 1, \lambda_2) - 3M(\lambda_2, 1, 1, \lambda_3) - M(\lambda_2, 1, \lambda_1, 1) + \\
& M(\lambda_2, 1, \lambda_1, \lambda_3) + M(\lambda_2, 1, \lambda_2, 1) - M(\lambda_2, 1, \lambda_2, \lambda_3) - M(\lambda_2, 1, \lambda_3, 0) - \\
& 3M(\lambda_2, 1, \lambda_3, 1) + M(\lambda_2, 1, \lambda_3, \lambda_1) - M(\lambda_2, 1, \lambda_3, \lambda_2) + 2M(\lambda_2, 1, \lambda_3, \lambda_3) - \\
& M(\lambda_2, \lambda_1, 0, 0) - M(\lambda_2, \lambda_1, 0, 1) + M(\lambda_2, \lambda_1, 0, \lambda_3) - M(\lambda_2, \lambda_1, 1, 0) - \\
& M(\lambda_2, \lambda_1, 1, 1) + M(\lambda_2, \lambda_1, 1, \lambda_3) + M(\lambda_2, \lambda_1, \lambda_3, 0) + M(\lambda_2, \lambda_1, \lambda_3, 1) - \\
& M(\lambda_2, \lambda_1, \lambda_3, \lambda_3) - M(\lambda_2, \lambda_2, 0, 0) - M(\lambda_2, \lambda_2, 0, 1) + M(\lambda_2, \lambda_2, 0, \lambda_3) - \\
& M(\lambda_2, \lambda_2, 1, 0) + M(\lambda_2, \lambda_2, 1, 1) - M(\lambda_2, \lambda_2, 1, \lambda_3) + M(\lambda_2, \lambda_2, \lambda_3, 0) - \\
& M(\lambda_2, \lambda_2, \lambda_3, 1) - M(\lambda_2, \lambda_2, \lambda_3, \lambda_3) + 3M(\lambda_2, \lambda_3, 0, 0) - 3M(\lambda_2, \lambda_3, 1, 1) + \\
& M(\lambda_2, \lambda_3, 1, \lambda_1) - M(\lambda_2, \lambda_3, 1, \lambda_2) + 2M(\lambda_2, \lambda_3, 1, \lambda_3) + M(\lambda_2, \lambda_3, \lambda_1, 1) - \\
& M(\lambda_2, \lambda_3, \lambda_1, \lambda_3) - M(\lambda_2, \lambda_3, \lambda_2, 1) - M(\lambda_2, \lambda_3, \lambda_2, \lambda_3) + 2M(\lambda_2, \lambda_3, \lambda_3, 1) - \\
& M(\lambda_2, \lambda_3, \lambda_3, \lambda_1) - M(\lambda_2, \lambda_3, \lambda_3, \lambda_2) - M(\lambda_3, 0, 0, \lambda_1) + M(\lambda_3, 0, 0, \lambda_2) - \\
& M(\lambda_3, 0, \lambda_1, 0) - M(\lambda_3, 0, \lambda_1, \lambda_3) + M(\lambda_3, 0, \lambda_2, 0) + M(\lambda_3, 0, \lambda_2, \lambda_3) -
\end{aligned}$$

$$\begin{aligned}
 &M(\lambda_3, 0, \lambda_3, \lambda_1) + M(\lambda_3, 0, \lambda_3, \lambda_2) + M(\lambda_3, 1, 1, \lambda_1) - M(\lambda_3, 1, 1, \lambda_2) + \\
 &M(\lambda_3, 1, \lambda_1, 1) - M(\lambda_3, 1, \lambda_1, \lambda_3) - M(\lambda_3, 1, \lambda_2, 1) + M(\lambda_3, 1, \lambda_2, \lambda_3) - \\
 &M(\lambda_3, 1, \lambda_3, \lambda_1) + M(\lambda_3, 1, \lambda_3, \lambda_2) - M(\lambda_3, \lambda_1, 0, 0) - M(\lambda_3, \lambda_1, 0, \lambda_3) + \\
 &M(\lambda_3, \lambda_1, 1, 1) - M(\lambda_3, \lambda_1, 1, \lambda_3) + 2M(\lambda_3, \lambda_1, \lambda_1, \lambda_3) - M(\lambda_3, \lambda_1, \lambda_3, 0) - \\
 &M(\lambda_3, \lambda_1, \lambda_3, 1) + 2M(\lambda_3, \lambda_1, \lambda_3, \lambda_1) + M(\lambda_3, \lambda_2, 0, 0) + M(\lambda_3, \lambda_2, 0, \lambda_3) - \\
 &M(\lambda_3, \lambda_2, 1, 1) + M(\lambda_3, \lambda_2, 1, \lambda_3) - 2M(\lambda_3, \lambda_2, \lambda_2, \lambda_3) + M(\lambda_3, \lambda_2, \lambda_3, 0) + \\
 &M(\lambda_3, \lambda_2, \lambda_3, 1) - 2M(\lambda_3, \lambda_2, \lambda_3, \lambda_2) - M(\lambda_3, \lambda_3, 0, \lambda_1) + M(\lambda_3, \lambda_3, 0, \lambda_2) - \\
 &M(\lambda_3, \lambda_3, 1, \lambda_1) + M(\lambda_3, \lambda_3, 1, \lambda_2) - M(\lambda_3, \lambda_3, \lambda_1, 0) - M(\lambda_3, \lambda_3, \lambda_1, 1) + \\
 &2M(\lambda_3, \lambda_3, \lambda_1, \lambda_1) + M(\lambda_3, \lambda_3, \lambda_2, 0) + M(\lambda_3, \lambda_3, \lambda_2, 1) - 2M(\lambda_3, \lambda_3, \lambda_2, \lambda_2) + \\
 &M(\lambda_2) \left( -\frac{1}{6} \ln^3 x_1 + \frac{1}{2} \ln x_2 \ln^2 x_1 - \ln^2 x_2 \ln x_1 - \frac{1}{6} \pi^2 \ln x_1 + \ln^3 x_2 + \right. \\
 &\left. \frac{1}{3} \pi^2 \ln x_2 - \zeta_3 \right) + M(\lambda_1) \left( \frac{1}{6} \ln^3 x_1 - \frac{1}{2} \ln x_2 \ln^2 x_1 + \ln^2 x_2 \ln x_1 + \frac{1}{6} \pi^2 \ln x_1 - \right. \\
 &\left. \ln^3 x_2 - \frac{1}{3} \pi^2 \ln x_2 + \zeta_3 \right) \Bigg\}.
 \end{aligned}$$

Note that  $\mathcal{I}_1^{(I)}$  is of uniform weight 4, as expected.

## M.2 Evaluation of the Mellin-Barnes integral in Region II

In this section we evaluate the pentagon in Region II. Since the Regions II(a) and II(b) are related simply by  $x_1 \leftrightarrow x_2$ , we only concentrate on Region II(a). The procedure is very similar to Region I, *i.e.* we start by deriving a twofold Mellin-Barnes representation for the pentagon in this region, which we then reduce to an Euler-type integral, and finally we express the result in terms of Goncharov’s multiple polylogarithms. Performing this rescaling (11.6) in the Mellin-Barnes representation (M.2) and after the change of variable

$$\begin{aligned}
 z_3 &\rightarrow z' - z_1 - z_2, \\
 z_4 &\rightarrow -z - 2z' + z_1,
 \end{aligned} \tag{M.41}$$

we find

$$\begin{aligned}
I_5^D(1, 1, 1, 1, 1; Q_i^2) &= \frac{-e^{\gamma_E \epsilon} (-s)^{-\epsilon-2}}{\Gamma(1-2\epsilon)} \frac{1}{(2\pi i)^4} \int_{-i\infty}^{+i\infty} dz dz' dz_1 dz_2 \\
&\times \left(\frac{s_1}{s}\right)^{-z-2z'+z_1} \left(\frac{s_2}{s}\right)^{z_1} \left(\frac{t_1}{s}\right)^{z_2} \left(\frac{t_2}{s}\right)^{-z_1-z_2+z'} \lambda^{-z} \\
&\times \Gamma(-z_1) \Gamma(-z_2) \Gamma(z_1+z_2+1) \Gamma(-\epsilon-z'-1) \Gamma(\epsilon-z+z_1-z'+2) \\
&\times \Gamma(-z-z_2-z'+1) \Gamma(z_1+z_2-z') \Gamma(-\epsilon+z+z'-1) \Gamma(-z_1+z'+1) \\
&\times \Gamma(z+z_1+2z_2+2(-z_1-z_2+z')).
\end{aligned} \tag{M.42}$$

We think of the integration over  $z$  as the last one, and we analyze how poles in  $\Gamma(\dots+z)$  with leading behavior  $\lambda^{-2}$  might arise. There is only one possibility, coming from the product  $\Gamma(-\epsilon-z'-1) \Gamma(-\epsilon+z+z'-1)$ . Taking the residues at  $z' = -1 - \epsilon + n'$ ,  $n' \in \mathbb{N}$ , we find

$$\lambda^{-z} \Gamma(-\epsilon+z+z'-1) \rightarrow \lambda^{-z} \Gamma(-2\epsilon-2+z+n'). \tag{M.43}$$

Taking the residues at  $z = 2 + 2\epsilon - n - v'$ ,  $n \in \mathbb{N}$ , we find

$$\lambda^z \Gamma(-2\epsilon-2+z+n') \rightarrow \lambda^{-2-2\epsilon+n+n'}. \tag{M.44}$$

Since we are only interested in the leading behavior in  $\lambda^{-2}$ , we only keep the terms in  $n = n' = 0$ . Hence, we find a twofold Mellin-Barnes representation for the pentagon in multi-Regge kinematics,

$$I_5^D(1, 1, 1, 1, 1; Q_i^2) = r_\Gamma e^{\gamma_E \epsilon} \frac{(-\kappa)^{-\epsilon}}{st_2} \mathcal{I}^{(IIa)}(\kappa, t_1, t_2) \tag{M.45}$$

with

$$\begin{aligned}
\mathcal{I}^{(IIa)}(\kappa, t_1, t_2) &= \frac{-y_1^\epsilon}{\Gamma(1+\epsilon)\Gamma(1-\epsilon)^2} \frac{1}{(2\pi i)^2} \int_{-i\infty}^{+i\infty} dz_1 dz_2 y_1^{z_1} y_2^{z_2} \\
&\times \Gamma(-\epsilon-z_1) \Gamma(-z_1)^2 \Gamma(z_1+1) \Gamma(-\epsilon-z_2) \Gamma(-z_2) \\
&\times \Gamma(z_1+z_2+1) \Gamma(\epsilon+z_1+z_2+1),
\end{aligned} \tag{M.46}$$

where  $y_1$  and  $y_2$  are defined in Eq. (11.18). The contours are taken following the usual Mellin-Barnes prescription, *i.e.*, the contour should separate the poles in  $\Gamma(\dots+z_i)$  from the poles in  $\Gamma(\dots-z_i)$ . We checked that if we close



the integration contours to the right, and take residues, we reproduce exactly the expression of the pentagon obtained from NDIM, Eq. (11.22).

We now evaluate the Mellin-Barnes representation (M.45) and we derive an Euler integral representation for the pentagon in multi-Regge kinematics. Let us concentrate only on the Mellin-Barnes integral. We can now use the identity (M.9), and we checked again numerically that we can exchange the Euler and the Mellin-Barnes integration. We find

$$\begin{aligned} \mathcal{I}^{(IIa)}(\kappa, t_1, t_2) &= \frac{-y_1^\epsilon}{\Gamma(1+\epsilon)\Gamma(1-\epsilon)^2} \frac{1}{2\pi i} \int_0^1 dv \int_{-i\infty}^{+i\infty} dz_1 (1-v)^{z_1-\epsilon} v^{\epsilon+z_1} \\ &\quad \times y_1^{z_1} (1-v(1-y_2))^{-z_1-1} \Gamma(-\epsilon-z_1) \Gamma(-z_1)^2 \Gamma(z_1+1)^3. \end{aligned} \tag{M.47}$$

Finally, we close the  $z_1$ -contour to the right and take residues at  $z_1 = n_1 - \epsilon, n_1 \in \mathbb{N}$ . As in the case of  $\mathcal{I}^{(I)}$ , we can sum up the series of residues and expand the integrand in a power series in  $\epsilon$ ,

$$\mathcal{I}^{(IIa)}(\kappa, t_1, t_2) = \mathcal{I}_0^{(IIa)}(y_1, y_2) + \epsilon \mathcal{I}_1^{(IIa)}(y_1, y_2) + \mathcal{O}(\epsilon^2). \tag{M.48}$$

We find

$$\mathcal{I}_0^{(IIa)}(y_1, y_2) = \int_0^1 dv \frac{j^{(0)}(y_1, y_2, v)}{(y_1 v^2 - y_1 v - y_2 v + v - 1)}, \tag{M.49}$$

and

$$\mathcal{I}_1^{(IIa)}(y_1, y_2) = \int_0^1 dv \frac{j^{(1)}(y_1, y_2, v)}{(y_1 v^2 - y_1 v - y_2 v + v - 1)}. \tag{M.50}$$

where  $j^{(0)}$  and  $j^{(1)}$  are functions depending on (poly)logarithms of weight 2 and 3 respectively in  $y_1, y_2$  and  $v$  (See Section M.4). Note that this implies that  $\mathcal{I}_0^{(IIa)}(y_1, y_2)$  and  $\mathcal{I}_1^{(IIa)}(y_1, y_2)$  will have uniform weight 3 and 4 respectively, as expected. Furthermore note that the poles in  $v = 0$  and  $v = 1$  have cancelled out. We need however still to be careful with the quadratic polynomial in the denominator of the integrand, since it might vanish in the integration region. We will analyze this situation in the rest of this section.

We know already that the phase space boundaries in Region II(a) require

$$-\sqrt{x_1} + \sqrt{x_2} > 1. \tag{M.51}$$

Since this implies  $x_2 > 1$  and  $x_2 > x_1$ , we get from Eq. (11.18) that  $0 < y_1, y_2 < 1$ . We now turn to the quadratic denominator in Eqs. (M.49) and (M.50). The roots of this quadratic polynomial are

$$\begin{aligned}\lambda'_1 &\equiv \lambda'_1(y_1, y_2) = \frac{1}{2y_1} \left( -1 + y_1 + y_2 - \sqrt{\lambda'_K} \right), \\ \lambda'_2 &\equiv \lambda'_1(y_1, y_2) = \frac{1}{2y_1} \left( -1 + y_1 + y_2 + \sqrt{\lambda'_K} \right),\end{aligned}\tag{M.52}$$

where  $\lambda'_K$  denotes the Källén function

$$\lambda'_K \equiv \lambda'_K(y_1, y_2) = \lambda(-y_1, y_2, 1) = 1 + y_1^2 + y_2^2 + 2y_1 - 2y_2 + 2y_1y_2.\tag{M.53}$$

First, let us note that  $\lambda'_K(y_1, y_2) > 0$  everywhere in Region II(a), and hence the square root in Eq. (M.52) is well-defined. Second, it is easy to show that we have,

$$-1 < \lambda'_1(y_1, y_2) < 0 \quad \text{and} \quad 1 < \lambda'_2(y_1, y_2) < 2.\tag{M.54}$$

For later convenience, let us note at this point the following useful identities

$$\begin{aligned}\lambda'_1 \lambda'_2 &= \frac{-1}{y_2}, \\ \lambda'_1 + \lambda'_2 &= \frac{-1 + y_1 - y_2}{y_1}, \\ \lambda'_1 - \lambda'_2 &= -\frac{\sqrt{\lambda'_K}}{y_1}, \\ \left(1 - \frac{1}{\lambda'_1}\right) \left(1 - \frac{1}{\lambda'_2}\right) &= y_2.\end{aligned}\tag{M.55}$$

From Eq. (M.54) it follows now immediately that the quadratic denominators in Eqs. (M.49) and (M.50) do not vanish in the whole integration  $v \in [0, 1]$ , and hence all the integrals in Eqs. (M.49) and (M.50) are convergent. Using partial fractioning and the relations (M.55) we can write

$$\begin{aligned}\mathcal{I}_0^{(IIa)}(y_1, y_2) &= \frac{-1}{\sqrt{\lambda'_K}} \int_0^1 dv \frac{j^{(0)}(y_1, y_2, v)}{v - \lambda_2} + \frac{1}{\sqrt{\lambda'_K}} \int_0^1 dv \frac{j^{(0)}(y_1, y_2, v)}{v - \lambda_1},\end{aligned}\tag{M.56}$$

and

$$\begin{aligned}\mathcal{I}_1^{(IIa)}(y_1, y_2) &= \frac{-1}{\sqrt{\lambda'_K}} \int_0^1 dv \frac{j^{(1)}(y_1, y_2, v)}{v - \lambda_2} + \frac{1}{\sqrt{\lambda'_K}} \int_0^1 dv \frac{j^{(1)}(y_1, y_2, v)}{v - \lambda_1}.\end{aligned}\tag{M.57}$$

Let us conclude this section by introducing the function

$$\lambda'_3 \equiv \lambda'_3(y_1, y_2) = \frac{1}{1 - y_2} = \frac{1}{1 - t_1/t_2} = \lambda_3. \tag{M.58}$$

This function appears in  $j^{(0)}$  and  $j^{(1)}$  through the logarithm

$$\ln(1 - v(1 - y_2)) = \ln\left(1 - \frac{v}{\lambda'_3}\right) = \int_0^v \frac{dt}{t - \lambda'_3}. \tag{M.59}$$

We now evaluate the integrals  $\mathcal{I}_0^{(IIa)}$  and  $\mathcal{I}_1^{(IIa)}$  explicitly. For  $\mathcal{I}_0^{(IIa)}$ , we find

$$\begin{aligned} \mathcal{I}_0^{(IIa)}(y_1, y_2) = & \\ & \frac{1}{\sqrt{\lambda'_k}} \left\{ \left( -\frac{1}{2} \ln^2 y_1 - \frac{\pi^2}{2} \right) M(\lambda'_1) + \left( \frac{1}{2} \ln^2 y_1 + \frac{\pi^2}{2} \right) M(\lambda'_2) - \ln y_1 M(\lambda'_1, 0) - \right. \\ & \ln y_1 M(\lambda'_1, 1) + \ln y_1 M(\lambda'_1, \lambda'_3) + \ln y_1 M(\lambda'_2, 0) + \ln y_1 M(\lambda'_2, 1) - \\ & \ln y_1 M(\lambda'_2, \lambda'_3) - M(\lambda'_1, 0, 0) - M(\lambda'_1, 0, 1) + M(\lambda'_1, 0, \lambda'_3) - M(\lambda'_1, 1, 0) - \\ & M(\lambda'_1, 1, 1) + M(\lambda'_1, 1, \lambda'_3) + M(\lambda'_1, \lambda'_3, 0) + M(\lambda'_1, \lambda'_3, 1) - M(\lambda'_1, \lambda'_3, \lambda'_3) + \\ & M(\lambda'_2, 0, 0) + M(\lambda'_2, 0, 1) - M(\lambda'_2, 0, \lambda'_3) + M(\lambda'_2, 1, 0) + M(\lambda'_2, 1, 1) - \\ & \left. M(\lambda'_2, 1, \lambda'_3) - M(\lambda'_2, \lambda'_3, 0) - M(\lambda'_2, \lambda'_3, 1) + M(\lambda'_2, \lambda'_3, \lambda'_3) \right\}. \end{aligned} \tag{M.60}$$

Note that this expression is of uniform weight 3, as expected.

The integration of  $\mathcal{I}_1^{(IIa)}$  can be done in a similar way as for  $\mathcal{I}_0^{(IIa)}$ . However, there is again a slight complication. The function  $j^{(1)}$  contains polylogarithms of the form

$$\text{Li}_n\left(\frac{y_2 v - v + 1}{v(v-1)y_1}\right). \tag{M.61}$$

In order to perform the integration in terms of  $G$ -functions, we have to express these functions in terms of objects of the form  $G(\dots; v)$ . In Appendix N.2 we show that the following identities hold:

$$\text{Li}_2\left(\frac{y_2 v - v + 1}{v(v-1)y_1}\right) = \tag{M.62}$$

$$\begin{aligned}
& -\frac{1}{2} \ln^2 \left( \frac{y_2}{y_1} \right) - G(0, 0; v) - G(0, 1; v) - G(0, \lambda'_1; 1) + G(0, \lambda'_1; v) - G(0, \lambda'_2; 1) + \\
& G(0, \lambda'_2; v) - G(1, 0; v) - G(1, 1; v) + G(1, \lambda'_1; v) + G(1, \lambda'_2; v) + G(\lambda'_1, 1; 1) + \\
& G(\lambda'_2, 1; 1) - G(\lambda'_3, 0; 1) + G(\lambda'_3, 0; v) - G(\lambda'_3, 1; 1) + G(\lambda'_3, 1; v) + \\
& G(\lambda'_3, \lambda'_1; 1) - G(\lambda'_3, \lambda'_1; v) + G(\lambda'_3, \lambda'_2; 1) - G(\lambda'_3, \lambda'_2; v) - G(0; v) \ln y_1 - \\
& G(1; v) \ln y_1 + G(\lambda'_3; v) \ln y_1 - \ln y_1 \ln y_2 - \frac{\pi^2}{6}.
\end{aligned}$$

$$\text{Li}_3 \left( \frac{y_2 v - v + 1}{v(v-1)y_1} \right) = \tag{M.63}$$

$$\begin{aligned}
& \frac{1}{6} \ln^3 \left( \frac{y_2}{y_1} \right) - \frac{1}{2} G(0; v) \ln^2 \left( \frac{y_2}{y_1} \right) - \frac{1}{2} G(1; v) \ln^2 \left( \frac{y_2}{y_1} \right) - \frac{1}{2} G(\lambda'_3; 1) \ln^2 \left( \frac{y_2}{y_1} \right) + \\
& \frac{1}{2} G(\lambda'_3; v) \ln^2 \left( \frac{y_2}{y_1} \right) + \frac{1}{6} \pi^2 \ln \left( \frac{y_2}{y_1} \right) - \frac{1}{6} \pi^2 G(0; v) - \frac{1}{6} \pi^2 G(1; v) - \frac{1}{6} \pi^2 G(\lambda'_3; 1) + \\
& \frac{1}{6} \pi^2 G(\lambda'_3; v) - G(0; v) G(0, \lambda'_1; 1) - G(1; v) G(0, \lambda'_1; 1) - G(\lambda'_3; 1) G(0, \lambda'_1; 1) + \\
& G(\lambda'_3; v) G(0, \lambda'_1; 1) - G(0; v) G(0, \lambda'_2; 1) - G(1; v) G(0, \lambda'_2; 1) - \\
& G(\lambda'_3; 1) G(0, \lambda'_2; 1) + G(\lambda'_3; v) G(0, \lambda'_2; 1) + G(0; v) G(\lambda'_1, 1; 1) + \\
& G(1; v) G(\lambda'_1, 1; 1) + G(\lambda'_3; 1) G(\lambda'_1, 1; 1) - G(\lambda'_3; v) G(\lambda'_1, 1; 1) + \\
& G(0; v) G(\lambda'_2, 1; 1) + G(1; v) G(\lambda'_2, 1; 1) + G(\lambda'_3; 1) G(\lambda'_2, 1; 1) - \\
& G(\lambda'_3; v) G(\lambda'_2, 1; 1) - G(0; v) G(\lambda'_3, 0; 1) - G(1; v) G(\lambda'_3, 0; 1) - \\
& G(\lambda'_3; 1) G(\lambda'_3, 0; 1) + G(\lambda'_3; v) G(\lambda'_3, 0; 1) - G(0; v) G(\lambda'_3, 1; 1) - \\
& G(1; v) G(\lambda'_3, 1; 1) - G(\lambda'_3; 1) G(\lambda'_3, 1; 1) + G(\lambda'_3; v) G(\lambda'_3, 1; 1) + \\
& G(0; v) G(\lambda'_3, \lambda'_1; 1) + G(1; v) G(\lambda'_3, \lambda'_1; 1) + G(\lambda'_3; 1) G(\lambda'_3, \lambda'_1; 1) - \\
& G(\lambda'_3; v) G(\lambda'_3, \lambda'_1; 1) + G(0; v) G(\lambda'_3, \lambda'_2; 1) + G(1; v) G(\lambda'_3, \lambda'_2; 1) + \\
& G(\lambda'_3; 1) G(\lambda'_3, \lambda'_2; 1) - G(\lambda'_3; v) G(\lambda'_3, \lambda'_2; 1) + G(0, 0, 0, 1) - G(0, 0, 0; v) - \\
& G(0, 0, 1; v) - G(0, 0, \lambda'_1; 1) + G(0, 0, \lambda'_1; v) - G(0, 0, \lambda'_2; 1) + G(0, 0, \lambda'_2; v) - \\
& G(0, 1, 0; v) - G(0, 1, 1; v) + G(0, 1, \lambda'_1; v) + G(0, 1, \lambda'_2; v) + G(0, \lambda'_1, 1; 1) + \\
& G(0, \lambda'_2, 1; 1) - G(0, \lambda'_3, 0; 1) + G(0, \lambda'_3, 0; v) - G(0, \lambda'_3, 1; 1) + G(0, \lambda'_3, 1; v) + \\
& G(0, \lambda'_3, \lambda'_1; 1) - G(0, \lambda'_3, \lambda'_1; v) + G(0, \lambda'_3, \lambda'_2; 1) - G(0, \lambda'_3, \lambda'_2; v) - \\
& G(1, 0, 0; v) - G(1, 0, 1; v) + G(1, 0, \lambda'_1; v) + G(1, 0, \lambda'_2; v) - G(1, 1, 0; v) - \\
& G(1, 1, 1; v) + G(1, 1, \lambda'_1; v) + G(1, 1, \lambda'_2; v) + G(1, \lambda'_3, 0; v) + G(1, \lambda'_3, 1; v) - \\
& G(1, \lambda'_3, \lambda'_1; v) - G(1, \lambda'_3, \lambda'_2; v) - G(\lambda'_1, 1, 1; 1) - G(\lambda'_2, 1, 1; 1) - G(\lambda'_3, 0, 0; 1) + \\
& G(\lambda'_3, 0, 0; v) + G(\lambda'_3, 0, 1; v) + G(\lambda'_3, 0, \lambda'_1; 1) - G(\lambda'_3, 0, \lambda'_1; v) + \\
& G(\lambda'_3, 0, \lambda'_2; 1) - G(\lambda'_3, 0, \lambda'_2; v) + G(\lambda'_3, 1, 0; v) + G(\lambda'_3, 1, 1; 1) + G(\lambda'_3, 1, 1; v) - \\
& G(\lambda'_3, 1, \lambda'_1; v) - G(\lambda'_3, 1, \lambda'_2; v) - G(\lambda'_3, \lambda'_1, 1; 1) - G(\lambda'_3, \lambda'_2, 1; 1) + \\
& G(\lambda'_3, \lambda'_3, 0; 1) - G(\lambda'_3, \lambda'_3, 0; v) + G(\lambda'_3, \lambda'_3, 1; 1) - G(\lambda'_3, \lambda'_3, 1; v) - \\
& G(\lambda'_3, \lambda'_3, \lambda'_1; 1) + G(\lambda'_3, \lambda'_3, \lambda'_1; v) - G(\lambda'_3, \lambda'_3, \lambda'_2; 1) + G(\lambda'_3, \lambda'_3, \lambda'_2; v) +
\end{aligned}$$

$$\begin{aligned}
 &G(0, 0, 1) \ln(y_1) - G(0, 0; v) \ln(y_1) - G(0, 1; v) \ln(y_1) - G(0, \lambda'_3; 1) \ln(y_1) + \\
 &G(0, \lambda'_3; v) \ln(y_1) - G(1, 0; v) \ln(y_1) - G(1, 1; v) \ln(y_1) + G(1, \lambda'_3; v) \ln(y_1) - \\
 &G(\lambda'_3, 0; 1) \ln(y_1) + G(\lambda'_3, 0; v) \ln(y_1) + G(\lambda'_3, 1; v) \ln(y_1) + \\
 &G(\lambda'_3, \lambda'_3; 1) \ln(y_1) - G(\lambda'_3, \lambda'_3; v) \ln(y_1) - G(0; v) \ln(y_1) \ln(y_2) - \\
 &G(1; v) \ln(y_1) \ln(y_2) - G(\lambda'_3; 1) \ln(y_1) \ln(y_2) + G(\lambda'_3; v) \ln(y_1) \ln(y_2).
 \end{aligned}$$

Using these identities we can express  $j^{(1)}$  completely in terms of  $G$  and  $M$ -functions, and perform the integration in exactly the same way as for  $\mathcal{I}_0^{(IIa)}$ . The result is

$$\begin{aligned}
 \mathcal{I}_1^{(IIa)}(y_1, y_2) = & \hspace{20em} \text{(M.64)} \\
 & \frac{1}{\sqrt{\lambda'_k}} \left\{ \left( -2 \ln^2 y_1 - \ln^2 y_2 - \frac{\pi^2}{2} \right) M(\lambda'_1, 0) + \left( -\ln^2 y_1 - \ln^2 y_2 + \frac{\pi^2}{2} \right) M(\lambda'_1, 1) + \right. \\
 & \left( -\frac{1}{2} \ln^2 y_1 - \frac{\pi^2}{2} \right) M(\lambda'_1, \lambda'_1) + \left( -\frac{1}{2} \ln^2 y_1 - \frac{\pi^2}{2} \right) M(\lambda'_1, \lambda'_2) + \\
 & \left( \frac{3}{2} \ln^2 y_1 + \frac{1}{2} \ln^2 y_2 + \frac{\pi^2}{3} \right) M(\lambda'_1, \lambda'_3) + \left( 2 \ln^2 y_1 + \ln^2 y_2 + \frac{\pi^2}{2} \right) M(\lambda'_2, 0) + \\
 & \left( \ln^2 y_1 + \ln^2 y_2 - \frac{\pi^2}{2} \right) M(\lambda'_2, 1) + \left( \frac{1}{2} \ln^2 y_1 + \frac{\pi^2}{2} \right) M(\lambda'_2, \lambda'_1) + \left( \frac{1}{2} \ln^2 y_1 + \right. \\
 & \left. \frac{\pi^2}{2} \right) M(\lambda'_2, \lambda'_2) + \left( -\frac{3}{2} \ln^2 y_1 - \frac{1}{2} \ln^2 y_2 - \frac{\pi^2}{3} \right) M(\lambda'_2, \lambda'_3) + \left( -\frac{1}{2} \ln^2 y_1 - \right. \\
 & \left. \frac{1}{2} \ln^2 y_2 - \frac{\pi^2}{6} \right) M(\lambda'_3, \lambda'_1) + \\
 & \left( \frac{1}{2} \ln^2 y_1 + \frac{1}{2} \ln^2 y_2 + \frac{\pi^2}{6} \right) M(\lambda'_3, \lambda'_2) - 2 \ln y_1 M(0, \lambda'_1, \lambda'_1) - \ln y_1 M(0, \lambda'_1, \lambda'_3) + \\
 & 2 \ln y_1 M(0, \lambda'_2, \lambda'_2) + \ln y_1 M(0, \lambda'_2, \lambda'_3) - \ln y_1 M(0, \lambda'_3, \lambda'_1) + \ln y_1 M(0, \lambda'_3, \lambda'_2) - \\
 & 4 \ln y_1 M(\lambda'_1, 0, 0) - 2 \ln y_1 M(\lambda'_1, 0, 1) - \ln y_1 M(\lambda'_1, 0, \lambda'_1) - \ln y_1 M(\lambda'_1, 0, \lambda'_2) + \\
 & 2 \ln y_1 M(\lambda'_1, 0, \lambda'_3) - 2 \ln y_1 M(\lambda'_1, 1, 0) + \ln y_1 M(\lambda'_1, 1, \lambda'_1) - \ln y_1 M(\lambda'_1, 1, \lambda'_2) + \\
 & \ln y_1 M(\lambda'_1, 1, \lambda'_3) - \ln y_1 M(\lambda'_1, \lambda'_1, 0) + \ln y_1 M(\lambda'_1, \lambda'_1, 1) + \ln y_1 M(\lambda'_1, \lambda'_1, \lambda'_3) - \\
 & \ln y_1 M(\lambda'_1, \lambda'_2, 0) - \ln y_1 M(\lambda'_1, \lambda'_2, 1) + \ln y_1 M(\lambda'_1, \lambda'_2, \lambda'_3) + \\
 & 2 \ln y_1 M(\lambda'_1, \lambda'_3, 0) + \ln y_1 M(\lambda'_1, \lambda'_3, 1) + \ln y_1 M(\lambda'_1, \lambda'_3, \lambda'_1) + \\
 & \ln y_1 M(\lambda'_1, \lambda'_3, \lambda'_2) - 2 \ln y_1 M(\lambda'_1, \lambda'_3, \lambda'_3) + 4 \ln y_1 M(\lambda'_2, 0, 0) + \\
 & 2 \ln y_1 M(\lambda'_2, 0, 1) + \ln y_1 M(\lambda'_2, 0, \lambda'_1) + \ln y_1 M(\lambda'_2, 0, \lambda'_2) - 2 \ln y_1 M(\lambda'_2, 0, \lambda'_3) + \\
 & 2 \ln y_1 M(\lambda'_2, 1, 0) + \ln y_1 M(\lambda'_2, 1, \lambda'_1) - \ln y_1 M(\lambda'_2, 1, \lambda'_2) - \ln y_1 M(\lambda'_2, 1, \lambda'_3) + \\
 & \ln y_1 M(\lambda'_2, \lambda'_1, 0) + \ln y_1 M(\lambda'_2, \lambda'_1, 1) - \ln y_1 M(\lambda'_2, \lambda'_1, \lambda'_3) + \ln y_1 M(\lambda'_2, \lambda'_2, 0) - \\
 & \ln y_1 M(\lambda'_2, \lambda'_2, 1) - \ln y_1 M(\lambda'_2, \lambda'_2, \lambda'_3) - 2 \ln y_1 M(\lambda'_2, \lambda'_3, 0) - \\
 & \ln y_1 M(\lambda'_2, \lambda'_3, 1) - \ln y_1 M(\lambda'_2, \lambda'_3, \lambda'_1) - \ln y_1 M(\lambda'_2, \lambda'_3, \lambda'_2) +
 \end{aligned}$$

$$\begin{aligned}
& 2 \ln y_1 M(\lambda'_2, \lambda'_3, \lambda'_3) - 2 \ln y_1 M(\lambda'_3, 0, \lambda'_1) + 2 \ln y_1 M(\lambda'_3, 0, \lambda'_2) - \\
& \ln y_1 M(\lambda'_3, 1, \lambda'_1) + \ln y_1 M(\lambda'_3, 1, \lambda'_2) - 2 \ln y_1 M(\lambda'_3, \lambda'_1, 0) - \\
& \ln y_1 M(\lambda'_3, \lambda'_1, 1) + 2 \ln y_1 M(\lambda'_3, \lambda'_1, \lambda'_1) + \ln y_1 M(\lambda'_3, \lambda'_1, \lambda'_3) + \\
& 2 \ln y_1 M(\lambda'_3, \lambda'_2, 0) + \ln y_1 M(\lambda'_3, \lambda'_2, 1) - 2 \ln y_1 M(\lambda'_3, \lambda'_2, \lambda'_2) - \\
& \ln y_1 M(\lambda'_3, \lambda'_2, \lambda'_3) + \ln y_1 M(\lambda'_3, \lambda'_3, \lambda'_1) - \ln y_1 M(\lambda'_3, \lambda'_3, \lambda'_2) - \\
& 2M(0, 0, \lambda'_1, \lambda'_1) + 2M(0, 0, \lambda'_2, \lambda'_2) - 3M(0, \lambda'_1, 0, \lambda'_1) - 3M(0, \lambda'_1, 0, \lambda'_2) - \\
& M(0, \lambda'_1, 1, \lambda'_1) - 3M(0, \lambda'_1, 1, \lambda'_2) - 4M(0, \lambda'_1, \lambda'_1, 0) - 2M(0, \lambda'_1, \lambda'_1, 1) + \\
& 2M(0, \lambda'_1, \lambda'_1, \lambda'_3) - M(0, \lambda'_1, \lambda'_3, 0) - M(0, \lambda'_1, \lambda'_3, 1) + M(0, \lambda'_1, \lambda'_3, \lambda'_1) + \\
& 3M(0, \lambda'_1, \lambda'_3, \lambda'_2) + 3M(0, \lambda'_2, 0, \lambda'_1) + 3M(0, \lambda'_2, 0, \lambda'_2) + 3M(0, \lambda'_2, 1, \lambda'_1) + \\
& M(0, \lambda'_2, 1, \lambda'_2) + 4M(0, \lambda'_2, \lambda'_2, 0) + 2M(0, \lambda'_2, \lambda'_2, 1) - 2M(0, \lambda'_2, \lambda'_2, \lambda'_3) + \\
& M(0, \lambda'_2, \lambda'_3, 0) + M(0, \lambda'_2, \lambda'_3, 1) - 3M(0, \lambda'_2, \lambda'_3, \lambda'_1) - M(0, \lambda'_2, \lambda'_3, \lambda'_2) - \\
& M(0, \lambda'_3, 0, \lambda'_1) + M(0, \lambda'_3, 0, \lambda'_2) - M(0, \lambda'_3, 1, \lambda'_1) + M(0, \lambda'_3, 1, \lambda'_2) - \\
& M(0, \lambda'_3, \lambda'_1, 0) - M(0, \lambda'_3, \lambda'_1, 1) + M(0, \lambda'_3, \lambda'_2, 0) + M(0, \lambda'_3, \lambda'_2, 1) - \\
& 4M(\lambda'_1, 0, 0, 0) - 2M(\lambda'_1, 0, 0, 1) - 3M(\lambda'_1, 0, 0, \lambda'_1) - 3M(\lambda'_1, 0, 0, \lambda'_2) + \\
& M(\lambda'_1, 0, 0, \lambda'_3) - 2M(\lambda'_1, 0, 1, 0) - M(\lambda'_1, 0, 1, \lambda'_3) - 2M(\lambda'_1, 0, \lambda'_1, 0) + \\
& M(\lambda'_1, 0, \lambda'_1, 1) + M(\lambda'_1, 0, \lambda'_1, \lambda'_3) - 2M(\lambda'_1, 0, \lambda'_2, 0) + M(\lambda'_1, 0, \lambda'_2, 1) + \\
& M(\lambda'_1, 0, \lambda'_2, \lambda'_3) - 2M(\lambda'_1, 0, \lambda'_3, 1) + 2M(\lambda'_1, 0, \lambda'_3, \lambda'_1) + 2M(\lambda'_1, 0, \lambda'_3, \lambda'_2) - \\
& 2M(\lambda'_1, 1, 0, 0) - M(\lambda'_1, 1, 0, \lambda'_3) + 2M(\lambda'_1, 1, 1, 1) + M(\lambda'_1, 1, 1, \lambda'_1) + \\
& 3M(\lambda'_1, 1, 1, \lambda'_2) - 3M(\lambda'_1, 1, 1, \lambda'_3) + 2M(\lambda'_1, 1, \lambda'_1, 0) + 3M(\lambda'_1, 1, \lambda'_1, 1) - \\
& M(\lambda'_1, 1, \lambda'_1, \lambda'_3) - 2M(\lambda'_1, 1, \lambda'_2, 0) + M(\lambda'_1, 1, \lambda'_2, 1) + M(\lambda'_1, 1, \lambda'_2, \lambda'_3) - \\
& M(\lambda'_1, 1, \lambda'_3, 0) - 3M(\lambda'_1, 1, \lambda'_3, 1) + M(\lambda'_1, 1, \lambda'_3, \lambda'_1) - M(\lambda'_1, 1, \lambda'_3, \lambda'_2) + \\
& 2M(\lambda'_1, 1, \lambda'_3, \lambda'_3) - M(\lambda'_1, \lambda'_1, 0, 0) + 3M(\lambda'_1, \lambda'_1, 0, 1) + M(\lambda'_1, \lambda'_1, 0, \lambda'_3) + \\
& 3M(\lambda'_1, \lambda'_1, 1, 0) + 5M(\lambda'_1, \lambda'_1, 1, 1) - M(\lambda'_1, \lambda'_1, 1, \lambda'_3) + M(\lambda'_1, \lambda'_1, \lambda'_3, 0) - \\
& M(\lambda'_1, \lambda'_1, \lambda'_3, 1) - M(\lambda'_1, \lambda'_1, \lambda'_3, \lambda'_3) - M(\lambda'_1, \lambda'_2, 0, 0) - M(\lambda'_1, \lambda'_2, 0, 1) + \\
& M(\lambda'_1, \lambda'_2, 0, \lambda'_3) - M(\lambda'_1, \lambda'_2, 1, 0) - M(\lambda'_1, \lambda'_2, 1, 1) + M(\lambda'_1, \lambda'_2, 1, \lambda'_3) + \\
& M(\lambda'_1, \lambda'_2, \lambda'_3, 0) + M(\lambda'_1, \lambda'_2, \lambda'_3, 1) - M(\lambda'_1, \lambda'_2, \lambda'_3, \lambda'_3) - M(\lambda'_1, \lambda'_3, 0, 0) - \\
& 2M(\lambda'_1, \lambda'_3, 0, 1) + 2M(\lambda'_1, \lambda'_3, 0, \lambda'_1) + 2M(\lambda'_1, \lambda'_3, 0, \lambda'_2) - 2M(\lambda'_1, \lambda'_3, 1, 0) - \\
& 3M(\lambda'_1, \lambda'_3, 1, 1) + M(\lambda'_1, \lambda'_3, 1, \lambda'_1) - M(\lambda'_1, \lambda'_3, 1, \lambda'_2) + 2M(\lambda'_1, \lambda'_3, 1, \lambda'_3) + \\
& 2M(\lambda'_1, \lambda'_3, \lambda'_1, 0) + M(\lambda'_1, \lambda'_3, \lambda'_1, 1) - M(\lambda'_1, \lambda'_3, \lambda'_1, \lambda'_3) + 2M(\lambda'_1, \lambda'_3, \lambda'_2, 0) - \\
& M(\lambda'_1, \lambda'_3, \lambda'_2, 1) - M(\lambda'_1, \lambda'_3, \lambda'_2, \lambda'_3) + 2M(\lambda'_1, \lambda'_3, \lambda'_3, 1) - M(\lambda'_1, \lambda'_3, \lambda'_3, \lambda'_1) - \\
& M(\lambda'_1, \lambda'_3, \lambda'_3, \lambda'_2) + 4M(\lambda'_2, 0, 0, 0) + 2M(\lambda'_2, 0, 0, 1) + 3M(\lambda'_2, 0, 0, \lambda'_1) + \\
& 3M(\lambda'_2, 0, 0, \lambda'_2) - M(\lambda'_2, 0, 0, \lambda'_3) + 2M(\lambda'_2, 0, 1, 0) + M(\lambda'_2, 0, 1, \lambda'_3) + \\
& 2M(\lambda'_2, 0, \lambda'_1, 0) - M(\lambda'_2, 0, \lambda'_1, 1) - M(\lambda'_2, 0, \lambda'_1, \lambda'_3) + 2M(\lambda'_2, 0, \lambda'_2, 0) - \\
& M(\lambda'_2, 0, \lambda'_2, 1) - M(\lambda'_2, 0, \lambda'_2, \lambda'_3) + 2M(\lambda'_2, 0, \lambda'_3, 1) - 2M(\lambda'_2, 0, \lambda'_3, \lambda'_1) -
\end{aligned}$$

$$\begin{aligned}
 & 2M(\lambda'_2, 0, \lambda'_3, \lambda'_2) + 2M(\lambda'_2, 1, 0, 0) + M(\lambda'_2, 1, 0, \lambda'_3) - 2M(\lambda'_2, 1, 1, 1) - \\
 & 3M(\lambda'_2, 1, 1, \lambda'_1) - M(\lambda'_2, 1, 1, \lambda'_2) + 3M(\lambda'_2, 1, 1, \lambda'_3) + 2M(\lambda'_2, 1, \lambda'_1, 0) - \\
 & M(\lambda'_2, 1, \lambda'_1, 1) - M(\lambda'_2, 1, \lambda'_1, \lambda'_3) - 2M(\lambda'_2, 1, \lambda'_2, 0) - 3M(\lambda'_2, 1, \lambda'_2, 1) + \\
 & M(\lambda'_2, 1, \lambda'_2, \lambda'_3) + M(\lambda'_2, 1, \lambda'_3, 0) + 3M(\lambda'_2, 1, \lambda'_3, 1) + M(\lambda'_2, 1, \lambda'_3, \lambda'_1) - \\
 & M(\lambda'_2, 1, \lambda'_3, \lambda'_2) - 2M(\lambda'_2, 1, \lambda'_3, \lambda'_3) + M(\lambda'_2, \lambda'_1, 0, 0) + M(\lambda'_2, \lambda'_1, 0, 1) - \\
 & M(\lambda'_2, \lambda'_1, 0, \lambda'_3) + M(\lambda'_2, \lambda'_1, 1, 0) + M(\lambda'_2, \lambda'_1, 1, 1) - M(\lambda'_2, \lambda'_1, 1, \lambda'_3) - \\
 & M(\lambda'_2, \lambda'_1, \lambda'_3, 0) - M(\lambda'_2, \lambda'_1, \lambda'_3, 1) + M(\lambda'_2, \lambda'_1, \lambda'_3, \lambda'_3) + M(\lambda'_2, \lambda'_2, 0, 0) - \\
 & 3M(\lambda'_2, \lambda'_2, 0, 1) - M(\lambda'_2, \lambda'_2, 0, \lambda'_3) - 3M(\lambda'_2, \lambda'_2, 1, 0) - 5M(\lambda'_2, \lambda'_2, 1, 1) + \\
 & M(\lambda'_2, \lambda'_2, 1, \lambda'_3) - M(\lambda'_2, \lambda'_2, \lambda'_3, 0) + M(\lambda'_2, \lambda'_2, \lambda'_3, 1) + M(\lambda'_2, \lambda'_2, \lambda'_3, \lambda'_3) + \\
 & M(\lambda'_2, \lambda'_3, 0, 0) + 2M(\lambda'_2, \lambda'_3, 0, 1) - 2M(\lambda'_2, \lambda'_3, 0, \lambda'_1) - 2M(\lambda'_2, \lambda'_3, 0, \lambda'_2) + \\
 & 2M(\lambda'_2, \lambda'_3, 1, 0) + 3M(\lambda'_2, \lambda'_3, 1, 1) + M(\lambda'_2, \lambda'_3, 1, \lambda'_1) - M(\lambda'_2, \lambda'_3, 1, \lambda'_2) - \\
 & 2M(\lambda'_2, \lambda'_3, 1, \lambda'_3) - 2M(\lambda'_2, \lambda'_3, \lambda'_1, 0) + M(\lambda'_2, \lambda'_3, \lambda'_1, 1) + M(\lambda'_2, \lambda'_3, \lambda'_1, \lambda'_3) - \\
 & 2M(\lambda'_2, \lambda'_3, \lambda'_2, 0) - M(\lambda'_2, \lambda'_3, \lambda'_2, 1) + M(\lambda'_2, \lambda'_3, \lambda'_2, \lambda'_3) - 2M(\lambda'_2, \lambda'_3, \lambda'_3, 1) + \\
 & M(\lambda'_2, \lambda'_3, \lambda'_3, \lambda'_1) + M(\lambda'_2, \lambda'_3, \lambda'_3, \lambda'_2) - M(\lambda'_3, 0, 0, \lambda'_1) + M(\lambda'_3, 0, 0, \lambda'_2) - \\
 & 3M(\lambda'_3, 0, \lambda'_1, 0) - 2M(\lambda'_3, 0, \lambda'_1, 1) + M(\lambda'_3, 0, \lambda'_1, \lambda'_3) + 3M(\lambda'_3, 0, \lambda'_2, 0) + \\
 & 2M(\lambda'_3, 0, \lambda'_2, 1) - M(\lambda'_3, 0, \lambda'_2, \lambda'_3) - M(\lambda'_3, 0, \lambda'_3, \lambda'_1) + M(\lambda'_3, 0, \lambda'_3, \lambda'_2) + \\
 & M(\lambda'_3, 1, 1, \lambda'_1) - M(\lambda'_3, 1, 1, \lambda'_2) - 2M(\lambda'_3, 1, \lambda'_1, 0) - M(\lambda'_3, 1, \lambda'_1, 1) + \\
 & M(\lambda'_3, 1, \lambda'_1, \lambda'_3) + 2M(\lambda'_3, 1, \lambda'_2, 0) + M(\lambda'_3, 1, \lambda'_2, 1) - M(\lambda'_3, 1, \lambda'_2, \lambda'_3) - \\
 & M(\lambda'_3, 1, \lambda'_3, \lambda'_1) + M(\lambda'_3, 1, \lambda'_3, \lambda'_2) - 5M(\lambda'_3, \lambda'_1, 0, 0) - 4M(\lambda'_3, \lambda'_1, 0, 1) + \\
 & 2M(\lambda'_3, \lambda'_1, 0, \lambda'_1) + 2M(\lambda'_3, \lambda'_1, 0, \lambda'_2) + M(\lambda'_3, \lambda'_1, 0, \lambda'_3) - 4M(\lambda'_3, \lambda'_1, 1, 0) - \\
 & 3M(\lambda'_3, \lambda'_1, 1, 1) + 2M(\lambda'_3, \lambda'_1, 1, \lambda'_1) + 2M(\lambda'_3, \lambda'_1, 1, \lambda'_2) + M(\lambda'_3, \lambda'_1, 1, \lambda'_3) + \\
 & 4M(\lambda'_3, \lambda'_1, \lambda'_1, 0) + 4M(\lambda'_3, \lambda'_1, \lambda'_1, 1) - 2M(\lambda'_3, \lambda'_1, \lambda'_1, \lambda'_3) + M(\lambda'_3, \lambda'_1, \lambda'_3, 0) + \\
 & M(\lambda'_3, \lambda'_1, \lambda'_3, 1) - 2M(\lambda'_3, \lambda'_1, \lambda'_3, \lambda'_2) + 5M(\lambda'_3, \lambda'_2, 0, 0) + 4M(\lambda'_3, \lambda'_2, 0, 1) - \\
 & 2M(\lambda'_3, \lambda'_2, 0, \lambda'_1) - 2M(\lambda'_3, \lambda'_2, 0, \lambda'_2) - M(\lambda'_3, \lambda'_2, 0, \lambda'_3) + 4M(\lambda'_3, \lambda'_2, 1, 0) + \\
 & 3M(\lambda'_3, \lambda'_2, 1, 1) - 2M(\lambda'_3, \lambda'_2, 1, \lambda'_1) - 2M(\lambda'_3, \lambda'_2, 1, \lambda'_2) - M(\lambda'_3, \lambda'_2, 1, \lambda'_3) - \\
 & 4M(\lambda'_3, \lambda'_2, \lambda'_2, 0) - 4M(\lambda'_3, \lambda'_2, \lambda'_2, 1) + 2M(\lambda'_3, \lambda'_2, \lambda'_2, \lambda'_3) - M(\lambda'_3, \lambda'_2, \lambda'_3, 0) - \\
 & M(\lambda'_3, \lambda'_2, \lambda'_3, 1) + 2M(\lambda'_3, \lambda'_2, \lambda'_3, \lambda'_1) - M(\lambda'_3, \lambda'_3, 0, \lambda'_1) + M(\lambda'_3, \lambda'_3, 0, \lambda'_2) - \\
 & M(\lambda'_3, \lambda'_3, 1, \lambda'_1) + M(\lambda'_3, \lambda'_3, 1, \lambda'_2) - M(\lambda'_3, \lambda'_3, \lambda'_1, 0) - M(\lambda'_3, \lambda'_3, \lambda'_1, 1) + \\
 & 2M(\lambda'_3, \lambda'_3, \lambda'_1, \lambda'_1) + M(\lambda'_3, \lambda'_3, \lambda'_2, 0) + M(\lambda'_3, \lambda'_3, \lambda'_2, 1) - 2M(\lambda'_3, \lambda'_3, \lambda'_2, \lambda'_2) + \\
 & M(\lambda'_1) \left( -\frac{2}{3} \ln^3 y_1 + \frac{1}{2} \ln y_2 \ln^2 y_1 - \ln^2 y_2 \ln y_1 - \frac{1}{2} \pi^2 \ln y_1 + \frac{1}{6} \ln^3 y_2 + \right. \\
 & \left. \frac{1}{6} \pi^2 \ln y_2 - \zeta_3 \right) + M(\lambda'_2) \left( \frac{2}{3} \ln^3 y_1 - \frac{1}{2} \ln y_2 \ln^2 y_1 + \ln^2 y_2 \ln y_1 + \frac{1}{2} \pi^2 \ln y_1 - \right. \\
 & \left. \frac{1}{6} \ln^3 y_2 - \frac{1}{6} \pi^2 \ln y_2 + \zeta_3 \right) \Bigg\}.
 \end{aligned}$$

Note that  $\mathcal{I}_1^{(IIa)}$  is of uniform weight 4, as expected.

### M.3 The analytic expressions of the functions $i^{(0)}$ and $i^{(1)}$

In this appendix we present the analytic expressions of the functions  $i^{(0)}$  and  $i^{(1)}$  that enter the integrals (M.13) and (M.14).

$$i^{(0)}(x_1, x_2) = \tag{M.65}$$

$$-\frac{1}{2} \ln^2 \left( 1 - v \left( 1 - \frac{x_1}{x_2} \right) \right) + \ln(1-v) \ln \left( 1 - v \left( 1 - \frac{x_1}{x_2} \right) \right) +$$

$$\ln(1-v) \ln x_2 + \ln v \ln \left( 1 - v \left( 1 - \frac{x_1}{x_2} \right) \right) + \ln v \ln x_2 - \ln x_2 \ln \left( 1 - v \left( 1 - \frac{x_1}{x_2} \right) \right) - \frac{1}{2} \ln^2(1-v) - \frac{\ln^2 v}{2} - \ln v \ln(1-v) - \frac{1}{2} \ln^2 x_2 - \frac{\pi^2}{2}.$$

$$i^{(1)}(x_1, x_2) = \tag{M.66}$$

$$\text{Li}_3 \left( \frac{vx_1 - vx_2 + x_2}{(v-1)v} \right) + \ln(1-v) \text{Li}_2 \left( \frac{vx_1 - vx_2 + x_2}{(v-1)v} \right) + \ln v \text{Li}_2 \left( \frac{vx_1 - vx_2 + x_2}{(v-1)v} \right) -$$

$$\text{Li}_2 \left( \frac{vx_1 - vx_2 + x_2}{(v-1)v} \right) \ln \left( 1 - v \left( 1 - \frac{x_1}{x_2} \right) \right) - \ln x_2 \text{Li}_2 \left( \frac{vx_1 - vx_2 + x_2}{(v-1)v} \right) -$$

$$\frac{1}{2} \ln^2(1-v) \ln \left( -v^2 + vx_1 - vx_2 + v + x_2 \right) - \frac{1}{2} \ln^2 v \ln \left( -v^2 + vx_1 - vx_2 + v + x_2 \right) -$$

$$\frac{1}{2} \ln^2 \left( 1 - v \left( 1 - \frac{x_1}{x_2} \right) \right) \ln \left( -v^2 + vx_1 - vx_2 + v + x_2 \right) -$$

$$\frac{1}{2} \ln^2 x_2 \ln \left( -v^2 + vx_1 - vx_2 + v + x_2 \right) - \ln v \ln(1-v) \ln \left( -v^2 + vx_1 - vx_2 + v + x_2 \right) +$$

$$\ln(1-v) \ln \left( 1 - v \left( 1 - \frac{x_1}{x_2} \right) \right) \ln \left( -v^2 + vx_1 - vx_2 + v + x_2 \right) +$$

$$\ln(1-v) \ln x_2 \ln \left( -v^2 + vx_1 - vx_2 + v + x_2 \right) +$$

$$\ln v \ln \left( 1 - v \left( 1 - \frac{x_1}{x_2} \right) \right) \ln \left( -v^2 + vx_1 - vx_2 + v + x_2 \right) +$$

$$\ln v \ln x_2 \ln \left( -v^2 + vx_1 - vx_2 + v + x_2 \right) -$$

$$\ln x_2 \ln \left( 1 - v \left( 1 - \frac{x_1}{x_2} \right) \right) \ln \left( -v^2 + vx_1 - vx_2 + v + x_2 \right) -$$

$$\frac{\pi^2}{2} \ln \left( -v^2 + vx_1 - vx_2 + v + x_2 \right) - 2 \ln^2(1-v) \ln \left( 1 - v \left( 1 - \frac{x_1}{x_2} \right) \right) -$$

$$\frac{3}{2} \ln^2(1-v) \ln x_2 + \ln(1-v) \ln^2 \left( 1 - v \left( 1 - \frac{x_1}{x_2} \right) \right) - \ln v \ln^2 x_2 + \ln^2 x_2 \ln \left( 1 - v \left( 1 - \frac{x_1}{x_2} \right) \right) + \frac{1}{2} \ln^2 v \ln x_2 + \frac{1}{2} \ln x_2 \ln^2 \left( 1 - v \left( 1 - \frac{x_1}{x_2} \right) \right) - 2 \ln v \ln(1-v)$$



$$\begin{aligned}
& v) \ln \left( 1 - v \left( 1 - \frac{x_1}{x_2} \right) \right) - \ln v \ln(1-v) \ln x_2 + \ln(1-v) \ln x_2 \ln \left( 1 - v \left( 1 - \frac{x_1}{x_2} \right) \right) \\
& + \frac{1}{6} \pi^2 \ln \left( 1 - v \left( 1 - \frac{x_1}{x_2} \right) \right) - \ln v \ln x_2 \ln \left( 1 - v \left( 1 - \frac{x_1}{x_2} \right) \right) + \\
& \ln^3(1-v) + 2 \ln v \ln^2(1-v) + \ln^2 v \ln(1-v) + \frac{5}{6} \pi^2 \ln(1-v) - \frac{1}{6} \pi^2 \ln v + \\
& \frac{1}{2} \ln^3 x_2 + \frac{2}{3} \pi^2 \ln x_2 - \zeta_3.
\end{aligned}$$

## M.4 The analytic expressions of the functions $j^{(0)}$ and $j^{(1)}$

In this appendix we present the analytic expressions of the functions  $j^{(0)}$  and  $j^{(1)}$  that enter the integrals (M.49) and (M.50).

$$j^{(0)}(y_1, y_2) = \tag{M.67}$$

$$\begin{aligned}
& \frac{1}{2} \ln^2 \left( v(y_2 - 1) + 1 \right) + \ln(1-v) \ln y_1 - \ln(1-v) \ln \left( v(y_2 - 1) + 1 \right) + \ln v \ln y_1 - \\
& \ln v \ln \left( v(y_2 - 1) + 1 \right) - \ln y_1 \ln \left( v(y_2 - 1) + 1 \right) + \frac{1}{2} \ln^2(1-v) + \frac{\ln^2 v}{2} + \\
& \ln v \ln(1-v) + \frac{1}{2} \ln^2 y_1 + \frac{\pi^2}{2}.
\end{aligned}$$

$$j^{(1)}(y_1, y_2) = \tag{M.68}$$

$$\begin{aligned}
& -\text{Li}_3 \left( \frac{v(y_2-1)+1}{(v-1)vy_1} \right) - \ln(1-v) \text{Li}_2 \left( \frac{v(y_2-1)+1}{(v-1)vy_1} \right) - \ln v \text{Li}_2 \left( \frac{v(y_2-1)+1}{(v-1)vy_1} \right) - \\
& \ln y_1 \text{Li}_2 \left( \frac{v(y_2-1)+1}{(v-1)vy_1} \right) + \text{Li}_2 \left( \frac{v(y_2-1)+1}{(v-1)vy_1} \right) \ln \left( v(y_2 - 1) + 1 \right) + \frac{1}{2} \ln^2(1-v) \ln \left( -v^2 y_1 + v(y_1 + y_2 - 1) + 1 \right) \\
& + \frac{1}{2} \ln^2 v \ln \left( -v^2 y_1 + v(y_1 + y_2 - 1) + 1 \right) + \frac{1}{2} \ln^2 y_1 \ln \left( -v^2 y_1 + v(y_1 + y_2 - 1) + 1 \right) \\
& + \frac{1}{2} \ln^2 \left( v(y_2 - 1) + 1 \right) \ln \left( -v^2 y_1 + v(y_1 + y_2 - 1) + 1 \right) + \\
& \ln v \ln(1-v) \ln \left( -v^2 y_1 + v(y_1 + y_2 - 1) + 1 \right) + \\
& \ln(1-v) \ln y_1 \ln \left( -v^2 y_1 + v(y_1 + y_2 - 1) + 1 \right) - \\
& \ln(1-v) \ln \left( v(y_2 - 1) + 1 \right) \ln \left( -v^2 y_1 + v(y_1 + y_2 - 1) + 1 \right) + \\
& \ln v \ln y_1 \ln \left( -v^2 y_1 + v(y_1 + y_2 - 1) + 1 \right) - \\
& \ln v \ln \left( v(y_2 - 1) + 1 \right) \ln \left( -v^2 y_1 + v(y_1 + y_2 - 1) + 1 \right) - \\
& \ln y_1 \ln \left( v(y_2 - 1) + 1 \right) \ln \left( -v^2 y_1 + v(y_1 + y_2 - 1) + 1 \right) + \\
& \frac{1}{2} \pi^2 \ln \left( -v^2 y_1 + v(y_1 + y_2 - 1) + 1 \right) - 2 \ln^2(1-v) \ln y_1 + 2 \ln^2(1-v) \ln \left( v(y_2 - 1) + 1 \right) \\
& - \ln(1-v) \ln^2 y_1 - \ln(1-v) \ln^2 \left( v(y_2 - 1) + 1 \right) - 2 \ln v \ln(1-v) \ln y_1 +
\end{aligned}$$

$$\begin{aligned}
& 2 \ln v \ln(1-v) \ln(v(y_2-1)+1) + 2 \ln(1-v) \ln y_1 \ln(v(y_2-1)+1) - \\
& \frac{1}{6} \pi^2 \ln(v(y_2-1)+1) - \ln^3(1-v) - 2 \ln v \ln^2(1-v) - \ln^2 v \ln(1-v) - \\
& \frac{5}{6} \pi^2 \ln(1-v) + \frac{1}{6} \pi^2 \ln v + \frac{1}{6} \pi^2 \ln y_1 + \zeta_3.
\end{aligned}$$

# Appendix N

## Reduction of the polylogarithms in terms of $G$ -functions

### N.1 Reduction of $\text{Li}_n$ in Region I

In this section we prove the reduction formulae of polylogarithms of the form  $\text{Li}_n\left(\frac{1}{a(x_1, x_2, v)}\right)$  to  $G$ -functions, where  $a(x_1, x_2, v) = \frac{v(v-1)}{v(x_1-x_2)+x_2}$ . We can see this polylogarithm as a Goncharov multiple polylogarithm

$$\begin{aligned} \text{Li}_n\left(\frac{1}{a(x_1, x_2, v)}\right) &= -M\left(\vec{0}_{n-1}, a(x_1, x_2, v)\right) \\ &= -\int_0^1 \left(\frac{dt}{t}\right)^{n-1} \circ \Omega(a(x_1, x_2, v)). \end{aligned} \tag{N.1}$$

We can now extract the dependence on the variable  $v$  using the reduction algorithm presented in Appendix G.4,

$$\begin{aligned} M\left(\vec{0}_{n-1}, a(x_1, x_2, v)\right) &= -\text{Li}_n\left(\frac{1}{a(x_1, x_2, v_0)}\right) + \int_{v_0}^v dv \int_0^1 \left(\frac{dt}{t}\right)^{n-1} \circ \frac{\partial}{\partial v'} \Omega(a(x_1, x_2, v')), \end{aligned} \tag{N.2}$$

and integrating back we find the expression of  $M\left(\vec{0}_{n-1}, a(x_1, x_2, v)\right)$  in terms of  $G$ -functions of the form  $G(\dots, v)$ . However, we still need to face the problem

of how to choose the value for  $v_0$ . The ‘best’ choice is of course  $v_0 = 1$ , since we know that at this point the  $G$ -functions collapse to  $M$ -functions, *i.e.* Goncharov’s multiple polylogarithm<sup>\*</sup>. However, it is easy to see that

$$\lim_{v \rightarrow 1} \operatorname{Li}_n \left( \frac{1}{a(x_1, x_2, v)} \right) = \infty. \quad (\text{N.3})$$

We therefore choose  $v_0 = 1 - \epsilon$ , and we compute

$$\begin{aligned} & M \left( \vec{0}_{n-1}, a(x_1, x_2, v) \right) \\ &= \lim_{\epsilon \rightarrow 0^+} \left\{ -\operatorname{Li}_n \left( \frac{1}{a(x_1, x_2, 1 - \epsilon)} \right) \right. \\ &\quad \left. - \int_0^{1-\epsilon} dv \int_0^1 \left( \frac{dt}{t} \right)^{n-1} \circ \frac{\partial}{\partial v'} \Omega(a(x_1, x_2, v')) \right\} \\ &\quad + \int_0^v dv \int_0^1 \left( \frac{dt}{t} \right)^{n-1} \circ \frac{\partial}{\partial v'} \Omega(a(x_1, x_2, v')). \end{aligned} \quad (\text{N.4})$$

We will show in the following that in the cases  $n \leq 3$  this limit is well-defined.

### N.1.1 Reduction of $\operatorname{Li}_1$

For  $n = 1$ , we do not need the machinery of the reduction algorithm, but the reduction can be performed in a straightforward way:

$$\begin{aligned} \operatorname{Li}_1 \left( \frac{1}{a(x_1, x_2, v)} \right) &= -\ln \left( 1 - \frac{v(x_1 - x_2) + x_2}{v(v-1)} \right) \\ &= \ln v + \ln(1-v) - \ln(v(1-v) + v(x_1 - x_2) + x_2) \\ &= \ln v + \ln(1-v) - \ln(-(\lambda_1 - v)(\lambda_2 - v)) \\ &= \ln v + \ln(1-v) - \ln(-\lambda_1 \lambda_2) - \ln \left( 1 - \frac{v}{\lambda_1} \right) - \ln \left( 1 - \frac{v}{\lambda_2} \right) \\ &= G(0; v) + G(1; v) - \ln x_2 - G(\lambda_1; v) - G(\lambda_2; v), \end{aligned} \quad (\text{N.5})$$

where the last step follows from Eq. (M.19).

---

<sup>\*</sup>We could of course choose another value, *e.g.*  $v_0 = 1/2$ , but then we need to face the problem how to obtain the values  $G(\dots; 1/2)$ .

### N.1.2 Reduction of $Li_2$

For  $n = 2$ , let us start by evaluating the second integral in Eq. (N.4). The last integral over  $v$  involves  $Li_1\left(\frac{1}{a(x_1, x_2, v)}\right)$ , which we know recursively from the previous paragraph. We immediately find

$$\begin{aligned} & \int_0^v dv \int_0^1 \frac{dt}{t} \circ \frac{\partial}{\partial v'} \Omega(a(x_1, x_2, v')) \\ &= G(0, 0; v) + G(0, 1; v) - G(0, \lambda_1; v) - G(0, \lambda_2; v) + G(1, 0; v) + G(1, 1; v) \\ & - G(1, \lambda_1; v) - G(1, \lambda_2; v) - G(\lambda_3, 0; v) - G(\lambda_3, 1; v) + G(\lambda_3, \lambda_1; v) \\ & + G(\lambda_3, \lambda_2; v) - G(0; v) \ln x_2 - G(1; v) \ln x_2 + G(\lambda_3; v) \ln x_2. \end{aligned} \tag{N.6}$$

We now turn to the limit. The integral is obtained immediately by putting  $v = 1 - \epsilon$  in the previous expression. As we are interested in the singular behavior around  $v = 1$ , we switch to the irreducible basis where this singular behavior is explicit (See Appendix G.4). Furthermore, since  $\epsilon$  is small, we can write

$$\begin{aligned} -Li_2\left(\frac{1}{a(x_1, x_2, 1 - \epsilon)}\right) &= \frac{1}{2} \ln^2 \epsilon - \ln x_1 \ln \epsilon + \frac{1}{2} \ln^2 x_1 + \frac{\pi^2}{6} + \mathcal{O}(\epsilon) \\ &= G(1, 1; 1 - \epsilon) - \ln x_1 G(1; 1 - \epsilon) + \frac{1}{2} \ln^2 x_1 + \frac{\pi^2}{6} + \mathcal{O}(\epsilon). \end{aligned} \tag{N.7}$$

We now find

$$\begin{aligned} & \lim_{\epsilon \rightarrow 0^+} \left\{ -Li_2\left(\frac{1}{a(x_1, x_2, 1 - \epsilon)}\right) - \int_0^{1-\epsilon} dv \int_0^1 \frac{dt}{t} \circ \frac{\partial}{\partial v'} \Omega(a(x_1, x_2, v')) \right\} \\ &= \lim_{\epsilon \rightarrow 0^+} \left\{ G(1, 1; 1 - \epsilon) - \ln x_1 G(1; 1 - \epsilon) - G(1, 1; 1 - \epsilon) \right. \\ & \quad \left. - G(1; 1 - \epsilon) [\ln(1 - \lambda_1) - \ln(-\lambda_1) + \ln(\lambda_2 - 1) - \ln \lambda_2 + \ln x_2] \right\} \\ & \quad + (finite) \\ &= (finite), \end{aligned} \tag{N.8}$$

where the last step follows from  $(1 - 1/\lambda_1)(1 - 1/\lambda_2) = x_1/x_2$ .

### N.1.3 Reduction of $\text{Li}_3$

For  $n = 3$ , let us start by evaluating the second integral. The last integral over  $v$  involves  $\text{Li}_2\left(\frac{1}{a(x_1, x_2, v)}\right)$ , which we know recursively from the previous paragraph. We immediately find

$$\int_0^v dv \int_0^1 \left(\frac{dt}{t}\right)^2 \circ \frac{\partial}{\partial v} \Omega(a(x_1, x_2, v')) = \tag{N.9}$$

$$\begin{aligned} & -\frac{1}{2}G(0; v) \ln^2 x_1 - \frac{1}{2}G(1; v) \ln^2 x_1 + \frac{1}{2}G(\lambda_3; v) \ln^2 x_1 + G(0; v) \ln(x_2) \ln x_1 + \\ & G(1; v) \ln(x_2) \ln x_1 - G(\lambda_3; v) \ln(x_2) \ln x_1 - G(0; v) \ln^2 x_2 - G(1; v) \ln^2 x_2 + \\ & G(\lambda_3; v) \ln^2 x_2 - \frac{1}{6}\pi^2 G(0; v) - \frac{1}{6}\pi^2 G(1; v) + \frac{1}{6}\pi^2 G(\lambda_3; v) - G(0; v)G(0, \lambda_1; 1) - \\ & G(1; v)G(0, \lambda_1; 1) + G(\lambda_3; v)G(0, \lambda_1; 1) - G(0; v)G(0, \lambda_2; 1) - \\ & G(1; v)G(0, \lambda_2; 1) + G(\lambda_3; v)G(0, \lambda_2; 1) + G(0; v)G(\lambda_1, 1; 1) + \\ & G(1; v)G(\lambda_1, 1; 1) - G(\lambda_3; v)G(\lambda_1, 1; 1) + G(0; v)G(\lambda_2, 1; 1) + \\ & G(1; v)G(\lambda_2, 1; 1) - G(\lambda_3; v)G(\lambda_2, 1; 1) - G(0; v)G(\lambda_3, 0; 1) - \\ & G(1; v)G(\lambda_3, 0; 1) + G(\lambda_3; v)G(\lambda_3, 0; 1) - G(0; v)G(\lambda_3, 1; 1) - \\ & G(1; v)G(\lambda_3, 1; 1) + G(\lambda_3; v)G(\lambda_3, 1; 1) + G(0; v)G(\lambda_3, \lambda_1; 1) + \\ & G(1; v)G(\lambda_3, \lambda_1; 1) - G(\lambda_3; v)G(\lambda_3, \lambda_1; 1) + G(0; v)G(\lambda_3, \lambda_2; 1) + \\ & G(1; v)G(\lambda_3, \lambda_2; 1) - G(\lambda_3; v)G(\lambda_3, \lambda_2; 1) - G(0, 0, 0; v) - G(0, 0, 1; v) + \\ & G(0, 0, \lambda_1; v) + G(0, 0, \lambda_2; v) - G(0, 1, 0; v) - G(0, 1, 1; v) + G(0, 1, \lambda_1; v) + \\ & G(0, 1, \lambda_2; v) + G(0, \lambda_3, 0; v) + G(0, \lambda_3, 1; v) - G(0, \lambda_3, \lambda_1; v) - \\ & G(0, \lambda_3, \lambda_2; v) - G(1, 0, 0; v) - G(1, 0, 1; v) + G(1, 0, \lambda_1; v) + G(1, 0, \lambda_2; v) - \\ & G(1, 1, 0; v) - G(1, 1, 1; v) + G(1, 1, \lambda_1; v) + G(1, 1, \lambda_2; v) + G(1, \lambda_3, 0; v) + \\ & G(1, \lambda_3, 1; v) - G(1, \lambda_3, \lambda_1; v) - G(1, \lambda_3, \lambda_2; v) + G(\lambda_3, 0, 0; v) + \\ & G(\lambda_3, 0, 1; v) - G(\lambda_3, 0, \lambda_1; v) - G(\lambda_3, 0, \lambda_2; v) + G(\lambda_3, 1, 0; v) + \\ & G(\lambda_3, 1, 1; v) - G(\lambda_3, 1, \lambda_1; v) - G(\lambda_3, 1, \lambda_2; v) - G(\lambda_3, \lambda_3, 0; v) - \\ & G(\lambda_3, \lambda_3, 1; v) + G(\lambda_3, \lambda_3, \lambda_1; v) + G(\lambda_3, \lambda_3, \lambda_2; v) + G(0, 0; v) \ln x_2 + \\ & G(0, 1; v) \ln x_2 - G(0, \lambda_3; v) \ln x_2 + G(1, 0; v) \ln x_2 + G(1, 1; v) \ln x_2 - \\ & G(1, \lambda_3; v) \ln x_2 - G(\lambda_3, 0; v) \ln x_2 - G(\lambda_3, 1; v) \ln x_2 + G(\lambda_3, \lambda_3; v) \ln x_2. \end{aligned}$$

We now turn to the limit. The integral is obtained immediately by putting  $v = 1 - \epsilon$  in the previous expression. As we are interested in the singular behavior around  $v = 1$ , we switch to the irreducible basis where this singular

behavior is explicit. Furthermore, since  $\epsilon$  is small, we can write

$$\begin{aligned}
-\text{Li}_2\left(\frac{1}{a(x_1, x_2, 1-\epsilon)}\right) &= -\frac{1}{6}\ln^3\epsilon + \frac{1}{2}\ln x_1 \ln^2\epsilon - \frac{1}{2}\ln^2 x_1 \ln\epsilon - \frac{1}{6}\pi^2 \ln\epsilon \\
&+ \frac{1}{6}\ln^3 x_1 + \frac{1}{6}\pi^2 \ln x_1 \\
&= \frac{1}{6}\ln^3 x_1 - \frac{1}{2}G(1; 1-\epsilon) \ln^2 x_1 + G(1, 1; 1-\epsilon) \ln x_1 \\
&+ \frac{1}{6}\pi^2 \ln x_1 - \frac{1}{6}\pi^2 G(1; 1-\epsilon) - G(1, 1, 1; 1-\epsilon).
\end{aligned} \tag{N.10}$$

We now find

$$\begin{aligned}
&\lim_{\epsilon \rightarrow 0^+} \left\{ -\text{Li}_3\left(\frac{1}{a(x_1, x_2, 1-\epsilon)}\right) \right. \\
&\quad \left. - \int_0^{1-\epsilon} dv \int_0^1 \left(\frac{dt}{t}\right)^2 \circ \frac{\partial}{\partial v'} \Omega(a(x_1, x_2, v')) \right\} \\
&= \lim_{\epsilon \rightarrow 0^+} \left\{ \frac{1}{6}\ln^3 x_1 - \frac{1}{2}G(1; 1-\epsilon) \ln^2 x_1 + G(1, 1; 1-\epsilon) \ln x_1 + \frac{1}{6}\pi^2 \ln x_1 \right. \\
&\quad - \frac{1}{6}\pi^2 G(1; 1-\epsilon) - G(1, 1, 1; 1-\epsilon) + G(1, 1, 1; 1-\epsilon) \\
&\quad + G(1, 1, 1; 1-\epsilon) [-G(\lambda_1; 1-\epsilon) - G(\lambda_2; 1-\epsilon) - \ln x_2] \\
&\quad + G(1; 1-\epsilon) \left[ \frac{1}{6}(3\ln^2 x_1 - 6\ln x_2 \ln x_1 + 6\ln^2 x_2 + \pi^2) \right. \\
&\quad \left. + G(\lambda_3; 1-\epsilon) \ln x_2 \right] \Big\} \\
&\quad + (finite) \\
&= (finite),
\end{aligned} \tag{N.11}$$

where the last step follows from Eq. (M.19), as well as

$$\begin{aligned}
G(\lambda_1; 1) &= \ln\left(1 - \frac{1}{\lambda_1}\right), \\
G(\lambda_2; 1) &= \ln\left(1 - \frac{1}{\lambda_2}\right), \\
G(\lambda_2; 1) &= \ln\left(1 - \frac{1}{\lambda_2}\right).
\end{aligned} \tag{N.12}$$

## N.2 Reduction of $\text{Li}_n$ in Region II

In this section we proof the reduction formulae of polylogarithms of the form  $\text{Li}_n\left(\frac{1}{a(y_1, y_2, v)}\right)$  to  $G$ -functions, where  $a(x_1, x_2, v) = \frac{v(v-1)y_1}{y_2 v - v + 1}$ . Since most of the discussion is exactly the same as in Appendix N.1, we will be brief on this. We can start by writing down an equation similar to Eq. (N.4). We then reduce the function  $\text{Li}_1$  in a straightforward way, and continue in a bootstrap to reduce  $\text{Li}_2$  and  $\text{Li}_3$ . Particular care is again needed when evaluating the limit that appears in Eq. (N.4). Let us illustrate the cancellation of the poles. For  $n = 2, 3$  we can write

$$\begin{aligned} -\text{Li}_2\left(\frac{1}{a(y_1, y_2, 1-\epsilon)}\right) &= \frac{1}{2}\ln^2\epsilon - \ln\left(\frac{y_2}{y_1}\right)\ln\epsilon + \frac{1}{2}\ln^2\left(\frac{y_2}{y_1}\right) + \frac{\pi^2}{6} + \mathcal{O}(\epsilon) \\ &= \frac{1}{2}\ln^2\left(\frac{y_2}{y_1}\right) - G(1; 1-\epsilon)\ln\left(\frac{y_2}{y_1}\right) + G(1, 1; 1-\epsilon) + \frac{\pi^2}{6} + \mathcal{O}(\epsilon). \end{aligned} \quad (\text{N.13})$$

$$\begin{aligned} -\text{Li}_3\left(\frac{1}{a(y_1, y_2, 1-\epsilon)}\right) &= \frac{1}{6}\ln^3\left(\frac{y_2}{y_1}\right) - \frac{1}{2}\ln\epsilon\ln^2\left(\frac{y_2}{y_1}\right) + \frac{1}{2}\ln^2\epsilon\ln\left(\frac{y_2}{y_1}\right) \\ &\quad + \frac{1}{6}\pi^2\ln\left(\frac{y_2}{y_1}\right) - \frac{\ln^3\epsilon}{6} - \frac{1}{6}\pi^2\ln\epsilon + \mathcal{O}(\epsilon) \\ &= \frac{1}{6}\ln^3\left(\frac{y_2}{y_1}\right) - \frac{1}{2}G(1; 1-\epsilon)\ln^2\left(\frac{y_2}{y_1}\right) + G(1, 1; 1-\epsilon)\ln\left(\frac{y_2}{y_1}\right) \\ &\quad + \frac{1}{6}\pi^2\ln\left(\frac{y_2}{y_1}\right) - \frac{1}{6}\pi^2G(1; 1-\epsilon) - G(1, 1, 1; 1-\epsilon) + \mathcal{O}(\epsilon). \end{aligned} \quad (\text{N.14})$$

Inserting these expressions into the limits that appear in Eq. (N.4), one can easily show that the limit is finite.



# Appendix O

## Results for tree-level Lipatov vertices

### O.1 NMHV-type vertices

#### O.1.1 Result for $V^{(0)}(q_1; 1^-, 2^+, 3^+, 4^+; q_2)$

$$\begin{aligned}
 N^{(1)}(q_1; 1^-, 2^+, 3^+, 4^+; q_2) &= -q_{1\perp}^* q_{2\perp} p_{1\perp}^3 x_2 x_3^{3/2}, \\
 D^{(1)}(q_1; 1^-, 2^+, 3^+, 4^+; q_2) &= \langle 12 \rangle \langle 23 \rangle (q_{1\perp} + p_{1\perp} + p_{2\perp}) (2q_{1\perp} + p_{1\perp} + p_{2\perp}) \\
 &\quad p_{4\perp} \sqrt{x_1} \left( q_{1\perp} q_{1\perp}^* x_1 x_2 + \left( |p_{2\perp}|^2 x_1 + |p_{1\perp}|^2 x_2 \right) x_3 \right),
 \end{aligned}$$

$$\begin{aligned}
 N^{(2)}(q_1; 1^-, 2^+, 3^+, 4^+; q_2) &= -|q_{1\perp}|^2 q_{2\perp} \sqrt{x_2}, \\
 D^{(2)}(q_1; 1^-, 2^+, 3^+, 4^+; q_2) &= \langle 23 \rangle \langle 34 \rangle (q_{1\perp} + p_{1\perp}) p_{2\perp} p_{1\perp}^* \sqrt{x_4},
 \end{aligned}$$

$$\begin{aligned}
 N^{(3)}(q_1; 1^-, 2^+, 3^+, 4^+; q_2) &= -q_{1\perp}^* q_{2\perp} p_{1\perp}^3 x_2^{3/2} \sqrt{x_3}, \\
 D^{(3)}(q_1; 1^-, 2^+, 3^+, 4^+; q_2) &= \langle 12 \rangle \langle 34 \rangle p_{2\perp} (p_{1\perp} + p_{2\perp}) (q_{1\perp} + p_{1\perp} + p_{2\perp}) \\
 &\quad \sqrt{x_1} \left( |p_{2\perp}|^2 x_1 + |p_{1\perp}|^2 x_2 \right) \sqrt{x_4},
 \end{aligned}$$

$$\begin{aligned}
N^{(4)}(q_1; 1^-, 2^+, 3^+, 4^+; q_2) &= |q_{1\perp}|^2 q_{2\perp} p_{1\perp}^3 x_2 x_3 x_4^{3/2}, \\
D^{(4)}(q_1; 1^-, 2^+, 3^+, 4^+; q_2) &= \langle 12 \rangle \langle 23 \rangle \langle 34 \rangle p_{4\perp} (q_{1\perp} + p_{1\perp} + p_{2\perp} + p_{4\perp}) \\
&\quad (2q_{1\perp} + p_{1\perp} + p_{2\perp} + p_{4\perp}) \sqrt{x_1} \\
&\quad \left( |p_{4\perp}|^2 x_1 x_2 x_3 + \left( q_{1\perp} q_{1\perp}^* x_1 x_2 + \left( |p_{2\perp}|^2 x_1 + |p_{1\perp}|^2 x_2 \right) x_3 \right) x_4 \right), \\
N^{(5)}(q_1; 1^-, 2^+, 3^+, 4^+; q_2) &= q_{1\perp} q_{2\perp} x_1^{5/2}, \\
D^{(5)}(q_1; 1^-, 2^+, 3^+, 4^+; q_2) &= \langle 12 \rangle \langle 23 \rangle \langle 34 \rangle \sqrt{x_4} x_{1234} (q_{1\perp} x_1 + p_{1\perp} x_{1234}), \\
N^{(6)}(q_1; 1^-, 2^+, 3^+, 4^+; q_2) &= -q_{1\perp}^* q_{2\perp} p_{1\perp}^3 \sqrt{x_2} (x_2 + x_3 + x_4)^3, \\
D^{(6)}(q_1; 1^-, 2^+, 3^+, 4^+; q_2) &= \langle 23 \rangle \langle 34 \rangle (q_{1\perp} + p_{1\perp}) \sqrt{x_4} (q_{1\perp} x_1 + p_{1\perp} x_{1234}) \\
&\quad (\sqrt{x_1 x_2} \langle 12 \rangle + q_{1\perp} x_2 + p_{2\perp} x_{1234}) (q_{1\perp} (q_{1\perp}^* + p_{1\perp}^*) x_1 \\
&\quad + p_{1\perp} (q_{1\perp}^* x_1 + p_{1\perp}^* x_{1234})), \\
N^{(7)}(q_1; 1^-, 2^+, 3^+, 4^+; q_2) &= q_{1\perp}^* q_{2\perp} x_2^{3/2}, \\
D^{(7)}(q_1; 1^-, 2^+, 3^+, 4^+; q_2) &= \langle 34 \rangle (p_{1\perp} + p_{2\perp}) [12] \sqrt{x_1} \sqrt{x_4} \Delta(3, 1, 2), \\
N^{(8)}(q_1; 1^-, 2^+, 3^+, 4^+; q_2) &= -q_{1\perp}^* q_{2\perp} p_{1\perp}^3 x_2^{3/2} \sqrt{x_3} (x_3 + x_4)^3, \\
D^{(8)}(q_1; 1^-, 2^+, 3^+, 4^+; q_2) &= \langle 12 \rangle \langle 34 \rangle (q_{1\perp} + p_{1\perp} + p_{2\perp}) \sqrt{x_1} \sqrt{x_4} \\
&\quad (\sqrt{x_1 x_2} \langle 12 \rangle + q_{1\perp} x_2 + p_{2\perp} x_{1234}) \left( x_2 \left( |p_{1\perp}|^2 x_1 + q_{1\perp}^* p_{1\perp} x_1 + |p_{1\perp}|^2 \right. \right. \\
&\quad \left. \left. x_4 + q_{1\perp} (q_{1\perp}^* + p_{1\perp}^* + p_{2\perp}^*) x_1 + \langle 12 \rangle [12] x_1 + |p_{1\perp}|^2 x_2 + |p_{1\perp}|^2 x_3 \right) \right. \\
&\quad \left. + p_{2\perp} x_1 (q_{1\perp}^* x_2 + p_{2\perp}^* x_{1234}) \right) (q_{1\perp} (x_1 + x_2 + 2x_3 + x_4) - \sqrt{x_3} \Delta(3, 1, 2)), \\
N^{(9)}(q_1; 1^-, 2^+, 3^+, 4^+; q_2) &= q_{1\perp}^* q_{2\perp} \Delta(1, 2, 3)^3, \\
D^{(9)}(q_1; 1^-, 2^+, 3^+, 4^+; q_2) &= s_{123} \langle 12 \rangle \langle 23 \rangle (q_{1\perp} + p_{1\perp} + p_{2\perp}) \sqrt{x_4} \\
&\quad \Delta(3, 1, 2) \Delta(4, 1, 3),
\end{aligned}$$

$$\begin{aligned}
N^{(10)}(q_1; 1^-, 2^+, 3^+, 4^+; q_2) &= -q_{1\perp}^* q_{2\perp} p_{1\perp}^3 x_2 x_3^{3/2} x_4^3, \\
D^{(10)}(q_1; 1^-, 2^+, 3^+, 4^+; q_2) &= \langle 12 \rangle \langle 23 \rangle (2q_{1\perp} + p_{1\perp} + p_{2\perp}) \sqrt{x_1} \\
&\quad (\sqrt{x_4} (\sqrt{x_4} q_{1\perp} - \langle 41 \rangle \sqrt{x_1} - \langle 42 \rangle \sqrt{x_2} - \langle 43 \rangle \sqrt{x_3}) + p_{4\perp} x_{1234}) \\
&\quad (q_{1\perp} x_1 x_2 ((p_{1\perp}^* + p_{2\perp}^*) x_3 \\
&\quad + q_{1\perp}^* (3x_3 + x_{1234})) + x_3 (p_{2\perp} x_1 (q_{1\perp}^* x_2 + p_{2\perp}^* x_{1234}) \\
&\quad + x_2 (p_{1\perp} (q_{1\perp}^* x_1 + p_{1\perp}^* x_{1234}) - s_{123} x_1)) (q_{1\perp} (x_3 + x_{1234}) \\
&\quad - \sqrt{x_3} \Delta(3, 1, 2)),
\end{aligned}$$

$$\begin{aligned}
N^{(11)}(q_1; 1^-, 2^+, 3^+, 4^+; q_2) &= q_{1\perp}^* q_{2\perp} \Delta(1, 2, 3)^3, \\
D^{(11)}(q_1; 1^-, 2^+, 3^+, 4^+; q_2) &= s_{123} \langle 12 \rangle \langle 23 \rangle (q_{1\perp} + p_{1\perp} + p_{2\perp}) \sqrt{x_4} \\
&\quad \Delta(3, 1, 2) \Delta(4, 1, 3).
\end{aligned}$$

### O.1.2 Result for $V^{(0)}(q_1; 1^+, 2^-, 3^+, 4^+; q_2)$

$$\begin{aligned}
N^{(1)}(q_1; 1^+, 2^-, 3^+, 4^+; q_2) &= -q_{1\perp}^* q_{2\perp} p_{2\perp}^4 x_1^{3/2} x_3^{3/2}, \\
D^{(1)}(q_1; 1^+, 2^-, 3^+, 4^+; q_2) &= (q_{1\perp} + p_{1\perp} + p_{2\perp}) (2q_{1\perp} + p_{1\perp} + p_{2\perp}) p_{4\perp} x_2 \\
&\quad \langle 12 \rangle \langle 23 \rangle p_{1\perp} \left( q_{1\perp} q_{1\perp}^* x_1 x_2 + (|p_{2\perp}|^2 x_1 + |p_{1\perp}|^2 x_2) x_3 \right), \\
N^{(2)}(q_1; 1^+, 2^-, 3^+, 4^+; q_2) &= -q_{1\perp}^* q_{2\perp} p_{2\perp}^3 x_1^{3/2} \sqrt{x_3}, \\
D^{(2)}(q_1; 1^+, 2^-, 3^+, 4^+; q_2) &= \langle 12 \rangle \langle 34 \rangle p_{1\perp} (p_{1\perp} + p_{2\perp}) (q_{1\perp} + p_{1\perp} + p_{2\perp}) \\
&\quad \sqrt{x_2} (|p_{2\perp}|^2 x_1 + |p_{1\perp}|^2 x_2) \sqrt{x_4},
\end{aligned}$$

$$\begin{aligned}
N^{(3)}(q_1; 1^+, 2^-, 3^+, 4^+; q_2) &= q_{1\perp} q_{1\perp}^* q_{2\perp} p_{2\perp}^4 x_1^{3/2} x_3 x_4^{3/2}, \\
D^{(3)}(q_1; 1^+, 2^-, 3^+, 4^+; q_2) &= \langle 12 \rangle \langle 23 \rangle \langle 34 \rangle p_{1\perp} p_{4\perp} (q_{1\perp} + p_{1\perp} + p_{2\perp} + p_{4\perp}) \\
&\quad (2q_{1\perp} + p_{1\perp} + p_{2\perp} + p_{4\perp}) x_2 \left( |p_{4\perp}|^2 x_1 x_2 x_3 + (q_{1\perp} q_{1\perp}^* x_1 x_2 \right. \\
&\quad \left. + (|p_{2\perp}|^2 x_1 + |p_{1\perp}|^2 x_2) x_3 \right) x_4,
\end{aligned}$$

$$N^{(4)}(q_1; 1^+, 2^-, 3^+, 4^+; q_2) = q_{1\perp} q_{2\perp} \sqrt{x_1} x_2^2$$

$$D^{(4)}(q_1; 1^+, 2^-, 3^+, 4^+; q_2) = \langle 12 \rangle \langle 23 \rangle \langle 34 \rangle \sqrt{x_4} x_{1234} (q_{1\perp} x_1 + p_{1\perp} x_{1234}),$$

$$N^{(5)}(q_1; 1^+, 2^-, 3^+, 4^+; q_2) = -q_{1\perp}^* q_{2\perp} (q_{1\perp} + p_{1\perp})^3 x_1^2 x_2^{5/2},$$

$$D^{(5)}(q_1; 1^+, 2^-, 3^+, 4^+; q_2) = \langle 23 \rangle \langle 34 \rangle p_{1\perp} \sqrt{x_4} (x_2 + x_3 + x_4) \\ (q_{1\perp} x_1 + p_{1\perp} x_{1234}) (\sqrt{x_1 x_2} \langle 12 \rangle + q_{1\perp} x_2 + p_{2\perp} x_{1234}) \\ (q_{1\perp} (q_{1\perp}^* + p_{1\perp}^*) x_1 + p_{1\perp} (q_{1\perp}^* x_1 + p_{1\perp}^* x_{1234})),$$

$$N^{(6)}(q_1; 1^+, 2^-, 3^+, 4^+; q_2) = q_{1\perp}^* q_{2\perp} x_1^{3/2},$$

$$D^{(6)}(q_1; 1^+, 2^-, 3^+, 4^+; q_2) = \langle 34 \rangle (p_{1\perp} + p_{2\perp}) [12] \sqrt{x_2} \sqrt{x_4} \Delta(3, 1, 2),$$

$$N^{(7)}(q_1; 1^+, 2^-, 3^+, 4^+; q_2) = -q_{1\perp}^* q_{2\perp} p_{2\perp}^4 x_1^{3/2} \sqrt{x_3} (x_3 + x_4)^3,$$

$$D^{(7)}(q_1; 1^+, 2^-, 3^+, 4^+; q_2) = \langle 12 \rangle \langle 34 \rangle p_{1\perp} (q_{1\perp} + p_{1\perp} + p_{2\perp}) \sqrt{x_2} \sqrt{x_4} \\ (\sqrt{x_1 x_2} \langle 12 \rangle + q_{1\perp} x_2 + p_{2\perp} x_{1234}) \left( x_2 \left( |p_{1\perp}|^2 x_1 + q_{1\perp}^* p_{1\perp} x_1 + |p_{1\perp}|^2 x_3 \right) \right. \\ \left. + p_{2\perp} x_1 (q_{1\perp}^* x_2 + p_{2\perp}^* x_{1234}) (q_{1\perp} (x_1 + x_2 + 2x_3 + x_4) - \sqrt{x_3} \Delta(3, 1, 2)) \right),$$

$$N^{(8)}(q_1; 1^+, 2^-, 3^+, 4^+; q_2) = -q_{1\perp}^* q_{2\perp} p_{2\perp}^4 x_1^{3/2} x_3^{3/2} x_4^3$$

$$D^{(8)}(q_1; 1^+, 2^-, 3^+, 4^+; q_2) = \langle 12 \rangle \langle 23 \rangle p_{1\perp} (2q_{1\perp} + p_{1\perp} + p_{2\perp}) x_2 \\ (\sqrt{x_4} (\sqrt{x_4} q_{1\perp} - \langle 41 \rangle \sqrt{x_1} - \langle 42 \rangle \sqrt{x_2} - \langle 43 \rangle \sqrt{x_3}) + p_{4\perp} x_{1234}) \\ (q_{1\perp} x_1 x_2 ((p_{1\perp}^* + p_{2\perp}^*) x_3 + q_{1\perp}^* (x_1 + x_2 + 4x_3 + x_4)) + \\ x_3 (p_{2\perp} x_1 (q_{1\perp}^* x_2 + p_{2\perp}^* x_{1234}) + x_2 (p_{1\perp} (q_{1\perp}^* x_1 + p_{1\perp}^* x_{1234}) - s_{123} x_1))) \\ (q_{1\perp} (x_1 + x_2 + 2x_3 + x_4) - \sqrt{x_3} \Delta(3, 1, 2)),$$

$$N^{(9)}(q_1; 1^+, 2^-, 3^+, 4^+; q_2) = -q_{1\perp}^* q_{2\perp} \Delta(2, 1, 4)^4$$

$$D^{(9)}(q_1; 1^+, 2^-, 3^+, 4^+; q_2) = s_{1234} \langle 12 \rangle \langle 23 \rangle \langle 34 \rangle (q_{1\perp} + p_{1\perp} + p_{2\perp} + p_{4\perp}) x_{1234} \\ \Delta(1, 2, 4) \Delta(4, 1, 3),$$

$$\begin{aligned}
N^{(10)}(q_1; 1^+, 2^-, 3^+, 4^+; q_2) &= q_{1\perp}^* q_{2\perp} \Delta(2, 1, 3)^4, \\
D^{(10)}(q_1; 1^+, 2^-, 3^+, 4^+; q_2) &= s_{123} \langle 12 \rangle \langle 23 \rangle (q_{1\perp} + p_{1\perp} + p_{2\perp}) \sqrt{x_4} \\
&\quad \Delta(1, 2, 3) \Delta(3, 1, 2) \Delta(4, 1, 3),
\end{aligned}$$

$$\begin{aligned}
N^{(11)}(q_1; 1^+, 2^-, 3^+, 4^+; q_2) &= q_{1\perp}^* q_{2\perp} \sqrt{x_1 x_3^{3/2}}, \\
D^{(11)}(q_1; 1^+, 2^-, 3^+, 4^+; q_2) &= p_{1\perp} [23] \sqrt{x_2} \sqrt{x_4} \Delta(1, 2, 3) \Delta(4, 2, 3),
\end{aligned}$$

$$\begin{aligned}
N^{(12)}(q_1; 1^+, 2^-, 3^+, 4^+; q_2) &= -q_{1\perp}^* q_{2\perp} \sqrt{x_1} \Delta(2, 3, 4)^3, \\
D^{(12)}(q_1; 1^+, 2^-, 3^+, 4^+; q_2) &= s_{234} \langle 23 \rangle \langle 34 \rangle p_{1\perp} (x_2 + x_3 + x_4) \\
&\quad \Delta(1, 2, 4) \Delta(4, 2, 3).
\end{aligned}$$

### O.1.3 Result for $V^{(0)}(q_1; 1^+, 2^+, 3^-, 4^+; q_2)$

$$\begin{aligned}
N^{(1)}(q_1; 1^+, 2^+, 3^-, 4^+; q_2) &= -q_{1\perp}^4 q_{1\perp}^* q_{2\perp} x_1^{3/2} x_2, \\
D^{(1)}(q_1; 1^+, 2^+, 3^-, 4^+; q_2) &= \langle 12 \rangle \langle 23 \rangle p_{1\perp} p_{4\perp} (q_{2\perp} + p_{4\perp}) (q_{1\perp} + q_{2\perp} + p_{4\perp}) \\
&\quad \sqrt{x_3} \left( q_{1\perp} q_{1\perp}^* x_1 x_2 + \left( |p_{2\perp}|^2 x_1 + |p_{1\perp}|^2 x_2 \right) x_3 \right),
\end{aligned}$$

$$\begin{aligned}
N^{(2)}(q_1; 1^+, 2^+, 3^-, 4^+; q_2) &= q_{1\perp}^5 q_{1\perp}^* \sqrt{x_1 x_4}, \\
D^{(2)}(q_1; 1^+, 2^+, 3^-, 4^+; q_2) &= (q_{1\perp} + q_{2\perp}) \langle 12 \rangle \langle 23 \rangle \langle 34 \rangle p_{1\perp} p_{4\perp} x_3^2 \\
&\quad \left( \frac{|q_{1\perp}|^2}{x_3} + \frac{|p_{1\perp}|^2}{x_1} + \frac{|p_{2\perp}|^2}{x_2} + \frac{|p_{4\perp}|^2}{x_4} \right),
\end{aligned}$$

$$\begin{aligned}
N^{(3)}(q_1; 1^+, 2^+, 3^-, 4^+; q_2) &= q_{1\perp}^4 q_{1\perp}^* x_1^{3/2} x_2 x_4^2, \\
D^{(3)}(q_1; 1^+, 2^+, 3^-, 4^+; q_2) &= \langle 12 \rangle \langle 23 \rangle p_{1\perp} (q_{2\perp} + p_{4\perp}) x_3 \\
&\quad (q_{2\perp} \sqrt{x_3} - \langle 34 \rangle \sqrt{x_4}) (q_{1\perp} x_1 x_2 ((p_{1\perp}^* + p_{2\perp}^*) x_3 + q_{1\perp}^* (3x_3 + x_{1234}))) \\
&\quad + x_3 (p_{2\perp} x_1 (q_{1\perp}^* x_2 + p_{2\perp}^* x_{1234}) \\
&\quad + x_2 (p_{1\perp} (q_{1\perp}^* x_1 + p_{1\perp}^* x_{1234}) - s_{123} x_1)),
\end{aligned}$$

$$\begin{aligned}
N^{(4)}(q_1; 1^+, 2^+, 3^-, 4^+; q_2) &= q_{2\perp} (q_{1\perp} + q_{2\perp} + p_{1\perp} + p_{2\perp} + p_{4\perp})^2 x_3^2, \\
D^{(4)}(q_1; 1^+, 2^+, 3^-, 4^+; q_2) &= q_{1\perp} \langle 12 \rangle \langle 23 \rangle \langle 34 \rangle \sqrt{x_4} x_{1234} \\
&\quad (\Delta(1, 2, 4) - q_{2\perp} \sqrt{x_1}),
\end{aligned}$$

$$\begin{aligned}
N^{(5)}(q_1; 1^+, 2^+, 3^-, 4^+; q_2) &= -q_{1\perp}^* q_{2\perp} \sqrt{x_1} x_4^{3/2}, \\
D^{(5)}(q_1; 1^+, 2^+, 3^-, 4^+; q_2) &= \langle 12 \rangle p_{1\perp} [34] \sqrt{x_3} (x_3 + x_4) \Delta(2, 3, 4),
\end{aligned}$$

$$\begin{aligned}
N^{(6)}(q_1; 1^+, 2^+, 3^-, 4^+; q_2) &= q_{1\perp}^* q_{2\perp} (q_{1\perp} + q_{2\perp} + p_{4\perp})^3 x_1^{3/2} x_2 x_3^2, \\
D^{(6)}(q_1; 1^+, 2^+, 3^-, 4^+; q_2) &= \langle 12 \rangle \langle 34 \rangle p_{1\perp} (\langle 34 \rangle \sqrt{x_4} - q_{2\perp} \sqrt{x_3}) \sqrt{x_4} \\
&\quad \left( x_2 \left( |p_{1\perp}|^2 x_1 + q_{1\perp}^* p_{1\perp} x_1 + q_{1\perp} (q_{1\perp}^* + p_{1\perp}^* + p_{2\perp}^*) x_1 + \langle 12 \rangle [12] x_1 \right. \right. \\
&\quad \left. \left. + |p_{1\perp}|^2 x_2 + |p_{1\perp}|^2 x_3 + |p_{1\perp}|^2 x_4 \right) + p_{2\perp} x_1 (q_{1\perp}^* x_2 + p_{2\perp}^* x_{1234}) \right) \\
&\quad (\Delta(2, 3, 4) - q_{2\perp} \sqrt{x_2}) (x_3 + x_4),
\end{aligned}$$

$$\begin{aligned}
N^{(7)}(q_1; 1^+, 2^+, 3^-, 4^+; q_2) &= q_{1\perp}^* q_{2\perp} (q_{1\perp} + q_{2\perp} + p_{2\perp} + p_{4\perp})^3 x_1^{3/2} x_3^2, \\
D^{(7)}(q_1; 1^+, 2^+, 3^-, 4^+; q_2) &= \langle 23 \rangle \langle 34 \rangle p_{1\perp} \sqrt{x_4} (x_2 + x_3 + x_4) \\
&\quad (q_{1\perp} (q_{1\perp}^* + p_{1\perp}^*) x_1 + p_{1\perp} (q_{1\perp}^* x_1 + p_{1\perp}^* x_{1234})) (\Delta(1, 2, 4) - q_{2\perp} \sqrt{x_1}) \\
&\quad (\Delta(2, 3, 4) - q_{2\perp} \sqrt{x_2}),
\end{aligned}$$

$$\begin{aligned}
N^{(8)}(q_1; 1^+, 2^+, 3^-, 4^+; q_2) &= q_{1\perp}^* q_{2\perp} \Delta(3, 1, 2)^3, \\
D^{(8)}(q_1; 1^+, 2^+, 3^-, 4^+; q_2) &= s_{123} \langle 12 \rangle \langle 23 \rangle (q_{1\perp} + p_{1\perp} + p_{2\perp}) \sqrt{x_4} \\
&\quad \Delta(1, 2, 3) \Delta(4, 1, 3),
\end{aligned}$$

$$\begin{aligned}
N^{(9)}(q_1; 1^+, 2^+, 3^-, 4^+; q_2) &= -q_{1\perp}^* q_{2\perp} \Delta(3, 1, 4)^4, \\
D^{(9)}(q_1; 1^+, 2^+, 3^-, 4^+; q_2) &= s_{1234} \langle 12 \rangle \langle 23 \rangle \langle 34 \rangle (q_{1\perp} + p_{1\perp} + p_{2\perp} + p_{4\perp}) \\
&\quad x_{1234} \Delta(1, 2, 4) \Delta(4, 1, 3),
\end{aligned}$$

$$\begin{aligned}
N^{(10)}(q_1; 1^+, 2^+, 3^-, 4^+; q_2) &= q_{1\perp}^* q_{2\perp} \sqrt{x_1} x_2^{3/2}, \\
D^{(10)}(q_1; 1^+, 2^+, 3^-, 4^+; q_2) &= p_{1\perp} [23] \sqrt{x_3} \sqrt{x_4} \Delta(1, 2, 3) \Delta(4, 2, 3)
\end{aligned}$$

$$\begin{aligned}
N^{(11)}(q_1; 1^+, 2^+, 3^-, 4^+; q_2) &= -q_{1\perp}^* q_{2\perp} \sqrt{x_1} \Delta(3, 2, 4)^4, \\
D^{(11)}(q_1; 1^+, 2^+, 3^-, 4^+; q_2) &= s_{234} \langle 23 \rangle \langle 34 \rangle p_{1\perp} (x_2 + x_3 + x_4) \Delta(1, 2, 4) \\
&\quad \Delta(2, 3, 4) \Delta(4, 2, 3).
\end{aligned}$$

#### O.1.4 Result for $V^{(0)}(q_1; 1^+, 2^+, 3^+, 4^-; q_2)$

$$\begin{aligned}
N^{(1)}(q_1; 1^+, 2^+, 3^+, 4^-; q_2) &= |q_{1\perp}|^2 p_{4\perp}^3 \sqrt{x_1}, \\
D^{(1)}(q_1; 1^+, 2^+, 3^+, 4^-; q_2) &= (q_{1\perp} + q_{2\perp}) \langle 12 \rangle \langle 23 \rangle \langle 34 \rangle p_{1\perp} \\
&\quad \left( \frac{q_{1\perp} q_{1\perp}^*}{x_3} + \frac{|p_{1\perp}|^2}{x_1} + \frac{|p_{2\perp}|^2}{x_2} + \frac{|p_{4\perp}|^2}{x_4} \right) x_4^{3/2}, \\
N^{(2)}(q_1; 1^+, 2^+, 3^+, 4^-; q_2) &= q_{1\perp}^* (q_{2\perp} + p_{4\perp})^3 x_1^{3/2} x_2 x_3, \\
D^{(2)}(q_1; 1^+, 2^+, 3^+, 4^-; q_2) &= \langle 12 \rangle \langle 23 \rangle p_{1\perp} (q_{2\perp} \sqrt{x_3} - \langle 34 \rangle \sqrt{x_4}) \\
&\quad (q_{1\perp} x_1 x_2 ((p_{1\perp}^* + p_{2\perp}^*) x_3 + q_{1\perp}^* (x_1 + x_2 + 4x_3 + x_4)) \\
&\quad + x_3 (p_{2\perp} x_1 (q_{1\perp}^* x_2 + p_{2\perp}^* x_{1234}) + x_2 (p_{1\perp} (q_{1\perp}^* x_1 + p_{1\perp}^* x_{1234}) \\
&\quad - s_{123} x_1))), \\
N^{(3)}(q_1; 1^+, 2^+, 3^+, 4^-; q_2) &= q_{2\perp} (q_{1\perp} + q_{2\perp} + p_{1\perp} + p_{2\perp} + p_{4\perp})^2 x_4^{3/2}, \\
D^{(3)}(q_1; 1^+, 2^+, 3^+, 4^-; q_2) &= q_{1\perp} \langle 12 \rangle \langle 23 \rangle \langle 34 \rangle x_{1234} (\Delta(1, 2, 4) - q_{2\perp} \sqrt{x_1}), \\
N^{(4)}(q_1; 1^+, 2^+, 3^+, 4^-; q_2) &= -q_{1\perp}^* q_{2\perp} \sqrt{x_1} x_3^{3/2}, \\
D^{(4)}(q_1; 1^+, 2^+, 3^+, 4^-; q_2) &= \langle 12 \rangle p_{1\perp} [34] \sqrt{x_4} (x_3 + x_4) \Delta(2, 3, 4), \\
N^{(5)}(q_1; 1^+, 2^+, 3^+, 4^-; q_2) &= q_{1\perp}^* q_{2\perp} (q_{1\perp} + q_{2\perp} + p_{4\perp})^3 x_1^{3/2} x_2 x_4^{3/2}, \\
D^{(5)}(q_1; 1^+, 2^+, 3^+, 4^-; q_2) &= \langle 12 \rangle \langle 34 \rangle p_{1\perp} (\langle 34 \rangle \sqrt{x_4} - q_{2\perp} \sqrt{x_3}) (x_3 + x_4) \\
&\quad \left( x_2 \left( |p_{1\perp}|^2 x_1 + q_{1\perp}^* p_{1\perp} x_1 + q_{1\perp} (q_{1\perp}^* + p_{1\perp}^* + p_{2\perp}^*) x_1 + \langle 12 \rangle [12] x_1 \right. \right. \\
&\quad \left. \left. + |p_{1\perp}|^2 x_2 + |p_{1\perp}|^2 x_3 + |p_{1\perp}|^2 x_4 \right) + p_{2\perp} x_1 (q_{1\perp}^* x_2 + p_{2\perp}^* x_{1234}) \right) \\
&\quad (\Delta(2, 3, 4) - q_{2\perp} \sqrt{x_2}),
\end{aligned}$$

$$\begin{aligned}
N^{(6)}(q_1; 1^+, 2^+, 3^+, 4^-; q_2) &= q_{1\perp}^* q_{2\perp} (q_{1\perp} + q_{2\perp} + p_{2\perp} + p_{4\perp})^3 x_1^{3/2} x_4^{3/2}, \\
D^{(6)}(q_1; 1^+, 2^+, 3^+, 4^-; q_2) &= \langle 23 \rangle \langle 34 \rangle p_{1\perp} (x_2 + x_3 + x_4) (q_{1\perp} (q_{1\perp}^* + p_{1\perp}^*) x_1 \\
&\quad + p_{1\perp} (q_{1\perp}^* x_1 + p_{1\perp}^* x_{1234})) (\Delta(1, 2, 4) - q_{2\perp} \sqrt{x_1}) (\Delta(2, 3, 4) - q_{2\perp} \sqrt{x_2}),
\end{aligned}$$

$$\begin{aligned}
N^{(7)}(q_1; 1^+, 2^+, 3^+, 4^-; q_2) &= -q_{1\perp}^* q_{2\perp} \Delta(4, 1, 3)^3, \\
D^{(7)}(q_1; 1^+, 2^+, 3^+, 4^-; q_2) &= s_{1234} \langle 12 \rangle \langle 23 \rangle \langle 34 \rangle (q_{1\perp} + p_{1\perp} + p_{2\perp} + p_{4\perp}) \\
&\quad x_{1234} \Delta(1, 2, 4),
\end{aligned}$$

$$\begin{aligned}
N^{(8)}(q_1; 1^+, 2^+, 3^+, 4^-; q_2) &= -q_{1\perp}^* q_{2\perp} \sqrt{x_1} \Delta(4, 2, 3)^3, \\
D^{(8)}(q_1; 1^+, 2^+, 3^+, 4^-; q_2) &= s_{234} \langle 23 \rangle \langle 34 \rangle p_{1\perp} (x_2 + x_3 + x_4) \\
&\quad \Delta(1, 2, 4) \Delta(2, 3, 4).
\end{aligned}$$



## O.2 NNMHV-type vertices

### O.2.1 Result for $V^{(0)}(q_1; 1^-, 2^-, 3^+, 4^+; q_2)$

$$N^{(1)}(q_1; 1^-, 2^-, 3^+, 4^+; q_2) = q_{1\perp}^* q_{2\perp} p_{2\perp}^3 x_1 x_3^{3/2},$$

$$D^{(1)}(q_1; 1^-, 2^-, 3^+, 4^+; q_2) = \langle 23 \rangle (q_{1\perp} + p_{2\perp}) (2q_{1\perp} + p_{1\perp} + p_{2\perp}) p_{4\perp} p_{1\perp}^* \sqrt{x_2} \\ \left( |q_{1\perp}|^2 x_1 x_2 + \left( |p_{2\perp}|^2 x_1 + |p_{1\perp}|^2 x_2 \right) x_3 \right),$$

$$N^{(2)}(q_1; 1^-, 2^-, 3^+, 4^+; q_2) = q_{1\perp}^* q_{2\perp} p_{2\perp} x_1 \sqrt{x_3},$$

$$D^{(2)}(q_1; 1^-, 2^-, 3^+, 4^+; q_2) = \langle 34 \rangle (q_{1\perp} + p_{1\perp} + p_{2\perp}) p_{1\perp}^* \\ \left( |p_{2\perp}|^2 x_1 + |p_{1\perp}|^2 x_2 \right) \sqrt{x_4},$$

$$N^{(3)}(q_1; 1^-, 2^-, 3^+, 4^+; q_2) = q_{1\perp}^* q_{2\perp} (p_{1\perp} + p_{2\perp}) \sqrt{x_1 x_2 x_3},$$

$$D^{(3)}(q_1; 1^-, 2^-, 3^+, 4^+; q_2) = \langle 34 \rangle (q_{1\perp} + p_{1\perp} + p_{2\perp}) [12] \\ \left( |p_{2\perp}|^2 x_1 + |p_{1\perp}|^2 x_2 \right) \sqrt{x_4},$$

$$N^{(4)}(q_1; 1^-, 2^-, 3^+, 4^+; q_2) = -|q_{1\perp}|^2 q_{2\perp} p_{2\perp}^3 x_1 x_3 x_4^{3/2},$$

$$D^{(4)}(q_1; 1^-, 2^-, 3^+, 4^+; q_2) = \langle 23 \rangle \langle 34 \rangle p_{4\perp} (q_{1\perp} + p_{2\perp} + p_{4\perp}) \\ \sqrt{x_2} \left( |p_{4\perp}|^2 x_1 x_2 x_3 + \left( q_{1\perp} q_{1\perp}^* x_1 x_2 + \left( |p_{2\perp}|^2 x_1 + |p_{1\perp}|^2 x_2 \right) x_3 \right) x_4 \right) \\ (2q_{1\perp} + p_{1\perp} + p_{2\perp} + p_{4\perp}) p_{1\perp}^*$$

$$N^{(5)}(q_1; 1^-, 2^-, 3^+, 4^+; q_2) = -|q_{1\perp}|^2 q_{2\perp} (q_{1\perp} + p_{1\perp}) x_1 x_2^{5/2},$$

$$D^{(5)}(q_1; 1^-, 2^-, 3^+, 4^+; q_2) = \langle 23 \rangle \langle 34 \rangle p_{1\perp}^* \sqrt{x_4} (x_2 + x_3 + x_4) \\ (q_{1\perp} (q_{1\perp}^* + p_{1\perp}^*) x_1 + p_{1\perp} (q_{1\perp}^* x_1 + p_{1\perp}^* x_{1234})) \\ (\sqrt{x_1 x_2} \langle 12 \rangle + q_{1\perp} x_2 + p_{2\perp} x_{1234}),$$

$$N^{(6)}(q_1; 1^-, 2^-, 3^+, 4^+; q_2) = -q_{1\perp} q_{2\perp} x_2^{5/2} (q_{1\perp} x_1 + p_{1\perp} x_{1234}),$$

$$D^{(6)}(q_1; 1^-, 2^-, 3^+, 4^+; q_2) = \langle 23 \rangle \langle 34 \rangle \sqrt{x_4} (x_2 + x_3 + x_4)$$

$$(q_{1\perp} (q_{1\perp}^* + p_{1\perp}^*) x_1 + p_{1\perp} (q_{1\perp}^* x_1 + p_{1\perp}^* x_{1234}))$$

$$(\sqrt{x_1 x_2} \langle 12 \rangle + q_{1\perp} x_2 + p_{2\perp} x_{1234}),$$

$$N^{(7)}(q_1; 1^-, 2^-, 3^+, 4^+; q_2) = |q_{1\perp}|^2 q_{2\perp} p_{1\perp}^3 \sqrt{x_2} x_3^{5/2},$$

$$D^{(7)}(q_1; 1^-, 2^-, 3^+, 4^+; q_2) = (q_{1\perp} + p_{2\perp}) (q_{1\perp} + p_{1\perp} + p_{2\perp})$$

$$(2q_{1\perp} + p_{1\perp} + p_{2\perp})$$

$$\left( q_{1\perp} q_{1\perp}^* x_1 x_2 + \left( |p_{2\perp}|^2 x_1 + |p_{1\perp}|^2 x_2 \right) x_3 \right) \Delta(1, 2, 3) p_{4\perp} [23] \sqrt{x_1},$$

$$N^{(8)}(q_1; 1^-, 2^-, 3^+, 4^+; q_2) = q_{1\perp}^* q_{2\perp} p_{1\perp}^3 \sqrt{x_2} x_3^{5/2} x_4^3,$$

$$D^{(8)}(q_1; 1^-, 2^-, 3^+, 4^+; q_2) = (2q_{1\perp} + p_{1\perp} + p_{2\perp}) [23] \sqrt{x_1} (\sqrt{x_4} (\sqrt{x_4} q_{1\perp}$$

$$- \langle 41 \rangle \sqrt{x_1} - \langle 42 \rangle \sqrt{x_2} - \langle 43 \rangle \sqrt{x_3}) + p_{4\perp} x_{1234})$$

$$(q_{1\perp} x_1 x_2 ((p_{1\perp}^* + p_{2\perp}^*) x_3 + q_{1\perp}^* (3x_3 + x_{1234}))$$

$$+ x_3 (p_{2\perp} x_1 (q_{1\perp}^* x_2 + p_{2\perp}^* x_{1234}) + x_2 (p_{1\perp} (q_{1\perp}^* x_1 + p_{1\perp}^* x_{1234})$$

$$- s_{123} x_1))) \Delta(1, 2, 3) (q_{1\perp} (x_1 + 2x_2 + 2x_3 + x_4) + p_{2\perp} x_{1234}$$

$$+ \sqrt{x_1} \Delta(1, 2, 3)),$$

$$N^{(9)}(q_1; 1^-, 2^-, 3^+, 4^+; q_2) = -q_{1\perp}^* q_{2\perp} (p_{1\perp} + p_{2\perp})^3 \sqrt{x_1 x_2} x_3^{3/2},$$

$$D^{(9)}(q_1; 1^-, 2^-, 3^+, 4^+; q_2) = \left( 2q_{1\perp}^2 + 3(p_{1\perp} + p_{2\perp}) q_{1\perp} + (p_{1\perp} + p_{2\perp})^2 \right)$$

$$\left( |q_{1\perp}|^2 x_1 x_2 + \left( |p_{2\perp}|^2 x_1 + |p_{1\perp}|^2 x_2 \right) x_3 \right) \Delta(3, 1, 2) p_{4\perp} [12],$$

$$N^{(10)}(q_1; 1^-, 2^-, 3^+, 4^+; q_2) = |q_{1\perp}|^2 q_{2\perp} (p_{1\perp} + p_{2\perp})^3 \sqrt{x_1 x_2} x_3 x_4^{3/2},$$

$$D^{(10)}(q_1; 1^-, 2^-, 3^+, 4^+; q_2) = \langle 34 \rangle p_{4\perp} [12] \Delta(3, 1, 2)$$

$$\left( 2q_{1\perp}^2 + 3(p_{1\perp} + p_{2\perp} + p_{4\perp}) q_{1\perp} + (p_{1\perp} + p_{2\perp} + p_{4\perp})^2 \right)$$

$$\left( |p_{4\perp}|^2 x_1 x_2 x_3 + \left( q_{1\perp} q_{1\perp}^* x_1 x_2 + \left( |p_{2\perp}|^2 x_1 + |p_{1\perp}|^2 x_2 \right) x_3 \right) x_4 \right),$$

$$\begin{aligned}
N^{(11)}(q_1; 1^-, 2^-, 3^+, 4^+; q_2) &= q_{1\perp} q_{2\perp} (x_1 + x_2)^4, \\
D^{(11)}(q_1; 1^-, 2^-, 3^+, 4^+; q_2) &= \langle 34 \rangle [12] \sqrt{x_1} \sqrt{x_2} \sqrt{x_4} x_{1234} \\
&\quad (q_{1\perp} (x_1 + x_2) + (p_{1\perp} + p_{2\perp}) x_{1234}) \Delta(3, 1, 2), \\
\\
N^{(12)}(q_1; 1^-, 2^-, 3^+, 4^+; q_2) &= |q_{1\perp}|^2 q_{2\perp} \langle 12 \rangle^3 (q_{1\perp} + p_{1\perp} + p_{2\perp}) x_1 x_2 x_3, \\
D^{(12)}(q_1; 1^-, 2^-, 3^+, 4^+; q_2) &= s_{123} \langle 23 \rangle (2q_{1\perp} + p_{1\perp} + p_{2\perp}) p_{4\perp} \\
&\quad \left( q_{1\perp} q_{1\perp}^* x_1 x_2 + \left( |p_{2\perp}|^2 x_1 + |p_{1\perp}|^2 x_2 \right) x_3 \right) \Delta(1, 2, 3) \Delta(3, 1, 2), \\
\\
N^{(13)}(q_1; 1^-, 2^-, 3^+, 4^+; q_2) &= q_{1\perp}^* q_{2\perp} \langle 12 \rangle^3 (q_{1\perp} + p_{1\perp} + p_{2\perp})^3 x_1 x_2 x_3 x_4^3, \\
D^{(13)}(q_1; 1^-, 2^-, 3^+, 4^+; q_2) &= s_{123} \langle 23 \rangle (2q_{1\perp} + p_{1\perp} + p_{2\perp}) \\
&\quad (\sqrt{x_4} (\sqrt{x_4} q_{1\perp} - \langle 41 \rangle \sqrt{x_1} - \langle 42 \rangle \sqrt{x_2} - \langle 43 \rangle \sqrt{x_3}) + p_{4\perp} x_{1234}) \\
&\quad ((p_{1\perp} + p_{2\perp}) x_{1234} + q_{1\perp} (x_1 + x_2 + x_3 + x_{1234})) \\
&\quad (q_{1\perp} x_1 x_2 ((p_{1\perp}^* + p_{2\perp}^*) x_3 + q_{1\perp}^* (3x_3 + x_{1234})) \\
&\quad + x_3 (p_{2\perp} x_1 (q_{1\perp}^* x_2 + p_{2\perp}^* x_{1234}) \\
&\quad + x_2 (p_{1\perp} (q_{1\perp}^* x_1 + p_{1\perp}^* x_{1234}) - s_{123} x_1)) \Delta(1, 2, 3) \Delta(3, 1, 2), \\
\\
N^{(14)}(q_1; 1^-, 2^-, 3^+, 4^+; q_2) &= -q_{1\perp} q_{2\perp} \langle 12 \rangle^3 x_1^{3/2} x_2^{3/2} \sqrt{x_3} (x_3 + x_4)^3, \\
D^{(14)}(q_1; 1^-, 2^-, 3^+, 4^+; q_2) &= \langle 34 \rangle \sqrt{x_4} (q_{1\perp} x_1 + p_{1\perp} x_{1234}) \\
&\quad (\sqrt{x_1 x_2} \langle 12 \rangle + q_{1\perp} x_2 + p_{2\perp} x_{1234}) \\
&\quad (q_{1\perp} (x_1 + x_2) + (p_{1\perp} + p_{2\perp}) x_{1234}) \\
&\quad \left( x_2 \left( |p_{1\perp}|^2 x_1 + q_{1\perp}^* p_{1\perp} x_1 + q_{1\perp} (q_{1\perp}^* + p_{1\perp}^* + p_{2\perp}^*) x_1 \right. \right. \\
&\quad \left. \left. + \langle 12 \rangle [12] x_1 + |p_{1\perp}|^2 x_2 + |p_{1\perp}|^2 x_3 + |p_{1\perp}|^2 x_4 \right) + p_{2\perp} x_1 (q_{1\perp}^* x_2 \right. \\
&\quad \left. + p_{2\perp}^* x_{1234}) \right) \\
&\quad (q_{1\perp} (x_1 + x_2 + 2x_3 + x_4) - \sqrt{x_3} \Delta(3, 1, 2)),
\end{aligned}$$

$$\begin{aligned}
N^{(15)}(q_1; 1^-, 2^-, 3^+, 4^+; q_2) &= |q_{1\perp}|^2 q_{2\perp} p_{2\perp}^3 x_1 x_3^{3/2} x_4^3, \\
D^{(15)}(q_1; 1^-, 2^-, 3^+, 4^+; q_2) &= \langle 23 \rangle (q_{1\perp} + p_{1\perp}) (2q_{1\perp} + p_{1\perp} + p_{2\perp}) p_{1\perp}^* \\
&\quad \sqrt{x_2} (\sqrt{x_4} (\sqrt{x_4} q_{1\perp} - \langle 41 \rangle \sqrt{x_1} - \langle 42 \rangle \sqrt{x_2} - \langle 43 \rangle \sqrt{x_3}) + p_{4\perp} x_{1234}) \\
&\quad (q_{1\perp} x_1 x_2 ((p_{1\perp}^* + p_{2\perp}^*) x_3 + q_{1\perp}^* (3x_3 + x_{1234})) + x_3 (p_{2\perp} x_1 \\
&\quad (q_{1\perp}^* x_2 + p_{2\perp}^* x_{1234}) + x_2 (p_{1\perp} (q_{1\perp}^* x_1 + p_{1\perp}^* x_{1234}) - s_{123} x_1))) \\
&\quad (q_{1\perp} (x_1 + x_2 + 2x_3 + x_4) \sqrt{x_3} \Delta(3, 1, 2)), \\
N^{(16)}(q_1; 1^-, 2^-, 3^+, 4^+; q_2) &= -q_{1\perp} q_{2\perp} \langle 12 \rangle^3 x_1^{3/2} x_2 x_3^{3/2} x_4^3, \\
D^{(16)}(q_1; 1^-, 2^-, 3^+, 4^+; q_2) &= \langle 23 \rangle (q_{1\perp} x_1 + p_{1\perp} x_{1234}) \\
&\quad (\sqrt{x_4} (\sqrt{x_4} q_{1\perp} - \langle 41 \rangle \sqrt{x_1} - \langle 42 \rangle \sqrt{x_2} - \langle 43 \rangle \sqrt{x_3}) + p_{4\perp} x_{1234}) \\
&\quad ((p_{1\perp} + p_{2\perp}) x_{1234} + q_{1\perp} (x_1 + x_2 + x_3 + x_{1234})) \\
&\quad (q_{1\perp} x_1 x_2 ((p_{1\perp}^* + p_{2\perp}^*) x_3 + q_{1\perp}^* (3x_3 + x_{1234})) + x_3 (p_{2\perp} x_1 \\
&\quad (q_{1\perp}^* x_2 + p_{2\perp}^* x_{1234}) + x_2 (p_{1\perp} (q_{1\perp}^* x_1 + p_{1\perp}^* x_{1234}) - s_{123} x_1))) \\
&\quad (q_{1\perp} (x_1 + x_2 + 2x_3 + x_4) - \sqrt{x_3} \Delta(3, 1, 2)), \\
N^{(17)}(q_1; 1^-, 2^-, 3^+, 4^+; q_2) &= q_{1\perp}^* q_{2\perp} p_{1\perp}^3 x_1 x_3^{3/2} x_4^3 \\
&\quad (\sqrt{x_1 x_2} \langle 12 \rangle + q_{1\perp} x_2 + p_{2\perp} x_{1234})^3, \\
D^{(17)}(q_1; 1^-, 2^-, 3^+, 4^+; q_2) &= \langle 23 \rangle (q_{1\perp} + p_{1\perp}) \sqrt{x_2} (q_{1\perp} x_1 + p_{1\perp} x_{1234}) \\
&\quad (\sqrt{x_4} (\sqrt{x_4} q_{1\perp} - \langle 41 \rangle \sqrt{x_1} - \langle 42 \rangle \sqrt{x_2} - \langle 43 \rangle \sqrt{x_3}) + p_{4\perp} x_{1234}) \\
&\quad (q_{1\perp} (q_{1\perp}^* + p_{1\perp}^*) x_1 + p_{1\perp} (q_{1\perp}^* x_1 + p_{1\perp}^* x_{1234})) \\
&\quad (q_{1\perp} x_1 x_2 ((p_{1\perp}^* + p_{2\perp}^*) x_3 + q_{1\perp}^* (3x_3 + x_{1234})) \\
&\quad + x_3 (p_{2\perp} x_1 (q_{1\perp}^* x_2 + p_{2\perp}^* x_{1234}) \\
&\quad + x_2 (p_{1\perp} (q_{1\perp}^* x_1 + p_{1\perp}^* x_{1234}) - s_{123} x_1))) \\
&\quad (q_{1\perp} (x_1 + 2x_2 + 2x_3 + x_4) + p_{2\perp} x_{1234} + \sqrt{x_1} \Delta(1, 2, 3)) \\
&\quad (q_{1\perp} (x_1 + x_2 + 2x_3 + x_4) - \sqrt{x_3} \Delta(3, 1, 2)),
\end{aligned}$$

$$\begin{aligned}
N^{(18)}(q_1; 1^-, 2^-, 3^+, 4^+; q_2) &= -q_{1\perp}^* q_{2\perp} (p_{1\perp} + p_{2\perp})^3 \sqrt{x_1 x_2 x_3} x_4^3, \\
D^{(18)}(q_1; 1^-, 2^-, 3^+, 4^+; q_2) &= (2q_{1\perp} + p_{1\perp} + p_{2\perp}) [12] \\
&\quad (\sqrt{x_4} (\sqrt{x_4} q_{1\perp} - \langle 41 \rangle \sqrt{x_1} - \langle 42 \rangle \sqrt{x_2} - \langle 43 \rangle \sqrt{x_3}) + p_{4\perp} x_{1234}) \\
&\quad (q_{1\perp} x_1 x_2 ((p_{1\perp}^* + p_{2\perp}^*) x_3 + q_{1\perp}^* (3x_3 + x_{1234})) + \\
&\quad x_3 (p_{2\perp} x_1 (q_{1\perp}^* x_2 + p_{2\perp}^* x_{1234}) + x_2 (p_{1\perp} (q_{1\perp}^* x_1 + p_{1\perp}^* x_{1234}) - s_{123} x_1))) \\
&\quad (q_{1\perp} (x_1 + x_2 + 2x_3 + x_4) - \sqrt{x_3} \Delta(3, 1, 2)) \Delta(3, 1, 2),
\end{aligned}$$

$$\begin{aligned}
N^{(19)}(q_1; 1^-, 2^-, 3^+, 4^+; q_2) &= |q_{1\perp}|^2 q_{2\perp} p_{2\perp}^3 x_1 \sqrt{x_3} (x_3 + x_4)^3, \\
D^{(19)}(q_1; 1^-, 2^-, 3^+, 4^+; q_2) &= \langle 34 \rangle (q_{1\perp} + p_{1\perp}) (q_{1\perp} + p_{1\perp} + p_{2\perp}) p_{1\perp}^* \sqrt{x_4} \\
&\quad (\sqrt{x_1 x_2} \langle 12 \rangle + q_{1\perp} x_2 + p_{2\perp} x_{1234}) \\
&\quad \left( x_2 \left( |p_{1\perp}|^2 x_1 + q_{1\perp}^* p_{1\perp} x_1 + q_{1\perp} (q_{1\perp}^* + p_{1\perp}^* + p_{2\perp}^*) x_1 \right. \right. \\
&\quad \left. \left. + \langle 12 \rangle [12] x_1 + |p_{1\perp}|^2 x_2 + |p_{1\perp}|^2 x_3 + |p_{1\perp}|^2 x_4 \right) + p_{2\perp} x_1 \right. \\
&\quad \left. (q_{1\perp}^* x_2 + p_{2\perp}^* x_{1234}) (q_{1\perp} (x_3 + x_{1234}) - \sqrt{x_3} \Delta(3, 1, 2)) \right),
\end{aligned}$$

$$\begin{aligned}
N^{(20)}(q_1; 1^-, 2^-, 3^+, 4^+; q_2) &= q_{1\perp}^* q_{2\perp} (p_{1\perp} + p_{2\perp})^3 \sqrt{x_1 x_2 x_3} (x_3 + x_4)^3, \\
D^{(20)}(q_1; 1^-, 2^-, 3^+, 4^+; q_2) &= \langle 34 \rangle (q_{1\perp} + p_{1\perp} + p_{2\perp}) [12] \sqrt{x_4} (q_{1\perp} (x_1 + x_2) \\
&\quad + (p_{1\perp} + p_{2\perp}) x_{1234}) (q_{1\perp} (x_3 + x_{1234}) - \sqrt{x_3} \Delta(3, 1, 2)) \\
&\quad \left( x_2 \left( |p_{1\perp}|^2 x_1 + q_{1\perp}^* p_{1\perp} x_1 + q_{1\perp} (q_{1\perp}^* + p_{1\perp}^* + p_{2\perp}^*) x_1 \right. \right. \\
&\quad \left. \left. + \langle 12 \rangle [12] x_1 + |p_{1\perp}|^2 x_2 + |p_{1\perp}|^2 x_3 + |p_{1\perp}|^2 x_4 \right) \right. \\
&\quad \left. + p_{2\perp} x_1 (q_{1\perp}^* x_2 + p_{2\perp}^* x_{1234}) \right),
\end{aligned}$$

$$\begin{aligned}
N^{(21)}(q_1; 1^-, 2^-, 3^+, 4^+; q_2) &= q_{1\perp}^* q_{2\perp} x_3^{3/2} \Delta(1, 2, 3), \\
D^{(21)}(q_1; 1^-, 2^-, 3^+, 4^+; q_2) &= s_{123} (q_{1\perp} + p_{1\perp} + p_{2\perp}) [23] \\
&\quad \sqrt{x_1} \sqrt{x_2} \sqrt{x_4} \Delta(4, 1, 3),
\end{aligned}$$

$$\begin{aligned}
N^{(22)}(q_1; 1^-, 2^-, 3^+, 4^+; q_2) &= q_{1\perp}^* q_{2\perp} p_{1\perp}^3 x_1 \sqrt{x_3} (x_3 + x_4)^3 \\
&\quad (\sqrt{x_1 x_2} \langle 12 \rangle + q_{1\perp} x_2 + p_{2\perp} x_{1234}), \\
D^{(22)}(q_1; 1^-, 2^-, 3^+, 4^+; q_2) &= \langle 34 \rangle (q_{1\perp} + p_{1\perp}) \sqrt{x_4} (q_{1\perp} x_1 + p_{1\perp} x_{1234}) \\
&\quad (q_{1\perp} (q_{1\perp}^* + p_{1\perp}^*) x_1 + p_{1\perp} (q_{1\perp}^* x_1 + p_{1\perp}^* x_{1234})) \\
&\quad \left( x_2 \left( |p_{1\perp}|^2 x_1 + q_{1\perp}^* p_{1\perp} x_1 + q_{1\perp} (q_{1\perp}^* + p_{1\perp}^* + p_{2\perp}^*) x_1 \right. \right. \\
&\quad \left. \left. + \langle 12 \rangle [12] x_1 + |p_{1\perp}|^2 x_2 + |p_{1\perp}|^2 x_3 + |p_{1\perp}|^2 x_4 \right) \right. \\
&\quad \left. + p_{2\perp} x_1 (q_{1\perp}^* x_2 + p_{2\perp}^* x_{1234}) \right) \\
&\quad (q_{1\perp} (x_3 + x_{1234}) - \sqrt{x_3} \Delta(3, 1, 2)),
\end{aligned}$$

$$\begin{aligned}
N^{(23)}(q_1; 1^-, 2^-, 3^+, 4^+; q_2) &= -|q_{1\perp}|^2 q_{2\perp} \langle 12 \rangle^3 (q_{1\perp} + p_{1\perp} + p_{2\perp} + p_{4\perp}) \\
&\quad x_1 x_2 x_3 x_4, \\
D^{(23)}(q_1; 1^-, 2^-, 3^+, 4^+; q_2) &= s_{1234} \langle 23 \rangle \langle 34 \rangle (2q_{1\perp} + p_{1\perp} + p_{2\perp} + p_{4\perp}) \\
&\quad \left( |p_{4\perp}|^2 x_1 x_2 x_3 \right. \\
&\quad \left. + \left( q_{1\perp} q_{1\perp}^* x_1 x_2 + \left( |p_{2\perp}|^2 x_1 + |p_{1\perp}|^2 x_2 \right) x_3 \right) x_4 \right) \\
&\quad \Delta(1, 2, 4) \Delta(4, 1, 3),
\end{aligned}$$

$$\begin{aligned}
N^{(24)}(q_1; 1^-, 2^-, 3^+, 4^+; q_2) &= -q_{1\perp} q_{2\perp} \langle 12 \rangle^3 x_{1234}, \\
D^{(24)}(q_1; 1^-, 2^-, 3^+, 4^+; q_2) &= s_{1234} \langle 23 \rangle \langle 34 \rangle (2q_{1\perp} + p_{1\perp} + p_{2\perp} + p_{4\perp}) \\
&\quad \Delta(1, 2, 4) \Delta(4, 1, 3),
\end{aligned}$$

$$\begin{aligned}
N^{(25)}(q_1; 1^-, 2^-, 3^+, 4^+; q_2) &= |q_{1\perp}|^2 q_{2\perp} \langle 12 \rangle^3 (q_{1\perp} + p_{1\perp} + p_{2\perp})^3 x_1 x_2 x_3 x_4^{3/2}, \\
D^{(25)}(q_1; 1^-, 2^-, 3^+, 4^+; q_2) &= s_{123} \langle 23 \rangle p_{4\perp} (2q_{1\perp}^2 + 3(p_{1\perp} + p_{2\perp} + p_{4\perp}) q_{1\perp} \\
&\quad + (p_{1\perp} + p_{2\perp} + p_{4\perp})^2) \left( |p_{4\perp}|^2 x_1 x_2 x_3 + (q_{1\perp} q_{1\perp}^* x_1 x_2 \right. \\
&\quad \left. + \left( |p_{2\perp}|^2 x_1 + |p_{1\perp}|^2 x_2 \right) x_3 \right) x_4 \\
&\quad \Delta(1, 2, 3) \Delta(3, 1, 2) \Delta(4, 1, 3),
\end{aligned}$$

$$N^{(26)}(q_1; 1^-, 2^-, 3^+, 4^+; q_2) = q_{1\perp} q_{2\perp} \langle 12 \rangle^3 (x_1 + x_2 + x_3)^4,$$

$$D^{(26)}(q_1; 1^-, 2^-, 3^+, 4^+; q_2) = s_{123} \langle 23 \rangle \sqrt{x_4} x_{1234} \\ ((p_{1\perp} + p_{2\perp}) x_{1234} + q_{1\perp} (x_1 + x_2 + x_3 + x_{1234})) \\ \Delta(1, 2, 3) \Delta(3, 1, 2) \Delta(4, 1, 3),$$

$$N^{(27)}(q_1; 1^-, 2^-, 3^+, 4^+; q_2) = -q_{1\perp}^* q_{2\perp} x_3^{3/2} \Delta(3, 1, 2),$$

$$D^{(27)}(q_1; 1^-, 2^-, 3^+, 4^+; q_2) = s_{123} (q_{1\perp} + p_{1\perp} + p_{2\perp}) [12] \\ \sqrt{x_1} \sqrt{x_2} \sqrt{x_4} \Delta(4, 1, 3),$$

$$N^{(28)}(q_1; 1^-, 2^-, 3^+, 4^+; q_2) = -q_{1\perp}^* q_{2\perp} (\sqrt{x_1 x_3} \langle 13 \rangle - \sqrt{x_4} \Delta(4, 1, 2) \\ + \langle 23 \rangle \sqrt{x_2 x_3})^3,$$

$$D^{(28)}(q_1; 1^-, 2^-, 3^+, 4^+; q_2) = s_{1234} \langle 34 \rangle (q_{1\perp} + p_{1\perp} + p_{2\perp} + p_{4\perp}) [12] \\ \sqrt{x_1} \sqrt{x_2} x_{1234} \Delta(3, 1, 2) \Delta(4, 1, 3),$$

$$N^{(29)}(q_1; 1^-, 2^-, 3^+, 4^+; q_2) = q_{1\perp}^* q_{2\perp} \langle 12 \rangle^3 x_4^{3/2} \Delta(4, 1, 3),$$

$$D^{(29)}(q_1; 1^-, 2^-, 3^+, 4^+; q_2) = s_{123} s_{1234} \langle 23 \rangle (q_{1\perp} + p_{1\perp} + p_{2\perp} + p_{4\perp}) x_{1234} \\ \Delta(1, 2, 3) \Delta(3, 1, 2),$$

$$N^{(30)}(q_1; 1^-, 2^-, 3^+, 4^+; q_2) = -|q_{1\perp}|^2 q_{2\perp} x_3^{3/2},$$

$$D^{(30)}(q_1; 1^-, 2^-, 3^+, 4^+; q_2) = (q_{1\perp} + p_{1\perp}) (q_{1\perp} + p_{2\perp}) p_{1\perp}^* [23] \\ \sqrt{x_2} \sqrt{x_4} \Delta(4, 2, 3),$$

$$\begin{aligned}
N^{(31)}(q_1; 1^-, 2^-, 3^+, 4^+; q_2) &= |q_{1\perp}|^2 q_{2\perp} p_{1\perp}^3 \sqrt{x_2} x_3^{5/2} x_4^{3/2}, \\
D^{(31)}(q_1; 1^-, 2^-, 3^+, 4^+; q_2) &= p_{4\perp} (2q_{1\perp}^2 + 3(p_{1\perp} + p_{2\perp} + p_{4\perp}) q_{1\perp} \\
&\quad + (p_{1\perp} + p_{2\perp} + p_{4\perp})^2) [23] \sqrt{x_1} \left( |p_{4\perp}|^2 x_1 x_2 x_3 + (q_{1\perp} q_{1\perp}^* x_1 x_2 \right. \\
&\quad \left. + (|p_{2\perp}|^2 x_1 + |p_{1\perp}|^2 x_2) x_3 \right) x_4 \Delta(1, 2, 3) \Delta(4, 2, 3),
\end{aligned}$$

$$\begin{aligned}
N^{(32)}(q_1; 1^-, 2^-, 3^+, 4^+; q_2) &= q_{1\perp} q_{2\perp} x_1^{5/2} x_3^{3/2}, \\
D^{(32)}(q_1; 1^-, 2^-, 3^+, 4^+; q_2) &= [23] \sqrt{x_2} \sqrt{x_4} x_{1234} (q_{1\perp} x_1 + p_{1\perp} x_{1234}) \\
&\quad \Delta(1, 2, 3) \Delta(4, 2, 3),
\end{aligned}$$

$$\begin{aligned}
N^{(33)}(q_1; 1^-, 2^-, 3^+, 4^+; q_2) &= -q_{1\perp}^* q_{2\perp} p_{1\perp}^3 x_3^{3/2} (x_2 + x_3 + x_4)^3, \\
D^{(33)}(q_1; 1^-, 2^-, 3^+, 4^+; q_2) &= (q_{1\perp} + p_{1\perp}) [23] \sqrt{x_2} \sqrt{x_4} (q_{1\perp} x_1 + p_{1\perp} x_{1234}) \\
&\quad (q_{1\perp} (q_{1\perp}^* + p_{1\perp}^*) x_1 + p_{1\perp} (q_{1\perp}^* x_1 + p_{1\perp}^* x_{1234})) (q_{1\perp} (x_{1234} + x_2 + x_3) \\
&\quad + p_{2\perp} x_{1234} + \sqrt{x_1} \Delta(1, 2, 3)) \Delta(4, 2, 3),
\end{aligned}$$

$$\begin{aligned}
N^{(34)}(q_1; 1^-, 2^-, 3^+, 4^+; q_2) &= |q_{1\perp}|^2 q_{2\perp} \Delta(2, 3, 4)^3, \\
D^{(34)}(q_1; 1^-, 2^-, 3^+, 4^+; q_2) &= s_{234} \langle 23 \rangle \langle 34 \rangle (q_{1\perp} + p_{1\perp}) (q_{1\perp} + p_{2\perp} + p_{4\perp}) p_{1\perp}^* \\
&\quad (x_2 + x_3 + x_4) \Delta(4, 2, 3),
\end{aligned}$$

$$\begin{aligned}
N^{(35)}(q_1; 1^-, 2^-, 3^+, 4^+; q_2) &= q_{1\perp}^* q_{2\perp} p_{1\perp}^3 (x_2 + x_3 + x_4)^2 \Delta(2, 3, 4)^3, \\
D^{(35)}(q_1; 1^-, 2^-, 3^+, 4^+; q_2) &= s_{234} \langle 23 \rangle \langle 34 \rangle (q_{1\perp} + p_{1\perp}) (q_{1\perp} x_1 + p_{1\perp} x_{1234}) \\
&\quad (\sqrt{x_1 x_2} \langle 12 \rangle + p_{4\perp} x_1 + p_{4\perp} x_2 + p_{4\perp} x_3 + p_{4\perp} x_4 \\
&\quad + q_{1\perp} (x_1 + 2(x_2 + x_3 + x_4)) \\
&\quad + p_{2\perp} x_{1234} + \langle 13 \rangle \sqrt{x_1 x_3} + \langle 14 \rangle \sqrt{x_1 x_4}) (q_{1\perp} (q_{1\perp}^* + p_{1\perp}^*) x_1 \\
&\quad + p_{1\perp} (q_{1\perp}^* x_1 + p_{1\perp}^* x_{1234})) \Delta(4, 2, 3),
\end{aligned}$$



$$\begin{aligned}
N^{(36)}(q_1; 1^-, 2^-, 3^+, 4^+; q_2) &= -|q_{1\perp}|^2 q_{2\perp} p_{1\perp}^3 x_2 x_3 x_4 \Delta(2, 3, 4)^3, \\
D^{(36)}(q_1; 1^-, 2^-, 3^+, 4^+; q_2) &= s_{234} \langle 23 \rangle \langle 34 \rangle (q_{1\perp} + p_{2\perp} + p_{4\perp}) \\
&\quad \left( 2q_{1\perp}^2 + 3(p_{1\perp} + p_{2\perp} + p_{4\perp}) q_{1\perp} + (p_{1\perp} + p_{2\perp} + p_{4\perp})^2 \right) \\
&\quad \sqrt{x_1} \left( |p_{4\perp}|^2 x_1 x_2 x_3 + \left( q_{1\perp} q_{1\perp}^* x_1 x_2 + \left( |p_{2\perp}|^2 x_1 + |p_{1\perp}|^2 x_2 \right) x_3 \right) x_4 \right) \\
&\quad \Delta(1, 2, 4) \Delta(4, 2, 3),
\end{aligned}$$

$$\begin{aligned}
N^{(37)}(q_1; 1^-, 2^-, 3^+, 4^+; q_2) &= -q_{1\perp} q_{2\perp} x_1^{5/2} \Delta(2, 3, 4)^3, \\
D^{(37)}(q_1; 1^-, 2^-, 3^+, 4^+; q_2) &= s_{234} \langle 23 \rangle \langle 34 \rangle (x_2 + x_3 + x_4) x_{1234} \\
&\quad (q_{1\perp} x_1 + p_{1\perp} x_{1234}) \Delta(1, 2, 4) \Delta(4, 2, 3),
\end{aligned}$$

$$\begin{aligned}
N^{(38)}(q_1; 1^-, 2^-, 3^+, 4^+; q_2) &= -q_{1\perp}^* q_{2\perp} \Delta(1, 2, 4) \Delta(2, 3, 4)^3, \\
D^{(38)}(q_1; 1^-, 2^-, 3^+, 4^+; q_2) &= s_{1234} s_{234} \langle 23 \rangle \langle 34 \rangle (q_{1\perp} + p_{1\perp} + p_{2\perp} + p_{4\perp}) \\
&\quad \sqrt{x_1} x_{1234} \Delta(4, 2, 3),
\end{aligned}$$

$$\begin{aligned}
N^{(39)}(q_1; 1^-, 2^-, 3^+, 4^+; q_2) &= -q_{1\perp}^* q_{2\perp} x_3^{3/2} \Delta(1, 2, 4)^3, \\
D^{(39)}(q_1; 1^-, 2^-, 3^+, 4^+; q_2) &= s_{1234} (q_{1\perp} + p_{1\perp} + p_{2\perp} + p_{4\perp}) [23] \sqrt{x_2} x_{1234} \\
&\quad \Delta(1, 2, 3) \Delta(4, 1, 3) \Delta(4, 2, 3).
\end{aligned}$$

## O.2.2 Result for $V^{(0)}(q_1; 1^-, 2^+, 3^-, 4^+; q_2)$

$$\begin{aligned}
N^{(1)}(q_1; 1^-, 2^+, 3^-, 4^+; q_2) &= q_{1\perp}^2 q_{1\perp}^* q_{2\perp} p_{1\perp}^3 \sqrt{x_1} x_2^{5/2}, \\
D^{(1)}(q_1; 1^-, 2^+, 3^-, 4^+; q_2) &= \langle 12 \rangle p_{2\perp} (p_{1\perp} + p_{2\perp}) (2q_{1\perp} + p_{1\perp} + p_{2\perp}) p_{4\perp} \\
&\quad \left( |p_{2\perp}|^2 x_1 + |p_{1\perp}|^2 x_2 \right) \left( |q_{1\perp}|^2 x_1 x_2 + \left( |p_{2\perp}|^2 x_1 + |p_{1\perp}|^2 x_2 \right) x_3 \right), \\
N^{(2)}(q_1; 1^-, 2^+, 3^-, 4^+; q_2) &= q_{1\perp}^4 q_{1\perp}^* q_{2\perp} x_1 x_2^{3/2}, \\
D^{(2)}(q_1; 1^-, 2^+, 3^-, 4^+; q_2) &= \langle 23 \rangle p_{2\perp} (q_{1\perp} + p_{2\perp}) (2q_{1\perp} + p_{1\perp} + p_{2\perp}) \\
&\quad p_{4\perp} p_{1\perp}^* \sqrt{x_3} \left( |q_{1\perp}|^2 x_1 x_2 + \left( |p_{2\perp}|^2 x_1 + |p_{1\perp}|^2 x_2 \right) x_3 \right), \\
N^{(3)}(q_1; 1^-, 2^+, 3^-, 4^+; q_2) &= |q_{1\perp}|^2 q_{2\perp} p_{1\perp}^3 x_2^{3/2} x_4^{3/2}, \\
D^{(3)}(q_1; 1^-, 2^+, 3^-, 4^+; q_2) &= \langle 12 \rangle p_{2\perp} (p_{1\perp} + p_{2\perp}) (q_{1\perp} + p_{1\perp} + p_{2\perp}) \\
&\quad (q_{1\perp} + p_{4\perp}) [34] \sqrt{x_1} \left( |p_{2\perp}|^2 x_1 + |p_{1\perp}|^2 x_2 \right) \sqrt{x_3} (x_3 + x_4), \\
N^{(4)}(q_1; 1^-, 2^+, 3^-, 4^+; q_2) &= -q_{1\perp}^5 q_{1\perp}^* q_{2\perp} x_1 x_2^{3/2} x_4^{3/2}, \\
D^{(4)}(q_1; 1^-, 2^+, 3^-, 4^+; q_2) &= \langle 23 \rangle \langle 34 \rangle p_{2\perp} p_{4\perp} (q_{1\perp} + p_{2\perp} + p_{4\perp}) \\
&\quad (2q_{1\perp} + p_{1\perp} + p_{2\perp} + p_{4\perp}) p_{1\perp}^* x_3 \\
&\quad \left( |p_{4\perp}|^2 x_1 x_2 x_3 + \left( |q_{1\perp}|^2 x_1 x_2 + \left( |p_{2\perp}|^2 x_1 + |p_{1\perp}|^2 x_2 \right) x_3 \right) x_4 \right), \\
N^{(5)}(q_1; 1^-, 2^+, 3^-, 4^+; q_2) &= -q_{1\perp}^4 q_{1\perp}^* q_{2\perp} p_{1\perp}^3 \sqrt{x_1} x_2^{5/2} x_4^{3/2}, \\
D^{(5)}(q_1; 1^-, 2^+, 3^-, 4^+; q_2) &= \langle 12 \rangle \langle 34 \rangle p_{2\perp} (p_{1\perp} + p_{2\perp}) p_{4\perp} (q_{1\perp} + p_{4\perp}) \\
&\quad (2q_{1\perp} + p_{1\perp} + p_{2\perp} + p_{4\perp}) \left( |p_{2\perp}|^2 x_1 + |p_{1\perp}|^2 x_2 \right) \sqrt{x_3} \\
&\quad \left( |p_{4\perp}|^2 x_1 x_2 x_3 + \left( |q_{1\perp}|^2 x_1 x_2 + \left( |p_{2\perp}|^2 x_1 + |p_{1\perp}|^2 x_2 \right) x_3 \right) x_4 \right), \\
N^{(6)}(q_1; 1^-, 2^+, 3^-, 4^+; q_2) &= -|q_{1\perp}|^2 q_{2\perp} (q_{1\perp} + p_{1\perp}) x_1 \sqrt{x_2} x_3^2, \\
D^{(6)}(q_1; 1^-, 2^+, 3^-, 4^+; q_2) &= \langle 23 \rangle \langle 34 \rangle p_{1\perp}^* \sqrt{x_4} (x_2 + x_3 + x_4) \\
&\quad (\sqrt{x_1 x_2} \langle 12 \rangle + q_{1\perp} x_2 + p_{2\perp} x_{1234}) \\
&\quad (q_{1\perp} (q_{1\perp}^* + p_{1\perp}^*) x_1 + p_{1\perp} (q_{1\perp}^* x_1 + p_{1\perp}^* x_{1234})),
\end{aligned}$$

$$\begin{aligned}
N^{(7)}(q_1; 1^-, 2^+, 3^-, 4^+; q_2) &= -q_{1\perp} q_{2\perp} \sqrt{x_2} x_3^2 (q_{1\perp} x_1 + p_{1\perp} x_{1234}), \\
D^{(7)}(q_1; 1^-, 2^+, 3^-, 4^+; q_2) &= (x_2 + x_3 + x_4) (\sqrt{x_1 x_2} \langle 12 \rangle + q_{1\perp} x_2 + p_{2\perp} x_{1234}) \\
&\quad \langle 23 \rangle \langle 34 \rangle \sqrt{x_4} (q_{1\perp} (q_{1\perp}^* + p_{1\perp}^*) x_1 + p_{1\perp} (q_{1\perp}^* x_1 + p_{1\perp}^* x_{1234})),
\end{aligned}$$

$$\begin{aligned}
N^{(8)}(q_1; 1^-, 2^+, 3^-, 4^+; q_2) &= q_{1\perp}^* q_{2\perp} p_{1\perp}^3 x_2^{3/2} x_4^{3/2} (x_3 + x_4)^2, \\
D^{(8)}(q_1; 1^-, 2^+, 3^-, 4^+; q_2) &= \langle 12 \rangle (q_{1\perp} + p_{1\perp} + p_{2\perp}) [34] \sqrt{x_1} \sqrt{x_3} \\
&\quad (\sqrt{x_1 x_2} \langle 12 \rangle + q_{1\perp} x_2 + p_{2\perp} x_{1234}) (\sqrt{x_1 x_3} \langle 13 \rangle + q_{1\perp} (x_{1234} + x_3 + x_4) \\
&\quad + p_{4\perp} x_{1234} + \langle 23 \rangle \sqrt{x_2 x_3} + \langle 14 \rangle \sqrt{x_1 x_4} + \langle 24 \rangle \sqrt{x_2 x_4}) \\
&\quad \left( x_2 \left( |p_{1\perp}|^2 x_{1234} + q_{1\perp}^* p_{1\perp} x_1 + q_{1\perp} (q_{1\perp}^* + p_{1\perp}^* + p_{2\perp}^*) x_1 + \langle 12 \rangle [12] x_1 \right) \right. \\
&\quad \left. + p_{2\perp} x_1 (q_{1\perp}^* x_2 + p_{2\perp}^* x_{1234}) \right),
\end{aligned}$$

$$\begin{aligned}
N^{(9)}(q_1; 1^-, 2^+, 3^-, 4^+; q_2) &= |q_{1\perp}|^2 q_{2\perp} p_{1\perp}^3 x_2^{5/2} \sqrt{x_3}, \\
D^{(9)}(q_1; 1^-, 2^+, 3^-, 4^+; q_2) &= (q_{1\perp} + p_{2\perp}) (q_{1\perp} + p_{1\perp} + p_{2\perp}) p_{4\perp} [23] \sqrt{x_1} \\
&\quad (2q_{1\perp} + p_{1\perp} + p_{2\perp}) \left( q_{1\perp} q_{1\perp}^* x_1 x_2 + \left( |p_{2\perp}|^2 x_1 + |p_{1\perp}|^2 x_2 \right) x_3 \right) \\
&\quad \Delta(1, 2, 3),
\end{aligned}$$

$$\begin{aligned}
N^{(10)}(q_1; 1^-, 2^+, 3^-, 4^+; q_2) &= q_{1\perp}^* q_{2\perp} p_{1\perp}^3 x_2^{5/2} \sqrt{x_3} x_4^3, \\
D^{(10)}(q_1; 1^-, 2^+, 3^-, 4^+; q_2) &= (2q_{1\perp} + p_{1\perp} + p_{2\perp}) [23] \sqrt{x_1} \\
&\quad (\sqrt{x_4} (\sqrt{x_4} q_{1\perp} - \langle 41 \rangle \sqrt{x_1} - \langle 42 \rangle \sqrt{x_2} - \langle 43 \rangle \sqrt{x_3}) + p_{4\perp} x_{1234}) \\
&\quad (q_{1\perp} x_1 x_2 ((p_{1\perp}^* + p_{2\perp}^*) x_3 + q_{1\perp}^* (3x_3 + x_{1234})) + \\
&\quad x_3 (p_{2\perp} x_1 (q_{1\perp}^* x_2 + p_{2\perp}^* x_{1234}) + x_2 (p_{1\perp} (q_{1\perp}^* x_1 + p_{1\perp}^* x_{1234}) - s_{123} x_1))) \\
&\quad (q_{1\perp} (x_1 + 2x_2 + 2x_3 + x_4) + p_{2\perp} x_{1234} + \sqrt{x_1} \Delta(1, 2, 3)) \\
&\quad \Delta(1, 2, 3),
\end{aligned}$$

$$\begin{aligned}
N^{(11)}(q_1; 1^-, 2^+, 3^-, 4^+; q_2) &= |q_{1\perp}|^2 q_{2\perp} \sqrt{x_2} x_4^{3/2}, \\
D^{(11)}(q_1; 1^-, 2^+, 3^-, 4^+; q_2) &= (q_{1\perp} + p_{1\perp}) p_{2\perp} p_{1\perp}^* [34] \sqrt{x_3} (x_3 + x_4) \\
&\quad \Delta(2, 3, 4),
\end{aligned}$$

$$\begin{aligned}
N^{(12)}(q_1; 1^-, 2^+, 3^-, 4^+; q_2) &= -|q_{1\perp}|^2 q_{2\perp} p_{1\perp}^3 x_2 \sqrt{x_3} x_4^{5/2}, \\
D^{(12)}(q_1; 1^-, 2^+, 3^-, 4^+; q_2) &= \langle 12 \rangle (q_{1\perp} + p_{4\perp}) (q_{1\perp} + p_{1\perp} + p_{2\perp} + p_{4\perp}) \\
&\quad (2q_{1\perp} + p_{1\perp} + p_{2\perp} + p_{4\perp}) [34] \sqrt{x_1} \Delta(2, 3, 4) \\
&\quad \left( |p_{4\perp}|^2 x_1 x_2 x_3 + \left( q_{1\perp} q_{1\perp}^* x_1 x_2 + \left( |p_{2\perp}|^2 x_1 + |p_{1\perp}|^2 x_2 \right) x_3 \right) x_4 \right), \\
N^{(13)}(q_1; 1^-, 2^+, 3^-, 4^+; q_2) &= -q_{1\perp} q_{2\perp} x_1^{5/2} x_4^{3/2}, \\
D^{(13)}(q_1; 1^-, 2^+, 3^-, 4^+; q_2) &= \langle 12 \rangle [34] \sqrt{x_3} (x_3 + x_4) x_{1234} \\
&\quad (q_{1\perp} x_1 + p_{1\perp} x_{1234}) \Delta(2, 3, 4), \\
N^{(14)}(q_1; 1^-, 2^+, 3^-, 4^+; q_2) &= q_{1\perp}^* q_{2\perp} p_{1\perp}^3 \sqrt{x_2} x_4^{3/2} (x_2 + x_3 + x_4)^3, \\
D^{(14)}(q_1; 1^-, 2^+, 3^-, 4^+; q_2) &= (q_{1\perp} + p_{1\perp}) [34] \sqrt{x_3} (x_3 + x_4) \\
&\quad (q_{1\perp} x_1 + p_{1\perp} x_{1234}) \Delta(2, 3, 4) \\
&\quad (\sqrt{x_1 x_2} \langle 12 \rangle + q_{1\perp} x_2 + p_{2\perp} x_{1234}) \\
&\quad (q_{1\perp} (q_{1\perp}^* + p_{1\perp}^*) x_1 + p_{1\perp} (q_{1\perp}^* x_1 + p_{1\perp}^* x_{1234})), \\
N^{(15)}(q_1; 1^-, 2^+, 3^-, 4^+; q_2) &= -q_{1\perp}^4 q_{1\perp}^* q_{2\perp} \sqrt{x_1} x_2^{5/2}, \\
D^{(15)}(q_1; 1^-, 2^+, 3^-, 4^+; q_2) &= (p_{1\perp} + p_{2\perp}) p_{4\perp} [12] \Delta(3, 1, 2) \\
&\quad \left( 2q_{1\perp}^2 + 3(p_{1\perp} + p_{2\perp}) q_{1\perp} + (p_{1\perp} + p_{2\perp})^2 \right) \\
&\quad \sqrt{x_3} \left( |q_{1\perp}|^2 x_1 x_2 + \left( |p_{2\perp}|^2 x_1 + |p_{1\perp}|^2 x_2 \right) x_3 \right), \\
N^{(16)}(q_1; 1^-, 2^+, 3^-, 4^+; q_2) &= q_{1\perp}^5 q_{1\perp}^* q_{2\perp} \sqrt{x_1} x_2^{5/2} x_4^{3/2}, \\
D^{(16)}(q_1; 1^-, 2^+, 3^-, 4^+; q_2) &= \langle 34 \rangle (p_{1\perp} + p_{2\perp}) p_{4\perp} [12] x_3 \Delta(3, 1, 2) \\
&\quad \left( 2q_{1\perp}^2 + 3(p_{1\perp} + p_{2\perp} + p_{4\perp}) q_{1\perp} + (p_{1\perp} + p_{2\perp} + p_{4\perp})^2 \right) \\
&\quad \left( |p_{4\perp}|^2 x_1 x_2 x_3 + \left( |q_{1\perp}|^2 x_1 x_2 + \left( |p_{2\perp}|^2 x_1 + |p_{1\perp}|^2 x_2 \right) x_3 \right) x_4 \right), \\
N^{(17)}(q_1; 1^-, 2^+, 3^-, 4^+; q_2) &= q_{1\perp} q_{2\perp} x_2^{3/2} x_3^2, \\
D^{(17)}(q_1; 1^-, 2^+, 3^-, 4^+; q_2) &= \langle 34 \rangle [12] \sqrt{x_1} \sqrt{x_4} x_{1234} \Delta(3, 1, 2) \\
&\quad (q_{1\perp} (x_1 + x_2) + (p_{1\perp} + p_{2\perp}) x_{1234}),
\end{aligned}$$

$$\begin{aligned}
N^{(18)}(q_1; 1^-, 2^+, 3^-, 4^+; q_2) &= |q_{1\perp}|^2 q_{2\perp} \langle 13 \rangle^4 (q_{1\perp} + p_{1\perp} + p_{2\perp}) x_1 x_2 x_3, \\
D^{(18)}(q_1; 1^-, 2^+, 3^-, 4^+; q_2) &= s_{123} \langle 12 \rangle \langle 23 \rangle \Delta(1, 2, 3) \Delta(3, 1, 2) \\
&\quad (2q_{1\perp} + p_{1\perp} + p_{2\perp}) p_{4\perp} \left( q_{1\perp} q_{1\perp}^* x_1 x_2 + (|p_{2\perp}|^2 x_1 + |p_{1\perp}|^2 x_2) x_3 \right),
\end{aligned}$$

$$\begin{aligned}
N^{(19)}(q_1; 1^-, 2^+, 3^-, 4^+; q_2) &= q_{1\perp}^* q_{2\perp} \langle 13 \rangle^4 (q_{1\perp} + p_{1\perp} + p_{2\perp})^3 x_1 x_2 x_3 x_4^3, \\
D^{(19)}(q_1; 1^-, 2^+, 3^-, 4^+; q_2) &= s_{123} \langle 12 \rangle \langle 23 \rangle (2q_{1\perp} + p_{1\perp} + p_{2\perp}) \\
&\quad (\sqrt{x_4} (\sqrt{x_4} q_{1\perp} - \langle 41 \rangle \sqrt{x_1} - \langle 42 \rangle \sqrt{x_2} - \langle 43 \rangle \sqrt{x_3}) + p_{4\perp} x_{1234}) \\
&\quad ((p_{1\perp} + p_{2\perp}) x_{1234} + q_{1\perp} (x_1 + x_2 + x_3 + x_{1234})) \\
&\quad (q_{1\perp} x_1 x_2 ((p_{1\perp}^* + p_{2\perp}^*) x_3 + q_{1\perp}^* (3x_3 + x_{1234})) + x_3 (p_{2\perp} \\
&\quad x_1 (q_{1\perp}^* x_2 + p_{2\perp}^* x_{1234}) + \\
&\quad x_2 (p_{1\perp} (q_{1\perp}^* x_1 + p_{1\perp}^* x_{1234}) - s_{123} x_1))) \Delta(1, 2, 3) \Delta(3, 1, 2),
\end{aligned}$$

$$\begin{aligned}
N^{(20)}(q_1; 1^-, 2^+, 3^-, 4^+; q_2) &= q_{1\perp}^4 q_{1\perp}^* q_{2\perp} p_{1\perp}^3 \sqrt{x_1} x_2^{5/2} x_4^3, \\
D^{(20)}(q_1; 1^-, 2^+, 3^-, 4^+; q_2) &= \langle 12 \rangle p_{2\perp} (p_{1\perp} + p_{2\perp}) \left( |p_{2\perp}|^2 x_1 + |p_{1\perp}|^2 x_2 \right) \\
&\quad \left( 2q_{1\perp}^2 + 3(p_{1\perp} + p_{2\perp}) q_{1\perp} + (p_{1\perp} + p_{2\perp})^2 \right) \\
&\quad (\sqrt{x_4} (\sqrt{x_4} q_{1\perp} - \langle 41 \rangle \sqrt{x_1} - \langle 42 \rangle \sqrt{x_2} - \langle 43 \rangle \sqrt{x_3}) + p_{4\perp} x_{1234}) \\
&\quad (q_{1\perp} x_1 x_2 ((p_{1\perp}^* + p_{2\perp}^*) x_3 + q_{1\perp}^* (3x_3 + x_{1234})) + x_3 (p_{2\perp} x_1 (q_{1\perp}^* x_2 \\
&\quad + p_{2\perp}^* x_{1234}) + x_2 (p_{1\perp} (q_{1\perp}^* x_1 + p_{1\perp}^* x_{1234}) - s_{123} x_1))) \\
&\quad (q_{1\perp} (x_1 + x_2 + 2x_3 + x_4) - \sqrt{x_3} \Delta(3, 1, 2)),
\end{aligned}$$

$$\begin{aligned}
N^{(21)}(q_1; 1^-, 2^+, 3^-, 4^+; q_2) &= q_{1\perp}^5 q_{1\perp}^* q_{2\perp} x_1 x_2^{3/2} x_4^3, \\
D^{(21)}(q_1; 1^-, 2^+, 3^-, 4^+; q_2) &= \langle 23 \rangle (q_{1\perp} + p_{1\perp}) p_{2\perp} (2q_{1\perp} + p_{1\perp} + p_{2\perp}) p_{1\perp}^* \\
&\quad \sqrt{x_3} (\sqrt{x_4} (\sqrt{x_4} q_{1\perp} - \langle 41 \rangle \sqrt{x_1} - \langle 42 \rangle \sqrt{x_2} - \langle 43 \rangle \sqrt{x_3}) + p_{4\perp} x_{1234}) \\
&\quad (q_{1\perp} x_1 x_2 ((p_{1\perp}^* + p_{2\perp}^*) x_3 + q_{1\perp}^* (3x_3 + x_{1234})) + x_3 (p_{2\perp} x_1 \\
&\quad (q_{1\perp}^* x_2 + p_{2\perp}^* x_{1234}) + x_2 (p_{1\perp} (q_{1\perp}^* x_1 + p_{1\perp}^* x_{1234}) - s_{123} x_1))) \\
&\quad (q_{1\perp} (x_1 + x_2 + 2x_3 + x_4) - \sqrt{x_3} \Delta(3, 1, 2)),
\end{aligned}$$

$$\begin{aligned}
N^{(22)}(q_1; 1^-, 2^+, 3^-, 4^+; q_2) &= -q_{1\perp} q_{2\perp} \langle 13 \rangle^4 x_1^{3/2} x_2 x_3^{3/2} x_4^3, \\
D^{(22)}(q_1; 1^-, 2^+, 3^-, 4^+; q_2) &= \langle 12 \rangle \langle 23 \rangle (q_{1\perp} x_1 + p_{1\perp} x_{1234}) \\
&\quad (\sqrt{x_4} (\sqrt{x_4} q_{1\perp} - \langle 41 \rangle \sqrt{x_1} - \langle 42 \rangle \sqrt{x_2} - \langle 43 \rangle \sqrt{x_3}) + p_{4\perp} x_{1234}) \\
&\quad ((p_{1\perp} + p_{2\perp}) x_{1234} + q_{1\perp} (x_1 + x_2 + x_3 + x_{1234})) \\
&\quad (q_{1\perp} x_1 x_2 ((p_{1\perp}^* + p_{2\perp}^*) x_3 + q_{1\perp}^* (3x_3 + x_{1234})) + x_3 \\
&\quad (p_{2\perp} x_1 (q_{1\perp}^* x_2 + p_{2\perp}^* x_{1234}) + x_2 (p_{1\perp} (q_{1\perp}^* x_1 + p_{1\perp}^* x_{1234}) - s_{123} x_1))) \\
&\quad (q_{1\perp} (x_1 + x_2 + 2x_3 + x_4) - \sqrt{x_3} \Delta(3, 1, 2)),
\end{aligned}$$

$$\begin{aligned}
N^{(23)}(q_1; 1^-, 2^+, 3^-, 4^+; q_2) &= q_{1\perp}^* q_{2\perp} p_{1\perp}^3 x_1 x_2^{3/2} x_4^3 \\
&\quad (\sqrt{x_1 x_3} \langle 13 \rangle + q_{1\perp} (x_1 + x_2 + 2x_3 + x_4))^4, \\
D^{(23)}(q_1; 1^-, 2^+, 3^-, 4^+; q_2) &= \langle 23 \rangle (q_{1\perp} + p_{1\perp}) \sqrt{x_3} (q_{1\perp} x_1 + p_{1\perp} x_{1234}) \\
&\quad (\sqrt{x_1 x_2} \langle 12 \rangle + q_{1\perp} x_2 + p_{2\perp} x_{1234}) \\
&\quad (\sqrt{x_4} (\sqrt{x_4} q_{1\perp} - \langle 41 \rangle \sqrt{x_1} - \langle 42 \rangle \sqrt{x_2} - \langle 43 \rangle \sqrt{x_3}) + p_{4\perp} x_{1234}) \\
&\quad (q_{1\perp} (q_{1\perp}^* + p_{1\perp}^*) x_1 + p_{1\perp} (q_{1\perp}^* x_1 + p_{1\perp}^* x_{1234})) \\
&\quad (q_{1\perp} x_1 x_2 ((p_{1\perp}^* + p_{2\perp}^*) x_3 + q_{1\perp}^* (3x_3 + x_{1234})) + \\
&\quad x_3 (p_{2\perp} x_1 (q_{1\perp}^* x_2 + p_{2\perp}^* x_{1234}) + x_2 (p_{1\perp} (q_{1\perp}^* x_1 + p_{1\perp}^* x_{1234}) - s_{123} x_1))) \\
&\quad (q_{1\perp} (x_1 + 2x_2 + 2x_3 + x_4) + p_{2\perp} x_{1234} + \sqrt{x_1} \Delta(1, 2, 3)) \\
&\quad (q_{1\perp} (x_{1234} + x_3) - \sqrt{x_3} \Delta(3, 1, 2)),
\end{aligned}$$

$$\begin{aligned}
N^{(24)}(q_1; 1^-, 2^+, 3^-, 4^+; q_2) &= -q_{1\perp}^4 q_{1\perp}^* q_{2\perp} \sqrt{x_1} x_2^{5/2} x_4^3, \\
D^{(24)}(q_1; 1^-, 2^+, 3^-, 4^+; q_2) &= (p_{1\perp} + p_{2\perp}) (2q_{1\perp} + p_{1\perp} + p_{2\perp}) [12] \sqrt{x_3} \\
&\quad (\sqrt{x_4} (\sqrt{x_4} q_{1\perp} - \langle 41 \rangle \sqrt{x_1} - \langle 42 \rangle \sqrt{x_2} - \langle 43 \rangle \sqrt{x_3}) + p_{4\perp} x_{1234}) \\
&\quad (q_{1\perp} x_1 x_2 ((p_{1\perp}^* + p_{2\perp}^*) x_3 + q_{1\perp}^* (3x_3 + x_{1234})) + \\
&\quad x_3 (p_{2\perp} x_1 (q_{1\perp}^* x_2 + p_{2\perp}^* x_{1234}) + x_2 (p_{1\perp} (q_{1\perp}^* x_1 + p_{1\perp}^* x_{1234}) - s_{123} x_1))) \\
&\quad \Delta(3, 1, 2) (q_{1\perp} (x_1 + x_2 + 2x_3 + x_4) - \sqrt{x_3} \Delta(3, 1, 2)),
\end{aligned}$$

$$\begin{aligned}
N^{(25)}(q_1; 1^-, 2^+, 3^-, 4^+; q_2) &= -|q_{1\perp}|^2 q_{2\perp} p_{1\perp}^3 (q_{1\perp} + p_{1\perp} + p_{2\perp}) \\
&\quad \sqrt{x_1 x_2}^{5/2} x_3^{5/2}, \\
D^{(25)}(q_1; 1^-, 2^+, 3^-, 4^+; q_2) &= \langle 12 \rangle \langle 34 \rangle p_{2\perp} (p_{1\perp} + p_{2\perp}) \sqrt{x_4} (x_3 + x_4) \\
&\quad \left( |p_{2\perp}|^2 x_1 + |p_{1\perp}|^2 x_2 \right) (q_{1\perp} (x_3 + x_{1234}) - \sqrt{x_3} \Delta(3, 1, 2)) \\
&\quad \left( x_2 \left( |p_{1\perp}|^2 x_1 + q_{1\perp}^* p_{1\perp} x_1 + q_{1\perp} (q_{1\perp}^* + p_{1\perp}^* + p_{2\perp}^*) x_1 + \langle 12 \rangle [12] x_1 + \right. \right. \\
&\quad \left. \left. |p_{1\perp}|^2 x_2 + |p_{1\perp}|^2 x_3 + |p_{1\perp}|^2 x_4 \right) + p_{2\perp} x_1 (q_{1\perp}^* x_2 + p_{2\perp}^* x_{1234}) \right),
\end{aligned}$$

$$\begin{aligned}
N^{(26)}(q_1; 1^-, 2^+, 3^-, 4^+; q_2) &= |q_{1\perp}|^2 q_{2\perp} (q_{1\perp} + p_{1\perp} + p_{2\perp})^3 x_1 x_2^2 x_3^{5/2}, \\
D^{(26)}(q_1; 1^-, 2^+, 3^-, 4^+; q_2) &= \langle 34 \rangle (q_{1\perp} + p_{1\perp}) p_{2\perp} p_{1\perp}^* \sqrt{x_4} (x_3 + x_4) \\
&\quad (\sqrt{x_1 x_2} \langle 12 \rangle + q_{1\perp} x_2 + p_{2\perp} x_{1234}) (q_{1\perp} (x_3 + x_{1234}) - \sqrt{x_3} \Delta(3, 1, 2)) \\
&\quad \left( x_2 \left( |p_{1\perp}|^2 x_1 + q_{1\perp}^* p_{1\perp} x_1 + q_{1\perp} (q_{1\perp}^* + p_{1\perp}^* + p_{2\perp}^*) x_1 \right. \right. \\
&\quad \left. \left. + \langle 12 \rangle [12] x_1 + |p_{1\perp}|^2 x_2 + |p_{1\perp}|^2 x_3 + |p_{1\perp}|^2 x_4 \right) \right. \\
&\quad \left. + p_{2\perp} x_1 (q_{1\perp}^* x_2 + p_{2\perp}^* x_{1234}) \right),
\end{aligned}$$

$$\begin{aligned}
N^{(27)}(q_1; 1^-, 2^+, 3^-, 4^+; q_2) &= q_{1\perp}^* q_{2\perp} (q_{1\perp} + p_{1\perp} + p_{2\perp})^3 \sqrt{x_1 x_2}^{5/2} x_3^{5/2}, \\
D^{(27)}(q_1; 1^-, 2^+, 3^-, 4^+; q_2) &= \langle 34 \rangle (p_{1\perp} + p_{2\perp}) [12] \sqrt{x_4} (x_3 + x_4) \\
&\quad (q_{1\perp} (x_1 + x_2) + (p_{1\perp} + p_{2\perp}) x_{1234}) (q_{1\perp} (x_3 + x_{1234}) - \sqrt{x_3} \Delta(3, 1, 2)) \\
&\quad \left( x_2 \left( |p_{1\perp}|^2 x_1 + q_{1\perp}^* p_{1\perp} x_1 + q_{1\perp} (q_{1\perp}^* + p_{1\perp}^* + p_{2\perp}^*) x_1 + \right. \right. \\
&\quad \left. \left. \langle 12 \rangle [12] x_1 + |p_{1\perp}|^2 x_2 + |p_{1\perp}|^2 x_3 + |p_{1\perp}|^2 x_4 \right) \right. \\
&\quad \left. + p_{2\perp} x_1 (q_{1\perp}^* x_2 + p_{2\perp}^* x_{1234}) \right),
\end{aligned}$$

$$\begin{aligned}
N^{(28)}(q_1; 1^-, 2^+, 3^-, 4^+; q_2) &= -q_{1\perp} q_{2\perp} x_2^{3/2} x_3^{5/2} \\
&\quad (-\sqrt{x_1 x_2} \langle 12 \rangle + q_{1\perp} x_1 + p_{1\perp} x_{1234})^4, \\
D^{(28)}(q_1; 1^-, 2^+, 3^-, 4^+; q_2) &= \langle 12 \rangle \langle 34 \rangle \sqrt{x_1} \sqrt{x_4} (x_3 + x_4) (q_{1\perp} x_1 + p_{1\perp} x_{1234}) \\
&\quad (\sqrt{x_1 x_2} \langle 12 \rangle + q_{1\perp} x_2 + p_{2\perp} x_{1234}) (q_{1\perp} (x_1 + x_2) + (p_{1\perp} + p_{2\perp}) x_{1234}) \\
&\quad \left( x_2 \left( |p_{1\perp}|^2 x_{1234} + q_{1\perp}^* p_{1\perp} x_1 + q_{1\perp} (q_{1\perp}^* + p_{1\perp}^* + p_{2\perp}^*) x_1 + \langle 12 \rangle [12] x_1 \right. \right. \\
&\quad \left. \left. + p_{2\perp} x_1 (q_{1\perp}^* x_2 + p_{2\perp}^* x_{1234}) \right) (q_{1\perp} (x_3 + x_{1234}) - \sqrt{x_3} \Delta(3, 1, 2)) \right),
\end{aligned}$$

$$\begin{aligned}
N^{(29)}(q_1; 1^-, 2^+, 3^-, 4^+; q_2) &= q_{1\perp}^* q_{2\perp} p_{1\perp}^3 x_1 x_2^2 x_3^{5/2} \\
&\quad (\sqrt{x_1 x_2} \langle 12 \rangle + q_{1\perp} x_2 + p_{2\perp} x_{1234}), \\
D^{(29)}(q_1; 1^-, 2^+, 3^-, 4^+; q_2) &= \langle 34 \rangle (q_{1\perp} + p_{1\perp}) \sqrt{x_4} (x_3 + x_4) \\
&\quad (q_{1\perp} x_1 + p_{1\perp} x_{1234}) (q_{1\perp} (q_{1\perp}^* + p_{1\perp}^*) x_1 + p_{1\perp} (q_{1\perp}^* x_1 + p_{1\perp}^* x_{1234})) \\
&\quad \left( x_2 \left( |p_{1\perp}|^2 x_{1234} + q_{1\perp}^* p_{1\perp} x_1 + q_{1\perp} (q_{1\perp}^* + p_{1\perp}^* + p_{2\perp}^*) x_1 + \langle 12 \rangle [12] x_1 \right) \right. \\
&\quad \left. + p_{2\perp} x_1 (q_{1\perp}^* x_2 + p_{2\perp}^* x_{1234}) \right) (q_{1\perp} (x_3 + x_{1234}) - \sqrt{x_3} \Delta(3, 1, 2)), \\
N^{(30)}(q_1; 1^-, 2^+, 3^-, 4^+; q_2) &= q_{1\perp}^* q_{2\perp} p_{1\perp}^3 \sqrt{x_1} x_2^{5/2} x_4^3 \\
&\quad (q_{1\perp} (x_3 + x_{1234}) - \sqrt{x_3} \Delta(3, 1, 2)), \\
D^{(30)}(q_1; 1^-, 2^+, 3^-, 4^+; q_2) &= \langle 12 \rangle (q_{1\perp} + p_{1\perp} + p_{2\perp}) \\
&\quad (\sqrt{x_1 x_2} \langle 12 \rangle + q_{1\perp} x_2 + p_{2\perp} x_{1234}) \\
&\quad (\sqrt{x_4} (\sqrt{x_4} q_{1\perp} - \langle 41 \rangle \sqrt{x_1} - \langle 42 \rangle \sqrt{x_2} - \langle 43 \rangle \sqrt{x_3}) + p_{4\perp} x_{1234}) \\
&\quad \left( x_2 \left( |p_{1\perp}|^2 x_1 + q_{1\perp}^* p_{1\perp} x_1 + q_{1\perp} (q_{1\perp}^* + p_{1\perp}^* + p_{2\perp}^*) x_1 + \langle 12 \rangle [12] x_1 \right) + \right. \\
&\quad \left. p_{2\perp} x_{1234} (q_{1\perp}^* x_2 + p_{2\perp}^* x_{1234}) \right) (q_{1\perp} x_1 x_2 ((p_{1\perp}^* + p_{2\perp}^*) x_3 + q_{1\perp}^* (3x_3 + \\
&\quad x_{1234})) + x_3 (p_{2\perp} x_1 (q_{1\perp}^* x_2 + p_{2\perp}^* x_{1234}) + x_2 (p_{1\perp} (q_{1\perp}^* x_1 + p_{1\perp}^* x_{1234}) \\
&\quad - s_{123} x_1))), \\
N^{(31)}(q_1; 1^-, 2^+, 3^-, 4^+; q_2) &= q_{1\perp}^* q_{2\perp} x_2^{3/2} x_4^{3/2}, \\
D^{(31)}(q_1; 1^-, 2^+, 3^-, 4^+; q_2) &= (p_{1\perp} + p_{2\perp}) [12] [34] \sqrt{x_1} \sqrt{x_3} (x_3 + x_4) \\
&\quad (\sqrt{x_1 x_3} \langle 13 \rangle - \sqrt{x_4} \Delta(4, 1, 2) + \langle 23 \rangle \sqrt{x_2 x_3}), \\
N^{(32)}(q_1; 1^-, 2^+, 3^-, 4^+; q_2) &= -q_{1\perp}^* q_{2\perp} x_4^{3/2} \Delta(1, 2, 4)^3, \\
D^{(32)}(q_1; 1^-, 2^+, 3^-, 4^+; q_2) &= s_{1234} \langle 12 \rangle (q_{1\perp} + p_{1\perp} + p_{2\perp} + p_{4\perp}) [34] \sqrt{x_3} \\
&\quad x_{1234} \Delta(2, 3, 4) (\sqrt{x_1 x_3} \langle 13 \rangle - \sqrt{x_4} \Delta(4, 1, 2) + \langle 23 \rangle \sqrt{x_2 x_3}), \\
N^{(33)}(q_1; 1^-, 2^+, 3^-, 4^+; q_2) &= q_{1\perp}^* q_{2\perp} x_2^{3/2} \Delta(1, 2, 3), \\
D^{(33)}(q_1; 1^-, 2^+, 3^-, 4^+; q_2) &= s_{123} (q_{1\perp} + p_{1\perp} + p_{2\perp}) [23] \\
&\quad \sqrt{x_1} \sqrt{x_3} \sqrt{x_4} \Delta(4, 1, 3),
\end{aligned}$$



$$N^{(34)}(q_1; 1^-, 2^+, 3^-, 4^+; q_2) = -|q_{1\perp}|^2 q_{2\perp} \langle 13 \rangle^4 (q_{1\perp} + p_{1\perp} + p_{2\perp} + p_{4\perp}) \\ x_1 x_2 x_3 x_4,$$

$$D^{(34)}(q_1; 1^-, 2^+, 3^-, 4^+; q_2) = s_{1234} \langle 12 \rangle \langle 23 \rangle \langle 34 \rangle (2q_{1\perp} + p_{1\perp} + p_{2\perp} + p_{4\perp}) \\ \left( |p_{4\perp}|^2 x_1 x_2 x_3 + \left( q_{1\perp} q_{1\perp}^* x_1 x_2 + \left( |p_{2\perp}|^2 x_1 + |p_{1\perp}|^2 x_2 \right) x_3 \right) x_4 \right) \\ \Delta(1, 2, 4) \Delta(4, 1, 3),$$

$$N^{(35)}(q_1; 1^-, 2^+, 3^-, 4^+; q_2) = -q_{1\perp} q_{2\perp} \langle 13 \rangle^4 x_{1234},$$

$$D^{(35)}(q_1; 1^-, 2^+, 3^-, 4^+; q_2) = s_{1234} \langle 12 \rangle \langle 23 \rangle \langle 34 \rangle (2q_{1\perp} + p_{1\perp} + p_{2\perp} + p_{4\perp}) \\ \Delta(1, 2, 4) \Delta(4, 1, 3),$$

$$N^{(36)}(q_1; 1^-, 2^+, 3^-, 4^+; q_2) = |q_{1\perp}|^2 q_{2\perp} \langle 13 \rangle^4 (q_{1\perp} + p_{1\perp} + p_{2\perp})^3 x_1 x_2 x_3 x_4^{3/2},$$

$$D^{(36)}(q_1; 1^-, 2^+, 3^-, 4^+; q_2) = s_{123} \langle 12 \rangle \langle 23 \rangle p_{4\perp} \Delta(1, 2, 3) \Delta(3, 1, 2) \Delta(4, 1, 3) \\ \left( 2q_{1\perp}^2 + 3(p_{1\perp} + p_{2\perp} + p_{4\perp}) q_{1\perp} + (p_{1\perp} + p_{2\perp} + p_{4\perp})^2 \right) \\ \left( |p_{4\perp}|^2 x_1 x_2 x_3 + \left( q_{1\perp} q_{1\perp}^* x_1 x_2 + \left( |p_{2\perp}|^2 x_1 + |p_{1\perp}|^2 x_2 \right) x_3 \right) x_4 \right),$$

$$N^{(37)}(q_1; 1^-, 2^+, 3^-, 4^+; q_2) = q_{1\perp} q_{2\perp} \langle 13 \rangle^4 (x_1 + x_2 + x_3)^4,$$

$$D^{(37)}(q_1; 1^-, 2^+, 3^-, 4^+; q_2) = s_{123} \langle 12 \rangle \langle 23 \rangle \sqrt{x_4} x_{1234} ((p_{1\perp} + p_{2\perp}) x_{1234} + \\ q_{1\perp} (x_1 + x_2 + x_3 + x_{1234})) \Delta(1, 2, 3) \Delta(3, 1, 2) \Delta(4, 1, 3),$$

$$N^{(38)}(q_1; 1^-, 2^+, 3^-, 4^+; q_2) = -q_{1\perp}^* q_{2\perp} x_2^{3/2} \Delta(3, 1, 2),$$

$$D^{(38)}(q_1; 1^-, 2^+, 3^-, 4^+; q_2) = s_{123} (q_{1\perp} + p_{1\perp} + p_{2\perp}) [12] \\ \sqrt{x_1} \sqrt{x_3} \sqrt{x_4} \Delta(4, 1, 3),$$

$$N^{(39)}(q_1; 1^-, 2^+, 3^-, 4^+; q_2) = -q_{1\perp}^* q_{2\perp} x_2^{3/2} \Delta(3, 1, 4)^4,$$

$$D^{(39)}(q_1; 1^-, 2^+, 3^-, 4^+; q_2) = s_{1234} \langle 34 \rangle (q_{1\perp} + p_{1\perp} + p_{2\perp} + p_{4\perp}) [12] \sqrt{x_1} x_{1234} \\ \left( \sqrt{x_1 x_3} \langle 13 \rangle - \sqrt{x_4} \Delta(4, 1, 2) + \langle 23 \rangle \sqrt{x_2 x_3} \right) \Delta(3, 1, 2) \Delta(4, 1, 3),$$

$$\begin{aligned}
N^{(40)}(q_1; 1^-, 2^+, 3^-, 4^+; q_2) &= q_{1\perp}^* q_{2\perp} \langle 13 \rangle^4 x_4^{3/2} \Delta(4, 1, 3), \\
D^{(40)}(q_1; 1^-, 2^+, 3^-, 4^+; q_2) &= s_{123} s_{1234} \langle 12 \rangle \langle 23 \rangle (q_{1\perp} + p_{1\perp} + p_{2\perp} + p_{4\perp}) x_{1234} \\
&\quad \Delta(1, 2, 3) \Delta(3, 1, 2),
\end{aligned}$$

$$\begin{aligned}
N^{(41)}(q_1; 1^-, 2^+, 3^-, 4^+; q_2) &= -|q_{1\perp}|^2 q_{2\perp} x_2^{3/2}, \\
D^{(41)}(q_1; 1^-, 2^+, 3^-, 4^+; q_2) &= (q_{1\perp} + p_{1\perp}) (q_{1\perp} + p_{2\perp}) p_{1\perp}^* [23] \\
&\quad \sqrt{x_3} \sqrt{x_4} \Delta(4, 2, 3),
\end{aligned}$$

$$\begin{aligned}
N^{(42)}(q_1; 1^-, 2^+, 3^-, 4^+; q_2) &= |q_{1\perp}|^2 q_{2\perp} p_{1\perp}^3 x_2^{5/2} \sqrt{x_3} x_4^{3/2}, \\
D^{(42)}(q_1; 1^-, 2^+, 3^-, 4^+; q_2) &= p_{4\perp} [23] \sqrt{x_1} \Delta(1, 2, 3) \Delta(4, 2, 3) \\
&\quad \left( 2q_{1\perp}^2 + 3(p_{1\perp} + p_{2\perp} + p_{4\perp}) q_{1\perp} + (p_{1\perp} + p_{2\perp} + p_{4\perp})^2 \right) \\
&\quad \left( |p_{4\perp}|^2 x_1 x_2 x_3 + \left( q_{1\perp} q_{1\perp}^* x_1 x_2 + \left( |p_{2\perp}|^2 x_1 + |p_{1\perp}|^2 x_2 \right) x_3 \right) x_4 \right),
\end{aligned}$$

$$\begin{aligned}
N^{(43)}(q_1; 1^-, 2^+, 3^-, 4^+; q_2) &= q_{1\perp} q_{2\perp} x_1^{5/2} x_2^{3/2}, \\
D^{(43)}(q_1; 1^-, 2^+, 3^-, 4^+; q_2) &= [23] \sqrt{x_3} \sqrt{x_4} x_{1234} (q_{1\perp} x_1 + p_{1\perp} x_{1234}) \\
&\quad \Delta(1, 2, 3) \Delta(4, 2, 3),
\end{aligned}$$

$$\begin{aligned}
N^{(44)}(q_1; 1^-, 2^+, 3^-, 4^+; q_2) &= -q_{1\perp}^* q_{2\perp} p_{1\perp}^3 x_2^{3/2} (x_2 + x_3 + x_4)^3, \\
D^{(44)}(q_1; 1^-, 2^+, 3^-, 4^+; q_2) &= (q_{1\perp} + p_{1\perp}) [23] \sqrt{x_3} \sqrt{x_4} (q_{1\perp} x_1 + p_{1\perp} x_{1234}) \\
&\quad (q_{1\perp} (q_{1\perp}^* + p_{1\perp}^*) x_1 + p_{1\perp} (q_{1\perp}^* x_1 + p_{1\perp}^* x_{1234})) \\
&\quad (q_{1\perp} (x_1 + 2x_2 + 2x_3 + x_4) + p_{2\perp} x_{1234} + \sqrt{x_1} \Delta(1, 2, 3)) \Delta(4, 2, 3),
\end{aligned}$$

$$\begin{aligned}
N^{(45)}(q_1; 1^-, 2^+, 3^-, 4^+; q_2) &= |q_{1\perp}|^2 q_{2\perp} \Delta(3, 2, 4)^4, \\
D^{(45)}(q_1; 1^-, 2^+, 3^-, 4^+; q_2) &= s_{234} \langle 23 \rangle \langle 34 \rangle (q_{1\perp} + p_{1\perp}) (q_{1\perp} + p_{2\perp} + p_{4\perp}) \\
&\quad p_{1\perp}^* (x_2 + x_3 + x_4) \Delta(2, 3, 4) \Delta(4, 2, 3),
\end{aligned}$$

$$\begin{aligned}
N^{(46)}(q_1; 1^-, 2^+, 3^-, 4^+; q_2) &= q_{1\perp}^* q_{2\perp} p_{1\perp}^3 (x_2 + x_3 + x_4)^2 \Delta(3, 2, 4)^4, \\
D^{(46)}(q_1; 1^-, 2^+, 3^-, 4^+; q_2) &= s_{234} \langle 23 \rangle \langle 34 \rangle (q_{1\perp} + p_{1\perp}) \Delta(2, 3, 4) \Delta(4, 2, 3) \\
&\quad (\sqrt{x_1 x_2} \langle 12 \rangle + q_{1\perp} x_1 + p_{2\perp} x_1 + p_{4\perp} x_1 + 2q_{1\perp} x_2 + p_{2\perp} x_2 + p_{4\perp} x_2 \\
&\quad + 2q_{1\perp} x_3 + p_{2\perp} x_3 + p_{4\perp} x_3 + 2q_{1\perp} x_4 + p_{2\perp} x_4 + p_{4\perp} x_4 + \langle 13 \rangle \sqrt{x_1 x_3} \\
&\quad + \langle 14 \rangle \sqrt{x_1 x_4}) (q_{1\perp} x_1 + p_{1\perp} x_{1234}) \\
&\quad (q_{1\perp} (q_{1\perp}^* + p_{1\perp}^*) x_1 + p_{1\perp} (q_{1\perp}^* x_1 + p_{1\perp}^* x_{1234})),
\end{aligned}$$

$$\begin{aligned}
N^{(47)}(q_1; 1^-, 2^+, 3^-, 4^+; q_2) &= -|q_{1\perp}|^2 q_{2\perp} p_{1\perp}^3 x_2 x_3 x_4 \Delta(3, 2, 4)^4, \\
D^{(47)}(q_1; 1^-, 2^+, 3^-, 4^+; q_2) &= s_{234} \langle 23 \rangle \langle 34 \rangle (q_{1\perp} + p_{2\perp} + p_{4\perp}) \sqrt{x_1} \\
&\quad (2q_{1\perp}^2 + 3(p_{1\perp} + p_{2\perp} + p_{4\perp}) q_{1\perp} + (p_{1\perp} + p_{2\perp} + p_{4\perp})^2) \\
&\quad (|p_{4\perp}|^2 x_1 x_2 x_3 + (q_{1\perp} q_{1\perp}^* x_1 x_2 + (|p_{2\perp}|^2 x_1 + |p_{1\perp}|^2 x_2) x_3) x_4) \\
&\quad \Delta(1, 2, 4) \Delta(2, 3, 4) \Delta(4, 2, 3),
\end{aligned}$$

$$\begin{aligned}
N^{(48)}(q_1; 1^-, 2^+, 3^-, 4^+; q_2) &= -q_{1\perp} q_{2\perp} x_1^{5/2} \Delta(3, 2, 4)^4, \\
D^{(48)}(q_1; 1^-, 2^+, 3^-, 4^+; q_2) &= s_{234} \langle 23 \rangle \langle 34 \rangle (x_2 + x_3 + x_4) x_{1234} \\
&\quad (q_{1\perp} x_1 + p_{1\perp} x_{1234}) \Delta(1, 2, 4) \Delta(2, 3, 4) \Delta(4, 2, 3),
\end{aligned}$$

$$\begin{aligned}
N^{(49)}(q_1; 1^-, 2^+, 3^-, 4^+; q_2) &= -q_{1\perp}^* q_{2\perp} \Delta(1, 2, 4) \Delta(3, 2, 4)^4, \\
D^{(49)}(q_1; 1^-, 2^+, 3^-, 4^+; q_2) &= s_{1234} s_{234} \langle 23 \rangle \langle 34 \rangle (q_{1\perp} + p_{1\perp} + p_{2\perp} + p_{4\perp}) \\
&\quad \sqrt{x_1} x_{1234} \Delta(2, 3, 4) \Delta(4, 2, 3),
\end{aligned}$$

$$\begin{aligned}
N^{(50)}(q_1; 1^-, 2^+, 3^-, 4^+; q_2) &= -q_{1\perp}^* q_{2\perp} x_2^{3/2} \Delta(1, 2, 4)^3, \\
D^{(50)}(q_1; 1^-, 2^+, 3^-, 4^+; q_2) &= s_{1234} (q_{1\perp} + p_{1\perp} + p_{2\perp} + p_{4\perp}) [23] \sqrt{x_3} \\
&\quad x_{1234} \Delta(1, 2, 3) \Delta(4, 1, 3) \Delta(4, 2, 3).
\end{aligned}$$

### O.2.3 Result for $V^{(0)}(q_1; 1^+, 2^-, 3^-, 4^+; q_2)$

$$\begin{aligned} N^{(1)}(q_1; 1^+, 2^-, 3^-, 4^+; q_2) &= x_1^{5/2} \sqrt{x_2} q_{1\perp}^2 p_{2\perp}^3 q_{2\perp} q_{1\perp}^*, \\ D^{(1)}(q_1; 1^+, 2^-, 3^-, 4^+; q_2) &= \langle 12 \rangle p_{1\perp} p_{4\perp} (p_{1\perp} + p_{2\perp}) (p_{1\perp} + 2q_{1\perp} + p_{2\perp}) \\ &\quad (x_2 p_{1\perp} p_{1\perp}^* + x_1 p_{2\perp} p_{2\perp}^*) (x_3 x_2 p_{1\perp} p_{1\perp}^* + x_1 x_2 q_{1\perp} q_{1\perp}^* + x_1 x_3 p_{2\perp} p_{2\perp}^*), \end{aligned}$$

$$\begin{aligned} N^{(2)}(q_1; 1^+, 2^-, 3^-, 4^+; q_2) &= x_1^{5/2} \sqrt{x_2} q_{1\perp}^4 q_{2\perp} q_{1\perp}^*, \\ D^{(2)}(q_1; 1^+, 2^-, 3^-, 4^+; q_2) &= [12] \sqrt{x_3} p_{4\perp} (p_{1\perp} + p_{2\perp}) (\sqrt{x_1} \langle 13 \rangle + \sqrt{x_2} \langle 23 \rangle) \\ &\quad (p_{1\perp} + q_{1\perp} + p_{2\perp}) (p_{1\perp} + 2q_{1\perp} + p_{2\perp}) \\ &\quad (x_3 x_2 p_{1\perp} p_{1\perp}^* + x_1 x_2 q_{1\perp} q_{1\perp}^* + x_1 x_3 p_{2\perp} p_{2\perp}^*), \end{aligned}$$

$$\begin{aligned} N^{(3)}(q_1; 1^+, 2^-, 3^-, 4^+; q_2) &= x_1^{3/2} \sqrt{x_2} \sqrt{x_3} q_{1\perp} q_{2\perp} q_{1\perp}^* (q_{1\perp} + p_{2\perp})^3, \\ D^{(3)}(q_1; 1^+, 2^-, 3^-, 4^+; q_2) &= [23] p_{1\perp} p_{4\perp} (\sqrt{x_2} \langle 12 \rangle + \sqrt{x_3} \langle 13 \rangle) \\ &\quad (p_{1\perp} + q_{1\perp} + p_{2\perp}) (p_{1\perp} + 2q_{1\perp} + p_{2\perp}) \\ &\quad (x_3 x_2 p_{1\perp} p_{1\perp}^* + x_1 x_2 q_{1\perp} q_{1\perp}^* + x_1 x_3 p_{2\perp} p_{2\perp}^*), \end{aligned}$$

$$\begin{aligned} N^{(4)}(q_1; 1^+, 2^-, 3^-, 4^+; q_2) &= x_1 x_2 x_3 \langle 23 \rangle^3 (-q_{1\perp}) q_{2\perp} q_{1\perp}^* (p_{1\perp} + q_{1\perp} + p_{2\perp}), \\ D^{(4)}(q_1; 1^+, 2^-, 3^-, 4^+; q_2) &= s_{123} \langle 12 \rangle p_{4\perp} (\sqrt{x_2} \langle 12 \rangle + \sqrt{x_3} \langle 13 \rangle) \\ &\quad (\sqrt{x_1} \langle 13 \rangle + \sqrt{x_2} \langle 23 \rangle) (p_{1\perp} + 2q_{1\perp} + p_{2\perp}) \\ &\quad (x_3 x_2 p_{1\perp} p_{1\perp}^* + x_1 x_2 q_{1\perp} q_{1\perp}^* + x_1 x_3 p_{2\perp} p_{2\perp}^*), \end{aligned}$$

$$\begin{aligned} N^{(5)}(q_1; 1^+, 2^-, 3^-, 4^+; q_2) &= x_1^{3/2} q_{2\perp} (\sqrt{x_1} \langle 13 \rangle + \sqrt{x_2} \langle 23 \rangle) (-q_{1\perp}^*), \\ D^{(5)}(q_1; 1^+, 2^-, 3^-, 4^+; q_2) &= [12] s_{123} \sqrt{x_2} \sqrt{x_3} \sqrt{x_4} (p_{1\perp} + q_{1\perp} + p_{2\perp}) \\ &\quad (\sqrt{x_1} \langle 14 \rangle + \sqrt{x_2} \langle 24 \rangle + \sqrt{x_3} \langle 34 \rangle), \end{aligned}$$

$$\begin{aligned} N^{(6)}(q_1; 1^+, 2^-, 3^-, 4^+; q_2) &= x_1^{3/2} q_{2\perp} (\sqrt{x_2} \langle 12 \rangle + \sqrt{x_3} \langle 13 \rangle) (-q_{1\perp}^*), \\ D^{(6)}(q_1; 1^+, 2^-, 3^-, 4^+; q_2) &= [23] s_{123} \sqrt{x_2} \sqrt{x_3} \sqrt{x_4} (p_{1\perp} + q_{1\perp} + p_{2\perp}) \\ &\quad (\sqrt{x_1} \langle 14 \rangle + \sqrt{x_2} \langle 24 \rangle + \sqrt{x_3} \langle 34 \rangle), \end{aligned}$$

$$\begin{aligned}
N^{(7)}(q_1; 1^+, 2^-, 3^-, 4^+; q_2) &= x_1^{3/2} x_4^{3/2} q_{1\perp} p_{2\perp}^3 q_{2\perp} q_{1\perp}^*, \\
D^{(7)}(q_1; 1^+, 2^-, 3^-, 4^+; q_2) &= [34] \sqrt{x_2} \sqrt{x_3} (x_3 + x_4) \langle 12 \rangle p_{1\perp} (p_{1\perp} + p_{2\perp}) \\
&\quad (p_{1\perp} + q_{1\perp} + p_{2\perp}) (q_{1\perp} + p_{4\perp}) (x_2 p_{1\perp} p_{1\perp}^* + x_1 p_{2\perp} p_{2\perp}^*), \\
N^{(8)}(q_1; 1^+, 2^-, 3^-, 4^+; q_2) &= x_1^{3/2} x_4^{3/2} q_{2\perp} q_{1\perp}^*, \\
D^{(8)}(q_1; 1^+, 2^-, 3^-, 4^+; q_2) &= [12][34] \sqrt{x_2} \sqrt{x_3} (x_3 + x_4) (p_{1\perp} + p_{2\perp}) \\
&\quad (\sqrt{x_1} \sqrt{x_3} \langle 13 \rangle + \sqrt{x_1} \sqrt{x_4} \langle 14 \rangle + \sqrt{x_2} \sqrt{x_3} \langle 23 \rangle + \sqrt{x_2} \sqrt{x_4} \langle 24 \rangle), \\
N^{(9)}(q_1; 1^+, 2^-, 3^-, 4^+; q_2) &= \sqrt{x_1} x_4^{3/2} q_{2\perp} (\sqrt{x_2} \langle 24 \rangle + \sqrt{x_3} \langle 34 \rangle) (-q_{1\perp}^*), \\
D^{(9)}(q_1; 1^+, 2^-, 3^-, 4^+; q_2) &= [23] s_{234} \sqrt{x_2} \sqrt{x_3} (x_2 + x_3 + x_4) p_{1\perp} \\
&\quad (\sqrt{x_2} \langle 12 \rangle + \sqrt{x_3} \langle 13 \rangle + \sqrt{x_4} \langle 14 \rangle), \\
N^{(10)}(q_1; 1^+, 2^-, 3^-, 4^+; q_2) &= \sqrt{x_1} x_4^{3/2} q_{2\perp} (\sqrt{x_3} \langle 23 \rangle + \sqrt{x_4} \langle 24 \rangle) (-q_{1\perp}^*), \\
D^{(10)}(q_1; 1^+, 2^-, 3^-, 4^+; q_2) &= [34] s_{234} \sqrt{x_2} \sqrt{x_3} (x_2 + x_3 + x_4) p_{1\perp} \\
&\quad (\sqrt{x_2} \langle 12 \rangle + \sqrt{x_3} \langle 13 \rangle + \sqrt{x_4} \langle 14 \rangle), \\
N^{(11)}(q_1; 1^+, 2^-, 3^-, 4^+; q_2) &= x_1^{3/2} \langle 23 \rangle^3 q_{2\perp} q_{1\perp}^* \\
&\quad (\sqrt{x_2} \langle 12 \rangle + \sqrt{x_3} \langle 13 \rangle + \sqrt{x_4} \langle 14 \rangle), \\
D^{(11)}(q_1; 1^+, 2^-, 3^-, 4^+; q_2) &= s_{1234} s_{234} x_{1234} \langle 34 \rangle \\
&\quad (\sqrt{x_3} \langle 23 \rangle + \sqrt{x_4} \langle 24 \rangle) (\sqrt{x_2} \langle 24 \rangle + \sqrt{x_3} \langle 34 \rangle) (p_{1\perp} + q_{1\perp} + p_{2\perp} + p_{4\perp}), \\
N^{(12)}(q_1; 1^+, 2^-, 3^-, 4^+; q_2) &= (\sqrt{x_1} \langle 13 \rangle + \sqrt{x_2} \langle 23 \rangle - \sqrt{x_4} \langle 34 \rangle)^4 \\
&\quad x_1^{3/2} q_{2\perp} (-q_{1\perp}^*), \\
D^{(12)}(q_1; 1^+, 2^-, 3^-, 4^+; q_2) &= [12] s_{1234} \sqrt{x_2} x_{1234} \langle 34 \rangle \\
&\quad (\sqrt{x_1} \langle 14 \rangle + \sqrt{x_2} \langle 24 \rangle + \sqrt{x_3} \langle 34 \rangle) (p_{1\perp} + q_{1\perp} + p_{2\perp} + p_{4\perp}) \\
&\quad (x_1 \sqrt{x_4} \langle 13 \rangle \langle 14 \rangle + 2 \sqrt{x_1} \sqrt{x_2} \sqrt{x_3} \langle 13 \rangle \langle 23 \rangle + \sqrt{x_1} \sqrt{x_2} \sqrt{x_4} \langle 13 \rangle \langle 24 \rangle + \\
&\quad x_1 \sqrt{x_3} \langle 13 \rangle^2 + \sqrt{x_1} \sqrt{x_2} \sqrt{x_4} \langle 14 \rangle \langle 23 \rangle + x_2 \sqrt{x_4} \langle 23 \rangle \langle 24 \rangle + x_2 \sqrt{x_3} \langle 23 \rangle^2),
\end{aligned}$$

$$\begin{aligned}
N^{(13)}(q_1; 1^+, 2^-, 3^-, 4^+; q_2) &= q_{2\perp} (-q_{1\perp}^*) (-\sqrt{x_1}\sqrt{x_2}\langle 12 \rangle - \sqrt{x_1}\sqrt{x_3}\langle 13 \rangle \\
&\quad + \sqrt{x_2}\sqrt{x_4}\langle 24 \rangle + \sqrt{x_3}\sqrt{x_4}\langle 34 \rangle)^4, \\
D^{(13)}(q_1; 1^+, 2^-, 3^-, 4^+; q_2) &= [23]s_{1234}\sqrt{x_2}\sqrt{x_3}x_{1234}(\sqrt{x_2}\langle 24 \rangle + \sqrt{x_3}\langle 34 \rangle) \\
&\quad (2\sqrt{x_2}\sqrt{x_3}\langle 12 \rangle\langle 13 \rangle + \sqrt{x_2}\sqrt{x_4}\langle 12 \rangle\langle 14 \rangle + x_2\langle 12 \rangle^2 + \sqrt{x_3}\sqrt{x_4}\langle 13 \rangle\langle 14 \rangle \\
&\quad + x_3\langle 13 \rangle^2)(\sqrt{x_1}\langle 14 \rangle + \sqrt{x_2}\langle 24 \rangle + \sqrt{x_3}\langle 34 \rangle)(p_{1\perp} + q_{1\perp} + p_{2\perp} + p_{4\perp}), \\
N^{(14)}(q_1; 1^+, 2^-, 3^-, 4^+; q_2) &= (\sqrt{x_1}\langle 14 \rangle + \sqrt{x_2}\langle 24 \rangle + \sqrt{x_3}\langle 34 \rangle) \\
&\quad x_4^{3/2}\langle 23 \rangle^3 q_{2\perp} q_{1\perp}^*, \\
D^{(14)}(q_1; 1^+, 2^-, 3^-, 4^+; q_2) &= s_{123}s_{1234}x_{1234}\langle 12 \rangle (\sqrt{x_2}\langle 12 \rangle + \sqrt{x_3}\langle 13 \rangle) \\
&\quad (\sqrt{x_1}\langle 13 \rangle + \sqrt{x_2}\langle 23 \rangle)(p_{1\perp} + q_{1\perp} + p_{2\perp} + p_{4\perp}), \\
N^{(15)}(q_1; 1^+, 2^-, 3^-, 4^+; q_2) &= (-\sqrt{x_1}\langle 12 \rangle + \sqrt{x_3}\langle 23 \rangle + \sqrt{x_4}\langle 24 \rangle)^4 \\
&\quad x_4^{3/2} q_{2\perp} (-q_{1\perp}^*), \\
D^{(15)}(q_1; 1^+, 2^-, 3^-, 4^+; q_2) &= [34]s_{1234}\sqrt{x_3}x_{1234}\langle 12 \rangle (\sqrt{x_3}\langle 23 \rangle + \sqrt{x_4}\langle 24 \rangle) \\
&\quad (\sqrt{x_2}\langle 12 \rangle + \sqrt{x_3}\langle 13 \rangle + \sqrt{x_4}\langle 14 \rangle)(p_{1\perp} + q_{1\perp} + p_{2\perp} + p_{4\perp}) \\
&\quad (\sqrt{x_1}\sqrt{x_3}\langle 13 \rangle + \sqrt{x_1}\sqrt{x_4}\langle 14 \rangle + \sqrt{x_2}\sqrt{x_3}\langle 23 \rangle + \sqrt{x_2}\sqrt{x_4}\langle 24 \rangle), \\
N^{(16)}(q_1; 1^+, 2^-, 3^-, 4^+; q_2) &= x_{1234}\langle 23 \rangle^3 q_{1\perp} q_{2\perp}, \\
D^{(16)}(q_1; 1^+, 2^-, 3^-, 4^+; q_2) &= s_{1234}\langle 12 \rangle\langle 34 \rangle (\sqrt{x_2}\langle 12 \rangle + \sqrt{x_3}\langle 13 \rangle + \sqrt{x_4}\langle 14 \rangle) \\
&\quad (\sqrt{x_1}\langle 14 \rangle + \sqrt{x_2}\langle 24 \rangle + \sqrt{x_3}\langle 34 \rangle)(p_{1\perp} + 2q_{1\perp} + p_{2\perp} + p_{4\perp}), \\
N^{(17)}(q_1; 1^+, 2^-, 3^-, 4^+; q_2) &= \sqrt{x_1}(x_2 + x_3)^4 (-q_{1\perp}) q_{2\perp}, \\
D^{(17)}(q_1; 1^+, 2^-, 3^-, 4^+; q_2) &= [23]\sqrt{x_2}\sqrt{x_3}\sqrt{x_4}x_{1234}(\sqrt{x_2}\langle 12 \rangle + \sqrt{x_3}\langle 13 \rangle) \\
&\quad (\sqrt{x_2}\langle 24 \rangle + \sqrt{x_3}\langle 34 \rangle)(x_1p_{1\perp} + x_2p_{1\perp} + x_3p_{1\perp} + x_4p_{1\perp} + x_1q_{1\perp}), \\
N^{(18)}(q_1; 1^+, 2^-, 3^-, 4^+; q_2) &= \sqrt{x_1}x_2^2x_4^{3/2}(-q_{1\perp}) q_{2\perp}, \\
D^{(18)}(q_1; 1^+, 2^-, 3^-, 4^+; q_2) &= [34]\sqrt{x_3}(x_3 + x_4)(\sqrt{x_3}\langle 23 \rangle + \sqrt{x_4}\langle 24 \rangle) \\
&\quad x_{1234}\langle 12 \rangle (x_1p_{1\perp} + x_2p_{1\perp} + x_3p_{1\perp} + x_4p_{1\perp} + x_1q_{1\perp}),
\end{aligned}$$

$$\begin{aligned}
N^{(19)}(q_1; 1^+, 2^-, 3^-, 4^+; q_2) &= \sqrt{x_1} (x_2 + x_3 + x_4)^3 \langle 23 \rangle^3 q_{1\perp} q_{2\perp}, \\
D^{(19)}(q_1; 1^+, 2^-, 3^-, 4^+; q_2) &= s_{234} x_{1234} \langle 34 \rangle (\sqrt{x_3} \langle 23 \rangle + \sqrt{x_4} \langle 24 \rangle) \\
&\quad (\sqrt{x_2} \langle 24 \rangle + \sqrt{x_3} \langle 34 \rangle) (x_1 p_{1\perp} + x_2 p_{1\perp} + x_3 p_{1\perp} + x_4 p_{1\perp} + x_1 q_{1\perp}) \\
&\quad (\sqrt{x_2} \langle 12 \rangle + \sqrt{x_3} \langle 13 \rangle + \sqrt{x_4} \langle 14 \rangle),
\end{aligned}$$

$$\begin{aligned}
N^{(20)}(q_1; 1^+, 2^-, 3^-, 4^+; q_2) &= x_1^{3/2} x_3^2 (-q_{1\perp}) q_{2\perp}, \\
D^{(20)}(q_1; 1^+, 2^-, 3^-, 4^+; q_2) &= [12] \sqrt{x_2} \sqrt{x_4} x_{1234} \langle 34 \rangle (\sqrt{x_1} \langle 13 \rangle + \sqrt{x_2} \langle 23 \rangle) \\
&\quad (x_{1234} p_{1\perp} + x_1 q_{1\perp} + x_2 q_{1\perp} + x_{1234} p_{2\perp}),
\end{aligned}$$

$$\begin{aligned}
N^{(21)}(q_1; 1^+, 2^-, 3^-, 4^+; q_2) &= (x_1 + x_2 + x_3)^4 \langle 23 \rangle^3 q_{1\perp} q_{2\perp}, \\
D^{(21)}(q_1; 1^+, 2^-, 3^-, 4^+; q_2) &= s_{123} \sqrt{x_4} x_{1234} \langle 12 \rangle (\sqrt{x_2} \langle 12 \rangle + \sqrt{x_3} \langle 13 \rangle) \\
&\quad (\sqrt{x_1} \langle 13 \rangle + \sqrt{x_2} \langle 23 \rangle) (\sqrt{x_1} \langle 14 \rangle + \sqrt{x_2} \langle 24 \rangle + \sqrt{x_3} \langle 34 \rangle) (x_{1234} p_{1\perp} \\
&\quad + 2x_1 q_{1\perp} + 2x_2 q_{1\perp} + 2x_3 q_{1\perp} + x_4 q_{1\perp} + x_{1234} p_{2\perp}),
\end{aligned}$$

$$\begin{aligned}
N^{(22)}(q_1; 1^+, 2^-, 3^-, 4^+; q_2) &= x_1^2 x_2^{5/2} x_4^{3/2} q_{2\perp} (p_{1\perp} + q_{1\perp})^3 q_{1\perp}^*, \\
D^{(22)}(q_1; 1^+, 2^-, 3^-, 4^+; q_2) &= [34] \sqrt{x_3} (x_3 + x_4) (x_2 + x_3 + x_4) p_{1\perp} \\
&\quad (\sqrt{x_3} \langle 23 \rangle + \sqrt{x_4} \langle 24 \rangle) (x_{1234} p_{1\perp} + x_1 q_{1\perp}) (x_1 p_{1\perp} q_{1\perp}^* + x_1 q_{1\perp} p_{1\perp}^* \\
&\quad + x_1 p_{1\perp} p_{1\perp}^* + x_2 p_{1\perp} p_{1\perp}^* + x_3 p_{1\perp} p_{1\perp}^* + x_4 p_{1\perp} p_{1\perp}^* + x_1 q_{1\perp} q_{1\perp}^*) \\
&\quad (x_2 q_{1\perp} + x_1 p_{2\perp} + x_2 p_{2\perp} + x_3 p_{2\perp} + x_4 p_{2\perp} + \sqrt{x_1} \sqrt{x_2} \langle 12 \rangle),
\end{aligned}$$

$$\begin{aligned}
N^{(23)}(q_1; 1^+, 2^-, 3^-, 4^+; q_2) &= x_1^2 (x_2 + x_3)^4 q_{2\perp} (p_{1\perp} + q_{1\perp})^3 q_{1\perp}^*, \\
D^{(23)}(q_1; 1^+, 2^-, 3^-, 4^+; q_2) &= [23] \sqrt{x_2} \sqrt{x_3} \sqrt{x_4} (x_2 + x_3 + x_4) p_{1\perp} \\
&\quad (\sqrt{x_2} \langle 24 \rangle + \sqrt{x_3} \langle 34 \rangle) (x_{1234} p_{1\perp} + x_1 q_{1\perp}) (x_1 p_{1\perp} q_{1\perp}^* + x_1 q_{1\perp} p_{1\perp}^* \\
&\quad + x_1 p_{1\perp} p_{1\perp}^* + x_2 p_{1\perp} p_{1\perp}^* + x_3 p_{1\perp} p_{1\perp}^* + x_4 p_{1\perp} p_{1\perp}^* + x_1 q_{1\perp} q_{1\perp}^*) \\
&\quad (x_1 q_{1\perp} + 2x_2 q_{1\perp} + 2x_3 q_{1\perp} + x_4 q_{1\perp} + x_1 p_{2\perp} + x_2 p_{2\perp} + \\
&\quad x_3 p_{2\perp} + x_4 p_{2\perp} + \sqrt{x_1} \sqrt{x_2} \langle 12 \rangle + \sqrt{x_1} \sqrt{x_3} \langle 13 \rangle),
\end{aligned}$$

$$\begin{aligned}
N^{(24)}(q_1; 1^+, 2^-, 3^-, 4^+; q_2) &= x_1^2 (x_2 + x_3 + x_4)^2 \langle 23 \rangle^3 q_{2\perp} \\
&\quad (p_{1\perp} + q_{1\perp})^3 (-q_{1\perp}^*), \\
D^{(24)}(q_1; 1^+, 2^-, 3^-, 4^+; q_2) &= s_{234} \langle 34 \rangle p_{1\perp} (\sqrt{x_3} \langle 23 \rangle + \sqrt{x_4} \langle 24 \rangle) \\
&\quad (\sqrt{x_2} \langle 24 \rangle + \sqrt{x_3} \langle 34 \rangle) (x_1 p_{1\perp} + x_2 p_{1\perp} + x_3 p_{1\perp} + x_4 p_{1\perp} + x_1 q_{1\perp}) \\
&\quad (x_1 p_{1\perp} q_{1\perp}^* + x_1 q_{1\perp} p_{1\perp}^* + x_1 p_{1\perp} p_{1\perp}^* + x_2 p_{1\perp} p_{1\perp}^* + x_3 p_{1\perp} p_{1\perp}^* \\
&\quad + x_4 p_{1\perp} p_{1\perp}^* + x_1 q_{1\perp} q_{1\perp}^*) (x_1 q_{1\perp} + 2x_2 q_{1\perp} + 2x_3 q_{1\perp} + 2x_4 q_{1\perp} + x_1 p_{2\perp} \\
&\quad + x_2 p_{2\perp} + x_3 p_{2\perp} + x_4 p_{2\perp} + x_1 p_{4\perp} + x_2 p_{4\perp} + x_3 p_{4\perp} \\
&\quad + x_4 p_{4\perp} + \sqrt{x_1} \sqrt{x_2} \langle 12 \rangle + \sqrt{x_1} \sqrt{x_3} \langle 13 \rangle + \sqrt{x_1} \sqrt{x_4} \langle 14 \rangle), \\
N^{(25)}(q_1; 1^+, 2^-, 3^-, 4^+; q_2) &= x_1^{5/2} \sqrt{x_2 x_3}^{5/2} (-q_{1\perp}) p_{2\perp}^3 q_{1\perp}^* \\
&\quad (p_{1\perp} + q_{1\perp} + p_{2\perp}), \\
D^{(25)}(q_1; 1^+, 2^-, 3^-, 4^+; q_2) &= \sqrt{x_4} (x_3 + x_4) \langle 12 \rangle \langle 34 \rangle p_{1\perp} (p_{1\perp} + p_{2\perp}) \\
&\quad (x_1 q_{1\perp} + x_2 q_{1\perp} + 2x_3 q_{1\perp} + x_4 q_{1\perp} + \sqrt{x_1} \sqrt{x_3} \langle 13 \rangle + \sqrt{x_2} \sqrt{x_3} \langle 23 \rangle) \\
&\quad (x_2 p_{1\perp} p_{1\perp}^* + x_1 p_{2\perp} p_{2\perp}^*) (x_2 x_1 p_{2\perp} q_{1\perp}^* + x_2 x_1 p_{1\perp} q_{1\perp}^* + x_2 x_1 q_{1\perp} p_{1\perp}^* \\
&\quad + x_2 x_1 p_{1\perp} p_{1\perp}^* + x_2^2 p_{1\perp} p_{1\perp}^* + x_2 x_3 p_{1\perp} p_{1\perp}^* + x_2 x_4 p_{1\perp} p_{1\perp}^* + x_2 x_1 q_{1\perp} q_{1\perp}^* \\
&\quad + x_2 x_1 q_{1\perp} p_{2\perp}^* + x_1^2 p_{2\perp} p_{2\perp}^* + x_2 x_1 p_{2\perp} p_{2\perp}^* + x_3 x_1 p_{2\perp} p_{2\perp}^* + \\
&\quad x_4 x_1 p_{2\perp} p_{2\perp}^* + [12] x_2 x_1 \langle 12 \rangle), \\
N^{(26)}(q_1; 1^+, 2^-, 3^-, 4^+; q_2) &= x_1^{5/2} \sqrt{x_2 x_3}^{5/2} q_{2\perp} q_{1\perp}^* (p_{1\perp} + q_{1\perp} + p_{2\perp})^3, \\
D^{(26)}(q_1; 1^+, 2^-, 3^-, 4^+; q_2) &= [12] \sqrt{x_4} (x_3 + x_4) \langle 34 \rangle (p_{1\perp} + p_{2\perp}) \\
&\quad (x_{1234} p_{1\perp} + x_1 q_{1\perp} + x_2 q_{1\perp} + x_{1234} p_{2\perp}) \\
&\quad (x_1 q_{1\perp} + x_2 q_{1\perp} + 2x_3 q_{1\perp} + x_4 q_{1\perp} + \sqrt{x_1} \sqrt{x_3} \langle 13 \rangle + \sqrt{x_2} \sqrt{x_3} \langle 23 \rangle) \\
&\quad (x_2 x_1 p_{2\perp} q_{1\perp}^* + x_2 x_1 p_{1\perp} q_{1\perp}^* + x_2 x_1 q_{1\perp} p_{1\perp}^* + x_2 x_1 p_{1\perp} p_{1\perp}^* + x_2^2 p_{1\perp} p_{1\perp}^* \\
&\quad + x_2 x_3 p_{1\perp} p_{1\perp}^* + x_2 x_4 p_{1\perp} p_{1\perp}^* + x_2 x_1 q_{1\perp} q_{1\perp}^* + x_2 x_1 q_{1\perp} p_{2\perp}^* + x_1^2 p_{2\perp} p_{2\perp}^* \\
&\quad + x_2 x_1 p_{2\perp} p_{2\perp}^* + x_3 x_1 p_{2\perp} p_{2\perp}^* x_4 x_1 p_{2\perp} p_{2\perp}^* + [12] x_2 x_1 \langle 12 \rangle),
\end{aligned}$$



$$\begin{aligned}
N^{(27)}(q_1; 1^+, 2^-, 3^-, 4^+; q_2) &= x_1^{3/2} x_3^{5/2} (-q_{1\perp}) q_{2\perp} \\
&\quad (x_2 q_{1\perp} + x_1 p_{2\perp} + x_2 p_{2\perp} + x_3 p_{2\perp} + x_4 p_{2\perp} + \sqrt{x_1} \sqrt{x_2} \langle 12 \rangle)^3, \\
D^{(27)}(q_1; 1^+, 2^-, 3^-, 4^+; q_2) &= \sqrt{x_2} \sqrt{x_4} (x_3 + x_4) \langle 12 \rangle \langle 34 \rangle (x_{1234} p_{1\perp} + x_1 q_{1\perp}) \\
&\quad (x_{1234} p_{1\perp} + x_1 q_{1\perp} + x_2 q_{1\perp} + x_{1234} p_{2\perp}) \\
&\quad (x_1 q_{1\perp} + x_2 q_{1\perp} + 2x_3 q_{1\perp} + x_4 q_{1\perp} + \sqrt{x_1} \sqrt{x_3} \langle 13 \rangle + \sqrt{x_2} \sqrt{x_3} \langle 23 \rangle) \\
&\quad (x_2 x_1 p_{2\perp} q_{1\perp}^* + x_2 x_1 p_{1\perp} q_{1\perp}^* + x_2 x_1 q_{1\perp} p_{1\perp}^* + x_2 x_1 p_{1\perp} p_{1\perp}^* + x_2^2 p_{1\perp} p_{1\perp}^* \\
&\quad + x_2 x_3 p_{1\perp} p_{1\perp}^* + x_2 x_4 p_{1\perp} p_{1\perp}^* + x_2 x_1 q_{1\perp} q_{1\perp}^* + x_2 x_1 q_{1\perp} p_{2\perp}^* + x_1^2 p_{2\perp} p_{2\perp}^* \\
&\quad + x_2 x_1 p_{2\perp} p_{2\perp}^* + x_3 x_1 p_{2\perp} p_{2\perp}^* x_4 x_1 p_{2\perp} p_{2\perp}^* + [12] x_2 x_1 \langle 12 \rangle),
\end{aligned}$$

$$\begin{aligned}
N^{(28)}(q_1; 1^+, 2^-, 3^-, 4^+; q_2) &= x_1^{3/2} x_4^{3/2} (x_3 + x_4)^2 p_{2\perp}^4 q_{2\perp} q_{1\perp}^*, \\
D^{(28)}(q_1; 1^+, 2^-, 3^-, 4^+; q_2) &= [34] \sqrt{x_2} \sqrt{x_3} \langle 12 \rangle p_{1\perp} (p_{1\perp} + q_{1\perp} + p_{2\perp}) \\
&\quad (x_2 q_{1\perp} + x_{1234} p_{2\perp} + \sqrt{x_1} \sqrt{x_2} \langle 12 \rangle) \\
&\quad (x_{1234} q_{1\perp} + x_3 q_{1\perp} + x_4 q_{1\perp} + x_1 p_{4\perp} + x_2 p_{4\perp} + x_3 p_{4\perp} + x_4 p_{4\perp} \\
&\quad + \sqrt{x_1} \sqrt{x_3} \langle 13 \rangle + \sqrt{x_1} \sqrt{x_4} \langle 14 \rangle + \sqrt{x_2} \sqrt{x_3} \langle 23 \rangle + \sqrt{x_2} \sqrt{x_4} \langle 24 \rangle) \\
&\quad (x_2 x_1 p_{2\perp} q_{1\perp}^* + x_2 x_1 p_{1\perp} q_{1\perp}^* + x_2 x_1 q_{1\perp} p_{1\perp}^* + x_2 x_1 p_{1\perp} p_{1\perp}^* + x_2^2 p_{1\perp} p_{1\perp}^* \\
&\quad + x_2 x_3 p_{1\perp} p_{1\perp}^* + x_2 x_4 p_{1\perp} p_{1\perp}^* + x_2 x_1 q_{1\perp} q_{1\perp}^* + x_2 x_1 q_{1\perp} p_{2\perp}^* + x_1^2 p_{2\perp} p_{2\perp}^* \\
&\quad + x_2 x_1 p_{2\perp} p_{2\perp}^* + x_3 x_1 p_{2\perp} p_{2\perp}^* + x_4 x_1 p_{2\perp} p_{2\perp}^* + [12] x_2 x_1 \langle 12 \rangle),
\end{aligned}$$

$$\begin{aligned}
N^{(29)}(q_1; 1^+, 2^-, 3^-, 4^+; q_2) &= x_1^3 x_3^{5/2} q_{2\perp} (p_{1\perp} + q_{1\perp})^3 q_{1\perp}^* \\
&\quad (x_2 q_{1\perp} + x_1 p_{2\perp} + x_2 p_{2\perp} + x_3 p_{2\perp} + x_4 p_{2\perp} + \sqrt{x_1} \sqrt{x_2} \langle 12 \rangle), \\
D^{(29)}(q_1; 1^+, 2^-, 3^-, 4^+; q_2) &= \sqrt{x_4} (x_3 + x_4) \langle 34 \rangle p_{1\perp} (x_{1234} p_{1\perp} + x_1 q_{1\perp}) \\
&\quad (x_1 q_{1\perp} + x_2 q_{1\perp} + 2x_3 q_{1\perp} + x_4 q_{1\perp} + \sqrt{x_1} \sqrt{x_3} \langle 13 \rangle + \sqrt{x_2} \sqrt{x_3} \langle 23 \rangle) \\
&\quad (x_1 p_{1\perp} q_{1\perp}^* + x_1 q_{1\perp} p_{1\perp}^* + x_1 p_{1\perp} p_{1\perp}^* + x_2 p_{1\perp} p_{1\perp}^* + x_3 p_{1\perp} p_{1\perp}^* + x_4 |p_{1\perp}|^2 \\
&\quad + x_1 q_{1\perp} q_{1\perp}^*) (x_2 x_1 p_{2\perp} q_{1\perp}^* + x_2 x_1 p_{1\perp} q_{1\perp}^* + x_2 x_1 q_{1\perp} p_{1\perp}^* + x_2 x_1 p_{1\perp} p_{1\perp}^* \\
&\quad + x_2^2 p_{1\perp} p_{1\perp}^* + x_2 x_3 p_{1\perp} p_{1\perp}^* + x_2 x_4 p_{1\perp} p_{1\perp}^* + x_2 x_1 q_{1\perp} q_{1\perp}^* + \\
&\quad x_2 x_1 q_{1\perp} p_{2\perp}^* + x_1^2 p_{2\perp} p_{2\perp}^* + x_2 x_1 p_{2\perp} p_{2\perp}^* + x_3 x_1 p_{2\perp} p_{2\perp}^* + x_4 x_1 p_{2\perp} p_{2\perp}^* \\
&\quad + [12] x_2 x_1 \langle 12 \rangle),
\end{aligned}$$

$$\begin{aligned}
N^{(30)}(q_1; 1^+, 2^-, 3^-, 4^+; q_2) &= x_1 x_2 x_3 x_4^3 \langle 23 \rangle^3 q_{2\perp} q_{1\perp}^* (p_{1\perp} + q_{1\perp} + p_{2\perp})^3, \\
D^{(30)}(q_1; 1^+, 2^-, 3^-, 4^+; q_2) &= s_{123} \langle 12 \rangle (\sqrt{x_2} \langle 12 \rangle + \sqrt{x_3} \langle 13 \rangle) \\
&\quad (\sqrt{x_1} \langle 13 \rangle + \sqrt{x_2} \langle 23 \rangle) (p_{1\perp} + 2q_{1\perp} + p_{2\perp}) \\
&\quad (x_1 p_{1\perp} + x_2 p_{1\perp} + x_3 p_{1\perp} + x_4 p_{1\perp} + 2x_1 q_{1\perp} + 2x_2 q_{1\perp} + 2x_3 q_{1\perp} + x_4 q_{1\perp} \\
&\quad + x_1 p_{2\perp} + x_2 p_{2\perp} + x_3 p_{2\perp} + x_4 p_{2\perp}) (x_4 q_{1\perp} + x_1 p_{4\perp} + x_2 p_{4\perp} + x_3 p_{4\perp} \\
&\quad + x_4 p_{4\perp} + \sqrt{x_1} \sqrt{x_4} \langle 14 \rangle + \sqrt{x_2} \sqrt{x_4} \langle 24 \rangle + \sqrt{x_3} \sqrt{x_4} \langle 34 \rangle) \\
&\quad (-x_2 x_3 x_1 p_{2\perp} q_{1\perp}^* - x_2 x_3 x_1 p_{1\perp} q_{1\perp}^* - x_2 x_3 x_1 q_{1\perp} p_{1\perp}^* - x_2 x_3 x_1 p_{1\perp} p_{1\perp}^* \\
&\quad - x_2 x_3^2 p_{1\perp} p_{1\perp}^* - x_2^2 x_3 p_{1\perp} p_{1\perp}^* - x_2 x_3 x_4 p_{1\perp} p_{1\perp}^* + x_2 x_1^2 (-q_{1\perp}) q_{1\perp}^* - \\
&\quad x_2^2 x_1 q_{1\perp} q_{1\perp}^* - 4x_2 x_3 x_1 q_{1\perp} q_{1\perp}^* - x_2 x_4 x_1 q_{1\perp} q_{1\perp}^* - x_2 x_3 x_1 q_{1\perp} p_{2\perp}^* \\
&\quad - x_3 x_1^2 p_{2\perp} p_{2\perp}^* - x_3^2 x_1 p_{2\perp} p_{2\perp}^* - x_2 x_3 x_1 p_{2\perp} p_{2\perp}^* - x_3 x_4 x_1 p_{2\perp} p_{2\perp}^* \\
&\quad + s_{123} x_2 x_3 x_1),
\end{aligned}$$

$$\begin{aligned}
N^{(31)}(q_1; 1^+, 2^-, 3^-, 4^+; q_2) &= x_1 x_2 x_3 x_4 \langle 23 \rangle^3 q_{1\perp} q_{2\perp} q_{1\perp}^* \\
&\quad (p_{1\perp} + q_{1\perp} + p_{2\perp} + p_{4\perp}), \\
D^{(31)}(q_1; 1^+, 2^-, 3^-, 4^+; q_2) &= s_{1234} \langle 12 \rangle \langle 34 \rangle (\sqrt{x_2} \langle 12 \rangle + \sqrt{x_3} \langle 13 \rangle + \sqrt{x_4} \langle 14 \rangle) \\
&\quad (\sqrt{x_1} \langle 14 \rangle + \sqrt{x_2} \langle 24 \rangle + \sqrt{x_3} \langle 34 \rangle) (p_{1\perp} + 2q_{1\perp} + p_{2\perp} + p_{4\perp}) \\
&\quad (x_2 x_4 x_3 p_{1\perp} p_{1\perp}^* + x_1 x_2 x_4 q_{1\perp} q_{1\perp}^* + x_1 x_4 x_3 p_{2\perp} p_{2\perp}^* + x_1 x_2 x_3 p_{4\perp} p_{4\perp}^*),
\end{aligned}$$

$$\begin{aligned}
N^{(32)}(q_1; 1^+, 2^-, 3^-, 4^+; q_2) &= x_1^{3/2} x_2 x_3 x_4 \langle 23 \rangle^3 q_{1\perp} q_{2\perp} q_{1\perp}^* (q_{1\perp} + p_{2\perp} + p_{4\perp})^3, \\
D^{(32)}(q_1; 1^+, 2^-, 3^-, 4^+; q_2) &= s_{234} \langle 34 \rangle p_{1\perp} (\sqrt{x_3} \langle 23 \rangle + \sqrt{x_4} \langle 24 \rangle) \\
&\quad (\sqrt{x_2} \langle 24 \rangle + \sqrt{x_3} \langle 34 \rangle) (\sqrt{x_2} \langle 12 \rangle + \sqrt{x_3} \langle 13 \rangle + \sqrt{x_4} \langle 14 \rangle) \\
&\quad (p_{1\perp} + q_{1\perp} + p_{2\perp} + p_{4\perp}) (p_{1\perp} + 2q_{1\perp} + p_{2\perp} + p_{4\perp}) \\
&\quad (x_2 x_4 x_3 p_{1\perp} p_{1\perp}^* + x_1 x_2 x_4 q_{1\perp} q_{1\perp}^* + x_1 x_4 x_3 p_{2\perp} p_{2\perp}^* + x_1 x_2 x_3 p_{4\perp} p_{4\perp}^*),
\end{aligned}$$

$$\begin{aligned}
N^{(33)}(q_1; 1^+, 2^-, 3^-, 4^+; q_2) &= x_1^{5/2} \sqrt{x_2} x_4^{3/2} (-q_{1\perp}^5) q_{2\perp} q_{1\perp}^*, \\
D^{(33)}(q_1; 1^+, 2^-, 3^-, 4^+; q_2) &= [12] x_3 \langle 34 \rangle p_{4\perp} (p_{1\perp} + p_{2\perp}) (\sqrt{x_1} \langle 13 \rangle + \sqrt{x_2} \langle 23 \rangle) \\
&\quad (p_{1\perp} + q_{1\perp} + p_{2\perp} + p_{4\perp}) (p_{1\perp} + 2q_{1\perp} + p_{2\perp} + p_{4\perp}) (x_2 x_4 x_3 p_{1\perp} p_{1\perp}^* \\
&\quad + x_1 x_2 x_4 q_{1\perp} q_{1\perp}^* + x_1 x_4 x_3 p_{2\perp} p_{2\perp}^* + x_1 x_2 x_3 p_{4\perp} p_{4\perp}^*),
\end{aligned}$$

$$\begin{aligned}
N^{(34)}(q_1; 1^+, 2^-, 3^-, 4^+; q_2) &= x_1^{5/2} \sqrt{x_2} x_4^{3/2} (-q_{1\perp}^4) p_{2\perp}^3 q_{2\perp} q_{1\perp}^*, \\
D^{(34)}(q_1; 1^+, 2^-, 3^-, 4^+; q_2) &= \sqrt{x_3} \langle 12 \rangle \langle 34 \rangle p_{1\perp} p_{4\perp} (p_{1\perp} + p_{2\perp}) (q_{1\perp} + p_{4\perp}) \\
&\quad (p_{1\perp} + 2q_{1\perp} + p_{2\perp} + p_{4\perp}) (x_2 p_{1\perp} p_{1\perp}^* + x_1 p_{2\perp} p_{2\perp}^*) \\
&\quad (x_2 x_4 x_3 p_{1\perp} p_{1\perp}^* + x_1 x_2 x_4 q_{1\perp} q_{1\perp}^* + x_1 x_4 x_3 p_{2\perp} p_{2\perp}^* + x_1 x_2 x_3 p_{4\perp} p_{4\perp}^*), \\
N^{(35)}(q_1; 1^+, 2^-, 3^-, 4^+; q_2) &= x_1^{3/2} \sqrt{x_2} \sqrt{x_3} x_4^{3/2} (-q_{1\perp}) q_{2\perp} q_{1\perp}^* (q_{1\perp} + p_{2\perp})^4, \\
D^{(35)}(q_1; 1^+, 2^-, 3^-, 4^+; q_2) &= [23] p_{1\perp} p_{4\perp} (\sqrt{x_2} \langle 12 \rangle + \sqrt{x_3} \langle 13 \rangle) \\
&\quad (\sqrt{x_2} \langle 24 \rangle + \sqrt{x_3} \langle 34 \rangle) (p_{1\perp} + q_{1\perp} + p_{2\perp} + p_{4\perp}) \\
&\quad (p_{1\perp} + 2q_{1\perp} + p_{2\perp} + p_{4\perp}) (x_2 x_4 x_3 p_{1\perp} p_{1\perp}^* + x_1 x_2 x_4 q_{1\perp} q_{1\perp}^* + \\
&\quad x_1 x_4 x_3 p_{2\perp} p_{2\perp}^* + x_1 x_2 x_3 p_{4\perp} p_{4\perp}^*), \\
N^{(36)}(q_1; 1^+, 2^-, 3^-, 4^+; q_2) &= x_1 x_2 x_3 x_4^{3/2} \langle 23 \rangle^3 q_{1\perp} q_{2\perp} q_{1\perp}^* (p_{1\perp} + q_{1\perp} + p_{2\perp})^3, \\
D^{(36)}(q_1; 1^+, 2^-, 3^-, 4^+; q_2) &= s_{123} \langle 12 \rangle p_{4\perp} (\sqrt{x_2} \langle 12 \rangle + \sqrt{x_3} \langle 13 \rangle) \\
&\quad (\sqrt{x_1} \langle 13 \rangle + \sqrt{x_2} \langle 23 \rangle) (\sqrt{x_1} \langle 14 \rangle + \sqrt{x_2} \langle 24 \rangle + \sqrt{x_3} \langle 34 \rangle) \\
&\quad (p_{1\perp} + q_{1\perp} + p_{2\perp} + p_{4\perp}) (p_{1\perp} + 2q_{1\perp} + p_{2\perp} + p_{4\perp}) \\
&\quad (x_2 x_4 x_3 p_{1\perp} p_{1\perp}^* + x_1 x_2 x_4 q_{1\perp} q_{1\perp}^* + x_1 x_4 x_3 p_{2\perp} p_{2\perp}^* + x_1 x_2 x_3 p_{4\perp} p_{4\perp}^*), \\
N^{(37)}(q_1; 1^+, 2^-, 3^-, 4^+; q_2) &= x_1^{3/2} \sqrt{x_3} x_4^{5/2} (-q_{1\perp}) p_{2\perp}^4 q_{2\perp} q_{1\perp}^*, \\
D^{(37)}(q_1; 1^+, 2^-, 3^-, 4^+; q_2) &= [34] x_2 \langle 12 \rangle p_{1\perp} (\sqrt{x_3} \langle 23 \rangle + \sqrt{x_4} \langle 24 \rangle) (q_{1\perp} + p_{4\perp}) \\
&\quad (p_{1\perp} + q_{1\perp} + p_{2\perp} + p_{4\perp}) (p_{1\perp} + 2q_{1\perp} + p_{2\perp} + p_{4\perp}) \\
&\quad (x_2 x_4 x_3 p_{1\perp} p_{1\perp}^* + x_1 x_2 x_4 q_{1\perp} q_{1\perp}^* + x_1 x_4 x_3 p_{2\perp} p_{2\perp}^* + x_1 x_2 x_3 p_{4\perp} p_{4\perp}^*),
\end{aligned}$$

$$\begin{aligned}
N^{(38)}(q_1; 1^+, 2^-, 3^-, 4^+; q_2) &= x_1^{5/2} \sqrt{x_2} x_4^3 q_{1\perp}^4 p_{2\perp}^3 q_{2\perp} q_{1\perp}^*, \\
D^{(38)}(q_1; 1^+, 2^-, 3^-, 4^+; q_2) &= \langle 12 \rangle p_{1\perp} (p_{1\perp} + p_{2\perp}) (p_{1\perp} + q_{1\perp} + p_{2\perp}) \\
&\quad (p_{1\perp} + 2q_{1\perp} + p_{2\perp}) (x_1 q_{1\perp} + x_2 q_{1\perp} + 2x_3 q_{1\perp} + x_4 q_{1\perp} + \sqrt{x_1} \sqrt{x_3} \langle 13 \rangle \\
&\quad + \sqrt{x_2} \sqrt{x_3} \langle 23 \rangle) (x_2 p_{1\perp} p_{1\perp}^* + x_1 p_{2\perp} p_{2\perp}^*) (x_4 q_{1\perp} + x_1 p_{4\perp} \\
&\quad + x_2 p_{4\perp} + x_3 p_{4\perp} + x_4 p_{4\perp} + \sqrt{x_1} \sqrt{x_4} \langle 14 \rangle + \sqrt{x_2} \sqrt{x_4} \langle 24 \rangle \\
&\quad + \sqrt{x_3} \sqrt{x_4} \langle 34 \rangle) (x_2 x_3 x_1 p_{2\perp} q_{1\perp}^* + x_2 x_3 x_1 p_{1\perp} q_{1\perp}^* + x_2 x_3 x_1 q_{1\perp} p_{1\perp}^* \\
&\quad + x_2 x_3 x_1 p_{1\perp} p_{1\perp}^* + x_2 x_3^2 p_{1\perp} p_{1\perp}^* + x_2^2 x_3 p_{1\perp} p_{1\perp}^* + x_2 x_3 x_4 p_{1\perp} p_{1\perp}^* \\
&\quad + x_2 x_1^2 q_{1\perp} q_{1\perp}^* + x_2^2 x_1 q_{1\perp} q_{1\perp}^* + 4x_2 x_3 x_1 q_{1\perp} q_{1\perp}^* + x_2 x_4 x_1 q_{1\perp} q_{1\perp}^* + \\
&\quad x_2 x_3 x_1 q_{1\perp} p_{2\perp}^* + x_3 x_1^2 p_{2\perp} p_{2\perp}^* + x_3^2 x_1 p_{2\perp} p_{2\perp}^* + x_2 x_3 x_1 p_{2\perp} p_{2\perp}^* \\
&\quad + x_3 x_4 x_1 p_{2\perp} p_{2\perp}^* - s_{123} x_2 x_3 x_1),
\end{aligned}$$

$$\begin{aligned}
N^{(39)}(q_1; 1^+, 2^-, 3^-, 4^+; q_2) &= x_1^{5/2} \sqrt{x_2} x_4^3 q_{1\perp}^4 q_{2\perp} q_{1\perp}^*, \\
D^{(39)}(q_1; 1^+, 2^-, 3^-, 4^+; q_2) &= [12] \sqrt{x_3} (p_{1\perp} + p_{2\perp}) (\sqrt{x_1} \langle 13 \rangle + \sqrt{x_2} \langle 23 \rangle) \\
&\quad (p_{1\perp} + 2q_{1\perp} + p_{2\perp}) (x_1 q_{1\perp} + x_2 q_{1\perp} + 2x_3 q_{1\perp} + x_4 q_{1\perp} + \sqrt{x_1} \sqrt{x_3} \langle 13 \rangle + \\
&\quad \sqrt{x_2} \sqrt{x_3} \langle 23 \rangle) (x_4 q_{1\perp} + x_1 p_{4\perp} + x_2 p_{4\perp} + x_3 p_{4\perp} + x_4 p_{4\perp} + \sqrt{x_1} \sqrt{x_4} \langle 14 \rangle \\
&\quad + \sqrt{x_2} \sqrt{x_4} \langle 24 \rangle + \sqrt{x_3} \sqrt{x_4} \langle 34 \rangle) (x_2 x_3 x_1 p_{2\perp} q_{1\perp}^* + x_2 x_3 x_1 p_{1\perp} q_{1\perp}^* + \\
&\quad x_2 x_3 x_1 q_{1\perp} p_{1\perp}^* + x_2 x_3 x_1 p_{1\perp} p_{1\perp}^* + x_2 x_3^2 p_{1\perp} p_{1\perp}^* + x_2^2 x_3 p_{1\perp} p_{1\perp}^* \\
&\quad + x_2 x_3 x_4 p_{1\perp} p_{1\perp}^* + x_2 x_1^2 q_{1\perp} q_{1\perp}^* + x_2^2 x_1 q_{1\perp} q_{1\perp}^* + 4x_2 x_3 x_1 q_{1\perp} q_{1\perp}^* \\
&\quad + x_2 x_4 x_1 q_{1\perp} q_{1\perp}^* + x_2 x_3 x_1 q_{1\perp} p_{2\perp}^* + x_3 x_1^2 p_{2\perp} p_{2\perp}^* + x_3^2 x_1 p_{2\perp} p_{2\perp}^* + \\
&\quad x_2 x_3 x_1 p_{2\perp} p_{2\perp}^* + x_3 x_4 x_1 p_{2\perp} p_{2\perp}^* - s_{123} x_2 x_3 x_1),
\end{aligned}$$

$$\begin{aligned}
N^{(40)}(q_1; 1^+, 2^-, 3^-, 4^+; q_2) &= x_1^{3/2} \sqrt{x_2} \sqrt{x_3} x_4^3 q_{2\perp} q_{1\perp}^* (q_{1\perp} + p_{2\perp})^4, \\
D^{(40)}(q_1; 1^+, 2^-, 3^-, 4^+; q_2) &= [23] p_{1\perp} (\sqrt{x_2} \langle 12 \rangle + \sqrt{x_3} \langle 13 \rangle) \\
&\quad (p_{1\perp} + 2q_{1\perp} + p_{2\perp}) (x_1 q_{1\perp} + 2x_2 q_{1\perp} + 2x_3 q_{1\perp} + x_4 q_{1\perp} + x_{1234} p_{2\perp} \\
&\quad + \sqrt{x_1} \sqrt{x_2} \langle 12 \rangle + \sqrt{x_1} \sqrt{x_3} \langle 13 \rangle) (x_4 q_{1\perp} + x_1 p_{4\perp} + x_2 p_{4\perp} + x_3 p_{4\perp} \\
&\quad + x_4 p_{4\perp} + \sqrt{x_1} \sqrt{x_4} \langle 14 \rangle + \sqrt{x_2} \sqrt{x_4} \langle 24 \rangle + \sqrt{x_3} \sqrt{x_4} \langle 34 \rangle) \\
&\quad (x_2 x_3 x_1 p_{2\perp} q_{1\perp}^* + x_2 x_3 x_1 p_{1\perp} q_{1\perp}^* + x_2 x_3 x_1 q_{1\perp} p_{1\perp}^* + x_2 x_3 x_1 p_{1\perp} p_{1\perp}^* + \\
&\quad x_2 x_3^2 p_{1\perp} p_{1\perp}^* + x_2^2 x_3 p_{1\perp} p_{1\perp}^* + x_2 x_3 x_4 p_{1\perp} p_{1\perp}^* + x_2 x_1^2 q_{1\perp} q_{1\perp}^* + x_2^2 x_1 |q_{1\perp}|^2 \\
&\quad + 4x_2 x_3 x_1 q_{1\perp} q_{1\perp}^* + x_2 x_4 x_1 q_{1\perp} q_{1\perp}^* + x_2 x_3 x_1 q_{1\perp} p_{2\perp}^* + x_3 x_1^2 p_{2\perp} p_{2\perp}^* \\
&\quad + x_3^2 x_1 p_{2\perp} p_{2\perp}^* + x_2 x_3 x_1 p_{2\perp} p_{2\perp}^* + x_3 x_4 x_1 p_{2\perp} p_{2\perp}^* - s_{123} x_2 x_3 x_1), \\
N^{(41)}(q_1; 1^+, 2^-, 3^-, 4^+; q_2) &= x_1^{3/2} x_2 x_3^{3/2} x_4^3 \langle 23 \rangle^3 (-q_{1\perp}) q_{2\perp}, \\
D^{(41)}(q_1; 1^+, 2^-, 3^-, 4^+; q_2) &= \langle 12 \rangle (x_1 p_{1\perp} + x_2 p_{1\perp} + x_3 p_{1\perp} + x_4 p_{1\perp} + x_1 q_{1\perp}) \\
&\quad (x_{1234} p_{1\perp} + 2x_1 q_{1\perp} + 2x_2 q_{1\perp} + 2x_3 q_{1\perp} + x_4 q_{1\perp} + x_{1234} p_{2\perp}) \\
&\quad (x_1 q_{1\perp} + x_2 q_{1\perp} + 2x_3 q_{1\perp} + x_4 q_{1\perp} + \sqrt{x_1} \sqrt{x_3} \langle 13 \rangle + \sqrt{x_2} \sqrt{x_3} \langle 23 \rangle) \\
&\quad (x_4 q_{1\perp} + x_{1234} p_{4\perp} + \sqrt{x_1} \sqrt{x_4} \langle 14 \rangle + \sqrt{x_2} \sqrt{x_4} \langle 24 \rangle + \sqrt{x_3} \sqrt{x_4} \langle 34 \rangle) \\
&\quad (x_2 x_3 x_1 p_{2\perp} q_{1\perp}^* + x_2 x_3 x_1 p_{1\perp} q_{1\perp}^* + x_2 x_3 x_1 q_{1\perp} p_{1\perp}^* + x_2 x_3 x_1 p_{1\perp} p_{1\perp}^* \\
&\quad + x_2 x_3^2 p_{1\perp} p_{1\perp}^* + x_2^2 x_3 p_{1\perp} p_{1\perp}^* + x_2 x_3 x_4 p_{1\perp} p_{1\perp}^* + x_2 x_1^2 q_{1\perp} q_{1\perp}^* \\
&\quad + x_2^2 x_1 q_{1\perp} q_{1\perp}^* + 4x_2 x_3 x_1 q_{1\perp} q_{1\perp}^* + x_2 x_4 x_1 q_{1\perp} q_{1\perp}^* + x_2 x_3 x_1 q_{1\perp} p_{2\perp}^* \\
&\quad + x_3 x_1^2 p_{2\perp} p_{2\perp}^* + x_3^2 x_1 p_{2\perp} p_{2\perp}^* + x_2 x_3 x_1 p_{2\perp} p_{2\perp}^* + x_3 x_4 x_1 p_{2\perp} p_{2\perp}^* \\
&\quad - s_{123} x_2 x_3 x_1),
\end{aligned}$$

$$\begin{aligned}
N^{(42)}(q_1; 1^+, 2^-, 3^-, 4^+; q_2) &= x_1^3 x_2^{3/2} x_3^{3/2} x_4^3 \langle 23 \rangle^3 q_{2\perp} (p_{1\perp} + q_{1\perp})^3 q_{1\perp}^*, \\
D^{(42)}(q_1; 1^+, 2^-, 3^-, 4^+; q_2) &= p_{1\perp} (x_1 p_{1\perp} + x_2 p_{1\perp} + x_3 p_{1\perp} + x_4 p_{1\perp} + x_1 q_{1\perp}) \\
&\quad (x_1 q_{1\perp} + x_2 q_{1\perp} + 2x_3 q_{1\perp} + x_4 q_{1\perp} + \sqrt{x_1} \sqrt{x_3} \langle 13 \rangle + \sqrt{x_2} \sqrt{x_3} \langle 23 \rangle) \\
&\quad (x_1 p_{1\perp} q_{1\perp}^* + x_1 q_{1\perp} p_{1\perp}^* + x_1 p_{1\perp} p_{1\perp}^* + x_2 p_{1\perp} p_{1\perp}^* + x_3 p_{1\perp} p_{1\perp}^* + x_4 |p_{1\perp}|^2 \\
&\quad + x_1 q_{1\perp} q_{1\perp}^*) (x_2 q_{1\perp} + x_1 p_{2\perp} + x_2 p_{2\perp} + x_3 p_{2\perp} + x_4 p_{2\perp} + \sqrt{x_1} \sqrt{x_2} \langle 12 \rangle) \\
&\quad (x_1 q_{1\perp} + 2x_2 q_{1\perp} + 2x_3 q_{1\perp} + x_4 q_{1\perp} + x_{1234} p_{2\perp} + \\
&\quad \sqrt{x_1} \sqrt{x_2} \langle 12 \rangle + \sqrt{x_1} \sqrt{x_3} \langle 13 \rangle) (x_4 q_{1\perp} + x_{1234} p_{4\perp} + \sqrt{x_1} \sqrt{x_4} \langle 14 \rangle) \\
&\quad + \sqrt{x_2} \sqrt{x_4} \langle 24 \rangle + \sqrt{x_3} \sqrt{x_4} \langle 34 \rangle) (x_2 x_3 x_1 p_{2\perp} q_{1\perp}^* + x_2 x_3 x_1 p_{1\perp} q_{1\perp}^* \\
&\quad + x_2 x_3 x_1 q_{1\perp} p_{1\perp}^* + x_2 x_3 x_1 p_{1\perp} p_{1\perp}^* + x_2 x_3^2 p_{1\perp} p_{1\perp}^* + x_2^2 x_3 p_{1\perp} p_{1\perp}^* \\
&\quad + x_2 x_3 x_4 p_{1\perp} p_{1\perp}^* + x_2 x_1^2 q_{1\perp} q_{1\perp}^* + x_2^2 x_1 q_{1\perp} q_{1\perp}^* + 4x_2 x_3 x_1 q_{1\perp} q_{1\perp}^* \\
&\quad + x_2 x_4 x_1 q_{1\perp} q_{1\perp}^* + x_2 x_3 x_1 q_{1\perp} p_{2\perp}^* + x_3 x_1^2 p_{2\perp} p_{2\perp}^* + x_3^2 x_1 p_{2\perp} p_{2\perp}^* + \\
&\quad x_2 x_3 x_1 p_{2\perp} p_{2\perp}^* + x_3 x_4 x_1 p_{2\perp} p_{2\perp}^* - s_{123} x_2 x_3 x_1),
\end{aligned}$$

$$\begin{aligned}
N^{(43)}(q_1; 1^+, 2^-, 3^-, 4^+; q_2) &= x_1^{5/2} \sqrt{x_2} x_4^3 p_{2\perp}^4 q_{2\perp} q_{1\perp}^* \\
&\quad (x_1 q_{1\perp} + x_2 q_{1\perp} + 2x_3 q_{1\perp} + x_4 q_{1\perp} + \sqrt{x_1} \sqrt{x_3} \langle 13 \rangle + \sqrt{x_2} \sqrt{x_3} \langle 23 \rangle), \\
D^{(43)}(q_1; 1^+, 2^-, 3^-, 4^+; q_2) &= \langle 12 \rangle p_{1\perp} (p_{1\perp} + q_{1\perp} + p_{2\perp}) (x_2 q_{1\perp} + x_{1234} p_{2\perp} \\
&\quad + \sqrt{x_1} \sqrt{x_2} \langle 12 \rangle) (x_4 q_{1\perp} + x_1 p_{4\perp} + x_2 p_{4\perp} + x_3 p_{4\perp} + x_4 p_{4\perp} \\
&\quad + \sqrt{x_1} \sqrt{x_4} \langle 14 \rangle + \sqrt{x_2} \sqrt{x_4} \langle 24 \rangle + \sqrt{x_3} \sqrt{x_4} \langle 34 \rangle) \\
&\quad (x_2 x_3 x_1 p_{2\perp} q_{1\perp}^* + x_2 x_3 x_1 p_{1\perp} q_{1\perp}^* + x_2 x_3 x_1 q_{1\perp} p_{1\perp}^* + x_2 x_3 x_1 p_{1\perp} p_{1\perp}^* \\
&\quad + x_2 x_3^2 p_{1\perp} p_{1\perp}^* + x_2^2 x_3 p_{1\perp} p_{1\perp}^* + x_2 x_3 x_4 p_{1\perp} p_{1\perp}^* + x_2 x_1^2 q_{1\perp} q_{1\perp}^* \\
&\quad + x_2^2 x_1 q_{1\perp} q_{1\perp}^* + 4x_2 x_3 x_1 q_{1\perp} q_{1\perp}^* + x_2 x_4 x_1 q_{1\perp} q_{1\perp}^* + x_2 x_3 x_1 q_{1\perp} p_{2\perp}^* \\
&\quad + x_3 x_1^2 p_{2\perp} p_{2\perp}^* + x_3^2 x_1 p_{2\perp} p_{2\perp}^* + x_2 x_3 x_1 p_{2\perp} p_{2\perp}^* + x_3 x_4 x_1 p_{2\perp} p_{2\perp}^* \\
&\quad - s_{123} x_2 x_3 x_1) (x_2 x_1 p_{2\perp} q_{1\perp}^* + x_2 x_1 p_{1\perp} q_{1\perp}^* + x_2 x_1 q_{1\perp} p_{1\perp}^* \\
&\quad + x_2 x_1 p_{1\perp} p_{1\perp}^* + x_2^2 p_{1\perp} p_{1\perp}^* + x_2 x_3 p_{1\perp} p_{1\perp}^* + x_2 x_4 p_{1\perp} p_{1\perp}^* \\
&\quad + x_2 x_1 q_{1\perp} q_{1\perp}^* + x_2 x_1 q_{1\perp} p_{2\perp}^* + x_1^2 p_{2\perp} p_{2\perp}^* + x_2 x_1 p_{2\perp} p_{2\perp}^* \\
&\quad + x_3 x_1 p_{2\perp} p_{2\perp}^* + x_4 x_1 p_{2\perp} p_{2\perp}^* + [12] x_2 x_1 \langle 12 \rangle),
\end{aligned}$$

# Bibliography

- [1] E. Witten, “Perturbative gauge theory as a string theory in twistor space,” *Commun. Math. Phys.*, vol. 252, pp. 189–258, 2004, [hep-th/0312171].
- [2] F. Cachazo, P. Svrcek, and E. Witten, “MHV vertices and tree amplitudes in gauge theory,” *JHEP*, vol. 09, p. 006, 2004, [hep-th/0403047].
- [3] R. Britto, F. Cachazo, and B. Feng, “New recursion relations for tree amplitudes of gluons,” *Nucl. Phys.*, vol. B715, pp. 499–522, 2005, [hep-th/0412308].
- [4] R. Britto, F. Cachazo, B. Feng, and E. Witten, “Direct proof of tree-level recursion relation in Yang-Mills theory,” *Phys. Rev. Lett.*, vol. 94, p. 181602, 2005, [hep-th/0501052].
- [5] Z. Bern, L. J. Dixon, D. C. Dunbar, and D. A. Kosower, “Fusing gauge theory tree amplitudes into loop amplitudes,” *Nucl. Phys.*, vol. B435, pp. 59–101, 1995, [hep-ph/9409265].
- [6] Z. Bern, L. J. Dixon, D. C. Dunbar, and D. A. Kosower, “One loop  $n$  point gauge theory amplitudes, unitarity and collinear limits,” *Nucl. Phys.*, vol. B425, pp. 217–260, 1994, [hep-ph/9403226].
- [7] C. F. Berger *et al.*, “An Automated Implementation of On-Shell Methods for One-Loop Amplitudes,” 2008, [arXiv:0803.4180].

- 
- [8] R. K. Ellis, W. T. Giele, and G. Zanderighi, “Semi-numerical evaluation of one-loop corrections,” *Phys. Rev.*, vol. D73, p. 014027, 2006, [hep-ph/0508308].
- [9] C. Anastasiou, Z. Bern, L. J. Dixon, and D. A. Kosower, “Planar amplitudes in maximally supersymmetric Yang-Mills theory,” *Phys. Rev. Lett.*, vol. 91, p. 251602, 2003, [hep-th/0309040].
- [10] Z. Bern, L. J. Dixon, and V. A. Smirnov, “Iteration of planar amplitudes in maximally supersymmetric Yang-Mills theory at three loops and beyond,” *Phys. Rev.*, vol. D72, p. 085001, 2005, [hep-th/0505205].
- [11] L. F. Alday and J. Maldacena, “Comments on gluon scattering amplitudes via AdS/CFT,” *JHEP*, vol. 11, p. 068, 2007, [arXiv:0710.1060].
- [12] Z. Bern *et al.*, “The Two-Loop Six-Gluon MHV Amplitude in Maximally Supersymmetric Yang-Mills Theory,” *Phys. Rev.*, vol. D78, p. 045007, 2008, [arXiv:0803.1465].
- [13] C. Anastasiou *et al.*, “Two-Loop Polygon Wilson Loops in  $\mathcal{N} = 4$  SYM,” 2009, [arXiv:0902.2245].
- [14] C. Duhr, S. Hoeche, and F. Maltoni, “Color-dressed recursive relations for multi-parton amplitudes,” *JHEP*, vol. 08, p. 062, 2006, [hep-ph/0607057].
- [15] D. A. Kosower, “Antenna factorization of gauge-theory amplitudes,” *Phys. Rev.*, vol. D57, pp. 5410–5416, 1998, [hep-ph/9710213].
- [16] D. A. Kosower, “Multiple singular emission in gauge theories,” *Phys. Rev.*, vol. D67, p. 116003, 2003, [hep-ph/0212097].
- [17] C. Duhr and F. Maltoni, “Antenna functions from MHV rules,” *JHEP*, vol. 11, p. 002, 2008, [arXiv:0808.3319].
- [18] T. G. Birthwright, E. W. N. Glover, V. V. Khoze, and P. Marquard, “Collinear limits in QCD from MHV rules,” *JHEP*, vol. 07, p. 068, 2005, [hep-ph/0505219].



- 
- [19] T. G. Birthwright, E. W. N. Glover, V. V. Khoze, and P. Marquard, “Multi-gluon collinear limits from MHV diagrams,” *JHEP*, vol. 05, p. 013, 2005, [hep-ph/0503063].
- [20] S. Catani and M. H. Seymour, “A general algorithm for calculating jet cross sections in NLO QCD,” *Nucl. Phys.*, vol. B485, pp. 291–419, 1997, [hep-ph/9605323].
- [21] G. Somogyi, Z. Trocsanyi, and V. Del Duca, “A subtraction scheme for computing QCD jet cross sections at NNLO: regularization of doubly-real emissions,” *JHEP*, vol. 01, p. 070, 2007, [hep-ph/0609042].
- [22] G. Somogyi and Z. Trocsanyi, “A subtraction scheme for computing QCD jet cross sections at NNLO: regularization of real-virtual emission,” *JHEP*, vol. 01, p. 052, 2007, [hep-ph/0609043].
- [23] G. Somogyi and Z. Trocsanyi, “A subtraction scheme for computing QCD jet cross sections at NNLO: integrating the subtraction terms I,” *JHEP*, vol. 08, p. 042, 2008, [arXiv:0807.0509].
- [24] G. Somogyi, “Subtraction with hadronic initial states: an NNLO-compatible scheme,” 2009, [arXiv:0903.1218].
- [25] V. Del Duca, A. Frizzo, and F. Maltoni, “Factorization of tree QCD amplitudes in the high-energy limit and in the collinear limit,” *Nucl. Phys.*, vol. B568, pp. 211–262, 2000, [hep-ph/9909464].
- [26] V. Del Duca and E. W. N. Glover, “Testing high-energy factorization beyond the next-to-leading-logarithmic accuracy,” *JHEP*, vol. 05, p. 056, 2008, [arXiv:0802.4445].
- [27] V. Del Duca, C. Duhr, and E. W. N. Glover, “Iterated amplitudes in the high-energy limit,” *JHEP*, vol. 12, p. 097, 2008, [arXiv:0809.1822].
- [28] V. Del Duca, C. Duhr, E. W. N. Glover, and V. A. Smirnov, “The one-loop pentagon to higher orders in epsilon,” 2009, [arXiv:0905.0097].
- [29] V. Del Duca, C. Duhr, and E. W. N. Glover, “The five-gluon amplitude in the high-energy limit,” 2009, [arXiv:0905.0100].

- [30] C. Duhr, “Twistor inspired techniques in QCD,” *AIP Conf. Proc.*, vol. 1038, pp. 295–304, 2008.
- [31] M. E. Peskin and D. V. Schroeder, *An Introduction to Quantum Field Theory*. Westview, 1995.
- [32] L. J. Dixon, “Calculating scattering amplitudes efficiently,” 1996, [hep-ph/9601359].
- [33] R. Kleiss and H. Kuijf, “Multi - Gluon Cross-Sections And Five Jet Production At Hadron Colliders,” *Nucl. Phys.*, vol. B312, p. 616, 1989.
- [34] Z. Bern, J. J. M. Carrasco, and H. Johansson, “New Relations for Gauge-Theory Amplitudes,” *Phys. Rev.*, vol. D78, p. 085011, 2008, [arXiv:0805.3993].
- [35] N. E. J. Bjerrum-Bohr, P. H. Damgaard, and P. Vanhove, “Minimal Basis for Gauge Theory Amplitudes,” 2009, [arXiv:0907.1425].
- [36] F. Maltoni, K. Paul, T. Stelzer, and S. Willenbrock, “Color-flow decomposition of QCD amplitudes,” *Phys. Rev.*, vol. D67, p. 014026, 2003, [hep-ph/0209271].
- [37] V. Del Duca, L. J. Dixon, and F. Maltoni, “New color decompositions for gauge amplitudes at tree and loop level,” *Nucl. Phys.*, vol. B571, pp. 51–70, 2000, [hep-ph/9910563].
- [38] C. Vergu, *Twisteurs, cordes et theories de jauge supersymetriques*. PhD thesis, Universite de Paris VI, 2008, [arXiv:0809.1807].
- [39] S. J. Parke and T. R. Taylor, “An Amplitude For  $n$  Gluon Scattering,” *Phys. Rev. Lett.*, vol. 56, p. 2459, 1986.
- [40] F. A. Berends and W. T. Giele, “Recursive Calculations For Processes With  $n$  Gluons,” *Nucl. Phys.*, vol. B306, p. 759, 1988.
- [41] R. Britto, B. Feng, R. Roiban, M. Spradlin, and A. Volovich, “All split helicity tree-level gluon amplitudes,” *Phys. Rev.*, vol. D71, p. 105017, 2005, [hep-th/0503198].

- [42] C. G. Papadopoulos and M. Worek, “Multi-parton Cross Sections at Hadron Colliders,” *Eur. Phys. J.*, vol. C50, pp. 843–856, 2007, [hep-ph/0512150].
- [43] S. D. Badger, E. W. N. Glover, V. V. Khoze, and P. Svrcek, “Recursion relations for gauge theory amplitudes with massive particles,” *JHEP*, vol. 07, p. 025, 2005, [hep-th/0504159].
- [44] S. D. Badger, E. W. N. Glover, and V. V. Khoze, “Recursion Relations for Gauge Theory Amplitudes with Massive Vector Bosons and Fermions,” *JHEP*, vol. 01, p. 066, 2006, [hep-th/0507161].
- [45] M.-x. Luo and C.-k. Wen, “Recursion relations for tree amplitudes in super gauge theories,” *JHEP*, vol. 03, p. 004, 2005, [hep-th/0501121].
- [46] K. J. Ozeren and W. J. Stirling, “Scattering amplitudes with massive fermions using BCFW recursion,” *Eur. Phys. J.*, vol. C48, pp. 159–168, 2006, [hep-ph/0603071].
- [47] K. Risager, “A direct proof of the CSW rules,” *JHEP*, vol. 12, p. 003, 2005, [hep-th/0508206].
- [48] S. D. Badger, E. W. N. Glover, and V. V. Khoze, “MHV rules for Higgs plus multi-parton amplitudes,” *JHEP*, vol. 03, p. 023, 2005, [hep-th/0412275].
- [49] J.-B. Wu and C.-J. Zhu, “MHV vertices and fermionic scattering amplitudes in gauge theory with quarks and gluinos,” *JHEP*, vol. 09, p. 063, 2004, [hep-th/0406146].
- [50] R. Boels and C. Schwinn, “CSW rules for a massive scalar,” *Phys. Lett.*, vol. B662, pp. 80–86, 2008, [arXiv:0712.3409].
- [51] F. Caravaglios, M. L. Mangano, M. Moretti, and R. Pittau, “A new approach to multi-jet calculations in hadron collisions,” *Nucl. Phys.*, vol. B539, pp. 215–232, 1999, [hep-ph/9807570].
- [52] T. Gleisberg and S. Hoeche, “Comix, a new matrix element generator,” *JHEP*, vol. 12, p. 039, 2008, [arXiv:0808.3674].

- [53] K. J. Ozeren and W. J. Stirling, “MHV techniques for QED processes,” *JHEP*, vol. 11, p. 016, 2005, [hep-th/0509063].
- [54] M. Dinsdale, M. Ternick, and S. Weinzierl, “A comparison of efficient methods for the computation of Born gluon amplitudes,” *JHEP*, vol. 03, p. 056, 2006, [hep-ph/0602204].
- [55] J. M. Campbell and E. W. N. Glover, “Double unresolved approximations to multiparton scattering amplitudes,” *Nucl. Phys.*, vol. B527, pp. 264–288, 1998, [hep-ph/9710255].
- [56] S. Catani and M. Grazzini, “Collinear factorization and splitting functions for next- to-next-to-leading order QCD calculations,” *Phys. Lett.*, vol. B446, pp. 143–152, 1999, [hep-ph/9810389].
- [57] S. Catani and M. Grazzini, “Infrared factorization of tree level QCD amplitudes at the next-to-next-to-leading order and beyond,” *Nucl. Phys.*, vol. B570, pp. 287–325, 2000, [hep-ph/9908523].
- [58] D. A. Kosower, “All-order collinear behavior in gauge theories,” *Nucl. Phys.*, vol. B552, pp. 319–336, 1999, [hep-ph/9901201].
- [59] Z. Bern, L. J. Dixon, and D. A. Kosower, “One loop corrections to two quark three gluon amplitudes,” *Nucl. Phys.*, vol. B437, pp. 259–304, 1995, [hep-ph/9409393].
- [60] Z. Bern, L. J. Dixon, and D. A. Kosower, “Two-loop  $g \rightarrow gg$  splitting amplitudes in QCD,” *JHEP*, vol. 08, p. 012, 2004, [hep-ph/0404293].
- [61] A. Vogt, S. Moch, and J. A. M. Vermaseren, “The three-loop splitting functions in QCD: The singlet case,” *Nucl. Phys.*, vol. B691, pp. 129–181, 2004, [hep-ph/0404111].
- [62] S. Moch, J. A. M. Vermaseren, and A. Vogt, “The three-loop splitting functions in QCD: The non-singlet case,” *Nucl. Phys.*, vol. B688, pp. 101–134, 2004, [hep-ph/0403192].
- [63] G. Somogyi and Z. Trocsanyi, “A new subtraction scheme for computing QCD jet cross sections at next-to-leading order accuracy,” 2006, [hep-ph/0609041].

- 
- [64] D. A. Kosower, “Antenna factorization in strongly-ordered limits,” *Phys. Rev.*, vol. D71, p. 045016, 2005, [hep-ph/0311272].
- [65] A. Gehrmann-De Ridder, T. Gehrmann, and E. W. N. Glover, “Antenna subtraction at NNLO,” *JHEP*, vol. 09, p. 056, 2005, [hep-ph/0505111].
- [66] A. Gehrmann-De Ridder, T. Gehrmann, and E. W. N. Glover, “Quark-gluon antenna functions from neutralino decay,” *Phys. Lett.*, vol. B612, pp. 36–48, 2005, [hep-ph/0501291].
- [67] A. Gehrmann-De Ridder, T. Gehrmann, and E. W. N. Glover, “Gluon-gluon antenna functions from Higgs boson decay,” *Phys. Lett.*, vol. B612, no. 49-60, 2005, [hep-ph/0502110].
- [68] D. Maitre and P. Mastrolia, “S@M, a Mathematica Implementation of the Spinor-Helicity Formalism,” 2007, [arXiv:0710.5559].
- [69] U. Aglietti, V. Del Duca, C. Duhr, G. Somogyi, and Z. Trocsanyi, “Analytic integration of real-virtual counterterms in NNLO jet cross sections I,” *JHEP*, vol. 09, p. 107, 2008, [arXiv:0807.0514].
- [70] W. L. van Neerven, “Dimensional Regularization of Mass and Infrared Singularities in Two Loop On-Shell Vertex Functions,” *Nucl. Phys.*, vol. B268, p. 453, 1986.
- [71] T. Huber and D. Maitre, “HypExp, a Mathematica package for expanding hypergeometric functions around integer-valued parameters,” *Comput. Phys. Commun.*, vol. 175, pp. 122–144, 2006, [hep-ph/0507094].
- [72] T. Huber and D. Maitre, “HypExp 2, Expanding Hypergeometric Functions about Half-Integer Parameters,” *Comput. Phys. Commun.*, vol. 178, pp. 755–776, 2008, [0708.2443].
- [73] M. Y. Kalmykov and B. A. Kniehl, “Towards all-order Laurent expansion of generalized hypergeometric functions around rational values of parameters,” *Nucl. Phys.*, vol. B809, pp. 365–405, 2009, [arXiv:0807.0567].
- [74] M. Y. Kalmykov, V. V. Bytev, B. A. Kniehl, B. F. L. Ward, and S. A. Yost, “Feynman Diagrams, Differential Reduction, and Hypergeometric Functions,” 2009, [arXiv:0901.4716].

- [75] S. Moch, P. Uwer, and S. Weinzierl, “Nested sums, expansion of transcendental functions and multi-scale multi-loop integrals,” *J. Math. Phys.*, vol. 43, pp. 3363–3386, 2002, [hep-ph/0110083].
- [76] S. Moch and P. Uwer, “XSummer: Transcendental functions and symbolic summation in Form,” *Comput. Phys. Commun.*, vol. 174, pp. 759–770, 2006, math-ph/0508008.
- [77] A. V. Kotikov, “Differential equations method: New technique for massive Feynman diagrams calculation,” *Phys. Lett.*, vol. B254, pp. 158–164, 1991.
- [78] A. V. Kotikov, “Differential equations method: The Calculation of vertex type Feynman diagrams,” *Phys. Lett.*, vol. B259, pp. 314–322, 1991.
- [79] A. V. Kotikov, “Differential equation method: The Calculation of N point Feynman diagrams,” *Phys. Lett.*, vol. B267, pp. 123–127, 1991.
- [80] M. Caffo, H. Czyz, S. Laporta, and E. Remiddi, “The master differential equations for the 2-loop sunrise selfmass amplitudes,” *Nuovo Cim.*, vol. A111, pp. 365–389, 1998, [hep-th/9805118].
- [81] M. Caffo, H. Czyz, S. Laporta, and E. Remiddi, “Master equations for master amplitudes,” *Acta Phys. Polon.*, vol. B29, pp. 2627–2635, 1998, [hep-th/9807119].
- [82] E. Remiddi, “Differential equations for Feynman graph amplitudes,” *Nuovo Cim.*, vol. A110, pp. 1435–1452, 1997, [hep-th/9711188].
- [83] P. Bolzoni, S. Moch, G. Somogyi, and Z. Trocsanyi, “Analytic integration of real-virtual counterterms in NNLO jet cross sections II,” 2009, [arXiv:0905.4390].
- [84] Z. Bern, M. Czakon, D. A. Kosower, R. Roiban, and V. A. Smirnov, “Two-loop iteration of five-point  $\mathcal{N} = 4$  super-Yang-Mills amplitudes,” *Phys. Rev. Lett.*, vol. 97, p. 181601, 2006, [hep-th/0604074].
- [85] L. F. Alday and J. M. Maldacena, “Gluon scattering amplitudes at strong coupling,” *JHEP*, vol. 06, p. 064, 2007, [arXiv:0705.0303].

- [86] E. A. Kuraev, L. N. Lipatov, and V. S. Fadin, “Multi - Reggeon Processes in the Yang-Mills Theory,” *Sov. Phys. JETP*, vol. 44, pp. 443–450, 1976.
- [87] V. Del Duca, “Equivalence of the Parke-Taylor and the Fadin-Kuraev-Lipatov amplitudes in the high-energy limit,” *Phys. Rev.*, vol. D52, pp. 1527–1534, 1995, [hep-ph/9503340].
- [88] L. N. Lipatov, “Reggeization of the Vector Meson and the Vacuum Singularity in Nonabelian Gauge Theories,” *Sov. J. Nucl. Phys.*, vol. 23, pp. 338–345, 1976.
- [89] L. N. Lipatov, “High-energy scattering in QCD and in quantum gravity and two-dimensional field theories,” *Nucl. Phys.*, vol. B365, pp. 614–632, 1991.
- [90] V. A. Smirnov, *Feynman Integral Calculus*. Springer, 2006.
- [91] V. S. Fadin and L. N. Lipatov, “Radiative corrections to QCD scattering amplitudes in a multi - Regge kinematics,” *Nucl. Phys.*, vol. B406, pp. 259–292, 1993.
- [92] V. Del Duca and C. R. Schmidt, “Virtual next-to-leading corrections to the impact factors in the high-energy limit,” *Phys. Rev.*, vol. D57, pp. 4069–4079, 1998, [hep-ph/9711309].
- [93] V. Del Duca and C. R. Schmidt, “Virtual next-to-leading corrections to the Lipatov vertex,” *Phys. Rev.*, vol. D59, p. 074004, 1999, [hep-ph/9810215].
- [94] J. Bartels, L. N. Lipatov, and A. S. Vera, “BFKL Pomeron, Reggeized gluons and Bern-Dixon-Smirnov amplitudes,” 2008, [arXiv:0802.2065].
- [95] R. C. Brower, H. Nastase, H. J. Schnitzer, and C.-I. Tan, “Implications of multi-Regge limits for the Bern-Dixon-Smirnov conjecture,” *Nucl. Phys.*, vol. B814, pp. 293–326, 2009, [arXiv:0801.3891].
- [96] R. C. Brower, H. Nastase, H. J. Schnitzer, and C.-I. Tan, “Analyticity for Multi-Regge Limits of the Bern-Dixon-Smirnov Amplitudes,” 2008, [arXiv:0809.1632].

- [97] A. Erdélyi, *Higher Transcendental Functions*, vol. 1 and 2. McGraw-Hill, 1954.
- [98] H. Exton, *Multiple Hypergeometric Functions and Applications*. Ellis Horwood, 1976.
- [99] J. A. M. Vermaseren, “Harmonic sums, Mellin transforms and integrals,” *Int. J. Mod. Phys.*, vol. A14, pp. 2037–2076, 1999, [hep-ph/9806280].
- [100] M. L. Mangano, M. Moretti, F. Piccinini, R. Pittau, and A. D. Polosa, “ALPGEN, a generator for hard multiparton processes in hadronic collisions,” *JHEP*, vol. 07, p. 001, 2003, [hep-ph/0206293].
- [101] N. Nielsen, “Der Eulersche Dilogarithmus und seine Verallgemeinerungen,” *Nova Acta Leopoldina*, vol. 90, p. 123, 1909.
- [102] E. Remiddi and J. A. M. Vermaseren, “Harmonic polylogarithms,” *Int. J. Mod. Phys.*, vol. A15, pp. 725–754, 2000, [hep-ph/9905237].
- [103] T. Gehrmann and E. Remiddi, “Numerical evaluation of harmonic polylogarithms,” *Comput. Phys. Commun.*, vol. 141, pp. 296–312, 2001, [hep-ph/0107173].
- [104] D. Maitre, “HPL, a Mathematica implementation of the harmonic polylogarithms,” *Comput. Phys. Commun.*, vol. 174, pp. 222–240, 2006, [hep-ph/0507152].
- [105] D. Maitre, “Extension of HPL to complex arguments,” 2007, [hep-ph/0703052].
- [106] T. Gehrmann and E. Remiddi, “Two-loop master integrals for  $\gamma^* \rightarrow 3$  jets: The planar topologies,” *Nucl. Phys.*, vol. B601, pp. 248–286, 2001, [hep-ph/0008287].
- [107] T. Gehrmann and E. Remiddi, “Numerical evaluation of two-dimensional harmonic polylogarithms,” *Comput. Phys. Commun.*, vol. 144, pp. 200–223, 2002, [hep-ph/0111255].
- [108] A. B. Goncharov, “Multiple polylogarithms, cyclotomy and modular complexes,” *Math. Research Letters*, vol. 5, pp. 497–516, July 1998.



- 
- [109] A. B. Goncharov, “Multiple polylogarithms and mixed Tate motives,” 2001, [math/0103059v4].
- [110] A. P. Prudnikov, Y. A. Brychkov, and O. Marichev, *Integrals and Series*. Gordon and Breach, 1990.
- [111] Appell, P. and Kampé de Fériet, J., *Fonctions Hypergéométriques et Hypersphériques, Polynômes d’Hermite*. Gauthiers-Villars, 1926.
- [112] K. G. Wilson, “Quantum field theory models in less than four- dimensions,” *Phys. Rev.*, vol. D7, pp. 2911–2926, 1973.
- [113] V. A. Smirnov, *Evaluating Feynman Integrals*. Springer Tracts Mod. Phys. **211**, 2004.
- [114] N. N. Bogoliubov and D. V. Shirkov, *Quantum Fields*. Benjamin Cummings Pub. Co., 1982.
- [115] C. Itzykson and J. B. Zuber, *Quantum Field Theory*. McGraw-Hill, 1980.
- [116] I. G. Halliday and R. M. Ricotta, “Negative Dimensional Integrals. 1. Feynman Graphs,” *Phys. Lett.*, vol. B193, p. 241, 1987.
- [117] R. M. Ricotta, “Negative Dimensions in Quantum Field Theory,” in *J.J. Giambiagi Festschrift* (H. Falomir, ed.), p. 350, 1990. IFT/P-33/89-SAO PAULO.
- [118] Z. Bern, M. Czakon, L. J. Dixon, D. A. Kosower, and V. A. Smirnov, “The Four-Loop Planar Amplitude and Cusp Anomalous Dimension in Maximally Supersymmetric Yang-Mills Theory,” *Phys. Rev.*, vol. D75, p. 085010, 2007, [hep-th/0610248].





